REFERENCE DATA FOR RADIO ENGINEERS

HOWARD W. SAMS & CO., INC.
A SUBSIDIARY OF
INTERNATIONAL TELEPHONE AND TELEGRAPH CORPORATION

ITT

REFERENCE DATA FOR RADIO ENGINEERS

CONTENTS OF THIS SIXTH EDITION

Frequency Data
International Telecommunication Recommendations
Units, Constants, and Conversion Factors
Properties of Materials
Components or Parts
Fundamentals of Networks
Filters, Image-Parameter Design
Filters, Modern-Network-Theory Design
Filters, Simple Band-Pass Design
Active Filter Design
Attenuators
Bridges and Impedance Measurements
Magnetic-Core Transformers and Reactors
Rectifiers and Filters
Magnetic Amplifiers
Feedback Control Systems
Electron Tubes
Electron-Tube Circuits
Semiconductors and Transistors
Transistor Circuits
Microminiature Electronics
Optoelectronics
Modulation
Transmission Lines
Waveguides and Resonators
Scattering Matrices
Antennas
Electromagnetic-Wave Propagation
Radio Noise and Interference
Broadcasting and Recording
Radar Fundamentals
Navigational Aids
Space Communication
Optical Communications
Wire Transmission
Switching Networks and Traffic Concepts
Electroacoustics
Nuclear Physics
Quantum Electronics
Digital Computers
Information Theory
Probability and Statistics
Reliability and Life Testing
Fourier Waveform Analysis
Maxwell's Equations
Mathematical Equations
Mathematical Tables
Miscellaneous Data

21218

ISBN: 0—672—21218—8

HOWARD W. SAMS & CO., INC.
A SUBSIDIARY OF
INTERNATIONAL TELEPHONE AND TELEGRAPH CORPORATION

REFERENCE DATA FOR RADIO ENGINEERS

SIXTH EDITION

Written by professionals for professionals, *Reference Data for Radio Engineers* is primarily a compilation of equations, graphs, tables, and similar data frequently needed in general radio engineering and design.

It began as a limited private edition used by engineers, mathematicians, and physicists of the worldwide International Telephone and Telegraph Corporation. Spurred on by immediate popular acceptance, it has grown into an intensely practical and compact encyclopedia of electronics, containing a very broad range of data not heretofore gathered together in one volume.

Reference Data for Radio Engineers has been accepted for classroom use in more than 200 of our leading colleges and universities.

$30.00

REFERENCE DATA FOR RADIO ENGINEERS
SIXTH EDITION

here are some comments about the previous editions.

"The book contains a great quantity of data, moreover, it is organized for ready retrieval." *IEEE SPECTRUM*

"Any engineer who has ever used "Reference Data" in the past will welcome this new edition with enthusiasm. For those not familiar with this "bible," this is a chance to acquire a complete reference library between two covers." *ELECTRONICS WORLD*

"Considering the extremely broad spectrum of subjects covered, the manual is easy reading and the information is well-presented." *EDN*

"It is a very practical supplement to the library of the practicing technician, engineer or educator . . . some institutions require (it) of their electrical engineering students and this alone should testify as to its usefulness in the profession." *Lyle C. Wilcox, College of Engineering, Clemson University.*

"Here's a book that for (many) years has provided the busy engineer with fast access to equations, graphs, tables, and other data . . . the engineer's bible." *ELECTRONICS*

REFERENCE DATA FOR RADIO ENGINEERS

REFERENCE DATA FOR RADIO ENGINEERS

HOWARD W. SAMS & CO., INC.
INDIANAPOLIS/KANSAS CITY/NEW YORK
A SUBSIDIARY OF
INTERNATIONAL TELEPHONE AND TELEGRAPH CORPORATION

WRH

SIXTH EDITION

FOURTH PRINTING—1981

Copyright © 1968, 1975 by Howard W. Sams & Co., Inc., Indianapolis, Indiana 46268; Copyright © 1956 by International Telephone and Telegraph Corp; Copyright © 1943, 1946, and 1949 by Federal Telephone and Radio Corp. Printed in the United States of America.

All rights reserved. Reproduction or use, without express permission, of editorial or pictorial content, in any manner, is prohibited. No patent liability is assumed with respect to the use of the information contained herein. While every precaution has been taken in the preparation of this book, the publisher assumes no responsibility for errors or omissions. Neither is any liability assumed for damages resulting from the use of the information contained herein.

International Standard Book Number: 0-672-21218-8
Library of Congress Catalog Card Number: 75-28960

FOREWORD

This sixth edition of *Reference Data for Radio Engineers* grew from a 60-page brochure of that title originally compiled by W. L. McPherson of ITT's Standard Telephones and Cables Limited, which company published it in England in 1942. Its immediate acceptance prompted the parent company, International Telephone and Telegraph Corporation, to arrange for a United States version that in five editions dated 1943, 1946, 1949, 1956, and 1968 had a total sale of 450,000 copies. The book has become a first place for the busy radio engineer to look for all kinds of data. It has also been widely used in colleges by both faculties and students.

To maintain a high standard in a book of such wide scope, it has been necessary to go outside of the ITT System for objective reviews of material to guide revisions, for critical reviews of manuscripts, and for the preparation of some new material. Such contributions are gratefully acknowledged from H. R. Romig; D. J. LeVine; N. Marchand of Marchand Laboratories; L. J. Lidofsky of Columbia University; Colin Cherry of London University; R. C. Barker of Yale University; J. D. Kraus of Ohio State University; J. A. Pierce of Harvard University; G. A. Deschamps of University of Illinois; J. R. Ragazzini of New York University; E. A. Guillemin of Massachusetts Institute of Technology; and from N. Marcuvitz, W. K. Kahn, and T. Tamir of Brooklyn Polytechnic Institute. The following persons from National Bureau of Standards and Environmental Science Services Administration also generously contributed to the book: J. W. Herbstreit, R. T. Disney, W. Q. Crichlow, P. L. Rice, D. D. Crombie, A. F. Barghausen, G. W. Haydon, R. S. Lawrence, and M. S. Cord.

Special acknowledgments are given to additional contributors to the sixth edition: D. Davis of Synergetic Audio Concepts, L. S. Golding of Digital Communications Corporation and J. E. D. Ball of Public Broadcasting Service, J. L. Hilburn and D. E. Johnson of Louisiana State University, F. M. Mims III, R. E. Taylor of the National Aeronautics and Space Administration, and J. L. Walters and R. J. Adams of the Naval Research Laboratory.

The difficulty in identifying the authors of material carried over during the more than 30-year history of the book makes it impossible for us to list their names despite the debt we owe them. However, special acknowledgment is made of the valuable contributions of A. G. Kandoian as Chairman of the Editorial Boards for the third through fifth editions and of H. P. Westman who edited the fourth and fifth editions. The following currently active International System personnel are acknowledged as contributors:

E. Baguley
E. E. Benham
R. A. Bones
T. Brown
J. H. Brundage
F. X. Bucher
J. A. Budek
H. G. Busignies
A. Casabona
R. Clayton
D. K. Coles
C. R. Cook
A. E. Cookson
M. Dishal
S. H. Dodington
J. G. Dunn
E. Eberhardt
J. A. Fingerett
M. T. Fujita
D. S. Girling
F. F. Hall

I. W. Hammer
D. E. Herrington
J. L. Jatlow
P. King
J. Kylander
P. Lighty
W. Litchman
J. G. Litterick
C. W. Moody
J. M. Moore
H. G. Nordlin
J. E. Obst
J. A. O'Connell
C. P. Oliphant
J. Polyzou
M. C. Poylo
L. G. Rado
D. S. Ridler
L. Rosenberg
J. E. Schlaikjer
H. H. Smith
R. Smith
T. L. Squires
J. L. Storr-Best
J. G. Tatum
L. F. Turner
R. Vachss
J. M. Valentine
R. Weber
A. K. Wing, Jr.
J. Youlios

TABLE OF CONTENTS

	Chapter
Frequency Data	1
International Telecommunication Recommendations	2
Units, Constants, and Conversion Factors	3
Properties of Materials	4
Components or Parts	5
Fundamentals of Networks	6
Filters, Image-Parameter Design	7
Filters, Modern-Network-Theory Design	8
Filters, Simple Band-Pass Design	9
Active Filter Design	10
Attenuators	11
Bridges and Impedance Measurements	12
Magnetic-Core Transformers and Reactors	13
Rectifiers and Filters	14
Magnetic Amplifiers	15
Feedback Control Systems	16
Electron Tubes	17
Electron-Tube Circuits	18
Semiconductors and Transistors	19
Transistor Circuits	20
Microminiature Electronics	21
Optoelectronics	22

Modulation 23

Transmission Lines 24

Waveguides and Resonators 25

Scattering Matrices 26

Antennas 27

Electromagnetic-Wave Propagation 28

Radio Noise and Interference 29

Broadcasting and Recording 30

Radar Fundamentals 31

Navigation Aids 32

Space Communication 33

Optical Communications 34

Wire Transmission 35

Switching Networks and Traffic Concepts 36

Electroacoustics 37

Nuclear Physics 38

Quantum Electronics 39

Digital Computers 40

Information Theory 41

Probability and Statistics 42

Reliability and Life Testing 43

Fourier Waveform Analysis 44

Maxwell's Equations 45

Mathematical Equations 46

Mathematical Tables 47

Miscellaneous Data 48

CHAPTER 1
FREQUENCY DATA

WAVELENGTH-FREQUENCY CONVERSION

Figure 1 permits conversion between frequency and wavelength; by use of multiplying factors shown, this graph will cover any portion of the electromagnetic-wave spectrum.

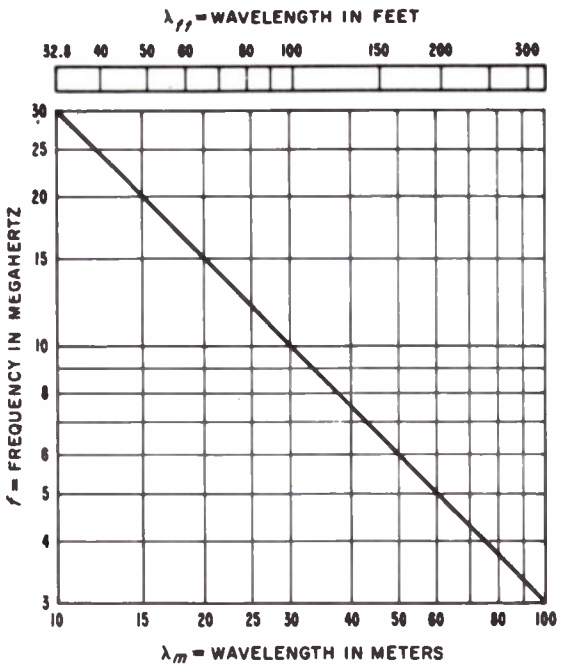

For Frequencies in Megahertz from	Multiply f by	Multiply λ by
0.03– 0.3	0.01	100
0.3 – 3.0	0.1	10
3.0 – 30	1.0	1.0
30 – 300	10	0.1
300 – 3 000	100	0.01
3 000 – 30 000	1 000	0.001
30 000 –300 000	10 000	0.0001

Fig. 1—Wavelength-frequency conversion.

Conversion Equations

Propagation velocity

$$c \approx 3 \times 10^8 \text{ meters/second}$$

Wavelength in meters

$$\lambda_m = \frac{300\,000}{f \text{ in kilohertz}} = \frac{300}{f \text{ in megahertz}}$$

Wavelength in centimeters

$$\lambda_{cm} = \frac{30}{f \text{ in gigahertz}}$$

Wavelength in feet

$$\lambda_{ft} = \frac{984\,000}{f \text{ in kilohertz}} = \frac{984}{f \text{ in megahertz}}$$

Wavelength in inches

$$\lambda_{in} = \frac{11.8}{f \text{ in gigahertz}}$$

1 angstrom unit $\text{Å} = 3.937 \times 10^{-9}$ inch
$= 1 \times 10^{-10}$ meter
$= 1 \times 10^{-4}$ micrometer

1 micrometer $\mu\text{m} = 3.937 \times 10^{-5}$ inch
$= 1 \times 10^{-6}$ meter
$= 1 \times 10^{4}$ angstrom units.

(Note that the term "micrometer" has superceded the term "micron.")

Nomenclature of Frequency Bands

Table 1 is adapted from the Radio Regulations of the International Telecommunication Union, Article 2, Section 11, Geneva; 1959.

Letter Designations for Frequency Bands

Letter designations commonly used for microwave bands (particularly in references to radar equipment) are shown in Table 2. These designations have no official international standing, and various engineers have used limits for the bands and subbands other than those listed in the table.

Subband code letters should be used as sub-

TABLE 1—NOMENCLATURE OF FREQUENCY BANDS.

Band Number*	Frequency Range	Metric Subdivision	Adjectival Designation
2	30 to 300 hertz	Megametric waves	ELF Extremely low frequency
3	300 to 3000 hertz	———	VF Voice frequency
4	3 to 30 kilohertz	Myriametric waves	VLF Very-low frequency
5	30 to 300 kilohertz	Kilometric waves	LF Low frequency
6	300 to 3000 kilohertz	Hectometric waves	MF Medium frequency
7	3 to 30 megahertz	Decametric waves	HF High frequency
8	30 to 300 megahertz	Metric waves	VHF Very-high frequency
9	300 to 3000 megahertz	Decimetric waves	UHF Ultra-high frequency
10	3 to 30 gigahertz	Centimetric waves	SHF Super-high frequency
11	30 to 300 gigahertz	Millimetric waves	EHF Extremely high frequency
12	300 to 3000 gigahertz or 3 terahertz	Decimillimetric waves	— —

* "Band Number N" extends from 0.3×10^N to 3×10^N hertz. The upper limit is included in each band; the lower limit is excluded.

scripts in designating particular frequency ranges; for example, L_x indicates the band between 0.950 and 1.150 gigahertz.

FREQUENCY ALLOCATIONS BY INTERNATIONAL TREATY

The following information is adapted from the Radio Regulations of the ITU, Geneva, 1959, corrected to July 1965. Some 400 footnotes describing special conditions pertaining to allocations within particular frequency bands and much other detailed information are not reproduced here. Copies of the Radio Regulations may be obtained from the Secretary General, International Telecommunication Union, Place des Nations, CH-1211, Geneva 20, Switzerland.*

For purposes of frequency allocations, the world has been divided into regions shown in Fig. 2.

See Article 5, Section 1 of the ITU Radio Regulations for definitions of the regions and of lines *A*, *B*, and *C*.

Frequency bands are allocated to services defined as follows:

Fixed: Radio communication between specified fixed points. Examples are point-to-point high-frequency circuits and microwave links.

Mobile: Radio communication between stations intended to be used while in motion or during halts at unspecified points or between such stations and fixed stations.

* In the official documents of ITU and FCC the following terms are combined as single words: radiobeacon, radiocommunication, radiodetermination, radiolocation, radionavigation, radiorange, radiosonde, radiotelegraphy, and radiotelephony.

Aeronautical Mobile: Radio communication between a land station and an aircraft or between aircraft. (*R* indicates frequency bands for communication within regions. *OR* indicates bands for communication between regions.)

Maritime Mobile: Radio communication between a coast station and a ship or between ships.

Land Mobile: Radio communication between a base station and land mobile station or between land mobile stations. Examples are radio communication with taxicabs and police vehicles.

Radio Navigation: The determination of position for purposes of navigation by means of the propagation properties of radio waves. This includes obstruction warning. An example is loran.

Aeronautical Radio Navigation: A radio navigation service intended for the benefit of aircraft. Examples are VOR and Tacan systems, aeronautical radio beacons, instrument landing systems, radio altimeters, and airborne obstruction-indicating radar.

Maritime Radio Navigation: A radio navigation service intended for the benefit of ships. Examples are coastal radio beacons, direction-finding stations, and shipboard radar.

Radio Location: The determination of position for purposes other than those of navigation by means of the propagation properties of radio waves. Examples are land radars, coastal radars, and tracking systems.

Broadcasting: Radio communication intended for direct reception by the general public. Examples are amplitude-modulation broadcasting on me-

TABLE 2—LETTER DESIGNATIONS FOR MICROWAVE BANDS.

Subband	Frequency in Gigahertz	Wavelength in Centimeters
	P Band	
	0.225	133.3
	0.390	76.9
	L Band	
	0.390	76.9
p	0.465	64.5
c	0.510	58.8
l	0.725	41.4
y	0.780	38.4
t	0.900	33.3
s	0.950	31.6
x	1.150	26.1
k	1.350	22.2
f	1.450	20.7
z	1.550	19.3
	S Band	
	1.55	19.3
e	1.65	18.3
f	1.85	16.2
t	2.00	15.0
c	2.40	12.5
q	2.60	11.5
y	2.70	11.1
g	2.90	10.3
s	3.10	9.67
a	3.40	8.32
w	3.70	8.10
h	3.90	7.69
*z**	4.20	7.14
d	5.20	5.77
	X Band	
	5.20	5.77
a	5.50	5.45
q	5.75	5.22
*y**	6.20	4.84
d	6.25	4.80
b	6.90	4.35
r	7.00	4.29
c	8.50	3.53
l	9.00	3.33
s	9.60	3.13
x	10.00	3.00
f	10.25	2.93
k	10.90	2.75
	K Band	
	10.90	2.75
p	12.25	2.45
s	13.25	2.26
e	14.25	2.10
c	15.35	1.95
u†	17.25	1.74
t	20.50	1.46
q†	24.50	1.22
r	26.50	1.13
m	28.50	1.05
n	30.70	0.977
l	33.00	0.909
a	36.00	0.834
	Q Band	
	36.0	0.834
a	38.0	0.790
b	40.0	0.750
c	42.0	0.715
d	44.0	0.682
e	46.0	0.652
	V Band	
	46.0	0.652
a	48.0	0.625
b	50.0	0.600
c	52.0	0.577
d	54.0	0.556
e	56.0	0.536
	W Band	
	56.0	0.536
	100.0	0.300

* *C* Band includes S_z through X_y (3.90–6.20 gigahertz).
† K_1 Band includes K_u through K_q (15.35–24.50 gigahertz).

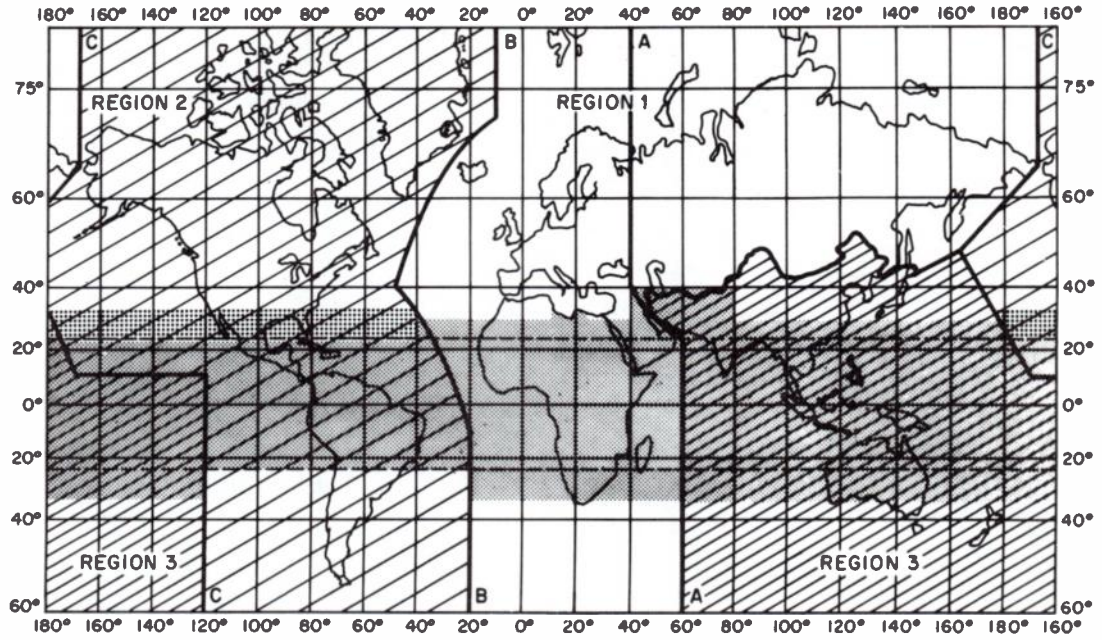

Fig. 2—Regions defined in table of frequency allocations. Shaded area represents tropical zone.

dium and high frequencies, frequency-modulation broadcasting, and television.

Amateur: Radio communication carried on by persons interested in the radio technique solely with a personal aim and without pecuniary interest.

Space: Radio communication between space stations.

Earth-Space: Radio communication between earth stations and space stations. An example is between the earth and a satellite.

Radio Astronomy: Astronomy based on the reception of radio waves of cosmic origin.

Standard Frequency: Radio transmission of specified frequencies of stated high precision, intended for general reception for scientific, technical, and other purposes.

The following allocations pertain to Region 2 (the western hemisphere). An asterisk (*) indicates that the allocation also pertains on a worldwide basis. Frequency assignments in the United States comply with the following table but they have been further divided (especially above 30 megahertz) among particular types of service as shown in the listings later in this chapter.

Services printed in small capitals (example: FIXED) are primary services.

Services printed in italics (example: *Radio location*) are permitted services and have equal rights with primary services except that the primary services have prior choice of frequencies.

Services printed in lower-case type (example: Mobile) are secondary services which shall not cause harmful interference to, or claim protection from, stations of a primary or permitted service.

The order of listing does not indicate relative priority within each category.

Kilohertz	Service
Below 10.00	(not allocated)*
10.00–14.00	RADIO NAVIGATION*
	Radio location*
14.00–19.95	FIXED*
	MARITIME MOBILE*
19.95–20.05	STANDARD FREQUENCY*
20.05–70.00	FIXED*
	MARITIME MOBILE*
70.00–90.00	FIXED
	MARITIME MOBILE
	MARITIME RADIO NAVIGATION
	Radio location
90.00–110.0	RADIO NAVIGATION
	FIXED
	Maritime mobile
110.0–130.0	FIXED
	MARITIME MOBILE
	MARITIME RADIO NAVIGATION
	Radio location
130.0–160.0	FIXED
	MARITIME MOBILE
160.0–200.0	FIXED
200.0–285.0	AERONAUTICAL RADIO NAVIGATION
	Aeronautical mobile
285.0–325.0	MARITIME RADIO NAVIGATION (radio beacons)
	Aeronautical radio navigation

Kilohertz	Service
325.0–405.0	AERONAUTICAL RADIO NAVIGATION*
	Aeronautical mobile*
405.0–415.0	MARITIME RADIO NAVIGATION
	(radio direction-finding)
	Aeronautical radio navigation
	Aeronautical mobile
415.0–490.0	MARITIME MOBILE*
	(radiotelegraphy only)
490.0–510.0	MOBILE*
	(distress and calling)
510.0–525.0	MOBILE
	Aeronautical radio navigation
525.0–535.0	MOBILE
	Broadcasting
	Aeronautical radio navigation
535.0–1605	BROADCASTING*
1605–1800	FIXED
	MOBILE
	AERONAUTICAL RADIO NAVIGATION
	Radio location
1800–2000	AMATEUR
	FIXED
	MOBILE EXCEPT AERONAUTICAL
	RADIO NAVIGATION
2000–2065	FIXED
	MOBILE
2065–2107	MARITIME MOBILE
2107–2170	FIXED
	MOBILE
2170–2194	MOBILE*
	(distress and calling)
2194–2300	FIXED
	MOBILE
2300–2495	FIXED
	MOBILE
	BROADCASTING
2495–2505	STANDARD FREQUENCY
2505–2850	FIXED
	MOBILE
2850–3025	AERONAUTICAL MOBILE (*R*)*

Megahertz	Service
3.025–3.155	AERONAUTICAL MOBILE (*OR*)*
3.155–3.200	FIXED*
	MOBILE EXCEPT AERONAUTICAL (*R*)*
3.200–3.400	FIXED*
	MOBILE EXCEPT AERONAUTICAL*
	BROADCASTING*
3.400–3.500	AERONAUTICAL MOBILE (*R*)*
3.500–4.000	AMATEUR
	FIXED
	MOBILE EXCEPT AERONAUTICAL (*R*)
4.000–4.063	FIXED*
4.063–4.438	MARITIME MOBILE*
4.438–4.650	FIXED
	MOBILE EXCEPT AERONAUTICAL (*R*)
4.650–4.700	AERONAUTICAL MOBILE (*R*)*
4.700–4.750	AERONAUTICAL MOBILE (*OR*)*

Megahertz	Service
4.750–4.850	FIXED
	BROADCASTING
4.850–4.995	FIXED*
	LAND MOBILE*
	BROADCASTING*
4.995–5.005	STANDARD FREQUENCY*
5.005–5.060	FIXED*
	BROADCASTING*
5.060–5.250	FIXED*
5.250–5.450	FIXED
	LAND MOBILE
5.450–5.680	AERONAUTICAL MOBILE (*R*)
5.680–5.730	AERONAUTICAL MOBILE (*OR*)*
5.730–5.950	FIXED*
5.950–6.200	BROADCASTING*
6.200–6.525	MARITIME MOBILE*
6.525–6.685	AERONAUTICAL MOBILE (*R*)*
6.685–6.765	AERONAUTICAL MOBILE (*OR*)*
6.765–7.000	FIXED*
7.000–7.300	AMATEUR
7.300–8.195	FIXED*
8.195–8.815	MARITIME MOBILE*
8.815–8.965	AERONAUTICAL MOBILE (*R*)*
8.965–9.040	AERONAUTICAL MOBILE (*OR*)*
9.040–9.500	FIXED*
9.500–9.775	BROADCASTING*
9.775–9.995	FIXED*
9.995–10.005	STANDARD FREQUENCY*
10.005–10.10	AERONAUTICAL MOBILE (*R*)*
10.10–11.175	FIXED*
11.175–11.275	AERONAUTICAL MOBILE (*OR*)*
11.275–11.40	AERONAUTICAL MOBILE (*R*)*
11.40–11.70	FIXED*
11.70–11.975	BROADCASTING*
11.975–12.33	FIXED*
12.33–13.20	MARITIME MOBILE*
13.20–13.26	AERONAUTICAL MOBILE (*OR*)*
13.26–13.36	AERONAUTICAL MOBILE (*R*)*
13.36–14.00	FIXED*
14.00–14.35	AMATEUR*
14.35–14.99	FIXED*
14.99–15.01	STANDARD FREQUENCY*
15.01–15.10	AERONAUTICAL MOBILE (*OR*)*
15.10–15.45	BROADCASTING*
15.45–16.46	FIXED*
16.46–17.36	MARITIME MOBILE*
17.36–17.70	FIXED*
17.70–17.90	BROADCASTING*
17.90–17.97	AERONAUTICAL MOBILE(*R*)*
17.97–18.03	AERONAUTICAL MOBILE (*OR*)*
18.03–18.052	FIXED*
18.052–18.068	FIXED*
	Space research*
18.068–19.99	FIXED*
19.99–20.01	STANDARD FREQUENCY*
20.01–21.00	FIXED*
21.00–21.45	AMATEUR*
21.45–21.75	BROADCASTING*
21.75–21.85	FIXED*

Megahertz	Service
21.85–21.87	RADIO ASTRONOMY*
21.87–22.00	AERONAUTICAL FIXED*
	AERONAUTICAL MOBILE (*R*)*
22.00–22.72	MARITIME MOBILE*
22.72–23.20	FIXED*
23.20–23.35	AERONAUTICAL FIXED*
	AERONAUTICAL MOBILE(*OR*)*
23.35–24.99	FIXED*
	LAND MOBILE*
24.99–25.01	STANDARD FREQUENCY*
25.01–25.07	FIXED*
	MOBILE EXCEPT AERONAUTICAL*
25.07–25.11	MARITIME MOBILE*
25.11–25.60	FIXED*
	MOBILE EXCEPT AERONAUTICAL*
25.60–26.10	BROADCASTING*
26.10–27.50	FIXED*
	MOBILE EXCEPT AERONAUTICAL*
27.50–28.00	METEOROLOGICAL AIDS
	FIXED
	MOBILE
28.00–29.70	AMATEUR*
29.70–30.005	FIXED*
	MOBILE*
30.005–30.01	FIXED*
	MOBILE*
	SPACE OPERATION*
	(satellite identification)
	SPACE RESEARCH*
30.01–37.75	FIXED*
	MOBILE*
37.75–38.25	FIXED*
	MOBILE*
	Radio astronomy*
38.25–50.00	FIXED
	MOBILE
50.00–54.00	AMATEUR
54.00–73.00	FIXED
	MOBILE
	BROADCASTING
73.00–74.60	RADIO ASTRONOMY
74.60–75.40	AERONAUTICAL RADIO NAVIGATION
75.40–88.00	FIXED
	MOBILE
	BROADCASTING
88.00–108.0	BROADCASTING
108.0–117.975	AERONAUTICAL RADIO NAVIGATION*
117.975–132.0	AERONAUTICAL MOBILE (*R*)*
132.0–136.0	AERONAUTICAL MOBILE*
136.0–137.0	SPACE RESEARCH
	(space to earth)
137.0–138.0	METEOROLOGICAL SATELLITE*
	SPACE OPERATION*
	(telemetering and tracking)
	SPACE RESEARCH*
	(space to earth)
138.0–143.6	FIXED
	MOBILE
	Radio location
	Space research
	(space to earth)
143.6–143.65	FIXED
	MOBILE
	SPACE RESEARCH
	(space to earth)
	Radio location
143.65–144.0	FIXED
	MOBILE
	Radio location
	Space research
	(space to earth)
144.0–148.0	AMATEUR
148.0–149.9	FIXED
	MOBILE
149.9–150.05	RADIO NAVIGATION-SATELLITE*
150.05–174.0	FIXED
	MOBILE
174.0–216.0	FIXED
	MOBILE
	BROADCASTING
216.0–220.0	FIXED
	MOBILE
	RADIO LOCATION
220.0–225.0	AMATEUR
	RADIO LOCATION
225.0–267.0	FIXED
	MOBILE
267.0–272.0	FIXED*
	MOBILE*
	Space operation*
	(telemetering)
272.0–273.0	FIXED*
	MOBILE*
	SPACE OPERATION*
	(telemetering)
273.0–328.6	FIXED*
	MOBILE*
328.6–335.4	AERONAUTICAL RADIO NAVIGATION*
	(glide-path systems)
335.4–399.9	FIXED*
	MOBILE*
399.9–400.05	RADIO NAVIGATION-SATELLITE*
400.05–400.15	STANDARD FREQUENCY SATELLITE*
400.15–401.0	METEOROLOGICAL AIDS*
	METEOROLOGICAL-SATELLITE*
	(maintenance telemetering)
	SPACE RESEARCH*
	(telemetering and tracking)
401.0–402.0	METEOROLOGICAL AIDS*
	SPACE OPERATION*
	(telemetering)
	Fixed*
	Meteorological satellite*
	(earth to space)
	Mobile except aeronautical*

Megahertz	Service
402.0–403.0	METEOROLOGICAL AIDS*
	Fixed*
	Meteorological Satellite* (earth to space)
	Mobile except aeronautical*
403.0–406.0	METEOROLOGICAL AIDS*
	Fixed*
	Mobile except aeronautical*
406.0–406.1	MOBILE SATELLITE* (earth to space)
406.1–410.0	FIXED*
	MOBILE EXCEPT AERONAUTICAL*
	RADIO ASTRONOMY*
410.0–420.0	FIXED*
	MOBILE EXCEPT AERONAUTICAL*
420.0–450.0	RADIO LOCATION
	Amateur
450.0–460.0	FIXED*
	MOBILE*
460.0–470.0	FIXED*
	MOBILE*
	Meteorological satellite*
470.0–890.0	BROADCASTING
890.0–942.0	FIXED
	RADIO LOCATION
942.0–960	FIXED
960.0–1215	AERONAUTICAL RADIO NAVIGATION*
1215–1300	RADIO LOCATION*
	Amateur*
1300–1350	AERONAUTICAL RADIO NAVIGATION*
	Radio location*
1350–1400	RADIO LOCATION
1400–1427	RADIO ASTRONOMY*
1427–1429	FIXED*
	MOBILE EXCEPT AERONAUTICAL*
	SPACE OPERATION* (telecommand)
1429–1435	FIXED
	MOBILE
1435–1525	MOBILE
	Fixed
1525–1535	SPACE OPERATION (telemetering)
	Fixed
	Mobile
	Earth Exploration Satellite
1535–1542.5	MARITIME MOBILE SATELLITE*
1542.5–1543.5	AERONAUTICAL MOBILE SATELLITE (R)*
	MARITIME MOBILE SATELLITE*
1543.5–1558.5	AERONAUTICAL MOBILE SATELLITE (R)*
1558.5–1636.5	AERONAUTICAL RADIO NAVIGATION*
1636.5–1644	MARITIME MOBILE SATELLITE*
1644–1645	AERONAUTICAL MOBILE SATELLITE (R)*
	MARITIME MOBILE SATELLITE*
1645–1660	AERONAUTICAL MOBILE SATELLITE (R)*
1660–1670	METEOROLOGICAL AIDS*
	RADIO ASTRONOMY*
1670–1690	METEOROLOGICAL AIDS*
	METEOROLOGICAL SATELLITE* (space to earth)
	FIXED*
	MOBILE EXCEPT AERONAUTICAL*
1690–1700	METEOROLOGICAL AIDS
	METEOROLOGICAL-SATELLITE (space to earth)
1700–1710	FIXED
	MOBILE
	SPACE RESEARCH (space to earth)
1710–1770	FIXED
	MOBILE
1770–1790	FIXED
	MOBILE
	Meteorological-satellite
1790–2290	FIXED
	MOBILE
2290–2300	SPACE RESEARCH (space to earth)
	FIXED
	MOBILE
2300–2450	RADIO LOCATION
	Amateur
	Fixed
	Mobile
2450–2500	FIXED
	MOBILE
	RADIO LOCATION
2500–2535	BROADCASTING SATELLITE
	FIXED
	FIXED SATELLITE (space to earth)
	MOBILE EXCEPT AERONAUTICAL
2535–2655	BROADCASTING SATELLITE
	FIXED
	MOBILE EXCEPT AERONAUTICAL
2655–2690	BROADCASTING SATELLITE
	FIXED
	FIXED-SATELLITE (earth to space)
	MOBILE EXCEPT AERONAUTICAL
2690–2700	RADIO ASTRONOMY*
2700–2900	AERONAUTICAL RADIO NAVIGATION*
	Radio location*
2900–3100	RADIO NAVIGATION* (ground-based radars)
	Radio location*

Gigahertz	Service
3.100–3.300	RADIO LOCATION*
3.300–3.400	RADIO LOCATION
	Amateur
3.400–3.500	RADIO LOCATION
	FIXED SATELLITE (space to earth)
	Amateur

Gigahertz	Service
3.500–3.700	FIXED
	MOBILE
	RADIO LOCATION
	FIXED SATELLITE
	(space to earth)
3.700–4.200	FIXED
	MOBILE
	FIXED SATELLITE
	(space to earth)
4.200–4.400	AERONAUTICAL RADIO NAVIGATION*
4.400–4.700	FIXED*
	MOBILE*
	FIXED SATELLITE*
	(earth to space)
4.700–4.990	FIXED*
	MOBILE*
4.990–5.000	RADIO ASTRONOMY
5.000–5.250	AERONAUTICAL RADIO NAVIGATION*
5.250–5.255	RADIO LOCATION*
	Space research*
5.255–5.350	RADIO LOCATION*
5.350–5.460	AERONAUTICAL RADIO NAVIGATION*
	Radio location*
5.460–5.470	RADIO NAVIGATION*
	Radio location*
5.470–5.650	MARITIME RADIO NAVIGATION*
	Radio location*
5.650–5.670	RADIO LOCATION*
	Amateur*
5.670–5.725	RADIO LOCATION*
	Amateur*
	Space research*
	(deep space)
5.725–5.925	RADIO LOCATION
	Amateur
5.925–6.425	FIXED*
	MOBILE*
	FIXED SATELLITE*
	(earth to space)
6.425–7.250	FIXED*
	MOBILE*
7.250–7.300	FIXED SATELLITE
	(space to earth)
7.300–7.450	FIXED*
	FIXED SATELLITE*
	(space to earth)
	MOBILE*
7.450–7.550	FIXED*
	FIXED SATELLITE*
	(space to earth)
	METEOROLOGICAL SATELLITE*
	(space to earth)
	MOBILE*
7.550–7.750	FIXED*
	FIXED SATELLITE*
	(space to earth)
	MOBILE*
7.750–7.900	FIXED*
	MOBILE*
7.900–7.975	FIXED*
	MOBILE*
	FIXED SATELLITE
	(earth to space)
7.975–8.025	FIXED SATELLITE
	(earth to space)
8.025–8.175	EARTH EXPLORATION SATELLITE
	(space to earth)
	FIXED
	FIXED SATELLITE
	(earth to space)
	MOBILE
8.175–8.215	EARTH EXPLORATION SATELLITE
	(space to earth)
	FIXED
	FIXED SATELLITE
	(earth to space)
	METEOROLOGICAL SATELLITE
	(earth to space)
	MOBILE
8.215–8.400	EARTH EXPLORATION SATELLITE
	(space to earth)
	FIXED
	FIXED SATELLITE
	(earth to space)
	MOBILE
8.400–8.500	FIXED*
	MOBILE*
	SPACE RESEARCH*
	(space to earth)
8.500–8.750	RADIO LOCATION*
8.750–8.850	RADIO LOCATION*
	AERONAUTICAL RADIO NAVIGATION*
	(airborne doppler aids)
8.850–9.000	RADIO LOCATION*
9.000–9.200	AERONAUTICAL RADIO NAVIGATION*
	(ground-based radars)
	Radio location*
9.200–9.300	RADIO LOCATION*
9.300–9.500	RADIO NAVIGATION*
	Radio location*
9.500–9.800	RADIO LOCATION*
9.800–10.00	RADIO LOCATION*
	Fixed*
10.00–10.50	RADIO LOCATION*
	Amateur*
10.50–10.55	RADIO LOCATION
	(continuous-wave systems only)
10.55–10.60	FIXED*
	MOBILE*
	Radio location*
10.60–10.68	FIXED*
	MOBILE*
	RADIO ASTRONOMY*
	Radio location*
10.68–10.70	RADIO ASTRONOMY*
10.70–10.95	FIXED*
	MOBILE*

Gigahertz	Service
10.95–11.20	FIXED
	FIXED SATELLITE (space to earth)
	MOBILE
11.20–11.45	FIXED*
	MOBILE*
11.45–11.70	FIXED*
	FIXED SATELLITE* (space to earth)
	MOBILE*
11.70–12.20	BROADCASTING
	BROADCASTING SATELLITE
	FIXED
	FIXED SATELLITE (space to earth)
	MOBILE EXCEPT AERONAUTICAL
12.20–12.50	BROADCASTING
	FIXED
	MOBILE EXCEPT AERONAUTICAL
12.50–12.75	FIXED
	FIXED SATELLITE (earth to space)
	MOBILE EXCEPT AERONAUTICAL
12.75–13.25	FIXED*
	MOBILE*
13.25–13.40	AERONAUTICAL RADIO NAVIGATION*
13.40–14.00	RADIO LOCATION*
14.00–14.30	RADIO NAVIGATION*
	FIXED SATELLITE (earth to space)
14.30–14.40	RADIO NAVIGATION SATELLITE*
	FIXED SATELLITE (earth to space)
14.40–14.50	FIXED*
	FIXED SATELLITE* (earth to space)
	MOBILE*
14.50–15.35	FIXED*
	MOBILE*
15.35–15.40	RADIO ASTRONOMY*
15.40–15.70	AERONAUTICAL RADIO NAVIGATION*
15.70–17.70	RADIO LOCATION*
17.70–19.70	FIXED*
	FIXED SATELLITE* (space to earth)
	MOBILE*
19.70–21.20	FIXED SATELLITE* (space to earth)
21.20–22.00	EARTH EXPLORATION SATELLITE* (space to earth)
	FIXED*
	MOBILE*
22.00–23.60	FIXED
	MOBILE
23.60–24.00	RADIO ASTRONOMY*
24.00–24.05	AMATEUR*
24.05–24.25	RADIO LOCATION*
	Amateur*
24.25–25.25	RADIO NAVIGATION*
25.25–27.50	FIXED*
	MOBILE*
27.50–29.50	FIXED*
	FIXED SATELLITE* (earth to space)
	MOBILE*
29.50–31.00	FIXED SATELLITE* (earth to space)
31.00–31.30	FIXED*
	MOBILE*
	Space research*
31.30–31.50	RADIO ASTRONOMY*
31.50–31.80	SPACE RESEARCH
31.80–32.30	RADIO NAVIGATION*
	Space research*
32.30–33.40	RADIO NAVIGATION
33.40–34.20	RADIO LOCATION*
34.20–35.20	RADIO LOCATION*
	Space research*
35.20–36.00	RADIO LOCATION*
36.00–40.00	FIXED*
	MOBILE*
40.00–41.00	FIXED SATELLITE (space to earth)
41.00–43.00	BROADCASTING SATELLITE
43.00–48.00	AERONAUTICAL MOBILE SATELLITE
	AERONAUTICAL RADIO NAVIGATION SATELLITE
	MARITIME MOBILE SATELLITE
	MARITIME RADIO NAVIGATION SATELLITE
48.00–50.00	Not allocated
50.00–51.00	FIXED SATELLITE (earth to space)
51.00–52.00	EARTH EXPLORATION SATELLITE
	SPACE RESEARCH
52.00–54.25	SPACE RESEARCH (Passive)
54.25–58.20	INTERSATELLITE
58.20–59.00	SPACE RESEARCH (Passive)
59.00–64.00	INTERSATELLITE
64.00–65.00	SPACE RESEARCH (Passive)
65.00–66.00	EARTH EXPLORATION SATELLITE
	SPACE RESEARCH
66.00–71.00	AERONAUTICAL MOBILE SATELLITE
	AERONAUTICAL RADIO NAVIGATION SATELLITE
	MARITIME MOBILE SATELLITE
	MARITIME RADIO NAVIGATION SATELLITE
71.00–84.00	Not allocated
84.00–86.00	BROADCASTING SATELLITE
86.00–92.00	RADIO ASTRONOMY
	SPACE RESEARCH (Passive)
92.00–95.00	FIXED SATELLITE (earth to space)
95.00–101.0	AERONAUTICAL MOBILE SATELLITE
	AERONAUTICAL RADIO NAVIGATION SATELLITE
	MARITIME MOBILE SATELLITE
	MARITIME RADIO NAVIGATION SATELLITE

Gigahertz	Service
101.0–102.0	SPACE RESEARCH (Passive)
102.0–105.0	FIXED SATELLITE (space to earth)
105.0–130.0	INTERSATELLITE
130.0–140.0	RADIO ASTRONOMY SPACE RESEARCH (Passive)
140.0–142.0	FIXED SATELLITE (earth to space)
142.0–150.0	AERONAUTICAL MOBILE SATELLITE AERONAUTICAL RADIO NAVIGATION SATELLITE MARITIME MOBILE SATELLITE MARITIME RADIO NAVIGATION SATELLITE
150.0–152.0	FIXED SATELLITE (space to earth)
152.0–170.0	Not allocated
170.0–182.0	INTERSATELLITE
182.0–185.0	SPACE RESEARCH (Passive)
185.0–190.0	INTERSATELLITE
190.0–200.0	AERONAUTICAL MOBILE SATELLITE AERONAUTICAL RADIO NAVIGATION SATELLITE MARITIME MOBILE SATELLITE MARITIME RADIO NAVIGATION SATELLITE
200.0–220.0	Not allocated
220.0–230.0	FIXED SATELLITE
230.0–240.0	RADIO ASTRONOMY SPACE RESEARCH (Passive)
240.0–250.0	Not allocated
250.0–265.0	AERONAUTICAL MOBILE SATELLITE AERONAUTICAL RADIO NAVIGATION SATELLITE MARITIME MOBILE SATELLITE MARITIME RADIO NAVIGATION SATELLITE
265.0–275.0	FIXED SATELLITE
Above 275.0	Not allocated

FREQUENCY ALLOCATIONS IN UNITED STATES

The following listings are abstracted from Part 2 of the Rules and Regulations of the Federal Communications Commission as revised to September 1974. Several hundred footnotes in the Regulations, describing special conditions for use and for assignment of many frequency bands or individual frequencies, have been omitted.

Since changes are frequently made in the Rules and Regulations, the latest issue always should be consulted. It may be obtained from the Superintendent of Documents, Government Printing Office, Washington, D.C. Additional guidance may be obtained from the Federal Communications Commission, Washington, D.C. [1]

[1] In the official documents of ITU and FCC the following terms are combined as single words: radiobeacon, radiocommunication, radiodetermination, radiolocation, radionavigation, radiorange, radiosonde, radiotelegraphy, and radiotelephony.

Aeronautical Mobile (Ground-air-ground and air-air communication.)

General

200.0 – 285.0 kHz
325.0 – 415.0
2850 –3155
3.400 – 3.500 MHz
4.650 – 4.750
5.450 – 5.730
6.525 – 6.765
8.815 – 9.040
10.005 – 10.10
11.175 – 11.40
13.20 – 13.36
15.01 – 15.10
17.90 – 18.03
21.87 – 22.00
23.20 – 23.35
123.5875– 136.0

Calling and Distress

500 kHz, telegraph calling frequency
2182 kHz, telephone calling frequency
156.8 MHz, telephone calling frequency
243.0 MHz, survival craft and equipment

Airdrome Control

118.0 –121.4 MHz

Aero Search and Rescue

123.1 MHz

Aero Utility

121.6 –121.925 MHz

Private Aircraft

121.975–123.075 MHz

Flight Test

123.125–123.275 MHz
123.325–123.475
123.525–123.575

Aviation Instructional

123.300 MHz
123.500

Civil Air Patrol

26.62 MHz
143.90
148.15

Telemetering

1435 –1535

Aeronautical Radio Navigation (Radio beacons, radio ranges, landing systems, airborne radar, etc.)

General

200.0 – 285.0 kHz
325.0 – 405.0
1605 –1715
960.0 –1215 MHz

1300 –1350 MHz
1558.5 –1636.5
5.000– 5.250 GHz
5.350– 5.460
9.000– 9.200
15.40 – 15.70

Direction Finding
405.0–415.0 kHz
(410 kHz is direction-finding frequency)

Marker–Beacon
74.60–75.40 MHz
(75.0 MHz is marker frequency)

VOR (omnidirectional range and localizer)
108.0–117.975 MHz

Glide Path
328.6 –335.4 MHz

Altimeter
4.200– 4.400 GHz

Airborne Doppler Radar
8.800 GHz (government)
13.25 – 13.40 GHz

Amateur

1800 –2000 kHz
3.500– 4.000 MHz
7.000– 7.300
14.00 – 14.35
21.00 – 21.45
28.00 – 29.70
50.00 – 54.00
144.0 – 148.0
220.0 – 225.0
420.0 – 450.0
1215 –1300
2300 –2450
3.300– 3.500 GHz
5.650– 5.925
10.00 – 10.50
24.00 – 24.25
48.00 – 50.00
71.00 – 84.00
152.0 – 170.0
200.0 – 220.0
240.0 – 250.0
Above 275.0

Broadcasting

Standard Amplitude-Modulation Broadcasting
535.0 –1605 kHz

Frequency-Modulation Broadcasting
88.00 – 108.0 MHz

Television Broadcasting
54.00 – 72.00 MHz
76.00 – 88.00
174.0 – 216.0
470.0 – 806.0

International Amplitude-Modulation Broadcasting
5.950– 6.200 MHz
9.500– 9.775
11.70 – 11.975
15.10 – 15.45
17.70 – 17.90
21.45 – 21.75
25.60 – 26.10

Citizens Radio (Personal radio services)

26.96 – 27.23 MHz
462.5375–462.7375
467.5375–467.7375

Fixed (Point-to-point radio services in which neither terminal is mobile)

International Fixed Public and Aeronautical Fixed
14.00 – 19.95 kHz (IFP only)
20.05 – 59.00 (IFP only)
61.00 – 90.00 (not Aero)
110.0 – 200.0 (not Aero)
1605 –1750
2107 –2170
2194 –2495
2505 –2850
3.155– 3.400 MHz
4.000– 4.063
4.438– 4.650
4.750– 4.995
5.005– 5.450
5.730– 5.950
6.765– 7.000
7.300– 8.195
9.040– 9.500
9.775– 9.995
10.10 – 11.175
11.40 – 11.70
11.975– 12.33
13.36 – 14.00
14.35 – 14.99
15.45 – 16.46
17.36 – 17.70
18.03 – 19.99
20.01 – 21.00
21.75 – 21.85
21.87 – 22.00 (Aero only)
22.72 – 23.20
23.20 – 23.35 (Aero only)
23.35 – 24.99
26.95 – 26.96 (IFP only)
29.80 – 29.89
29.91 – 30.00

Fixed in Alaska, Hawaii, and United States Possessions
110.0 – 200.0 kHz (Alaska)
1605 –1750 (Alaska)
2107 –2170 (Alaska)

2194 –2495 kHz (Alaska)
2505 –2850 (Alaska)
3.155– 3.200 MHz (Alaska and Puerto Rico)
3.200– 3.400 (Alaska)
4.000– 4.063 (Alaska)
4.438– 4.650 (Alaska)
4.750– 4.995 (Alaska)
5.005– 5.450 (Alaska)
5.730– 5.950 (Alaska)
6.765– 7.000 (Alaska)
7.300– 8.195 (Alaska)
9.040– 9.500 (Alaska)
947.0 – 952.0 (Alaska, Hawaii, and U.S. possessions)
952.0 – 960.0 (Puerto Rico and Virgin Islands)

Disaster
1750 –1800 kHz

Zone and Interzone Police
5.005– 5.450 MHz
7.300– 8.195

Omnidirectional (Point-to-Point)
2150 –2180 MHz

Domestic Fixed Public (Point-to-point services by common carriers within United States)
2110 –2130 MHz
2160 –2180
3.700– 4.200 GHz
5.925– 6.425
10.70 – 11.70
17.70 – 19.70
21.2 – 23.6

Operational Fixed and International Control (Point-to-point services not for public use, as well as links between control centers and stations for international service)
72.00 – 73.00 MHz (Operational Fixed only)
75.40 – 76.00 (Operational Fixed only)
952.0 – 960.0
1850 –1990
2130 –2150
2180 –2200
2500 –2690 (Not International Control)
6.525– 6.575 GHz (Operational Fixed only)
6.575– 6.875
12.20 – 12.70

*Aural Broadcast (Studio-transmitter link)**
947.0 – 952.0 MHz

Instructional Television
2500 –2690 MHz

* See Broadcast Remote Pickup under Land Mobile.

Television Pickup (Intercity relay and studio-transmitter link)
1990 –2110 MHz
6.875– 7.125 GHz
12.70 – 13.20

Cable Television Relay
12.70 – 12.95 GHz

Industrial, Scientific, and Medical Equipment
13.56 MHz
27.12
40.68 (government)
915.0 (government)
5.800 GHz
24.125

Government (Armed Forces and other departments of the national government)

General
510.0 – 535.0 kHz
25.33 – 25.60 MHz
27.54 – 28.00
29.89 – 29.91
30.00 – 30.56
32.00 – 33.00
34.00 – 35.00
36.00 – 37.00
38.00 – 39.00
40.00 – 42.00
46.60 – 47.00
49.60 – 50.00
138.0 – 144.0
148.0 – 149.9
150.05 – 150.8
157.0375– 157.1875
173.4 – 174.0
225.0 – 328.6
335.4 – 399.9
410.0 – 420.0
902.0 – 928.0
1350 –1400
1429 –1435
1710 –1850
2200 –2290
2700 –2900
4.400 – 4.990 GHz
7.125 – 8.400
14.5 – 15.35
20.2 – 21.2
25.25 – 27.5
30.0 – 31.0
36.0 – 38.6
54.25 – 58.2
59.0 – 64.0
92.0 – 93.0
102.0 – 103.0
105.0 – 110.0
117.5 – 122.5
140.0 – 141.0
150.0 – 151.0
170.0 – 175.0
189.0 – 190.0

Land Mobile (Communication on land between base stations and mobile stations or between mobile stations)

Public Safety (Police, fire, highway, forestry, and emergency services)

1605 –1750 kHz
2107 –2170
2194 –2495
2505 –2850
3.155 – 3.400 MHz
30.56 – 32.00
33.01 – 33.11
33.41 – 34.00
35.19 – 35.69
37.01 – 37.43
37.89 – 38.00
39.00 – 40.00
42.00 – 42.95
43.19 – 43.69
44.61 – 46.60
47.00 – 47.69
150.98 – 151.4825
153.7325– 154.46
154.6375– 156.25
158.715 – 159.48
162.0125– 173.2
451.0 – 454.0
456.0 – 459.0
460.0 – 462.5375
462.7375– 467.5375
467.7375– 512.0
1427 –1435

Zone and Interzone Police

2804 kHz
2808
2812
5005–5450
7300–8195

Disaster

1750–1800 kHz

Industrial (Power, petroleum, pipeline, forest products, factories, builders, ranchers, motion picture, press relay, etc.)

1605 –1750 kHz
2107 –2170
2194 –2495
2505 –2850
3.155 – 3.400 MHz
4.438 – 4.650
25.01 – 25.33
27.28 – 27.54
29.70 – 29.80
30.56 – 32.00
33.11 – 33.41
35.00 – 35.19
35.69 – 36.00
37.00 – 37.01
37.43 – 37.89
42.95 – 43.19
47.43 – 49.60 MHz
151.4975– 152.0
152.465 – 152.495
152.855 – 153.7325
154.46 – 154.6375
157.725 – 157.755
158.115 – 158.475
173.2 – 173.4
216.0 – 220.0
451.0 – 454.0
456.0 – 459.0
460.0 – 462.5375
462.7375– 465.5375
467.7375– 512.0

Land Transportation (Taxis, trucks, buses, railroads)

30.56 – 32.00 MHz
33.00 – 34.00
43.68 – 44.61
150.8 – 150.98
152.255 – 152.465
157.45 – 157.725
159.48 – 161.575
451.0 – 454.0
456.0 – 459.0
460.0 – 462.5375
462.7375– 467.5375
467.7375– 512.0
1427 –1435

Operational Land and Operational Mobile

6.525 – 6.575 GHz
10.55 – 10.68

Domestic Public

35.19 – 35.69 MHz
43.19 – 43.69
152.0 – 152.255
152.495 – 152.855
157.755 – 158.115
158.475 – 158.715
454.0 – 455.0
459.0 – 460.0
470.0 – 512

Broadcast Remote Pickup

1605 –1715 kHz
26.10 – 26.48 MHz
161.625 – 161.775
166.25
170.15
450.0 – 451.0
455.0 – 456.0

Television Pickup

1990 –2110 MHz
6.875 – 7.125 GHz
12.70 – 13.20

Common Carrier

6.425 – 6.525 GHz
11.70 – 12.20
27.5 – 29.5

Maritime Mobile (Communication between coast stations and ships, or between ships)

General

110.0 – 160.0 kHz
415.0 – 490.0 (telegraphy)
1605 –1750
2000 –2035
2092.5 –2170
2190.5 –2495
2505 –2850
3.155 – 3.400 MHz
4.1395– 4.166
6.2104– 6.2165
6.2445– 6.248
8.2812– 8.288
8.328 – 8.3315
12.421 – 12.4315
12.4795– 12.483
16.565 – 16.576
16.6365– 16.640
22.0945– 22.112
22.1605– 22.164

Calling, Safety, and Distress

500 kHz, telegraph calling frequency
2182 kHz, telephone calling frequency
156.8 MHz, telephone calling frequency
243.0 MHz, survival craft and equipment

Coast Stations (Telegraphy and facsimile)

2035 –2065 kHz (Telegraphy only)
4.231 – 4.361 MHz
6.3455– 6.514
8.4595– 8.7285
12.689 – 13.1075
16.9175– 17.255
22.374 – 22.6245

Ship Stations (Telegraphy)

4.166 – 4.178 MHz
4.187 – 4.231
6.248 – 6.267
6.2805 – 6.3455
8.34175– 8.356
8.374 – 8.4595
12.483 – 12.534
12.561 – 12.689
16.640 – 16.712
16.748 – 16.9175
22.164 – 22.2225
22.2675 – 22.374

Ship Stations (Wide-band telegraphy, facsimile, and special)

2068.5 –2078.5 kHz
6.2165– 6.2445 MHz
8.288 – 8.328
12.4315– 12.4795
16.576 – 16.6365
22.112 – 22.1605

Coast Stations (Telephony)

2065 –2068.5 kHz
2078.5 –2089.5
2173.5 –2190.5
4.1395– 4.1425
4.361 – 4.438
6.2104– 6.2165
6.514 – 6.525
8.2812– 8.288
8.7285– 8.815
12.421 – 12.4315
13.1075– 13.20
16.565 – 16.576
17.255 – 17.360
22.0945– 22.112
22.6245– 22.720
156.250 – 157.0375
161.575 – 161.625
161.775 – 162.0125

Ship Stations (Telephony)

2065 –2068.5 kHz
2078.5 –2089.5
2170 –2190.5
4.063 – 4.1395 MHz
6.200 – 6.2104
8.195 – 8.2812
12.330 – 12.421
16.460 – 16.565
22.000 – 22.0945
156.250 – 157.0375
157.1875– 157.450

Ship Calling (Telegraphy)

2089.5 –2092.5 kHz
4.178 – 4.187 MHz
6.267 – 6.2805
8.356 – 8.374
12.534 – 12.561
16.712 – 16.748
22.2225– 22.2675

Intership (Telephony)

2638 kHz
2738

Meteorological Aids

Radiosondes

400.15 – 406.0 MHz
1660 –1700

Ground-Based Radars

5.600– 5.650 GHz
9.300– 9.500

Meteorological Satellite

137.0–138.0 MHz

Radio Astronomy

21.850– 21.870 MHz
73.00 – 74.60
406.1 – 410
1400 –1427
1660 –1670
2690 –2700
4.990– 5.000 GHz
10.68 – 10.70
15.35 – 15.40
23.6 – 24.0
31.20 – 31.50
86.0 – 92.0
130.0 – 140.0
230.0 – 240.0

Standard Frequencies

19.95 – 20.05 kHz
59.00 – 61.00
2495 –2505
4.995– 5.005 MHz
9.995– 10.005
14.99 – 15.01
19.99 – 20.01
24.99 – 25.01

Radio Location (Coastal radar, tracking systems, etc.)

70.00 – 90.00 kHz
110.0 – 130.0
1605 –1800
2450 –2500 MHz
2900 –3700
5.250– 5.650 GHz
8.5 – 10.55
13.4 – 14.0
15.7 – 17.7
33.4 – 36.0

Radio Navigation (Radio beacons, shipboard radar, navigational systems, direction finding, etc.)*

General

10.00 – 14.00 kHz
90.00 – 110.0
5.460– 5.470 GHz
9.300– 9.500
14.00 – 14.30
24.25 – 25.25
31.80 – 33.40

Maritime Radio Navigation

285.0 – 325.0 kHz
2900 –3100 MHz
5.470– 5.650 GHz

* See listings under Aeronautical Radio Navigation.

Maritime Direction Finding

405.0 – 415.0 kHz (410 kHz is the direction-finding frequency)

Loran

90.0 – 110.0 kHz (100 kHz is Loran *C* frequency)
1800 –2000 (Loran *A*)

Land Radio Navigation

1638 kHz
1708

Satellites

Aeronautical Mobile

1542.5–1558.5 MHz
1644.0–1660.0
43.0– 48.0 GHz
66.0– 71.0
95.0– 101.0
142.0– 150.0
190.0– 200.0
250.0– 265.0

Aeronautical Radionavigation

43.0– 48.0 GHz
66.0– 71.0
95.0–101.0
142.0–150.0
190.0–200.0
250.0–265.0

Broadcasting

2500 –2690 MHz
41.0– 43.0 GHz
84.0– 86.0

Earth Exploration

21.2–22.0 GHz
51.0–52.0
65.0–66.0

Fixed

2500 –2535 MHz
2655 –2690
3700 –4200
5925 –6425
6625 –6875
10.95– 11.2 GHz
11.45– 12.2
12.5– 12.75
14.0 – 14.5
17.7 – 20.2
27.5 – 30.0
40.0 – 41.0
50.0 – 51.0
93.0 – 95.0
103.0 – 105.0
141.0 – 142.0
151.0 – 152.0
220.0 – 230.0
265.0 – 275.0

Intersatellite

110.0–117.5 GHz
122.5–130.0
175.0–182.0
185.0–189.0

Maritime Mobile

1535 –1543.5 MHz
1636.5–1645
43.0– 48.0 GHz
66.0– 71.0
95.0– 101.0
142.0– 150.0
190.0– 200.0
250.0– 265.0

Maritime Radionavigation

43.0– 48.0 GHz
66.0– 71.0
95.0–101.0
142.0–150.0
190.0–200.0
250.0–265.0

Meteorological

401– 403 MHz
1670–1710

Radionavigation

149.9–150.05 MHz
399.9–400.05

Standard Frequency

400.05–400.15 MHz

Space

Operation

137.0– 138.0 MHz
401.0– 402.0
1427 –1429

Research

136.0 – 138.0 MHz
400.15– 401
1700 –1710
2290 –2300
8400 –8500
13.4 – 14.0 GHz
14.4 – 14.5
31.5 – 31.8
51.0 – 52.0
52.0 – 54.25 (Passive)
58.2 – 59.0 (Passive)
64.0 – 65.0 (Passive)
65.0 – 66.0
86.0 – 92.0 (Passive)
101.0 – 102.0 (Passive)
130.0 – 140.0 (Passive)
182.0 – 185.0 (Passive)
230.0 – 240.0 (Passive)

INTERNATIONAL CALL-SIGN PREFIXES

AAA–ALZ	United States
AMA–AOZ	Spain
APA–ASZ	Pakistan
ATA–AWZ	India
AXA-AXZ	Australia
AYA–AZZ	Argentina
A2A–A2Z	Botswana
A3A–A3Z	Tonga
A5A–A5Z	Bhutan
BAA–BZZ	China
CAA-CEZ	Chile
CFA–CKZ	Canada
CLA–CMZ	Cuba
CNA–CNZ	Morocco
COA–COZ	Cuba
CPA–CPZ	Bolivia
CQA–CRZ	Portuguese Territories
CSA–CUZ	Portugal
CVA–CXZ	Uruguay
CYA–CZZ	Canada
C2A–C2Z	Nauru
C3A–C3Z	Andorra
DAA–DTZ	Germany
DUA–DZZ	Philippines
EAA–EHZ	Spain
EIA–EJZ	Ireland
EKA–EKZ	USSR
ELA–ELZ	Liberia
EMA–EOZ	USSR
EPA–EQZ	Iran
ERA–ERZ	USSR
ESA–ESZ	Estonia (USSR)
ETA–ETZ	Ethiopia
EUA–EWZ	Belorussia (USSR)
EXA–EZZ	USSR
FAA–FZZ	France and Territories
GAA–GZZ	United Kingdom
HAA–HAZ	Hungary
HBA–HBZ	Switzerland
HCA–HDZ	Ecuador
HEA–HEZ	Switzerland
HFA–HFZ	Poland
HGA–HGZ	Hungary
HHA–HHZ	Haiti
HIA–HIZ	Dominican Republic
HJA–HKZ	Colombia
HLA–HMZ	Korea
HNA–HNZ	Iraq
HOA–HPZ	Panama
HQA–HRZ	Honduras
HSA–HSZ	Thailand
HTA–HTZ	Nicaragua
HUA–HUZ	El Salvador
HVA–HVZ	Vatican State
HWA–HYZ	France and Territories
HZA–HZZ	Saudi Arabia
IAA–IZZ	Italy and Territories
JAA–JSZ	Japan
JTA–JVZ	Mongolia

JWA–JXZ	Norway
JYA–JYZ	Jordan
JZA–JZZ	West Irian
KAA–KZZ	United States
LAA–LNZ	Norway
LOA–LWZ	Argentina
LXA–LXZ	Luxembourg
LYA–LYZ	Lithuania (USSR)
LZA–LZZ	Bulgaria
L2A–L9Z	Argentina
MAA–MZZ	United Kingdom
NAA–NZZ	United States
OAA–OCZ	Peru
ODA–ODZ	Lebanon
OEA–OEZ	Austria
OFA–OJZ	Finland
OKA–OMZ	Czechoslovakia
ONA–OTZ	Belgium
OUA–OZZ	Denmark
PAA–PIZ	Netherlands
PJA–PJZ	Netherlands West Indies
PKA–POZ	Indonesia
PPA–PYZ	Brazil
PZA–PZZ	Surinam
QAA–QZZ	(Service abbreviations)
RAA–RZZ	(USSR)
SAA–SMZ	Sweden
SNA–SRZ	Poland
SSA–SSM	Egypt
SSN–STZ	Sudan
SUA–SUZ	Egypt
SVA–SZZ	Greece
TAA–TCZ	Turkey
TDA–TDZ	Guatemala
TEA–TEZ	Costa Rica
TFA–TFZ	Iceland
TGA–TGZ	Guatemala
THA–THZ	France and Territories
TIA–TIZ	Costa Rica
TJA–TJZ	Cameroon
TKA–TKZ	France and Territories
TLA–TLZ	Central African Republic
TMA–TMZ	France and Territories
TNA–TNZ	Congo
TOA–TQZ	France and Territories
TRA–TRZ	Gabon
TSA–TSZ	Tunisia
TTA–TTZ	Chad
TUA–TUZ	Ivory Coast
TVA–TXZ	France and Territories
TYA–TYZ	Dahomey
TZA–TZZ	Mali
UAA–UQZ	USSR
URA–UTZ	Ukraine (USSR)
UUA–UZZ	USSR
VAA–VGZ	Canada
VHA–VNZ	Australia
VOA–VOZ	Canada
VPA–VSZ	British Territories
VTA–VWZ	India
VXA–VYZ	Canada
VZA–VZZ	Australia
WAA–WZZ	United States
XAA–XIZ	Mexico
XJA–XOZ	Canada
XPA–XPZ	Denmark
XQA–XRZ	Chile
XSA–XSZ	China
XTA–XTZ	Upper Volta
XUA–XUZ	Khmer Republic
XVA–XVZ	Vietnam
XWA–XWZ	Laos
XXA–XXZ	Portuguese Territories
XYA–XZZ	Burma
YAA–YAZ	Afghanistan
YBA–YHZ	Indonesia
YIA–YIZ	Iraq
YJA–YJZ	New Hebrides
YKA–YKZ	Syria
YLA–YLZ	Latvia (USSR)
YMA–YMZ	Turkey
YNA–YNZ	Nicaragua
YOA–YRZ	Romania
YSA–YSZ	El Salvador
YTA–YUZ	Yugoslavia
YVA–YYZ	Venezuela
YZA–YZZ	Yugoslavia
ZAA–ZAZ	Albania
ZBA–ZJZ	British Territories
ZKA–ZMZ	New Zealand
ZNA–ZOZ	British Territories
ZPA–ZPZ	Paraguay
ZQA–ZQZ	British Territories
ZRA–ZUZ	South Africa
ZVA–ZZZ	Brazil
2AA–2ZZ	United Kingdom
3AA–3AZ	Monaco
3BA–3BZ	Mauritius
3CA–3CZ	Equatorial Guinea
3DA–3DM	Swaziland
3DN–3DZ	Fiji
3EA–3FZ	Panama
3GA–3GZ	Chile
3HA–3UZ	China
3VA–3VZ	Tunisia
3WA–3WZ	Vietnam
3XA–3XZ	Guinea
3YA–3YZ	Norway
3ZA–3ZZ	Poland
4AA–4CZ	Mexico
4DA–4IZ	Philippines
4JA–4LZ	USSR
4MA–4MZ	Venezuela
4NA–4OZ	Yugoslavia
4PA–4SZ	Sri Lanka
4TA–4TZ	Peru
4UA–4UZ	United Nations
4VA–4VZ	Haiti
4WA–4WZ	Yemen (YAR)
4XA–4XZ	Israel
4YA–4YZ	International Civil Aviation Organization

4ZA–4ZZ	Israel
5AA–5AZ	Libya
5BA–5BZ	Cyprus
5CA–5GZ	Morocco
5HA–5IZ	Tanzania
5JA–5KZ	Colombia
5LA–5MZ	Liberia
5NA–5OZ	Nigeria
5PA–5QZ	Denmark
5RA–5SZ	Malagasy Republic
5TA–5TZ	Mauretania
5UA–5UZ	Niger
5VA–5VZ	Togo
5WA–5WZ	Western Samoa
5XA–5XZ	Uganda
5YA–5ZZ	Kenya
6AA–6BZ	Egypt
6CA–6CZ	Syria
6DA–6JZ	Mexico
6KA–6NZ	Korea
6OA–6OZ	Somali Republic
6PA–6SZ	Pakistan
6TA–6UZ	Sudan
6VA–6WZ	Senegal
6XA–6XZ	Malagasy Republic
6YA–6YZ	Jamaica
6ZA–6ZZ	Liberia
7AA–7IZ	Indonesia
7JA–7NZ	Japan
7OA–7OZ	Yemen (PDRY)
7PA–7PZ	Lesotho
7QA–7QZ	Malawi
7RA–7RZ	Algeria
7SA–7SZ	Sweden
7TA–7YZ	Algeria
7ZA–7ZZ	Saudi Arabia
8AA–8IZ	Indonesia
8JA–8NZ	Japan
8OA–8OZ	Botswana
8PA–8PZ	Barbados
8QA–8QZ	Maldive Islands
8RA–8RZ	Guyana
8SA–8SZ	Sweden
8TA–8YZ	India
8ZA–8ZZ	Saudi Arabia
9AA–9AZ	San Marino
9BA–9DZ	Iran
9EA–9FZ	Ethiopia
9GA–9GZ	Ghana
9HA–9HZ	Malta
9IA–9JZ	Zambia
9KA–9KZ	Kuwait
9LA–9LZ	Sierra Leone
9MA–9MZ	Malaysia
9NA–9NZ	Nepal
9OA–9TZ	Zaire
9UA–9UZ	Burundi
9VA–9VZ	Singapore
9WA–9WZ	Malaysia
9XA–9XZ	Rwanda
9YA–9ZZ	Trinidad and Tobago

DESIGNATION OF EMISSIONS

The full designation of an emission consists of the symbol for that emission, as given in Table 3, preceded by a number indicating the necessary bandwidth in kilohertz. Bandwidths are generally expressed to a maximum of 3 significant figures. Necessary bandwidth and examples of designations are shown in Table 4.

Emissions are classified and symbolized according to the type of modulation, type of transmission, and supplementary characteristics.

NECESSARY BANDWIDTHS*

The necessary bandwidth is the minimum value of bandwidth sufficient to ensure the transmission of information at the rate and with the quality required for the system employed. Emissions needed for satisfactory functioning of the receiving equipment such as the carrier in reduced-carrier systems, or a vestigial sideband, are included in the necessary bandwidth.

For the determination of necessary bandwidth, Table 4 may be considered a guide. In formulating the table, the following terms have been employed:

B_n = Necessary bandwidth in hertz
B = Telegraph speed in bauds
N = Maximum possible number of black plus white elements to be transmitted per second, in facsimile and television
M = Maximum modulation frequency in hertz
C = Subcarrier frequency in hertz
D = Half the difference between the maximum and minimum values of the instantaneous frequency: Instantaneous frequency is the rate of change of phase
t = Pulse duration in seconds
K = An overall numerical factor which varies according to the emission and which depends on the allowable signal distortion
N_c = Number of baseband telephone channels in radio systems employing multichannel multiplex telephony
P = Continuity pilot subcarrier frequency in hertz (may exceed value of M)
R = Maximum transmission speed in binary digits (bits) per second
S = Number of equivalent nonredundant signaling states

FREQUENCY TOLERANCES

The following information is abstracted from the Radio Regulations of the International Telecommunication Union, Geneva, 1959, Appendix 3.

* From FCC Rules and Regulations, Vol. 2, 1972.

TABLE 3—DESIGNATION OF EMISSIONS.

Type of Modulation of Main Carrier	Type of Transmission	Supplementary Characteristics	Symbol
Amplitude modulation	With no modulation	—	A0
	Telegraphy without the use of a modulating audio frequency (by on-off keying)	—	A1
	Telegraphy by the on-off keying of an amplitude-modulating audio frequency or audio frequencies, or by the on-off keying of the modulated emission (special case: an unkeyed emission amplitude modulated)	—	A2
	Telephony	Double sideband, full carrier Single sideband, reduced carrier Single sideband, suppressed carrier Two independent sidebands, reduced carrier	A3 A3A A3J A3B
	Facsimile (with modulation of main carrier either directly or by a frequency-modulated subcarrier)	— Single sideband, reduced carrier	A4 A4A
	Television	Vestigial sideband	A5C
	Multichannel voice-frequency telegraphy	Single sideband, reduced carrier	A7A
	Cases not covered by the above, such as a combination of telephony and telegraphy	Two independent sidebands	A9B
Frequency (or phase) modulation	With no modulation	—	F0
	Telegraphy by frequency-shift keying without the use of a modulating audio frequency: one of two frequencies being emitted at any instant	—	F1
	Telegraphy by the on-off keying of a frequency-modulating audio frequency or by the on-off keying of a frequency-modulated emission (special case: an unkeyed emission, frequency modulated)	—	F2
	Telephony	—	F3
	Facsimile by direct frequency modulation of the carrier	—	F4
	Television	—	F5
	Four-frequency diplex telegraphy	—	F6
	Cases not covered by the above, in which the main carrier is frequency modulated	—	F9
Pulse modulation	A pulsed carrier without any modulation intended to carry information, for example, radar	—	P0

TABLE 3—*Continued*

Type of Modulation of Main Carrier	Type of Transmission	Supplementary Characteristics	Symbol
	Telegraphy by the on-off keying of a pulsed carrier without the use of a modulating audio frequency	—	P1D
	Telegraphy by the on-off keying of a modulating audio frequency or audio frequencies, or by the on-off keying of a modulated pulsed carrier (special case: an unkeyed modulated pulsed carrier)	Audio frequency or audio frequencies modulating the amplitude of the pulses	P2D
		Audio frequency or audio frequencies modulating the width (or duration) of the pulses	P2E
		Audio frequency or audio frequencies modulating the phase (or position) of the pulses	P2F
	Telephony	Amplitude modulated pulses	P3D
		Width (or duration) modulated pulses	P3E
		Phase (or position) modulated pulses	P3F
		Code modulated pulses (after sampling and quantization)	P3G
	Cases not covered by the above in which the main carrier is pulse modulated	—	P9

Applicable dates and certain exceptions which appear in the Regulations have been omitted.

Frequency tolerance is defined as the maximum permissible departure by the center frequency of the frequency band occupied by an emission from the assigned frequency or, by the characteristic frequency of an emission from the reference frequency. The frequency tolerance is expressed in parts in 10^6 or in some cases, in hertz.

The power shown for the various categories of stations is the mean power defined as power supplied to the antenna transmission line by a transmitter during normal operation, averaged over a time sufficiently long compared with the period of the lowest frequency encountered in the modulation. A time of 0.1 second during which the mean power is greatest will be selected normally.

Radio determination stations include radio navigation stations such as radio beacons, marker beacons, instrument landing systems, navigational radio, loran, decca, et cetera, and it also includes radio location stations such as radar used for purposes other than radio navigation. Where specific frequencies are not assigned to radar stations, the bandwidth occupied by the emission shall be maintained wholly within the band allocated to the service and the indicated tolerance does not apply.

Frequency Bands and Station Categories	Tolerance (Parts in 10^6)
Band: 10–535 kHz	
Fixed stations:	
10–50 kilohertz	1000
50–535 kilohertz	200
Land stations:	
Coast stations	
Power $\leq$200 watts	500
Power $>$200 watts	200
Aeronautical stations	100
Mobile stations:	
Ship stations	1000
Aircraft stations	500
Emergency ship transmitters	5000
Survival-craft stations	5000
Radio determination stations	100
Broadcasting stations	10 Hz
Band: 535–1605 kHz	
Broadcasting stations	10 Hz
Stations covered by the North American Regional Broadcasting Agreement	20 Hz
Band: 1605–4000 kHz	
Fixed stations:	
Power $\leq$200 watts	100
Power $>$200 watts	50

Frequency Bands and Station Categories	Tolerance (Parts in 10^6)
Land stations:	
Power ≤200 watts	100
Power >200 watts	50
Mobile stations:	
Ship stations	200
Aircraft stations	100
Survival-craft stations	300
Land mobile stations	200
Radio determination stations:	
Power ≤200 watts	100
Power >200 watts	50
Broadcasting stations	20
Band: 4–29.7 MHz	
Fixed stations:	
Power ≤500 watts	50
Power >500 watts	15
Land stations:	
Coast stations:	
Power ≤500 watts	50
Power >500 <5000 watts	30
Power >5000 watts	15
Aeronautical stations:	
Power ≤500 watts	100
Power >500 watts	50
Base stations:	
Power ≤500 watts	100
Power >500 watts	50
Mobile stations:	
Ship stations:	
Class A1 emission	200
Emission other than class A1	50
Aircraft stations	100
Survival-craft stations	200
Land mobile stations	200
Broadcasting stations	15
Band: 29.7–100 MHz	
Fixed stations:	
Power ≤200 watts	50
Power >200 watts	30
Land stations:	
Power ≤15 watts	50
Power >15 watts	20
Mobile stations:	
Power ≤5 watts	100
Power >5 watts	50
Radio determination stations	200
Broadcasting stations (other than television):	
Power ≤50 watts	50
Power >50 watts	20
Television broadcasting stations:	
Power ≤50 watts	100
Power >50 watts	1000 Hz
Band: 100 – 470 MHz	
Fixed stations:	
Power ≤50 watts	50
Power >50 watts	20
Land stations:	
Coast stations	20
Aeronautical stations	50
Base stations:	
Power ≤5 watts	50
Power >5 watts	20
Mobile stations:	
Ship and survival-craft stations:	
In the band 156–174 megahertz	20
Outside this band	50
Aircraft stations	50
Land mobile stations:	
Power ≤5 watts	50
Power >5 watts	20
Radio determination stations	50
Broadcasting stations (other than television)	20
Television broadcasting stations:	
Power ≤100 watts	100
Power >100 watts	1000 Hz
Band: 470–2450 MHz	
Fixed stations:	
Power ≤100 watts	300
Power >100 watts	100
Land stations	300
Mobile stations	300
Radio determination stations	500
Broadcasting stations (other than television)	100
Television broadcasting stations:	
Power ≤100 watts	100
Power >100 watts	1000 Hz
Band: 2450–10 500 MHz	
Fixed stations:	
Power ≤100 watts	300
Power >100 watts	100
Land stations	300
Mobile stations	300
Radio determination stations	2000
Band: 10.5–40 GHz	
Fixed stations	500
Radio determination stations	7500

NOTE: Requirements in the USA with respect to frequency tolerances are in all cases at least as restrictive (and for some services more restrictive) than the tolerances specified by the International Convention. For details, consult the Rules and Regulations of the Federal Communications Commission.

Spurious-Emission Tolerances (ITU, Geneva, 1959)

Spurious emission occurs on a frequency or frequencies outside the necessary band, and the level of this spurious emission may be reduced without affecting transmission of information.

TABLE 4—DETERMINATION OF NECESSARY BANDWIDTH.

Description and Class of Emission	Necessary Bandwidth in Hertz	Examples: Details	Examples: Designation of Emission
	Amplitude Modulation		
Continuous-wave telegraphy, A1	$B_n = BK$ where $K = 5$ for fading circuits $K = 3$ for nonfading circuits	Morse code at 25 words per minute, $B = 20$, $K = 5$ Bandwidth: 100 hertz	0.1A1
		Four-channel time-division multiplex, 7-unit code, 42.5 bauds per channel, $B = 170$, $K = 5$ Bandwidth: 850 hertz	0.85A1
Telegraphy, modulated by an audio frequency, A2	$B_n = BK + 2M$ where $K = 5$ for fading circuits $K = 3$ for nonfading circuits	Morse code at 25 words per minute, $B = 20$, $M = 1000$, $K = 5$ Bandwidth: 2100 hertz	2.1A2
Telephony, A3	$B_n = M$ for single sideband	Double-sideband telephony, $M = 3000$ Bandwidth: 6000 hertz	6A3
	$B_n = 2M$ for double sideband	Single-sideband telephony, reduced carrier, $M = 3000$ Bandwidth: 3000 hertz	3A3A
		Telephony, two independent sidebands, $M = 3000$ Bandwidth: 6000 hertz	6A3B
Sound broadcasting, A3	$B_n = 2M$ M may vary between 4000 and 10 000 depending on quality desired.	Speech and music, $M = 4000$ Bandwidth: 8000 hertz	8A3
Facsimile, carrier modulated by tone and by keying, A4	$B_n = KN + 2M$ where $K = 1.5$	The total number of picture elements (black plus white) transmitted per second is equal to the circumference of the cylinder multiplied by the number of lines per unit length and by the speed of rotation of the cylinder in revolutions per second. Diameter of cylinder = 70 millimeters Number of lines per millimeter = 5 Speed of rotation = 1 rotation per second $N = 1100$ $M = 1900$ Bandwidth: 5450 hertz	5.45A4

TABLE 4—*Continued*

Description and Class of Emission	Necessary Bandwidth in Hertz	Examples: Details	Examples: Designation of Emission
Television (visual and aural), A5 and F3	Refer to relevant CCIR documents for the bandwidths of the commonly used television systems.	Number of lines = 525 Number of lines per second = 15 750 Video bandwidth: 4.2 megahertz Total visual bandwidth: 5.75 megahertz FM aural bandwidth including guard bands: 250 000 hertz Total bandwidth: 6 megahertz	5750A5C 250F3
Composite transmission, A9	$B_n = 2M$ (double sideband)	Television relay, video limited to 4 megahertz, audio on 6.5 megahertz FM subcarrier, subcarrier deviation = 50 kilohertz M = subcarrier frequency plus its maximum deviation = 6.55×10^6. Bandwidth: 13.1×10^6 hertz	13 100A9
Composite transmission, A9	$B_n = 2M$ (double sideband)	Microwave relay system providing 10 telephone channels occupying baseband between 4 and 164 kilohertz $M = 164\ 000$ Bandwidth: 328 000 hertz	328A9
Composite transmission A9Y, digital modulation using DSB–AM	$B_n = \frac{2RK}{\log_2 S}$	Microwave radio relay specifications: digital modulation used to send 5 megabits per second by use of amplitude modulation of the main carrier with four signaling states. $R = 5 \times 10^6$ bits per second $K = 1$ $S = 4$ $B_n = 5$ MHz	5000A9Y
	Frequency Modulation		
Frequency-shift telegraphy, F1	$B_n = 2.6D + 0.55B$ for $1.5 \leq 2D/B \leq 5.5$ $B_n = 2.1D + 1.9B$ for $5.5 \leq 2D/B \leq 20$	Four-channel time-division multiplex with 7-unit code, 42.5 bauds per channel, $B = 170$, $D = 200$; $2D/B = 2.35$; therefore the first equation in column 2 applies Bandwidth: 613 hertz	0.6F1

TABLE 4—*Continued*

Description and Class of Emission	Necessary Bandwidth in Hertz	Examples	
		Details	Designation of Emission
Commercial telephony, F3	$B_n = 2M + 2DK$ K is normally 1 but under certain conditions a higher value may be necessary.	For an average case of commercial telephony, $D = 15\ 000$, $M = 3000$. Bandwidth: 36 000 hertz	36F3
Sound broadcasting, F3	$B_n = 2M + 2DK$	D = 75 000, $M = 15\ 000$ and assuming $K = 1$ Bandwidth: 180 000 hertz	180F3
Facsimile, F4	$B_n = KN + 2M + 2D$ where $K = 1.5$	(See facsimile, amplitude modulation) Diameter of cylinder = 70 millimeters Number of lines per millimeter = 5 Speed of rotation = 1 rotation per second $N = 1100$. $M = 1900$ $D = 10\ 000$ Bandwidth: 25 450 hertz	25.5F4
Four-frequency diplex telegraphy, F6	If the channels are not synchronized, $B_n = 2.6D + 2.75B$, where B is the speed of the higher-speed channel. If the channels are synchronized the bandwidth is as for F1, B being the speed of either channel.	Four-frequency diplex system with 400-hertz spacing between frequencies, channels not synchronized, 170 bauds keying in each channel, $D = 600$, $B = 170$ Bandwidth: 2027 hertz	2.05F6
Composite transmission, F9	$B_n = 2P + 2DK$ where $K = 1$	Microwave radio relay system specifications: 60 telephone channels occupying baseband between 60 and 300 kHz; rms per-channel deviation 200 kHz; continuity pilot at 331 kHz produces 100 kHz rms deviation of main carrier. $D = (200 \times 10^3 \times 3.76 \times 2.02)$ Hz $= 1.52 \times 10^6$ Hz; $P = 0.331 \times 10^6$ Hz. Bandwidth: 3.702×10^6 Hz.	3700F9

TABLE 4—*Continued*

Designation and Class of Emission	Necessary Bandwidth in Hertz	Examples	
		Details	Designation of Emission
Composite transmission, F9	$B_n = 2M + 2DK$ where $K = 1$	Microwave radio relay system specifications: 960 telephone channels occuping baseband between 60 and 4028 kHz; rms per-channel deviation 200 kHz; continuity pilot at 4715 kHz produces 140 kHz rms deviation of main carrier. $D = (200 \times 10^3 \times 3.76 \times 5.5)$ Hz $= 4.13 \times 10^6$ Hz; $M = 4.028 \times 10^6$ Hz; $P = 4.715 \times 10^6$ Hz; $(2M + 2DK) > 2P$. Bandwidth: 16.32×10^6 Hz.	16 300F9
Composite transmission, F9	$B_n = 2P$	Microwave radio relay system specifications: 600 telephone channels occupying baseband between 60 and 2540 kHz; rms per-channel deviation 200 kHz; continuity pilot at 8500 kHz produces 140 kHz rms deviation of main carrier. $D = (200 \times 10^3 \times 3.76 \times 4.36)$ Hz $= 3.28 \times 10^6$ Hz; $M = 2.54 \times 10^6$ Hz; $K = 1$; $P = 8.5 \times 10^6$ Hz; $(2M + 2DK) < 2P$. Bandwidth: 17×10^6 Hz.	17 000F9
Composite transmission, F9	$B_n = 2M + 2DK$ where $K = 1$	TV microwave relay system specifications: Aural program on 7.5 MHz, aural subcarrier deviation ± 150 kHz; continuity pilot at 8.5 MHz produces 140 kHz rms deviation of main carrier; $D = 3.7 \times 10^6$ Hz (visual) plus 0.3×10^6 Hz (aural). $M = (7.5 + 0.15) \times 10^6$ Hz; $P = 8.5 \times 10^6$ Hz; $D = (3.7 + 0.3) \times 10^6$ Hz; $(2M + 2DK) > 2P$. Bandwidth: 23.3×10^6 Hz.	23 300F9
Composite transmission, F9	$B_n = 2P$	TV microwave relay system specifications: Aural program on 6.0 MHz subcarrier; aural subcarrier deviation ± 150 kHz; continuity pilot at 8.5 MHz produces 50 kHz rms deviation of main carrier; $D = 2 \times 10^6$ Hz (visual) plus 0.2×10^6 Hz (aural). $D = (2.0 + 0.2) \times 10^6$ Hz; $M = 6.15 \times 10^6$ Hz; $K = 1$; $P = 8.5 \times 10^6$ Hz; $(2M + 2DK) < 2P$. Bandwidth: 17×10^6 Hz.	17 000F9

TABLE 4—*Continued*

Description and Class of Emission	Necessary Bandwidth in Hertz	Examples: Details	Examples: Designation of Emission
Composite transmission, F9	$B_n = 2M + 2DK$ where $K = 1$	Stereophonic FM broadcasting (United States system) with multiplexed subsidiary communications subcarrier, $M =$ 75 000, $D = 75$ 000 Bandwidth: 300 000 hertz	300F9
Composite transmission, F9Y, digital modulation using PSK	$B_n = \frac{2RK}{\log_2 S}$	Microwave radio relay system specifications: digital modulation used to send 10 megabits per second by use of phase-shift keying with four signaling states. $R = 10 \times 10^6$ bits per second $K = 1$ $S = 4$ $B_n = 10$ MHz	10 000F9Y
Composite transmission, F9Y, digital modulation using FSK	$B_n = \frac{R}{\log_2 S} + 2DK$	Microwave radio relay system specifications: digital modulation used to send 10 megabits per second by use of frequency-shift keying with four signaling states and 2-MHz peak deviation of the main carrier. $R = 10 \times 10^6$ bits per second $D = 2$ MHz $K = 1$ $S = 4$ $B_n = 9$ MHz	9000F9Y
	Pulse Modulation		
Unmodulated pulse, P0	$B_n = 2K/t$ K depends on the ratio of pulse duration to pulse rise time. Its value usually falls between 1 and 10 and in many cases it does not need to exceed 6.	$t = 3 \times 10^{-6}$, $K = 6$ Bandwidth: 4×10^6 hertz	4000P0
Modulated pulse, P2 or P3	The bandwidth depends on the particular types of modulation used, many of these being still in the development stage.		
Composite transmission, P9	$B_n = 2K/t$ where $K = 1.6$	Microwave relay, pulse-position modulated by 36-channel baseband; pulse width at half amplitude = 0.4 microsecond Bandwidth: 8×10^6 hertz	8000P9

Spurious emissions include harmonics, parasitic emissions, and intermodulation products.

The mean power of any spurious emission supplied to the antenna transmission line shall not exceed the values specified below. Spurious radiation from any other part of the installation shall not have an effect greater than would occur if the antenna system were supplied with the maximum permissible spurious power.

Fundamental Frequency	Below Mean Power of Fundamental (dB)	Maximum Power of Spurious Emissions
Below 30 MHz:		
Transmitter power ≤50 kW	40	50 mW
Transmitter power >50 kW	60	50 mW
30 MHz to 235 MHz:		
Transmitter power ≤25 W	40	10 μW
Transmitter power >25 W	60	1 mW
Above 235 MHz	As low as practicable	

STANDARD FREQUENCY SOURCES

There are the following general types of stable oscillators:

(A) Free-running crystal oscillators.

(B) Crystal oscillators locked to an atomic transition frequency.

(C) Atomic beam devices (using cesium or thallium).

(D) Gas-cell devices (using mostly rubidium).

Some of these types, such as the atomic beam devices and the hydrogen maser, have excellent reproducibility because of the small interactions between the atoms and the environment. They are suitable for primary standards. In other devices, mostly gas cells, the frequency of atomic transition is affected by interaction between the atoms and the buffer gas or the walls of the cell, and the frequency of transition must be calibrated since it cannot be reproduced with sufficient accuracy. These devices, however, can be very useful as secondary, or working, standards if they have good stability and good reliability.

The performances of the types of oscillators most commonly used as sources for standard frequencies are given in Tables 5 and 6.

TIME SCALES

Ephemeris Time

In 1956 the International Committee of Weights and Measures defined the fundamental unit of time, the second, as 1/31 556 925.9747 of the tropical year for 12^h ephemeris time January 0, 1900 (January 0, 1900= December 31, 1899). The tropical year is the interval between two consecutive returns of the sun to the vernal equinox. It consisted of 365 days, 5 hours, 48 minutes, and 46 seconds at that time and has been decreasing by about 5.3 milliseconds per year.

A constant second has thus been defined in relation to the tropical year at a particular time. Although the ephemeris second has been defined very exactly, it cannot be measured by astronomical observations with anything like the precision implied by so many digits, but actually only to parts in 10^9.

In practice, ephemeris time is determined by observations of the moon and subsequent reference to lunar ephemeris tables.

Atomic Time

Atomic resonance can be used to provide time scales which are presumably uniform. The agreement between groups of measurements of certain atomic transition frequencies by different instruments is of the order of 5 parts in 10^{12}. The frequency standard maintained by the National Bureau of Standards consists of atomic standards which are stable to 1 part in 10^{12}.

The zero-field (4,0)–(3,0) transition for cesium has been measured in terms of the ephemeris second to be 9 192 631 770±20 hertz. The uncertainty of 2 parts in 10^9 is avoided by temporarily defining the standard to be used in determining the second to be exactly equal to the above number of vibrations with no uncertainty. This standard was adopted at the 12th General Conference of Weights and Measures in 1964. Other standards may be adopted in future years if more-precise measurements can be made using them. The frequency of the hydrogen maser has been measured as 1 420 405 751.73±0.03 hertz on this time scale.

Sidereal Time (θ)

This time scale is based on the mean time of rotation of the earth about its axis in relation to the vernal-equinox point in the sky. It is determined by observing the meridian transits of stars. The mean sidereal day is 23 hours, 56 minutes, 4.09 seconds. Because of variations in the rotational speed of the earth as outlined below, sidereal time is not perfectly uniform.

Universal-Time Scales (UT)

A universal-time scale, also known as Greenwich Mean Time or Greenwich Civil Time, is based on the mean angle of rotation of the earth about its axis in relation to the sun. It is referred to the

TABLE 5—CHARACTERISTICS OF ATOMIC FREQUENCY STANDARDS.

Characteristic	Hydrogen Maser	Cesium Beam (24-Inch) Controlled Oscillator	Rubidium Gas Cell Controlled Oscillator
Intrinsic reproducibility of present devices	No general published results Measured: $\pm 2\times10^{-12}$ and less	$\pm 3\times10^{-12}$	Does not apply
Stability (rms deviation from the mean):			
One second	5×10^{-13}	5×10^{-11}	1×10^{-11}
One minute	6×10^{-11}	6×10^{-12}	2×10^{-12}
One hour	3×10^{-14}	8×10^{-13}	1×10^{-12}
One day	2×10^{-14}	3×10^{-13}	5×10^{-12}
Systematic drift	None detectable with resolution of 1×10^{-12} per year	$<3\times10^{-12}$ per year	$<3\times10^{-11}$ per month
Volume (with power supply)	16.4 ft^3	1.6 ft^3	0.6 ft^3
Weight (with power supply)	800 lb	64 lb	20 lb
Power demand (115 volts ac)	200 watts	60 watts	40 watts
Relative cost	5.5	1.5	1.0

TABLE 6—PHYSICAL DATA OF AVAILABLE ATOMIC FREQUENCY STANDARDS.

Characteristic	Hydrogen Maser	Cesium Beam (24-Inch) Controlled Oscillator	Rubidium Gas Cell Controlled Oscillator
Nominal resonance frequency	1420.405 751 MHz	9192.631 770 MHz	6834.682 608 MHz
Resonance width	1 Hz	250 Hz	200 Hz (typical)
Atomic interaction time	0.5 second	2.5×10^{-3} second. Interaction length, L–25 (typical)	2×10^{-3} second (typical)
Atomic resonance events per second	10^{12}	10^{6}	10^{12}
Principal frequency offsets:			
Magnetic	$f-f_o=2750B^2$ (gauss) 5×10^{-13} (typical)	$f-f_o=427B^2$ (gauss) 1×10^{-10} (typical)	$f-f_o=574B^2$ (gauss) 1×10^{-9} (typical)
2nd-order doppler	4×10^{-11} ($\Delta f/f$/°T= 1.4×10^{-13}/K)	3×10^{-13}	8×10^{-13}
Collisions	2×10^{-11}	None	3×10^{-7} (typical)
State selection method	Atomic beam deflection in hexapole magnets	Atomic beam reflection in dipole or multi-pole magnets	Optical pumping
Resonance detection method	Atomic microwave radiation (active maser oscillation)	Surface ionization of deflected atoms	Optical absorption
Temperature of resonating atoms	300 K	360 K	330 K

TABLE 7—SERVICES PROVIDED BY RADIO STATIONS OF THE NATIONAL BUREAU OF STANDARDS.

Services	*WWV*	*WWVH*	*WWVB*
Standard radio frequencies:			
60 kilohertz			×
2.5 megahertz	×	×	
5 megahertz	×	×	
10 megahertz	×	×	
15 megahertz	×	×	
20 megahertz	×	×	
25 megahertz	×		
Standard audio frequencies:			
440 hertz	×	×	
500 hertz	×	×	
600 hertz	×	×	
Standard time intervals	×	×	×
Time signals	×	×	×
Time code	×	×	×
*UT*1 corrections	×	×	×
Radio propagation forecasts	×		
Geophysical alerts	×	×	

The station locations and radiated powers are as follows:
WWV—Fort Collins, Colorado (10 kilowatts for 5, 10, and 15 MHz; 2.5 kilowatts for 2.5, 20, and 25 MHz)
40°40′49″N, 105°02′27″W.
WWVH—Kekaha, Kauai, Hawaii (10 kilowatts for 5, 10, and 15 MHz; 5 kilowatts for 2.5 MHz; 2.5 kilowatts for 20 MHz)
21°59′26″N, 159°46′00″W.
WWVB—Fort Collins, Colorado (13 kilowatts)
40°40′28.3″N, 105°02′39.5″W.
WWVL—Fort Collins, Colorado
40°40′51.3″N, 105°03′00.0″W.

prime meridian that passes through Greenwich, England.

Since actual solar days vary throughout the year, a mean solar day of 24 hours is used to denote one revolution. Determinations of the earth's rotation relative to the sun are made by observing mean sidereal rotation of the earth and converting it to mean solar rotation by ephemeris tables based on the accumulated data of many astronomical observatories.

Mean solar rotation derived from uncorrected astronomical observations is denoted *UT*0.

Annual variations occur in the speed of rotation of the earth and are probably due to seasonal changes in the wind patterns of the Northern and Southern Hemispheres. There is also a semiannual variation due chiefly to tidal action of the sun, which distorts the shape of the earth slightly. The cumulative effect of these variations is that the earth is late about 30 milliseconds or 0.45 arc second near June 1 and is ahead about 30 milliseconds or 0.45 arc second near October 1 each year. *UT*0 corrected for these periodic variations is denoted *UT*1.

Irregular variations in the speed of rotation of the earth also occur. They may be due to turbulent motions in the core of the earth. In addition, friction of the ocean tides causes a decrease in speed of about one millisecond per century. Observations of these effects throughout the world are reported to the Bureau International de l'Heure at Paris, which issues corrections for *UT*1 to establish *UT*2.

For navigators and space scientists, time signals must be correlated with the earth's rotation, and for this reason most radio time signals include *UT*2 or earth rotation information.

"Standard Times"

"Standard times" are based on *UT* or on *UT*2. Although the term "standard time" is a misnomer, as implied by the foregoing, common usage dictates its retention in this section.

The world is divided into 24 zones, each 15° of longitude, or 1 hour angle, apart. The meridian of Greenwich, England, is the center of the zero zone which extends to 7.5° east and west. Proceeding

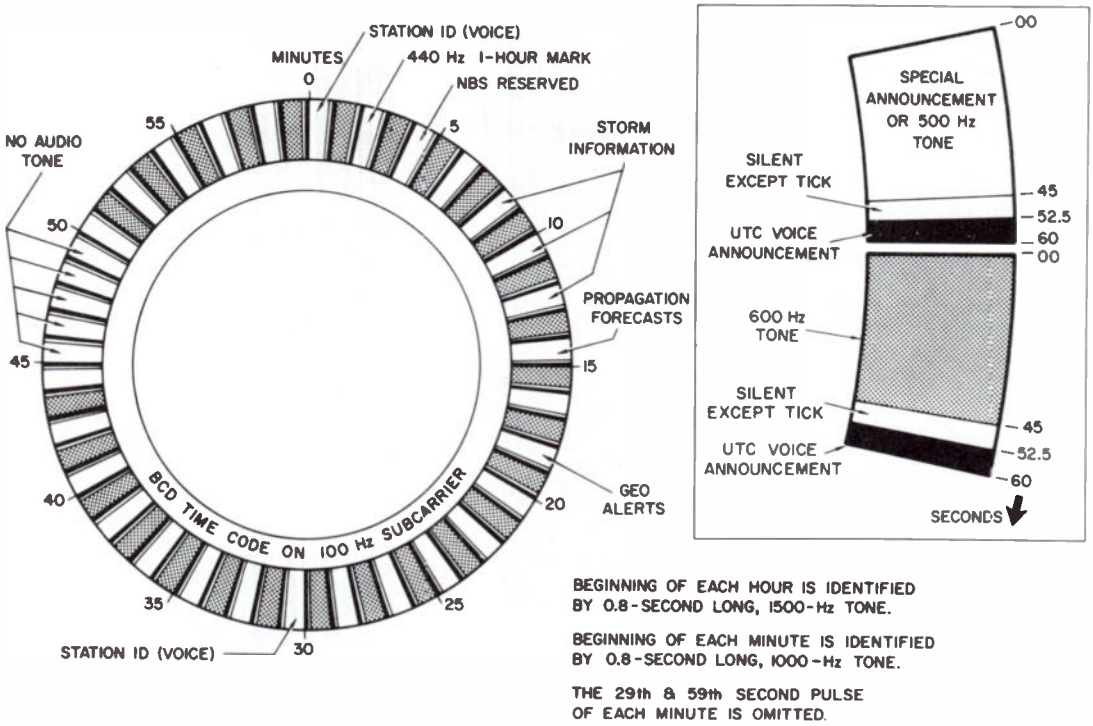

(A) *WWV*.

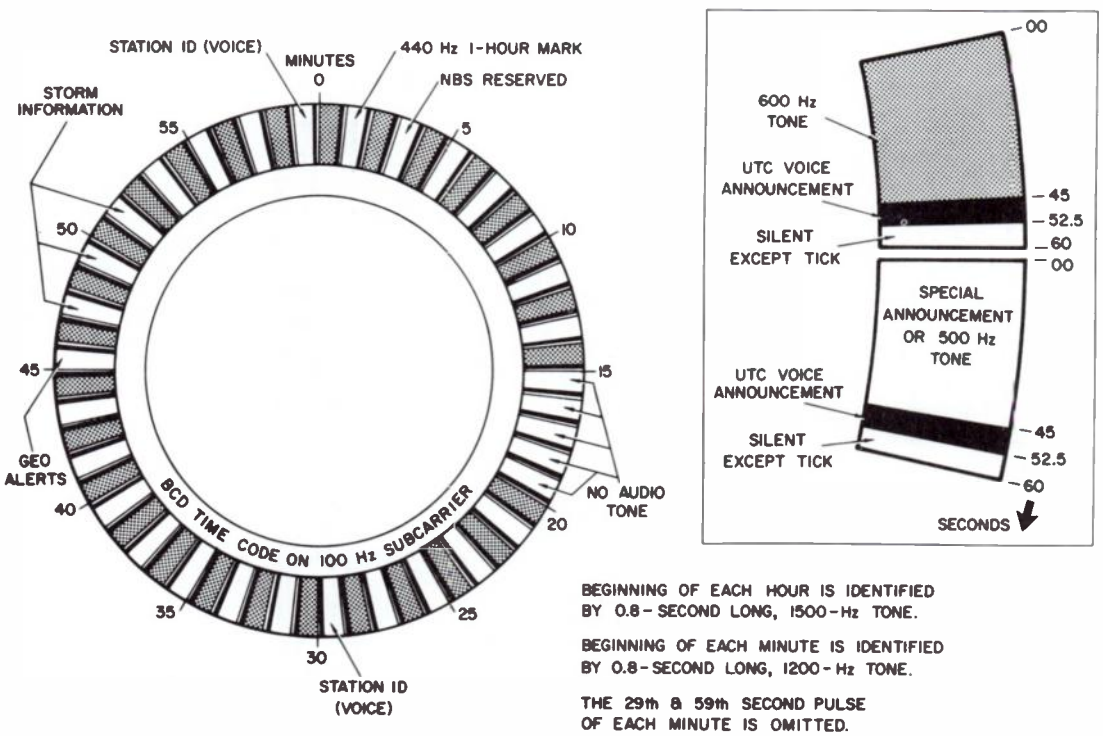

(B) *WWVH*.

Fig. 3—Hourly broadcast schedules of *WWV* and *WWVH*.

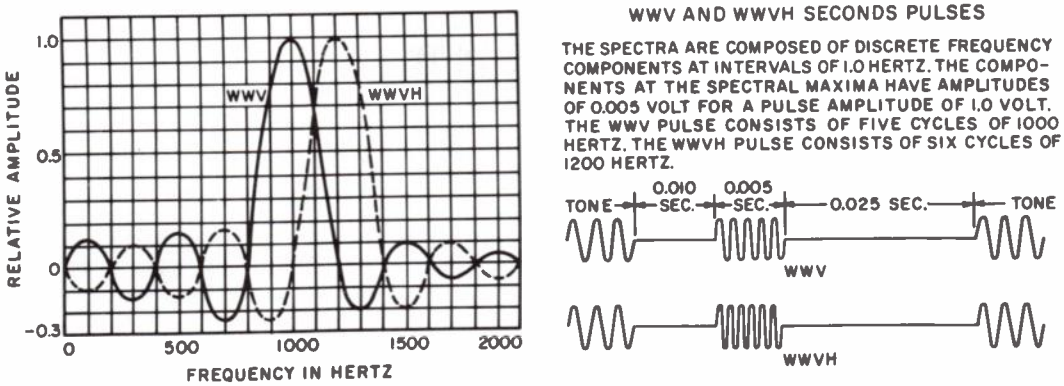

Fig. 4—Waveforms and pulse durations of *WWV* and *WWVH*.

eastward from Greenwich the zones are numbered 1 to 12 with the prefix "plus" to indicate the hour angle to be added to universal time to obtain local "standard time." Proceeding westward, the zones are numbered 1 to 12 with the prefix "minus" to indicate the hour angle to be subtracted from universal time to obtain local "standard time." For example, Washington, D.C., at longitude 77° West, is in time zone −5.

The actual boundaries of time zones are defined by law or custom in the various countries and generally do not coincide with the theoretical zone, even in some places at sea. In many areas local legal "standard time" differs by 60 or 30 minutes from theoretical standard time. A chart in Chapter 48 shows "standard time" in principal cities, and most atlases contain time-zone maps.

STANDARD FREQUENCIES AND TIME SIGNALS

The national Bureau of Standards operates standard frequency and time stations WWV, WWVB, and WWVL at Fort Collins, Colorado, and WWVH at Kekaha, Kauai, Hawaii.* The services provided by WWV, WWVH, and WWVB are listed in Table 7. WWVL is a vlf station broadcasting experimental programs, usually involving multiple frequencies, on an intermittent basis only.

WWV and WWVH

The program from WWV and WWVH is continuous, 24 hours a day. The content is summarized in Fig. 3. In addition to off-the-air reception, the broadcasts of WWV may be heard via telephone by dialing (303) 499-7111, Boulder, Colorado. The telephone user will hear the broadcasts as transmitted from the station. Because of the instabilities and variable delays of propagation by telephone, the accuracy of the telephone time signals should not be expected to be better than 30 milliseconds. This service is automatically limited to 3 minutes per call. Similar time-of-day broadcasts from WWVH can be heard by dialing (808) 355-4363 on the Island of Kauai. (Neither of the listed telephone numbers is a toll-free number.)

All carrier and modulation frequencies at WWV and WWVH are derived from cesium-controlled oscillators and are accurate to within ± 1 part in 10^{11}. Deviations are normally less than 1 part in 10^{12} from day to day. Changes in the propagation medium (causing Doppler shifts, diurnal shifts, etc.) result in fluctuations in the received carrier frequencies which may be much greater than the uncertainties of the frequencies as transmitted.

In conformity with the UTC scale, the carrier and modulation frequencies of WWV and WWVH are no longer offset significantly from nominal values. The frequency offset of UTC was made permanently zero relative to International Atomic Time (TAI) effective 0000 hours UTC January 1, 1972. Previously, the fractional frequency offset was -150 parts in 10^{10} during 1960 and 1961; -130 parts in 10^{10} during 1962 and 1963; -150 parts in 10^{10} during 1964 and 1965; and -300 parts in 10^{10} from 1966 through 1971.

Standard Time Intervals: Seconds pulses at precise intervals are derived from the same frequency standard that controls the radio carrier frequencies; for example, they commence at intervals of 5,000,000 cycles of the 5-MHz carrier. The 1-second markers are transmitted throughout all programs of WWV and WWVH except that the 29th and 59th markers of each minute are omitted. Details of these pulses are shown in Fig. 4. (Compositions of the hour and minute markers are listed in Fig. 3.)

Both WWV and WWVH broadcast voice announcements of Coordinated Universal Time

* Information on these services may be obtained from the Frequency-Time Broadcast Services Section, Time and Frequency Division, NBS, Boulder, CO 80302.

(UTC) each minute. The reference time scale is the Coordinated Time Scale maintained by the National Bureau of Standards, UTC(NBS). The UTC(NBS) scale includes small frequency offsets relative to the NBS primary frequency standard for coordination purposes.

The 24-hour system is used. Numbering starts with 0000 for midnight at the Greenwich Meridian (longitude zero). The first two figures give the hour, and the last two figures give the number of minutes past the hour when the next 800-millisecond tone begins after the announcement.

Time Corrections: Prior to January 1, 1972, time signals broadcast from WWV and WWVH were kept in close agreement with UT2 (astronomical time) by making step adjustments of 100 milliseconds as necessary. On December 31, 1971 at 23 hours 59 minutes 60.107600 seconds UTC, the UTC(NBS) scale was retarded 0.107600 second to give it an initial difference of exactly 10 seconds late with respect to the International Atomic Time (TAI) scale as maintained by the Bureau International d l'Heure (BIH).

Since the new UTC rate (effective January 1, 1972) is no longer adjusted periodically to agree with the earth's rotation rate, UTC departs more rapidly than before from earth rotation time (known as UT1), gaining about 1 second per year. Corrections to UTC are now made in step adjustments of exactly 1 second (called a leap second) as directed by BIH. The leap-second adjustments ensure that UTC signals as broadcast never differ from UT1 by more than about +0.7 second. (The corrections no longer relate to UT2.)

The leap-second adjustments are made as necessary at the end of the UTC month, preferably on December 31 or June 30. Thus, when required, a leap second is inserted between the end of the 60th second of the last minute of the last day of a month and the beginning of the next minute. The minute during which the correction is made contains either 59 or 61 seconds, depending on whether the correction is negative or positive.

For those applications in which it is necessary to date events on the UT1 time scale to better than ±0.7 second, coded corrections are provided in the broadcast formats to give UT1-UTC values to a resolution of 0.1 second. The method involves the use of a system of double second pulses. Doubling of the first through the seventh seconds pulses indicates a "plus" correction; doubling the ninth through the fifteenth pulses indicates a "minus" correction. The eighth seconds pulse is not used. The amount of correction in units of 0.1 second is determined by counting the number of seconds pulses that are doubled. For example, if the first, second, and third seconds pulses are doubled, the UT1 correction is "plus 0.3 second." Or if the ninth, tenth, eleventh, twelfth, thirteenth, and fourteenth seconds pulses are doubled, the UT1 correction is "minus 0.6 second." To obtain UT1, add the numerical correction to the time broadcast if "plus" is transmitted; subtract the correction if "minus" is transmitted. Thus, a clock keeping step with the time signals broadcast will be early with respect to UT1 if a "minus" is broadcast. The corrections are revised as necessary; the new value appears for the first time during the hour after 0000 UTC.

UT1 corrections are also encoded in the time code (described later in connection with Fig. 5) transmitted continuously on a 100-Hz subcarrier from WWV and WWVH. The value of the correction is indicated by the weight of the control functions that occur at the end of the code frame. The "plus and minus" indication is encoded in the first control function. If the first control function is a binary one, the correction is positive; if it is a binary zero, the correction is negative. The correction is expressed to the nearest 0.1 second.

Propagation Forecasts: A forecast of radio propagation conditions is broadcast from WWV in voice at 14 minutes after each hour. The announcements are short-term forecasts for propagation along paths in the North Atlantic area. The announcement consists of the statement, "The radio propagation quality forecast at ... (0100, 0700, 1300, or 1900 UTC) is ... (excellent, very good, good, fair-to-good, fair, poor-to-fair, poor, very poor, or useless). Current geomagnetic activity is ... (quiet, unsettled, or disturbed)." The propagation forecast announcements are repeated in synoptic form, consisting of a phonetic and a numeral. The phonetic identifies the radio quality at the time the forecast is made. The numeral indicates the radio propagation quality expected during the six-hour period after the forecast is issued. The meanings of the phonetics and numerals are:

Phonetic	*Meaning*
Whiskey	Disturbed
Uniform	Unsettled
November	Normal
Numeral	
One	Useless
Two	Very poor
Three	Poor
Four	Poor-to-fair
Five	Fair
Six	Fair-to-good
Seven	Good
Eight	Very good
Nine	Excellent

For example, if propagation conditions are normal and expected to be good during the next six hours, the coded forecast announcement would be "November Seven."

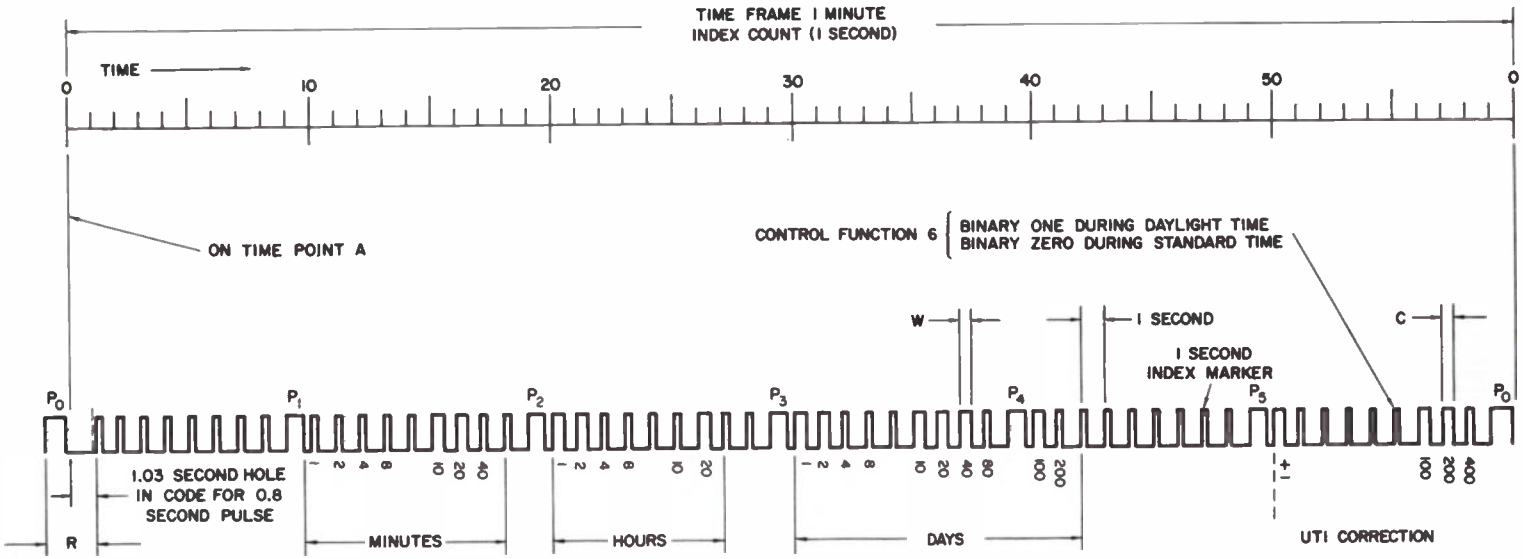

R FRAME REFERENCE MARKER (P_0 AND 1.03 SECOND "HOLE")

P_0-P_5 POSITION IDENTIFIERS (0.8 SECOND DURATION)

W WEIGHTED CODE DIGIT (0.5 SECOND DURATION)

C WEIGHTED CONTROL ELEMENT (0.5 SECOND DURATION)

DURATION OF INDEX MARKERS, UNWEIGHTED CODE AND CONTROL ELEMENTS = 0.2 SECOND

IN THIS EXAMPLE:

UTC AT POINT A = 173 DAYS, 21 HOURS, 10 MINUTES

UT1 AT POINT A = 173 DAYS, 21 HOURS, 10 MINUTES, 0.3 SECOND

Fig. 5—Time code format of *WWV* and *WWVH*.

Geophysical Alerts: Current geophysical alerts declared by the World Warning Agency of the International Ursigram and World Days Service (IUWDS) are broadcast in voice from WWV at 18 minutes after each hour and from WWVH at 45 minutes after each hour. The messages are changed daily at 0400 UTC with provisions to broadcast real-time data alerts of outstanding occurring events. These are followed by a summary of selected solar and geophysical events during the previous 24 hours.

Weather Information: WWV broadcasts information about major storms in the western North Atlantic and eastern North Pacific, and WWVH broadcasts information about major storms in the eastern and central North Pacific. These announcements are given in voice from WWV at 8, 10, and 12 minutes after each hour and from WWVH at 17, 19, and 51 minutes after each hour. The brief messages are designed to tell mariners of storm threats in their areas. If there are no warnings in the designated areas, the broadcasts so indicate.

WWV/WWVH Time Code: The time code in Fig. 5 is transmitted continuously by WWV and WWVH. The code format is a modified IRIG-H time code. The code is produced at a 1-pps rate and is carried on a 100-Hz subcarrier that is synchronous with the code pulses so that 10-millisecond resolution is readily obtained.

The code contains UTC time-of-year information in minutes, hours, and day of year. Coded time-of-day information refers to time at the beginning of the frame. Seconds information may be obtained by counting the pulses.

Each minute contains seven binary-coded decimal (BCD) groups, in the following order: two groups for minutes, two groups for hours, and three groups for day of year. The digit weighting is 1-2-4-8 for each BCD group, multiplied by 1, 10, or 100 as appropriate. A complete time frame is 1 minute. The binary groups follow the 1-minute reference marker.

"On-time" occurs at the leading edge of a pulse. A binary zero pulse consists of 20 cycles of 100-Hz amplitude modulation; a binary one pulse consists of 50 cycles of 100-Hz amplitude modulation. Because of the 10-millisecond hole that accompanies each seconds marker in the WWV/WWVH format, however, the leading 30-millisecond portion of each marker in the WWV/WWVH time code is deleted. The leading edge of each pulse coincides with a positive-going zero-axis crossing of the 100-Hz modulating frequency.

The code contains six position identification markers per minute and a minute reference marker. Each 6-per-minute position identification marker consists of an 0.8-second pulse preceding a code group. The 1-per-minute reference marker consists of a 0.8-second pulse followed by a 1.03-second hole in the code and eight binary zero pulses in succession. The minute begins with the 1.03-second hole preceding the first binary zero.

UT1 corrections to the nearest 0.1 second are encoded by means of control-function pulses that occur during the final ten seconds of the frame. Control function 1, which occurs as the 50th second pulse, is a binary zero when the UT1 correction is negative and a binary one when the correction is positive. Control functions 7, 8, and 9, which occur as the 56th, 57th, and 58th second pulses, identify the magnitude of the UT1 correction.

Control function 6, which occurs as the 55th second pulse, is programmed as a binary one throughout those weeks when Daylight Saving Time is in effect and as binary zero when Standard Time is in effect. The setting of this function is changed at 0000 UTC on the date of change as specified by Congress.

WWVB Broadcast Services

WWVB broadcasts a standard radio carrier frequency of 60 kHz with no offset. It also broadcasts a time code consistent with the internationally coordinated time scale UTC(NBS). The frequency of WWVB is normally within its prescribed value to better than 1 part in 10^{11}. Deviations from day to day are less than 5 parts in 10^{12}. Effects of the propagation medium on received signals are relatively minor at low frequencies, and the accuracy of the transmitted signals may be fully utilized if proper receiving and averaging techniques are employed.

WWVB broadcasts time information continuously using a carrier-level-shift BCD time code (Fig. 6). The code pulses are synchronized with the 60-kHz carrier signal. Identification of WWVB is accomplished by advancing the carrier phase 45° at 10 minutes after the hour and returning to the normal phase at 15 minutes after the hour. The station also can be identified by the time code.

As shown in Fig. 6, the time-code signal consists of 60 markers each minute, with one marker occurring each second. Each marker is generated by reducing the power of the carrier by 10 decibels at the beginning of a second and restoring it 0.2 second later for an uncoded marker or binary zero, 0.5 second later for a binary one, and 0.8 second later for a 10-second position marker or for a minute reference marker. Several examples of binary "ones" are indicated by I in Fig. 6.

The 10-second position markers are blackened and labeled P0 to P5 on the diagram. Uncoded markers occur periodically in the 5th, 15th, 25th, 35th, 45th, and 55th seconds of each minute; they are shaded in the figure. Other uncoded markers occur in the 11th, 12th, 21st, 22nd, 36th, 56th, 57th, 58th, and 59th seconds as indicated by *U* in

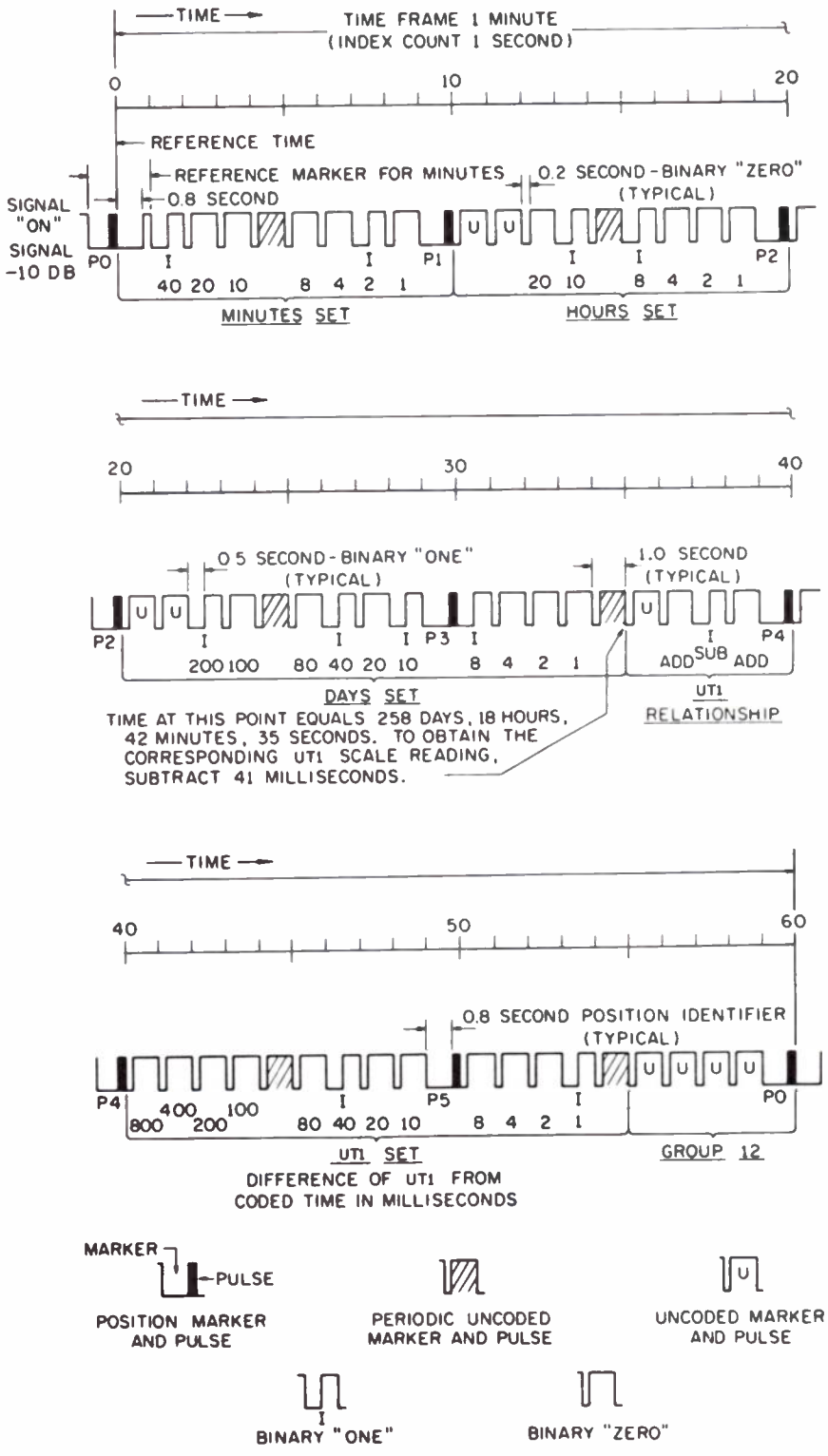

Fig. 6—Time code format of *WWVB*.

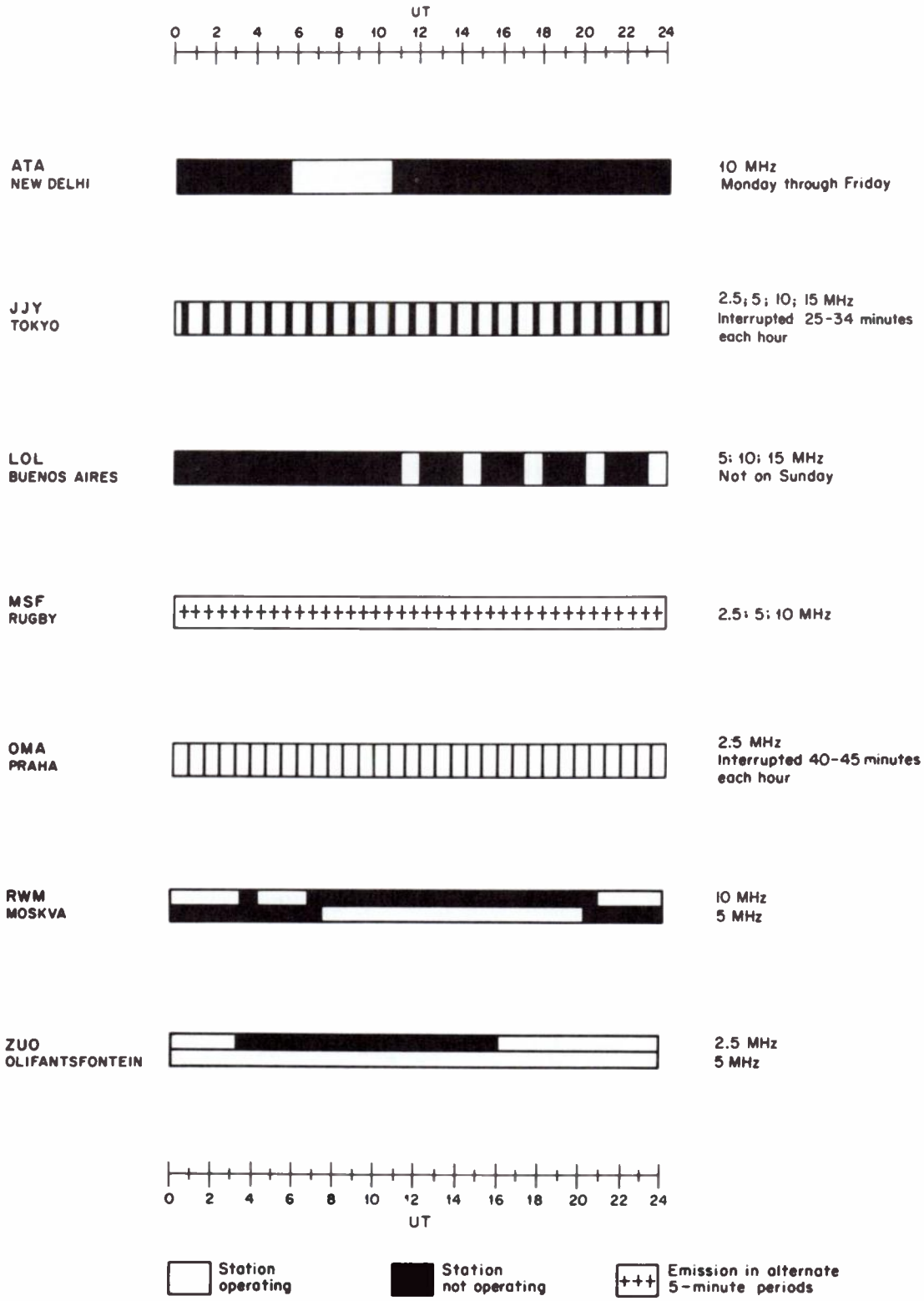

Fig. 7—Daily emission schedules of standard frequency and time stations (other than National Bureau of Standards) operating on high frequency.

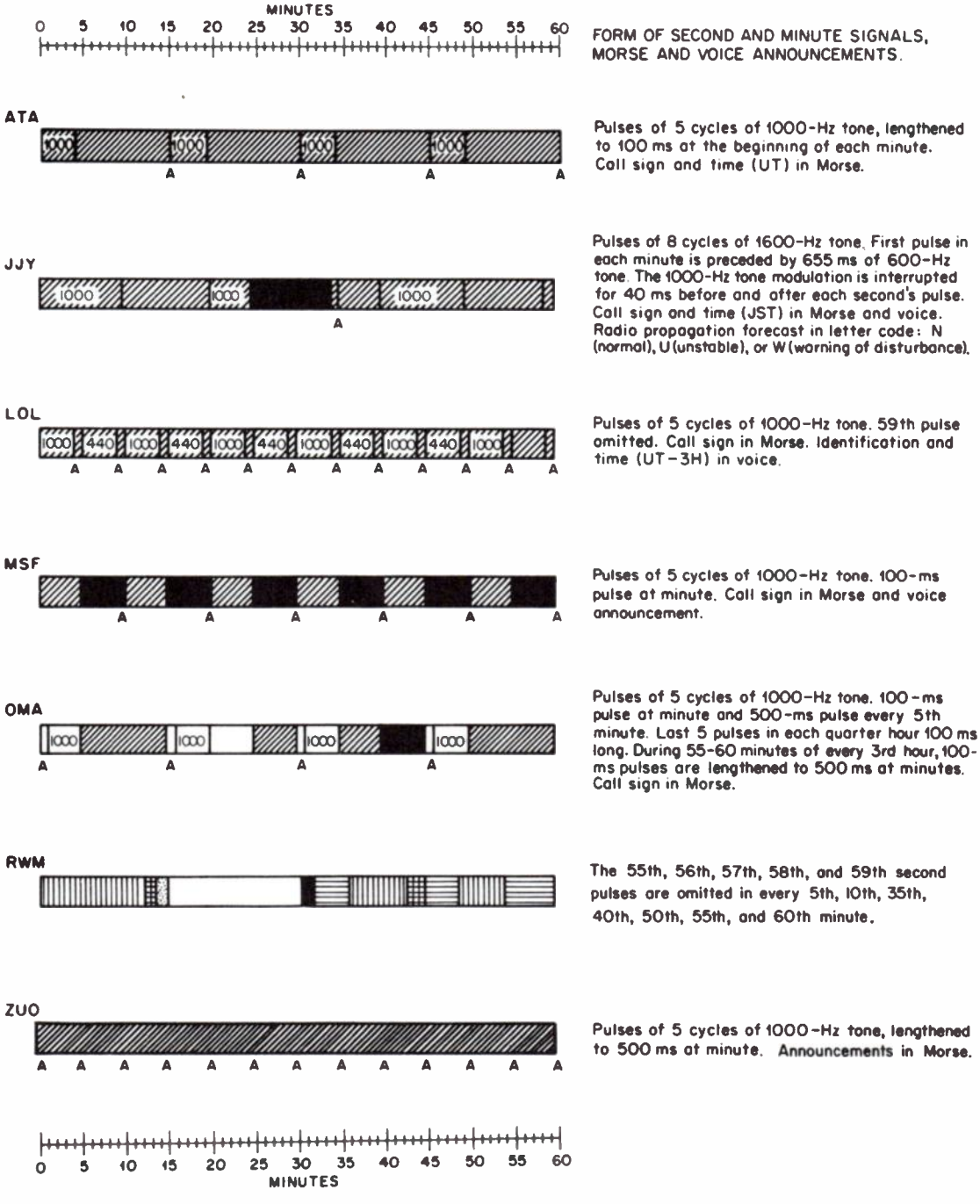

Fig. 8—Hourly modulation schedules of stations in Fig. 7.

TABLE 8—ADDITIONAL STANDARD FREQUENCY AND TIME STATIONS OPERATING ON HIGH FREQUENCY (FIGS. 7 AND 8). Refer to footnotes in Table 9.

Call Sign	Place	Latitude and Longitude	Carrier Frequency (Megahertz)	Carrier Power (Kilowatts)	Modulation (Hertz)	Accuracy (Parts in 10^{10})
ATA	New Delhi, India	28°34′N 77°19′E	10	2	1; 1000	100
CHU (2)	Ottawa, Canada	45°18′N 75°45′W	3.330 7.335 14.670	3 10 3	1 (8)	0.05
JJY (1)	Tokyo, Japan	35°42′N 139°31′E	2.5 5 10 15	2	1; 1000 (9)	0.5
LOL (1)	Buenos Aires, Argentina	34°37′S 58°21′W	5 10 15	2	1; 440; 1000	0.2
MSF (1)	Rugby, United Kingdom	52°22′N 01°11′W	2.5 5 10	0.5	1	1
OMA (1)	Praha, Czechoslovak S.R.	50°07′N 14°35′E	2.5	1	1; 1000 (10)	10
RWM (1)	Moscow, U.S.S.R.	55°19′N 38°41′E	10 15	8	1; 10	0.5
VNG (2)	Lyndhurst, Victoria, Australia	38°03′S 145°16′E	4.5 7.5 12	10	1; 1000 (11)	1
ZUO (1)	Olifantsfontein, Republic of South Africa	24°58′S 28°14′E	2.5 5	4	1	0.1

Fig. 6. Thus, every minute contains twelve groups of five binary-coded-decimal markers, each group ending either with a position marker or an uncoded marker.

The four coded markers in a binary-coded-decimal group are indexed 8-4-2-1, in that order. Sometimes only the last two or three coded markers are needed, as in the first group in the minutes, hours, and days sets. The indices of the first group in each set which contains two groups are multiplied by 10, and those of the second group are multiplied by 1. The indices of the first group in each set which contains three groups are multiplied by 100, those of the second group by 10, and those of the third group by 1.

The first two binary-coded-decimal groups in each minute form a set which specifies the minute of the hour; the third and fourth groups make up a set which specifies the hour of the day; the fifth, sixth, and seventh groups form a set which specifies the day of the year. The relationship of the UT1 scale to the time as coded is indicated by the eighth group. If UT1 is late with respect to UTC, a binary 1 is sent in the eighth group in the 38th second. If UT1 is early with respect to the code time, binary ones are sent in the eighth group in the 37th and 39th seconds. A set, made up of the ninth, tenth, and eleventh binary-coded-decimal groups, specifies the number of milliseconds to be added or subtracted from the code time as broadcast in order to obtain UT1. The twelfth group is not used to convey information at present.

Other Standard Frequency and Time Stations

Standard frequency and time stations in Argentina, Australia, Canada, Japan, Republic of South Africa, United Kingdom, and other countries, as well as the United States Navy, are listed in Tables 8 and 9.

TABLE 9—ADDITIONAL PRINCIPAL STANDARD FREQUENCY AND TIME STATIONS OPERATING ON LOW FREQUENCY AND VERY-LOW FREQUENCY.

Call Sign	Place	Latitude and Longitude	Carrier Frequency (kHz)	Power to Antenna (kW)	Estimated Radiated Power (kW)	Modulation (Hz)	Time Signal	Accuracy (Parts in 10^{10})
DCF 77 (2)	Mainflingen, West Germany	50°01′N 09°00′E	77.5	38	—	1	Continuous (14)	0.1
GBR (2)(3)	Rugby, United Kingdom	52°22′N 01°11′W	15.95 16	750	60 (6)	1 (12)	4×5 min per day (15)	0.2
Loran-*C*	Carolina Beach, North Carolina	34°04′N 77°55′W	100	—	1000 (7)	(19)	Continuous	0.05
MSF	Rugby, United Kingdom	52°22′N 01°11′W	60	50	—	1 (13)	Continuous	0.1
NAA (2)(4)(5)	Cutler, Maine	44°38′N 67°16′W	17.8	2000	1000 (6)	nil	nil	0.1
NBA (2)(4)(5)	Balboa, Panama Canal Zone	09°03′N 79°38′W	24	300	150 (6)	nil	(16)	0.1
NLK (2)(5)	Jim Creek, Washington	48°12′N 121°55′W	18.6	1200	250 (6)	nil	nil,	0.1
NPM (2)(4)(5)	Lualualei, Hawaii	21°25′N 158°09′W	23.4	1000	140 (6)	nil	nil	0.1
NSS (2) (5)	Annapolis, Maryland	38°59′N 76°27′W	21.4	1000	85 (2)	nil	(17)	0.1
OMA	Podebrady, Czechoslovak S.R.	50°08′N 15°08′E	50	5	—	1 (12)	23 hours per day (18)	10

Notes Associated with Tables of Standard Frequency and Time Stations

(1) Station follows UTC system as specified in ITU Recommendation 460-1. Time signals remain within about 0.8 second of UT1 by means of occasional 1-second steps as directed by BIH.

(2) Station follows one of the systems referred to in ITU Recommendation 460-1.

(3) FSK is used alternately with CW; both carriers are frequency controlled.

(4) FSK is used. Phase stable on assigned frequency.

(5) Station primarily for communication purposes; data subject to change.

(6) Estimated radiated power.

(7) Peak radiated power.

(8) Seconds pulses consist of 300 cycles of 1000-Hz tone. The first pulse in each second is prolonged.

(9) Seconds pulses consist of 8 cycles of 1600-Hz tone; first pulse of each minute is preceded by 655 ms of 600-Hz tone. There is 1000-Hz modulation between minutes 0–10, 20–25, 34–35, 40–50, and 59–60 except 40 ms before and after each seconds pulse.

(10) Audio-frequency modulation is replaced by time signals during the period 1800–0600 hours UT.

(11) Seconds pulses consist of 50 cycles of 1000-Hz tone, shortened to 5 cycles from the 55th to the 58th second (59th pulse is omitted). At the 5th, 10th, 15th, etc., minutes, pulses from the 50th to the 58th second are shortened to 5 cycles. Voice identification is given between the 20th and 50th pulses in the 15th, 30th, 45th, and 60th minutes.

(12) A1 telegraphy signals.

(13) The carrier is interrupted for 100 ms at each second and 500 ms at each minute. From 1430 to 1530 hours UT, A2 pulses are transmitted in the same form as for MSF high-frequency transmission.

(14) 100-ms carrier interruptions at beginning of each second except 59th second of each minute. Minute, hour, day, month, year, and day of week are transmitted each minute in BCD code beginning with 20th second and ending with 58th second; binary zero is 0.1-s wide second marker, and binary one is 0.2-s wide marker.

(15) 0255–0300, 0855–0900, 1455–1500, and 2055–2100 hours UT.

(16) Time signal on FSK 5 minutes before each even hour except 2355 to 2400 hours UTC.

(17) Temporarily suspended; FSK time signals planned.

(18) From 1000 to 1100 hours UT, transmissions without keying except for call sign at beginning of each quarter hour.

(19) Pulse repetition, 99 300 microseconds. Time pulses appear in groups of 9.

CHAPTER 2
INTERNATIONAL TELECOMMUNICATION RECOMMENDATIONS

INTERNATIONAL STANDARDS

Administrations and operating companies throughout the world carry on studies of technical and other problems related to the interworking of their respective national telecommunication systems to provide a worldwide telecommunications network. Two international committees exist for this purpose: The International Telegraph and Telephone Consultative Committee (CCITT), and The International Radio Consultative Committee (CCIR). They operate under the auspices of the International Telecommunication Union (ITU). They promulgate their decisions in the form of Recommendations, which are published by the ITU. Generally, these Recommendations cover features of international circuits, but where essential, they deal with relevant characteristics of the national systems which may form part of international connections. This compendium collects, in condensed form, major Recommendations dealing with telephone, telegraph, and data-transmission circuits and equipment.

Recommendations of the CCITT

The CCITT develops new Recommendations, and updates existing ones, through the activities of Study Groups, whose reports are acted on at Plenary Assemblies, which meet at intervals of 3 or 4 years. The resulting Recommendations of the Second Plenary Assembly, New Delhi, 1960, were published by the ITU in a number of volumes, called collectively the Red Book. The subsequent study periods culminated in the Third Plenary Assembly, Geneva, 1964 (Blue Book); the Fourth Plenary Assembly, Mar del Plata, 1968 (White Book); and the Fifth Plenary Assembly, Geneva, 1972 (Green Book). This compendium refers to Green Book Recommendations, designated thus: (G.101), (H.31), (V.2), etc.

Recommendations of the CCIR

The CCIR also functions with Study Groups and Plenary Assemblies. The Eleventh Plenary Assembly was held at Oslo in 1966, the Twelfth Plenary Assembly at New Delhi in 1970, and the Thirteenth Plenary Assembly at Geneva in 1974. After each Plenary Assembly, the ITU publishes volumes which contain the currently accepted Recommendations, including such Recommendations of the Plenary Assemblies at London (1953), Warsaw (1956), Los Angeles (1959), and Geneva (1963) which are still in effect. No color coding is used. This compendium deals with those Recommendations which treat point-to-point radio relay systems. A purpose of those Recommendations is to make the performance of such systems compatible with metallic line systems which follow the CCITT Recommendations. References to the CCIR Recommendations are made thus: (CCIR, 391).

ZERO-RELATIVE-LEVEL POINTS AND RELATIVE LEVELS

Many CCITT and CCIR Recommendations specify signal or noise levels at "a point of zero relative level," or in dBm0 or pWp0, etc., where "0" (zero) stands for "measured at or referred to a point of zero relative level."

(A) In 2-wire switching systems, the sending end terminals of a long-distance circuit have long been considered to be at a point of zero relative level. The relative levels of all other points are calculated from this reference point, as the algebraic sum of all transmission losses and gains from it to the point in question. Any point in a circuit with the same relative level as the sending terminals is a point of zero relative level, which may be written 0 dBr (*dB* relative level). The American term for *relative level* is *transmission level*. Thus: "Zero-transmission-level point" (0TLP).

For convenience in comparing circuit noise performance, it is customary to convert absolute noise measurements made at the receiving ends of circuits having various relative levels, to absolute power levels at a zero-relative-level point. For example, −50 dBmp of noise at a −7-dBr point would be reported as −43 dBm0p. Signaling-tone levels are

TABLE 1—RELATIVE LEVELS, PLUS LEVELS OF ABSOLUTE AND REFERRED POWER, FOR A 2-WIRE CIRCUIT.

	Sending Point	Circuit Loss: 5 dB Direction→ 2-Wire Circuit	Receiving Point
Relative levels, or transmission levels	0 dBr		−5 dBr
"Milliwatt" test tone	0 dBm		−5 dBm absolute power
At any point	0 dBm0		0 dBm0 referred power
Signaling tone	−10 dBm		−15 dBm absolute power
At any point	−10 dBm0		−10 dBm0 referred power
Circuit noise, picked up along circuit	—		−65 dBmp absolute power
Circuit noise, referred to 0-dBr point	—		−60 dBm0p referred power

similarly expressed. For example, a tone introduced at a −3.5-dBr point with an absolute power level of −18.5 dBm may be referred to as a −15-dBm0 signal. The latter designation would apply to such a tone no matter where it appeared; the "0" denotes that its level is referred to a point of zero relative level. (Refer to Table 1.)

Statistics of speech power, requirements for linearity and limiting, system loading factors, crosstalk, and noise have become well known in terms of their values at points of zero relative level. The proper performance of voice repeaters, carrier terminal and line equipment, radio relay systems, etc., depends on adherence to the relative levels for which they were designed. Many relative levels associated with such equipment have been standardized.

(B) In 4-wire switching systems, it is often considered desirable to handle speech and signaling at lower values of absolute power through the switching equipment than is customary in 2-wire systems. In 1964, the CCITT adopted a relative level of −3.5 dBr for the sending end of a 4-wire circuit, at the "virtual" switching points. These are theoretical points; their exact location depends on national practice, and the CCITT considers it unnecessary to define them. (In the American commercial system, −2 dBr is widely used.) (G.101, Section B)

Therefore, to ensure that carrier and other transmission equipment will be subjected to the same absolute speech and signaling power levels as in 2-wire systems, determination of relative levels in 4-wire circuits must take into account the relative level of the virtual switching points. In a 4-wire circuit, there may be no actual point of zero relative level. Nevertheless, standards will continue to refer many requirements to a zero relative point. (Refer to Table 2.)

Currently, many transmission measurements are made with a standard 800- or 1000-hertz test tone, with an absolute power of 1 milliwatt at a zero-

TABLE 2—RELATIVE LEVELS, PLUS LEVELS OF ABSOLUTE AND REFERRED POWER, FOR ONE DIRECTION OF A 4-WIRE CIRCUIT.

	Sending Point	Circuit Loss: 5 dB Direction→ One Side of 4-Wire Circuit	Receiving Point
Relative levels, or transmission levels	−3.5 dBr		−8.5 dBr
"Milliwatt" test tone	−3.5 dBm		−8.5 dBm absolute power
At any point	0 dBm0		0 dBm0 referred power
Signaling tone	−13.5 dBm		−18.5 dBm absolute power
At any point	−10 dBm0		−10 dBm0 referred power
Circuit noise, picked up along circuit	—		−68.5 dBmp absolute power
Circuit noise, referred to 0-dBr point	—		−60 dBm0p referred power

relative-level point: a power of 0 dBm0. The actual level applied is adjusted to the relative level of the sending point. The test-tone level in dBm will be numerically equal to the relative level in dBr at any point in the circuit, but it is not proper to express *relative* levels in dBm, since dBm represents absolute power levels. If the standard-test-tone power is ever changed to another value, such as −10 dBm0, as has been tentatively proposed, the distinction between relative levels and test-tone levels will be more apparent.

PSOPHOMETRIC NOISE AND POWER

Psophometric Noise Weighting

The CCITT calls a noise measuring set a "psophometer." A psophometer includes a device for measuring power through a weighting network. For measurements on commercial telephone circuits, a weighting characteristic is used which results in the objective instrument measurements approximately parallelling the results of subjective tests with human observers using modern telephone sets. The CCITT weighting characteristic for commercial circuits is nominally identical with the American F1A line weighting. Psophometric noise power may be expressed in dBm0 "psophometrically weighted," or dBm0p. The conventional conversion equation used between dBm0p and dBa0 (F1A) is

$$\text{dBm0p} = \text{dBa0} - 84.$$

Psophometric Weighting for Commercial Telephone Circuits:

Frequency (hertz)	Level (dB)	Frequency (hertz)	Level (dB)
100	−41.0	1350	−0.65
150	−29.0	1500	−1.30
200	−21.0	1750	−2.22
250	−15.0	2000	−3.00
300	−10.6	2250	−3.60
400	−6.3	2500	−4.20
500	−3.6	2750	−4.87
600	−2.0	3000	−5.60
700	−0.9	3500	−8.5
800	0.0	4000	−15.0
900	+0.6	4200	−18.7
1000	+1.0	4500	−25.0
1100	+0.6	4700	−29.4
1200	0.0	5000	−36.0

(Extracted from G.223, which gives weighting for 84 frequencies.)

Psophometric Weighting Factor: If uniform-spectrum random noise is measured in a 3.1-kilohertz band with a flat attenuation/frequency characteristic, the noise level must be reduced by 2.5 decibels to obtain the psophometric power level. For another bandwidth B, the weighting factor will be equal to

$$2.5 + 10 \log_{10}(B/3.1) \text{ decibels.}$$

When $B = 4$ kilohertz, for example, this gives a weighting factor of 3.6 decibels. (G.223)

Psophometric Power: Where power addition of noise can be assumed, it has been found convenient for calculations and design of international circuits to use the concept of "psophometric power."

psophometric power

= (psophometric voltage)^2/600

= (psophometric emf)^2/(4×600).

A convenient unit is the picowatt (pW) = 10^{-12} watt, so that

psophometric power in pW

= (psophometric voltage in mV)^2/0.0024. (G.212)

CONVENTIONAL TELEPHONE SIGNAL

For the calculation or measurement of crosstalk noise between adjacent channels, of the balance return loss for echo, and generally speaking, when it is desired to simulate the speech currents transmitted by a telephone channel, the CCITT recommends the use of a conventional telephone signal. This signal may be produced by passing the output of a generator of a uniform-spectrum random noise signal ("white noise") through a weighting network with a characteristic as shown in Fig. 1. The amount of this signal that appears in another circuit because of crosstalk, etc., is measured with a psophometer or weighted-noise measuring set, with standard psophometric weighting for commercial telephone circuits. (G.227)

TELEPHONE CIRCUIT LOADING

Nominal Mean Power During Busy Hour

To simplify calculations when designing carrier systems on cables or radio links, the CCITT has adopted a *conventional* value to represent the *mean absolute power level*, at a point of zero relative level, of the speech-plus-signaling currents, etc., transmitted over a telephone channel in one direction of transmission during the busy hour, which is −15 dBm (−1.73 nepers) (mean power = 31.6 microwatts); this is the mean with time and the mean for a large batch of circuits. This total mean power of about 32 microwatts is conventionally distributed as follows (nominal mean power): 10 microwatts, all signaling and tones; 22 microwatts,

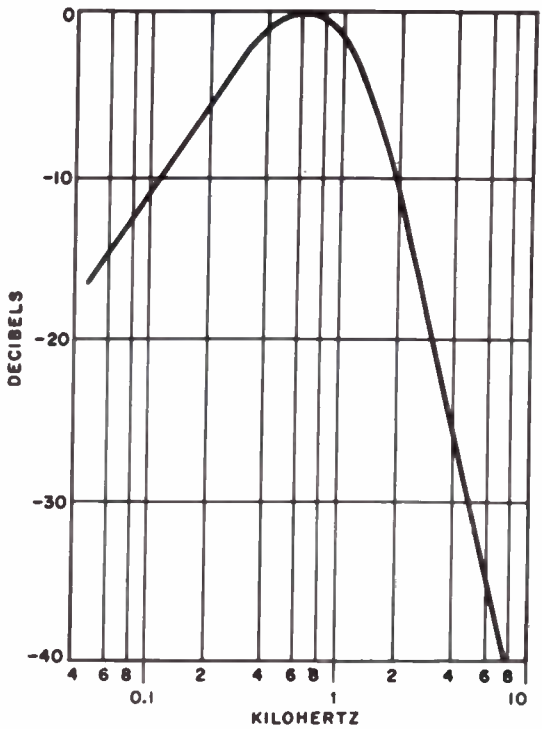

Fig. 1—Relative response curve for the weighting network of the conventional telephone signal generator. (G. 227)

to include speech currents (including echoes), carrier leak, and telegraph signals, based on a speech activity factor of 0.25 for one direction of a telephone channel. No account is taken of pilot signals, which are assumed to be an integral part of the carrier system, not affecting telephone channel power. (G.223, Section 1)

Conventional Load

It will be assumed for the calculation of intermodulation noise below the overload point that the multiplex signal during the busy hour can be represented by a uniform-spectrum random noise signal, the mean absolute power level of which, at a zero-relative-level point, $n(\bar{P})$, is given by

$$n(\bar{P}) = -15 + 10 \log_{10} N \text{ dB}$$

for $N = 240$ or more

and

$$n(\bar{P}) = -1 + 4 \log_{10} N \text{ dB}$$

for values of N between 12 and 240

where N is the total number of telephone channels in the system.

Typical values so calculated are as follows

N	$n(\bar{P})$, dB
12	3.3
24	4.5
36	5.2
48	5.7
60	6.1
120	7.3
⋮	⋮
240	8.8
300	9.8
600	12.8
960	14.8
1800	17.5
2700	19.3

Assumed: No pre-emphasis, and use of independent amplifiers for each direction. (G.223, Section 2)

POWER LEVELS

Maximum Power Level for Signaling Pulses

For crosstalk reasons, each component of a short-duration signal should not exceed the following absolute power levels, at a zero-relative-level point.

Signaling Frequency (hertz)	Absolute Power Level at Zero-Relative-Level Point (dBm0)
800	−1
1200	−3
1600	−4
2000	−5
2400	−6
2800, 3200	−8

(G.224)

Private Telegraph Transmission on a Rented International Circuit, with Alternative Private Telephone Service

The frequency of 1500 hertz is recommended for private telegraph transmission between subscribers permanently connected via a rented international circuit. The permissible power for a continuously transmitted telegraph marking signal is 0.3 milliwatt at a zero-relative-level point (−5 dBm0). (H.31)

Simultaneous Communication by Telephony and Telegraphy on a Telephone Circuit

A continuously transmitted telegraph signal should not exceed a level of −13 dBm0. There should not be more than 3 telephone circuits of this type per group, nor more than the number of supergroups in a wide-band system. (H.32)

Phototelegraphy Transmissions Over Telephone Circuits which are Entirely 4-Wire Between Phototelegraph Stations

The sent voltage for the phototelegraph signal corresponding to maximum amplitude should be so adjusted that the absolute power level of the signal, at a zero-relative-level point, is 0 dBm0 for amplitude-modulation facsimile, and −10 dBm0 for frequency-modulation facsimile. In the former, the "black" level is about 30 decibels lower than the "white" level. (H.41)

Power Levels for Data Transmission Over Telephone Circuits

Private Wires on Carrier Systems:

(A) Maximum power output of subscriber's apparatus into line: 1 milliwatt.

(B) Continuous-tone systems (for example, frequency modulation): Maximum power level at zero-relative-level point: −10 dBm0, to be reduced to or below −20 dBm0 when data transmission is discontinued for any appreciable time.

(C) Noncontinuous-tone systems (for example, amplitude modulation): Maximum power level at zero-relative-level point: −6 dBm0, provided that busy-hour mean power in both directions of transmission added does not exceed 64 microwatts (−15 dBm0 mean level in each direction simultaneously). Also, the level of tones above 2400 hertz should conform to recommendations for signaling tones in G.224. (H.51)

Switched Telephone Network:

(A) Maximum power output of subscriber's apparatus into line: 1 milliwatt.

(B) Continuous-tone systems (for example frequency- or phase-modulation systems): The power level at the subscriber's equipment should be adjusted not to exceed −10 dBm0 (simplex operation) or −13 dBm0 (duplex operation).

(C) Noncontinuous-tone systems (for example amplitude-modulation or multifrequency systems): Higher levels may be used, if mean power at international-circuit input is limited to 64 microwatts in any hour (both directions), i.e., −15 dBm0 in each direction simultaneously. (H.51)

HYPOTHETICAL REFERENCE CIRCUITS

General Definitions (G.212)

Hypothetical Reference Circuit: A hypothetical circuit of defined length and with a specified number of terminal and intermediate equipments, this number being sufficient but not excessive. It forms the basis for the study of certain characteristics of long-distance circuits, for example, noise.

Hypothetical Reference Circuit for Telephony: This is a complete telephone circuit, between audio-frequency terminals, established on a hypothetical international telephone carrier system and having a specified length and a specified number of modulations and demodulations of the groups, supergroups, and mastergroups, these numbers being reasonably great but not having their maximum possible values.

Various hypothetical reference circuits for telephony have been defined by the CCITT and CCIR to allow the coordination of the different specifications concerning the constituent parts of the multichannel carrier telephone systems, so that the complete telephone circuits set up on these systems can meet CCITT standards.

Homogeneous Section: A section without diversion or modulation of any one of the mastergroups, supergroups, groups, or channels established on the system being considered, except for those modulations or demodulations defined at the ends of the section. All the hypothetical reference circuits defined below consist of homogeneous sections of equal length (6 or 9 sections). It is assumed that at the end of each homogeneous section, the channels, groups, supergroups, and mastergroups, as appropriate, are connected through at random.

Important Hypothetical Reference Circuits Defined by CCITT and CCIR

Hypothetical Reference Circuit on Symmetric Cable Pairs: This circuit is 2500 kilometers long and is set up on a symmetric-cable-pair carrier system. For each direction of transmission, it has a total of 3 pairs of channel modulators and demodulators, 6 pairs of group modulators and demodulators, and 6 pairs of supergroup modulators and demodulators.

Figure 2*A* shows that there are 15 modulations and 15 demodulations for each direction of transmission, assuming that single-stage translations are used. There are 6 homogeneous sections of equal length. (G.322)

Hypothetical Reference Circuit for 4-Megahertz Systems on Coaxial Cable: This circuit is 2500 kilometers long and is set up on a 4-megahertz

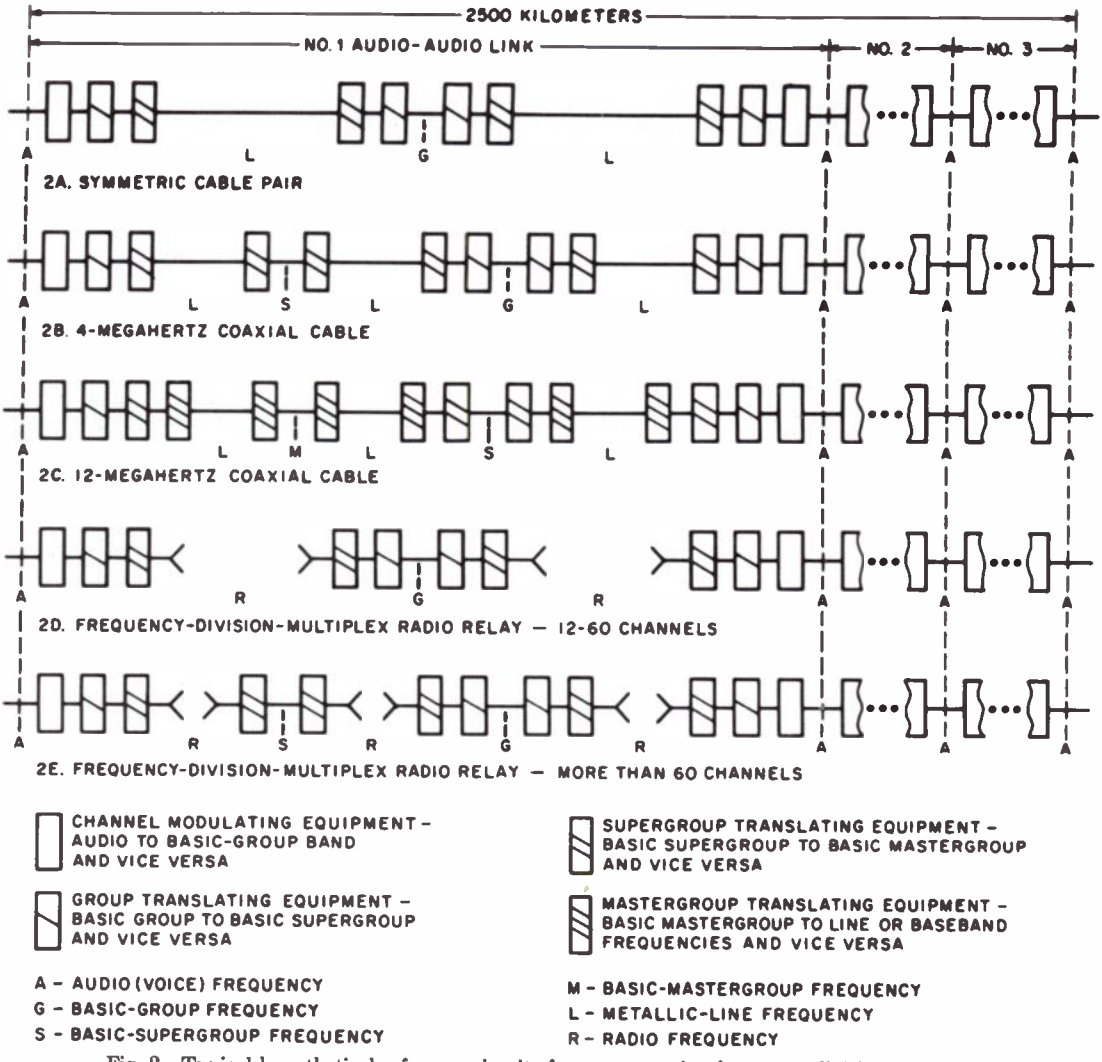

Fig. 2—Typical hypothetical reference circuits for systems using frequency-division multiplex.

carrier system on 0.104/0.375-inch coaxial cable pairs. For each direction of transmission, it has a total of 3 pairs of channel modulators and demodulators, 6 pairs of group modulators and demodulators, and 9 pairs of supergroup modulators and demodulators.

Figure 2*B* shows that there are 18 modulations and 18 demodulations for each direction of transmission, assuming that single-stage translations are used. There are 9 homogeneous sections of equal length. (G.338)

Hypothetical Reference Circuit for 12-Megahertz Systems on Coaxial Cable: This circuit is 2500 kilometers long and is set up on a 12-megahertz carrier system on 0.104/0.375-inch coaxial cable pairs. For each direction of transmission, it has a total of 3 pairs of channel modulators and demodulators, 3 pairs of group modulators and demodulators, 6 pairs of supergroup modulators and demodulators, and 9 pairs of mastergroup modulators and demodulators.

Figure 2*C* shows that there are 21 modulations and 21 demodulations for each direction of transmission, assuming that single-stage translations are used. There are 9 homogeneous sections of equal length. (G.332)

Hypothetical Reference Circuit over Radio Relay Systems with Frequency-Division Multiplex, Providing 12 to 60 Channels: This circuit is 2500 kilometers long and is set up on a carrier system providing 12 to 60 channels per radio channel over line-of-sight and near-line-of-sight radio relay systems. For each direction of transmission it has a total of 3 sets of channel modulators and demodulators, 6 sets of group modulators and demodulators, 6 sets of supergroup modulators and demodulators, and 6 sets of radio modulators and demodulators. The circuit is divided into 6 homogeneous sections of equal length. (See Fig. 2*D*.) (CCIR, 391)

Hypothetical Reference Circuit over Radio Relay

Systems with Frequency-Division Multiplex, Providing More than 60 Channels: This circuit is 2500 kilometers long, and is set up on a carrier system providing more than 60 channels per radio channel over line-of-sight or near-line-of-sight radio relay systems. For each direction of transmission it has a total of 3 sets of channel modulators and demodulators, 6 sets of group modulators and demodulators, 9 sets of supergroup modulators and demodulators, and 9 sets of radio modulators and demodulators. The circuit is divided into 9 homogeneous sections of equal length. (See Fig. 2*E*.) (CCIR, 392)

Hypothetical Reference Circuit over Transhorizon Radio Relay Systems: This circuit is 2500 kilometers long and is set up over a transhorizon radio relay system for telephony using frequency-division multiplex. For each direction of transmission it has a total of 3 sets of channel modulators and demodulators, 6 sets of group modulators and demodulators, and 9 sets of supergroup modulators and demodulators.

It is recommended that the hypothetical reference circuit not be divided into homogeneous sections of fixed length, because these systems, as distinct from line-of-sight systems, are usually composed of long radio sections, the lengths of which depend on local conditions and may vary considerably (between 100 and 400 kilometers). If a radio section under study is L kilometers long, the hypothetical reference circuit should be composed of $(2500/L)$ sections of this type in tandem, the value $(2500/L)$ being taken to the nearest whole number. (CCIR, 396-1)

Hypothetical Reference Circuit over Active Intercontinental Communication-Satellite Systems. This circuit has no fixed length. For intercontinental connections, satellite links should be capable of spanning 7500 kilometers. For great-circle distances up to 25 000 kilometers, it will be necessary to connect two or three satellite links in tandem. The basic hypothetical reference circuit shall consist of one earth–satellite–earth link, as shown in Fig. 3. It shall contain one pair of modulation and demodulation equipments for translation from the baseband to the radio-frequency carrier and back. (CCIR, 352-2)

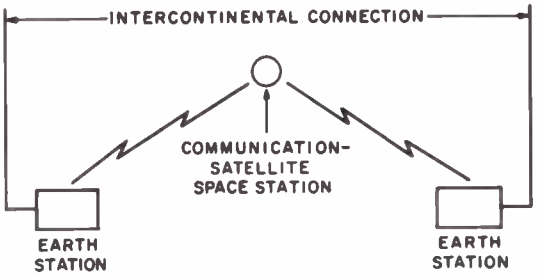

Fig. 3—Basic hypothetical reference circuit, active intercontinental communication-satellite system (CCIR, 352-2).

TELEPHONE CIRCUIT CHARACTERISTICS

Impedance of International and National Trunks

All circuits (whether international circuits or national 2-wire or 4-wire trunk circuits) terminating at the same trunk exchange should have the same nominal value of impedance as seen from the switchboard or selectors. The preferred value is 600 ohms. (G.232, Section L)

One-Way Propagation Time

The 1-way propagation time of connections when echo sources exist and echo suppressors are used is considered to be: acceptable without reservation, 0–150 milliseconds; provisionally acceptable, 150–400 milliseconds; and provisionally unacceptable, 400 milliseconds or higher (should not be used except under extraordinary circumstances).

On National Extension Circuits: Probable propagation time, most distant subscriber to international center: 12 plus (0.0064×distance in statute miles) milliseconds or 12 plus (0.004×distance in kilometers) milliseconds.

International Circuits, Terrestrial (Including Submarine Cable): 100 statute miles (160 kilometers) per millisecond, including effects of terminal or intermediate multiplex equipment.

International Circuits, Communication-Satellite Systems: Moving satellite, altitude 8700 miles (14 000 kilometers): 110 milliseconds. Geostationary satellite, altitude 22 500 miles (36 000 kilometers): 260 milliseconds. (G.114)

Group Delay Distortion

The permissible differences, for a worldwide chain of 12 circuits, between the minimum group delay throughout the frequency band transmitted, and the group delay at the upper and lower limits of this band in milliseconds are as follows:

Facility	At the Limits of the Frequency Band: Lower Limit	Upper Limit
International chain	30	15
Each of the national 4-wire extensions	15	7.5
Entire 4-wire chain	60	30

(G.113, P.13)

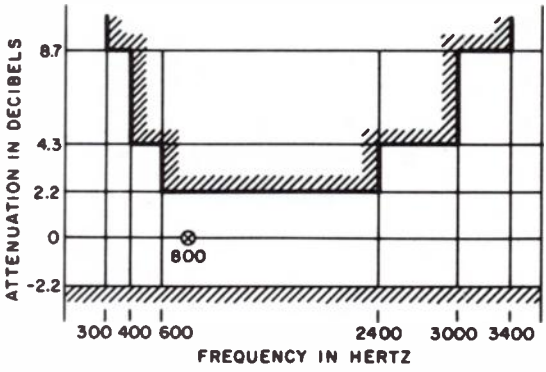

Fig. 4—Attenuation vs. frequency objective for worldwide chain of 12 circuits in terminal service (G. 132).

The CCITT does not recommend limiting values for the group delay at different frequencies, but offers information on typical values reported by four Administrations. Values are in milliseconds measured on a pair of equipments.

	Frequency (hertz)				
Administration	300	400	2000	3000	3400
Belgium (b)	4.0	2.7	1.0	1.3	2.6
France (b)	4.2	2.9	1.0	1.4	2.8
Federal Republic of Germany (b)	3.9	2.7	1.2	1.6	3.0
United Kingdom (a)	2.6	2.2	1	1.4	2.6
(b)	4.2	2.7	1.2	1.8	3.4
For 12 pairs (c)	50	35	14	22	41

(a) With in-band signaling.
(b) With out-band signaling.
(c) Typical maximum values in milliseconds for 12 pairs of equipments.

(G.232, Section C)

Attenuation Distortion in Worldwide Chain

The objectives for the variation with frequency of transmission loss in the terminal condition of a worldwide chain of 12 circuits (international plus national extensions), each one routed over a single group link, are shown in Fig. 4, which assumes that no use is made of high-frequency radio circuits or 3-kilohertz channel equipment. (G.132)

Variation of Transmission Loss with Time

(A) The standard deviation for the variation in transmission loss of a circuit should not exceed 1 decibel. This can be met for circuits on single-group links with automatic regulation, and it should be met on any national circuit whether regulated or not. For other international circuits, the standard deviation should not exceed 1.5 decibels. Standard deviation is sometimes called "distribution grade."

(B) The difference between the mean value of the transmission loss and the nominal value (that is, the bias) should not exceed 0.5 decibel. (G.151, Section C)

Linear Crosstalk

(A) Between circuits, the near-end or far-end crosstalk ratio (intelligible only), measured at audio frequency at a national or international center between two complete circuits in terminal service, should not be less than 58 decibels for 90 percent of all 2-circuit combinations, and 52 decibels for all combinations. 58 dB is the planning objective for modern systems for all combinations.

(B) Between the go and return channels of a 4-wire circuit, the near-end crosstalk ratio must be at least 43 decibels.

Note: The above refers to telephone circuits which are not equipped with (or used in conjunction with) modern echo suppressors designed for long propagation times. Circuits which can form part of switched connections with a long propagation time and lie between terminal half-echo suppressors of modern design should conform to high standards. (G.151, Section D)

Frequency Accuracy of Virtual Carrier Frequencies on an International Circuit

As the channel of any international telephone circuit should be suitable for voice-frequency telegraphy, the accuracy of the virtual carrier frequencies should be such that the difference between an audio frequency applied to one end of the circuit and the frequency received at the other end should not exceed 2 hertz, even when there are intermediate modulating and demodulating processes.

Considering either the hypothetical reference circuit proper to each system or the worldwide hypothetical reference connection, the accuracy of restitution of frequency which is recommended above should be assured if the channel and group carrier frequencies of the various stages have the following accuracies.

Virtual channel carrier frequencies in a group	$\pm 10^{-6}$
Group and supergroup carrier frequencies	$\pm 10^{-7}$
Mastergroup and supermastergroup carrier frequencies	
for 12-MHz system	$\pm 5 \times 10^{-8}$
for 60-MHz system	$\pm 10^{-8}$

(G.225, Section a)

For 12-channel open wire carrier systems, channel carriers (G.311) $\pm 5 \times 10^{-6}$

CIRCUIT NOISE OBJECTIVES

Noise Characteristics for 2500-Kilometer Hypothetical Reference Circuits

The following design objectives should apply to any telephone channel provided by multichannel carrier systems on cable and radio relay links, having the same composition as the appropriate hypothetical reference circuit of 2500 kilometers. The noise is to be measured at or referred to a point of zero relative level. The objectives are intended to ensure adequate speech and signaling performance. They include an allowance of 2500 pWp0 due to frequency-division-multiplex equipment. (See Fig. 5.)

(A) The mean psophometric power during any hour shall not exceed 10 000 pWp0.

(B) The mean noise power over 1 minute shall not exceed 10 000 pWp0 for more than 20 percent of any month.

(C) The mean noise power over 1 minute shall not exceed 50 000 pWp0 for more than 0.1 percent of any month.

(D) The unweighted noise power, measured or calculated with an integrating time of 5 milliseconds, shall not exceed 1 000 000 pW0 (10^6 pW0) for more than 0.01 percent (10^{-4}) of any month. However, this is reduced to 0.001 percent (10^{-5}) of any month, or 0.1 percent of any hour, if the telephone channel is to be used for 50-baud amplitude-modulated voice-frequency telegraph, if recommended quality of telegraph operation is to be obtained. This stiffer requirement need not apply to frequency-modulated voice-frequency telegraph systems operating at 50 bauds.

In a part of a hypothetical reference circuit consisting of one or more homogeneous sections, the values of noise power in (A) and (B) above, and the small percentages of time in (C) and (D) above, shall be considered to be proportional to the number of homogeneous sections involved.

These are design objectives, "and it is not intended that they be quoted in specifications for equipment or used for acceptance tests." (G.222, and CCIR, 393-2)

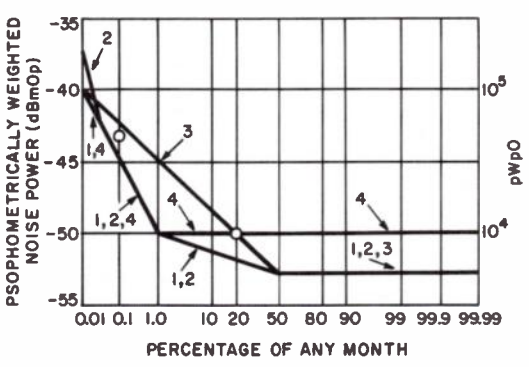

Fig. 5—Examples of distribution curves for the psophometrically weighted 1-minute mean noise power at the end of the hypothetical reference circuit (CCIR, 393–2).

Noise Characteristics for Long Circuits Not More than 2500 Kilometers in Length

Circuits on Land, in Submarine-Cable Systems, or on Radio Relay Systems: The mean psophometric power during any hour should be of the order of 4 pWp0 per kilometer, including noise due to frequency-division-multiplex equipment, except for very short circuits or those with a very complicated composition. (G.151, Section A)

Circuits on Transhorizon Relay Systems: The CCIR divides transhorizon systems into two classes, from the viewpoint of performance.

Transhorizon systems of the first class are those intended to operate between two points which might, without excessive difficulty, be connected by line-of-sight radio relay or cable systems. The hypothetical reference circuit described for transhorizon systems applies to this class. The noise power at the end of this circuit will be calculated by statistical combination of the noise power in each of its radio sections. The statistical noise distribution curve should meet requirements (A) through (D) above.

Transhorizon systems of the second class are those used between points for which other transmission systems cannot be used without excessive difficulty. If the design objectives given above cannot be met without excessive difficulty, the calculated noise-power distribution should meet the following objectives: The mean psophometric power during 1 minute must not exceed 25 000 pWp0 for more than 20 percent of any month, nor exceed 63 000 pWp0 for more than 0.5 percent of any month. Also, the unweighted noise power (integrated over 5 milliseconds) stated in (D) above, should not be exceeded for more than 0.05 percent of the most unfavorable month.

The objectives for both classes are provisional. (CCIR, 397–2)

Noise Characteristics for International Circuits More than 2500 Kilometers in Length

Circuits in Cable or Radio Relay Systems, with no Long Submarine-Cable Section: Such circuits, be-

tween 2500 and 25 000 kilometers in length, are generally carried in land cable or radio relay systems designed to 2500-kilometer objectives, and the number of channel demodulations seldom exceeds that in the corresponding part of the world-wide hypothetical reference chain. Automatic regulation should be used on each group link. The noise objectives are:

(**A**) The mean psophometric noise power during any hour, due to the line, should not exceed 3 pWp0 per kilometer; preferably 2 pWp0 per kilometer or even less. It is noted that in some countries, long overland systems (5000 kilometers or more) have the same objectives as the submarine-cable system (1 pWp0/km).

(**B**) For systems up to about 7500 kilometers long, the 1-minute mean power should not exceed 50 000 pWp0 for more than 0.3 percent of any month.

(**C**) For systems up to about 7500 kilometers long, the unweighted noise power, measured or calculated with an integrating time of 5 milliseconds, should not exceed 1 000 000 pW0 for more than 0.03 percent of any month.

Note: (**B**) and (**C**) are prorated from 2500-kilometer objectives, and proportional values should be used for lengths between 2500 and 7500 kilometers. The CCITT does not yet recommend short-term objectives for systems longer than 7500 kilometers. (G.153, Section A)

Circuits with a Long Submarine-Cable Section: The circuit noise attributable to the submarine section, without compandors, should not exceed a mean psophometric noise value of 3 pWp0 per kilometer in the worst hour on the worst channel. The mean noise power for each direction of transmission, over all channels used for the longest circuits, should not exceed 1 pWp0 per kilometer. No objectives are given for circuits equipped with compandors. The other parts of the circuit should conform to normal 2500-kilometer objectives. (G.153, Section B)

Circuits on Communication-Satellite Systems: The psophometrically weighted noise power at a point of zero relative level in any telephone circuit in the basic hypothetical reference circuit (as defined in Recommendation 352) should not exceed the provisional values of 10 000 pWp0 mean in any hour, 10 000 pWp0 one-minute mean for more than 20 percent of any month, 50 000 pWp0 one-minute mean for more than 0.3 percent of any month, and 1 000 000 pW0 (5-millisecond integrating time) for more than 0.03 percent of any month. The multiplex noise is not included in these figures. (CCIR, 353-2)

Circuits on Open Wire Carrier Systems: In systems of about 10 000 kilometers in length, with lines of strict regularity of construction, accurately operating automatic line regulators, adjustment of line levels to take account of special climatic conditions, and carefully chosen repeater spacings, the following objectives may apply: The mean psophometric power, during any hour, at the end of a circuit of about 10 000 kilometers, taking into account all noise that exists, with the exception of noise due to radio transmitters, should not exceed 50 000 pWp0. This is for a reasonable distribution of wet weather in the territory crossed by the circuit. (G.153, Section D)

Noise in Actual Circuits

Radio Relay Circuits, 280 to 2500 Kilometers in Length: In a telephone channel of an actual radio relay system using frequency-division multiplex, whose composition does not differ appreciably from the hypothetical reference circuit and whose length L is between 280 and 2500 kilometers, the psophometrically weighted noise power, excluding multiplex noise, should not exceed (A) $3L$ pWp0 mean power in any hour, (B) $3L$ pWp0 one-minute mean power for more than 20 percent of any month, and (C) 47 500 pWp0 one-minute mean power for more than $(L/2500)\times 0.1$ percent of any month, as a planning objective. (CCIR, 359–3)

Radio Relay Circuits, Over Real Links, 50 to 2500 Kilometers in Length: If, for planning reasons, the composition of a real link differs substantially from the hypothetical reference circuit, the noise power of a circuit of length L, carried in one or more baseband sections of frequency-division-multiplex radio links, should not exceed the following values.

Length of System (km)	Mean Power in Any Hour	1-Minute Mean Power for More Than 20% of Any Month	1-Minute Mean Power of 47 500 pWp0, for More Than Stated % of Any Month
50–280	$3L$ pWp0 + 200 pWp0	$3L$ pWp0 + 200 pWp0	(280/2500) × 0.1%
280–840	$3L$ pWp0 + 200 pWp0	$3L$ pWp0 + 200 pWp0	(L/2500) × 0.1%
840–1670	$3L$ pWp0 + 400 pWp0	$3L$ pWp0 + 400 pWp0	(L/2500) ×0.1%
1670–2500	$3L$ pWp0 + 600 pWp0	$3L$ pWp0 + 600 pWp0	(L/2500) × 0.1%

Note 1: Frequency-division-multiplex noise is not included.

Note 2: The hourly mean-noise-power objective and its subdivision are under study.

National Circuits on Carrier Systems over Very Short Distances: Assuming that circuits in an international connection, making use of frequency-division-multiplex carrier systems over very short distances, can be limited in number to 4, the mean psophometric power should not exceed 2000 pWp0 per circuit during any hour, including crosstalk.

For CCITT Recommendations for pulse-code-modulation systems see G.123.

Design Objectives for Noise Produced by Modulating Equipments

The mean psophometric power, which corresponds to the noise produced by all modulating equipment mentioned in the definition of the hypothetical reference circuit in question, should not exceed 2500 pWp0. This value includes noise due to various causes, such as thermal noise, intermodulation, crosstalk, power supplies, etc. Its allocation between the various equipments can be left somewhat to the discretion of designers, but the following values are given as a guide to the target design values.

	pWp0
One pair of channel modulators	200–400
One pair of group modulators	60–100
One pair of supergroup modulators	60–100
One pair of mastergroup modulators	40–60

(G.222, Section d)

CCITT AND TELEGRAPHY

The CCITT Blue Book contains the Recommendations adopted by the Third Plenary Assembly in Geneva, in 1964. The Recommendations on Telegraph Technique are included in Volume VII, and those on Data Transmission are included in Volume VIII. The Recommendations on Telegraph Operations and Tariffs are contained in Volume II of the Red Book and in Documents AP III–64, –67, and –74. The latter (AP III–74) has been importantly revised by CCITT Circular No. 15 dated 12 November 1964 entitled "List of Destination Indicators."

Numbering

There is a worldwide system of Destination Indicators for the telegraph-message retransmission network. These indicators consist of two letters signifying the country and its telegraph network (if more than one) followed by two letters signifying the town on that network. Examples: Vienna AUWI, Panama City (Tropical Radio) PAPA, Balboa (ITTCACR) PZBA, Stockholm SWSM, San Francisco (ITT Worldcom) UISF.

The CCITT has approved a worldwide numbering system for telex services. The telex destination code consists of 2 or 3 numerical digits signifying the country or network within the country. The destination code is followed by the telex subscriber's national number, also consisting of numerical digits.

The telex system provides also for *designation* codes, for identifying the country and network of

TABLE 3—CCITT SIGNALING SYSTEMS.

No.	Systems
1	500/20-hertz system used in the international manual service (ringdown).
2	600/750-hertz 2-frequency system. Never used in international service.
	International Automatic and Semiautomatic Systems
3	For unidirectional operation of circuits. Uses 1 in-band frequency (2280 hertz) for the transmission of both line and interregister signals; used for terminal traffic; in general not to be used for new installations.
4	For unidirectional operation of circuits (circuits seized from one end only). Uses 2 in-band frequencies (2040 and 2400 hertz) for the end-to-end transmission of both line and register signals; used for international intracontinental traffic; suitable for terminal and transit traffic; in the latter case 2 or 3 circuits equipped with System No. 4 may be switched in tandem. Suitable for submarine- or land-cable circuits and microwave radio circuits; not applicable to TASI-equipped systems. Capable of interworking with System No. 5.
5	For both-way operation of circuits. Uses 2 in-band signaling frequencies (2400 and 2600 hertz) for the link-by-link transmission of line signals, and 6 in-band frequencies (700, 900, 1100, 1300, 1500, and 1700 hertz) in a 2-out-of-6 code (numerical information transmitted *en bloc*) for the link-by-link transmission of register signals; used for intercontinental traffic. Suitable for submarine- or land-cable circuits and microwave links, whether or not TASI is used; suitable for terminal or transit traffic—in the latter case, 2 or more circuits equipped with System No. 5 may be switched in tandem but are subject to possible undesirable delays if all are TASI-equipped. Capable of interworking with System No. 4.
6	A proposed system to be free from some limitations of Systems No. 3, 4, and 5; expected to use voice channel for interregister signaling, plus a separate channel for line signaling and "management" signaling (changing of routing, et cetera); not expected to be in use before 1970.

TABLE 4—LINE SIGNALS IN CCITT SYSTEMS.

Signal	Direction	CCITT No. 3 (1*VF*)	CCITT No. 4 (2*VF*)	CCITT No. 5 (2*VF*)
Seize, terminal	→	*X*	*PX*	*X*
Seize, transit	→		*PY*	
Start pulsing, terminal	←	*X*	*X*	*Y*
Start pulsing, transit	←		*Y*	
End of pulsing (ST)	→	250 ms*	*xSxSxSx**	1500+1700 herts*
Busy	←	*XX*	*PX*	*Y*
Acknowledge	→			*X*
Answer	←	*XSX*	*PY*	*X*
Acknowledge	→			*X*
Clear back (on-hook)	←	*XX*	*PX*	*Y*
Acknowledge	→			*X*
Ring forward	→	*XSX*	*PYY*	*Y*(850±200 ms)
Clear forward (disconnect)	→	*XXSXX*	*PXX*	*X*+*Y*
Release guard (disconnect acknowledge)	←	*XXSXX*	*PYY*	*X*+*Y*
		X: 2280±6 herts, 150±30 ms *XX*: 2280±6 herts, 600±120 ms *S*: 100±20 ms silence	*X*: 2040±6 herts, 100±20 ms *Y*: 2400±6 herts, 100±20 ms *XX*: 350±70 ms *YY*: 350±70 ms *S*: 35±7 ms; *x*: 2040 herts, 35 ms *P*: (2040 herts, 2400 herts), 150+30 ms	*X*: 2400±6 herts *Y*: 2600±6 herts

* Combination No. 15 of address code.

the originator of a communication. The designation code consists of two letters, the same two letters that compose the first half of the message-retransmission-system *destination* indicator.

Examples of destination codes are:

North and Central America: 200 Cuba, 205 Puerto Rico (RCA), 206 Puerto Rico (ITTWC), 207 Puerto Rico (C & W), 21 Canada (except TWX), 22 Mexico, 25 USA (TWX), 271 Guatemala, 275 British Honduras, 290 Bermuda, 292 Virgin Islands.

South America: 304 Surinam, 305 Paraguay, 31 Venezuela, 36 Peru, 381 Brazil (Radio Brazil), 383 Brazil (PTT), 387 Argentina (ITTCM), 390 Netherlands Antilles, 391 Trinidad.

Europe: 400 Canary Islands, 403 Spain, 409 Algeria, 41 Germany, 46 Belgium, 492 Syria, 496 Kuwait, 501 Iceland, 51 United Kingdom, 57 Finland.

Eastern Europe: 601 Greece, 606 Israel, 61 Hungary, 64 USSR, 65 Romania.

Pacific: 702 Guam, 704 Hawaii (RCA), 705 Hawaii (ITTWC), 71 Australia, 72 Japan, 75 Philippines.

Asia: 801 Korea, 802 Hong Kong, 81 India, 85 China, 88 Iran.

Africa: 901 Libya, 907 Southern Rhodesia, 91 United Arab Republic, 94 Ghana, 95 South Africa, 972 Dahomey, 975 Niger, 981 Congo (Brazzaville), 982 Congo (Leopoldville), 991 Angola, 992 Mozambique.

CCITT AND TELEPHONY

International Country Codes

The addressing signals of worldwide automatic telephony consist of the national telephone number, as used for long-distance dialing within a country, prefixed by a country code. Country codes are grouped by continental regions; for example, the country codes of all South American countries begin with "5." Where the national numbering system includes more than one country, the country code may also include the countries included in the national system. Thus the country code for the United States—"1"—includes Canada and some other countries. The following are examples of some country codes, grouped by world numbering regions or zones as assigned by the Third Plenary Assembly of the CCITT in Geneva in 1964.

Zone 1—Code 1: USA, Canada, Mexico and Central America, Bahamas, Bermuda, Jamaica, French Antilles, Netherlands Antilles.

Zone 2—Africa: 51 countries, 48 country codes (Algeria, Morocco, Tunisia, Libya in one group—the Maghreb— code 21). United Arab Republic 20, South Africa 27, 45 three-digit codes.

Zones 3 and 4—Europe, Iceland, Malta, Cyprus: 17 two-digit and 13 three-digit country codes. Examples: France 33, Spain 34, Italy 39, United Kingdom 44, Germany 49, Iceland 354, Finland 401, Hungary 402.

Zone 5—South America and Cuba: 6 two-digit and 8 three-digit country codes. Examples: Cuba 53, Argentina 54, Brazil 55, Chile 56, Colombia 57, Venezuela 58, Peru 596.

Zone 6—Southwestern Pacific: 6 two-digit and 14 three-digit country codes. Examples: Malaysia 60, Australia 61, Indonesia 62, Philippines 63, New Zealand 64, Thailand 66, Guam 682.

Zone 7—Country code 7: Soviet Union.

Zone 8—Northwestern Pacific: 4 two-digit and 6 three-digit country codes. Examples: Japan 81, Korea 82, Vietnam 84, China (Formosa) 85, Hong Kong 852, Mongolia 854, Laos 856.

Zone 9—East: 5 two-digit and 15 three-digit country codes. Examples: India 91, Burma 95, Iran 98, Lebanon 961, Saudi Arabia 966, Israel 972, Nepal 977.

TELEPHONE SIGNALING

CCITT signaling systems have been standardized for international use. General descriptions are

TABLE 5—MULTIFREQUENCY NUMERICAL CODE USED BY CCITT (2-OUT-OF-6).

Digit	Frequencies	Weighting
1	700+ 900	0+ 1
2	700+1100	0+ 2
3	900+1100	1+ 2
4	700+1300	0+ 4
5	900+1300	1+ 4
6	1100+1300	2+ 4
7	700+1500	0+ 7
8	900+1500	1+ 7
9	1100+1500	2+ 7
0	1300+1500	4+ 7
Code 11	700+1700	0+11 for inward
Code 12	900+1700	1+11 operators
KP	1100+1700	2+11 start of pulsing
KP2	1300+1700	4+11 transit traffic
ST	1500+1700	7+11 end of pulsing

TABLE 6—NUMERICAL 4-BY-4 MULTIFREQUENCY CODE.

Touch-Tone or Touch Calling

Low group (hertz)					
697	1	2	3		
770	4	5	6		
852	7	8	9		
941	spare	0	spare		
	1209	1336	1477	(1633)	High group (hertz)

US Air Force 412L

Low group (hertz)					
1020	1	2	3		
1140	4	5	6		
1260	7	8	9		
1380		0			
	1620	1740	1860	(1980)	High group (hertz)

Note: Each digit is composed of one frequency from the low group and one frequency from the high group. The frequencies have been chosen to minimize voice simulation.

given in Table 3, and some of the signaling characteristics are given in Table 4.

Signals in communications are used for passing information, for identifying the called subscriber or addressee (with resulting internal system signals concerned with the establishment of a connection), and for supervising and controlling the connection once it has been established.

Information Signals may be analog (voice, telemetry, or facsimile) or digital (teleprinter or data).

Addressing Signals may be dial pulse, multifrequency, or binary. They are not needed once a communication has been established.

TABLE 7—US ARMY TA-341/PT NUMERICAL CODE.

Digit	Frequencies
1	2100+2300
2	2300+2500
3	1900+2700
4	1900+2100
5	2500+2700
6	2300+2700
7	2100+2500
8	1900+2300
9	2100+2700
0	1900+2500

(A) *Dial Pulse* signals consist of a series of from 1 to 10 pulses representing the corresponding numerical digits 1 to 9 and 0. The pulses are breaks in a continuous direct current on the line, usually lasting from 58 to 67 percent of the time interval between the starts of successive pulses. These breaks in direct current may have to be converted into pulses in a tone, or to frequency

TABLE 8—NUMERICAL CODE, 2-VOICE-FREQUENCY SIGNALING SYSTEM, CCITT No. 4.

Digit	Successive Elements			
	1	2	3	4
1	y	y	y	x
2	y	y	x	y
3	y	y	x	x
4	y	x	y	y
5	y	x	y	x
6	y	x	x	y
7	y	x	x	x
8	x	y	y	y
9	x	y	y	x
0	x	y	x	y

Note: The 2 frequencies are sent one at a time, with a silent space between pulses. The duration of both frequency and silent periods is 35±7 milliseconds. Frequencies: $x=2040\pm6$ hertz; $y=2400\pm6$ hertz. Power level: −9 decibels.

shifts between tones, in order to pass through some media or multiplexing systems. Dial pulse speeds are usually 10 pulses per second, although high-speed dials of nearly twice that speed are sometimes used.

(B) *Multifrequency* signals represent numerical digits by 1 pulse (or sometimes 4 pulses) of a specific frequency combination. The 2-out-of-6 and 4-by-4 multifrequency codes are shown in Tables 5 and 6. Inherent in both is the constant-ratio error-control principle (the simultaneous receipt of 3 or more, or 1 only, frequencies indicates an error). Table 7 shows the US Army 2-out-of-5 numerical code. The CCITT 2-voice-frequency code, consisting of 2 frequencies sent one at a time in 4 pulses, is given in Table 8.

(C) *Binary* signals for addressing are usually in a numeric or alphanumeric code used also for information signals, such as in telegraph addresses or headings. Multifrequency signals are sometimes directly converted to binary signals by changing the 2-frequencies-out-of-6 code to a corresponding 2-time-slots-out-of-6 synchronous 6-element binary code. Another example of a binary code used only for addressing is the CCITT 1-voice-frequency code, a 4-element start-stop code given in Table 9. (The CCITT 2-voice-frequency code is not truly binary since it uses a third condition—no tone—in addition to the 2 tones.)

TABLE 9—NUMERICAL CODE, 1-VOICE-FREQUENCY SIGNALING SYSTEM, CCITT No. 3.

	Time Elements					
Digit	Start	1	2	3	4	Stop
1	1				1	
2	1			1		
3	1			1	1	
4	1		1			
5	1		1		1	
6	1		1	1		
7	1		1	1	1	
8	1	1				
9	1	1			1	
0	1	1		1		

Note: "1" signifies frequency present. Length of each time element is 50 milliseconds±1 percent. Frequency: 2280±6 hertz. Power level: −6 decibels.

Supervisory or Line Signals

Supervisory or line signals cannot be generated exclusively by registers because they are required during the entire use of the connection, after the registers that established the connection have been disconnected. Supervisory signals are an extension of the original basic signals of ringing and of closing a line loop to allow direct current to flow. Supervisory signals may be classified as spurt (discontinuous) and continuous.

Continuous Signals are based on conditions of on-hook and off-hook, representing the condition of blocked or flowing direct current on the subscriber's line, and their extension to trunk signaling is given in Table 10. Either condition is continuous and may be detected at any time. On the other hand, discontinuous signals must be recorded, and the condition represented is presumed to continue until a new signal is sent. Supervisory signaling in

TABLE 10—ON-HOOK AND OFF-HOOK SIGNALS.

Direct Current Telephone Line	Trunk
On-hook signifies loop is open to direct current supplied from other end.	If idle, signals on-hook to other end. Seizure at calling end signals off-hook to called end. While calling end awaits answer, called end signals on-hook to calling end.
Off-hook signifies loop is closed, allowing relay at other end to operate. Signaling in reverse direction is ring-down.	Answer results in signaling off-hook from called end.
	If called end is not ready to receive address signals when seized, it signals off-hook to calling end until ready.

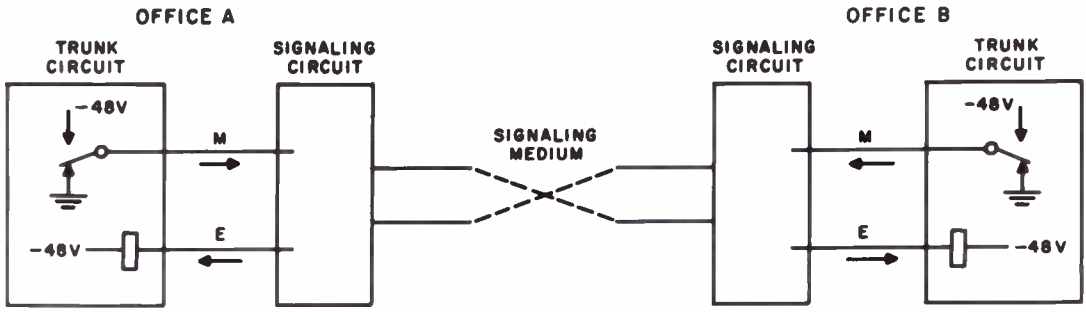

SIGNAL A TO B	SIGNAL B TO A	CONDITION AT SIGNALING CIRCUIT A		CONDITION AT SIGNALING CIRCUIT B	
		M LEAD	E LEAD	M LEAD	E LEAD
ON-HOOK	ON-HOOK	GROUND	OPEN	GROUND	OPEN
OFF-HOOK	ON-HOOK	BATTERY	OPEN	GROUND	GROUND
ON-HOOK	OFF-HOOK	GROUND	GROUND	BATTERY	OPEN
OFF-HOOK	OFF-HOOK	BATTERY	GROUND	BATTERY	GROUND

Fig. 6—*E* and *M* signaling. The *E* lead receives open or ground signals from the signaling circuit. The *M* lead sends ground or battery signals to the signaling circuit.

a backward direction (toward the calling end) is also needed in automatic working and is also described as on-hook or off-hook, although on 2-wire metallic circuits the signaling condition is usually a reversal of flow of the direct current rather than an interruption.

Continuous supervisory signaling over longer distances is effected by use of signaling paths distinct from the voice path. These signaling paths may be telegraph legs of a composite telegraph system, simplexing of the voice pair, or special tones inside or outside of the voice channel. Whatever the paths, they are extensions of separate direct-current leads from the trunk circuits, known as *E* and *M* leads. The relation between the conditions of these leads and the on-hook or off-hook signaling conditions they represent is shown in Fig. 6. The usual method of extending the *E* and *M* leads over tone channels is shown in Fig. 7. The frequency of the tone used is preferably higher than 2000 hertz and is usually 2600 hertz on 4-wire circuits. A 3825-hertz signaling system is known as "out-of-band," and must be built into the carrier system using it.

SIGNAL	TONE	OPERATION	LEAD	CONDITION
ON-HOOK	ON	SENDING	M	GROUND
		RECEIVING	E	OPEN
OFF-HOOK	OFF	SENDING	M	BATTERY
		RECEIVING	E	GROUND

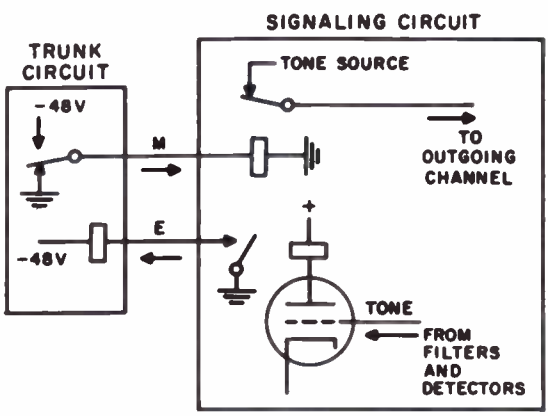

Fig. 7—Tone signaling.

Spurt Signaling avoids the necessity of using distinct signaling paths. For manual operation, ringdown signaling is usually satisfactory. For semiautomatic or automatic operation, however, more-elaborate systems are required. Voice-frequency signals are used and they are distinguished from voice transmissions by filters and timing. Single-frequency systems use 1 or 2 long or short pulses of the specific signaling frequency, with the pulses carefully timed to within minimum and maximum limits. Two-frequency systems use a gate-opening prefix pulse of the 2 frequencies together, followed, without a silent period, by a long or short pulse of either of the 2 frequencies. The submarine-cable signaling system (CCITT No. 5) uses 2 frequencies in the "compel" mode, wherein the signal frequencies are sent until acknowledged, and the acknowledging signal is sent until the original signal is stopped. No gate-opening prefix is used.

TABLE 11—TABLE OF PROPOSED STANDARD OF AUDIBLE TONES IN NORTH AMERICA (FROM CCITT DOCUMENT AP III-84).

Use	Frequencies§ (hertz) 350	440	480	620	Power per Frequency at Exchange Where Tone is Applied (dBm0)	Cadence
Dial tone	x	x			−13	Continuous
Busy tone			x	x	−24	0.5 second on 0.5 second off
Reorder tone*			x	x	−24	0.2 second on 0.3 second off or 0.3 second on 0.2 second off
Audible ringing tone		x	x		−16	2 seconds on 4 seconds off
High tone†			x		−16	Varies according to use
Pre-emption tone‡		x		x	−18	Single 200/500-ms pulse
Call-waiting tone		x			−13	Single 500-ms pulse

Notes:

* A possible alternative is the use of a call-failure tone, which would identify the office and type of condition that prevented the successful completion of the call.

† High tone is used in many ways. For example:

(A) Spurts of tone to indicate specific orders to operators in the manual service (order tones).

(B) To inform operators of lines that are temporarily out of service (permanent signal tone).

(C) To alert customers that their services are in a permanent off-hook condition.

‡ Pre-emption tones are used in certain private switched networks which may interconnect with national networks.

§ Frequency limits are ±0.5 percent of nominal.

Ringdown Signals

Ringdown signals are spurts of ringing current (16 to 25 hertz) applied usually through the ringing key of an operator and intended to operate a bell, ringer, or drop at the called end. The current may be generated by a manually operated magneto or by a ringing machine with or without automatically inserted silent periods. Ringing to telephone subscribers in automatic central offices is stopped or "tripped" automatically by relay action resulting from the subscriber's off-hook condition. Ringing signals may be converted to 500 or 1000 hertz, usually interrupted at a 20-hertz rate, to pass through voice channels of carrier equipment. A ringing signal to a manual switchboard usually lights a switchboard lamp, which can be darkened again only by local action and not by stopping or repeating the ringing signal. This characteristic makes ringdown operation unsuitable for fully automatic operation. Ringdown signaling over carrier circuits has the advantages of simplicity and of not requiring the distinct signaling channels of *E* and *M* systems.

Tones

A special case of signaling is that of information in the form of tones to the subscriber of a telephone system. The basic tones are dial tone, busy tone, and ring-back tone (representing the ringing of the called subscriber's line). The dial tone is generated at the subscriber's local switching center,

but the busy tone and ring-back tone, plus special tones such as no-such-number and line-out-of-order, are generated at the called subscriber's switching center and should be standardized for universal intelligibility. A proposal by the American Telephone and Telegraph Company for standard tones is described in Table 11. On some international calls, the busy and ring-back tones are generated locally in accordance with spurt supervisory signals from the called end.

Alternative Routing

Switching systems in which the complete called number is recorded in the first center to which the subscriber is connected permit a translation of digits from those identifying the called subscriber to those most conveniently used by the switching mechanism to establish the desired connection. This translation of digits permits the controlling mechanism to use a variety of routes in such a way that if the first-choice route is occupied or disabled a second-choice route may be tried, etc. Safeguards are required to prevent doubling back of routes and dead-end choices. In the near future many sophisticated plans may be expected that depend on rapid analysis of network possibilities by data-transmission means. The signals used for this purpose are interregister signals and are classed with addressing signals in that they are used in establishing a connection to the desired addressee, not being needed after a connection has been established.

CHAPTER 3
UNITS, CONSTANTS, AND CONVERSION FACTORS

SYMBOLS FOR UNITS

Unit symbols are letters, combinations of letters, or other characters that may be used in place of the names of the units. The following list covers symbols for *units* only. It does not cover letter symbols for physical *quantities*.

> Example: In the expression $I = 150$ mA, I is the symbol for a physical quantity (current) and mA is the symbol for a unit (milliamperes) of that quantity.

The symbols in the list at the end of this section are consistent in nearly all respects with the recommendations of the International Organization for Standardization (ISO). Most of the list and much of the text material in this section have been taken from ANSI Y10.19-1969.*

The basic symbols are short; thus multiplication and division may be indicated in ways that resemble those used with algebraic quantities. When an unfamiliar unit symbol is first used in text, it should be followed by its name in parentheses; only the symbol need be used thereafter.

Symbols for units are written in lower-case letters, except for the first letter if the name of the unit is derived from a proper name, and except for a very few that are not formed from letters. Every effort should be made to follow the distinction between upper- and lower-case letters, even if the symbols appear in applications where the other lettering is in upper-case style.

Symbols for units are printed in roman (upright) type. Their form is the same for both singular and plural, and they are not followed by a period. When there is risk of confusion in using the standard symbols "in" for inch and "l" for liter, the name of the unit should be spelled out.

When a compound unit is formed by multiplication of two or more other units, its symbol consists of the symbols for the separate units joined by a raised dot (for example, N·m for newton meter). The dot may be omitted in the case of familiar compounds (such as watthour, whose symbol is Wh), if no confusion would result.* Hyphens should not be used in symbols for compound units.

Positive and negative exponents may be used with unit symbols, but care must be taken in text to avoid confusion with superscripts that indicate footnotes or references.

When a compound unit is formed by division of one unit by another, its symbol consists of the symbols for the separate units either separated by a solidus (for example, m/s for meter per second) or multiplied using negative powers (for example, $m \cdot s^{-1}$ for meter per second). In simple cases use of the solidus is recommended, but in no case should more than one solidus on the same line, or a solidus followed by a product, be included in such a combination unless parentheses are inserted to avoid ambiguity. In complicated cases negative powers should be used.

The following prefixes are used to indicate multiples or submultiples of units:

Multiple	Prefix	Symbol
10^{18}	exa	E
10^{15}	peta	P
10^{12}	tera	T
10^{9}	giga	G
10^{6}	mega	M
10^{3}	kilo	k
10^{2}	hecto	h
10	deka	da
10^{-1}	deci	d
10^{-2}	centi	c
10^{-3}	milli	m
10^{-6}	micro	μ†
10^{-9}	nano	n
10^{-12}	pico	p
10^{-15}	femto	f
10^{-18}	atto	a

* Extracted from American National Standard *Letter Symbols for Units Used in Science and Technology*, ANSI Y10.19-1969, with permission of the publisher, The American Society of Mechanical Engineers, United Engineering Center, 345 East 47th Street, New York, New York 10017.

* When a unit symbol prefix is identical to a unit symbol, special care must be taken. m·N indicates the product of the units *meter* and *newton*, while mN is the symbol for *millinewton*.

† Lower-case u is frequently used in typing.

Symbols for prefixes are printed in roman type, without space between the prefix and the symbol for the unit. The distinctions between upper- and lower-case letters must be observed.

Compound prefixes should not be used:

Use		Do not use	
tera	T	megamega	MM
giga	G	kilomega	kM
nano	n	millimicro	mμ
pico	p	micromicro	$\mu\mu$

When a symbol representing a unit that has a prefix carries an exponent, this indicates that the multiple (or submultiple) unit is raised to the power expressed by the exponent. For example:

$$2\ \mathrm{cm}^3 = 2(\mathrm{cm})^3 = 2(10^{-2}\mathrm{m})^3 = 2 \cdot 10^{-6}\mathrm{m}^3$$

$$1\ \mathrm{ms}^{-1} = 1(\mathrm{ms})^{-1} = 1(10^{-3}\mathrm{s})^{-1} = 10^3\mathrm{s}^{-1}$$

Numerical Values

To facilitate the reading of numbers, the digits may be separated into groups of three, counting from the decimal sign toward the left and the right. The groups should be separated by a small space, but not by a comma or a point. In numbers of four digits, the space is usually not necessary. For example:

2.141 596 73 772 7372 0.133 47

In English-language documents the recommended decimal sign is a period. (The British recommended decimal sign is a raised period (·).) For all other languages the recommended decimal sign is a comma.

If the magnitude of a number is less than unity, the decimal sign should be preceded by a zero.

The sign of multiplication of numbers is a cross (×) or a raised dot (·).

SI Units

In the following list some units are identified as SI units. These units belong to the International System of Units (Système International d'Unités), which is the name given in 1960 by the Conférence Générale des Poids et Mesures to the coherent system of units based on the following basic units and quantities:

Unit	Quantity
meter	length
kilogram	mass
second	time
ampere	electric current
kelvin	temperature
candela	luminous intensity
mole	amount of substance

The SI units include as subsystems the MKS system of units, which covers mechanics, and the MKSA (*M*eter *K*ilogram *S*econd *A*mpere) or Georgi system, which covers mechanics, electricity, and magnetism.

Letter Symbols Alphabetically by Name of Unit

Unit	Symbol	Notes
ampere	A	SI unit of electric current
ampere (turn)	At	SI unit of magnetomotive force
ampere-hour	Ah	
ampere per meter	A/m	SI unit of magnetic field strength
angstrom	Å	1 Å = 10^{-10} m
apostilb	asb	1 asb = $(1/\pi)$ cd/m^2 A unit of luminance. The SI unit, candela per square meter, is preferred.
atmosphere:		
standard atmosphere	atm	1 atm = 101 325 N/m^2
technical atmosphere	at	1 at = 1 kgf/cm^2
atomic mass unit (unified)	u	The (unified) atomic mass unit is defined as one-twelfth of the mass of an atom of the ^{12}C nuclide. Use of the old atomic mass unit (amu), defined by reference to oxygen, is deprecated.
bar	bar	1 bar = 100 000 N/m^2
barn	b	1 b = 10^{-28} m^2
baud	Bd	Unit of signaling speed equal to one element per second.
becquerel	Bq	1 Bq = 1 s^{-1} SI unit of radioactivity.
bel	B	
billion electronvolts		The name *billion electronvolts* is deprecated; see *gigaelectronvolt* (GeV).
bit	b	

Unit	Symbol	Notes
British thermal unit	Btu	
calorie (International Table calorie)	cal_{IT}	1 cal°–=4.1868 J The 9th Conférence Générale des Poids et Mesures adopted the joule as the unit of heat, avoiding the use of the calorie as far as possible.
calorie (thermochemical calorie)	cal	1 cal=4.1840 J (See note for International Table calorie.)
candela	cd	SI unit of luminous intensity.
candela per square inch	cd/in^2	Use of the SI unit, candela per square meter, is preferred.
candela per square meter	cd/m^2	SI unit of luminance. The name nit has been used.
candle		The unit of luminous intensity has been given the name *candela*; use of the word *candle* for this purpose is deprecated.
centimeter	cm	
circular mil	cmil	1 cmil= $(\pi/4)\cdot 10^{-6}$ in^2
coulomb	C	SI unit of electric charge.
cubic centimeter	cm^3	
cubic foot	ft^3	
cubic foot per minute	ft^3/min	
cubic foot per second	ft^3/s	
cubic inch	in^3	
cubic meter	m^3	
cubic meter per second	m^3/s	
cubic yard	yd^3	
curie	Ci	Unit of activity in the field of radiation dosimetry.
cycle	c	
cycle per second	c/s	Deprecated. Use hertz
decibel	dB	
degree (plane angle)	°	
degree (temperature):		Note that there is no space between the symbol ° and the letter. The use of the word *centigrade* for the Celsius temperature scale was abandoned by the Conférence Générale des Poids et Mesures in 1948.
degree Celsius	°C	
degree Fahrenheit	°F	
degree Kelvin		See Kelvin.
degree Rankine	°R	
dyne	dyn	
electronvolt	eV	
erg	erg	
erlang	E	Unit of telephone traffic.
farad	F	SI unit of capacitance.
foot	ft	
footcandle	fc	The name *lumen per square foot* (lm/ft^2) is recommended for this unit. Use of the SI unit of illuminance, the lux (lumen per square meter), is preferred.
footlambert	fL	If luminance is to be measured in English units, the candela per square inch (cd/in^2) is recommended. Use of the SI unit, the candela per square meter, is preferred.
foot per minute	ft/min	
foot per second	ft/s	
foot per second squared	ft/s^2	
foot pound-force	$ft\cdot lb_f$	
gal	Gal	1 Gal=1 cm/s^2
gallon	gal	The gallon, quart, and pint differ in the US and the UK, and their use is deprecated.

Unit	Symbol	Notes
gauss	G	The gauss is the electromagnetic CGS (Centimeter Gram Second) unit of magnetic flux density. The SI unit, tesla, is preferred.
gigaelectronvolt	GeV	
gigahertz	GHz	
gilbert	Gb	The gilbert is the electromagnetic CGS (Centimeter Gram Second) unit of magnetomotive force. Use of the SI unit, the ampere (or ampere-turn), is preferred.
grain	gr	
gram	g	
gray	Gy	1 Gy = 1 J/kg SI unit of absorbed dose.
henry	H	
hertz	Hz	SI unit of frequency.
horsepower	hp	Use of the SI unit, the watt, is preferred.
hour	h	Time may be designated as in the following example: $9^h46^m30^s$.
inch	in	
inch per second	in/s	
joule	J	SI unit of energy.
joule per Kelvin	J/K	SI unit of heat capacity and entropy.
Kelvin	K	SI unit of temperature (formerly called *degree Kelvin*). The symbol K is now used without the symbol °.
kiloelectronvolt	keV	
kilogauss	kG	
kilogram	kg	SI unit of mass.
kilogram-force	kg_f	In some countries the name *kilopond* (kp) has been adopted for this unit.
kilohertz	kHz	
kilojoule	kJ	
kilohm	kΩ	
kilometer	km	
kilometer per hour	km/h	
kilopond	kp	See kilogram-force.
kilovar	kvar	
kilovolt	kV	
kilovoltampere	kVA	
kilowatt	kW	
kilowatthour	kWh	
knot	kn	1 kn = 1 nmi/h
lambert	L	The lambert is the CGS (Centimeter Gram Second) unit of luminance. The SI unit, candela per square meter, is preferred.
liter	l	
liter per second	l/s	
lumen	lm	SI unit of luminous flux.
lumen per square foot	lm/ft^2	Use of the SI unit, the lumen per square meter, is preferred.
lumen per square meter	lm/m^2	SI unit of luminous exitance.
lumen per watt	lm/W	SI unit of luminous efficacy.
lumen second	lm·s	SI unit of quantity of light.
lux	lx	1 lx = 1 lm/m^2. SI unit of illuminance.
maxwell	Mx	The maxwell is the electromagnetic CGS (Centimeter Gram Second) unit of magnetic flux. Use of the SI unit, the weber, is preferred.
megaelectronvolt	MeV	
megahertz	MHz	

Unit	Symbol	Notes
megavolt	MV	
megawatt	MW	
megohm	MΩ	
meter	m	SI unit of length.
mho	mho	1 mho = 1 Ω^{-1} = 1 S
microampere	μA	
microbar	μbar	
microfarad	μF	
microgram	μg	
microhenry	μH	
micrometer	μm	
micron		The name *micrometer* (μm) is preferred.
microsecond	μs	
microwatt	μW	
mil	mil	1 mil = 0.001 in.
mile		
nautical	nmi	
statute	mi	
mile per hour	mi/h	
milliampere	mA	
millibar	mbar	mb may be used.
milligal	mGal	
milligram	mg	
millihenry	mH	
milliliter	ml	
millimeter	mm	
conventional millimeter of mercury	mm Hg	1 mm Hg = 133.322 N/m².
millimicron		The name *nanometer* (nm) is preferred.
millisecond	ms	
millivolt	mV	
milliwatt	mW	
minute (plane angle)	...′	
minute (time)	min	Time may be designated as in the following example: $9^h46^m30^s$.
mole	mol	SI unit of amount of substance.
nanoampere	nA	
nanofarad	nF	
nanometer	nm	
nanosecond	ns	
nanowatt	nW	
nautical mile	nmi	
neper	Np	
newton	N	SI unit of force.
newton meter	N·m	
newton per square meter	N/m²	See pascal.
nit	nt	1 nt = 1 cd/m² See candela per square meter.
oersted	Oe	The oersted is the electromagnetic CGS (Centimeter Gram Second) unit of magnetic field strength. Use of the SI unit, the ampere per meter, is preferred.
ohm	Ω	SI unit of electric resistance.
ounce (avoirdupois)	oz	
pascal	Pa	SI unit of pressure or stress. 1 Pa = 1 N/m²
picoampere	pA	
picofarad	pF	
picosecond	ps	
picowatt	pW	
pint	pt	The gallon, quart, and pint differ in the US and the UK, and their use is deprecated.

Unit	Symbol	Notes
pound	lb	
poundal	pdl	
pound-force	lb_f	
pound-force foot	$lb_f \cdot ft$	
pound-force per square inch	lb_f/in^2	
pound per square inch		Although use of the abbreviation psi is common, it is not recommended. See pound-force per square inch.
quart	qt	The gallon, quart, and pint differ in the US and the UK, and their use is deprecated.
rad	rd	Unit of absorbed dose in the field of radiation dosimetry.
radian	rad	SI unit of plane angle.
rem	rem	Unit of dose equivalent in the field of radiation dosimetry.
revolution per minute	r/min	Although use of the abbreviation rpm is common, it is not recommended.
revolution per second	r/s	
roentgen	R	Unit of exposure in the field of radiation dosimetry.
second (plane angle)	...″	
second (time)	s	SI unit of time. Time may be designated as in the following example: $9^h46^m30^s$.
siemens	S	SI unit of conductance. 1 S = 1 Ω^{-1}
square foot	ft^2	
square inch	in^2	
square meter	m^2	
square yard	yd^2	
steradian	sr	SI unit of solid angle.
stilb	sb	1 sb = 1 cd/cm^2 A CGS unit of luminance. Use of the SI unit, the candela per square meter, is preferred.
tesla	T	SI unit of magnetic flux density. 1 T = 1 Wb/m^2.
tonne	t	1 t = 1000 kg.
(unified) atomic mass unit	u	See atomic mass unit (unified).
var	var	Unit of reactive power.
volt	V	SI unit of electromotive force.
voltampere	VA	SI unit of apparent power.
watt	W	SI unit of power.
watthour	Wh	
watt per steradian	W/sr	SI unit of radiant intensity.
watt per steradian square meter	$W/(sr \cdot m^2)$	SI unit of radiance.
weber	Wb	SI unit of magnetic flux. 1 Wb = 1 V·s.
yard	yd	

CONVERSION FACTORS

To Convert	Into	Multiply by	Conversely, Multiply by
acres	square feet	4.356×10^4	2.296×10^{-5}
acres	square meters	4047	2.471×10^{-4}
acres	square yards	4.84×10^3	2.066×10^{-4}
acres	hectares	0.4047	2.471
ampere-hours	coulombs	3600	2.778×10^{-4}
amperes per sq cm	amperes per sq inch	6.452	0.1550
ampere-turns	gilberts	1.257	0.7958
ampere-turns per cm	ampere-turns per inch	2.540	0.3937
angstroms	nanometers	10^{-1}	10
ares	square meters	10^2	10^{-2}

To Convert	Into	Multiply by	Conversely, Multiply by
atmospheres	bars	1.0133	0.9869
atmospheres	mm of mercury at 0°C	760	1.316×10^{-3}
atmospheres	feet of water at 4°C	33.90	2.950×10^{-2}
atmospheres	inches of mercury at 0°C	29.92	3.342×10^{-2}
atmospheres	kg per sq meter	1.033×10^{4}	9.678×10^{-5}
atmospheres	newtons per sq meter	1.0133×10^{5}	0.9869×10^{-5}
atmospheres	pounds per sq inch	14.70	6.804×10^{-2}
barns	square meters	10^{-28}	10^{28}
bars	newtons per square meter	10^{5}	10^{-5}
bars	hectopiezes	1	1
bars	baryes (dyne per sq cm)	10^{6}	10^{-6}
bars	pascals (newtons per sq meter)	10^{5}	10^{-5}
baryes	newtons per sq meter	10^{-1}	10
Btu	foot-pounds	778.3	1.285×10^{-3}
Btu	joules	1054.8	9.480×10^{-4}
Btu	kilogram-calories	0.2520	3.969
Btu	horsepower-hours	3.929×10^{-4}	2545
bushels	cubic feet	1.2445	0.8036
calories (I.T.)	joules	4.1868	0.238
calories (thermochem)	joules	4.184	0.239
carats (metric)	grams	0.2	5
Celsius (centigrade)	Fahrenheit	°C×9/5=°F−32 (°C+40)×9/5=(°F+40)	
chains (surveyor's)	feet	66	1.515×10^{-2}
circular mils	square centimeters	5.067×10^{-6}	1.973×10^{5}
circular mils	square mils	0.7854	1.273
cords	cubic meters	3.625	0.2758
cubic feet	cords	7.8125×10^{-3}	128
cubic feet	gallons (liq US)	7.481	0.1337
cubic feet	liters	28.32	3.531×10^{-2}
cubic inches	cubic centimeters	16.39	6.102×10^{-2}
cubic inches	cubic feet	5.787×10^{-4}	1728
cubic inches	cubic meters	1.639×10^{-5}	6.102×10^{4}
cubic inches	gallons (liq US)	4.329×10^{-3}	231
cubic meters	cubic feet	35.31	2.832×10^{-2}
cubic meters	cubic yards	1.308	0.7646
degrees (angle)	radians	1.745×10^{-2}	57.30
dynes	pounds	2.248×10^{-6}	4.448×10^{5}
dynes	newtons	10^{-5}	10^{5}
electron volts	joules	1.602×10^{-19}	0.624×10^{19}
ergs	foot-pounds	7.376×10^{-8}	1.356×10^{7}
ergs	joules	10^{-7}	10^{7}
fathoms	feet	6	0.16667
fathoms	meters	1.8288	0.5467
feet	centimeters	30.48	3.281×10^{-2}
feet	varas	0.3594	2.782
feet of water at 4°C	inches of mercury at 0°C	0.8826	1.133
feet of water at 4°C	kg per sq meter	304.8	3.281×10^{-3}
feet of water at 4°C	pounds per sq foot	62.43	1.602×10^{-2}
fermis	meters	10^{-15}	10^{15}
footcandles	lumens per sq meter	10.764	0.0929
footlamberts	candelas per sq meter	3.4263	2.919×10^{-1}
foot-pounds	horsepower-hours	5.050×10^{-7}	1.98×10^{6}
foot-pounds	kilogram-meters	0.1383	7.233
foot-pounds	kilowatt-hours	3.766×10^{-7}	2.655×10^{6}
gallons (liq US)	cubic meters	3.785×10^{-3}	264.2
gallons (liq US)	gallons (liq Br Imp) (Canada)	0.8327	1.201
gammas	teslas	10^{-9}	10^{9}
gausses	lines per sq inch	6.452	0.1550

To Convert	Into	Multiply by	Conversely, Multiply by
gausses	teslas	10^{-4}	10^{4}
gilberts	amperes	7.9577×10^{-1}	1.257
grains (for humidity calculations)	pounds (avoirdupois)	1.429×10^{-4}	7000
grams	dynes	980.7	1.020×10^{-3}
grams	grains	15.43	6.481×10^{-2}
grams	ounces (avoirdupois)	3.527×10^{-2}	28.35
grams	poundals	7.093×10^{-2}	14.10
grams per cm	pounds per inch	5.600×10^{-3}	178.6
grams per cu cm	pounds per cu inch	3.613×10^{-2}	27.68
grams per sq cm	pounds per sq foot	2.0481	0.4883
hectares	square meters	10^{4}	10^{-4}
hectares	acres	2.471	0.4047
horsepower (boiler)	Btu per hour	3.347×10^{4}	2.986×10^{-5}
horsepower (metric) (542.5 ft-lb per second)	Btu per minute	41.83	2.390×10^{-2}
horsepower (metric) (542.5 ft-lb per second)	foot-lb per minute	3.255×10^{4}	3.072×10^{-5}
horsepower (metric) (542.5 ft-lb per second)	kg-calories per minute	10.54	9.485×10^{-2}
horsepower (550 ft-lb per second)	Btu per minute	42.41	2.357×10^{-2}
horsepower (550 ft-lb per second)	foot-lb per minute	3.3×10^{4}	3.030×10^{-5}
horsepower (550 ft-lb per second)	kilowatts	0.745	1.342
horsepower (metric) (542.5 ft-lb per second)	horsepower (550 ft-lb per second)	0.9863	1.014
horsepower (550 ft-lb per second)	kg-calories per minute	10.69	9.355×10^{-2}
inches	centimeters	2.540	0.3937
inches	feet	8.333×10^{-2}	12
inches	miles	1.578×10^{-5}	6.336×10^{4}
inches	mils	1000	0.001
inches	yards	2.778×10^{-2}	36
inches of mercury at 0°C	lbs per sq inch	0.4912	2.036
inches of water at 4°C	kg per sq meter	25.40	3.937×10^{-2}
inches of water at 4°C	ounces per sq inch	0.5782	1.729
inches of water at 4°C	pounds per sq foot	5.202	0.1922
inches of water at 4°C	in of mercury	7.355×10^{-2}	13.60
inches per ounce	meters per newton (compliance)	9.136×10^{-2}	10.95
joules	foot-pounds	0.7376	1.356
joules	ergs	10^{7}	10^{-7}
kilogram-calories	kilogram-meters	426.9	2.343×10^{-3}
kilogram-calories	kilojoules	4.186	0.2389
kilogram-meters	joules	0.102	9.81
kilogram force	newtons	9.81	0.102
kilograms	tons, long (avdp 2240 lb)	9.842×10^{-4}	1016
kilograms	tons, short (avdp 2000 lb)	1.102×10^{-3}	907.2
kilograms	pounds (avoirdupois)	2.205	0.4536
kilograms per kilometer	pounds (avdp) per mile (stat)	3.548	0.2818
kg per sq meter	pounds per sq foot	0.2048	4.882
kilometers	feet	3281	3.048×10^{-4}
kilopond force	newtons	9.81	0.102
kilowatt-hours	Btu	3413	2.930×10^{-4}
kilowatt-hours	foot-pounds	2.655×10^{6}	3.766×10^{-7}
kilowatt-hours	joules	3.6×10^{6}	2.778×10^{-7}
kilowatt-hours	kilogram-calories	860	1.163×10^{-3}

To Convert	Into	Multiply by	Conversely, Multiply by
kilowatt-hours	kilogram-meters	3.671×10^{5}	2.724×10^{-6}
kilowatt-hours	pounds carbon oxidized	0.235	4.26
kilowatt-hours	pounds water evaporated from and at 212°F	3.53	0.283
kilowatt-hours	pounds water raised from 62° to 212°F	22.75	4.395×10^{-2}
kips	newtons	4.448×10^{3}	2.248×10^{-4}
knots* (naut mi per hour)	feet per second	1.688	0.5925
knots	meters per minute	30.87	0.03240
knots	miles (stat) per hour	1.1508	0.8690
lamberts	candelas per sq cm	0.3183	3.142
lamberts	candelas per sq inch	2.054	0.4869
lamberts	candelas per sq meter	3.183×10^{3}	3.142×10^{-4}
leagues	miles (approximately)	3	0.33
links (surveyor's)	chains	0.01	100
links	inches	7.92	0.1263
liters	bushels (dry US)	2.838×10^{-2}	35.24
liters	cubic centimeters	1000	0.001
liters	cubic meters	0.001	1000
liters	cubic inches	61.02	1.639×10^{-2}
liters	gallons (liq US)	0.2642	3.785
liters	pints (liq US)	2.113	0.4732
$\log_e$ or ln	$\log_{10}$	0.4343	2.303
lumens per sq foot	foot-candles	1	1
lux	lumens per sq foot	0.0929	10.764
maxwells	webers	10^{-8}	10^{8}
meters	yards	1.094	0.9144
meters	varas	1.179	0.848
meters per min	feet per minute	3.281	0.3048
meters per min	kilometers per hour	0.06	16.67
microhms per cu cm	microhms per inch cube	0.3937	2.540
microhms per cu cm	ohms per mil foot	6.015	0.1662
microns	meters	10^{-6}	10^{6}
miles (nautical)*	feet	6076.1	1.646×10^{-4}
miles (nautical)	meters	1852	5.400×10^{-4}
miles (nautical)	miles (statute)	1.1508	0.8690
miles (statute)	feet	5280	1.894×10^{-4}
miles (statute)	kilometers	1.609	0.6214
miles per hour	kilometers per minute	2.682×10^{-2}	37.28
miles per hour	feet per minute	88	1.136×10^{-2}
miles per hour	kilometers per hour	1.609	0.6214
millibars	inches of mercury (32°F)	0.02953	33.86
millibars (10^3 dynes per sq cm)	pounds per sq foot	2.089	0.4788
mils	meters	2.54×10^{-5}	3.94×10^{4}
nepers	decibels	8.686	0.1151
newtons	dynes	10^{5}	10^{-5}
newtons	kilograms	0.1020	9.807
newtons	poundals	7.233	0.1383
newtons	pounds (avoirdupois)	0.2248	4.448
oersteds	amperes per meter	7.9577×10	1.257×10^{-2}
ounce-inches	newton-meters	7.062×10^{-3}	1.416×10^{2}
ounces (fluid)	quarts	3.125×10^{-2}	32
ounces (avoirdupois)	pounds	6.25×10^{-2}	16
pascals	newtons per sq meter	1	1
pascals	pounds per sq inch	1.45×10^{-4}	6.895×10^{3}
piezes	newtons per sq meter	10^{3}	10^{-3}
piezes	sthenes per sq meter	1	1

To Convert	Into	Multiply by	Conversely, Multiply by
pints	quarts (liq US)	0.50	2
poises	newton-seconds per sq meter	10^{-1}	10
pounds of water (dist)	cubic feet	1.603×10^{-2}	62.38
pounds of water (dist)	gallons	0.1198	8.347
pounds per inch	kg per meter	17.86	0.05600
pounds per foot	kg per meter	1.488	0.6720
pounds per mile (statute)	kg per kilometer	0.2818	3.548
pounds per cu foot	kg per cu meter	16.02	6.243×10^{-2}
pounds per cu inch	pounds per cu foot	1728	5.787×10^{-4}
pounds per sq foot	pounds per sq inch	6.944×10^{-3}	144
pounds per sq foot	kg per sq meter	4.882	0.2048
pounds per sq inch	kg per sq meter	703.1	1.422×10^{-3}
poundals	dynes	1.383×10^{4}	7.233×10^{-5}
poundals	pounds (avoirdupois)	3.108×10^{-2}	32.17
quarts	gallons (liq US)	0.25	4
rods	feet	16.5	6.061×10^{-2}
slugs (mass)	pounds (avoirdupois)	32.174	3.108×10^{-2}
sq inches	circular mils	1.273×10^{6}	7.854×10^{-7}
sq inches	sq centimeters	6.452	0.1550
sq feet	sq meters	9.290×10^{-2}	10.76
sq miles	sq yards	3.098×10^{6}	3.228×10^{-7}
sq miles	acres	640	1.562×10^{-3}
sq miles	sq kilometers	2.590	0.3861
sq millimeters	circular mils	1973	5.067×10^{-4}
steres	cubic meters	1	1
stokes	sq meters per second	10^{-4}	10^{4}
(temp rise, °C)×(U.S. gal water)/minute	watts	264	3.79×10^{-3}
tonnes	kilograms	10^{3}	10^{-3}
tons, short (avoir 2000 lb)	tonnes (1000 kg)	0.9072	1.102
tons, long (avoir 2240 lb)	tonnes (1000 kg)	1.016	0.9842
tons, long (avoir 2240 lb)	tons, short (avoir 2000 lb)	1.120	0.8929
tons (US shipping)	cubic feet	40	0.025
torrs	newtons per sq meter	133.32	7.5×10^{-3}
watts	Btu per minute	5.689×10^{-2}	17.58
watts	ergs per second	10^{7}	10^{-7}
watts	foot-lb per minute	44.26	2.260×10^{-2}
watts	horsepower (550 ft-lb per second)	1.341×10^{-3}	745.7
watts	horsepower (metric) (542.5 ft-lb per second)	1.360×10^{-3}	735.5
watts	kg-calories per minute	1.433×10^{-2}	69.77
watt-seconds (joules)	gram-calories (mean)	0.2389	4.186
webers per sq meter	gausses	10^{4}	10^{-4}
yards	feet	3	0.3333

* Conversion factors for the nautical mile and, hence, for the knot, are based on the International Nautical Mile which was adopted by the U.S. Department of Defense and the U.S. Department of Commerce, effective 1 July 1954, See, "Adoption of International Nautical Mile," *National Bureau of Standards Technical News Bulletin*, vol. 38, p. 122; August 1954. The International Nautical Mile has been in use by many countries for various lengths of time.

Note: Pounds are avoirdupois in every entry except where otherwise indicated.

Examples

(A) Required, the conversion factor for pounds (avoirdupois) to grams. Duplication of entries in the table has been reduced to the minimum. An entry will be found for kilograms to pounds, from which the required factor is obviously 453.6.

(B) Convert inches per pound to meters per kilogram. A number of conversions have been collected under the name, pounds. The desired factor appears under pounds per inch. Since the reciprocal is tabulated, the factors must be interchanged, so the desired one is 0.05600.

FUNDAMENTAL PHYSICAL CONSTANTS†

Quantity	Symbol	Value	Error (ppm)	Units: SI	Units: cgs
Velocity of light	c	2.9979250(10)	0.33	10^{8} m sec^{-1}	10^{10} cm sec^{-1}
Fine structure constant, $[\mu_0 c^3/4\pi](e^2/\hbar c)$	α α^{-1}	7.297351(11) 137.03602(21)	1.5 1.5	10^{-3}	10^{-3}
Electron charge	e	1.6021917(70) 4.803250(21)	4.4 4.4	10^{-19} C	10^{-20} emu 10^{-10} esu
Planck's constant	h $\hbar = h/2\pi$	6.626196(50) 1.0545919(80)	7.6 7.6	10^{-34} J·sec 10^{-34} J·sec	10^{-27} erg·sec 10^{-27} erg·sec
Avogadro's number	N	6.022169(40)	6.6	10^{26} kmole^{-1}	10^{23} mole^{-1}
Atomic mass unit	amu	1.660531(11)	6.6	10^{-27} kg	10^{-24} g
Electron rest mass	m_e m_e*	9.109558(54) 5.485930(34)	6.0 6.2	10^{-31} kg 10^{-4} amu	10^{-28} g 10^{-4} amu
Proton rest mass	M_p M_p*	1.672614(11) 1.00727661(8)	6.6 0.08	10^{-27} kg amu	10^{-24} g amu
Neutron rest mass	M_n M_n*	1.674920(11) 1.00866520(10)	6.6 0.10	10^{-27} kg amu	10^{-24} g amu
Ratio of proton mass to electron mass	M_p/m_e	1836.109(11)	6.2		
Electron charge to mass ratio	e/m_e	1.7588028(54) 5.272759(16)	3.1 3.1	10^{11} C kg^{-1}	10^{7} emu g^{-1} 10^{17} esu g^{-1}
Magnetic flux quantum, $[c]^{-1}(hc/2e)$	Φ_0 h/e	2.0678538(69) 4.135708(14) 1.3795234(46)	3.3 3.3 3.3	10^{-15} T·m^2 10^{-15} J·sec C^{-1}	10^{-7} G·cm^2 10^{-7} erg·sec emu^{-1} 10^{-17} erg·sec esu^{-1}
Quantum of circulation	$h/2m_e$ h/m_e	3.636947(11) 7.273894(22)	3.1 3.1	10^{-4} J·sec kg^{-1} 10^{-4} J·sec kg^{-1}	erg·sec g^{-1} erg·sec g^{-1}
Faraday constant, Ne	F	9.648670(54) 2.892599(16)	5.5 5.5	10^{7} C kmole^{-1}	10^{3} emu mole^{-1} 10^{14} esu mole^{-1}

Quantity	Symbol	Value	Error (ppm)	Units SI	Units cgs
Rydberg constant, $[\mu_0 c^2/4\pi]^2(m_e e^4/4\pi\hbar^3 c)$	R_∞	1.09737312(11)	0.10	10^7 m^{-1}	10^5 cm^{-1}
Bohr radius, $[\mu_0 c^2/4\pi]^{-1}(\hbar^2/m_e e^2) = \alpha/4\pi R_\infty$	α_0	5.2917715(81)	1.5	10^{-11} m	10^{-9} cm
Classical electron radius $[\mu_0 c^2/4\pi](e^2/m_e c^2) = \alpha^2/4\pi R_\infty$	r_0	2.817939(13)	4.6	10^{-15} m	10^{-13} cm
Electron magnetic moment in Bohr magnetons	μ_e/μ_B	1.0011596389(31)	0.0031		
Bohr magneton, $[c](e\hbar/2m_e c)$	μ_B	9.274096(65)	7.0	10^{-24} J T^{-1}	10^{-21} erg G^{-1}
Electron magnetic moment	μ_e	9.284851(65)	7.0	10^{-24} J T^{-1}	10^{-21} erg G^{-1}
Gyromagnetic ratio of protons in H_2O	γ'_p $\gamma'_p/2\pi$	2.6751270(82) 4.257597(13)	3.1 3.1	10^8 rad sec^{-1}·T^{-1} 10^7 Hz T^{-1}	10^4 rad sec^{-1}·G^{-1} 10^3 Hz G^{-1}
γ'_p corrected for diamagnetism of H_2O	γ_p $\gamma_p/2\pi$	2.6751965(82) 4.257707(13)	3.1 3.1	10^8 rad sec^{-1}·T^{-1} 10^7 Hz T^{-1}	10^4 rad sec^{-1}·G^{-1} 10^3 Hz G^{-1}
Magnetic moment of protons in H_2O in Bohr magnetons	μ'_p/μ_B	1.52099312(10)	0.066	10^{-3}	10^{-3}
Proton magnetic moment in Bohr magnetons	μ_p/μ_B	1.52103264(46)	0.30	10^{-3}	10^{-3}
Proton magnetic moment	μ_p	1.4106203(99)	7.0	10^{-26} J T^{-1}	10^{-23} erg G^{-1}
Magnetic moment of protons in H_2O in nuclear magnetons	μ'_p/μ_n	2.792709(17)	6.2		
μ'_p/μ_n corrected for diamagnetism of H_2O	μ_p/μ_n	2.792782(17)	6.2		
Nuclear magneton, $[c](e\hbar/2M_p c)$	μ_n	5.050951(50)	10	10^{-27} J T^{-1}	10^{-24} erg G^{-1}

Compton wavelength of the electron, $h/m_e c$	λ_C	2.4263096(74)	3.1	10^{-12} m	10^{-10} cm
	$\lambda_C/2\pi$	3.861592(12)	3.1	10^{-13} m	10^{-11} cm
Compton wavelength of the proton, $h/M_p c$	$\lambda_{C,p}$	1.3214409(90)	6.8	10^{-15} m	10^{-13} cm
	$\lambda_{C,p}/2\pi$	2.103139(14)	6.8	10^{-16} m	10^{-14} cm
Compton wavelength of the neutron, $h/M_n c$	$\lambda_{C,n}$	1.3196217(90)	6.8	10^{-15} m	10^{-13} cm
	$\lambda_{C,n}/2\pi$	2.100243(14)	6.8	10^{-16} m	10^{-14} cm
Gas constant	R_0	8.31434(35)	42	10^{3} J kmole^{-1}·K^{-1}	10^{7} erg mole^{-1}·K^{-1}
Boltsman's constant R_0/N	k	1.380622(59)	43	10^{-23} J K^{-1}	10^{-16} erg K^{-1}
Stefan–Boltsman constant, $\pi^2 k^4/60\hbar^3 c^2$	σ	5.66961(96)	170	10^{-8} W m^{-2} K^{4}	10^{-5} erg sec^{-1}·cm^{-2}·K^{-4}
First radiation constant, $8\pi hc$	c_1	4.992579(38)	7.6	10^{-24} J·m	10^{-15} erg·cm
Second radiation constant, hc/k	c_2	1.438833(61)	43	10^{-2} m·K	cm·K
Gravitational constant	G	6.6732(31)	460	10^{-11} N·m^2 kg^{-2}	10^{-8} dyn·cm^2 g^{-2}
kx-unit-to-angstrom conversion factor, $\Lambda = \lambda(\text{Å})/\lambda(\text{kxu})$; $\lambda(\text{Cu}K\alpha_1) \equiv 1.537400$ kxu	Λ	1.0020764(53)	5.3		
Å-to-angstrom conversion factor, $\Lambda = \lambda(\text{Å})/\lambda(\text{Å}^*)$; $\lambda(\text{W}K\alpha_1) \equiv 0.2090100$ Å*	Λ^*	1.0000197(56)	5.6		

† Compiled by B. N. Taylor, W. H. Parker, and D. N. Langenberg. Reprinted from *Reviews of Modern Physics*, vol. 41, p. 375, 1969.

Note that the unified atomic mass scale $^{12}C \equiv 12$ has been used throughout, that amu = atomic mass unit, C = coulomb, G = gauss, Hz = hertz = cycles/sec, J = joule, K = kelvin (degrees kelvin), T = tesla (10^4 G), V = volt, and W = watt. In cases where formulas for constants are given (e.g., R_∞), the relations are written as the product of two factors. The second factor, in parentheses, is the expression to be used when all quantities are expressed in cgs units, with the electron charge in electrostatic units. The first factor, in brackets, is to be included only if all quantities are expressed in SI units. With the exception of the auxiliary constants which have been taken to be exact, the uncertainties of these constants are correlated, and therefore the general law of error propagation must be used in calculating additional quantities requiring two or more of these constants. The numbers in parentheses are the standard-deviation uncertainties in the last digits of the quoted value, computed on the basis of internal consistency.

ENERGY CONVERSION FACTORS†

Quantity	Value	Unit	Error (ppm)
1 kg	5.609538(24)	10^{29} MeV	4.4
1 amu	931.4812(52)	MeV	5.5
Electron mass	0.5110041(16)	MeV	3.1
Proton mass	938.2592(52)	MeV	5.5
Neutron mass	939.5527(52)	MeV	5.5
1 electron volt	1.6021917(70)	10^{-19} J	4.4
		10^{-12} erg	
	2.4179659(81)	10^{14} Hz	3.3
	8.065465(27)	10^{5} m^{-1}	3.3
		10^{3} cm^{-1}	
	1.160485(49)	10^{4} K	42
Energy-wavelength conversion	1.2398541(41)	10^{-6} eV·m	3.3
		10^{-4} eV·cm	
Rydberg constant, R_∞	2.179914(17)	10^{-18} J	7.6
		10^{-11} erg	
	13.605826(45)	eV	3.3
	3.2898423(11)	10^{15} Hz	0.35
	1.578936(67)	10^{5} K	43
Bohr magneton, μ_B	5.788381(18)	10^{-5} eV T^{-1}	3.1
	1.3996108(43)	10^{10} Hz T^{-1}	3.1
	46.68598(14)	m^{-1}·T^{-1}	3.1
		10^{-2} cm^{-1}·T^{-1}	
	0.671733(29)	K T^{-1}	43
Nuclear magneton, μ_n	3.152526(21)	10^{-8} eV T^{-1}	6.8
	7.622700(42)	10^{6} Hz T^{-1}	5.5
	2.542659(14)	10^{-2} m^{-1}·T^{-1}	5.5
		10^{-4} cm^{-1}·T^{-1}	
	3.65846(16)	10^{-4} K T^{-1}	44
Gas constant, R_0	8.20562(35)	10^{-2} m^3·atm $kmole^{-1}$·K^{-1}	42
Standard volume of ideal gas, V_0	22.4136	m^3 $kmole^{-1}$	

† Compiled by B. N. Taylor, W. H. Parker, and D. N. Langenberg. Reprinted from *Reviews of Modern Physics*, vol. 41, 1969.

The numbers in parentheses are the standard-deviation uncertainties in the last digits of the quoted value, computed on the basis of internal consistency.

DECIBELS AND POWER, VOLTAGE, AND CURRENT RATIOS

The decibel, abbreviated dB, is a unit used to express the ratio between two amounts of power, P_1 and P_2, existing at two points. By definition number of dB $= 10 \log_{10} (P_1/P_2)$. It is also used to express voltage and current ratios: number of dB $= 20 \log_{10} (V_1/V_2) = 20 \log_{10} (I_1/I_2)$.

Strictly, it can be used to express voltage and current ratios only when the voltages or currents in question are measured at places having identical impedances.

Power Ratio	Voltage and Current Ratio	Decibels	Nepers	Power Ratio	Voltage and Current Ratio	Decibels	Nepers
1.0233	1.0116	0.1	0.01	19.953	4.4668	13.0	1.50
1.0471	1.0233	0.2	0.02	25.119	5.0119	14.0	1.61
1.0715	1.0351	0.3	0.03	31.623	5.6234	15.0	1.73
1.0965	1.0471	0.4	0.05	39.811	6.3096	16.0	1.84
1.1220	1.0593	0.5	0.06	50.119	7.0795	17.0	1.96
1.1482	1.0715	0.6	0.07	63.096	7.9433	18.0	2.07
1.1749	1.0839	0.7	0.08	79.433	8.9125	19.0	2.19
1.2023	1.0965	0.8	0.09	100.00	10.0000	20.0	2.30
1.2303	1.1092	0.9	0.10	158.49	12.589	22.0	2.53
1.2589	1.1220	1.0	0.12	251.19	15.849	24.0	2.76
1.3183	1.1482	1.2	0.14	398.11	19.953	26.0	2.99
1.3804	1.1749	1.4	0.16	630.96	25.119	28.0	3.22
1.4454	1.2023	1.6	0.18	1000.0	31.623	30.0	3.45
1.5136	1.2303	1.8	0.21	1584.9	39.811	32.0	3.68
1.5849	1.2589	2.0	0.23	2511.9	50.119	34.0	3.91
1.6595	1.2882	2.2	0.25	3981.1	63.096	36.0	4.14
1.7378	1.3183	2.4	0.28	6309.6	79.433	38.0	4.37
1.8197	1.3490	2.6	0.30	10^4	100.000	40.0	4.60
1.9055	1.3804	2.8	0.32	$10^4 \times 1.5849$	125.89	42.0	4.83
1.9953	1.4125	3.0	0.35	$10^4 \times 2.5119$	158.49	44.0	5.06
2.2387	1.4962	3.5	0.40	$10^4 \times 3.9811$	199.53	46.0	5.29
2.5119	1.5849	4.0	0.46	$10^4 \times 6.3096$	251.19	48.0	5.52
2.8184	1.6788	4.5	0.52	10^5	316.23	50.0	5.76
3.1623	1.7783	5.0	0.58	$10^5 \times 1.5849$	398.11	52.0	5.99
3.5481	1.8836	5.5	0.63	$10^5 \times 2.5119$	501.19	54.0	6.22
3.9811	1.9953	6.0	0.69	$10^5 \times 3.9811$	630.96	56.0	6.45
5.0119	2.2387	7.0	0.81	$10^5 \times 6.3096$	794.33	58.0	6.68
6.3096	2.5119	8.0	0.92	10^6	1 000.00	60.0	6.91
7.9433	2.8184	9.0	1.04	10^7	3 162.3	70.0	8.06
10.0000	3.1623	10.0	1.15	10^8	10 000.0	80.0	9.21
12.589	3.5481	11.0	1.27	10^9	31 623	90.0	10.36
15.849	3.9811	12.0	1.38	10^{10}	100 000	100.0	11.51

To convert:

Decibels to nepers, multiply by 0.1151

Decibels per statute mile to nepers per kilometer, multiply by 7.154×10^{-2}

Decibels per nautical mile to nepers per kilometer, multiply by 6.215×10^{-2}

Nepers to decibels, multiply by 8.686

Nepers per kilometer to decibels per statute mile, multiply by 13.978

Nepers per kilometer to decibels per nautical mile, multiply by 16.074.

Where the power ratio is less than unity, it is usual to invert the fraction and express the answer as a decibel loss.

UNIT CONVERSION TABLE*

Quantity	Symbol	Equation in MKS(R) (Rationalized) Units	MKS(R) (Rationalized) Unit	Equivalent Number of: MKS (NR) Units	Pract Units	esu	emu	MKS(NR) (Nonrationalized) Unit
length	l		meter (m)	1	10^2	10^2	10^2	meter (m)
mass	m		kilogram	1	10^3	10^3	10^3	kilogram
time	t		second	1	1	1	1	second
force	F	$F=ma$	newton	1	10^5	10^5	10^5	newton
work, energy	W	$W=Fl$	joule	1	1	10^7	10^7	joule
power	P	$P=W/t$	watt	1	1	10^7	10^7	watt
electric charge	q		coulomb	1	1	3×10^9	10^{-1}	coulomb
volume charge density	ρ	$\rho=q/v$	coulomb/m^3	1	10^{-6}	3×10^3	10^{-7}	coulomb/m^3
surface charge density	σ	$\sigma=q/A$	coulomb/m^2	1	10^{-4}	3×10^5	10^{-5}	coulomb/m^2
electric dipole moment	p	$\mathrm{p}=ql$	coulomb-meter	1	10^2	3×10^{11}	10	coulomb-meter
polarization	P	$\mathbf{P}=\mathrm{p}/v$	coulomb/m^2	1	10^{-4}	3×10^5	10^{-5}	coulomb/m^2
electric field strength	E	$\mathbf{E}=\mathbf{F}/q$	volt/m	1	10^{-2}	$10^{-4}/3$	10^6	volt/m
permittivity	ϵ	$F=q^2/4\pi\epsilon l^2$	farad/m	4π	$4\pi\times10^{-9}$	$36\pi\times10^9$	$4\pi\times10^{-11}$	
displacement	D	$\mathbf{D}=\epsilon\mathbf{E}$	coulomb/m^2	4π	$4\pi\times10^{-4}$	$12\pi\times10^5$	$4\pi\times10^{-5}$	
displacement flux	Ψ	$\Psi=DA$	coulomb	4π	4π	$12\pi\times10^9$	$4\pi\times10^{-1}$	
emf, electric potential	V	$V=El$	volt	1	1	$10^{-2}/3$	10^8	volt
current	I	$I=q/t$	ampere	1	1	3×10^9	10^{-1}	ampere
volume current density	J	$\mathbf{J}=I/A$	ampere/m^2	1	10^{-4}	3×10^5	10^{-5}	ampere/m^2
surface current density	K	$\mathbf{K}=I/l$	ampere/m	1	10^{-2}	3×10^7	10^{-3}	ampere/m
resistance	R	$R=V/I$	ohm	1	1	$10^{-11}/9$	10^9	ohm
conductance	G	$G=1/R$	mho	1	1	9×10^{11}	10^{-9}	mho
resistivity	ρ	$\rho=RA/l$	ohm-meter	1	10^2	$10^{-9}/9$	10^{11}	ohm-meter
conductivity	γ	$\gamma=1/\rho$	mho/meter	1	10^{-2}	9×10^9	10^{-11}	mho/meter
capacitance	C	$C=q/V$	farad	1	1	9×10^{11}	10^{-9}	farad
elastance	S	$S=1/C$	daraf	1	1	$10^{-11}/9$	10^9	daraf
magnetic charge	m		weber	$1/4\pi$	$10^8/4\pi$	$10^{-2}/12\pi$	$10^8/4\pi$	
magnetic dipole moment	m	$\mathrm{m}=ml$	weber-meter	$1/4\pi$	$10^{10}/4\pi$	$1/12\pi$	$10^{10}/4\pi$	
magnetization	M	$\mathbf{M}=\mathrm{m}/v$	weber/m^2	$1/4\pi$	$10^4/4\pi$	$10^{-6}/12\pi$	$10^4/4\pi$	
magnetic field strength	H	$\mathbf{H}=nI/l$	ampere-turn/m	4π	$4\pi\times10^{-3}$	$12\pi\times10^7$	$4\pi\times10^{-3}$	
permeability	μ	$F=m^2/4\pi\mu l^2$	henry/m	$1/4\pi$	$10^7/4\pi$	$10^{-13}/36\pi$	$10^7/4\pi$	
induction	B	$\mathbf{B}=\mu\mathbf{H}$	weber/m^2	1	10^4	$10^{-6}/3$	10^4	weber/m^2
induction flux	Φ	$\Phi=\mathbf{B}A$	weber	1	10^8	$10^{-2}/3$	10^8	weber
mmf, magnetic potential	M	$M=\mathrm{H}l$	ampere-turn	4π	$4\pi\times10^{-1}$	$12\pi\times10^9$	$4\pi\times10^{-1}$	
reluctance	$\mathcal{R}$	$\mathcal{R}=M/\Phi$	amp-turn/weber	4π	$4\pi\times10^{-9}$	$36\pi\times10^{11}$	$4\pi\times10^{-9}$	
permeance	$\mathcal{P}$	$\mathcal{P}=1/\mathcal{R}$	weber/amp-turn	$1/4\pi$	$10^9/4\pi$	$10^{-11}/36\pi$	$10^9/4\pi$	
inductance	L	$L=\Phi/I$	henry	1	1	$10^{-11}/9$	10^9	henry

* Compiled by J. R. Ragazzini and L. A. Zadeh, Columbia University, New York.
(G) = Gaussian unit.

Equivalent Number of			Practical (CGS) Unit	Equivalent Number of			Equivalent Number of		
Pract Units	esu	emu		esu	emu	esu		emu	emu
10^2	10^2	10^2	centimeter (cm)	1	1	centimeter (cm) (G)	1		centimeter (cm)
10^3	10^3	10^3	gram	1	1	gram (G)	1		gram
1	1	1	second	1	1	second (G)	1		second
10^5	10^5	10^5	dyne	1	1	dyne (G)	1		dyne
1	10^7	10^7	joule	10^7	10^7	erg (G)	1		erg
1	10^7	10^7	watt	10^7	10^7	erg/second (G)	1		erg/second
1	3×10^9	10^{-1}	coulomb	3×10^9	10^{-1}	statcoulomb (G)	$10^{-10}/3$		abcoulomb
10^{-6}	3×10^3	10^{-7}	coulomb/cm^3	3×10^9	10^{-1}	statcoulomb/cm^3 (G)	$10^{-10}/3$		abcoulomb/cm^3
10^{-4}	3×10^5	10^{-5}	coulomb/cm^2	3×10^9	10^{-1}	statcoulomb/cm^2 (G)	$10^{-10}/3$		abcoulomb/cm^2
10^2	3×10^{11}	10	coulomb-cm	3×10^9	10^{-1}	statcoulomb-cm (G)	$10^{-10}/3$		abcoulomb-cm
10^{-4}	3×10^5	10^{-5}	coulomb/cm^2	3×10^9	10^{-1}	statcoulomb/cm^2 (G)	$10^{-10}/3$		abcoulomb/cm^2
10^{-2}	$10^{-4}/3$	10^6	volt/cm	$10^{-2}/3$	10^8	statvolt/cm (G)	3×10^{10}		abvolt/cm
10^{-9}	9×10^9	10^{-11}		9×10^{18}	10^{-2}	(G)	$10^{-20}/9$		
10^{-4}	3×10^5	10^{-5}		3×10^9	10^{-1}	(G)	$10^{-10}/3$		
1	3×10^9	10^{-1}		3×10^9	10^{-1}	(G)	$10^{-10}/3$		
1	$10^{-2}/3$	10^8	volt	$10^{-2}/3$	10^8	statvolt (G)	3×10^{10}		abvolt
1	3×10^9	10^{-1}	ampere	3×10^9	10^{-1}	statampere (G)	$10^{-10}/3$		abampere
10^{-4}	3×10^5	10^{-5}	ampere/cm^2	3×10^9	10^{-1}	statampere/cm^2 (G)	$10^{-10}/3$		abampere/cm^2
10^{-2}	3×10^7	10^{-3}	ampere/cm	3×10^9	10^{-1}	statampere/cm (G)	$10^{-10}/3$		abampere/cm
1	$10^{-11}/9$	10^9	ohm	$10^{-11}/9$	10^9	statohm (G)	9×10^{20}		abohm
1	9×10^{11}	10^{-9}	mho	9×10^{11}	10^{-9}	statmho (G)	$10^{-20}/9$		abmho
10^2	$10^{-9}/9$	10^{11}	ohm-cm	$10^{-11}/9$	10^9	statohm-cm (G)	9×10^{20}		abohm-cm
10^{-2}	9×10^9	10^{-11}	mho/cm	9×10^{11}	10^{-9}	statmho/cm (G)	$10^{-20}/9$		abmho/cm
1	9×10^{11}	10^{-9}	farad	9×10^{11}	10^{-9}	statfarad (cm) (G)	$10^{-20}/9$		abfarad
1	$10^{-11}/9$	10^9	daraf	$10^{-11}/9$	10^9	statdaraf (G)	9×10^{20}		abdaraf
10^8	$10^{-2}/3$	10^8		$10^{-10}/3$	1		3×10^{10}	unit pole	(G)
10^{10}	1/3	10^{10}		$10^{-10}/3$	1		3×10^{10}	pole-cm	(G)
10^4	$10^{-6}/3$	10^4		$10^{-10}/3$	1		3×10^{10}	pole/cm^2	(G)
10^{-3}	3×10^7	10^{-3}	oersted	3×10^{10}	1		$10^{-10}/3$	oersted	(G)
10^7	$10^{-13}/9$	10^7	gauss/oersted	$10^{-20}/9$	1		9×10^{20}	gauss/oersted	(G)
10^4	$10^{-6}/3$	10^4	gauss	$10^{-10}/3$	1		3×10^{10}	gauss	(G)
10^8	$10^{-2}/3$	10^8	maxwell (line)	$10^{-10}/3$	1		3×10^{10}	maxwell (line)	(G)
10^{-1}	3×10^9	10^{-1}	gilbert	3×10^{10}	1		$10^{-10}/3$	gilbert	(G)
10^{-9}	9×10^{11}	10^{-9}	gilbert/maxwell	9×10^{20}	1		$10^{-20}/9$	gilbert/maxwell	(G)
10^9	$10^{-11}/9$	10^9	maxwell/gilbert	$10^{-20}/9$	1		9×10^{20}	maxwell/gilbert	(G)
1	$10^{-11}/9$	10^9	henry	$10^{-11}/9$	10^9	stathenry (G)	9×10^{20}	abhenry (cm)	(G)

The velocity of light was taken as 3×10^{10} centimeters/second in computing the conversion factors. Equations in the third column are for dimensional purposes only.

GREEK ALPHABET

Name	Capital	Small	Commonly Used to Designate
Alpha	A	α	Angles, coefficients, attenuation constant, absorption factor, area
Beta	B	β	Angles, coefficients, phase constant
Gamma	Γ	γ	Complex propagation constant (cap), specific gravity, angles, electrical conductivity, propagation constant
Delta	Δ	δ	Increment or decrement (cap or small), determinant (cap), permittivity (cap), density, angles
Epsilon	E	ϵ	Dielectric constant, permittivity, base of natural logarithms, electric intensity
Zeta	Z	ζ	Coordinates, coefficients
Eta	H	η	Intrinsic impedance, efficiency, surface charge density, hysteresis, coordinates
Theta	Θ	$\vartheta\ \theta$	Angular phase displacement, time constant, reluctance, angles
Iota	I	ι	Unit vector
Kappa	K	κ	Susceptibility, coupling coefficient
Lambda	Λ	λ	Permeance (cap), wavelength, attenuation constant
Mu	M	μ	Permeability, amplification factor, prefix micro
Nu	N	ν	Reluctivity, frequency
Xi	Ξ	ξ	Coordinates
Omicron	O	o	
Pi	Π	π	3.1416
Rho	P	ρ	Resistivity, volume charge density, coordinates
Sigma	Σ	σ	Summation (cap), surface charge density, complex propagation constant, electrical conductivity, leakage coefficient, deviation
Tau	T	τ	Time constant, volume resistivity, time-phase displacement, transmission factor, density
Upsilon	Υ	υ	
Phi	Φ	$\phi\ \varphi$	Scalar potential (cap), magnetic flux, angles
Chi	X	χ	Electric susceptibility, angles
Psi	Ψ	ψ	Dielectric flux, phase difference, coordinates, angles
Omega	Ω	ω	Resistance in ohms (cap), solid angle (cap), angular velocity

Note: Small letter is used except where capital (Cap) is indicated.

USEFUL NUMERICAL DATA

1 cubic foot of water at 4°C (weight)	62.43 lb
1 foot of water at 4°C (pressure)	0.4335 lb/in.^{2}
Velocity of light in vacuum, c	186 280 mi/second $= 2.998 \times 10^{10}$ cm/second
Velocity of sound in dry air at 20°C, 760 mm Hg	1127 ft/second
Degree of longitude at equator	68.703 statute miles, 59.661 nautical miles
Acceleration due to gravity at sea level, 40° latitude, g	32.1578 ft/second^2
$(2g)^{1/2}$	8.020
1 inch of mercury at 4°C	1.132 ft water $= 0.4908$ lb/in.^{2}
Base of natural logs ϵ	2.718
1 radian	$180° \div \pi = 57.3°$
360 degrees	2π radians
π	3.1416
Sin 1′	0.00029089
Arc 1°	0.01745 radian
Side of square	0.707 × (diagonal of square)

FRACTIONS OF AN INCH WITH METRIC EQUIVALENTS

Fractions of an inch	Decimals of an inch	Millimeters	Fractions of an inch	Decimals of an inch	Millimeters
1/64	0.0156	0.397	33/64	0.5156	13.097
1/32	0.0313	0.794	17/32	0.5313	13.494
3/64	0.0469	1.191	35/64	0.5469	13.891
1/16	0.0625	1.588	9/16	0.5625	14.288
5/64	0.0781	1.984	37/64	0.5781	14.684
3/32	0.0938	2.381	19/32	0.5938	15.081
7/64	0.1094	2.778	39/64	0.6094	15.478
1/8	0.1250	3.175	5/8	0.6250	15.875
9/64	0.1406	3.572	41/64	0.6406	16.272
5/32	0.1563	3.969	21/32	0.6563	16.669
11/64	0.1719	4.366	43/64	0.6719	17.066
3/16	0.1875	4.763	11/16	0.6875	17.463
13/64	0.2031	5.159	45/64	0.7031	17.859
7/32	0.2188	5.556	23/32	0.7188	18.256
15/64	0.2344	5.953	47/64	0.7344	18.653
1/4	0.2500	6.350	3/4	0.7500	19.050
17/64	0.2656	6.747	49/64	0.7656	19.447
9/32	0.2813	7.144	25/32	0.7813	19.844
19/64	0.2969	7.541	51/64	0.7969	20.241
5/16	0.3125	7.938	13/16	0.8125	20.638
21/64	0.3281	8.334	53/64	0.8281	21.034
11/32	0.3438	8.731	27/32	0.8438	21.431
23/64	0.3594	9.128	55/64	0.8594	21.828
3/8	0.3750	9.525	7/8	0.8750	22.225
25/64	0.3906	9.922	57/64	0.8906	22.622
13/32	0.4063	10.319	29/32	0.9063	23.019
27/64	0.4219	10.716	59/64	0.9219	23.416
7/16	0.4375	11.113	15/16	0.9375	23.813
29/64	0.4531	11.509	61/64	0.9531	24.209
15/32	0.4688	11.906	31/32	0.9688	24.606
31/64	0.4844	12.303	63/64	0.9844	25.003
1/2	0.5000	12.700	—	1.0000	25.400

TEMPERATURE CONVERSION TABLE

To use the table, find the temperature reading you have in the middle column. If the reading you have is in degrees Celsius (Centigrade), read the Fahrenheit equivalent in the right-hand column. If the reading you have is in degrees Fahrenheit, read the Celsius equivalent in the left-hand column.

−459.4 to 0			0 to 100					
C		F	C		F	C		F
−273	−459.4		−17.8	0	32	10.0	50	122.0
−268	−450		−17.2	1	33.8	10.6	51	123.8
−262	−440		−16.7	2	35.6	11.1	52	125.6
−257	−430		−16.1	3	37.4	11.7	53	127.4
−251	−420		−15.6	4	39.2	12.2	54	129.2
−246	−410		−15.0	5	41.0	12.8	55	131.0
−240	−400		−14.4	6	42.8	13.3	56	132.8
−234	−390		−13.9	7	44.6	13.9	57	134.6
−229	−380		−13.3	8	46.4	14.4	58	136.4
−223	−370		−12.8	9	48.2	15.0	59	138.2
−218	−360		−12.2	10	50.0	15.6	60	140.0
−212	−350		−11.7	11	51.8	16.1	61	141.8
−207	−340		−11.1	12	53.6	16.7	62	143.6
−201	−330		−10.6	13	55.4	17.2	63	145.4
−196	−320		−10.0	14	57.2	17.8	64	147.2
−190	−310		− 9.4	15	59.0	18.3	65	149.0
−184	−300		− 8.9	16	60.8	18.9	66	150.8
−179	−290		− 8.3	17	62.6	19.4	67	152.6
−173	−280		− 7.8	18	64.4	20.0	68	154.4
−169	−273	−459.4	− 7.2	19	66.2	20.6	69	156.2
−168	−270	−454	− 6.7	20	68.0	21.1	70	158.0
−162	−260	−436	− 6.1	21	69.8	21.7	71	159.8
−157	−250	−418	− 5.6	22	71.6	22.2	72	161.6
−151	−240	−400	− 5.0	23	73.4	22.8	73	163.4
−146	−230	−382	− 4.4	24	75.2	23.3	74	165.2
−140	−220	−364	− 3.9	25	77.0	23.9	75	167.0
−134	−210	−346	− 3.3	26	78.8	24.4	76	168.8
−129	−200	−328	− 2.8	27	80.6	25.0	77	170.6
−123	−190	−310	− 2.2	28	82.4	25.6	78	172.4
−118	−180	−292	− 1.7	29	84.2	26.1	79	174.2
−112	−170	−274	− 1.1	30	86.0	26.7	80	176.0
−107	−160	−256	− 0.6	31	87.8	27.2	81	177.8
−101	−150	−238	0.0	32	89.6	27.8	82	179.6
− 96	−140	−220	0.6	33	91.4	28.3	83	181.4
− 90	−130	−202	1.1	34	93.2	28.9	84	183.2
− 84	−120	−184	1.7	35	95.0	29.4	85	185.0
− 79	−110	−166	2.2	36	96.8	30.0	86	186.8
− 73	−100	−148	2.8	37	98.6	30.6	87	188.6
− 68	− 90	−130	3.3	38	100.4	31.1	88	190.4
− 62	− 80	−112	3.9	39	102.2	31.7	89	192.2
− 57	− 70	− 94	4.4	40	104.0	32.2	90	194.0
− 51	− 60	− 76	5.0	41	105.8	32.8	91	195.8
− 46	− 50	− 58	5.6	42	107.6	33.3	92	197.6
− 40	− 40	− 40	6.1	43	109.4	33.9	93	199.4
− 34	− 30	− 22	6.7	44	111.2	34.4	94	201.2
− 29	− 20	− 4	7.2	45	113.0	35.0	95	203.0
− 23	− 10	+ 14	7.8	46	114.8	35.6	96	204.8
− 17.8	− 0	+ 32	8.3	47	116.6	36.1	97	206.6
			8.9	48	118.4	36.7	98	208.4
			9.4	49	120.2	37.2	99	210.2
						37.8	100	212.0

Notes:

1. Kelvins (Celsius absolute) = °C + 273.18.

100 to 1000						1000 to 2000					
C		F	C		F	C		F	C		F
38	100	212	260	500	932	538	1000	1832	816	1500	2732
43	110	230	266	510	950	543	1010	1850	821	1510	2750
49	120	248	271	520	968	549	1020	1868	827	1520	2768
54	130	266	277	530	986	554	1030	1886	832	1530	2786
60	140	284	282	540	1004	560	1040	1904	838	1540	2804
66	150	302	288	550	1022	566	1050	1922	843	1550	2822
71	160	320	293	560	1040	571	1060	1940	849	1560	2840
77	170	338	299	570	1058	577	1070	1958	854	1570	2858
82	180	356	304	580	1076	582	1080	1976	860	1580	2876
88	190	374	310	590	1094	588	1090	1994	866	1590	2894
93	200	392	316	600	1112	593	1100	2012	871	1600	2912
99	210	410	321	610	1130	599	1110	2030	877	1610	2930
100	212	413.6	327	620	1148	604	1120	2048	882	1620	2948
104	220	428	332	630	1166	610	1130	2066	888	1630	2966
110	230	446	338	640	1184	616	1140	2084	893	1640	2984
116	240	464	343	650	1202	621	1150	2102	899	1650	3002
121	250	482	349	660	1220	627	1160	2120	904	1660	3020
127	260	500	354	670	1238	632	1170	2138	910	1670	3038
132	270	518	360	680	1256	638	1180	2156	916	1680	3056
138	280	536	366	690	1274	643	1190	2174	921	1690	3074
143	290	554	371	700	1292	649	1200	2192	927	1700	3092
149	300	572	377	710	1310	654	1210	2210	932	1710	3110
154	310	590	382	720	1328	660	1220	2228	938	1720	3128
160	320	608	388	730	1346	666	1230	2246	943	1730	3146
166	330	626	393	740	1364	671	1240	2264	949	1740	3164
171	340	644	399	750	1382	677	1250	2282	954	1750	3182
177	350	662	404	760	1400	682	1260	2300	960	1760	3200
182	360	680	410	770	1418	688	1270	2318	966	1770	3218
188	370	698	416	780	1436	693	1280	2336	971	1780	3236
193	380	716	421	790	1454	699	1290	2354	977	1790	3254
199	390	734	427	800	1472	704	1300	2372	982	1800	3272
204	400	752	432	810	1490	710	1310	2390	988	1810	3290
210	410	770	438	820	1508	716	1320	2408	993	1820	3308
216	420	788	443	830	1526	721	1330	2426	999	1830	3326
221	430	806	449	840	1544	727	1340	2444	1004	1840	3344
227	440	824	454	850	1562	732	1350	2462	1010	1850	3362
232	450	842	460	860	1580	738	1360	2480	1016	1860	3380
238	460	860	466	870	1598	743	1370	2498	1021	1870	3398
243	470	878	471	880	1616	749	1380	2516	1027	1880	3416
249	480	896	477	890	1634	754	1390	2534	1032	1890	3434
254	490	914	482	900	1652	760	1400	2552	1038	1900	3452
			488	910	1670	766	1410	2570	1043	1910	3470
			493	920	1688	771	1420	2588	1049	1920	3488
			499	930	1706	777	1430	2606	1054	1930	3506
			504	940	1724	782	1440	2624	1060	1940	3524
			510	950	1742	788	1450	2642	1066	1950	3542
			516	960	1760	793	1460	2660	1071	1960	3560
			521	970	1778	799	1470	2678	1077	1970	3578
			527	980	1796	804	1480	2696	1082	1980	3596
			532	990	1814	810	1490	2714	1088	1990	3614
			538	1000	1832				1093	2000	3632

2. Degrees Rankine (Fahrenheit absolute) = °F + 459.72.

TIME CONVERSION NOMOGRAPH*

The duration of component and equipment tests and requirements for equipment reliability are usually stated in hours. Such figures become more meaningful when converted to days, months, or years. For example, Fig. 1 shows that a "1000-hour test" requires approximately 42 days for completion.

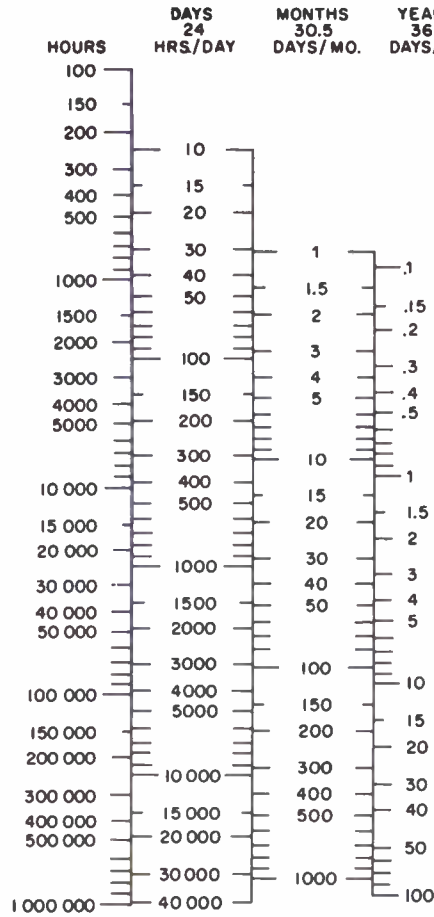

Fig. 1—Time conversion nomograph. *From R. F. Graf, "'Reliability' in Terms of Time," Electronic Industries, p. 95; April 1958. © 1958, Chilton Company, Philadelphia, Pa.*

* Extracted from: R. F. Graf, "'Reliability' in Terms of Time," *Electronic Industries*, p. 95; April 1958. *© 1958, Chilton Company, Philadelphia, Pa.*

CHAPTER 4
PROPERTIES OF MATERIALS

GENERAL PROPERTIES OF THE ELEMENTS (TABLE 1)*

Atomic Number Z represents the number of protons per atom.

Mass Number $Z+N$ is equal to the number of protons Z plus the number of neutrons N present in the nuclei. Mass numbers of the most abundant isotopes are given in order of decreasing abundance. For example, Cadmium Cd-48 mass numbers 114–112 means that cadmium atoms of greater abundance (28.86%) have a mass number of 114; that is, that the nucleus of Cd^{114} has $114-48=66$ neutrons while isotope Cd^{112} of lower abundance (24.07%) has $112-48=64$ neutrons.

Atomic Radii. The values listed provide a comparison of sizes (deduced from interatomic spacing of bound atoms).

Gram Atomic Volume in cubic centimeters gives the volume occupied in the solid state by an atom at its melting point. The gram atomic volume contains the Avogadro number of atoms (6.0225×10^{23}).

Electronegativity represents the relative tendency of an atom to attract shared electron pairs. The highest electronegativity is assigned to fluorine with the value 3.90.

* Tables 1 through 6 of this chapter are partly based on data from the following sources: "Textbook of Chemistry", McGraw-Hill Book Company; 1961. "Handbook of Chemistry and Physics," 55th ed., CRC Press, Inc.; 1974. "Fundamentals of Chemistry," John Wiley & Sons. "The Encyclopedia of Electrochemistry," Reinhold Publishing Corp.; 1964. "American Institute of Physics Handbook," 3rd ed., McGraw-Hill Book Co.; 1972. "Lange's Handbook of Chemistry," 11th ed., McGraw-Hill Book Co.; 1973.

First Ionization Potential is the work in electron-volts required to pull 1 electron off an isolated neutral atom.

$$1 \text{ electron-volt} = 3.8\times 10^{-20} \text{ calorie}$$

$$= 1.602\times 10^{-12} \text{ erg}$$

$$= 1.602\times 10^{-19} \text{ joules.}$$

Electron Work Function, expressed in electron-volts, represents the energy that must be supplied to an electron to cross over the surface barrier of a metal. That energy may be supplied by heat (thermionic work function), by light (photo-electric work function), or by contact with a dissimilar metal (contact potential).

Electrochemical Equivalents are expressed in ampere-hours per gram liberated at the electrode.

PERIODIC CLASSIFICATION OF THE ELEMENTS (TABLE 2)

Oxidation Number is defined as the charge which an atom appears to have in a compound when electrons are counted according to certain rules:

(A) In the free elements each atom has an oxidation number of 0.

(B) Electrons shared between two unlike atoms are counted with the more electronegative atom.

(C) Electrons shared between two like atoms are divided equally between the sharing atoms.

When an atom loses an electron its oxidation number increases by one.

Groups 1A and 2A of the periodic table having respectively oxidation numbers 1 and 2 (in all compounds) form only +1 ions (group 1A) and +2 ions (group 2A).

TABLE 1—PROPERTIES

	Symbol	Atomic Number Z	Mass Number $Z+N$	Atomic Weight	Atomic Radii (angstrom units)	Gram Atomic Volume (cm^3)
Actinium	Ac	89	227	227		
Aluminum	Al	13	27	26.98	1.25	10
Americium	Am	95	243	243		
Antimony	Sb	51	121–123	121.75	1.41	18
Argon	Ar or A	18	40	39.948	1.74	24
Arsenic	As	33	75	74.92	1.21	16
Astatine	At	85	210	210		
Barium	Ba	56	138	137.34	1.98	38
Berkelium	Bk	97	247	247		
Beryllium	Be	4	9	9.012	0.89	5
Bismuth	Bi	83	209	208.98	1.52	21
Boron	B	5	11	10.81	0.88	5
Bromine	Br	35	79–81	79.904	1.14	23
Cadmium	Cd	48	114–112	112.40	1.41	13
Calcium	Ca	20	40	40.08	1.74	26
Californium	Cf	98	251	251		
Carbon	C	6	12	12.011	0.77	5
Cerium	Ce	58	140	140.12	1.65	21
Cesium	Cs	55	133	132.905	2.35	71
Chlorine	Cl	17	35	35.453	0.99	19
Chromium	Cr	24	52	51.996	1.17	7
Cobalt	Co	27	59	58.933	1.16	7
Copper	Cu	29	63	63.546	1.17	7
Curium	Cm	96	247	247		
Dysprosium	Dy	66	164–162–163	162.50	1.59	19
Einsteinium	Es or E	99	254	254		
Erbium	Er	68	166–168–167	167.26	1.57	18
Europium	Eu	63	153–151	151.96	1.85	29
Fermium	Fm	100	257	257		
Fluorine	F	9	19	18.998	0.64	15
Francium	Fr	87	223	223		
Gadolinium	Gd	64	158–160–156	157.25	1.61	20
Gallium	Ga	31	69–71	69.72	1.25	12
Germanium	Ge	32	74–72–70	72.59	1.22	13
Gold	Au	79	197	196.967	1.34	10
Hafnium	Hf	72	180–178–177	178.49	1.44	13
Helium	He	2	4	4.003		32
Holmium	Ho	67	165	164.93	1.58	19
Hydrogen	H	1	1	1.008	0.37	13
Indium	In	49	115	114.82	1.50	16
Iodine	I	53	127	126.904	1.33	26
Iridium	Ir	77	193–191	192.22	1.26	9
Iron	Fe	26	56	55.847	1.17	7
Krypton	Kr	36	84–86	83.80	1.89	33
Lanthanum	La	57	139	138.905	1.69	22
Lawrencium	Lw	103	257	257		
Lead	Pb	82	208–206–207	207.2	1.54	18
Lithium	Li	3	7	6.940	1.23	13
Lutetium	Lu	71	175	174.97	1.56	18
Magnesium	Mg	12	24	24.305	1.36	14
Manganese	Mn	25	55	54.938	1.17	7

OF THE ELEMENTS.

Electro-negativity, Relative Scale	First Ionization Potential (electron volts)	Electron Work Function			Electrochemical Equivalent	
		Thermionic	Photoelectric	Contact	Valence* Involved	Amp-Hours per Gram
1.1	6.9				3	0.35
1.5	5.98		4.08	3.38	3	2.98
	6.05					
2.05	8.64		4.01	4.14	5	1.1
0	15.76				n	0.67
2.0	9.81		5.11		5	1.79
2.2						
0.9	5.21	2.11	2.48	1.73	2	0.39
1.5	9.32		3.92	3.10	2	5.94
1.9	7.29		4.25	4.17	5	0.64
2.0	8.3		4.5		3	7.43
2.85	11.81				1	0.335
1.7	8.99		4.07	4.0	2	0.477
1.0	6.11	2.24	2.706	3.33	2	1.337
2.6	11.26	4.34	4.81		4	8.93
1.1	5.6	2.6	2.84		3	0.574
0.7	3.89	1.81	1.92	4.46	1	0.2
3.15	12.97				1	0.756
1.6	6.76	4.60	4.37	4.38	3	1.546
1.8	7.86	4.40	4.20	4.21	2	0.91
1.9	7.72	4.26	4.18	4.46	2	0.84
1.2	5.93				3	0.495
1.2	6.10				3	0.48
1.1	5.67				3	0.53
3.9	17.42				1	1.41
0.65						
1.1	6.16				3	0.513
1.6	5.99	4.12		3.80	3	1.15
1.9	7.89		4.5	4.5	4	1.48
2.4	9.22	4.32	4.82	4.46	3	0.41
1.3	7.0	3.53			4	0.600
0	24.59				n	6.698
1.2	6.02				3	0.488
2.2	13.59				1	26.59
1.7	5.78				3	0.700
2.65	10.45		6.8		1	0.211
2.2	9.1	5.3		4.57	4	0.555
1.8	7.87	4.25	4.33	4.40	3	1.440
0	13.99				n	0.32
1.1	5.61	3.3			3	0.579
1.8	7.42		4.05	3.94	4	0.517
1.0	5.39		2.35	2.49	1	3.862
1.2	6.15				3	0.46
1.2	7.64		3.68	3.63	2	2.204
1.5	7.43	3.83	3.76	4.14	4	1.952

TABLE 1—

	Symbol	Atomic Number Z	Mass Number $Z+N$	Atomic Weight	Atomic Radii (angstrom units)	Gram Atomic Volume (cm^3)
Mendelevium	Md or Mv	101	256	256		
Mercury	Hg	80	202–200–199	200.59	1.44	14
Molybdenum	Mo	42	98–96–92–95	95.94	1.29	9
Neodymium	Nd	60	142–144–146	144.24	1.64	21
Neon	Ne	10	20	20.179	1.31	17
Neptunium	Np	93	237	237.048		
Nickel	Ni	28	58	58.71	1.15	6
Niobium	Nb	41	93	92.906	1.34	11
Nitrogen	N	7	14	14.007	0.70	14
Nobelium	No	102	254	254		
Osmium	Os	76	192–190–189	190.2	1.26	9
Oxygen	O	8	16	15.999	0.66	11
Palladium	Pd	46	108–106–105	106.4	1.28	9
Phosphorus	P	15	31	30.974	1.10	17
Platinum	Pt	78	195–194–196	195.09	1.29	9
Plutonium	Pu	94	242	242		
Polonium	Po	84	209	210	1.53	
Potassium	K	19	39	39.098	2.03	46
Praseodymium	Pr	59	141	140.907	1.65	21
Promethium	Pm	61	145	145		
Protactinium	Pa	91	231	231.036		
Radium	Ra	88	226	226.025		45
Radon	Rn	86	222	222	2.14	50
Rhenium	Re	75	187–185	186.2	1.28	9
Rhodium	Rh	45	103	102.905	1.25	8
Rubidium	Rb	37	85–87	85.468	2.16	56
Ruthenium	Ru	44	102–104–101	101.07	1.24	8
Samarium	Sm	62	152–154–147	150.35	1.66	20
Scandium	Sc	21	45	44.956	1.44	15
Selenium	Se	34	80–78	78.96	1.17	16
Silicon	Si	14	28	28.086	1.17	12
Silver	Ag	47	107–109	107.868	1.34	10
Sodium	Na	11	23	22.99	1.57	24
Strontium	Sr	38	88	87.62	1.92	34
Sulfur	S	16	32	32.064	1.04	16
Tantalum	Ta	73	181	180.948	1.34	11
Technetium	Tc	43	99	98.906		
Tellurium	Te	52	130–128–126	127.60	1.37	21
Terbium	Tb	65	159	158.925	1.59	19
Thallium	Tl	81	205–203	204.37	1.55	17
Thorium	Th	90	232	232.038	1.65	20
Thulium	Tm	69	169	168.934	1.56	18
Tin	Sn	50	120–118	118.69	1.40	16
Titanium	Ti	22	48	47.90	1.32	11
Tungsten	W	74	184–186–182	183.85	1.30	10
Uranium	U	92	238	238.029	1.42	13
Vanadium	V	23	51	50.94	1.22	8
Xenon	Xe	54	132–129–131	131.30	2.09	43
Ytterbium	Yb	70	174–172–173	173.04	1.70	25
Yttrium	Y	39	89	88.906	1.62	21
Zinc	Zn	30	64–66–68	65.38	1.25	9
Zirconium	Zr	40	90–94–92	91.22	1.45	14

CONTINUED.

Electro-negativity, Relative Scale	First Ionization Potential (electron volts)	Electron Work Function			Electrochemical Equivalent	
		Thermionic	Photoelectric	Contact	Valence* Involved	Amp-Hours per Gram
1.9	10.43		4.53	4.50	2	0.267
1.8	7.10	4.20	4.25	4.28	6	1.67
1.1	5.49	3.3			3	0.557
0	21.56				n	1.33
1.3	5.8					
1.8	7.63	5.03	5.01	4.96	2	0.913
1.6	6.88	4.01	4.5			
3.05	14.53				5	9.57
2.2	8.7			4.55	4	0.56
3.5	13.62				2	3.35
2.2	8.33	4.99	4.97	4.49	4	1.005
2.15	10.48				5	4.33
2.2	9.0	5.32	5.22	5.36	4	0.549
	5.8					
2.0	8.43				6	0.766
0.8	4.34		2.24	1.60	1	0.685
1.1	5.42	2.7			3	0.571
1.1	5.55					
1.5					5	0.580
0.9	5.28				2	0.237
0	10.75				n	0.121
1.9	7.87	5.1	5.0		7	1.007
2.2	7.46	4.80	4.57	4.52	4	1.042
0.8	4.18		2.09		1	0.314
2.2	7.37			4.52	4	1.054
1.1	5.63	3.2			3	0.535
1.3	6.54				3	1.783
2.45	9.75		4.8	4.42	6	2.037
1.9	8.15	3.59	4.52	4.2	4	3.821
1.9	7.57	3.56	4.73	4.44	1	0.248
0.9	5.14		2.28	1.9	1	1.166
1.0	5.69		2.74		2	0.612
2.6	10.36				6	5.01
1.3	7.88	4.19	4.14	4.1	5	0.741
1.9	7.28					
2.3	9.01		4.76	4.70	6	1.260
1.2	5.98				3	0.505
1.8	6.11		3.68	3.84	3	0.393
1.3	6.95	3.35	3.47	3.46	4	0.462
1.2	6.18				3	0.475
1.8	7.34		4.38	4.09	4	0.903
1.5	6.82	3.95	4.06	4.14	4	2.238
1.7	7.98	4.52	4.49	4.38	6	0.874
1.7	6.08	3.27	3.63	4.32	6	0.676
1.6	6.74	4.12	3.77	4.44	5	2.63
0	12.13				n	0.204
1.2	6.25				3	0.465
1.3	6.38				3	0.904
1.6	9.39		3.73	3.78	2	0.820
1.6	6.84	4.21	3.82	3.60	4	1.175

* n = nonvalent

TABLE 2—PERIODIC CLASSIFICATION OF THE ELEMENTS.

PERIOD	GROUP 1A	2A	3B	4B	5B	6B	7B	8	1B	2B	3A	4A	5A	6A	7A	0
1	+1 -1 H 1															0 He 2
	LIGHT METALS						HEAVY METALS					NON METALS			INERT GAS	
2	+1 Li 3	+2 Be 4	BRITTLE					DUCTILE		LOW-MELTING	+3 B 5	+2 -4 +4 C 6	+1 -1 +2 +3 N -2 -3 +4 +5 7	-2 O 8	-1 F 9	0 Ne 10
3	+1 Na 11	+2 Mg 12									+3 Al 13	+2 -4 +4 Si 14	+3 -3 +5 P 15	+4 -2 +6 S 16	+1 -1 +5 +7 Cl 17	0 Ar 18
4	+1 K 19	+2 Ca 20	+3 Sc 21	+2 +3 +4 Ti 22	+2 +3 +4 +5 V 23	+2 +3 +6 Cr 24	+2 +3 +4 +7 Mn 25	+2 +3 Fe 26	+2 +3 Co 27	+2 +3 Ni 28	+1 +2 Cu 29	+2 Zn 30	+3 Ga 31	+2 +4 Ge 32	+3 -3 +5 As 33	+4 -2 +6 Se 34	+1 -1 +5 Br 35	0 Kr 36
5	+1 Rb 37	+2 Sr 38	+3 Y 39	+4 Zr 40	+3 +5 Nb 41	+6 Mo 42	+4 +6 +7 Tc 43	+3 Ru 44	+3 Rh 45	+2 +4 Pd 46	+1 Ag 47	+2 Cd 48	+3 In 49	+2 +4 Sn 50	+3 -3 +5 Sb 51	+4 -2 +6 Te 52	+1 -1 +5 +7 I 53	0 Xe 54
6	+1 Cs 55	+2 Ba 56	♦ 57-71	+4 Hf 72	+5 Ta 73	+6 W 74	+4 +6 +7 Re 75	+3 +4 Os 76	+3 +4 Ir 77	+2 +4 Pt 78	+1 +3 Au 79	+1 +2 Hg 80	+1 +3 Tl 81	+2 +4 Pb 82	+3 +5 Bi 83	+2 +4 Po 84	At 85	0 Rn 86
7	+1 Fr 87	+2 Ra 88	★ 89-103	— 104	— 105											

TRANSITION ELEMENTS { BETWEEN GROUPS 2A AND 3A.

♦ LANTHANIDES (RARE EARTHS)	+3 La 57	+3 +4 Ce 58	+3 Pr 59	+3 Nd 60	+3 Pm 61	+2 +3 Sm 62	+2 +3 Eu 63	+3 Gd 64	+3 Tb 65	+3 Dy 66	+3 Ho 67	+3 Er 68	+3 Tm 69	+2 +3 Yb 70	+3 Lu 71
★ ACTINIDES	+3 Ac 89	+4 Th 90	+4 +5 Pa 91	+3 +4 +5 +6 U 92	+3 +4 +5 +6 Np 93	+3 +4 +5 +6 Pu 94	+3 +4 +5 +6 Am 95	+3 Cm 96	+3 +4 Bk 97	+3 Cf 98	Es 99	Fm 100	Md 101	No 102	Lw 103

KEY TO CHART: OXIDATION NUMBERS { +2 +4 −4 — OXIDATION NUMBER; Si — SYMBOL; 14 — ATOMIC NUMBER

ELECTRONIC CONFIGURATION OF THE ELEMENTS (TABLE 3)

n = principal quantum number

Maximum electron population of any energy level = $2n^2$.

OXIDATION POTENTIALS OF THE ELEMENTS

In all galvanic cells the observed voltage E_c arises from two independent voltages: oxidation potential E_{ox} and reduction potential E_{red}.

$$E_c = E_{ox} + E_{red}.$$

To determine independently the oxidation potential E_{ox} of a single electrode, the potential of the standard hydrogen electrode at 25°C (H_2 pressure 1 atmosphere and 1mH^+ concentration) is given arbitrarily the value 0. Then in a cell with the standard hydrogen electrode, the measured voltage is attributed to the half reaction at the other electrode.

The standard hydrogen electrode can play the role of an anode (oxidation process) or a cathode (reduction process) for electrode elements having respectively a negative or positive oxidation number.

Lithium (Li) is the best reducing agent since it has the highest tendency (+3.045 volts) to give up electrons (oxidation process). The fluoride ion (F^-) is the worst reducing agent.

The reducing agents arranged in decreasing order as in Table 4 are also called electromotive series.

TABLE 3.

Period	Atomic Number Z	Elements	n Shells	1 K	2 L		3 M			4 N				5 O				6 P				7 Q
			Subshells	s	s	p	s	p	d	s	p	d	f	s	p	d	f	s	p	d	f	s
I	1	H		1																		
	2	He		2																		
II	3	Li		2	1																	
	4	Be		2	2																	
	5	B		2	2	1																
	6	C		2	2	2																
	7	N		2	2	3																
	8	O		2	2	4																
	9	F		2	2	5																
	10	Ne		2	2	6																
III	11	Na		2	2	6	1															
	12	Mg		2	2	6	2															
	13	Al		2	2	6	2	1														
	14	Si		2	2	6	2	2														
	15	P		2	2	6	2	3														
	16	S		2	2	6	2	4														
	17	Cl		2	2	6	2	5														
	18	Ar		2	2	6	2	6														
IV	19	K		2	2	6	2	6		1												
	20	Ca		2	2	6	2	6		2												
	21	Sc		2	2	6	2	6	1	2												
	22	Ti		2	2	6	2	6	2	2												
	23	V		2	2	6	2	6	3	2												
	24	Cr		2	2	6	2	6	5	1												
	25	Mn		2	2	6	2	6	5	2												
	26	Fe		2	2	6	2	6	6	2												
	27	Co		2	2	6	2	6	7	2												
	28	Ni		2	2	6	2	6	8	2												
	29	Cu		2	2	6	2	6	10	1												
	30	Zn		2	2	6	2	6	10	2												
	31	Ga		2	2	6	2	6	10	2	1											
	32	Ge		2	2	6	2	6	10	2	2											
	33	As		2	2	6	2	6	10	2	3											
	34	Se		2	2	6	2	6	10	2	4											
	35	Br		2	2	6	2	6	10	2	5											
	36	Kr		2	2	6	2	6	10	2	6											
V	37	Rb		2	2	6	2	6	10	2	6			1								
	38	Sr		2	2	6	2	6	10	2	6			2								
	39	Y		2	2	6	2	6	10	2	6	1		2								
	40	Zr		2	2	6	2	6	10	2	6	2		2								
	41	Nb		2	2	6	2	6	10	2	6	4		1								
	42	Mo		2	2	6	2	6	10	2	6	5		1								
	43	Tc		2	2	6	2	6	10	2	6	6		1								
	44	Ru		2	2	6	2	6	10	2	6	7		1								
	45	Rh		2	2	6	2	6	10	2	6	8		1								
	46	Pd		2	2	6	2	6	10	2	6	10										
	47	Ag		2	2	6	2	6	10	2	6	10		1								
	48	Cd		2	2	6	2	6	10	2	6	10		2								
	49	In		2	2	6	2	6	10	2	6	10		2	1							
	50	Sn		2	2	6	2	6	10	2	6	10		2	2							
	51	Sb		2	2	6	2	6	10	2	6	10		2	3							

TABLE 3—CONTINUED.

Period	Atomic Number Z	Elements	n shells	1 K	2 L		3 M			4 N				5 O				6 P				7 Q
			subshells	s	s	p	s	p	d	s	p	d	f	s	p	d	f	s	p	d	f	s
	52	Te		2	2	6	2	6	10	2	6	10		2	4							
	53	I		2	2	6	2	6	10	2	6	10		2	5							
	54	Xe		2	2	6	2	6	10	2	6	10		2	6							
VI	55	Cs		2	2	6	2	6	10	2	6	10		2	6			1				
	56	Ba		2	2	6	2	6	10	2	6	10		2	6			2				
	57	La		2	2	6	2	6	10	2	6	10		2	6	1		2				
	58	Ce		2	2	6	2	6	10	2	6	10	2	2	6			2				
	59	Pr		2	2	6	2	6	10	2	6	10	3	2	6			2				
	60	Nd		2	2	6	2	6	10	2	6	10	4	2	6			2				
	61	Pm		2	2	6	2	6	10	2	6	10	5	2	6			2				
	62	Sm		2	2	6	2	6	10	2	6	10	6	2	6			2				
	63	Eu		2	2	6	2	6	10	2	6	10	7	2	6			2				
	64	Gd		2	2	6	2	6	10	2	6	10	7	2	6	1		2				
	65	Tb		2	2	6	2	6	10	2	6	10	9	2	6			2				
	66	Dy		2	2	6	2	6	10	2	6	10	10	2	6			2				
	67	Ho		2	2	6	2	6	10	2	6	10	11	2	6			2				
	68	Er		2	2	6	2	6	10	2	6	10	12	2	6			2				
	69	Tm		2	2	6	2	6	10	2	6	10	13	2	6			2				
	70	Yb		2	2	6	2	6	10	2	6	10	14	2	6			2				
	71	Lu		2	2	6	2	6	10	2	6	10	14	2	6	1		2				
	72	Hf		2	2	6	2	6	10	2	6	10	14	2	6	2		2				
	73	Ta		2	2	6	2	6	10	2	6	10	14	2	6	3		2				
	74	W		2	2	6	2	6	10	2	6	10	14	2	6	4		2				
	75	Re		2	2	6	2	6	10	2	6	10	14	2	6	5		2				
	76	Os		2	2	6	2	6	10	2	6	10	14	2	6	6		2				
	77	Ir		2	2	6	2	6	10	2	6	10	14	2	6	7		2				
	78	Pt		2	2	6	2	6	10	2	6	10	14	2	6	9		1				
	79	Au		2	2	6	2	6	10	2	6	10	14	2	6	10		1				
	80	Hg		2	2	6	2	6	10	2	6	10	14	2	6	10		2				
	81	Tl		2	2	6	2	6	10	2	6	10	14	2	6	10		2	1			
	82	Pb		2	2	6	2	6	10	2	6	10	14	2	6	10		2	2			
	83	Bi		2	2	6	2	6	10	2	6	10	14	2	6	10		2	3			
	84	Po		2	2	6	2	6	10	2	6	10	14	2	6	10		2	4			
	85	At		2	2	6	2	6	10	2	6	10	14	2	6	10		2	5			
	86	Rn		2	2	6	2	6	10	2	6	10	14	2	6	10		2	6			
VII	87	Fr		2	2	6	2	6	10	2	6	10	14	2	6	10		2	6			1
	88	Ra		2	2	6	2	6	10	2	6	10	14	2	6	10		2	6			2
	89	Ac		2	2	6	2	6	10	2	6	10	14	2	6	10		2	6	1		2
	90	Th		2	2	6	2	6	10	2	6	10	14	2	6	10		2	6	2		2
	91	Pa		2	2	6	2	6	10	2	6	10	14	2	6	10	2	2	6	1		2
	92	U		2	2	6	2	6	10	2	6	10	14	2	6	10	3	2	6	1		2
	93	Np		2	2	6	2	6	10	2	6	10	14	2	6	10	4	2	6	1		2
	94	Pu		2	2	6	2	6	10	2	6	10	14	2	6	10	6	2	6			2
	95	Am		2	2	6	2	6	10	2	6	10	14	2	6	10	7	2	6			2
	96	Cm		2	2	6	2	6	10	2	6	10	14	2	6	10	7	2	6	1		2
	97	Bk		2	2	6	2	6	10	2	6	10	14	2	6	10	9	2	6			2
	98	Cf		2	2	6	2	6	10	2	6	10	14	2	6	10	10	2	6			2
	99	Es		2	2	6	2	6	10	2	6	10	14	2	6	10	11	2	6			2
	100	Fm		2	2	6	2	6	10	2	6	10	14	2	6	10	12	2	6			2
	101	Md		2	2	6	2	6	10	2	6	10	14	2	6	10	13	2	6			2
	102	No		2	2	6	2	6	10	2	6	10	14	2	6	10	14	2	6			2
	103	Lw		2	2	6	2	6	10	2	6	10	14	2	6	10	14	2	6	1		2

TABLE 4—OXIDATION POTENTIALS OF ELEMENTS.

Element or Reducing Agent	Reaction	E_{ox} (volts)	Element or Reducing Agent	Reaction	E_{ox} (volts)
Lithium	$Li \rightarrow Li^{+} + 1e$	+3.045	Manganese	$Mn \rightarrow Mn^{++} + 2e$	+1.18
Potassium	$K \rightarrow K^{+} + 1e$	+2.925	Vanadium	$V \rightarrow V^{++} + 2e$	+1.18
Rubidium	$Rb \rightarrow Rb^{+} + 1e$	+2.925	Niobium	$Nb \rightarrow Nb^{+++} + 3e$	+1.1
Cesium	$Cs \rightarrow Cs^{+} + 1e$	+2.923	Tellurium	$Te^{--} \rightarrow Te + 2e$	+0.92
Radium	$Ra \rightarrow Ra^{++} + 2e$	+2.92	Selenium	$Se^{--} \rightarrow Se + 2e$	+0.78
Barium	$Ba \rightarrow Ba^{++} + 2e$	+2.90	Zinc	$Zn \rightarrow Zn^{++} + 2e$	+0.763
Strontium	$Sr \rightarrow Sr^{++} + 2e$	+2.89	Chromium	$Cr \rightarrow Cr^{++} + 2e$	+0.56
Calcium	$Ca \rightarrow Ca^{++} + 2e$	+2.87	Gallium	$Ga \rightarrow Ga^{+++} + 3e$	+0.56
Sodium	$Na \rightarrow Na^{+} + 1e$	+2.714	Sulfur	$S^{--} \rightarrow S + 2e$	+0.51
Lanthanum	$La \rightarrow La^{+++} + 3e$	+2.52	Iron	$Fe \rightarrow Fe^{++} + 2e$	+0.44
Cerium	$Ce \rightarrow Ce^{+++} + 3e$	+2.48	Cadmium	$Cd \rightarrow Cd^{++} + 2e$	+0.403
Neodymium	$Nd \rightarrow Nd^{+++} + 3e$	+2.44	Indium	$In \rightarrow In^{+++} + 3e$	+0.345
Samarium	$Sm \rightarrow Sm^{+++} + 3e$	+2.41	Thallium	$Tl \rightarrow Tl^{+} + 1e$	+0.336
Gadolinium	$Gd \rightarrow Gd^{+++} + 3e$	+2.40	Cobalt	$Co \rightarrow Co^{++} + 2e$	+0.277
Magnesium	$Mg \rightarrow Mg^{++} + 2e$	+2.37	Nickel	$Ni \rightarrow Ni^{++} + 2e$	+0.246
Yttrium	$Y \rightarrow Y^{+++} + 3e$	+2.37	Molybdenum	$Mo \rightarrow Mo^{+++} + 3e$	+0.2
Dysprosium	$Dy \rightarrow Dy^{+++} + 3e$	+2.35	Tin	$Sn \rightarrow Sn^{++} + 2e$	+0.136
Ytterbium	$Yb \rightarrow Yb^{+++} + 3e$	+2.27	Lead	$Pb \rightarrow Pb^{++} + 2e$	+0.126
Lutetium	$Lu \rightarrow Lu^{+++} + 3e$	+2.25	Hydrogen	$H_2 \rightarrow 2H^{+} + 2e$	0.000
Hydrogen	$H^{-} \rightarrow \frac{1}{2}H_2 + 1e$	+2.25	Copper	$Cu \rightarrow Cu^{++} + 2e$	−0.337
Scandium	$Sc \rightarrow Sc^{+++} + 3e$	+2.08	Iodine	$2I^{-} \rightarrow I_2 + 2e$	−0.536
Plutonium	$Pu \rightarrow Pu^{+++} + 3e$	+2.02	Rhodium	$Rh \rightarrow Rh^{+} + 1e$	−0.6
Thorium	$Th \rightarrow Th^{++++} + 4e$	+1.90	Silver	$Ag \rightarrow Ag^{+} + 1e$	−0.7995
Neptunium	$Np \rightarrow Np^{+++} + 3e$	+1.86	Mercury	$Hg \rightarrow Hg^{++} + 2e$	−0.854
Beryllium	$Be \rightarrow Be^{++} + 2e$	+1.85	Palladium	$Pd \rightarrow Pd^{++} + 2e$	−0.987
Uranium	$U \rightarrow U^{+++} + 3e$	+1.80	Bromine	$2Br^{-} \rightarrow Br_2(liq) + 2e$	−1.065
Hafnium	$Hf \rightarrow Hf^{++++} + 4e$	+1.70	Platinum	$Pt \rightarrow Pt^{++} + 2e$	−1.2
Aluminum	$Al \rightarrow Al^{+++} + 3e$	+1.66	Chlorine	$2Cl^{-} \rightarrow Cl_2 + 2e$	−1.36
Titanium	$Ti \rightarrow Ti^{++} + 2e$	+1.63	Gold	$Au \rightarrow Au^{+} + 1e$	−1.68
Zirconium	$Zr \rightarrow Zr^{++++} + 4e$	+1.53	Fluorine	$2F^{-} \rightarrow F_2 + 2e$	−2.87

TABLE 5—PHYSICAL PROPERTIES

	Symbol	Atomic Number	Density at 20°C (gr/cm³)	Relative Hardness	Melting Point (°C)	Boiling Point (°C)
Actinium	Ac	89			1 050	3 200
Aluminum	Al	13	2.70	2.9	660	2 467
Americium	Am	95	13.67		994	2 600
Antimony	Sb	51	6.62	3	630.5	1 750
Argon	Ar or A	18	1.78*		−189.2	−185.7
Arsenic (gray)	As	33	5.73	3.5	820‡	615¶
Astatine	At	85			302	337
Barium	Ba	56	3.5		725	1 640
Berkelium	Bk	97				
Beryllium	Be	4	1.82	3	1 278	2 970
Bismuth	Bi	83	9.80	2.5	271.3	1 560
Boron	B	5	2.46	9.5	2 300	2 550¶
Bromine	Br	35	3.12		−7.2	58.8
Cadmium	Cd	48	8.65	2.0	320.9	765
Calcium	Ca	20	1.54		842	1 487
Californium	Cf	98				
Carbon	C	6	2.22	10†	>3 500	4 827
Cerium	Ce	58	6.9	2.5	795	3 468
Cesium	Cs	55	1.87	0.2	28.5	690
Chlorine	Cl	17	3.21*		−100.98	−34.7
Chromium	Cr	24	7.14	9	1 890	2 672
Cobalt	Co	27	8.9	5	1 495	2 900
Copper	Cu	29	8.96	3	1 083	2 595
Curium	Cm	96	13.51		1 340	
Dysprosium	Dy	66	8.54		1 407	2 600
Einsteinium	Es or E	99				
Erbium	Er	68	9.05		1 497	2 900
Europium	Eu	63	5.26		826	1 439
Fermium	Fm	100				
Fluorine	F	9	1.69* at 15°C		−220	−188
Francium	Fr	87			27	677
Gadolinium	Gd	64	7.89		1 312	3 000
Gallium	Ga	31	5.91	1.5	29.78	2 403
Germanium	Ge	32	5.36	6.2	937.4	2 830
Gold	Au	79	19.3	2.5	1 063	2 966
Hafnium	Hf	72	13.31		2 220	4 602
Helium	He	2	0.1664*		<−272§	−268.94
Holmium	Ho	67	8.803		1 461	2 600
Hydrogen	H	1	0.08375*		−259.14	−252.8
Indium	In	49	7.31	1.2	156	2 050
Iodine	I	53	4.93		113.5	184.3
Iridium	Ir	77	22.4	6.15	2 410	4 527
Iron	Fe	26	7.87	4	1 535	3 000
Krypton	Kr	36	3.448*		−156.6	−152.3
Lanthanum	La	57	6.15		920	3 469
Lawrencium	Lw	103				
Lead	Pb	82	11.34	1.5	327.4	1 744
Lithium	Li	3	0.53	0.6	179	1 336
Lutetium	Lu	71	9.84		1 652	3 327
Magnesium	Mg	12	1.74	2	651	1 100
Manganese	Mn	25	7.44	5.0	1 244	2 097
Mendelevium	Md or Mv	101				
Mercury	Hg	80	13.55	1.5	−38.87	356.9

OF THE ELEMENTS.

Latent Heat of Fusion (cal/gr)	Specific Heat at 20°C (cal/gr °C)	Thermal Conductivity at 20°C (watts/cm °C)	Linear Thermal Expansion per °C at 20°C ($\times 10^{-6}$)	Elasticity Modulus (kg/mm²)	Tensile Strength (kg/mm²)
93	0.226	2.18	22.9	7 250	6.3
38.3	0.049	0.19	8.5–10.8	7 900	1.05
6.7	0.125	1.7×10^{-4}			
	0.082		4.7		
324	0.425	1.64	12	30 000	12.0
12.5	0.0294	0.084	13.3	3 200	
	0.307		2		
16.2	0.107				
13.2	0.055	0.91	29.8	5 500	7.2
	0.145		25	2 100	5.7
	0.165	0.24	0.6–4.3	500	
	0.042				9.05
3.8	0.052		97		
23	0.226	0.072×10^{-4}			
75.6	0.11	0.69	6.2		
58.4	0.1001	0.69	12.3	21 000	24.4
50.6	0.0921	3.94	16.5	11 000	22.5
10.1					
19.2	0.079		18		
	0.073				
16.1	0.031	2.96	14.2	7 300	11.5
	1.25	13.9×10^{-4}			
15	3.415	17×10^{-4}			
	0.057	0.24	33		0.3
15.8	0.052	43.5×10^{-4}	93		
33	0.032	1.4	6.5	52 500	
65	0.108	0.79	11.7	20 000	20.5
		0.89×10^{-4}			
	0.045				
6.3	0.030	0.35	28.7	1 800	1.33
159	0.79	0.71	56		
88	0.249	1.55	25.2	4 600	9.15
64.8	0.107		23	16 000	39.0
2.7	0.033	0.084			

TABLE 5–

	Symbol	Atomic Number	Density at 20°C (gr/cm³)	Relative Hardness	Melting Point (°C)	Boiling Point (°C)
Molybdenum	Mo	42	10.2	6	2 610	4 800
Neodymium	Nd	60	7.05		1 024	3 027
Neon	Ne	10	0.8387*		−248.7	−245.9
Neptunium	Np	93	20.45		640	3 902
Nickel	Ni	28	8.9	5	1 453	2 732
Niobium	Nb	41	8.57		2 468	5 127
Nitrogen	N	7	1.1649*		−209.9	−195.8
Nobelium	No	102				
Osmium	Os	76	22.48	7.0	3 000	5 000
Oxygen	O	8	1.3318*		−218.4	−183
Palladium	Pd	46	12	4.8	1 552	2 927
Phosphorus	P	15	1.82		44.1	280
Platinum	Pt	78	21.45	4.3	1 769	3 827
Plutonium	Pu	94	19.82		639.5	3 235
Polonium	Po	84	9.2		254	962
Potassium	K	19	0.86	0.5	63.65	774
Praseodymium	Pr	59	6.63		935	3 127
Promethium	Pm	61			1 027	2 027
Protactinium	Pa	91	15.37		1 227	4 027
Radium	Ra	88	5		700	1 525
Radon	Rn	86	4.40*		−71	−61.8
Rhenium	Re	75	20		3 180	5 627
Rhodium	Rh	45	12.44	6	1 966	3 727
Rubidium	Rb	37	1.53	0.3	38.5	688
Ruthenium	Ru	44	12.2	6.5	2 250	3 900
Samarium	Sm	62	7.7		1 072	1 900
Scandium	Sc	21	2.5		1 539	2 727
Selenium	Se	34	4.81	2	217	685
Silicon	Si	14	2.4	7	1 410	2 355
Silver	Ag	47	10.49	2.7	960.8	2 212
Sodium	Na	11	0.97	0.4	97	892
Strontium	Sr	38	2.6	1.8	769	1 384
Sulfur	S	16	2.07	2.0	116	444.6
Tantalum	Ta	73	16.6	7	2 996	5 425
Technetium	Tc	43	11.49		2 200	4 700
Tellurium	Te	52	6.24	2.3	449.5	990
Terbium	Tb	65	8.27		1 356	2 800
Thallium	Tl	81	11.85	1.2	303.5	1 457
Thorium	Th	90	11.5		1 800	4 200
Thulium	Tm	69	9.33		1 545	1 727
Tin	Sn	50	7.3	1.8	231.89	2 270
Titanium	Ti	22	4.54	4	1 675	3 260
Tungsten	W	74	19.3	7	3 410	5 660
Uranium	U	92	18.7		1 133	3 818
Vanadium	V	23	5.68		1 890	3 400
Xenon	Xe	54	5.495*		−111	−107
Ytterbium	Yb	70	6.98		824	1 427
Yttrium	Y	39	5.51		1 495	2 927
Zinc	Zn	30	7.14	2.5	419.4	907
Zirconium	Zr	40	6.4	4.7	1 852	4 377

* per liter. † diamond ‡ 36 atm § 26 atm ¶ sublimes

CONTINUED.

Latent Heat of Fusion (cal/gr)	Specific Heat at 20°C (cal/gr °C)	Thermal Conductivity at 20°C (watts/cm °C)	Linear Expansion per °C at 20°C ($\times 10^6$)	Elasticity Modulus (kg/mm²)	Tensile Strength (kg/mm²)
69.0	0.065	1.46	4.9	35 000	120.0
	0.045				
		4.57×10^{-4}			
73.8	0.112	0.9	13.3	21 000	32.3
68.0	0.064	0.52	7.1		
6.2	0.247				
34.0	0.031	0.61	5		
3.3	0.218				
34.2	0.059	0.70	11.8	12 000	14.0
5.0	0.177		125		
27.1	0.032	0.69	8.9	15 000	16
3.0	0.032	0.08	54		
14.5	0.177	0.99	83		
	0.458				
	0.035				
50.0	0.060	1.5	8.1	3 000	
6.1	0.080		90		
	0.061		9.1		
16.0	0.077	0.005	37		
430.0	0.176	0.84	2.8–7.3	11 000	
24.3	0.056	4.08	18.9	7 200	15.1
27.5	0.295	1.35	71		
25					
9.3	0.175	26.4×10^{-4}	6.4		
41.0	0.036	0.54	6.6	19 000	50
25.3	0.047	0.060	16.8	2 100	1.12
7.2	0.031	0.39	28		
17.0	0.028	0.41	11.1		56
14.4	0.054	0.64	23	41 100	1.4
100.0	0.142	0.2	8.5	8 500	
44.0	0.034	1.99	4.3	35 000	270
12.0	0.028	0.25	13.4		
98.0	0.115	0.60	8		
		5.9×10^{-4}			
24.1	0.09	1.1	17–39	8 400	10.5
	0.066		5.6	7 500	30

In air all the metals from lithium down to copper rust with comparative ease. The metals below copper do not rust.

All metals in the series above hydrogen (H_2) are found in nature in the combined state as sulfides, carbonates, etc. Metals below hydrogen (H_2) are frequently found in the free state.

PHYSICAL PROPERTIES OF THE ELEMENTS (TABLE 5)

GALVANIC SERIES IN SEA WATER

Two dissimilar metals connected by a conductor form in sea water a galvanic cell. If the two metals are in different groups of Table 6 (separated by spaces), the metal coming first in the series—starting from corroded end to protected end—will be anodic, (i.e., corroded by the metal contained in the group farther from the corroded end) If the two metals are in the same group, no appreciable corrosive action will take place.

TEMPERATURE–EMF CHARACTERISTICS OF THERMOCOUPLES* (FIG. 1)

Electromotive Force and Other Properties (Tables 7–8)

* R. L. Weber, "Temperature Measurement and Control," Blakiston Co., Philadelphia, Pennsylvania; 1941: pp. 68–71.

TABLE 6—GALVANIC SERIES IN SEA WATER.

Corroded end (anodic)

Magnesium
Magnesium alloys

Zinc
Galvanized steel
Galvanized wrought iron

Aluminum:
52SH, 4S, 3S, 2S, 53ST
Aluminum clad

Cadmium

Aluminum:
A17ST, 17ST, 24ST

Mild steel
Wrought iron
Cast iron

Ni-resist

13% chromium stainless steel
(type 410–active)

50–50 lead–tin solder

18–8 stainless steel type 304
(active)
18–8–3 stainless steel type 316
(active)

Lead
Tin

Muntz metal
Manganese bronze
Naval brass

Nickel (active)
Inconel (active)

Yellow brass
Admiralty brass
Aluminum bronze
Red brass
Copper
Silicon bronze
Ambrac
70–30 copper–nickel
Comp. G, bronze
Comp. M, bronze

Nickel (passive)
Inconel (passive)

Monel

18–8 stainless steel type 304
(passive)
18–8–3 stainless steel type 316
(passive)

Protected end (cathodic or most noble)

Table 7—Thermocouples and Their Characteristics.

Type	Copper/Constantan		Iron/Constantan		Chromel/Constantan		Chromel/Alumel		Platinum/Platinum Rhodium (10)		Platinum/Platinum Rhodium (13)		Carbon/Silicon Carbide	
Composition, percent	100 Cu/60 Cu 40 Ni		100 Fe/60 Cu 40 Ni		90 Ni 10 Cr/55 Cu 45 Ni		90 Ni 10 Cr/94 Ni 2 Al 3 Mn 1 Si		Pt/90 Pt 10 Rh		Pt/87 Pt 13 Rh		C/SiC	
*Range of application, °C	−200 to +300		−200 to +1100		0 to +1100		−200 to +1200		0 to +1450		0 to +1450		0 to +2000	
Resistivity, microhm-cm	1.75	49	10	49	70	49	70	29.4	10	21				
Temperature coefficient of resistivity, per °C	0.0039	0.00001	0.005	0.00001	0.00035	0.0002	0.00035	0.000125	0.0030	0.0018				
Melting temperature, °C	1085	1190	1535	1190	1400	1190	1400	1430	1755	1700			3000	2700
emf in millivolts; reference junction at 0°C	100°C	4.24mV	100°C	5.28mV	100°C	6.3mV	100°C	4.1mV	100°C	0.643mV	100°C	0.646mV	1210°C	353.6mV
	200	9.06	200	10.78	200	13.3	200	8.13	200	1.436	200	1.464	1300	385.2
	300	14.42	400	21.82	400	28.5	400	16.39	400	3.251	400	3.398	1360	403.2
			600	33.16	600	44.3	600	24.90	600	5.222	600	5.561	1450	424.9
			800	45.48			800	33.31	800	7.330	800	7.927		
			1000	58.16			1000	41.31	1000	9.569	1000	10.470		
							1200	48.85	1200	11.924	1200	13.181		
							1400	55.81	1400	14.312	1400	15.940		
									1600	16.674	1600	18.680		
Influence of temperature and gas atmosphere	Subject to oxidation and alteration above 400°C due Cu, above 600° due constantan wire. Ni-plating of Cu tube gives protection in acid-containing gas. Contamination of Cu affects calibration greatly. Resistance to oxid. atm. good. Resistance to reducing atm. good. Requires protection from acid fumes.		Oxidizing and reducing atmosphere have little effect on accuracy. Best used in dry atmosphere. Resistance to oxidation good to 400°C. Resistance to reducing atmosphere good. Protect from oxygen, moisture, sulphur.		Chromel attacked by sulphurous atmosphere. Resistance to oxidation good. Resistance to reducing atmosphere poor.		Resistance to oxidizing atmosphere very good. Resistance to reducing atmosphere poor. Affected by sulphur, reducing or sulphurous gas, SO_2 and H_2S.		Resistance to oxidizing atmosphere very good. Resistance to reducing atmosphere poor. Susceptible to chemical alteration by As, Si, P vapor in reducing gas (CO_2, H_2, H_2S, SO_2). Pt corrodes easily above 1000°. Used in gas-tight protecting tube.				Used as tube element. Carbon sheath chemically inert.	
Particular applications	Low temperature, industrial. Internal-combustion engine. Used as a tube element for measurements in steam line.		Low temperature, industrial. Steel annealing, boiler flues, tube stills. Used in reducing or neutral atmosphere.				Used in oxidizing atmosphere. Industrial. Ceramic kilns, tube stills, electric furnaces.		International Standard 630 to 1065°C.		Similar to Pt/PtRh-(10) but has higher emf.		Steel furnace and ladle temperatures. Laboratory measurements.	

* For prolonged use; can be used at higher temperature for short periods.

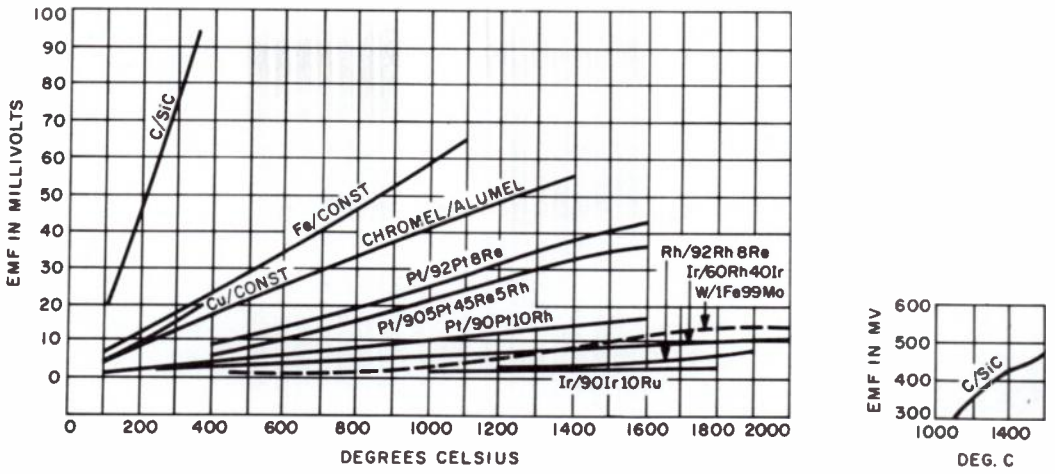

Fig. 1.

TABLE 8—THERMAL ELECTROMOTIVE FORCE OF PLATINUM–RHODIUM ALLOYS VERSUS PLATINUM. *From "Smithsonian Physical Tables," 9th revised edition, vol. 120, Smithsonian Institution, Washington, D. C.; 1969.*

	Electromotive Force (millivolts)							
	Percent Rhodium							
Temp., °C	0.5	1.0	5.0	10.0	20.0	40.0	80.0	100.0
0	0.00	0.00	0.00	0.00	0.00	0.00	0.00	0.00
100	+0.10	+0.18	+0.54	+0.64	+0.63	+0.65	+0.62	+0.70
200	0.20	0.37	1.16	1.43	1.44	1.52	1.49	1.61
300	0.29	0.57	1.82	2.32	2.40	2.55	2.55	2.68
400	0.39	0.76	2.49	3.25	3.47	3.70	3.77	3.91
500	0.48	0.94	3.17	4.22	4.63	4.97	5.12	5.28
600	0.58	1.12	3.86	5.22	5.87	6.36	6.60	6.77
700	0.67	1.30	4.55	6.26	7.20	7.85	8.20	8.40
800	0.76	1.48	5.25	7.33	8.59	9.45	9.92	10.16
900	0.85	1.66	5.96	8.43	10.06	11.16	11.76	12.04
1000	0.94	1.84	6.68	9.57	11.58	12.98	13.73	14.05
1100	1.03	2.02	7.42	10.74	13.17	14.90	15.81	16.18
1200	1.13	2.20	8.16	11.93	14.84	16.91	17.99	18.42

TABLE 9—MELTING POINTS OF MIXTURES OF METALS. *From "Smithsonian Physical Tables," 9th revised edition, vol. 120, Smithsonian Institution, Washington, D. C.; 1969.*

	Melting Points, °C										
	Percentage of second metal in metals column										
Metals	0	10	20	30	40	50	60	70	80	90	100
Pb Sn	327	295	276	262	240	220	190	185	200	216	232
Bi	327	290	—	—	179	145	126	168	205	—	271
Te	327	710	790	880	917	760	600	480	410	425	452
Ag	327	460	545	590	620	650	705	775	840	905	961
Na	327	360	420	400	370	330	290	250	200	130	97.5
Cu	327	870	920	925	945	950	955	985	1005	1020	1083
Sb	327	250	275	330	395	440	490	525	560	600	631
Al Sb	660	750	840	925	945	950	970	1000	1040	1010	631
Cu	660	630	600	560	540	580	610	755	930	1055	1083
Au	660	675	740	800	855	915	970	1025	1055	675	1063
Ag	660	625	615	600	590	580	575	570	650	750	961
Zn	660	640	620	600	580	560	530	510	475	425	419
Fe	660	860	1015	1110	1145	1145	1220	1315	1425	1500	1533
Sn	660	645	635	625	620	605	590	570	560	540	232
Sb Bi	631	610	590	575	555	540	520	470	405	330	271
Ag	631	595	570	545	520	500	505	545	680	850	961
Sn	631	600	570	525	480	430	395	350	310	255	232
Zn	631	555	510	540	570	565	540	525	510	470	419
Ni Sn	1453	1380	1290	1200	1235	1290	1305	1230	1060	800	232
Na Bi	97.5	425	520	590	645	690	720	730	715	570	271
Cd	97.5	125	185	245	285	325	330	340	360	390	321
Cd Ag	321	420	520	610	700	760	805	850	895	940	961
Tl	321	300	285	270	262	258	245	230	210	235	303
Zn	321	280	270	295	313	327	340	355	370	390	419
Au Cu	1063	910	890	895	905	925	975	1000	1025	1060	1083
Ag	1063	1062	1061	1058	1054	1049	1039	1025	1006	982	961
Pt	1063	1125	1190	1250	1320	1380	1455	1530	1610	1685	1769
K Na	63	17.5	−10	−3.5	5	11	26	41	58	77	97.5
Hg	63	—	—	—	—	90	110	135	162	265	—
Tl	63	133	165	188	205	215	220	240	280	305	303
Cu Ni	1083	1180	1240	1290	1320	1335	1380	1410	1430	1440	1453
Ag	1083	1035	990	945	910	870	830	788	814	875	961
Sn	1083	1005	890	755	725	680	630	580	530	440	232
Zn	1083	1040	995	930	900	880	820	780	700	580	419
Ag Zn	961	850	755	705	690	660	630	610	570	505	419
Sn	961	870	750	630	550	495	450	420	375	300	232
Na Hg	97.5	90	80	70	60	45	22	55	95	215	—

TABLE 10—MELTING POINTS IN °C OF LOW-MELTING-POINT ALLOYS. *From "Smithsonian Physical Tables," 9th revised edition, vol. 120, Smithsonian Institution, Washington, D. C.; 1969.*

	Percent						
Cadmium	10.8	10.2	14.8	13.1	6.2	7.1	6.7
Tin	14.2	14.3	7.0	13.8	9.4	—	—
Lead	24.9	25.1	26.0	24.3	34.4	39.7	43.4
Bismuth	50.1	50.4	52.2	48.8	50.0	53.2	49.9
Solidification at	65.5°	67.5°	68.5°	68.5°	76.5°	89.5°	95°

	Percent									
Lead	32.0	25.8	25.0	43.0	33.3	10.7	50.0	35.8	20.0	70.9
Tin	15.5	19.8	15.0	14.0	33.3	23.1	33.0	52.1	60.0	9.1
Bismuth	52.5	54.4	60.0	43.0	33.3	66.2	17.0	12.1	20.0	20.0
Solidification at	96°	101°	125°	128°	145°	148°	161°	181°	182°	234°

TEMPERATURE CHARTS OF METALS (TABLES 9–10)

SURFACE TENSIONS OF MATERIALS

To extend the surface of a liquid, some molecules from the interior must be brought to the surface and some work must be done against the inward attractive forces.

In extending the surface of a liquid, the work per unit area extended is by definition the surface tension of the liquid. The work per unit area expressed in ergs/cm² may also be expressed in dynes/cm. Then the concept of work per unit area can be replaced by a hypothetical tension γ, which is the normal tensile force per unit of length traced on the surface of the liquid.

Surface tensions of liquids and particularly solids at melting point play an important role in zone-leveling and zone-refining processes, in which the material in rod form is often in a vertical position and the molten zone is held in place by its surface tension. The maximum height of the stable molten zone is given by

$$h_z(\text{cm}) = 2.8(\gamma/\rho g)^{1/2}$$

from Heywang, ρ being the density in gr/cm³, and g=gravity.

As the molten zone is moving along the rod, the impurity will travel in the same direction as the molten zone if the impurity depresses the freezing point and in the opposite direction if the impurity raises the freezing point.

Some values of γ, ρ, and h_z are given in Table 11.

Surface tensions of some liquids at room temperature are given below (in dynes/cm).

Water	71.9
Alcohol	21.8
Mercury	513
Mercury under water	392
Turpentine	28.8
Glycerine	63

Rise in capillarity tube, diameter=$2r$ (Fig. 2)

$$h = 2\gamma/\rho g r.$$

Angle of contact α

$$\cos\alpha = r\rho g h/2\gamma.$$

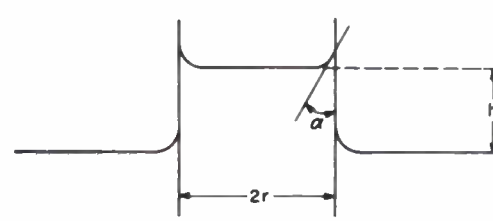

Fig. 2.

TABLE 11—SURFACE TENSIONS OF ELEMENTS AND OTHER CONSTANTS. Taylor's (1954) estimated values are given in parentheses ( ) where no experimental values were available. Room temperature values for density and italicized values for surface tension were used in calculating the surface tension/density ratios and the Heywang zone lengths. Various tables of reference (Honig, 1962; Taylor, 1954) were used to obtain many values for the other physical constants.

Element	Atomic Number	Density, ρ(g/cm³) Room Temp.	Density, ρ(g/cm³) Melting Point	Surface Tension γ at Melting Point (dynes/cm)	Ratio: Surface Tension/Density	Stable Zone Height h_z(cm) from Heywang's Equation
Ag	47	10.49	9.3	800	76	0.78
Al	13	2.70	2.37	*840*, 915	311	1.58
As	33	5.72	—	—	—	—
Au	79	19.32	—	*580*, 1000	30	0.49
B	5	2.34	2.08	1060	453	1.91
Ba	56	3.5	—	224	64	0.72
Be	4	1.85	—	(1620)	876	2.64
Bi	83	9.80	10.06	388	40	0.56
C	6	2.25	—	—	—	—
Ca	20	1.55	—	*337*	218	1.32
Cd	48	8.65	8.02	*630*, 550	73	0.76
Ce	58	6.77	—	(610)	90	0.84
Co	27	8.85	—	*1880*	212	1.30
Cr	24	7.19	—	(1420)	198	1.25
Cs	55	1.90	1.84	(55)	29	0.48
Cu	29	8.96	—	*1265*, 1103	141	1.06
Dy	66	8.55	—	—	—	—
Er	68	9.15	—	—	—	—
Eu	63	5.24	—	—	—	—
Fe	26	7.87	—	*1754*, 1510	223	1.34
Ga	31	5.91	—	*358*, 735	61	0.70
Gd	64	7.86	—	—	—	—
Ge	32	5.32	5.575	600	113	0.95
Hf	72	13.09	—	1460	112	0.95
Ho	67	8.80	—	—	—	—
I	53	4.94	—	—	—	—
In	49	7.31	7.03	*513*, 599	70	0.75
Ir	77	22.5	—	(2310)	103	0.90
K	19	0.86	—	86	100	0.89
La	57	6.19	—	—	—	—
Li	3	0.534	0.51	(430)	805	2.54
Lu	71	9.85	—	—	—	—
Mg	12	1.74	1.57	*556*, 987	320	1.60
Mn	25	7.43	6.54	(1050)	141	1.06
Mo	42	10.22	—	2080	204	1.28

TABLE 11—CONTINUED.

Element	Atomic Number	Density, ρ(g/cm³) Room Temp.	Density, ρ(g/cm³) Melting Point	Surface Tension γ at Melting Point (dynes/cm)	Ratio: Surface Tension/Density	Stable Zone Height h_s(cm) from Heywang's Equation
Na	11	0.97	0.93	192.2	198	1.26
Nb	41	8.57	—	(2030)	237	1.38
Nd	60	7.00	—	688	98	0.89
Ni	28	8.9	—	*1735*, 1660, 1670	195	1.25
Os	76	22.57	—	(2450)	108	0.93
P	15	1.82	—	—	—	—
Pb	82	11.4	10.6	440	39	0.56
Pd	46	12.02	—	1470	122	0.99
Pr	59	6.77	—	—	—	—
Pt	78	21.45	—	1819 (at 2000°C)	85	0.83
Ra	88	5.00	—	—	—	—
Rb	37	1.53	—	(75)	49	0.63
Re	75	21.04	—	(2480)	118	0.97
Rh	45	12.44	10.65	1940	156	1.12
Ru	44	12.2	—	—	—	—
S	16	2.07	—	—	—	—
Sb	51	6.62	6.50	383	58	0.68
Sc	21	2.99	—	—	—	—
Se	34	4.79	—	*720*, 712, 732	150	1.57
Si	14	2.33	—	*72*	30.9	0.35
Sm	62	7.49	—	—	—	—
Sn	50	7.30	—	*566*, 625	78	0.79
Sr	38	2.60	—	288	111	0.94
Ta	73	16.6	—	*1910*, 2300	115	0.96
Tb	65	8.25	—	—	—	—
Te	52	6.24	—	(300)	48	0.62
Th	90	11.66	—	(1075)	92	0.86
Ti	22	4.51	—	*1390*, 1588, 1460	309	1.57
Tl	81	11.85	11.29	*465*, 401	39	0.56
Tm	69	9.31	—	—	—	—
U	92	19.07	—	(1020)	53	0.65
V	23	6.1	—	(1710)	280	1.50
W	74	19.3	—	2300	119	0.98
Y	39	4.47	—	—	—	—
Yb	70	6.96	—	—	—	—
Zn	30	7.13	6.7	824	116	0.96
Zr	40	6.49	—	*1400*, 1390	216	1.32

CONDUCTING MATERIALS (TABLES 12–14)

Conducting materials (Table 12) can be classified as follows:

Conductors: Resistivities from 10^{-6} to 10^{-4} ohm-cm (1 to 100 microhm-cm). Conductivities from 10^{4} to 10^{6} mho-cm^{-1}.

Semiconductors: Resistivities from 10^{-4} to 10^{9} ohm-cm. Conductivities from 10^{-9} to 10^{4} mho-cm^{-1}.

Insulators: Resistivities from 10^{9} to 10^{25} ohm-cm. Conductivities from 10^{-25} to 10^{-9} mho-cm^{-1}.

TABLE 12—RESISTIVITIES OF METALS AND ALLOYS.

Material	Form	Resistivity (ohm-cm×10^{-6})	Temperature (°C)	Temperature Coefficient
Alumel	solid	33.3	0	0.0012
Aluminum	liquid	20.5	670	
	solid	2.62	20	0.0039
Antimony	liquid	123	800	
	solid	39.2	20	0.0036
Arsenic	solid	35	0	0.0042
Beryllium		4.57	20	
Bismuth	liquid	128.9	300	
	solid	115	20	0.004
Boron		1.8×10^{12}	0	
Brass (66 Cu 34 Zn)		3.9	20	0.002
Cadmium	liquid	34	400	
	solid	7.5	20	0.0038
Carbon	diamond	5×10^{20}	15	
	graphite	1400	20	−0.0005
Cerium		78	20	
Cesium	liquid	36.6	30	
	solid	20	20	
		18.83	0	
Chromax (15 Cr, 35 Ni, balance Fe)		100	20	0.00031
Chromel	solid	70–110	0	0.00011–0.000054
Chromium		2.6	0	
Cobalt		9.7	20	0.0033
Constantan (55 Cu, 45 Ni)		44.2	20	+0.0002
Copper (commercial annealed)	liquid	21.3	1083	
	solid	1.7241	20	0.0039
Gallium	liquid	27	30	
	solid	53	0	
Germanium		45	20	
German silver (18% Ni)		33	20	0.0004
Gold	liquid	30.8	1063	
	solid	2.44	20	0.0034
		2.19	0	
Hafnium		32.1	20	
Indium	liquid	29	157	
	solid	9	20	0.00498
Iridium		5.3	20	0.0039
Iron		9.71	20	0.0052–0.0062
Kovar A (29 Ni, 17 Co, 0.3 Mn, balance Fe)		45–85	20	
Lead	liquid	98	400	
	solid	21.9	20	0.004
PbO_2		92		

TABLE 12—CONTINUED.

Material	Form	Resistivity (ohm-cm×10^{-6})	Temperature (°C)	Temperature Coefficient
Lithium	liquid	45	230	0.003
	solid	9.3	20	0.005
Magnesium		4.46	20	0.004
Manganese		5	20	
Manganin (84 Cu, 12 Mn, 4 Ni)		44	20	±0.0002
Mercury	liquid	95.8	20	0.00089
	solid	21.3	−50	
Molybdenum		5.17	0	
		4.77	20	0.0033
MnO_2		6 000 000	20	
Monel metal (67 Ni, 30 Cu, 1.4 Fe, 1 Mn)	solid	42	20	0.002
Neodymium	solid	79	18	
Nichrome (65 Ni, 12 Cr, 23 Fe)	solid	100	20	0.00017
Nickel	solid	6.9	20	0.0047
Nickel–silver (64 Cu, 18 Zn, 18 Ni)	solid	28	20	0.00026
Niobium		12.4	20	
Osmium		9	20	0.0042
Palladium		10.8	20	0.0033
Phosphor bronze (4 Sn, 0.5 P, balance Cu)		9.4	20	0.003
Platinum		10.5	20	0.003
Plutonium		150	20	
Potassium	liquid	13	62	
	solid	7	20	0.006
Praseodymium		68	25	
Rhenium		19.8	20	
Rhodium		5.1	20	0.0046
Rubidium		12.5	20	
Ruthenium		10	20	
Selenium	solid	1.2	20	
Silicon		85×10^{3}	20	
Silver		1.62	20	0.0038
Sodium	liquid	9.7	100	
	solid	4.6	20	
Steel (0.4–0.5 C, balance Fe)		13–22	20	0.003
Steel, manganese (13 Mn, 1 C, 86 Fe)		70	20	0.001
Steel, stainless (0.1 C, 18 Cr, 8 Ni, balance Fe)		90	20	
Strontium		23	20	
Sulfur		2×10^{23}	20	
Tantalum		13.1	20	0.003
Thallium		18.1	20	0.004
Thorium		18	20	0.0021
Tin		11.4	20	0.0042
Titanium		47.8	25	
Tungsten		5.48	20	0.0045
Tophet A (80 Ni, 20 Cr)		108	20	0.00014
Uranium		29	0	0.0021
W_2O_5		450	20	
WO_3		2×10^{11}	20	
Zinc	liquid	35.3	420	
	solid	6	20	0.0037
Zirconium		40	20	0.0044

SEMICONDUCTING MATERIALS (TABLES 15–18)

INSULATING MATERIALS

The permittivity ϵ of an insulating material is defined by

$$\epsilon = \epsilon_0 + (P/E)$$

where ϵ_0 = permittivity of free space, P = flux density from dipoles within the dielectric medium, E = electric-field intensity, and P/E = electric susceptibility.

(*Continued on p. 4-27*)

TABLE 13—ELECTRICAL RESISTIVITY OF ROCKS AND SOILS. *From "Smithsonian Physical Tables," 9th revised edition, vol. 120, Smithsonian Institution, Washington, D. C.; 1969.*

Igneous Rocks	Resistivity (ohm-cm)
Granite	10^7–10^9
Lava flow (basic)	10^6–10^7
Lava, fresh	3×10^5–10^6
Quartz vein, massive	$>10^6$
Metamorphic Rocks	
Marble, white	10^{10}
Marble	4×10^8
Marble, yellow	10^{10}
Schist, mica	10^7
Shale, Nonesuch	10^4
Shale, bed	10^5
Sedimentary Rocks	
Limestone	10^4
Limestone, Cambrian	10^4–10^5
Sandstone, eastern	3×10^3–10^4
Sandstone	10^5
Unconsolidated Materials	
Clay, blue	2×10^4
Clayey earth	10^4–4×10^4
Clay, fire	2×10^5
Gravel	10^5
Sand, dry	10^5–10^6
Sand, moist	10^5–10^6

TABLE 14—SUPERCONDUCTIVITY OF SOME METALS, ALLOYS, AND COMPOUNDS.

Material	Critical Temperature (K)
NbC	10.1
Niobium	9.22
TaC	9.2
Pb–As–Bi	9.0
Pb–Bi–Sb	8.9
Pb–Sn–Bi	8.5
Pb–As	8.4
MoC	7.7
Lead	7.2
N_2Pb_5	7.2
Bi_6Tl_3	6.5
Sb_2Tl_7	5.5
Lanthanum	5.2
Tantalum	4.4
Vanadium	4.3
TaSi	4.2
Mercury	4.15
PbS	4.1
Hg_5Tl_7	3.8
Tin	3.71
Indium	3.38
ZrB	2.82
WC	2.8
Rhenium	2.57
Mo_2C	2.4
Thallium	2.4
W_2C	2.05
Au_2Bi	1.84
CuS	1.6
TiN	1.4
Thorium	1.32
VN	1.3
Aluminum	1.15
Gallium	1.12
TiC	1.1
Zinc	0.95
Uranium	0.75
Osmium	0.71
Zirconium	0.54
Cadmium	0.54
Titanium	0.53
Ruthenium	0.47
Hafnium	0.35

TABLE 15—PROPERTIES OF ELEMENTAL SEMICONDUCTORS. *From Clauser et al, "Encyclopedia of Engineering Materials and Processes," Reinhold Publishing Corporation, New York; 1963.*

Element	Crystal Structure	Density (gm/cm^3)	Melting Point (°C)	Linear Coefficient of Expansion (10^{-6}/°C)	Energy Band Gap at 300 K, (eV)	Electron Mobility (cm^2/volt sec)	Hole Mobility	
							Light Mass (cm^2/volt sec)	Heavy Mass (cm^2/volt sec)
B	—	2.34	2 075	—	1.4	1	—	2
C (diamond)	Cub. (f.c.), O^7_h	3.51	3 800	1.18	5.3	1 800	—	1 600
Si	Cub. (f.c.), O^7_h	2.33	1 417	4.2	1.09	1 500	1 500	480
Ge	Cub. (f.c.), O^7_h	5.32	937	6.1	0.66	3 900	14 000	1 860
α–Sn	Cub. (f.c.), O^7_h	5.75	231.9	—	0.08	144 000*	—	1 600*
As	Hex. (rhomb.), D^5_{3d}	5.73	814	3.86	1.2	—	—	—
Sb	Hex. (rhomb.), D^5_{3d}	6.68	630.5	10.88	0.11	—	—	—
α–S	Rhomb. (f.c.), V^{24}_h	2.07	112.8	64.1	2.6	—	—	—
Se	Hex., D^4_3	4.79	217	36.8	1.8	—	—	1
Se	Amorphous	4.82	—	—	2.3	0.005	—	0.15
Te	Hex., D^4_3	6.25	452	16.8	0.38	1 100	10 000	700

* Values for carrier mobilities are experimental values obtained at 300 K, except in the case of gray tin where the 77 K values are given.

TABLE 16—III–V COMPOUNDS AND THEIR PROPERTIES. *From Clauser et al, "Encyclopedia of Engineering Materials and Processes," Reinhold Publishing Corporation, New York; 1963.*

Compound	Crystal Structure	Density (gm/cm^3)	Melting Point (°C)	Linear Coefficient of Expansion (10^{-6}/°C)	Energy Band Gap at 300 K (eV)	Electron Mobility* (cm^2/volt sec)		Hole Mobility* (cm^2/volt sec)	
						Light Mass	Heavy Mass	Light Mass	Heavy Mass
BN	Hex. (graphite), D^4_{6h}	2.2	3 000	—	—	—	—	—	—
BN	Cub. (ZnS), T^2_d	—	—	—	4.6	—	—	—	—
BP	Cub. (ZnS), T^2_d	—	>3 000	—	—	—	—	—	500–1000
BAs	Cub. (ZnS), T^2_d	—	—	—	—	—	—	—	—
AlN	Hex., C^4_{6v}	3.26	>2 700	—	—	—	—	—	—
AlP	Cub. (ZnS), T^2_d	—	>2 100	—	2.42	—	—	—	—
AlAs	Cub. (ZnS), T^2_d	—	1 600	—	2.16	—	—	—	—
AlSb	Cub. (ZnS), T^2_d	4.28	1 065	—	1.6	—	180–230	—	420–500
GaN	Hex., C^4_{6v}	—	1 500	—	3.25	—	—	—	150–250
GaP	Cub. (ZnS), T^2_d	4.13	1 450	5.3	2.25	—	120–300	—	70–150
GaAs	Cub. (ZnS), T^2_d	5.32	1 238	5.7	1.43	8 600–11 000	1 000	3 000	426–500
GaSb	Cub. (ZnS), T^2_d	5.62	706	6.9	0.70	5 000–40 000	1 000	7 000	700–1 200
InN	Hex., C^4_{6v}	—	1 200	—	—	—	—	—	—
InP	Cub. (ZnS), T^2_d	4.79	1 062	4.5	1.27	4 800–6 800	—	—	150–200
InAs	Cub. (ZnS), T^2_d	5.67	942	5.3	0.33	33 000–40 000	—	8 000	450–500
InSb	Cub. (ZnS), T^2_d	5.78	530	5.5	0.17	78 000	—	12 000	750

* Since InSb is the only III–V compound which has been prepared with an impurity concentration low enough that the characteristic lattice carrier mobility can be determined, the best experimental value is given followed by the theoretical estimate for higher-purity material. All mobility values are for 300 K.

TABLE 17—SEMICONDUCTOR APPLICATIONS AND MATERIALS USED (INCLUDING SOME INSULATORS). *From Clauser et al, "Encyclopedia of Engineering Materials and Processes," Reinhold Publishing Corporation, New York; 1963.*

1. TRANSISTORS, DIODES, RECTIFIERS, and RELATED DEVICES	
Transistors	Ge, Si, GaAs
Diodes	
Switching Diodes	Ge, Si, GaAs
Varactor Diodes	Ge, Si, GaAs
Tunnel Diodes	Ge, Si, GaAs, GaSb
Photodiodes	Ge, Si, GaAs
Zener Diodes	Ge, Si, GaAs
Microwave Diodes	Ge, Si, GaAs
Magnetodiodes	InSb
Power Rectifiers	Cu_2O, Se, Si, Ge
Varistors	SiC, Cu_2O
2. LUMINESCENT DEVICES	
Electroluminescence	ZnS, ZnO
Phosphors	ZnS, CdS, ZnO, $ZnSiO_3$, $MgWO_3$, $SrWO_4$
Lasers	Al_2O_3, CaF_2, $CaWO_4$, BaF_2, $SrMoO_4$, SrF_2, LaF_2, LaF_3, As_2S_3, $CaMoO_4$, $KMgF_3$, $(BaMg)_2P_2O_7$
3. FERRITES	
Soft	ZnO, MnO, NiO, Fe_2O_3
Permanent	$BaFe_{12}O_{19}$
4. SPECIAL RESISTORS	
Thermistors	B, U_3O_8, Si, $(NiMn)O_2$
Photoconductors	Ge, Se, CdS, CdSe, GaAs, InSb, PbSe, PbTe
Particle Detectors	CdS, Diamond, Si, GaAs
Magnetoresistors	InSb, InAs
Piezoresistors	Si, PbTe, GaSb
Cryosars	Ge
Bokotrons	Ge
Helicons	Fe_2S
Oscillistors	Ge, Si, InSb
Chargistors	Ge, Si
5. PHOTOVOLTAIC AND HALL EFFECT	
Photovoltaic Cells	Se, Si, GaAs
Photoelectromagnetic Cells	InSb, InAs
Hall Effect Devices	InSb, InAs, GaAs
6. OPTICAL MATERIALS	
Infrared Lenses and Domes	Ge, Si, Se, Al_2O_3, As_2S_3, MgO, TiO_2, $SrTiO_3$
7. THERMOELECTRIC DEVICES	
Generators	PbTe, Bi_2Te_3, ZnSb, GeTe, MnTe, CeS
Refrigerators	Bi_2Te_3
8. PIEZOELECTRIC DEVICES	$BaTiO_3$, $PbTiO_3$, $(PbZr)TiO_3$, $PbNbO_2$, CdS, GaAs
9. XEROGRAPHY	Se, ZnO
10. ELECTRON EMISSION	BaO, SrO

TABLE 18—COMPOUND SEMICONDUCTORS. *From Clauser et al, "Encyclopedia of Engineering Materials and Processes," Reinhold Publishing Corporation, New York; 1963*

Formula No.	Typical Compounds
I-V	KSb, K_3Sb, CsSb, Cs_3Sb, Cs_3Bi
I-VI	Ag_2S, Ag_2Se, Cu_2S, Cu_2Te
II-IV	Mg_2Si, Mg_2Ge, Mg_2Sn, Ca_2Si, Ca_2Sn, Ca_2Pb, $MnSi_2$, $CrSi_2$
II-V	ZnSb, CdSb, Mg_3Sb_2, Zn_3As_2, Cd_3P_2, Cd_3As_2
II-VI	CdS, CdSe, CdTe, ZnS, ZnSe, ZnTe, HgS, HgSe, HgTe, $MoTe_2$, $RuTe_2$, $MnTe_2$, BeS, MgS, CaS
III-VI	Al_2S_3, Ga_2S_3, Ga_2Se_3, Ga_2Te_3, In_2S_3, In_2Se_3, In_2Te_3, GaS, GaSe, GaTe, InS, InSe, InTe
IV-IV	SiC
IV-VI	PbS, PbSe, PbTe, TiS_2, GeTe
V-VI	Sb_2S_3, Sb_2Se_3, Sb_2Te_3, As_2Se_3, As_2Te_3, Bi_2S_3, Bi_2Se_3, Bi_2Te_3, Ce_2S_3, Gd_2Se_3
$A^IB^{II}C_2^{VI}$	$CuFeS_2$
$A^IB^{III}C_2^{VI}$	C_4AlS_2, $CuInS_2$, $CuInSe_2$, $CuInTe_2$, $AgInSe_2$, $AgInTe_2$, $CuGaTe_2$
$A^IB^VC_2^{VI}$	$AgSbSe_2$, $AgSbTe_2$, $AgBiS_2$, $AgBiSe_2$, $AgBiTe_2$, $AuSbTe_2$, $Au(SbBi)Te_2$
$A_3^IB^VC_3^{VI}$	Cu_3SbS_3, Cu_3AsS_3
$A_3^IB^VC_4^{VI}$	Cu_3AsSe_4
$A^{II}B^{IV}C_2^V$	$ZnSnAs_2$
Oxides	SrO, BaO, MnO, NiO, Fe_2O_3, $BaFe_{12}O_{19}$, Al_2O_3, In_2O_3, TiO_2, BeO, MgO, CaO, CdO, ZnO, SiO_2, GeO_2, $ZnSiO_3$, $MgWO_3$, CuO

To deal with a dimensionless coefficient, it is customary to use the relative dielectric constant ϵ_r defined by

$$\epsilon_r = \epsilon/\epsilon_0.$$

The relative dielectric constant ϵ_r is a function of temperature and frequency. From Table 19, which gives the values of ϵ_r as a function of frequencies at room temperature, it is easy to get

$$\epsilon = \epsilon_r \epsilon_0.$$

In the MKS rationalized system of units the permittivity of vacuum is equal to

$$\epsilon_0 = 10^{-9}/36\pi = 8.854 \times 10^{-12} \text{ farad/meter}$$

and we have

Coulomb Law

$$F = (1/4\pi\epsilon_0\epsilon_r)(q_1q_2/R^2)$$

Gauss Law

$$\Phi = (\epsilon_0\epsilon_r)^{-1} \sum q_i.$$

The dissipation factor of an insulating material (Table 19) is defined as the ratio of the energy dissipated to the energy stored in the dielectric per hertz, or as the tangent of the loss angle. For dissipation factors less than 0.1, the dissipation factor may be considered equal to the power factor of the dielectric, which is the cosine of the phase angle by which the current leads the voltage.

Many of the materials listed are characterized by a peak dissipation factor occurring somewhere in the frequency range, this peak being accompanied by a rapid change in the dielectric constant. These effects are the result of a resonance phenomenon occurring in polar materials. The position of the dissipation-factor peak in the frequency spectrum is very sensitive to temperature. An increase in the temperature increases the frequency at which the peak occurs, as illustrated qualitatively in Fig. 3. Nonpolar materials have very low losses without a noticeable peak; the dielectric constant remains essentially unchanged over the frequency range.

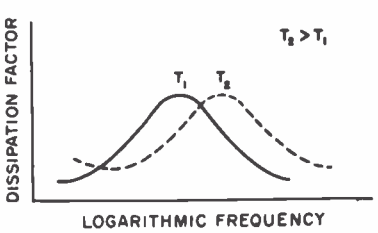

Fig. 3.

TABLE 19—CHARACTERISTICS

Material Composition	T°C	Dielectric Constant at (Frequency in Herts) 60	10^3	10^6	10^8	3×10^9	2.5×10^{10}
Ceramics:							
Aluminum oxide	25	—	8.83	8.80	8.80	8.79	—
Barium titanate†	26	1250	1200	1143	—	600	100
Calcium titanate	25	168	167.7	167.7	167.7	165	—
Magnesium oxide	25	—	9.65	9.65	9.65	—	—
Magnesium silicate	25	6.00	5.98	5.97	5.96	5.90	—
Magnesium titanate	25	—	13.9	13.9	13.9	13.8	13.7
Oxides of aluminum, silicon, magnesium, calcium, barium	24	—	6.04	6.04	—	5.90	—
Porcelain (dry process)	25	5.5	5.36	5.08	5.04	—	—
Steatite 410	25	5.77	5.77	5.77	5.77	5.7	—
Strontium titanate	25	—	233	232	232	—	—
Titanium dioxide (rutile)	26	—	100	100	100	—	—
Glasses:							
Iron-sealing glass	24	8.41	8.38	8.30	8.20	7.99	7.84
Soda-borosilicate	25	—	4.97	4.84	4.84	4.82	4.65
100% silicon dioxide (fused quarts)	25	3.78	3.78	3.78	3.78	3.78	3.78
Plastics:							
Alkyd resin	25	—	5.10	4.76	4.55	4.50	—
Cellulose acetate-butyrate, plasticized	26	3.60	3.48	3.30	3.08	2.91	—
Cresylic acid-formaldehyde, 50% α-cellulose	25	5.45	4.95	4.51	3.85	3.43	3.21
Cross-linked polystyrene	25	2.59	2.59	2.58	2.58	2.58	—
Epoxy resin (Araldite CN-501)	25	—	3.67	3.62	3.35	3.09	—
Epoxy resin (Epon resin RN-48)	25	—	3.63	3.52	3.32	3.04	—
Foamed polystyrene, 0.25% filler	25	1.03	1.03	1.03	—	1.03	1.03
Melamine—formaldehyde, α-cellulose	24	—	7.57	7.00	6.0	4.93	—
Melamine—formaldehyde, 55% filler	26	—	6.00	5.75	5.5	—	—
Phenol—formaldehyde (Bakelite BM 120)	25	4.90	4.74	4.36	3.95	3.70	3.55
Phenol—formaldehyde, 50% paper laminate	26	5.25	5.15	4.60	4.04	3.57	—
Phenol—formaldehyde, 65% mica, 4% lubricants	24	5.1	5.03	4.78	4.72	4.71	—
Polycarbonate	—	3.17	3.02	2.96	—	—	—
Polychlorotrifluoroethylene	25	2.72	2.63	2.42	2.32	2.29	2.28
Polyethylene	25	2.26	2.26	2.26	2.26	2.26	2.26
Polyethylene-terephthalate	—	3.16	3.12	2.98	—	—	—
Polyethylmethacrylate	22	—	2.75	2.55	2.52	2.51	2.5
Polyhexamethylene-adipamide (nylon)	25	3.7	3.50	3.14	3.0	2.84	2.73
Polyimide	—	—	3.5	3.4	—	—	—
Polyisobutylene	25	2.23	2.23	2.23	2.23	2.23	—
Polymer of 95% vinyl-chloride, 5% vinyl-acetate	20	—	3.15	2.90	2.8	2.74	—
Polymethyl methacrylate	27	3.45	3.12	2.76	—	2.60	—
Polyphenylene oxide	—	2.55	2.55	2.55	—	2.55	—
Polypropylene	—	2.25	2.25	2.55	—	—	—
Polystyrene	25	2.56	2.56	2.56	2.55	2.55	2.54
Polytetrafluoroethylene (teflon)	22	2.1	2.1	2.1	2.1	2.1	2.08
Polyvinylcyclohexane	24	—	2.25	2.25	2.25	2.25	—
Polyvinyl formal	26	3.20	3.12	2.92	2.80	2.76	2.7
Polyvinylidene fluoride	—	8.4	8.0	6.6	—	—	—
Urea-formaldehyde, cellulose	27	6.6	6.2	5.65	5.1	4.57	—
Urethane elastomer	—	6.7–7.5	6.7–7.5	6.5–7.1	—	—	—
Vinylidene-vinyl chloride copolymer	23	5.0	4.65	3.18	2.82	2.71	—
100% aniline-formaldehyde (Dilectene-100)	25	3.70	3.68	3.58	3.50	3.44	—
100% phenol-formaldehyde	24	8.6	7.15	5.4	4.4	3.64	—
100% polyvinyl-chloride	20	3.20	3.10	2.88	2.85	2.84	—
Organic Liquids:							
Aviation gasoline (100 octane)	25	—	—	1.94	1.94	1.92	—
Benzene (pure, dried)	25	2.28	2.28	2.28	2.28	2.28	2.28

OF INSULATING MATERIALS.*

Dissipation Factor at (Frequency in Herts)						Dielectric Strength in Volts/Mil at 25°C	DC Volume Resistivity in Ohm-cm at 25°C	Thermal Expansion (Linear) in Parts/°C	Softening Point in °C	Moisture Absorption in Percent
60	10^3	10^6	10^8	3×10^9	2.5×10^{10}					
—	0.00057	0.00033	0.00030	0.0010	—	—	—	—	—	—
0.056	0.0130	0.0105	—	0.30	0.60	75	10^{12}–10^{13}	—	1400–1430	0.1
0.006	0.00044	0.0002	—	0.0023	—	100	10^{13}–10^{14}	—	1510	<0.1
—	<0.0003	<0.0003	<0.0003	—	—	—	—	—	—	—
0.012	0.0034	0.0005	0.0004	0.0012	—	—	$>10^{14}$	9.2×10^{-6}	1350	0.1–1
—	0.0011	0.0004	0.0005	0.0017	0.0065	—	—	—	—	—
—	0.0019	0.0011	—	0.0024	—	—	—	7.7×10^{-6}	1325	—
0.03	0.0140	0.0075	0.0078	—	—	—	—	—	—	—
—	0.0030	0.0007	0.0006	0.00089	—	—	—	—	—	—
—	0.0011	0.0002	0.0001	—	—	100	10^{13}–10^{14}	—	1510	0.1
—	0.0015	0.0003	0.00025	—	—	—	—	—	—	—
—	0.0004	0.0005	0.0009	0.00199	0.0112	—	10^{16} at 250°	132×10^{-7}	484	Poor
—	0.0055	0.0036	0.0030	0.0054	0.0090	—	7×10^{7} at 250°	50×10^{-7}	693	—
0.0009	0.00075	0.0001	0.0002	0.00006	0.00025	410 (0.25″)	$>10^{16}$	5.7×10^{-7}	1667	—
—	0.0236	0.0149	0.0138	0.0108	—	—	—	—	—	—
0.0045	0.0097	0.018	0.017	0.028	—	250–400 (0.125″)	—	11–17$\times10^{-6}$	60–121	2.3
0.098	0.033	0.036	0.055	0.051	0.038	1020 (0.033″)	3×10^{13}	3×10^{-5}	>125	1.2
0.0004	0.0005	0.0016	0.0020	0.0019	—	—	—	—	—	—
—	0.0024	0.019	0.034	0.027	—	405 (0.125″)	$>3.8\times10^{7}$	4.77×10^{-6}	109 (distortion)	0.14
—	0.0038	0.0142	0.0264	0.021	—	—	—	—	—	—
<0.0002	<0.0001	<0.0002	—	0.0001	—	—	—	—	85	low
—	0.0122	0.041	0.085	0.103	—	300–400	—	—	99 (stable)	0.4–0.6
—	0.0119	0.0115	0.020	—	—	—	—	1.7×10^{-5}	—	0.6
0.08	0.0220	0.0280	0.0380	0.0438	0.0390	300 (0.125″)	10^{11}	30–40$\times10^{-6}$	<135 (distortion)	<0.6
0.025	0.0165	0.034	0.057	0.060	—	—	—	—	—	—
0.015	0.0104	0.0082	0.0115	0.0126	—	—	—	—	—	—
0.009	0.0021	0.010	—	—	—	364 (0.125″)	2×10^{16}	7×10^{-5}	135 (deflection)	—
0.015	0.0270	0.0082	—	0.0028	0.0053	—	10^{18}	—	—	—
<0.0002	<0.0002	<0.0002	0.0002	0.00331	0.0006	1200 (0.033″)	10^{17}	19×10^{-5} (varies)	95–105 (distortion)	0.03
0.0021	0.0047	0.016	—	—	—	4000 (0.002″)	←	—	—	—
—	0.0294	0.0090	—	0.0075	0.0083	—	—	—	60 (distortion)	low
0.018	0.0186	0.0218	0.0200	0.0117	0.0105	400 (0.125″)	8×10^{14}	10.3×10^{-5}	65 (distortion)	1.5
—	0.002	0.003	—	—	—	570	—	—	—	—
0.0004	0.0001	0.0001	0.0003	0.00047	—	600 (0.010″)	—	—	25 (distortion)	low
—	0.0165	0.0150	0.0080	0.0059	—	—	—	—	—	—
0.064	0.0465	0.0140	—	0.0057	—	990 (0.030″)	$>5\times10^{16}$	8–9$\times10^{-5}$	70–75 (distortion)	0.3–0.6
0.0004	0.0003	0.0007	—	0.0011	—	500 (0.125″)	10^{17}	5.3×10^{-5}	195 (deflection)	—
<0.0005	<0.0005	<0.0005	—	—	—	650 (0.125″)	6×10^{16}	6–8.5$\times10^{-5}$	99–116 (deflection)	—
<0.00005	<0.00005	0.00007	<0.0001	0.00033	0.0012	500–700 (0.125″)	10^{18}	6–8$\times10^{-5}$	82 (distortion)	0.05
<0.0005	<0.0003	<0.0002	<0.0002	0.00015	0.0006	1000–2000 (0.005″–0.012″)	10^{17}	9.0×10^{-5}	66 (distortion) (stable to 300)	0.00
—	0.0002	<0.0002	<0.0002	0.00018	—	—	—	—	—	—
0.003	0.0100	0.019	0.013	0.0113	0.0115	860 (0.034″)	$>5\times10^{16}$	7.7×10^{-5}	190	1.3
0 049	0.018	0.17	—	—	—	260 (0.125″)	2×10^{14}	12×10^{-5}	148 (deflection)	—
0.032	0.024	0.027	0.050	0.0555	—	375 (0.085″)	—	2.6×10^{-5}	152 (distortion)	2
0.016	0.055	—	—	—	—	450–500 (0.125″)	2×10^{11}	10–20$\times10^{-5}$	—	—
0.042	0.063	0.057	0.0180	0.0072	—	300 (0.125″)	10^{14}–10^{16}	15.8$\times10^{-6}$	150	<0.1
0.0033	0.0032	0.0061	0.0033	0.0026	—	810 (0.068″)	10^{16}	5.4×10^{-5}	125	0.06–0.08
0.15	0.082	0.060	0.077	0.052	—	277 (0.125″)	—	8.3–13$\times10^{-5}$	50 (distortion)	0.42
0.0115	0.0185	0.0160	0.0081	0.0055	—	400 (0.125″)	10^{14}	6.9×10^{-6}	54 (distortion)	0.05–0.15
—	—	—	0.0001	0.0014	—	—	—	—	—	—
<0.0001	<0.0001	<0.0001	<0.0001	<0.0001	<0.0001	—	—	—	—	—

TABLE 19—

Material Composition	T°C	Dielectric Constant at (Frequency in Herts) 60	10^3	10^6	10^8	3×10^9	2.5×10^{10}
Organic Liquids:—Continued							
Carbon tetrachloride	25	2.17	2.17	2.17	2.17	2.17	—
Ethyl alcohol (absolute)	25	—	—	24.5	23.7	6.5	—
Ethylene glycol	25	—	—	41	41	12	—
Jet fuel (JP-3)	25	—	—	2.08	2.08	2.04	—
Methyl alcohol (absolute analytical grade)	25	—	—	31	31.0	23.9	—
Methyl or ethyl siloxane polymer (1000 cs)	22	2.78	2.78	2.78	—	2.74	—
Monomeric styrene	22	2.40	2.40	2.40	2.40	2.40	—
Transil oil	26	2.22	2.22	2.22	2.20	2.18	—
Vaseline	25	2.16	2.16	2.16	2.16	2.16	—
Waxes:							
Beeswax, yellow	23	2.76	2.66	2.53	2.45	2.39	—
Dichloronaphthalenes	23	3.14	3.04	2.98	2.93	2.89	—
Polybutene	25	2.34	2.34	2.34	2.30	2.27	—
Vegetable and mineral waxes	25	2.3	2.3	2.3	2.3	2.25	—
Rubbers:							
Butyl rubber	25	2.39	2.38	2.35	2.35	2.35	—
GR-S rubber	25	2.96	2.96	2.90	2.82	2.75	—
Gutta-percha	25	2.61	2.60	2.53	2.47	2.40	—
Hevea rubber (pale crepe)	25	2.4	2.4	2.4	2.4	2.15	—
Hevea rubber, vulcanised (100 pts pale crepe, 6 pts sulfur)	27	2.94	2.94	2.74	2.42	2.36	—
Neoprene rubber	24	6.7	6.60	6.26	4.5	4.00	4.0
Organic polysulfide, fillers	23	—	2260	110	30	16	13.6
Silicone-rubber compound	25	—	3.35	3.20	3.16	3.13	—
Woods:‡							
Balsawood	26	1.4	1.4	1.37	1.30	1.22	—
Douglas fir	25	2.05	2.00	1.93	1.88	1.82	1.78
Douglas fir, plywood	25	2.1	2.1	1.90	—	—	1.6
Mahogany	25	2.42	2.40	2.25	2.07	1.88	1.6
Yellow birch	25	2.9	2.88	2.70	2.47	2.13	1.87
Yellow poplar	25	1.85	1.79	1.75	—	1.50	1.4
Miscellaneous:							
Amber (fossil resin)	25	2.7	2.7	2.65	—	2.6	—
DeKhotinsky cement	23	3.95	3.75	3.23	—	2.96	—
Gilsonite (99.9% natural bitumen)	26	2.69	2.66	2.58	2.56	—	—
Shellac (natural XL)	28	3.87	3.81	3.47	3.10	2.86	—
Mica, glass-bonded	25	—	7.45	7.39	—	—	—
Mica, glass, titanium dioxide	24	—	9.3	9.0	—	—	—
Ruby mica	26	5.4	5.4	5.4	5.4	5.4	—
Paper, royalgrey	25	3.30	3.29	2.99	2.77	2.70	—
Selenium (amorphous)	25	—	6.00	6.00	6.00	6.00	6.00
Asbestos fiber–chrysotile paper	25	—	4.80	3.1	—	—	—
Sodium chloride (fresh crystals)	25	—	5.90	5.90	—	—	5.90
Soil, sandy dry	25	—	2.91	2.59	2.55	2.55	—
Soil, loamy dry	25	—	2.83	2.53	2.48	2.44	—
Ice (from pure distilled water)	−12	—	—	4.15	3.45	3.20	—
Freshly fallen snow	−20	—	3.33	1.20	1.20	1.20	—
Hard-packed snow followed by light rain	−6	—	—	1.55	—	1.5	—
Water (distilled)	25	—	—	78.2	78	76.7	34

* Mostly taken from "Tables of Dielectric Materials," vols. I–IV, prepared by the Laboratory for Insulation Research of the Massachusetts Institute of Technology, Cambridge, Massachusetts, January 1953; from "Dielectric Materials and Applications," A. R. von Hippel, editor, John Wiley & Sons, New York, N. Y., 1954; and from "Modern Plastics Encyclopedia," Joel Frados, editor, 1301 Avenue of the Americas, New York, N. Y., 1962. Materials listed are typical of a class. Further data should be sought for a particular material of interest.

CONTINUED.

Dissipation Factor at (Frequency in Herts)						Dielectric Strength in Volts/Mil at 25°C	DC Volume Resistivity in Ohm-cm at 25°C	Thermal Expansion (Linear) in Parts/°C	Softening Point in °C	Moisture Absorption in Percent
60	10^3	10^6	10^8	3×10^9	2.5×10^{10}					
0.007	0.0008	<0.00004	<0.0002	0.0004	—	—	—	—	—	—
—	—	0.090	0.062	0.250	—	—	—	—	—	—
—	—	0.030	0.045	1.00	—	—	—	—	—	—
—	—	0.0001	—	0.0055	—	—	—	—	—	—
—	—	0.20	0.038	0.64	—	—	—	—	—	—
0.0001	0.00008	<0.0003	—	0.0096	—	—	—	—	—	—
0.01	0.005	<0.0003	—	0.0020	—	300 (0.100″)	3×10^{12}	—	—	0.06
0.001	<0.00001	<0.0005	0.0048	0.0028	—	300 (0.100″)	—	—	−40 (pour point)	—
0.0004	0.0002	<0.0001	<0.0004	0.00066	—	—	—	—	—	—
—	0.0140	0.0092	0.0090	0.0075	—	—	—	—	45–64 (melts)	—
0.10	0.0110	0.0003	0.0017	0.0037	—	—	—	—	35–63 (melts)	nil
0.0002	0.0003	0.00133	0.00133	0.0009	—	—	—	—	—	—
0.0009	0.0006	0.0004	0.0004	0.00046	—	—	—	—	57	—
0.0034	0.0035	0.0010	0.0010	0.0009	—	—	—	—	—	—
0.0008	0.0024	0.0120	0.0080	0.0057	—	870 (0.040″)	2×10^{15}	—	—	—
0.0005	0.0004	0.0042	0.0120	0.0060	—	—	10^{15}	—	—	—
0.0030	0.0018	0.0018	0.0050	0.0030	—	—	—	—	—	—
0.005	0.0024	0.0446	0.0180	0.0047	—	—	—	—	—	—
0.018	0.011	0.038	0.090	0.034	0.025	300 (0.125″)	8×10^{12}	—	—	nil
—	1.29	0.39	0.28	0.22	0.10	—	—	—	—	—
—	0.0067	0.0030	0.0032	0.0097	—	—	—	—	—	—
0.058	0.0040	0.0120	0.0135	0.100	—	—	—	—	—	—
0.004	0.0080	0.026	0.033	0.027	0.032	—	—	—	—	—
0.012	0.0105	0.0230	—	—	0.0220	—	—	—	—	—
0.008	0.0120	0.025	0.032	0.025	0.020	—	—	—	—	—
0.007	0.0090	0.029	0.040	0.033	0.026	—	—	—	—	—
0.004	0.0054	0.019	—	0.015	0.017	—	—	—	—	—
0.001	0.0018	0.0056	—	0.0090	—	2300 (0.125″)	Very high	—	200	—
0.049	0.0335	0.024	—	0.021	—	—	—	9.8×10^{-5}	80–85	—
0.006	0.0035	0.0016	0.0011	—	—	—	—	—	155 (melts)	—
0.006	0.0074	0.031	0.030	0.0254	—	—	10^{16}	—	80	low after baking
—	0.0019	0.0013	—	—	—	—	—	—	—	—
—	0.0125	0.0026	—	0.0040	—	—	—	—	400	<0.5
0.005	0.0006	0.0003	0.0002	0.0003	—	3800–5600 (0.040″)	5×10^{13}	—	—	—
0.010	0.0077	0.038	0.066	0.056	—	202 (0.125″)	—	—	—	—
—	0.0004	<0.0003	<0.0002	0.00018	0.0013	—	—	—	—	—
—	0.15	0.025	—	—	—	—	—	—	—	—
—	<0.0001	<0.0002	—	—	<0.0005	—	—	—	—	—
—	0.08	0.017	—	0.0062	—	—	—	—	—	—
—	0.05	0.018	—	0.0011	—	—	—	—	—	—
—	—	0.12	0.035	0.0009	—	—	—	—	—	—
—	0.492	0.0215	—	0.00029	—	—	—	—	—	—
—	—	0.29	—	0.0009	—	—	—	—	—	—
—	—	0.040	0.005	0.157	0.2650	—	10^6	—	—	—

† Dielectric constant and dissipation factor depend on electrical field strength.

‡ Field perpendicular to grain.

Another effect that contributes to dielectric losses is that of ionic or electronic conduction. This loss, if present, is important usually at the lower end of the frequency range only, and is distinguished by the fact that the dissipation factor varies inversely with frequency. Increase in temperature increases the loss due to ionic conduction because of increased ionic mobility.

The data given on dielectric strength are accompanied by the thickness of the specimen tested because the dielectric strength, expressed in volts/mil, varies inversely with the square root of thickness, approximately.

The direct-current volume resistivity of many materials is influenced by changes in temperature or humidity. The values given in the table may be reduced several decades by raising the temperature toward the higher end of the working range of the material, or by raising the relative humidity of the air surrounding the material to above 90 percent.

MAGNETIC MATERIALS (TABLES 20–22)

The permeability μ of a magnetic material is defined by

$$\mu = \mu_0 + (M/H)$$

where μ_0 = permeability of free space, M = flux density or magnetic polarization, H = magnetic-field strength, and M/H = magnetic susceptibility.

To deal with a dimensionless coefficient, it is customary to use the relative permeability μ_r defined by

$$\mu_r = \mu/\mu_0 = 1 + M/\mu_0 H.$$

The relative permeability μ_r of magnetic materials is given in Table 20. We have $\mu = \mu_0\mu_r$, with $\mu_0 = 1.257 \times 10^{-6}$ henry per meter in the MKS rationalized system of units.

For ferromagnetic materials μ_r is larger than 1, for paramagnetic materials μ_r is slightly larger than 1, and for diamagnetic materials μ_r is less than 1.

Applications in Rationalized Systems

Coulomb Law

$$F = (1/4\pi\mu_r\mu_0)(m_1m_2/r^2).$$

Field Strength

$$H = (1/4\pi\mu_r\mu_0)(m/r^2).$$

F is in newtons if m_1 and m_2 are in webers and r in meters. H is in ampere-turns per meter if m is in webers and r in meters.

In ferromagnetic materials the permeability is a function of temperature, pressure, frequency, and magnetic strength.

In paramagnetic and diamagnetic materials the permeability is independent of magnetic strength but depends also on temperature, pressure, and frequency.

FERRITES

Ferrite is the common term applied to a wide range of different ceramic ferromagnetic materials

(*Continued on p. 4-36*)

TABLE 20—RELATIVE PERMEABILITY μ_r OF VARIOUS MATERIALS.

	μ_r Maximum	μ_r at Small Magnetization
Ferromagnetic:		
Cobalt	60	60
Nickel	50	50
Cast iron	90	60
Silicon iron	7 000	3 500
Transformer iron	5 500	3 000
Very pure iron	8 000	4 000
Machine steel	450	300
Paramagnetic:		
Aluminum	1.000 000 65	
Beryllium	1.000 000 79	
$MnSO_4$	1.000 100	
NiCl	1.000 040	
Diamagnetic:		
Bismuth	0.999 998 600	
Paraffin	0.999 999 42	
Silver	0.999 999 81	
Wood	0.999 999 50	

TABLE 21—PROPERTIES OF HIGH-PERMEABILITY MATERIALS. These properties are expressed in the CGS electromagnetic system (typical values).*

Name	Composition, %	Permeability		Coercivity, H_c (Oe)	Retentivity, B_r (G)	B (max) (G)	Resistivity ($\mu\Omega$-cm)
		Initial	Maximum				
Iron, pure (laboratory conditions)	Annealed	25 000	350 000	0.05	12 000	14 000	9.7
Iron, Swedish		250	5 500	1.0	13 000	21 000	10
Iron, cast		100	600	4.5	5 300	20 000	30
Iron, silicon	4 Si, bal. Fe (hot rolled)	500	7 000	0.3	7 000	20 000	50
Rhometal	36 Ni, bal. Fe	1 000	5 000	0.5	3 600	10 000	90
Permalloy 45	45 Ni, bal. Fe	2 500	25 000	0.3		16 000	45
Mumetal	71–78 Ni, 4.3–6 Cu, 0–2 Cr, bal. Fe	20 000	100 000	0.05	6 000	7 200	25–50
Supermalloy	79 Ni, 5 Mo, bal. Fe	100 000	1 000 000	0.002		8 000	60
HyMu80	80 Ni, bal. Fe	20 000	100 000	0.05		8 700	57
Alfenol	16 Al, bal. Fe	3 450	116 000	0.025	3 800	7 825	150
Permendure	50 Co, 1–2 V, bal Fe	800	4 500	2.0	14 000	24 000	26
Sendust	10 Si, 5 Al, bal. Fe (cast)	30 000	120 000	0.05	5 000	10 000	60–80
Ferroxcube 3	Mn-Zn-Ferrite	1 000	1 500	0.1	1 000	3 000	$>10^6$
Ferroxcube 101	Ni-Zn-Ferrite	1 100		0.18	1 100	2 300	$>10^5$

* The above values are approximate only and vary with heat treatment and mechanical working of the material. Data sources include: P. R. Bardell, "Magnetic Materials in the Electrical Industry," courtesy Philosophical Library, New York; 1955. R. M. Bozorth, "Ferromagnetism," D. Van Nostrand Company, Inc., Princeton, N.J.; 1951. Technical catalog data by Allegheny Ludlum Steel Corporation, Pittsburgh; and Ferroxcube Corporation, Saugerties, N.Y.

TABLE 22—TYPICAL PROPERTIES OF HIGH-REMANENCE MAGNETIC MATERIALS (CGS electromagnetic system).*

Name and Composition, %	H(max) (Oe)	B(max) (G)	Retentivity B_r(G)	Coercivity H_c(Oe)	Ext. energy B_dH_d (max)	Form†	Resistivity ($\mu\Omega$-cm)
Carbon steel 1 C, 0.5 Mn, bal. Fe	300	14 800	8 600	48	180 000	Bar F-P-M	
Tungsten steel 5 W, 1 C, bal. Fe	300	14 500	10 300	70	320 000	Bar H-F-M	
Chromium steel 3.5 Cr, 1 C, bal. Fe	300	13 500	9 000	63	290 000	Bar H-F-M	
Cobalt steel 36 Co, 35 Cr, 3 W, 0.85 C, bal. Fe	1 000	15 500	9 000	210	936 000	Bar F-P-M	
Alnico 1 12 Al, 20 Ni, 5 Co, bal. Fe	2 000	12 350	7 100	400	1 300 000	Cast H-B	75
Alnico 2 (sintered) 10 Al, 17 Ni, 12.5 Co, 6 Cu, bal. Fe	2 000	12 000	6 900	520	1 430 000	Sintered H	
Alnico 2 (cast) 10 Al, 17 Ni, 12.5 Co, 6 Cu, bal. Fe	2 000	12 600	7 200	540	1 600 000	Cast H-B	65
Alnico 3 (section over $\frac{5}{8}'' \times \frac{3}{8}''$) 12 Al, 25 Ni, bal. Fe	2 000	12 000	6 700	450	1 380 000	Cast H-B	60
Alnico 4 (cast and sintered) 12 Al, 28 Ni, 5 Co, bal. Fe	3 000	11 850	5 200	700	1 200 000	C or S H-B	75
Alnico 5 8 Al, 14 Ni, 24 Co, 3 Cu, bal. Fe	2 000	15 700	12 000	575	4 500 000	Cast H-B	47
Alnico 6 8 Al, 15 Ni, 24 Co, 3 Cu, 1.25 Ti, bal. Fe	3 000	14 300	10 000	750	3 500 000	Cast H-B	
Alnico 12 6 Al, 18 Ni, 35 Co, 8 Ti, bal. Fe	3 000	12 800	5 800	950	1 500 000	Cast H-B	
Cunife I 60 Cu, 20 Ni, 20 Fe	2 400	8 400	5 800	600	1 960 000	Wire-Tape D-M	45

TABLE 22—CONTINUED.

Name and Composition, %	H(max) (Oe)	B(max) (G)	Retentivity B_r(G)	Coercivity H_c(Oe)	Ext. energy B_dH_d (max)	Form†	Resistivity ($\mu\Omega$-cm)
Cunife II 50 Cu, 20 Ni, 2.5 Co, bal. Fe	2 400	8 000	7 300	260	780 000	D-M	
Cunico 50 Cu, 20 Ni, 29 Co	3 200	8 000	3 400	660	800 000	Strip D-M	
Vectolite 30 Fe_2O_3, 44 Fe_3O_4, 26 Co_2O_3	3 000	4 800	1 600	1 000	600 000	Sintered B	
Sintered oxide 30 Fe_2O_3, 40 Fe_3O_4, 26 Co_2O_3	3 000	4 800	900	1 000	500 000	Powder B-weak	10^{12}
Silmanal 86.75 Ag, 8.8 Mn, 4.45 Al	20 000	20 830 B_i=830	550	6 000	75 600	Rod W	26
77% platinum alloy 77 Pt, 23 Co	15 000	22 900	4 500	2 000	3 800 000		50
Vicalloy 52 Co, 11 V, 37 Fe			14 100 9 400	200 400	1 350 000 2 400 000	Wire strip	
Remalloy or Comol 17 Mo, 12 Co, bal. Fe	1 000	17 000	10 500	250	1 100 000	Rolled F-M-P	
17% Cobalt 17 Co, 0.75 C, 3 Na, 2.5 Cr, 8 W	1 000	15 000	9 500	150	650 000	Rolled H-A-F	
Iron oxide powder 8 Fe_2O_3, Fe_3O_4	Density 2.81 g/cm³		2 265	550			
Iron oxide powder 8 Fe_2O_3, Fe_3O_4	Density 4.96 g/cm³		7 480	395			
Magnetite Plated coating 80 Co, 20 Ni	Density 2.62 g/cm³		1 600 10 000	190 250			

* The values are approximate only. Data sources include R. M. Bozorth, "Ferromagnetism," D. Van Nostrand Company, Inc., Princeton, N. J.; 1951.

† A—Annealed for machining; B—Brittle; D—Ductile; F—Hot Forged; H—Hard; M—Machinable; P—Punch; W—Workable.

TABLE 23—FERRITE CHARACTERISTICS.

Ferrite	Saturation Moment in Gauss	Curie Temperature in °C	Saturation Moment in Bohr Magnetons n_B	X-ray Density	Lattice Constant	First-Order Anisotropy Constant K_1	Saturation Magnetostriction $\lambda_s \times 10^6$
$NiFe_2O_4$	3400	585	2.3	5.38	8.34	−0.06	−22
$Ni_{0.8}Zn_{0.2}Fe_2O_4$	4600	460	3.5	—	—	—	−18.5
$Ni_{0.6}Zn_{0.4}Fe_2O_4$	5800	360	4.8	—	—	—	−15.0
$Ni_{0.5}Zn_{0.4}Fe_2O_4$	5500	290	5.0	—	—	—	−8.3
$Ni_{0.2}Zn_{0.5}Fe_2O_4$	2600	85	4.0	—	—	−0.004	−1.0
$MnFe_2O_4$	5200	300	0	5.00	8.50	−0.04	−14
$Mn_{0.5}Zn_{0.5}Fe_2O_4$	—	100	6.0	—	—	−0.004	—
$FeFe_2O_4$	6000	585	4.1	5.24	8.39	−0.135	+41
$CoFe_2O_4$	5000	520	3.8	5.29	8.38	+2000	−250
$CuFe_2O_4$	1700	455	1.3	5.35	$\begin{cases} a=8.24 \\ c=8.68 \end{cases}$	—	—
$Li_{0.5}Fe_{2.5}O_4$	3900	670	2.6	4.75	8.33	—	—
$MgFe_2O_4$	1400	440	1.1	4.52	8.36	−0.05	—
$MgAlFeO_4$	—	—	0.3	—	—	—	—
$NiAl_{0.25}Fe_{1.75}O_4$	1300	506	1.30	—	8.31	—	—
$NiAl_{0.45}Fe_{1.55}O_4$	900	465	0.61	—	8.28	—	—
$NiAl_{0.62}Fe_{1.38}O_4$	0	360	0	—	8.25	—	—
$NiAlFeO_4$	900	198	0.64	5.00	8.20	—	—

Specifically, the term applies to those materials with the spinel crystal structures having the general formula XFe_2O_4, where X is any divalent metallic ion having the proper ionic radius to fit in the spinel structure. Several ceramic ferromagnetic materials have been prepared that do not have the basic formula XFe_2O_4 but common usage has included them in the family of ferrite materials.

The behavior of the conductivity and dielectric constant of ferrites is not well understood. They behave as if they consisted of large regions of fairly low-resistance material separated by thin layers of a relatively poor conductor. Therefore, the dielectric constant and conductivity show a relaxation as a function of frequency with the relaxation frequency varying from 1000 to several million hertz. Most ferrites appear to have relatively high resistivities ($\approx 10^6$ ohm-centimeters) if they are prepared carefully so as to avoid the presence of any divalent iron in the material. However, if the ferrite is prepared with an appreciable amount of divalent iron, then both the

conductivity and dielectric constant are very high. Relative dielectric constants as high as 100 000 and resistivities less than 1 ohm-centimeter have been measured in several ferrites having a small amount of divalent iron in their composition.

Tables 23, 24, and 25 list some of the pertinent information with respect to the more-important ferrites. Properties such as electrical conductivity and dielectric constant, which are extremely structure-sensitive, are not listed since slight changes in method of preparation can cause these properties to change by several orders of magnitude. Also not included is the initial permeability of ferrite materials since this is also a structure-sensitive property. The initial permeability of most ferrites lies between 100 and 2000. In general, the ferrites listed in the tables have the following properties in common.

Thermal conductivity

$= 1.5 \times 10^{-2}$ calorie/second/centimeter^2/degree C

Specific heat

$= 0.2$ calorie/gram/degree C

Young's modulus

$= 1.5 \times 10^{12}$ dynes/centimeter^2.

MAGNETOSTRICTION (FIG. 4)

The static strain $\Delta l/l$ produced by a direct-current polarizing flux density B_0 is given by

$$\Delta l/l = cB_0^2$$

c being a material constant expressed in m^4/weber^2.

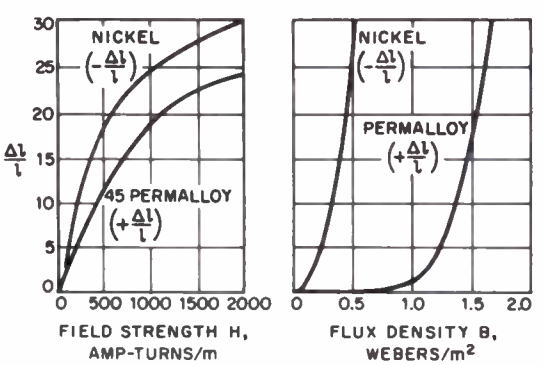

Fig. 4—Strain versus field strength (left) and versus flux density (right). *From "Sonics," p. 173, editors T. F. Hueter and R. H. Bolt, John Wiley & Sons, Inc., New York; 1955.*

If a small alternating-current driving field is superimposed on a large constant polarizing field B_0, we have

$$d(\Delta l/l) = 2cB_0B = \beta B.$$

The magnetostriction stress constant Λ in newtons/weber is

$$\Lambda = \beta Y_0 = 2cB_0Y_0$$

Y_0 being the Young's modulus for a free bar.

Nickel contracts with increasing B so Λ is negative. Permalloy and Alfer expand and their Λ is positive.

Table 26 gives values for the three important transducer materials in both MKS and CGS units: annealed nickel, 45 *Permalloy* (45-percent nickel, 55-percent iron) and *Alfer* (an alloy of 13-percent aluminum and 87-percent iron). For nickel the values for two different polarizing conditions are given: 160 ampere-turns and 1200 ampere-turns, the latter appearing in parentheses. Table 27 compares properties of six magnetostriction materials.

PIEZOELECTRICITY (TABLES 28–29)

Table 28 lists piezoelectric strain coefficients* d_{nm}, which are ratios of piezoelectric polarization components to components of applied stress at constant electric field (direct piezoelectric effect) and also ratios between piezoelectric strain components to applied electric field components at constant mechanical stress (converse effect). The subscripts $n = 1$ to 3 indicate electric field components, $m = 1$ to 6 mechanical stress or strain components. These components are referred to orthogonal coordinate axes. For correlation of these to crystallographic axes, we follow Standards on Piezoelectric Crystals.

In the monoclinic system, indices 2 and 5 refer to the symmetry (b) axis, in distinction from the older convention relating indices 3 and 6 to the symmetry axis. Crystal classes are designated by international (Hermann–Mauguin) symbols. A dash in place of a coefficient indicates that it is equal by symmetry from another listed coefficient; a blank space indicates that the coefficient is zero by sym-

(*Continued on p. 4-54*)

* The coefficient d_{14} of Rochelle salt is extremely dependent on temperature and on amplitude. The ratio of d_{14} to dielectric constant K is, however, nearly constant; $4\pi d_{14}/K = g_{14} = 6.4 \times 10^{-7}$ statvolt cm/dyne.

TABLE 24—FERROXCUBE TYPE FERRITES.

(A) General Applications for Commercial Materials*

Designation	$MnFe_2O_4$, mole %	$ZnFe_2O_4$, mole %	μ_0	B, gauss ($H=10$ Oe) 20°C	B, gauss ($H=10$ Oe) 100°C	B_r, G	H_c, Oe	Loss factor† $\tan\delta/\mu\times10^6$ 100 kHz	Loss factor† $\tan\delta/\mu\times10^6$ 1 MHz	ρ, Ω-cm‡	TF $\times10^{-6}$§	T_c/°C§	Density, g/cm³
3B¶	57.5	42.5	900	3450	2300	1500	0.5	—	—	20	3	150	4.9
3B7	—	—	2300	3400	—	900	0.2	5	120	100	0	170	4.8
3B9	—	—	1800	—	—	1200	0.3	6	120	300	1.8	145	—
3B11	—	—	1500	—	—	—	—	15	—	—	1.4	125	—
3C5	—	—	800	4300	3500	2200	0.2	20	350	60	—	200	4.9
3D3	67	33	750	—	—	—	—	8	30	150	2	150	4.9
3E1	54	46	2700	3500	—	1600	0.15	15	—	30	4	125	4.9
3E2A	—	—	5000	4200	2800	700	0.08	15	—	10	—	170	4.8
3H1	61	39	2300	3500	—	—	—	5	—	100	1.5	170	4.9
	$NiFe_2O_4$, mole %	$ZnFe_2O_4$, mole %											
4A	36	64	600	2900	2700	1800	0.4	22	100	10^5	6	125	4.9
4B	50	50	250	3300	2700	1950	1.9	35	70	10^5	8	250	4.6
4C	64	36	125	2800	2500	2000	3	105	120	10^5	12	350	4.2
4C4	—	—	125	3000	—	2350	3	40	40	10^5	−5	350	4.3
4D	80	20	50	2500	2300	1500	5	160	160	10^5	15	400	4.1
4E	100	0	15	1900	1800	1100	12	300	300	10^5	15	500	4.0

* Courtesy of Ferroxcube Corporation, Saugerties, N.Y.

† $\tan\delta/\mu=1/\mu Q$.

‡ Minimum value.

§ TF = temperature factor $=\Delta\mu/\mu_0{}^2T$. When used with magnetic circuit with air gap and effective permeability μ_{eff}, then the temperature coefficient of the magnetic circuit TC is given by $TC=\mu_{eff}\times TF$.

¶ All varieties of Ferroxcube 3 include in the compositions controlled amounts of ferrous ferrite.

TABLE 24—CONTINUED.

(B) Special Applications for Microwave Devices*

[Applications based on (1) Faraday rotation (F.R.), (2) ferromagnetic resonance (Res.), (3) field displacement (F.D.)]

Designation	Basic composition†	T_c, °C	ρ, MΩ-cm	$4\pi M_s$, G	Proposed use (F.R., Res., F.D.)	Freq., MHz
5B1	$MnO \cdot XAl_2O_3 \cdot (1-x)Fe_2O_3$‡	140	17	1 000	F.R. and F.D.	2 000–3 500
5A1	$MnO \cdot XAl_2O_3 \cdot (1-x)Fe_2O_3$‡	160	0.12	1 200	Res.	2 000–5 000
					F.R. and F.D.	3 500–4 200
5A2	$MnO \cdot XAl_2O_3 \cdot (1-x)Fe_2O_3$‡	180	3.4	1 450	F.R. and F.D.	4 200–6 000
5D3	$NiFe_2O_4$ 80%, $CuFe_2O_4$ 20%§	500	21	2 900	Res.	>5 000
					F.R. and F.D.	>9 000
5D1	$NiFe_2O_4$ 80%, $ZnFe_2O_4$ 20%	460	0.1	3 900	Res. (low power)	>8 000
5E1	$NiFe_2O_4$ 57%, $ZnFe_2O_4$ 43%	280	5 000	4 900	Res. (high power)	>8 000
					F.R. and F.D.	>14 000

* From "American Institute of Physics Handbook," 2nd edition, McGraw-Hill Book Co.; 1963.
† May have minor amounts of other components.
‡ The fraction x of Al_2O_3 adjusted to produce the desired properties.
§ Percentages are mole percentages.

(C) Special Applications for Magnetostrictive Transducers*

Designation	Basic Composition†	T_c, °C	Optimum Magnetostrictive Coupling Coef K_{opt}	Mechanical Quality Factor Q_{mech}	Biasing Field for Max K (oersteds)
7A1	$Ni_{(1-x)}Cu_xFe_2O_4$	530	0.25–0.32	>2 000	12–19
7A2	$Ni_{(1-x)}Cu_xFe_2O_4$	530	0.20–0.26	>2 500	9–15
7B	$NiFe_2O_4$	590	0.19–0.22	>4 000	25–50

* From "American Institute of Physics Handbook," 2nd edition, McGraw-Hill Book Co.; 1963.
† Contains controlled amounts of cobalt ferrite (see C. M. v. d. Burgt, *Philips Tech. Rev.*, vol. 18, pp. 285–298; 1957).

TABLE 25—NOMINAL FERRITE VALUES.

Material Code	Q-2	Q-3	Q-4	MF-6784	2285	2285A	C-10	C-20	K-12	U-17	U-60	SF	J	W
Manufacturer	1	1	1	1	2	2	3	3	4	4	4	5	5	5
Recommended frequency range in megahertz	10–80	50–225	200–500	10–75	30–80	30–300	30–80	30–80	3–40	10–220		10–250	40–250	40–500
Initial permeability, μ'	40	16	4.5	35	13.3	7.5	15	10	24	10	9			
Magnetic loss tangent, $\tan\delta_m$	0.006	0.02	0.010	0.0125			0.005	0.006	0.09	0.009	0.06			
Dielectric constant, ϵ'	10				10.5	10.5	11.0	11.0	11	11	11			
Dielectric loss tangent, $\tan\delta_d$	0.005						0.002	0.001						
Quality factor, μQ	5900	2380			2300	2500								
Temperature coefficient, $\%\Delta\mu/°C$	0.10	0.10		0.05	0.36	0.36			0.0144			0.003	0.017	0.013
Saturation magnetization, B_s in gauss	2400	2600			2100		2600	1900	1450		1100			
Residual magnetization, B_r in gauss	750	1470			1600									
Maximum permeability, μ_{max}	115	42			38									
Coercivity, H_c in oersteds	4.7	21			21				12	15	10			

Manufacturer code

1. Indiana General, Electronics Division
2. Stackpole Carbon Co., Electronic Components Division
3. Orbit Industries, Division of Countis Industries
4. Siemens America Inc., Components Division
5. Arnold Engineering Co.

TABLE 26—MAGNETOMECHANICAL COEFFICIENTS OF THREE IMPORTANT MAGNETOSTRICTIVE MATERIALS AT INTERNAL POLARIZING FIELD H_0*. *From "Sonics," p. 175, editors T. F. Hueter and R. H. Bolt, John Wiley & Sons, Inc., New York; 1955.*

Coefficient	Annealed Nickel†		45 Permalloy		Alfer (13% Al, 87% Fe)	
	MKS	CGS	MKS	CGS	MKS	CGS
H_0						
Amp/m	160 (1200)		600		800	
Oersted		2 (15)		7.5		10
B_0						
Volt·sec/m²	0.25 (0.51)		1.43		1.15	
Gauss		2500 (5100)		14 300		11 500
μ	1250 (340)		1900		1150	
μ_i	137 (41)		230		190	
$\Delta l/l$ at H_0	-8×10^{-6} (-26×10^{-6})		14×10^{-6}		26×10^{-6}	
ζ						
m⁴/weber²	-1×10^{-4}		6.9×10^{-6}		19.5×10^{-6}	
Gauss^{-2}		-1×10^{-12}		6.9×10^{-14}		19.5×10^{-14}
A						
Newton/weber	-4.8×10^{6} (-20×10^{6})		2.7×10^{6}		6.7×10^{6}	
Dynes/gauss·cm²		-4.8×10^{3} (-20×10^{3})		2.7×10^{3}		6.7×10^{3}
Y_0						
Newtons/m²	20×10^{10}		13.8×10^{10}		15×10^{10}	
Dynes/m²		20×10^{11}		13.8×10^{11}		15×10^{11}
ρ						
kg/m³	8.7×10^{3}		8.25×10^{3}		6.7×10^{3}	
g/cm³		8.7		8.25		6.7
k_c% (electromechanical coupling factor)	14 (31)		12.4		27	
ρ_e						
Ohm·m	7×10^{-8}		7×10^{-7}		9×10^{-7}	
Ohm·cm		7×10^{-6}		7×10^{-5}		9×10^{-5}

* The number of external ampere-turns per meter required to produce H_0 depends on the shape of the core. For closed magnetic loops H_{ext} is equal to H_0. For rod-shaped cores external fields larger than H_0 are necessary to compensate for the demagnetizing effect of the poles at the free ends.

† The values for two different polarizing conditions are given: 160 and 1200 ampere-turns/meter, the latter in parentheses.

TABLE 27—OTHER CONSTANTS FOR SOME MAGNETOSTRICTION MATERIALS.

Composition	$\Delta l/l$ at Saturation of B	Λ (newtons/weber)	μ_i (henries/meter)	Young's modulus (newtons/m²)	k_c (%)	Curie Temperature (°C)
99.9% Ni annealed	-33×10^{-6}	-20×10^{6}	4.3×10^{-6}	2.0×10^{11}	31	358
2V 49 Co 49 Fe (2V Permadur)	$+70\times10^{-6}$	—	—	1.7×10^{11}	20–37	980
45 Ni 55 Fe (45 Permalloy)	$+27\times10^{-6}$	2.7×10^{6}	2.9×10^{-4}	1.4×10^{11}	12	440
13 Al 87 Fe (13 Alfer)	+40	6.7×10^{6}	2.4×10^{-4}	1.5×10^{11}	27	500
Fe_3O_4	+40	-90×10^{6}	1.9×10^{-2}	1.8×10^{11}	3	190
Ferrite 7 Al	−28	-28 to -44×10^{6}	$4\text{–}5\times10^{-6}$	1.68 to 1.75×10^{11}	25–30	640

TABLE 28—PIEZOELECTRIC STRAIN COEFFICIENTS FOR VARIOUS MATERIALS. *From "Smithsonian Physical Tables," 9th revised edition, vol. 120, p. 432, Smithsonian Institution, Washington, D. C.; 1969.*

(A) Cubic and Tetragonal Crystals	Composition	Class	d_{14}	d_{36}
Sphalerite	ZnS	43	9.7	—
Sodium chlorate	$NaClO_3$	23	5.2	—
Sodium bromate	$NaBrO_3$	23	7.3	—
"ADP"	NH_4H_2PO	$\bar{4}2$	−1.5	+48.0
"KDP"	KH_2PO_4	$\bar{4}2$	+1.3	+21
"ADA"	$NH_4H_2AsO_4$	$\bar{4}2$	+41	+31
"KDA"	KH_2AsO_4	$\bar{4}2$	+23.5	+22

(B) Trigonal Crystals	Class	d_{11}	d_{14}	d_{15}	d_{22}	d_{31}	d_{33}
Quartz	32	+6.9	−2.0				
Tourmaline	3			+11.0	−0.94	+0.96	+5.4

(C) Orthorhombic Crystals	Class	d_{14}	d_{25}	d_{36}
Epsomite	222	−6.2	−8.2	−11.5
Iodic acid	222	57	46	70
Rochelle salt (30°C)	222	+1500	−160	+35
$NaNH_4$ tartrate	222	+56	−150	+28
LiK tartrate	222	9.6	33.6	22.8
$LiNH_4$ tartrate	222	13.2	19.6	14.8
$(NH_4)_2$ oxalate	222	50	11	25

	d_{15}	d_{24}	d_{31}	d_{32}	d_{33}
K pentaborate	9.5	1.7	−5.4	0	+5.6

TABLE 28—CONTINUED.

(D) Monoclinic Crystals (Class 2)	d_{14}	d_{16}	d_{21}	d_{22}	d_{23}	d_{25}	d_{34}	d_{36}
Lithium sulfate	+14.0	−12.5	+11.6	−45.0	−5.5	+16.5	−26.4	+10.0
Tartaric acid	+24.0	+15.8	−2.3	−6.5	−6.3	+1.1	−32.4	+35.0
K_2 tartrate (DKT)	−25	+6.5	−2.2	+8.5	−10.4	−22.5	+29.4	−66.0
$(NH_4)_2$ tartrate	+9.3	−8.5	+17.6	−26.2	+1.8	−5.9	−14.0	+5.6
EDT (ethylene diamine tartrate)	−31.1	−36.5	+30.6	+6.6	−33.8	−54.3	−51	−56.9
Cane sugar	−3.7	−7.2	+4.4	−10	+2.2	−2.6	−1.3	+1.3

(E) Polarized Polycrystalline Substance	d_{15}	d_{31}	d_{33}
Barium titanate ceramic K=1700	750	−235	+570

Note: If the sign of a coefficient is not given, it is unknown (not necessarily positive).

TABLE 29—CONSTANTS OF SOME PIEZOELECTRIC MATERIALS.* *From J. R. Frederick, "Ultrasonic Engineering," p. 66, John Wiley & Sons, Inc., New York; 1965.*

Physical Property	Quartz 0° X-cut	Lithium Sulfate 0° Y-cut	Barium Titanate Type B	Lead Zirconate-Titanate PZT-4	Lead Zirconate-Titanate PZT-5	Lead Meta-Niobate	Units
Density ρ	2.65	2.06	5.6	7.6	7.7	5.8	10^3 kg/m^3
Acoustic impedance ρc	15.2	11.2	24	30.0	28.0	16	10^6 kg/m^{2}s
Frequency thickness constant ft	2870	2730	2740	2000	1800	1400	kHz/mm
Maximum operating temperature	550	75	70–90	250	290	500	°C
Dielectric constant	4.5	10.3	1700	1300	1700	225	—
Electromechanical coupling factor for thickness mode k_{33}	0.1	0.35	0.48	0.64	0.675	0.42	—
Electromechanical coupling factor for radial mode k_p	0.1	—	0.33	0.58	0.60	0.07	—
Elastic quality factor Q	10^6	—	400	500	75	11	—
Piezoelectric modulus for thickness mode d_{33}	2.3	16	149	285	374	85	10^{-12} m/V
Piezoelectric pressure constant g_{33}	58	175	14.0	26.1	24.8	42.5	10^{-3}(V/m)/(N/m^2)
Volume resistivity at 25°C	$>10^{12}$	—	$>10^{11}$	$>10^{12}$	$>10^{13}$	10^9	—
Curie temperature	575	—	115	320	365	550	°C
Young's modulus E	8.0	—	11.8	8.15	6.75	2.9	10^{10} N/m^2
Rated dynamic tensile strength	—	—	—	3500	4000	—	psi

* The properties of the ceramic materials can vary with slight changes in composition and processing, and hence the values that are shown should not be taken as exact.

TABLE 30—SIMPLIFIED EQUATIONS FOR SOUND INTENSITY. *From "Sonics", p. 125, editors T. F. Hueter and R. H. Bolt, John Wiley & Sons, Inc. New York; 1955.*

Material	Mode of Vibration	Crystal Cut	Effective* Piezo Modulus H (coulombs/m^2)	Sound Velocity c (m/sec)	Density ρ(kg/m^3)	Sound Intensity in Water for Airbacked Transducer† $\mathcal{G}$ (watts/m^2)	Units (rms values for V and E)
Quartz	Thickness	X	$H=e_{11}$ $=5.2\times10^4$ esu $=0.17$ coulomb/m^2	5.72×10^3	2.65×10^3	$f_0^2V^2\times10^4$	V in kV f in MHz
	Longitudinal	X	$H=d_{11}/s'$ $=5.4\times10^4$ esu $=0.18$ coulomb/m^2	5.44×10^3	2.65×10^3	$0.087\times E^2\times10^4$	E in kV/cm
Ammonium dihydrogen phosphate (ADP)	Longitudinal	45°Z	$H=d_{36}/2s'$ $=1.4\times10^4$ esu $=0.042$ coulomb/m^2	3.28×10^3	1.8×10^3	$0.6E^2\times10^4$	E in kV/cm
Rochelle salt (0°C)	Longitudinal	45°X	$H=d_{14}/2s'$ $=1.7\times10^6$ esu $=5.67$ coulombs/m^2	3.4×10^3	1.77×10^3	$85E^2\times10^4$	E in kV/cm
Barium titanate (40°C)	Thickness	Polarized normal to thickness	$H=e_{33}$ $=3$ to 5×10^6 esu $=10$ to 17 coulombs/m^2	5×10^3	5.5×10^3	$0.005f_0^2V^2\times10^4$ to $0.014f_0^2V^2\times10^4$	V in volts f in MHz

* The quantity s' in the relationship $H=d_{ik}/s'$ is the effective compliance in the direction of longitudinal vibration.
† Without the factor 10^4, this column gives the sound intensity in watts/cm^2.

TABLE 31—VELOCITIES, DENSITIES, AND CHARACTERISTIC IMPEDANCES OF VARIOUS METALS. *From J. R. Frederick, "Ultrasonic Engineering," p. 363, John Wiley & Sons., Inc., New York; 1965.*

Metals	Velocities: Longitudinal: Bulk m/s	Velocities: Longitudinal: Bulk in./s	Velocities: Longitudinal: Bar m/s	Velocities: Longitudinal: Bar in./s	Velocities: Shear m/s	Velocities: Shear in./s	Density ρ (kg/m³)	Characteristic impedance ρc Bulk (kg/m²s)
	×10³	×10⁵	×10³	×10⁵	×10³	×10⁵	×10³	×10⁶
Aluminum	6.40	2.50	5.15	2.03	3.13	1.24	2.7	17.3
Beryllium	12.89	17.	...	...	8.88	3.51	1.8	23.2
Brass, 70–30	4.37	1.73	3.40	1.34	2.10	0.83	8.5	37.0
Cast iron	3.50–5.60	1.38–2.22	3.0–4.7	1.19–1.86	2.2–3.2	0.87–1.31	7.2	25.0–40.0
Copper	4.80	1.90	3.65	1.45	2.33	0.92	8.9	42.5
Gold	3.24	1.28	2.03	...	1.20	0.47	19.3	63.0
Iron	5.96	2.35	5.18	2.05	3.22	1.28	7.9	46.8
Lead	2.40	0.95	1.25	0.49	0.79	0.31	11.3	27.2
Magnesium	5.74	2.27	4.90	1.94	3.08	1.22	1.7	9.9
Mercury	1.45	0.57	...	...	...	...	13.6	19.6
Molybdenum	6.25	2.47	...	...	3.35	1.33	10.2	63.7
Nickel	5.48	2.17	4.70	1.86	2.99	1.19	8.9	48.5
Platinum	3.96	1.57	2.80	1.11	1.67	0.66	21.4	85.0
Steel, mild	6.10	2.41	5.05	2.00	3.24	1.29	7.9	46.7
Silver	3.70	1.46	2.67	1.06	1.70	0.67	10.5	36.9
Tin	3.38	1.34	2.74	1.09	1.61	0.66	7.3	24.7
Titanium	5.99	2.37	...	...	3.12	1.24	4.50	27.0
Tungsten	5.17	2.04	...	...	2.88	1.14	19.3	100.0
Uranium	3.37	1.33	...	...	2.02	0.80	18.7	63.0
Zinc	4.17	1.65	3.81	1.51	2.48	0.98	7.1	29.6
Zirconium	4.65	1.84	...	...	2.30	0.91	6.4	29.8
Other Solid Materials:								
Crown glass	5.66	2.24	5.30	2.10	3.42	1.35	2.5	14.0
Granite	...	...	3.95	1.56	...	...	2.75	...
Ice	3.98	1.58	...	...	1.99	0.79	0.9	3.6
Nylon	1.8–2.2	0.71–0.87	...	...	...	...	1.1–1.2	2.0–2.7
Paraffin, hard	2.2	0.87	...	...	...	...	0.83	1.8
Plexiglas or Lucite	2.68	1.06	1.8	0.71	1.32	0.52	1.20	3.2
Polystyrene	2.67	1.06	...	...	...	...	1.06	2.8
Quartz, fused	5.57	2.21	5.37	2.12	3.52	1.39	2.6	14.5
Teflon	1.35	0.53	...	...	...	...	2.2	3.0
Tungsten carbide	6.66	2.64	...	...	3.98	1.57	10.0–15.0	66.5–98.5
Wood, oak	...	...	4.1	1.62	...	...	0.8	...
Fluids:								
Benzene	1.32	0.52	...	...	...	...	0.88	1.16
Castor oil	1.54	0.61	...	...	...	...	0.95	1.45
Glycerine	1.92	0.76	...	...	...	...	1.26	2.5
Methyl iodide	0.98	0.39	...	...	...	...	3.23	3.2
Oil, SAE 20	1.74	0.69	...	...	...	...	0.87	1.5
Water, fresh	1.48	0.59	...	...	...	...	1.00	1.48

Note: The values that are shown should not be taken as exact values because of the effects of variations in composition and processing. They are adequate for most practical purposes, however.

TABLE 32—ADHESIVES CLASSIFIED BY CHEMICAL COMPOSITION. *From Clauser et al, "Encyclopedia of Engineering Materials and Processes," Reinhold Publishing Corporation, New York; 1963.*

Group→	Natural	Thermoplastic	Thermosetting	Elastomeric	Alloys*
Types within group	Casein, blood albumin, hide, bone, fish, starch (plain and modified); rosin, shellac, asphalt; inorganic (sodium silicate, litharge-glycerin)	Polyvinyl acetate, polyvinyl alcohol, acrylic, cellulose nitrate, asphalt, oleoresin	Phenolic, resorcinol, phenol-resorcinol, epoxy, epoxy-phenolic, urea, melamine, alkyd	Natural rubber, reclaim rubber, butadiene-styrene (GR-S), neoprene, acrylonitrile-butadiene (Buna-N), silicone	Phenolic-polyvinyl butyral, phenolic-polyvinyl formal, phenolic-neoprene rubber, phenolic-nitrile rubber, modified epoxy
Most used form	Liquid, powder	Liquid, some dry film	Liquid, but all forms common	Liquid, some film	Liquid, paste, film
Common further classifications	By vehicle (water emulsion is most common but many types are solvent dispersions)	By vehicle (most are solvent dispersions or water emulsions)	By cure requirements (heat and/or pressure most common but some are catalyst types)	By cure requirements (all are common); also by vehicle (most are solvent dispersions or water emulsions)	By cure requirements (usually heat and pressure except some epoxy types); by vehicle (most are solvent dispersions or 100% solids); and by type of adherends or end-service conditions

Bond characteristics	Wide range, but generally low strength; good resistance to heat, chemicals; generally poor moisture resistance	Good to 200–500 F; poor creep strength; fair peel strength	Good to 200–500 F; good creep strength; fair peel strength	Good to 150–400 F; never melt completely; low strength; high flexibility	Balanced combination of properties of other chemical groups depending on formulation; generally higher strength over wider temperature range
Major type of use†	Household, general purpose, quick set, long shelf life	Unstressed joints; designs with caps, overlaps, stiffeners	Stressed joints at slightly elevated temperature	Unstressed joints on lightweight materials; joints in flexure	Where highest and strictest end-service conditions must be met; sometimes regardless of cost, as military uses
Materials most commonly bonded	Wood (furniture), paper, cork, liners, packaging (food), textiles, some metals and plastics. Industrial uses giving way to other groups	Formulation range covers all materials, but emphasis on nonmetallics—especially wood, leather, cork, paper, etc.	Epoxy-phenolics for structural uses of most materials; others mainly for wood; alkyds for laminations; most epoxies are modified (alloys)	Few used "straight" for rubber, fabric, foil, paper, leather, plastics, films; also as tapes. Most modified with synthetic resins	Metals, ceramics, glass, thermosetting plastics; nature of adherends often not as vital as design or end-service conditions (i.e., high strength, temperature)

* "Alloy," as used here, refers to formulations containing resins from two or more *different* chemical groups. There are also formulations which benefit from compounding two resin types from the same chemical group (e.g., epoxy-phenolic).

† Although some uses of the "nonalloyed" adhesives absorb a large percentage of the quantity of adhesives sold, the uses are narrow in scope; from the standpoint of diversified applications, by far the most important use of any group is the forming of adhesive alloys.

TABLE 33—SOLID COPPER—COMPARISON OF GAUGES.

American (B & S) Wire Gauge	Birmingham (Stubs') Iron Wire Gauge	British Standard (NBS) Wire Gauge	Diameter		Area			Weight	
			Mils	Millimeters	Circular Mils	Square Millimeters	Square Inches	per 1000 Feet in Pounds	per Kilometer in Kilograms
—	0	—	340.0	8.636	115 600	58.58	0.09079	350	521
0	—	—	324.9	8.251	105 500	53.48	0.08289	319	475
—	—	0	324.0	8.230	105 000	53.19	0.08245	318	472
—	1	1	300.0	7.620	90 000	45.60	0.07069	273	405
1	—	—	289.3	7.348	83 690	42.41	0.06573	253	377
—	2	—	284.0	7.214	80 660	40.87	0.06335	244	363
—	—	—	283.0	7.188	80 090	40.58	0.06290	242	361
—	—	2	276.0	7.010	76 180	38.60	0.05963	231	343
—	3	—	259.0	6.579	67 080	33.99	0.05269	203	302
2	—	—	257.6	6.544	66 370	33.63	0.05213	201	299
—	—	3	252.0	6.401	63 500	32.18	0.04988	193	286
—	4	—	238.0	6.045	56 640	28.70	0.04449	173	255
—	—	4	232.0	5.893	53 820	27.27	0.04227	163	242
3	—	—	229.4	5.827	52 630	26.67	0.04134	159	237
—	5	—	220.0	5.588	48 400	24.52	0.03801	147	217
—	—	5	212.0	5.385	44 940	22.77	0.03530	136	202
4	—	—	204.3	5.189	41 740	21.18	0.03278	126	188
—	6	—	203.0	5.156	41 210	20.88	0.03237	125	186
—	—	6	192.0	4.877	36 860	18.68	0.02895	112	166
5	—	—	181.9	4.621	33 100	16.77	0.02600	100	149
—	7	—	180.0	4.572	32 400	16.42	0.02545	98.0	146
—	—	7	176.0	4.470	30 980	15.70	0.02433	93.6	139
—	8	—	165.0	4.191	27 220	13.86	0.02138	86.2	123
6	—	—	162.0	4.116	26 250	13.30	0.02062	79.5	118
—	—	8	160.0	4.064	25 600	12.97	0.02011	77.5	115
—	9	—	148.0	3.759	21 900	11.10	0.01720	66.3	98.6
7	—	—	144.3	3.665	20 820	10.55	0.01635	63.0	93.7
—	—	9	144.0	3.658	20 740	10.51	0.01629	62.8	93.4
—	10	—	134.0	3.404	17 960	9.098	0.01410	54.3	80.8
8	—	—	128.8	3.264	16 510	8.366	0.01297	50.0	74.4
—	—	10	128.0	3.251	16 380	8.302	0.01267	49.6	73.8
—	11	—	120.0	3.048	14 400	7.297	0.01131	43.6	64.8

TABLE 33—CONTINUED.

American (B & S) Wire Gauge	Birmingham (Stubs') Iron Wire Gauge	British Standard (NBS) Wire Gauge	Diameter		Area			Weight	
			Mils	Millimeters	Circular Mils	Square Millimeters	Square Inches	per 1000 Feet in Pounds	per Kilometer in Kilograms
—	—	11	116.0	2.946	13 460	6.818	0.01057	40.8	60.5
9	—	—	114.4	2.906	13 090	6.634	0.01028	39.6	58.9
—	12	—	109.0	2.769	11 880	6.020	0.009331	35.9	53.5
—	—	12	104.0	2.642	10 820	5.481	0.008495	32.7	48.7
10	—	—	101.9	2.588	10 380	5.261	0.008155	31.4	46.8
—	13	—	95.00	2.413	9 025	4.573	0.007088	27.3	40.6
—	—	13	92.00	2.337	8 464	4.289	0.006648	25.6	38.1
11	—	—	90.74	2.305	8 234	4.172	0.006467	24.9	37.1
—	14	—	83.00	2.108	6 889	3.491	0.005411	20.8	31.0
12	—	—	80.81	2.053	6 530	3.309	0.005129	19.8	29.4
—	—	14	80.00	2.032	6 400	3.243	0.005027	19.4	28.8
—	15	15	72.00	1.829	5 184	2.627	0.004072	16.1	23.4
13	—	—	71.96	1.828	5 178	2.624	0.004067	15.7	23.3
—	16	—	65.00	1.651	4 225	2.141	0.003318	12.8	19.0
14	—	—	64.08	1.628	4 107	2.081	0.003225	12.4	18.5
—	—	16	64.00	1.626	4 096	2.075	0.003217	12.3	18.4
—	17	—	58.00	1.473	3 364	1.705	0.002642	10.2	15.1
15	—	—	57.07	1.450	3 257	1.650	0.002558	9.86	14.7
—	—	17	56.00	1.422	3 136	1.589	0.002463	9.52	14.1
16	—	—	50.82	1.291	2 583	1.309	0.002028	7.82	11.6
—	18	—	49.00	1.245	2 401	1.217	0.001886	7.27	10.8
—	—	18	48.00	1.219	2 304	1.167	0.001810	6.98	10.4
17	—	—	45.26	1.150	2 048	1.038	0.001609	6.20	9.23
—	19	—	42.00	1.067	1 764	0.8938	0.001385	5.34	7.94
18	—	—	40.30	1.024	1 624	0.8231	0.001276	4.92	7.32
—	—	19	40.00	1.016	1 600	0.8107	0.001257	4.84	7.21
—	—	20	36.00	0.9144	1 296	0.6567	0.001018	3.93	5.84
19	—	—	35.89	0.9116	1 288	0.6527	0.001012	3.90	5.80
—	20	—	35.00	0.8890	1 225	0.6207	0.0009621	3.71	5.52
—	21	21	32.00	0.8128	1 024	0.5189	0.0008042	3.11	4.62
20	—	—	31.96	0.8118	1 022	0.5176	0.0008023	3.09	4.60

TABLE 34—ANNEALED COPPER.

AWG B & S Gauge	Diameter in Mils	Cross Section: Circular mils	Cross Section: Square Inches	Ohms per 1000 Ft at 20° C (68° F)	Lb per 1000 Ft	Ft per Lb	Ft per ohm at 20° C (68° F)	Ohms per Lb at 20° C (68° F)
0000	460.0	211 600	0.1662	0.04901	640.5	1.561	20 400	0.0000765
000	409.6	167 800	0.1318	0.06180	507.9	1.968	16 180	0.0001217
00	364.8	133 100	0.1045	0.07793	402.8	2.482	12 830	0.0001935
0	324.9	105 500	0.08289	0.09827	319.5	3.130	10 180	0.0003076
1	289.3	83 690	0.06573	0.1239	253.3	3.947	8 070	0.0004891
2	257.6	66 370	0.05213	0.1563	200.9	4.977	6 400	0.0007778
3	229.4	52 640	0.04134	0.1970	159.3	6.276	5 075	0.001237
4	204.3	41 740	0.03278	0.2485	126.4	7.914	4 025	0.001966
5	181.9	33 100	0.02600	0.3133	100.2	9.980	3 192	0.003127
6	162.0	26 250	0.02062	0.3951	79.46	12.58	2 531	0.004972
7	144.3	20 820	0.01635	0.4982	63.02	15.87	2 007	0.007905
8	128.5	16 510	0.01297	0.6282	49.98	20.01	1 592	0.01257
9	114.4	13 090	0.01028	0.7921	39.63	25.23	1 262	0.01999
10	101.9	10 380	0.008155	0.9989	31.43	31.82	1 001	0.03178
11	90.74	8 234	0.006467	1.260	24.92	40.12	794	0.05053
12	80.81	6 530	0.005129	1.588	19.77	50.59	629.6	0.08035
13	71.96	5 178	0.004067	2.003	15.68	63.80	499.3	0.1278
14	64.08	4 107	0.003225	2.525	12.43	80.44	396.0	0.2032
15	57.07	3 257	0.002558	3.184	9.858	101.4	314.0	0.3230
16	50.82	2 583	0.002028	4.016	7.818	127.9	249.0	0.5136
17	45.26	2 048	0.001609	5.064	6.200	161.3	197.5	0.8167
18	40.30	1 624	0.001276	6.385	4.917	203.4	156.6	1.299
19	35.89	1 288	0.001012	8.051	3.899	256.5	124.2	2.065
20	31.96	1 022	0.0008023	10.15	3.092	323.4	98.50	3.283
21	28.46	810.1	0.0006363	12.80	2.452	407.8	78.11	5.221
22	25.35	642.4	0.0005046	16.14	1.945	514.2	61.95	8.301
23	22.57	509.5	0.0004002	20.36	1.542	648.4	49.13	13.20
24	20.10	404.0	0.0003173	25.67	1.223	817.7	38.96	20.99
25	17.90	320.4	0.0002517	32.37	0.9699	1 031.0	30.90	33.37
26	15.94	254.1	0.0001996	40.81	0.7692	1 300	24.50	53.06
27	14.20	201.5	0.0001583	51.47	0.6100	1 639	19.43	84.37
28	12.64	159.8	0.0001255	64.90	0.4837	2 067	15.41	134.2
29	11.26	126.7	0.00009953	81.83	0.3836	2 607	12.22	213.3
30	10.03	100.5	0.00007894	103.2	0.3042	3 287	9.691	339.2
31	8.928	79.70	0.00006260	130.1	0.2413	4 145	7.685	539.3
32	7.950	63.21	0.00004964	164.1	0.1913	5 227	6.095	857.6
33	7.080	50.13	0.00003937	206.9	0.1517	6 591	4.833	1 364
34	6.305	39.75	0.00003122	260.9	0.1203	8 310	3.833	2 168
35	5.615	31.52	0.00002476	329.0	0.09542	10 480	3.040	3 448
36	5.000	25.00	0.00001964	414.8	0.07568	13 210	2.411	5 482
37	4.453	19.83	0.00001557	523.1	0.06001	16 660	1.912	8 717
38	3.965	15.72	0.00001235	659.6	0.04759	21 010	1.516	13 860
39	3.531	12.47	0.000009793	831.8	0.03774	26 500	1.202	22 040
40	3.145	9.888	0.000007766	1049.0	0.02993	33 410	0.9534	35 040

TABLE 35—HARD-DRAWN COPPER.

AWG B & S Gauge	Wire Diameter in Inches	Breaking Load in Pounds	Tensile Strength in lb/in.²	Weight		Maximum Resistance (ohms per 1000 feet at 68° F)	Cross-Sectional Area	
				Pounds per 1000 Feet	Pounds per Mile		Circular Mils	Square Inches
4/0	0.4600	8 143	49 000	640.5	3 382	0.05045	211 600	0.1662
3/0	0.4096	6 722	51 000	507.9	2 682	0.06361	167 800	0.1318
2/0	0.3648	5 519	52 800	402.8	2 127	0.08021	133 100	0.1045
1/0	0.3249	4 517	54 500	319.5	1 687	0.1011	105 500	0.08289
1	0.2893	3 688	56 100	253.3	1 338	0.1287	83 690	0.06573
2	0.2576	3 003	57 600	200.9	1 061	0.1625	66 370	0.05213
3	0.2294	2 439	59 000	159.3	841.2	0.2049	52 630	0.04134
4	0.2043	1 970	60 100	126.4	667.1	0.2584	41 740	0.03278
5	0.1819	1 591	61 200	100.2	529.1	0.3258	33 100	0.02600
—	0.1650	1 326	62 000	82.41	435.1	0.3961	27 225	0.02138
6	0.1620	1 280	62 100	79.46	419.6	0.4108	26 250	0.02062
7	0.1443	1 030	63 000	63.02	332.7	0.5181	20 820	0.01635
—	0.1340	894.0	63 400	54.35	287.0	0.6006	17 956	0.01410
8	0.1285	826.0	63 700	49.97	263.9	0.6533	16 510	0.01297
9	0.1144	661.2	64 300	39.63	209.3	0.8238	13 090	0.01028
—	0.1040	550.4	64 800	32.74	172.9	0.9971	10 816	0.008495
10	0.1019	529.2	64 900	31.43	165.9	1.039	10 380	0.008155
11	0.09074	422.9	65 400	24.92	131.6	1.310	8 234	0.006467
12	0.08081	337.0	65 700	19.77	104.4	1.652	6 530	0.005129
13	0.07196	268.0	65 900	15.68	82.77	2.083	5 178	0.004067
14	0.06408	213.5	66 200	12.43	65.64	2.626	4 107	0.003225
15	0.05707	169.8	66 400	9.858	52.05	3.312	3 257	0.002558
16	0.05082	135.1	66 600	7.818	41.28	4.176	2 583	0.002028
17	0.04526	107.5	66 800	6.200	32.74	5.266	2 048	0.001609
18	0.04030	85.47	67 000	4.917	25.96	6.640	1 624	0.001276

TABLE 36—TENSILE STRENGTH OF COPPER WIRE.

AWG B & S Gauge	Wire Diameter in Inches	Hard Drawn		Medium-Hard Drawn		Soft or Annealed	
		Minimum Tensile Strength lb/in.²	Breaking Load in Pounds	Minimum Tensile Strength lb/in.²	Breaking Load in Pounds	Maximum Tensile Strength lb/in.²	Breaking Load in Pounds
1	0.2893	56 100	3 688	46 000	3 024	37 000	2 432
2	0.2576	57 600	3 003	47 000	2 450	37 000	1 929
3	0.2294	59 000	2 439	48 000	1 984	37 000	1 530
4	0.2043	60 100	1 970	48 330	1 584	37 000	1 213
5	0.1819	61 200	1 591	48 660	1 265	37 000	961.9
—	0.1650	62 000	1 326	—	—	—	—
6	0.1620	62 100	1 280	49 000	1 010	37 000	762.9
7	0.1443	63 000	1 030	49 330	806.6	37 000	605.0
—	0.1340	63 400	894.0	—	—	—	—
8	0.1285	63 700	826.0	49 660	643.9	37 000	479.8
9	0.1144	64 300	661.2	50 000	514.2	37 000	380.5
—	0.1040	64 800	550.4	—	—	—	—
10	0.1019	64 900	529.2	50 330	410.4	38 500	314.0
11	0.09074	65 400	422.9	50 660	327.6	38 500	249.0
12	0.08081	65 700	337.0	51 000	261.6	38 500	197.5

TABLE 37—COPPER-CLAD STEEL

AWG B & S Gauge	Diam Inch	Cross-Sectional Area		Weight			Resistance Ohms/1000 ft at 68°F		Breaking Load Pounds		Attenuation in Decibels/Mile*				Characteristic Impedance*	
											40% Cond		30% Cond			
		Circular Mils	Square Inch	Pounds per 1000 Feet	Pounds per Mile	Feet per Pound	40% Conduct	30% Conduct	40% Conduct	30% Conduct	Dry	Wet	Dry	Wet	40% Cond	30% Cond
4	0.2043	41 740	0.03278	115.8	611.6	8.63	0.6337	0.8447	3 541	3 934	—	—	—	—	—	—
5	0.1819	33 100	0.02600	91.86	485.0	10.89	0.7990	1.065	2 938	3 250	—	—	—	—	—	—
6	0.1620	26 250	0.02062	72.85	384.6	13.73	1.008	1.343	2 433	2 680	0.078	0.086	0.103	0.109	650	686
7	0.1443	20 820	0.01635	57.77	305.0	17.31	1.270	1.694	2 011	2 207	0.093	0.100	0.122	0.127	685	732
8	0.1285	16 510	0.01297	45.81	241.9	21.83	1.602	2.136	1 660	1 815	0.111	0.118	0.144	0.149	727	787
9	0.1144	13 090	0.01028	36.33	191.8	27.52	2.020	2.693	1 368	1 491	0.132	0.138	0.169	0.174	776	852
10	0.1019	10 380	0.008155	28.81	152.1	34.70	2.547	3.396	1 130	1 231	0.156	0.161	0.196	0.200	834	920
11	0.0907	8 234	0.006467	22.85	120.6	43.76	3.212	4.28	896	975	0.183	0.188	0.228	0.233	910	1 013
12	0.0808	6 530	0.005129	18.12	95.68	55.19	4.05	5.40	711	770	0.216	0.220	0.262	0.266	1 000	1 120
13	0.0720	5 178	0.004067	14.37	75.88	69.59	5.11	6.81	490	530						
14	0.0641	4 107	0.003225	11.40	60.17	87.75	6.44	8.59	400	440						
15	0.0571	3 257	0.002558	9.038	47.72	110.6	8.12	10.83	300	330						
16	0.0508	2 583	0.002028	7.167	37.84	139.5	10.24	13.65	250	270						
17	0.0453	2 048	0.001609	5.684	30.01	175.9	12.91	17.22	185	205						
18	0.0403	1 624	0.001276	4.507	23.80	221.9	16.28	21.71	153	170						
19	0.0359	1 288	0.001012	3.575	18.87	279.8	20.53	27.37	122	135						
20	0.0320	1 022	0.0008023	2.835	14.97	352.8	25.89	34.52	100	110						
21	0.0285	810.1	0.0006363	2.248	11.87	444.8	32.65	43.52	73.2	81.1						
22	0.0253	642.5	0.0005046	1.783	9.413	560.9	41.17	54.88	58.0	64.3						
23	0.0226	509.5	0.0004002	1.414	7.465	707.3	51.92	69.21	46.0	51.0						
24	0.0201	404.0	0.0003173	1.121	5.920	891.9	65.46	87.27	36.5	40.4						
25	0.0179	320.4	0.0002517	0.889	4.695	1 125	82.55	110.0	28.9	32.1						
26	0.0159	254.1	0.0001996	0.705	3.723	1 418	104.1	138.8	23.0	25.4						
27	0.0142	201.5	0.0001583	0.559	2.953	1 788	131.3	175.0	18.2	20.1						
28	0.0126	159.8	0.0001255	0.443	2.342	2 255	165.5	220.6	14.4	15.9						
29	0.0113	126.7	0.0000995	0.352	1.857	2 843	208.7	278.2	11.4	12.6						
30	0.0100	100.5	0.0000789	0.279	1.473	3 586	263.2	350.8	9.08	10.0						
31	0.0089	79.70	0.0000626	0.221	1.168	4 521	331.9	442.4	7.20	7.95						
32	0.0080	63.21	0.0000496	0.175	0.926	5 701	418.5	557.8	5.71	6.30						
33	0.0071	50.13	0.0000394	0.139	0.734	7 189	527.7	703.4	4.53	5.00						
34	0.0063	39.75	0.0000312	0.110	0.582	9 065	665.4	887.0	3.59	3.97						
35	0.0056	31.52	0.0000248	0.087	0.462	11 430	839.0	1 119	2.85	3.14						
36	0.0050	25.00	0.0000196	0.069	0.366	14 410	1 058	1 410	2.26	2.49						
37	0.0045	19.83	0.0000156	0.055	0.290	18 180	1 334	1 778	1.79	1.98						
38	0.0040	15.72	0.0000123	0.044	0.230	22 920	1 682	2 243	1.42	1.57						
39	0.0035	12.47	0.00000979	0.035	0.183	28 900	2 121	2 828	1.13	1.24						
40	0.0031	9.89	0.00000777	0.027	0.145	36 440	2 675	3 566	0.893	0.986						

* DP insulators, 12-inch wire spacing at 1000 herts.

TABLE 38—CONDUCTOR SIZE FOR 2-PERCENT VOLTAGE DROP.

Current in Amperes	Distance in Feet									Distance in Feet								
	25	50	75	100	150	200	300	400	500	25	50	75	100	150	200	300	400	500
	Single-phase—110 volts									Single-phase—220 volts								
1	—	—	—	—	—	—	14	12	10	—	—	—	—	—	—	—	—	14
1.5	—	—	—	—	14	14	12	10	10	—	—	—	—	—	—	14	14	12
2	—	—	—	—	14	12	10	10	8	—	—	—	—	—	—	14	12	12
3	—	—	14	14	12	10	8	8	6	—	—	—	—	14	14	12	10	10
4	—	—	14	12	10	10	8	6	6	—	—	—	—	14	12	10	10	8
5	—	14	12	12	10	8	6	6	4	—	—	—	14	12	12	10	8	8
6	—	14	12	10	8	8	6	4	4	—	—	14	14	12	10	8	8	6
7	—	14	12	10	8	8	6	4	2	—	—	14	14	12	10	8	8	6
8	—	12	10	10	8	6	4	2	2	—	—	14	12	10	10	8	6	6
9	—	12	10	8	8	6	4	2	2	—	14	14	12	10	8	8	6	4
10	14	12	10	8	6	6	4	2	2	—	14	12	12	10	8	6	6	4
12	14	10	8	8	6	4	2	1	1	—	14	12	10	8	8	6	4	4
14	14	10	8	8	6	4	2	0	0	—	14	12	10	8	8	6	4	2
16	12	10	8	6	4	4	2	0	00	—	12	10	10	8	6	4	4	2
18	12	8	8	6	4	2	1	00	00	14	12	10	8	8	6	4	2	2
20	12	8	6	6	4	2	1	00	000	14	12	10	8	6	6	4	2	2
25	10	8	6	4	2	2	0	000	0000	14	10	8	8	6	4	2	2	1
30	10	6	4	4	2	1	00	—	—	12	10	8	6	4	4	2	1	0
35	10	6	4	2	2	0	000	—	—	12	10	8	6	4	2	2	0	00
40	8	6	4	2	1	00	0000	—	—	12	8	6	6	4	2	1	00	0000
45	8	4	4	2	0	00	—	—	—	10	8	6	4	4	2	0	00	0000
50	8	4	2	2	0	000	—	—	—	10	8	6	4	2	2	0	000	0000
60	6	4	2	1	00	0000	—	—	—	10	6	4	4	2	1	00	0000	—
70	6	2	2	0	000	—	—	—	—	10	6	4	2	2	0	000	—	—
80	6	2	1	00	0000	—	—	—	—	8	6	4	2	1	00	0000	—	—
90	4	2	0	00	—	—	—	—	—	8	4	4	2	0	00	—	—	—
100	4	2	0	000	—	—	—	—	—	8	4	2	2	0	000	—	—	—
120	4	1	00	0000	—	—	—	—	—	6	4	2	1	00	0000	—	—	—
	Three-phase—220 volts									Three-phase—440 volts								
1	—	—	—	—	—	—	—	—	—	—	—	—	—	—	—	—	—	—
1.5	—	—	—	—	—	—	—	14	14	—	—	—	—	—	—	—	—	—
2	—	—	—	—	—	—	14	14	12	—	—	—	—	—	—	—	—	—
3	—	—	—	—	—	14	12	12	10	—	—	—	—	—	—	—	14	14
4	—	—	—	—	14	14	12	10	10	—	—	—	—	—	—	14	14	12
5	—	—	—	—	14	12	10	10	8	—	—	—	—	—	—	14	12	12
6	—	—	—	14	12	12	10	8	8	—	—	—	—	—	14	12	12	10
7	—	—	14	14	12	10	8	8	6	—	—	—	—	14	14	12	10	10
8	—	—	14	14	12	10	8	6	6	—	—	—	—	14	14	12	10	10
9	—	—	14	12	10	10	8	6	6	—	—	—	—	14	12	10	10	8
10	—	—	14	12	10	10	8	6	6	—	—	—	—	14	12	10	10	8
12	—	14	12	12	10	8	6	6	4	—	—	—	14	12	12	10	8	8
14	—	14	12	10	8	8	6	4	4	—	—	14	14	12	10	8	8	6
16	—	14	12	10	8	8	6	4	2	—	—	14	14	12	10	8	8	6
18	—	12	10	10	8	6	4	4	2	—	—	14	12	10	10	8	6	6
20	—	12	10	10	8	6	4	2	2	—	—	14	12	10	10	8	6	6
25	14	12	10	8	6	6	4	2	1	—	14	12	12	10	8	6	6	4
30	14	10	8	8	6	4	2	2	0	—	14	12	10	8	8	6	6	4
35	12	10	8	6	4	4	2	1	0	—	12	10	10	8	6	4	4	4
40	12	10	8	6	4	2	2	0	00	—	12	10	10	8	6	4	2	2
45	12	8	6	6	4	2	1	0	000	14	12	10	8	6	6	4	2	2
50	12	8	6	4	4	2	0	00	000	14	12	10	8	6	6	4	2	1
60	10	8	6	4	2	2	0	000	—	14	10	8	8	6	4	2	2	0
70	10	6	4	4	2	1	00	0000	—	12	10	8	6	4	4	2	1	0
80	10	6	4	2	2	0	000	—	—	12	10	8	6	4	2	2	0	00
90	8	6	4	2	1	0	0000	—	—	12	8	6	6	4	2	1	0	000
100	8	6	4	2	0	00	—	—	—	12	8	6	6	4	2	0	00	000
120	8	4	2	2	0	0000	—	—	—	10	8	6	4	2	2	0	000	0000

metry. If the sign of a coefficient is not given it is unknown, not necessarily positive.

Unit for $d_{nm} = 10^{-8}$ statcoulomb/dyne
$= \frac{1}{3} \times 10^{-12}$ coulomb/newton
$= 10^{-8}$ cm/statvolt
$= \frac{1}{3} \times 10^{-12}$ meter/volt.

Coupling factor k is defined practically by

k^2 = (mechanical energy converted into electric charge)/(mechanical energy put into the crystal)

The converse effect is also true. The same type of relationship holds and the coupling coefficient

TABLE 39—FUSING CURRENTS IN AMPERES. *Courtesy of Automatic Electric Company; Chicago, Ill.*

AWG B & S Gauge	Diam d in Inches	Copper ($K = 10\,244$)	Aluminum ($K = 7585$)	German Silver ($K = 5230$)	Iron ($K = 3148$)	Tin ($K = 1642$)
40	0.0031	1.77	1.31	0.90	0.54	0.28
38	0.0039	2.50	1.85	1.27	0.77	0.40
36	0.0050	3.62	2.68	1.85	1.11	0.58
34	0.0063	5.12	3.79	2.61	1.57	0.82
32	0.0079	7.19	5.32	3.67	2.21	1.15
30	0.0100	10.2	7.58	5.23	3.15	1.64
28	0.0126	14.4	10.7	7.39	4.45	2.32
26	0.0159	20.5	15.2	10.5	6.31	3.29
24	0.0201	29.2	21.6	14.9	8.97	4.68
22	0.0253	41.2	30.5	21.0	12.7	6.61
20	0.0319	58.4	43.2	29.8	17.9	9.36
19	0.0359	69.7	51.6	35.5	21.4	11.2
18	0.0403	82.9	61.4	42.3	25.5	13.3
17	0.0452	98.4	72.9	50.2	30.2	15.8
16	0.0508	117	86.8	59.9	36.0	18.8
15	0.0571	140	103	71.4	43.0	22.4
14	0.0641	166	123	84.9	51.1	26.6
13	0.0719	197	146	101	60.7	31.7
12	0.0808	235	174	120	72.3	37.7
11	0.0907	280	207	143	86.0	44.9
10	0.1019	333	247	170	102	53.4
9	0.1144	396	293	202	122	63.5
8	0.1285	472	349	241	145	75.6
7	0.1443	561	416	287	173	90.0
6	0.1620	668	495	341	205	107

is numerically identical to what it was before, namely

k^2= (electrical energy converted into mechanical energy)/(electrical energy put into the crystal)

d is the measure of the deflection caused by an applied voltage or the amount of charge produced by a given force (units= meters per volt or coulomb per newton)

g denotes a field produced in a piezoelectric crystal by an applied stress unit:

$$\frac{\text{volts/meter}}{\text{newtons/square meter}}.$$

Relations between g and d are

$$g=d/\epsilon_r\epsilon_0$$

where ϵ_r= relative permittivity of the dielectric, ϵ_0= permittivity of free space= 8.85×10^{-12} farad/meter, E= Young's modulus, and $k^2=gdE$.

ACOUSTIC PROPERTIES OF SOME MATERIALS (TABLES 30–31)

ADHESIVES (TABLE 32)

SHOP DATA

Wire Tables

Temperature coefficient of resistance: The resistance of a conductor at temperature T in degrees Celsius is given by

$$R=R_{20}[1+\alpha_{20}(T-20)]$$

where R_{20} is the resistance at 20 degrees Celsius and α_{20} is the temperature coefficient of resistance at 20 degrees Celsius. For copper, α_{20}= 0.00393. That is, the resistance of a copper conductor increases approximately $\frac{4}{10}$ of 1 percent per degree Celsius rise in temperature.

Modulus of elasticity is 17 000 000 lb/inch^2. Coefficient of linear expansion is 0.0000094/degree Fahrenheit.

Weights are based on a density of 8.89 grams/cm^3 at 20 degrees Celsius (equivalent to 0.00302699 lb/circular mil/1000 feet).

The resistances are maximum values for hard-drawn copper and are based on a resistivity of 10.674 ohms/circular-mil foot at 20 degrees Celsius (97.16 percent conductivity) for sizes 0.325 inch and larger, and 10.785 ohms/circular-mil foot at 20 degrees Celsius (96.16 percent conductivity) for sizes 0.324 inch and smaller. (Refer to Tables 33–37.)

Voltage Drop in Long Circuits

Table 38 shows the conductor size (AWG or B&S gauge) necessary to limit the voltage drop to 2 percent maximum for various loads and distances. The calculations are for alternating-current circuits in conduit.

Fusing Currents of Wires

The current I in amperes at which a wire will melt can be calculated from

$$I=Kd^{3/2}$$

where d is the wire diameter in inches and K is a constant that depends on the metal concerned. Table 39 gives the fusing currents in amperes for 5 commonly used types of wire. Owing to the wide variety of factors that can influence the rate of heat loss, these figures must be considered as only approximations.

TABLE 40—PHYSICAL PROPERTIES OF VARIOUS WIRES. *Reprinted by permission from*

Property		Copper		Aluminum 99 Percent Pure
		Annealed	Hard-Drawn	
Conductivity, Matthiessen's standard in percent		99 to 102	96 to 99	61 to 63
Ohms/mil-foot at 68° F = 20° C		10.36	10.57	16.7
Circular-mil-ohms/mile at 68° F = 20° C		54 600	55 700	88 200
Pounds/mile-ohm at 68° F = 20° C		875	896	424
Mean temp coefficient of resistivity/°F		0.00233	0.00233	0.0022
Mean temp coefficient of resistivity/°C		0.0042	0.0042	0.0040
Mean specific gravity		8.89	8.94	2.68
Pounds/1000 feet/circular mil		0.003027	0.003049	0.000909
Weight in pounds/inch^3		0.320	0.322	0.0967
Mean specific heat		0.093	0.093	0.214
Mean melting point in °F		2 012	2 012	1 157
Mean melting point in °C		1 100	1 100	625
Mean coefficient of linear expansion/°F		0.00000950	0.00000950	0.00001285
Mean coefficient of linear expansion/°C		0.0000171	0.0000171	0.0000231
Solid wire (Values in pounds/in.^{2})	Ultimate tensile strength	30 000 to 42 000	45 000 to 68 000	20 000 to 35 000
	Average tensile strength	32 000	60 000	24 000
	Elastic limit	6 000 to 16 000	25 000 to 45 000	14 000
	Average elastic limit	15 000	30 000	14 000
	Modulus of elasticity	7 000 000 to 17 000 000	13 000 000 to 18 000 000	8 500 000 to 11 500 000
	Average modulus of elasticity	12 000 000	16 000 000	9 000 000
Concentric strand (Values in pounds/in.^{2})	Tensile strength	29 000 to 37 000	43 000 to 65 000	25 800
	Average tensile strength	35 000	54 000	—
	Elastic limit	5 800 to 14 800	23 000 to 42 000	13 800
	Average elastic limit	—	27 000	—
	Modulus of elasticity	5 000 000 to 12 000 000	12 000 000	Approx 10 000 000

"Transmission Towers," American Bridge Company, Pittsburgh, Pa.; 1925: p. 169.

Iron (Ex BB)	Steel (Siemens-Martin)	Crucible Steel, High Strength	Plow Steel, Extra-High Strength	Copper-Clad	
				30% Cond	40% Cond
16.8	8.7	—	—	29.4	39.0
62.9	119.7	122.5	125.0	35.5	26.6
332 000	632 000	647 000	660 000	187 000	140 000
4 700	8 900	9 100	9 300	2.775	2.075
0.0028	0.00278	0.00278	0.00278	0.0024	—
0.0050	0.00501	0.00501	0.00501	0.0044	0.0041
7.77	7.85	7.85	7.85	8.17	8.25
0.002652	0.002671	—	—	0.00281	0.00281
0.282	0.283	0.283	0.283	0.298	0.298
0.113	0.117	—	—	—	—
2 975	2 480	—	—	—	—
1 635	1 360	—	—	—	—
0.00000673	0.00000662	—	—	0.0000072	0.0000072
0.0000120	0.0000118	—	—	0.0000129	0.0000129
50 000 to 55 000	70 000 to 80 000	—	—	—	—
55 000	75 000	125 000	187 000	60 000	100 000
25 000 to 30 000	35 000 to 50 000	—	—	—	—
30 000	38 000	69 000	130 000	30 000	50 000
22 000 000 to 27 000 000	22 000 000 to 29 000 000	—	—	—	—
26 000 000	29 000 000	30 000 000	30 000 000	19 000 000	21 000 000
—	74 000 to 98 000	85 000 to 165 000	140 000 to 245 000	70 000 to 97 000	—
—	80 000	125 000	180 000	80 000	—
—	37 000 to 49 000	—	—	—	—
—	40 000	70 000	110 000	—	—
—	12 000 000	15 000 000	15 000 000	—	—

Physical Properties (Tables 40–41)

TABLE 41—PHYSICAL PROPERTIES OF STRANDED COPPER (AWG)*.

Circular Mils	AWG B & S Gauge	Number of Wires	Individual Wire Diam in Inches	Cable Diam in Inches	Area in Square Inches	Weight in Lb per 1000 Ft	Weight in Lb per Mile	*Maximum Resistance in Ohms/1000 Ft at 20° C
211 600	4/0	19	0.1055	0.528	0.1662	653.3	3 450	0.05093
167 800	3/0	19	0.0940	0.470	0.1318	518.1	2 736	0.06422
133 100	2/0	19	0.0837	0.419	0.1045	410.9	2 170	0.08097
105 500	1/0	19	0.0745	0.373	0.08286	325.7	1 720	0.1022
83 690	1	19	0.0664	0.332	0.06573	258.4	1 364	0.1288
66 370	2	7	0.0974	0.292	0.05213	204.9	1 082	0.1624
52 640	3	7	0.0867	0.260	0.04134	162.5	858.0	0.2048
41 740	4	7	0.0772	0.232	0.03278	128.9	680.5	0.2582
33 100	5	7	0.0688	0.206	0.02600	102.2	539.6	0.3256
26 250	6	7	0.0612	0.184	0.02062	81.05	427.9	0.4105
20 820	7	7	0.0545	0.164	0.01635	64.28	339.4	0.5176
16 510	8	7	0.0486	0.146	0.01297	50.98	269.1	0.6528
13 090	9	7	0.0432	0.130	0.01028	40.42	213.4	0.8233
10 380	10	7	0.0385	0.116	0.008152	32.05	169.2	1.038
6 530	12	7	0.0305	0.0915	0.005129	20.16	106.5	1.650
4 107	14	7	0.0242	0.0726	0.003226	12.68	66.95	2.624
2 583	16	7	0.0192	0.0576	0.002029	7.975	42.11	4.172
1 624	18	7	0.0152	0.0456	0.001275	5.014	26.47	6.636
1 022	20	7	0.0121	0.0363	0.0008027	3.155	16.66	10.54

* The resistance values in this table are trade maxima for soft or annealed copper wire and are higher than the average values for commercial cable. The following values for the conductivity and resistivity of copper at 20 degrees Celsius were used:

Conductivity in terms of International Annealed Copper Standard: 98.16 percent

Resistivity in pounds per mile-ohm: 891.58

The resistance of hard-drawn copper is slightly greater than the values given, being about 2 percent to 3 percent greater for sizes from 4/0 to 20 AWG.

TABLE 42—MACHINE-SCREW DIMENSIONS AND OTHER DATA.

Screw		Threads/in.		Clearance Drill*		Tap Drill†			Head					Hex Nut			Washer		
							Diameter		Round		Flat	Fillister							
No.	Diam	Coarse	Fine	No.	Diam	No.	Inches	mm	Max OD	Max Height	Max OD	Max OD	Max Height	Across Flat	Across Corner	Thick-ness	OD	ID	Thick-ness
0	0.060	—	80	52	0.064	56	0.047	1.2	0.113	0.053	0.119	0.096	0.059	0.156	0.171	0.046	—	—	—
1	0.073	64	72	47	0.079	53	0.060	1.5	0.138	0.061	0.146	0.118	0.070	0.156	0.171	0.046	—	—	—
2	0.086	56	64	42	0.094	50	0.070	1.8	0.162	0.070	0.172	0.140	0.083	0.187	0.205	0.062	¼	0.093	0.032
3	0.099	48 / —	— / 56	37	0.104	47 / 45	0.079 / 0.082	2.0 / 2.1	0.187	0.078	0.199	0.161	0.095	0.187	0.205	0.062	¼	0.105	0.020
4	0.112	40 / —	— / 48	31	0.120	43 / 42	0.089 / 0.094	2.3 / 2.4	0.211	0.086	0.225	0.183	0.107	0.250	0.275	0.093	5/16	0.125	0.032
5	0.125	40 / —	— / 44	29	0.136	38 / 37	0.102 / 0.104	2.6 / 2.6	0.236	0.095	0.252	0.205	0.120	0.312	0.344	0.109	3/8	0.140	0.032
6	0.138	32 / —	— / 40	27	0.144	36 / 33	0.107 / 0.113	2.7 / 2.9	0.260	0.103	0.279	0.226	0.132	0.312	0.344	0.109	5/16 / 3/8	0.156	0.026 / 0.046
8	0.164	32 / —	— / 36	18	0.170	29 / 29	0.136 / 0.136	3.5 / 3.5	0.309	0.119	0.332	0.270	0.156	0.344	0.373	0.125	3/8 / 7/16	0.186	0.032 / 0.046
10	0.190	24 / —	— / 32	9	0.196	25 / 21	0.150 / 0.159	3.8 / 4.0	0.359	0.136	0.385	0.313	0.180	0.375	0.413	0.125	7/16 / ½	0.218	0.036 / 0.063
12	0.216	24 / —	— / 28	2	0.221	16 / 14	0.177 / 0.182	4.5 / 4.6	0.408	0.152	0.438	0.357	0.205	0.437	0.488	0.156	½ / 9/16	0.250	0.063
¼	0.250	20 / —	— / 28	—	17/64	7 / 3	0.201 / 0.213	5.1 / 5.5	0.472	0.174	0.507	0.414	0.237	0.437 / 0.500	0.488 / 0.577	0.203 / 0.250	9/16 / 5/8	0.281	0.040 / 0.063

All dimensions in inches except where noted.

* Clearance-drill sizes are practical values for use of the engineer or technician doing his own shop work.

† Tap-drill sizes are for use in hand tapping material such as brass or soft steel. For copper, aluminum, Norway iron, cast iron, bakelite, or for very thin material, the drill should be a size or two larger in diameter than shown.

TABLE 43—DRILL SIZES. *From New Departure Handbook.*

Drill	Inches	Drill	Inches	Drill	Inches	Drill	Inches
0.10 mm	0.003937	no 59	0.041000	no 41	0.096000	4.30 mm	0.169291
0.15 mm	0.005905	1.05 mm	0.041338	2.45 mm	0.096456	no 18	0.169500
0.20 mm	0.007874	no 58	0.042000	no 40	0.098000	11/64 in.	0.171875
0.25 mm	0.009842	no 57	0.043000	2.50 mm	0.098425	no 17	0.173000
0.30 mm	0.011811	1.10 mm	0.043307	no 39	0.099500	4.40 mm	0.173228
no 80	0.013000	1.15 mm	0.045275	no 38	0.101500	no 16	0.177000
no 79½	0.013500	no 56	0.046500	2.60 mm	0.102362	4.50 mm	0.177165
0.35 mm	0.013779	3/64 in.	0.046875	no 37	0.104000	no 15	0.180000
no 79	0.014000	1.20 mm	0.047244	2.70 mm	0.106299	4.60 mm	0.181102
no 78½	0.014500	1.25 mm	0.049212	no 36	0.106500	no 14	0.182000
no 78	0.015000	1.30 mm	0.051181	2.75 mm	0.108267	no 13	0.185000
1/64 in.	0.015625	no 55	0.052000	7/64 in.	0.109375	4.70 mm	0.185039
0.40 mm	0.015748	1.35 mm	0.053149	no 35	0.110000	4.75 mm	0.187007
no 77	0.016000	no 54	0.055000	2.80 mm	0.110236	3/16 in.	0.187500
0.45 mm	0.017716	1.40 mm	0.055118	no 34	0.111000	4.80 mm	0.188976
no 76	0.018000	1.45 mm	0.057086	no 33	0.113000	no 12	0.189000
0.50 mm	0.019685	1.50 mm	0.059055	2.90 mm	0.114173	no 11	0.191000
no 75	0.020000	no 53	0.059500	no 32	0.116000	4.90 mm	0.192913
no 74½	0.021000	1.55 mm	0.061023	3.00 mm	0.118110	no 10	0.193500
0.55 mm	0.021653	1/16 in.	0.062500	no 31	0.120000	no 9	0.196000
no 74	0.022000	1.60 mm	0.062992	3.10 mm	0.122047	5.00 mm	0.196850
no 73½	0.022500	no 52	0.063500	1/8 in.	0.125000	no 8	0.199000
no 73	0.023000	1.65 mm	0.064960	3.20 mm	0.125984	5.10 mm	0.200787
0.60 mm	0.023622	1.70 mm	0.066929	3.25 mm	0.127952	no 7	0.201000
no 72	0.024000	no 51	0.067000	no 30	0.128500	13/64 in.	0.203125
no 71½	0.025000	1.75 mm	0.068897	3.30 mm	0.129921	no 6	0.204000
0.65 mm	0.025590	no 50	0.070000	3.40 mm	0.133858	5.20 mm	0.204724
no 71	0.026000	1.80 mm	0.070866	no 29	0.136000	no 5	0.205500
no 70	0.027000	1.85 mm	0.072834	3.50 mm	0.137795	5.25 mm	0.206692
0.70 mm	0.027559	no 49	0.073000	no 28	0.140500	5.30 mm	0.208661
no 69½	0.028000	1.90 mm	0.074803	9/64 in.	0.140625	no 4	0.209000
no 69	0.029000	no 48	0.076000	3.60 mm	0.141732	5.40 mm	0.212598
no 68½	0.029250	1.95 mm	0.076771	no 27	0.144000	no 3	0.213000
0.75 mm	0.029527	5/64 in.	0.078125	3.70 mm	0.145669	5.50 mm	0.216535
no 68	0.030000	no 47	0.078500	no 26	0.147000	7/32 in.	0.218750
no 67	0.031000	2.00 mm	0.078740	3.75 mm	0.147637	5.60 mm	0.220472
1/32 in.	0.031250	2.05 mm	0.080708	no 25	0.149500	no 2	0.221000
0.80 mm	0.031496	no 46	0.081000	3.80 mm	0.149606	5.70 mm	0.224409
no 66	0.032000	no 45	0.082000	no 24	0.152000	5.75 mm	0.226377
no 65	0.033000	2.10 mm	0.082677	3.90 mm	0.153543	no 1	0.228000
0.85 mm	0.033464	2.15 mm	0.084645	no 23	0.154000	5.80 mm	0.228346
no 64	0.035000	no 44	0.086000	5/32 in.	0.156250	5.90 mm	0.232283
0.90 mm	0.035433	2.20 mm	0.086614	no 22	0.157000	ltr A	0.234000
no 63	0.036000	2.25 mm	0.088582	4.00 mm	0.157480	15/64 in.	0.234375
no 62	0.037000	no 43	0.089000	no 21	0.159000	6.00 mm	0.236220
0.95 mm	0.037401	2.30 mm	0.090551	no 20	0.161000	ltr B	0.238000
no 61	0.038000	2.35 mm	0.092519	4.10 mm	0.161417	6.10 mm	0.240157
no 60½	0.039000	no 42	0.093500	4.20 mm	0.165354	ltr C	0.242000
1.00 mm	0.039370	3/32 in.	0.093750	no 19	0.166000	6.20 mm	0.244094
no 60	0.040000	2.40 mm	0.094488	4.25 mm	0.167322	ltr D	0.246000

TABLE 43—CONTINUED.

Drill	Inches	Drill	Inches	Drill	Inches	Drill	Inches
6.25 mm	0.246062	ltr O	0.316000	10.00 mm	0.393700	17.50 mm	0.688975
6.30 mm	0.248031	8.10 mm	0.318897	ltr X	0.397000	45/64 in.	0.703125
ltr E, 1/4 in.	0.250000	8.20 mm	0.322834	ltr Y	0.404000	18.00 mm	0.708660
		ltr P	0.323000	13/32 in.	0.406250	23/32 in.	0.718750
6.40 mm	0.251968	8.25 mm	0.324802	ltr Z	0.413000	18.50 mm	0.728345
6.50 mm	0.255905	8.30 mm	0.326771	10.50 mm	0.413385	47/64 in.	0.734375
ltr F	0.257000	21/64 in.	0.328125	27/64 in.	0.421875	19.00 mm	0.748030
6.60 mm	0.259842	8.40 mm	0.330708	11.00 mm	0.433070	3/4 in.	0.750000
ltr G	0.261000	ltr Q	0.332000	7/16 in.	0.437500	49/64 in.	0.765625
6.70 mm	0.263779	8.50 mm	0.334645	11.50 mm	0.452755	19.50 mm	0.767715
17/64 in.	0.265625	8.60 mm	0.338582	29/64 in.	0.453125	25/32 in.	0.781250
6.75 mm	0.265747	ltr R	0.339000	15/32 in.	0.468750	20.00 mm	0.787400
ltr H	0.266000	8.70 mm	0.342519	12.00 mm	0.472440	51/64 in.	0.796875
6.80 mm	0.267716	11/32 in.	0.343750	31/64 in.	0.484375	20.50 mm	0.807085
6.90 mm	0.271653	8.75 mm	0.344487	12.50 mm	0.492125	13/16 in.	0.812500
ltr I	0.272000	8.80 mm	0.346456	1/2 in.	0.500000	21.00 mm	0.826770
7.00 mm	0.275590	ltr S	0.348000	13.00 mm	0.511810	53/64 in.	0.828125
ltr J	0.277000	8.90 mm	0.350393	33/64 in.	0.515625	27/32 in.	0.843750
7.10 mm	0.279527	9.00 mm	0.354330	17/32 in.	0.531250	21.50 mm	0.846455
ltr K	0.281000	ltr T	0.358000	13.50 mm	0.531495	55/64 in.	0.859375
9/32 in.	0.281250	9.10 mm	0.358267	35/64 in.	0.546875	22.00 mm	0.866140
7.20 mm	0.283464	23/64 in.	0.359375	14.00 mm	0.551180	7/8 in.	0.875000
7.25 mm	0.285432	9.20 mm	0.362204	9/16 in.	0.562500	22.50 mm	0.885825
7.30 mm	0.287401	9.25 mm	0.364172	14.50 mm	0.570865	57/64 in.	0.890625
ltr L	0.290000	9.30 mm	0.366141	37/64 in.	0.578125	23.00 mm	0.905510
7.40 mm	0.291338	ltr U	0.368000	15.00 mm	0.590550	29/32 in.	0.906250
ltr M	0.295000	9.40 mm	0.370078	19/32 in.	0.593750	59/64 in.	0.921875
7.50 mm	0.295275	9.50 mm	0.374015	39/64 in.	0.609375	23.50 mm	0.925195
19/64 in.	0.296875	3/8 in.	0.375000	15.50 mm	0.610235	15/16 in.	0.937500
7.60 mm	0.299212	ltr V	0.377000	5/8 in.	0.625000	24.00 mm	0.944880
ltr N	0.302000	9.60 mm	0.377952	16.00 mm	0.629920	61/64 in.	0.953125
7.70 mm	0.303149	9.70 mm	0.381889	41/64 in.	0.640625	24.50 mm	0.964565
7.75 mm	0.305117	9.75 mm	0.383857	16.50 mm	0.649605	31/32 in.	0.968750
7.80 mm	0.307086	9.80 mm	0.385826	21/32 in.	0.656250	25.00 mm	0.984250
7.90 mm	0.311023	ltr W	0.386000	17.00 mm	0.669290	63/64 in.	0.984375
5/16 in.	0.312500	9.90 mm	0.389763	43/64 in.	0.671875	1 in.	1.000000
8.00 mm	0.314960	25/64 in.	0.390625	11/16 in.	0.687500		

Machine Screws and Drill Sizes (Tables 42–43)

Head Styles—Method of Length Measurement (Fig. 5)

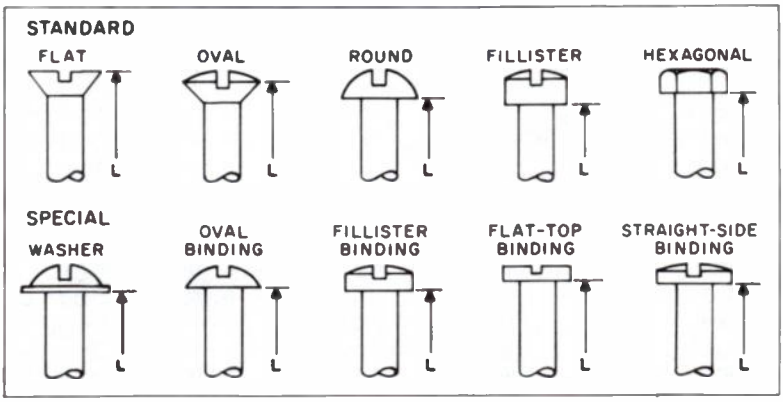

Fig. 5.

Sheet-Metal Gauges

Systems in Use: Materials are customarily made to certain gauge systems. While materials can usually be had specially in any system, some usual practices are shown in Tables 44 and 45.

TABLE 44—COMMON GAUGE PRACTICES.

Material	Sheet	Wire
Aluminum	B&S	AWG (B&S)
Brass, bronze, sheet	B&S	—
Copper	B&S	AWG (B&S)
Iron, steel, band, and hoop	BWG	—
Iron, steel, telephone, and telegraph wire	—	BWG
Steel wire, except telephone and telegraph	—	W&M
Steel sheet	US	—
Tank steel	BWG	—
Zinc sheet	"Zinc gauge" proprietary	—

TABLE 45—COMPARISON OF GAUGES. *Courtesy of Whitehead Metal Products Co., Inc.*

Gauge	AWG B&S	Birmingham or Stubs BWG	Wash. & Moen W&M	British Standard NBS SWG	London or Old English	United States Standard US	American Standard Preferred Thickness*
0000000	—	—	0.490	0.500	—	0.50000	—
000000	0.5800	—	0.460	0.464	—	0.46875	—
00000	0.5165	—	0.430	0.432	—	0.43750	—
0000	0.4600	0.454	0.3938	0.400	0.454	0.40625	—
000	0.4096	0.425	0.3625	0.372	0.425	0.37500	—
00	0.3648	0.380	0.3310	0.348	0.380	0.34375	—
0	0.3249	0.340	0.3065	0.324	0.340	0.31250	—
1	0.2893	0.300	0.2830	0.300	0.300	0.28125	—
2	0.2576	0.284	0.2625	0.276	0.284	0.265625	—
3	0.2294	0.259	0.2437	0.252	0.259	0.250000	0.224
4	0.2043	0.238	0.2253	0.232	0.238	0.234375	0.200
5	0.1819	0.220	0.2070	0.212	0.220	0.218750	0.180
6	0.1620	0.203	0.1920	0.192	0.203	0.203125	0.160
7	0.1443	0.180	0.1770	0.176	0.180	0.187500	0.140
8	0.1285	0.165	0.1620	0.160	0.165	0.171875	0.125
9	0.1144	0.148	0.1483	0.144	0.148	0.156250	0.112
10	0.1019	0.134	0.1350	0.128	0.134	0.140625	0.100
11	0.09074	0.120	0.1205	0.116	0.120	0.125000	0.090
12	0.08081	0.109	0.1055	0.104	0.109	0.109375	0.080
13	0.07196	0.095	0.0915	0.092	0.095	0.093750	0.071
14	0.06408	0.083	0.0800	0.080	0.083	0.078125	0.063
15	0.05707	0.072	0.0720	0.072	0.072	0.0703125	0.056
16	0.05082	0.065	0.0625	0.064	0.065	0.0625000	0.050
17	0.04526	0.058	0.0540	0.056	0.058	0.0562500	0.045
18	0.04030	0.049	0.0475	0.048	0.049	0.0500000	0.040
19	0.03589	0.042	0.0410	0.040	0.040	0.0437500	0.036
20	0.03196	0.035	0.0348	0.036	0.035	0.0375000	0.032
21	0.02846	0.032	0.03175	0.032	0.0315	0.0343750	0.028
22	0.02535	0.028	0.02860	0.028	0.0295	0.0312500	0.025
23	0.02257	0.025	0.02580	0.024	0.0270	0.0281250	0.022
24	0.02010	0.022	0.02300	0.022	0.0250	0.0250000	0.020
25	0.01790	0.020	0.02040	0.020	0.0230	0.0218750	0.018
26	0.01594	0.018	0.01810	0.018	0.0205	0.0187500	0.016
27	0.01420	0.016	0.01730	0.0164	0.0187	0.0171875	0.014
28	0.01264	0.014	0.01620	0.0148	0.0165	0.0156250	0.012
29	0.01126	0.013	0.01500	0.0136	0.0155	0.0140625	0.011
30	0.01003	0.012	0.01400	0.0124	0.01372	0.0125000	0.010
31	0.008928	0.010	0.01320	0.0116	0.01220	0.01093750	0.009
32	0.007950	0.009	0.01280	0.0108	0.01120	0.01015625	0.008
33	0.007080	0.008	0.01180	0.0100	0.01020	0.00937500	0.007
34	0.006305	0.007	0.01040	0.0092	0.00950	0.00859375	0.006
35	0.005615	0.005	0.00950	0.0084	0.00900	0.00781250	—
36	0.005000	0.004	0.00900	0.0076	0.00750	0.007031250	—
37	0.004453	—	0.00850	0.0068	0.00650	0.006640625	—
38	0.003965	—	0.00800	0.0060	0.00570	0.006250000	—
39	0.003531	—	0.00750	0.0052	0.00500	—	—
40	0.003145	—	0.00700	0.0048	0.00450	—	—

* These thicknesses are intended to express the desired thickness in decimal fractions of an inch. They have no relation to gauge numbers; they are approximately related to the AWG sizes 3–34.

Antifreeze Solutions (Table 46)

TABLE 46—COMMERCIAL ANTIFREEZE SOLUTIONS.

Percent by Volume	Percent by Volume in Water with Freezing Points and Specific Gravities				
	10	20	30	40	50
Typical commercial methanol antifreeze	−5.2°C	−12.0°C	−21.1°C	−32.2°C	−45.0°C
Sp. gr. at 15°C/15°C*	0.986	0.975	0.963	0.950	0.935
Typical commercial ethanol antifreeze	−3.3°C	−7.7°C	−14.2°C	−22.0°C	−30.6°C
Sp. gr. at 15°C/15°C*	0.988	0.977	0.967	0.955	0.938
Commercial glycerine† antifreeze	−1.6°C	−4.7°C	−9.5°C	−15.4°C	−23.0°C
Sp. gr. at 15°C/15°C*	1.023	1.048	1.074	1.101	1.128
Typical commercial ethylene glycol† antifreeze	−3.8°C	−8.8°C	−15.5°C	−24.3°C	−36.5°C
Sp. gr. at 15°C/15°C*	1.015	1.030	1.045	1.060	1.074

* Specific gravity is measured for mixture at 15°C referred to water at 15°C.

† Glycerine and ethylene glycol are practically nonvolatile. All types must be suitably inhibited to prevent cooling-system corrosion. Commercial antifreeze solutions based on ethylene glycol and on glycerine are in use at the present time.

CHAPTER 5
COMPONENTS OR PARTS

GENERAL STANDARDS

Standardization of electronic components or parts is handled by several cooperating agencies.

In the US, the Electronic Industries Association (EIA)*, and the American National Standards Institute (ANSI)† are active in the commercial field. Electron-tube and semiconductor-device standards are handled by the Joint Electron Device Engineering Council (JEDEC), a cooperative effort of EIA and the National Electrical Manufacturers Association (NEMA)‡. Military (MIL) standards are issued by the US Department of Defense or one of its agencies such as the Defense Electronics Supply Center (DESC).

International standardization in the electronics field is carried out by the various Technical Committees of the International Electrotechnical Commission (IEC)§. A list of the available IEC Recommendations is included in the ANSI Index (outside the US, consult the national standardization agency or the IEC). IEC documents may be used directly or their recommendations may be incorporated in whole or in part in national standards issued by the EIA or ANSI. A few broad areas may be covered by standards issued by the International Standards Organization (ISO).

These organizations establish standards for electronic components or parts (and in some cases, for equipments) to provide interchangeability among different products regarding size, performance, and identification; minimum number of sizes and designs; and uniform testing of products for acceptance. This chapter presents a brief outline of the requirements, characteristics, and designations for the major types of component parts used in electronic equipment. Such standardization offers economic advantages to both the parts user and the parts manufacturer, but is not intended to prevent the manufacture and use of other parts under special conditions.

There is a trend away from circuits assembled of separate components and wiring and toward integrated circuits that have the various resistors, capacitors, inductors, and semiconductor devices deposited on a common substrate. Such integrated circuits offer advantages of minimum size, good stability (with proper protection), and economical manufacture in large quantities. However, field repair and revisions of the circuit values after manufacture are not possible—failure of any portion of an integrated circuit necessitates replacement of the entire unit. As of this printing (1975) integrated-circuit standards are still being developed; however, standard outlines, systems of nomenclature, methods of reporting technical characteristics, and some standards for testing procedures have been established.

Color Coding

The color code of Table 1 is used for marking electronic parts.

Tolerance

The maximum deviation allowed from the specified nominal value is known as the tolerance. It is usually given as a percentage of the nominal value, though for very small capacitors the tolerance may be specified in picofarads (pF). For critical applications it is important to specify the permissible tolerance; where no tolerance is specified, components are likely to vary by ±20 percent from the nominal value.

Do not assume that a given lot of components will have values distributed throughout the acceptable range of values. A lot ordered with a

* EIA Engineering Dept., Washington, D. C. Index of standards is available. EIA was formerly Radio-Electronics-Television Manufacturers' Association (RETMA).

† ANSI, New York, New York. Index of standards is available. ANSI was formerly the USA Standards Institute (USASI).

‡ NEMA, New York, New York. Index of standards is available.

§ IEC, Central Office; Geneva, Switzerland. The US National Committee for the IEC operates within the ANSI.

TABLE 1—STANDARD COLOR CODE OF ELECTRONICS INDUSTRY.

Color	Significant Figure	Decimal Multiplier	Tolerance in Percent*	Voltage Rating	Characteristic
Black	0	1	±20 (M)	—	A
Brown	1	10	±1 (F)	100	B
Red	2	100	±2 (G)	200	C
Orange	3	1 000	±3	300	D
Yellow	4	10 000	GMV‡	400	E
Green	5	100 000	±5(J)†, (0.50(D))§	500	F
Blue	6	1 000 000	±6, (0.25(C))§	600	G
Violet	7	10 000 000	±12.5, (0.10(B))§	700	—
Gray	8	0.01†	±30, (0.05(N))§	800	I
White	9	0.1†	±10†	900	J
Gold	—	0.1	±5 (J), (0.50(E))‖	1 000	—
Silver	—	0.01	±10 (K)	2 000	—
No Color	—	—	±20	500	—

* Tolerance letter symbol as used in type designations has tolerance meaning as shown. ±3, ±6, ±12.5, and ±30 percent are tolerances for USA Std 40-, 20-, 10-, and 5-step series, respectively.
† Optional coding where metallic pigments are undesirable.
‡ GMV is −0 to +100-percent tolerance or Guaranteed Minimum Value.
§ For some film and other resistors only.
‖ For some capacitors only.

±20% tolerance may include *no* parts having values within 5% of the desired nominal value; these may have been sorted out before shipment. The manufacturing process for a given lot may produce parts in a narrow range of values only, not necessarily centered in the acceptable tolerance range.

Preferred Values

To maintain an orderly progression of sizes, preferred numbers are frequently used for the nominal values. A further advantage is that all parts manufactured are salable as one or another of the preferred values. Each preferred value differs from its predecessor by a constant multiplier, and the final result is conveniently rounded to two significant figures.

ANSI Standard Z17.1-1973 covers a series of preferred numbers based on $(10)^{1/5}$ and $(10)^{1/10}$ as listed in Table 2. This series has been widely used for fixed wire-wound power-type resistors and for time-delay fuses.

Because of the established practice of using ±20-, ±10-, and ±5-percent tolerances, a series of values based on $(10)^{1/6}$, $(10)^{1/12}$, and $(10)^{1/24}$ has been adopted by the EIA, and is now an ANSI Standard (C83.2-1971) (EIA RS-385). It is widely used for such small electronic components as fixed composition resistors and fixed ceramic, mica, and molded paper capacitors. These values are listed in Table 2. (For series with smaller steps, consult the ANSI or EIA Standard.)

Voltage Rating

Distinction must be made between the breakdown-voltage rating (test volts) and the working-voltage rating. The maximum voltage that may be applied (usually continuously) over a long period of time without causing the part to fail determines the working-voltage rating. Application of the test voltage for more than a very few minutes, or even repeated applications of short duration, may result in permanent damage or failure of the part.

Characteristic

This term is frequently used to include various qualities of a part such as temperature coefficient of capacitance or resistance, Q value, maximum permissible operating temperature, stability when subjected to repeated cycles of high and low temperature, and deterioration when it is subjected to moisture either as humidity or water immersion.

TABLE 2—PREFERRED VALUES*.

	USA Standard Z17.1-1973†		USA Standard C83.2-1971‡		
Name of Series	"5"	"10"	±20%(E6)	±10%(E12)	±5%(E24)
Percent step size	60	25	≈40	20	10
Step multiplier	$(10)^{1/5}=1.58$	$(10)^{1/10}=1.26$	$(10)^{1/6}=1.46$	$(10)^{1/12}=1.21$	$(10)^{1/24}=1.10$
Values in the series (Use decimal multipliers for smaller or larger values)	10	10	10	10	10
	—	12.5	—	—	11
	—	(12)	—	12	12
	—	—	—	—	13
	—	—	15	15	15
	16	16	—	—	16
	—	—	—	18	18
	—	20	—	—	20
	—	—	22	22	22
	—	—	—	—	24
	25	25	—	—	—
	—	—	—	27	27
	—	31.5	—	—	30
	—	(32)	—	—	—
	—	—	33	33	33
	—	—	—	—	36
	—	—	—	39	39
	40	40	—	—	—
	—	—	—	—	43
	—	—	47	47	47
	—	50	—	—	—
	—	—	—	—	51
	—	—	—	56	56
	—	—	—	—	62
	63	63	—	—	—
	—	—	68	68	68
	—	—	—	—	75
	—	80	—	—	—
	—	—	—	82	82
	—	—	—	—	91
	100	100	100	100	100

* ANSI Standard C83.2-1971 applies to most electronics components. It is the same as EIA Standard RS-385 (formerly GEN-102) and agrees with IEC Publication 63. ANSI Standard Z17.1-1973 covers preferred numbers and agrees with ISO 3 and ISO 497.

† "20" series with 12-percent steps ($(10)^{1/20}=1.22$ multiplier) and a "40" series with 6-percent steps ($(10)^{1/40}=1.059$ multiplier) are also standard.

‡ Associate the tolerance ±20%, ±10%, or ±5% only with the values listed in the corresponding column. Thus, 1200 ohms may be either ±10 or ±5, but not ±20 percent; 750 ohms may be ±5, but neither ±20 nor ±10 percent.

One or two letters are assigned in EIA or MIL type designations, and the characteristic may be indicated by color coding on the part. An explanation of the characteristics applicable to a component or part will be found in the following sections covering that part.

ENVIRONMENTAL TEST METHODS

Since many component parts and equipments have the same environmental exposure, environmental test methods are becoming standardized. The principal standards follow.

EIA Standard RS-186-D (*ANSI C83.58-1972*): Standard Test Methods for Passive Electronic Component Parts.

IEC Publication 68: Basic Environmental Testing Procedures for Electronic Components and Electronic Equipment (published in several parts).

MIL-STD-202E: Military Standard Test Methods for Electronic and Electrical Component Parts.

MIL-STD-810C: Military Standard Environmental Test Methods.

ASTM Standard Test Methods*—Primarily applicable to the materials used in electronic component parts.

Wherever the test methods in these standards are reasonably applicable, they should be specified in preference to other methods. This simplifies testing of a wide variety of parts, testing in widely separated locations, and comparison of data.

When selecting destructive environmental tests to determine the probable life of a part, distinguish between the environment prevailing during normal equipment operation and the environment used to accelerate deterioration. During exposure to the latter environment, the item may be out of tolerance with respect to its parameters in its normal operating-environment range. Accelerated tests are most meaningful if some relation between the degree of acceleration and component life is known. Such acceleration factors are known for many insulation systems.

STANDARD AMBIENT CONDITIONS FOR MEASUREMENT

	Standard	Temperature (°C)	Relative Humidity (%)	Barometric Pressure	
				mm Hg	mbar
Normal range	RS-186-D	15–35	45–75	650–800	860–1060
	IEC-68	15–35	45–75	(645–795)	860–1060
	MIL-STD-202E	15–35	45–75	650–800	(866–1066)
	MIL-STD-810C	13–33	20–80	650–775	(866–1033)
Closely controlled range	IEC-68	20±1	65±2	(645–795)	860–1060
	IEC-68	23±1	50±2	(645–795)	860–1060
	MIL-STD-202E	23±1	50±2	650–800	(866–1066)
	MIL-STD-810C	23±1.4	50±5	650–775	(866–1033)
	IEC-68	27±1	65±2	(645–795)	860–1060
	RS-186-D	25±2	50±2	650–800	860–1060

Notes:

1. Use the closely controlled range only if the properties are sensitive to temperature or humidity variations, or for referee conditions in case of a dispute. The three temperatures 20°, 23°, and 27°C correspond to normal laboratory conditions in various parts of the world.
2. Rounded derived values are shown in parentheses ( ).
3. 25±2°C, 20 to 50% relative humidity (RH) has been widely used as a closely controlled ambient for testing electronics components.

OTHER STANDARD ENVIRONMENTAL TEST CONDITIONS

Ambient Temperature

Dry heat, °C: +30, +40, (+49), +55, (+68), +70, (+71), +85, +100, +125, +155, +200 (values in parentheses not universally used).

Cold, °C: −10, −25, −40, −55, −65.

* ASTM = American Society for Testing and Materials; Philadelphia, Pa. Index of standards is available.

Constant-Humidity Tests

40°C, 90 to 95% RH; 4, 10, 21, or 56 days.

66°C, ≈100% RH: 48, 96, or 240 hours (primarily for small items).

Cycling Humidity Tests

Figure 1 shows a number of cycling humidity tests. (See applicable chart in standard for full details.) Preconditioning is customary before starting cycle series. RH = relative humidity.

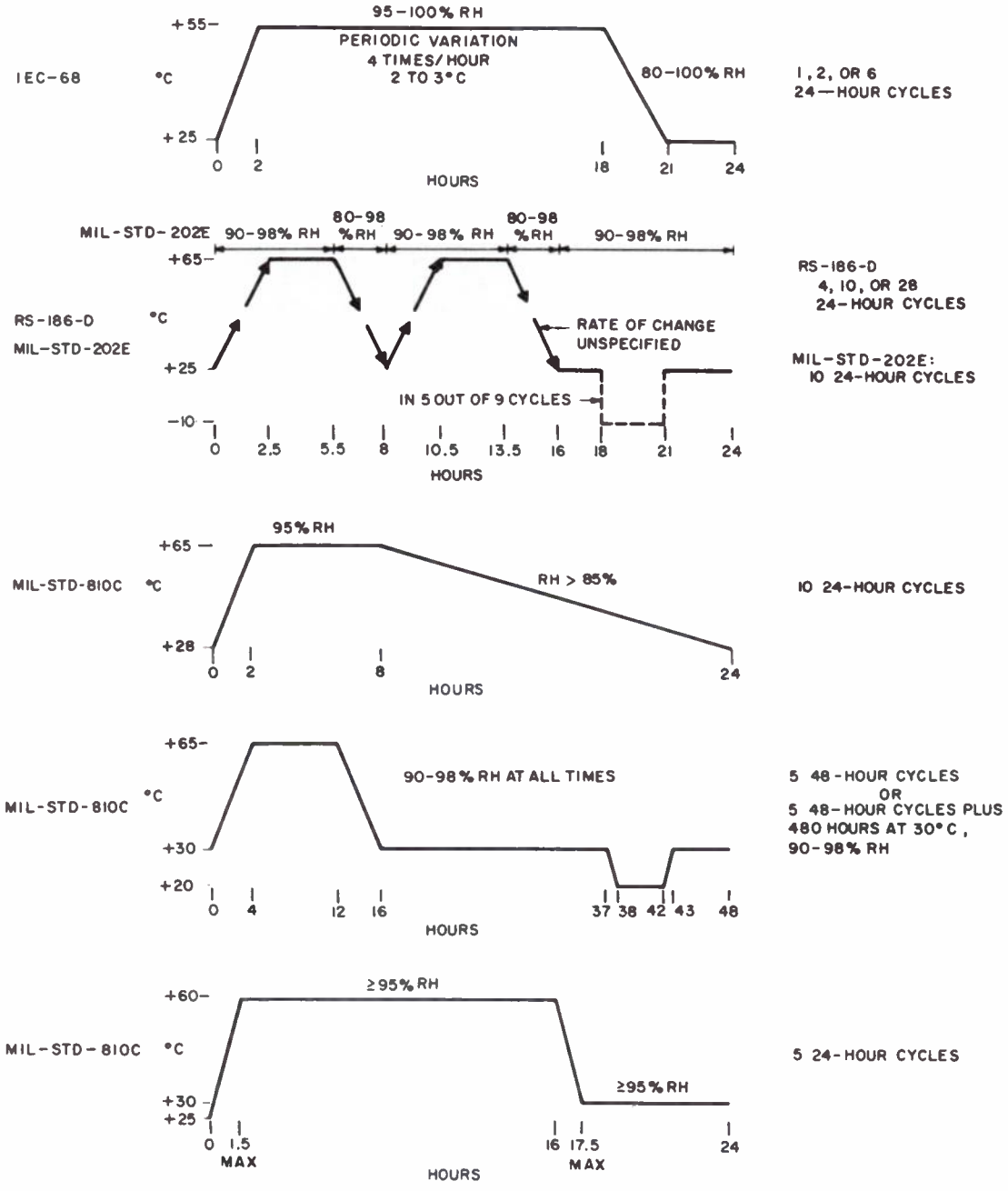

Fig. 1—Cycling humidity tests. Relative humidity for RS-186-D is 90–95% but may be uncontrolled during temperature changes.

High Altitude Tests

Pressure			Approximate Corresponding Altitude		
mbar	mm Hg	in. Hg	feet	meters	Standard
700	*525*	*20.67*	*7 218*	2 200	IEC
600	*450*	*17.72*	*11 483*	3 500	IEC
533	*400*	*15.74*	*14 108*	4 300	IEC
586	439	17.3	15 000	4 572	MIL-202
466	*349*	13.75	20 000	*6 096*	RS-186
300	*225*	*8.86*	*27 900*	8 500	IEC
300	226	8.88	30 000	9 144	MIL-202, RS-186
116	87.0	3.44	50 000	15 240	MIL-202, RS-186
85	*63.8*	*2.51*	*52 500*	16 000	IEC
44	*33.0*	*1.30*	*65 600*	20 000	IEC
44.4	33.0	1.31	70 000	21 336	MIL-202
20	*17.2*	*0.677*	*85 300*	26 000	IEC
10.6	8.00	0.315	100 000	30 480	MIL-202
1.28	1.09	0.043	150 000	45 720	MIL-202
3.18×10⁻⁶	2.40×10^{-6}	9.44×10^{-8}	656 000	200 000	MIL-202

Notes:
1. The inconsistency in the pressure–altitude relation arises from the use of different model atmospheres. For testing purposes always specify the desired pressure rather than an elevation in feet or meters.
2. Values in italics are derived from the values specified in the associated standard.

Vibration Tests

The purposes of vibration tests are:

(A) Search for resonance.
(B) Determination of endurance (life) at resonance (or at specific frequencies).
(C) Determination of deterioration resulting from long exposure to swept frequency (or random vibration).

Recommended Frequency Ranges for Tests:
Hertz: 1 to 10, 5 to 35, 10 to 55, 10 to 150, 10 to 500, 10 to 2000, 10 to 5000.

Recommended Combinations of Amplitude and Frequency: IEC Publication 68 recommends testing at constant amplitude below and constant acceleration above the crossover frequency (57 to 62 hertz). MIL-STD-202 and MIL-STD-810 also follow this principle but use different crossover points and low-frequency severities. The choice of frequency range and vibration amplitude or acceleration should bear some relation to the actual service environment. Successful completion of 10^7 vibration cycles indicates a high probability of no failures in a similar service environment. Resonances may make the equipment output unusable, although the mechanical life may be adequate.

COMPONENT VALUE CODING

Axial-lead and some other components are often color coded by circumferential bands to indicate the resistance, capacitance, or inductance value and its tolerance. Usually the value may be decoded as indicated in Fig. 2 and Table 1.

Sometimes, instead of circumferential bands, colored dots are used as shown in Fig. 3 and examples.

Examples:

Component Value	Band or Dot Color			
	A	B	C	D
3300±20%	Orange	Orange	Red	Black or omitted
5.1±10%	Green	Brown	Gold or white	Silver
1.8 megohms ±5% (as applied to a resistor)	Brown	Gray	Green	Gold

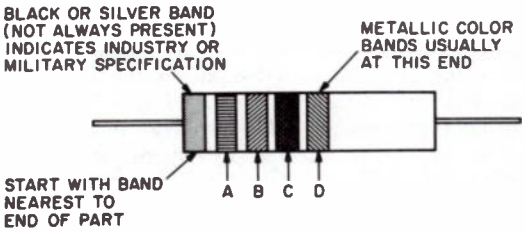

Fig. 2—Component value coding. The code of Table 1 determines values. Band A color = First significant figure of value in ohms, picofarads, or microhenries. Band B color = Second significant figure of value. Band C color = Decimal multiplier for significant figures. Band D color = Tolerance in % (if omitted, the broadest tolerance series of the part applies).

Semiconductor-Diode Type Number Coding

The sequential number portion (following the "1N" of the assigned industry type number) may be indicated by color bands* as shown in Fig. 4.

Colors have the numerical significance given in Table 1.

Bands J, K, L, M represent the digits in the sequential number (for 2-digit numbers, band J is black).

Band N is used to designate the suffix letter as follows.

Color	Suffix Letter	Number
Black	—	0
Brown	A	1
Red	B	2
Orange	C	3
Yellow	D	4
Green	E	5
Blue	F	6
Violet	G	7
Gray	H	8
White	J	9

Band N may be omitted in 2- or 3-digit number coding if not required, but will always be present on 4-digit number coding (black if no suffix letter is required).

Example:

Band	Band Color		
J	Red	Red	Orange
K	Green	Green	Blue
L	Yellow	Yellow	Violet
M	—	—	Red
N	—	Red	Black
	1N254	1N254B	1N3672

A single band indicates the cathode end of a diode or rectifier.

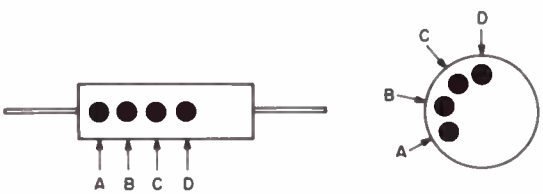

Fig. 3—Alternative methods of component value coding.

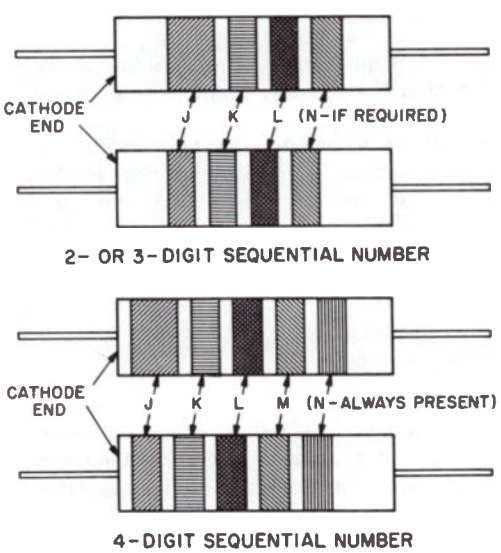

Fig. 4—Semiconductor-diode value coding.

* EIA Standard RS-236-B.

RESISTORS

Definitions

Wattage Rating: The maximum power that the resistor can dissipate, assuming (A) a specific life, (B) a standard ambient temperature, and (C) a stated long-term drift from its no-load value. Increasing the ambient temperature or reducing the allowable deviation from the initial value (more-stable resistance value) requires derating the allowable dissipation. With few exceptions, resistors are derated linearly from full wattage at rated temperature to zero wattage at the maximum temperature.

Temperature Coefficient (Resistance–Temperature Characteristic): The magnitude of change in resistance due to temperature, usually expressed in percent per degree Celsius or parts per million per degree Celsius (ppm/°C). If the changes are linear over the operating temperature range, the parameter is known as "temperature coefficient"; if nonlinear, the parameter is known as "resistance–temperature characteristic". A large temperature coefficient and a high hot-spot temperature cause a large deviation from the nominal condition; e.g., 500 ppm/°C and 275°C result in a resistance change of over 12 percent.

Maximum Working Voltage: The maximum voltage that may be applied across the resistor (maximum working voltage) is a function of (A) the materials used, (B) the allowable resistance deviation from the low-voltage value, and (C) the physical configuration of the resistor. Carbon composition resistors are more voltage-sensitive than other types.

Noise: An unwanted voltage fluctuation generated within the resistor. Total noise of a resistor always includes Johnson noise, which depends only on resistance value and the temperature of the resistance element. Depending on type of element and construction, total noise may also include noise caused by current flow and noise caused by cracked bodies and loose end caps or leads. For adjustable resistors, noise may also be caused by jumping of the contact over turns of wire and by imperfect electrical path between contact and resistance element.

Hot-Spot Temperature: The maximum temperature measured on the resistor due to both internal heating and the ambient operating temperature. The allowable maximum hot-spot temperature is predicated on thermal limits of the materials and the design. Since the maximum hot-spot temperature may not be exceeded under normal operating conditions, the wattage rating of the resistor must be lowered if it is operated at an ambient temperature higher than that at which the wattage rating was established. At zero dissipation, the maximum ambient around the resistor may be its maximum hot-spot temperature. The ambient temperature for a resistor is affected by surrounding heat-producing devices; resistors stacked together do not experience the ambient surrounding the stack except under forced cooling.

Critical Resistance Value: A resistor of specified power and voltage ratings has a critical resistance value above which the allowable voltage limits the permissible power dissipation. Below the critical resistance value, the maximum permitted voltage across the resistor is never reached at rated power.

Inductance and Other Frequency Effects: For other than wire-wound resistors, the best high-frequency performance is secured if (A) the ratio of resistor length to cross section is a maximum, and (B) dielectric losses are kept low in the base material and a minimum of dielectric binder is used in composition types.

Carbon composition types exhibit little change in effective dc resistance up to frequencies of about 100 kHz. Resistance values above 0.3 megohm start to decrease in resistance at approximately 100 kHz. Above 1 MHz all resistance values decrease.

Wire-wound types have inductive and capacitive effects and are unsuited for use above 50 kHz, even when specially wound to reduce the inductance and capacitance. Wire-wound resistors usually exhibit an increase in resistance at high frequencies because of "skin" effect.

Film types have the best high-frequency performance. The effective dc resistance for most resistance values remains fairly constant up to 100 MHz and decreases at higher frequencies. In general, the higher the resistance value the greater the effect of frequency.

Established-Reliability Resistors: Some resistor styles can be purchased with maximum-failure-rate guarantees. Standard-failure-rate levels are:

%/1000 hours—1.0; 0.1; 0.01; 0.001.

Resistance Value and Tolerance Choice: A calculated circuit-resistance nominal value should be checked to determine the allowable deviation in that value under the most unfavorable circuit, ambient, and life conditions. A resistor type, resistance value, and tolerance should be selected considering (A) standard resistance values (specials are uneconomical in most cases), (B) purchase tolerance, (C) resistance value changes caused by temperature, humidity, voltage, etc., and (D) long-term drift.

RESISTORS—FIXED COMPOSITION

Color Code

EIA-standard and MIL-specification requirements for color coding of fixed composition resistors are identical (see Fig. 2). The exterior body color of insulated axial-lead composition resistors is usually tan, but other colors (except black) are permitted. Noninsulated axial-lead composition resistors have a black body color.

If 3 significant figures are required, Fig. 5 shows the resistor markings (EIA Std RS-279).

Another form of resistor color coding (MIL-STD-1285A) is shown in Fig. 6. Colors have the following significance.

	Brown	Red	Orange	Yellow	Green	White
Failure Rate Level:						
Letter	M	P	R	S	—	—
Rate (%/1000 hrs)	1.0	0.1	0.01	0.001	—	—
Terminal	—	—	—	—	—	Solderable
Special	—	—	—	—	Fig. 6	—

Tolerance

Standard resistors are furnished in ±20-, ±10-, and ±5-percent tolerances, and in the preferred-value series of Table 2. "Even" values, such as 50 000 ohms, may be found in old equipment, but they are seldom used in new designs.

Temperature and Voltage Coefficients

Resistors are rated for maximum wattage at an ambient temperature of 70 degrees Celsius; above these temperatures up to the maximum allowable hot-spot temperature of 130 or 150 degrees Celsius, it is necessary to operate at reduced wattage ratings. Resistance values are a function of voltage as well as temperature; present specifications allow a maximum voltage coefficient of resistance as given in Table 3 and permit a resistance–temperature characteristic as in Table 4.

A 1000-hour rated-load life test should not cause a change in resistance greater than 12% for $\frac{1}{8}$-watt resistors and 10% for all other ratings. A severe cycling humidity test may cause resistance changes of 10% average and 15% maximum; 250 hours at 40°C and 95% relative humidity may cause up to 10% change. Five temperature-change cycles, −55°C to +85°C, should not change the resistance value by more than 4% from the 25°C value. Soldering the resistor in place may cause a resistance change of 3%. Always allow $\frac{1}{4}$-inch-minimum lead length; use heat-dissipating clamps when soldering confined assemblies. The preceding summary indicates that close tolerances cannot be maintained over a wide range of load and ambient conditions.

Noise

Composition resistors above 1 megohm have high Johnson noise levels, precluding their use in critical applications.

RF Effects

The end-to-end shunted capacitance effect may be noticeable because of the short resistor bodies

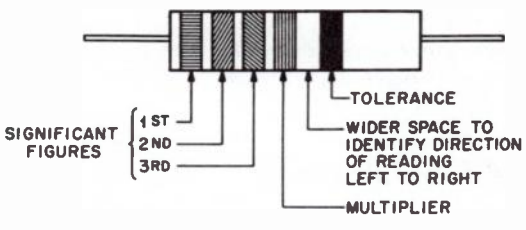

Fig. 5—Resistor value color code for 3 significant figures. Colors of Table 1 determine values.

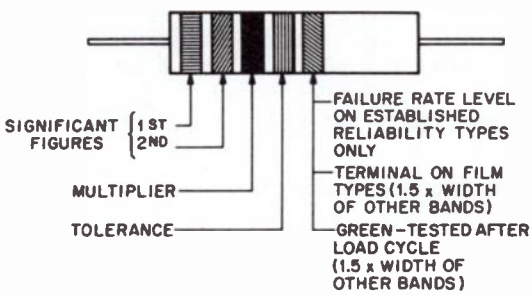

Fig. 6—Resistor color code per MIL-STD-1285A.

TABLE 3—STANDARD RATINGS FOR COMPOSITION RESISTORS.

Watts	Working Volts (maximum)	Hot-Spot Temperature (°C) (maximum)	Critical Resistance (megohms)	Voltage Coefficient* (%/Volt) (maximum)
$\frac{1}{8}$	150	150	0.22	0.05
$\frac{1}{4}$	250	130	0.25	0.035
$\frac{1}{2}$	350	130	0.25	0.035
1	500	130	0.25	0.02
2	500	130	0.12	0.02

* Applicable only to resistors of 1000 ohms and over.

and small internal distance between the ends. Operation at VHF or higher frequencies reduces the effective resistance because of dielectric losses (Boella effect).

Good Design Practice

Operate at $\frac{1}{2}$ allowable wattage dissipation for expected ambient temperature. Provide adequate heat sink. Mount no other heat-dissipating parts within 1 diameter. Use only in applications where 15% change from installed value is permissible or where environment is controlled to reduce resistance value change.

RESISTORS—FIXED WIRE-WOUND

Fixed wire-wound resistors are available as low-power insulated types, precision types, and power types.

EIA Low-Power Insulated Resistors†

These resistors are furnished with power ratings from 1 watt through 15 watts, in tolerances of ±5 and ±10 percent, and in resistance values from 0.1 ohm to 30 000 ohms in the preferred-value series of Table 2. They may be color coded as described in Fig. 2, but band A will be twice the width of the other bands. They may also be typographically marked in accordance with the EIA Standard.

The stability of these resistors is somewhat better than that of composition resistors, and they may be preferred except where a noninductive resistor is required.

EIA Precision Resistors‡

These resistors are furnished in ±1.0-, ±0.5-, ±0.25-, ±0.1-, and ±0.05-percent tolerances and in any value from 1.0 ohm to 1.0 megohm in the preferred-value series of Table 2. Power rating range from 0.1 watt to 0.5 watt. The maximum ambient temperature for full-wattage rating is 125°C. If the resistor is mounted in a confined area or may be required to operate in higher ambient temperatures (145°C maximum), the allowable dissipation must be reduced in accordance with the EIA Standard.

These resistors have an inherently low noise level, approaching the thermal agitation level, and their stability is excellent—the typical change in resistance for the lifetime of the resistor will not exceed 50 percent of the initial resistance tolerance when used within the specified design limits of the EIA Standard.

The temperature coefficient of resistance over the range −55°C to +145°C, referred to 25°C may have maximums as follows:

Value	EIA Standard
Above 10 ohms	±0.002%/°C
5 ohms to 10 ohms	±0.006%/°C
Below 5 ohms	±0.010%/°C

Where required, temperature coefficients of less than ±20 ppm/°C can be obtained by special selection of the resistance wire. Temperature coefficients of ±10 ppm/°C may be obtained by limiting the range of temperatures for testing from −40°C to +105°C. The application of temperature coefficient to resistors should be limited, where possible, to the actual temperatures at which the equipment will operate.

*EIA Power Resistors**

These resistors are furnished in 3 styles (strip, tubular, open end; and axial lead) and 24 power ratings ranging from 1 watt to 210 watts in toler-

† EIA Standard RS-344.

‡ EIA Standard RS-229-A.

* EIA Standard RS-155-B.

ances of ±1.0 percent and ±5 percent. Resistance values range from 1.0 ohm to 182 kilohms in the preferred-value series of Table 2.

Axial-lead types are available in 2 general inductance classifications—inductive winding and noninductive winding. The noninductive styles have a maximum resistance value of 1/2 the maximum resistance of inductive styles because of the special manner in which they are wound. The inductance of noninductive styles must not exceed 0.5 microhenry when measured at a test frequency of 1.0 megahertz ±5%. However, these resistors should not be used in very-high-frequency circuits where the inductance may affect circuit operation.

The maximum ambient temperature for full wattage rating for these resistors is 25°C. When the resistors are operated at ambient temperatures above 25°C, the wattage dissipation must be reduced in accordance with the EIA Standard.

RESISTORS—FIXED FILM

Film-type resistors use a thin layer of resistive material deposited on an insulating core. The low-power types are more stable than the usual composition resistors. Except for very high-precision requirements, film-type resistors are a good alternative to accurate wire-wound resistors, being both smaller and less expensive and having excellent noise characteristics.

The power types are similar in size and performance to conventional wire-wound power resistors. While their 200°C maximum operating temperature limits the power rating, the maximum resistance value available for a given physical size is much higher than that of the corresponding wire-wound resistor.

Construction

For low-resistance values, a continuous film is applied to the core, a range of values being obtained by varying the film thickness. Higher resistances are achieved by the use of a spiral pattern, a coarse spiral for intermediate values and a fine spiral for high resistance. Thus, the inductance is greater in high values, but it is likely to be far less than in wire-wound resistors. Special high-frequency units having greatly reduced inductance are available.

Resistive Films

Resistive-material films presently used are microcrystalline carbon, boron–carbon, and various metallic oxides or precious metals.

Deposited-carbon resistors have a negative temperature coefficient of 0.01 to 0.05 percent/°C for low resistance values and somewhat larger for higher values. Cumulative permanent resistance changes of 1 to 5 percent may result from soldering, overload, low-temperature exposure, and aging. Additional changes up to 5 percent are possible from moisture penetration and temperature cycling.

The introduction of a small percentage of boron in the deposited-carbon film results in a more stable unit. A negative temperature coefficient of 0.005 to 0.02 percent/°C is typical. Similarly, a metallic dispersion in the carbon film provides a negative coefficient of 0.015 to 0.03 percent/°C. In other respects, these materials are similar to standard deposited carbon. Carbon and boron–carbon resistive elements have the highest random noise of the film-type resistors.

Metallic-oxide and precious-metal-alloy films permit higher operating temperatures. Their noise characteristics are excellent. Temperature coefficients are predominantly positive, varying from 0.03 to as little as 0.0025 percent/°C.

Applications

Power ratings of film resistors are based on continuous direct-current or on root-mean-square operation. Power derating is necessary for operation at ambient temperatures above the rated temperature. In pulse applications, the power dissipated during each pulse and the pulse duration are more significant than average power conditions. Short high-power pulses may cause instantaneous local heating sufficient to alter or destroy the film. Excessive peak voltages may result in flashover between turns of the film element. Derating under these conditions must be determined experimentally.

Film resistors are fairly stable up to about 10 megahertz. Because of the extremely thin resistive film, skin effect is small. At frequencies above 10 megahertz, it is advisable to use only unspiraled units if inductive effects are to be minimized (these are available in low resistance values only).

Under extreme exposure, deposited-carbon resistors deteriorate rapidly unless the element is protected. Encapsulated or hermetically sealed units are preferred for such applications. Open-circuiting in storage as the result of corrosion under the end caps has been reported in all types of film resistors. Silver-plated caps and core ends effectively overcome this problem.

Technical Characteristics

Stable equivalents for composition resistors; axial leads; data for MIL "RL" series.

WRH

Watts	¼	½	1	2
Voltage rating	250	350	500	500
Critical resistance (megohms)	0.25	0.25	0.25	0.12

Maximum temp for full load—70°C; for 0 load—150°C

Resistance–temperature characteristic: ±200 ppm/°C maximum

Life-test resistance change: ±2% maximum

Moisture resistance test: ±1.5% maximum change

Resistance values: E24 series, same as composition resistors; tolerances 2% or 5%.

The MIL "RN" series of film resistors is more stable than the "RL" series and is available in a wider range of ratings. Commercial equivalents are also offered. Where stability and reliability are desired, the "RN" series is economically very competitive with the "RC" or "RL" series.

High-stability film resistors; axial leads; data for MIL "RD" series. Uninsulated commercial versions have lower temperature limits and greater resistance change. Color coding is the same as previously indicated for composition resistors.

	Watts							
	1/20	1/10	⅛	¼	½	¾	1	2
Characteristic	Voltage Rating							
B	—	—	—	—	—	—	500	750
D	—	—	200	300	350	500	—	—
C, E	200	200	250	300	350	—	500	—

	Characteristic			
	B	C	D	E
Maximum temp (°C):				
Full load	70	125	70	125
0 load	150	175	165	175
Life-test resistance change (max)	±1%	±0.5%	±1%	±0.5%
Resistance-temperature characteristic (max ppm/°C)	±500	±50	+200 −500	±25
Moisture resistance test (max change)	±1.5%	±0.5%	±1.5%	±0.5%

Resistance Values: E96 series (E48 preferred): 1% tolerance;
E192 series (E96 preferred): 0.5%, 0.25%, 0.1% tolerances.

Power-type film resistors, uninsulated.

	Axial-Lead and MIL "RD" Series			Commercial Tab-Terminal Styles				
Watts	2	4	8	7	23	25	55	115
Voltage rating	350	500	750	525	1380	2275	3675	7875
Critical resistance (kilohms)	61	62	70	39	83	208	245	540
Maximum temperature (°C):								
Full load	25	25	25	25	25	25	25	25
0 load	235	235	235	235	235	235	235	235
	275 (MIL)	275 (MIL)	275 (MIL)					

Life-test resistance change: ±5% maximum
Resistance–temperature characteristic: ±500 ppm/°C maximum
Moisture resistance test: ±3% maximum change
Resistance values: E12 series (approx. for MIL)
Tolerances: Axial lead: ½%, 1%, 2% (MIL "RD" Series), 5%, 10%.
Tab lead: 1%, 2%, 5%, 10%, 20%.

TABLE 4—TEMPERATURE COEFFICIENT OF RESISTANCE FOR COMPOSITION RESISTORS.

	Characteristic*	Percent Maximum Allowable Change from Resistance at 25 Degrees Celsius†					
At −55°C ambient	F	±6.5	±10	±13	±15	±20	±25
At +105°C ambient	F	±5	±6	±7.5	±10	±15	±15
Nominal resistance in ohms		0 to 1 000	>1 000 to 10 000	>10 000 to 0.1 meg	>0.1 meg to 1.0 meg	>1 meg to 10 meg	>10 meg

* Resistance—temperature.
† Up to 1 megohm, data also apply to MIL Established Reliability characteristic *G* (= former *GF*).

RESISTORS, ADJUSTABLE

General

Adjustable resistors are available with several types of resistance elements: carbon composition, wire-wound, and metallic film.

The wattage rating of an adjustable resistor is based on using the full resistance element; if only a portion of the element is used, the allowable wattage is reduced approximately in the same proportion as the resistance (for a linear-resistance-vs-rotation characteristic).

At the extremes of movable-contact travel there is a residual (hop-off) resistance between the end contact and the movable contact having a maximum value (for linear tapers) approximately as follows:

Element Type	Residual Resistance (ohms)
Composition, linear taper:	
100 000 ohms	0.05 % total *R*
25 000, 50 000 ohms	35*
5000, 10 000 ohms	25*
Wire-wound, low power, 1 turn	1 ohm or 0.5%* of total *R*†
Wire-wound, low power, 1 turn, reliable	1 ohm or 3% of total *R*†
Wire-wound, lead-screw actuated	1 ohm or 2% of total *R*†
Wire-wound, lead-screw actuated, reliable	1 ohm or 0.25% of total *R*†
Wire-wound, precision	5 ohms or 1% of total *R*†
Wire-wound, power, 1 turn	0.2 ohm or 0.2% of total *R*†
Nonwire-wound, lead-screw actuated	20 ohms or 2% of total *R*†

*EIA standard.
†Whichever is greater.

The usual form is a movable arm attached to a rotating shaft with an angular travel (electrical rotation) of about 300°. Multi-turn lead-screw-actuated movable-contact resistors are available with linear or circular resistance elements; locking is less essential in high shock or vibration environments for this construction. Multi-turn movable-arm styles are available for high-resistance or high-resolution applications.

The common low-power resistors may be fitted with a power switch that is actuated in the first 20° of mechanical motion preceding the electrical rotation.

Composition Resistors

Carbon composition elements may be formed on an insulating base such as paper-base phenolic laminate, or they may be hot molded integral with a molded base; the latter is more durable. Thin-layer composition elements may be noisy and tend to wear away with frequent use. The resistance change is continuous.

In addition to a linear-rotation-vs-resistance characteristic, composition elements can have a wide range of nonlinear curves (tapers). Standard tapers are shown in Fig. 7. Commercial units are available with 2 taps in addition to the usual 3 terminals, permitting frequency-sensitive circuit adjustments such as are required for tone controls.

Usual ratings are as follows:

	Single-Turn Shaft				Lead-Screw Actuated
Watts at 70°C*	½	¾	2, 3	5	¼
Max operating temp	120°C	120°C	120°C	120°C	125°C
Case size in inches (nominal, typical)	0.50 dia	0.72 dia	1.15 dia	1.62×2.15	0.28×0.33×1.25
Resistance range (min ohms to max megohms)	100 to 5	500 to 2.5	50 to 5	50 to 2.5	100 to 2.5
Life expectancy–shaft rotations:					
Hot-molded	25 000	—	>25 000	100 000	25 000
EIA RS-303	10 000	—	10 000	—	—

* Derate 50% for other than linear taper, plus 50% if not mounted on metal panel (e.g., printed-wiring board).

Hot-molded elements may change up to 5% in resistance value after 100 hours at 40°C, 95% relative humidity.

Film- and Ceramic-Element Resistors

Adjustable resistors using a metallic-film or conductive-ceramic element are stepless and have less inherent noise than units using a composition element.

They are available as linear and circular lead-screw-actuated resistors and as single-turn resistors. They may be operated from −65°C to +150°C, but operation above 150°C is limited primarily by the lubricant requirements for the moving parts, and by the housing material. Life expectancies are of the order of 10^7 shaft revolutions for precision single-turn designs.

Usual ratings for nonwire-wound lead-screw-actuated adjustable resistors are as follows:

	Linear Type–Rectangular Case		Circular Type–Square Case		
Watts	¾	¼	½	½	0.2
Temp for rated watts	85°C	25°C	85°C	85°C	85°C
Max operating temp	150°C	85°C	150°C	150°C	150°C
Case size in inches (nominal)	0.30×0.37×1.25 0.20×0.33×1.25	0.28×0.36×1.00 0.16×0.31×0.75	0.50 sq	0.38 sq	0.25 sq
Resistance range (min ohms to max megohms)	10 to 1	10 to 1	10 to 1	10 to 1	10 to 1
Life expectancy–end-to-end travel of wiper on resistance element (cycles)	200	200	200	200	200

Wire-Wound Resistors

These are available as general-purpose low-power resistors, precision resistors, and power resistors.

Wire-wound elements are usually not suitable for frequency-sensitive rf circuits because of inductive and capacitive effects. High-resistance wire-wound units are more subject to winding damage because of the fine wire required; they are impractical above a resistance value determined by the winding space available and the smallest resistance wire that can be space-wound.

Resistors wound with wire smaller than 0.001 inch in diameter are not as rugged as those using larger-diameter wire; composition or film elements may be more suitable for high resistance values.

The usual rotation-vs-resistance characteristic is linear, but by tapering or otherwise shaping the winding card, a limited amount of taper, log characteristic, sine wave, or similar function can be generated. By changing the resistance wire size or material, different linear tapers may be obtained on a uniform-width winding card.

Wire-wound elements, with rare exceptions, change value in steps. There may be 20 steps in a small low-resistance unit or 2000 steps (turns) in a single-turn high-resistance unit; in some cases this abrupt step characteristic may provide an unwanted signal in the circuit. Noise arises from motion of the wiper from turn to turn. Resolution may be improved by using multi-turn adjustable resistors. (If the desired resistance value is low enough, resolution may also be improved by using a resistor in which the wiper is in continuous contact with a single-turn wire.)

Usual ratings follow (linear tapers).

Wire-Wound Low-Power Adjustable Resistors:

	Bushing-Mounted Single-Turn Shaft		
Watts	1*	2*	4*
Temp for rated watts	40°C	40°C	40°C
Max operating temp	105°C	105°C	105°C
Case size in inches (nominal)	0.75 dia	1.30 dia	1.72 dia
Resistance range (min ohms to max megohms)	15 to 0.0025	3 to 0.015	3 to 0.025
Wire diameter in inches	0.00156	0.00156	0.00156
Rotational life–shaft turns	25 000	25 000	25 000

	Lead-Screw Actuated			
	Linear Type—Rectangular Case		Circular Type—Square Case	
Watts	¾	¾	¾	¾
Temp for rated watts	85°C	85°C	85°C	85°C
Max operating temp	105°C	150°C	150°C	150°C
Case size in inches (nominal)	0.19×0.32×1.00	0.20×0.32×1.25	0.20×0.50 sq	0.15×0.38 sq
Resistance range (min ohms to max megohms)	100 to 0.005	10 to 0.01	10 to 0.01	10 to 0.005
Wire diameter (inches)	0.001	0.001	0.001	0.001
Rotational life–shaft turns	2 500	4 000	4 000	3 000

	Multi-Turn Shaft		
	10*t*	10*t*	40*t*
Watts	1.5	5	20
Temp for rated watts	40°C	40°C	40°C
Max operating temp	85°C	85°C	85°C
Case size in inches (nominal)	0.88 dia	1.82 dia	3.32 dia
Resistance range (min ohms to max megohms)	10 to 0.125	10 to 0.648	125 to 5.3
Rotational life–shaft turns	2×10^6	2×10^6	2×10^6

* At 40°C, derate 50% for other than linear tapers, plus additional for other than metal panel mounting.

Wire-Wound High-Power Adjustable Resistors:

Watts at 25°C:					
MIL	6	25	50	75	100
EIA	12.5	25	50	75	100
Max operating temp	340°C	340°C	340°C	340°C	340°C
Body diameter in inches	0.90	1.68	2.41	2.81	3.19
Resistance range* (min ohms to max megohms)	1 to 0.0035	2 to 0.005	1 to 0.01	2 to 0.01	2 to 0.01

* Based on 0.0024-inch-diameter wire.

CAPACITORS

Definitions

Dielectric: A dielectric is a material that can withstand high electric stress without appreciable conduction. When such stress is applied, energy in the form of an electric charge is held by the dielectric. Most of this stored energy is recovered when the stress is removed. The only perfect dielectric in which no conduction occurs and from which the whole of the stored energy may be recovered is a perfect vacuum.

Relative Capacitivity: The relative capacitivity or relative permittivity or dielectric constant is the ratio by which the capacitance is increased when another dielectric replaces a vacuum between two electrodes.

Dielectric Absorption: Dielectric absorption is the absorption of charge by a dielectric when subjected to an electric field by other than normal polarization. This charge is not recovered instantaneously when the capacitor is short-circuited, and a decay current will continue for many minutes. If the capacitor is short-circuited momentarily a new voltage will build up across the terminals afterward. This is the source of some danger with high-voltage dc capacitors or with ac capacitors not fitted with a discharge resistor. The phenomenon may be used as a measure of dielectric absorption.

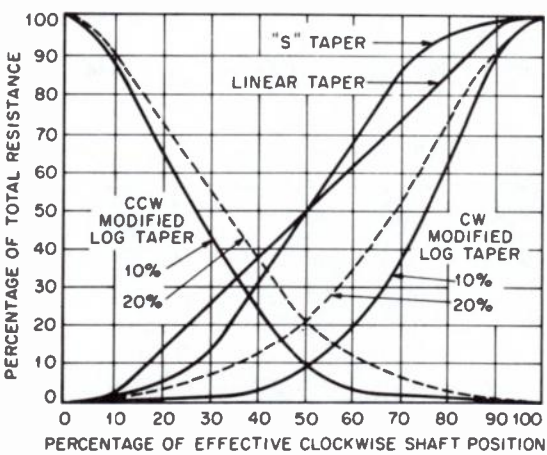

Fig. 7—Nominal resistance-vs-rotation characteristics for standard tapers.

Tangent of Loss Angle: This is a measure of the energy loss in the capacitor. It is expressed as $\tan\delta$ and is the power loss of the capacitor divided by its reactive power at a sinusoidal voltage of specified frequency. (This term also includes power factor, loss factor, and dielectric loss. The true power factor is $\cos(90-\delta)$.)

Insulation Resistance: This is a measure of the conduction in the dielectric. Because this conduction takes a very long time to reach a stable value, it is usually measured after 1 minute of electrification for nonelectrolytic types and 3 minutes for electrolytics. It is measured preferably at the rated working voltage or at a standardized voltage.

The insulation resistance is usually multiplied by the capacitance to give the ohm-farad value, which is the apparent discharge time constant (seconds). This is a figure of merit for the dielectric, although for small capacitances a maximum value of insulation resistance is usually also specified.

In electrolytics the conduction is expressed as leakage current at rated working voltage. It is calculated as $\mu A/\mu FV$, which is the reciprocal of the ohm-farad value. In this case a maximum value of leakage current is specified for small capacitances.

Leakage Current: The current flowing between two or more electrodes by any path other than the interelectrode space is termed the leakage current, and the ratio of this to the test voltage is the insulation resistance.

Impedance: Impedance is the ratio of voltage to current at a specified frequency. At high frequencies the inductance of leads becomes a limiting factor, in which case a transfer impedance method may be employed. This then measures the impedance of the shunt path only.

DC or AC Capacitor: A dc capacitor is designed to operate on direct current only. It is normally not suitable for use above 200 volts ac because of the occurrence of discharges in internal gas bubbles. An ac capacitor is designed to have freedom from internal discharges and low tangent of loss angle to minimize internal heating. It is normally not suitable for use on dc.

Rated Voltage and Temperature: The rated voltage is the direct operating voltage that may be applied continuously to a capacitor at the rated temperature.

Category Voltage and Temperature: The category voltage is the voltage which may be applied to the capacitor at the maximum category temperature. It differs from the rated voltage by a derating factor.

Ripple Voltage: If alternating voltages are present in addition to direct voltage, the working voltage of the capacitor is taken as the sum of the direct voltage and the peak alternating voltages. This sum must not exceed the value of the rated voltage.

In electrolytics the permissible ripple may be expressed as a rated ripple current.

Surge Voltage: This is a voltage above the rated voltage which the capacitor will withstand for a short time.

Voltage Proof Test: This is the highest possible voltage that may be applied without breakdown to a capacitor during qualification approval testing to prove the dielectric. The repeated application of this voltage may cause failure.

Forming Voltage (Electrolytics): The voltage at which the anodic oxide has been formed. The thickness of the oxide layer is proportional to this voltage.

Burnout Voltage (Metallized Types): The voltage at which metallized types burn out during manufacture.

Self-Healing Failure (Metallized Types): A momentary partial discharge of a capacitor resulting from a localized failure of the dielectric. Burning away the metallized electrode isolates the fault and effectively restores the properties of the capacitor.

Volt-Ampere Rating (VA): This is the reactive power in a capacitor when an ac voltage is applied. VA $\cos\theta$ gives the amount of heat generated in the capacitor. Since the amount of heat that can be dissipated is limited, the VA must also be limited and in some cases a VA rating is quoted. (Note that $\cos\theta = \cos(90-\delta) \approx \tan\delta$, when δ is small.)

Scintillation: Minute and rapid fluctuations of capacitance formerly exhibited by silvered mica or silvered ceramic types but overcome by modern manufacturing techniques.

Internal Discharge: Partial discharge of a capacitor due to ionization of the gas in a bubble in the dielectric. On ac this may occur in unsuitable dielectrics above 200 volts and is a major cause of failure. On dc such discharges are very infrequent and normally are not a cause of failure.

CLASSES OF CAPACITORS

Modern electronics circuits require the smallest possible capacitors, which are usually made with the thinnest possible dielectric material since they are for operation at low voltages. There are three broad classes of capacitors.

(A) Low-loss capacitors with good capacitance stability. These are usually of mica, glass, ceramic, or a low-loss plastic such as polystyrene.

(B) Capacitors of medium loss and medium stability, usually required to operate over a fairly wide range of ac and dc voltages. This need is met by paper, plastic film, or high-K ceramic types. The first two of these may have electrodes of metal foil or electrodes of evaporated metal which have a self-healing characteristic.

(C) Capacitors of the highest possible capacitance per unit volume. These are the electrolytics, which are normally made either of aluminum or tantalum. Both of these metals form extremely thin anodic oxide layers of high dielectric constant and good electrical characteristics. Contact with this oxide layer is normally by means of a liquid electrolyte that has a marked influence on the characteristics of the capacitor. In solid tantalum the function of the electrolyte is performed by a manganese-dioxide semiconductor.

PLASTIC FILM CAPACITORS

Advances in organic chemistry have made it possible to produce materials of high molecular weight. These are formed by joining together a number of basic elements (monomers) to produce a polymer. Some of these have excellent dielectric characteristics.

Physically they can be classified as thermoplastic or thermosetting. In the former case the molecule consists of long chains with little or no branching, while in the latter the molecules are crosslinked. Thermosetting materials have no clearly defined melting point and are usually hard and brittle, making them unsuitable for the manufacture of plastic films. A cast film is usually amorphous but by extrusion, stretching, and heat treatment, oriented crystalline films are produced with good flexibility and dielectric characteristics.

The electrical properties of these plastics depend on the structure of the molecule. If the molecule is not symmetrical it will have a dipole moment giving increased dielectric constant. On the other hand, the dielectric constant and tanδ are then dependent on frequency. Generally speaking, nonpolar materials have electrical characteristics that are independent of frequency, while polar materials exhibit a decrease in capacitance with increasing frequency, and tanδ may pass through a maximum in the frequency range.

Figures 8, 9, and 10 show some characteristics of several types of capacitors. At the present time two classes of plastic film capacitors are recognized.

(A) *Polystyrene Capacitors.* Polystyrene is a nonpolar plastic and has excellent electrical characteristics which are independent of frequency.

(B) *Polyester Films.* Strictly speaking these are the polyethylene terephthalates (Mylar, Melinex, Hostaphan) but the polycarbonates are now included in this group because they have similar electrical characteristics.

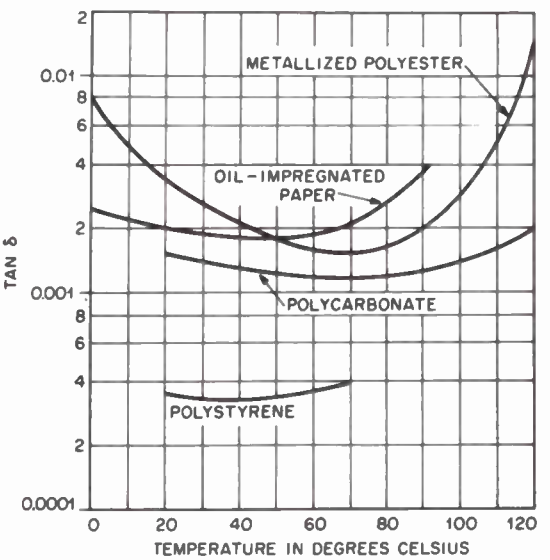

Fig. 8—Typical capacitance characteristics of various capacitors as a function of temperature. Measured on 0.1-microfarad capacitors at 1000 hertz.

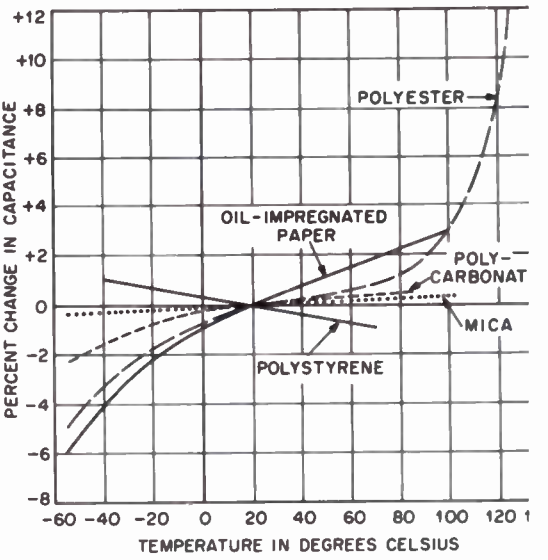

Fig. 9—Variation of tan δ with temperature for variou plastic films compared with oil-impregnated paper

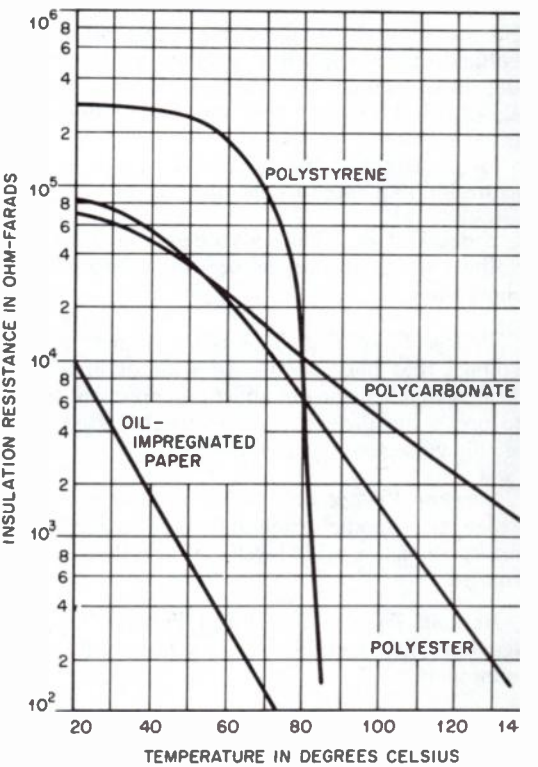

Fig. 10—Variation of insulation resistance with temper ature for various plastic films compared with oil-im pregnated paper.

Plastic films for capacitor manufacture are usually of the oriented crystalline type because of their good combinations of characteristics. One important feature of some of these films is that they tend to shrink back to their original shape after being heated. This fact is sometimes exploited in manufacturing the capacitor.

Moisture usually has little effect on the dielectric properties of plastic films, and capacitors made from them require less protection than paper or mica types. This, together with simple processing, has permitted them to be mass-produced at relatively low cost.

The electrical characteristics of capacitors made with these materials depend on the construction employed. The resistance of metallized electrodes and the shape and method of connection to the unit are particularly important.

Many plastic materials are being used in the manufacture of capacitors for which there are no internationally agreed specifications. In this case it is necessary to obtain the relevant data from the manufacturer. There is no doubt that in the future the range of plastic film capacitors will be considerably extended.

Polystyrene Film Capacitors with Foil Electrodes

Polystyrene has excellent electrical characteristics. The film employed is of the oriented crystalline type, which makes it flexible and suitable for forming into thin films. On heat treatment the film shrinks considerably and this is used in the manufacturing process to obtain capacitance stability. The film is affected by greases and solvents, and care must be taken both in manufacture and in use to ensure that capacitors do not come into contact with these materials.

The power factor of polystyrene is low over the whole frequency range, but the resistance of the electrodes may result in an increase of power factor at high frequencies in the larger values, as shown in Table 5.

Polyester Film Capacitors with Foil Electrodes

This generic title is usually used to apply to polyethylene terephthalate. It is a slightly polar plastic film suitable for operation up to temperatures of 125°C. Capacitors are available with foil electrodes.

TABLE 5—POWER FACTOR OF POLYSTYRENE AT VARIOUS FREQUENCIES.

	Nominal Capacitance (*p*F)			
Frequency (hertz)	Up to 1 000	1 000 to 10 000	10 000 to 100 000	Above 100 000
800	0.0003	0.0003	0.0003	0.0003
10 000	0.0003	0.0003	0.0003	0.001
100 000	0.0003	0.0005	0.001–0.003	—
1 000 000	0.001	0.002	0.005–0.02	—

Plastic Film Capacitors with Metallized Electrodes

These are tending to supersede metallized paper capacitors on dc applications because of superior electrical characteristics, less tendency for self-healing to occur during service, higher and more stable insulation resistance, and approximately the same space factors. Two types of film are generally used, polyethylene terephthalate and polycarbonate. For some purposes these are comparable, but polycarbonate has a lower loss angle and smaller change of capacitance with temperature. Polycarbonate is also available in thinner films, giving an advantage of space factor.

ELECTROLYTIC CAPACITORS

Electrolytic capacitors (Fig. 11) employ for at least one of their electrodes a "valve metal". This metal, when operated in an electrolytic cell as the

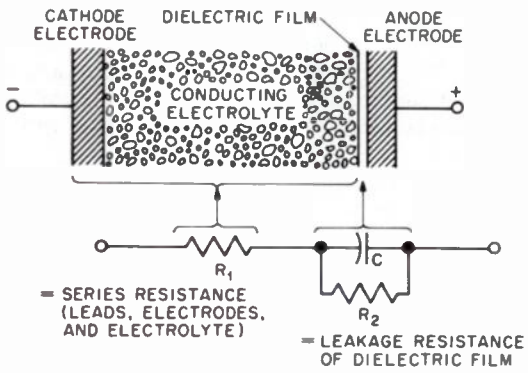

Fig. 11—Basic cell and simplified equivalent circuit for polar electrolytic capacitor.

anode, forms a layer of dielectric oxide. The most commonly used metals are aluminum or tantalum. The valve-metal behavior of these metals was known about 1850. Tantalum electrolytic capacitors were introduced in the 1950's because of the need for highly reliable miniature capacitors in transistor circuits over a wide temperature range. These capacitors were made possible by improved refining and powder metallurgy techniques.

The term "electrolytic capacitor" is applied to any capacitor in which the dielectric layer is formed by an electrolytic method. The capacitor does not necessarily contain an electrolyte.

The oxide layer is formed by placing the metal in a bath containing a suitable forming electrolyte, and applying voltage between the metal as anode and another electrode as cathode. The oxide grows at a rate determined by the current flowing, but this rate of growth decreases until the oxide has reached a limiting thickness determined by the voltage. For most practical purposes it may be assumed that the thickness of the oxide is proportional to the forming voltage.

Properties of aluminum and tantalum and their oxides follow.

Metal	Density	Principal Oxide	Dielectric Constant	Thickness (Å/V)
Aluminum	2.7	Al_2O_3	8	13.5
Tantalum	16.6	Ta_2O_5	27.6	17

The structure of these oxide layers plays an important part in determining their performance. Ideally they are amorphous but aluminum tends to form two distinct layers, the outer one being porous. Tantalum normally forms an amorphous oxide which, under conditions of a high field strength of the oxide layer, may become crystalline. Depending on the forming electrolyte and the surface condition of the metal, there is an upper limit of voltage beyond which the oxide breaks down. The working voltage is between 25 and 90 percent (according to type) of the forming voltage at which stable operation of the oxide layer can be obtained.

To produce a capacitor it is necessary to make contact to the oxide layer on the anode, and there are two distinct methods of doing this. The first is to use a working electrolyte that has sufficient conductivity over the temperature range to give a good power factor. There are many considerations in choosing the working electrolyte, and the choice is usually a compromise between high and low temperature performance. The working electrolyte also provides a rehealing feature in that any faults in the oxide layer will be repaired by further anodization.

In aluminum electrolytic capacitors the working electrolyte must be restricted to those materials in which aluminum and its oxide are inert. Corrosion can be minimized by using the highest possible purity of aluminum. This also reduces the tendency of the oxide layer to dissolve in the electrolyte, giving a better shelf life.

Tantalum, on the other hand, is very inert and therefore allows a wider choice of electrolyte. Since there is no gas evolution, better methods of sealing can be employed. The characteristics of aluminum and tantalum capacitors are shown in Figs. 12 and 13.

A major problem with all electrolytic capacitors is to ensure that the electrolyte is retained within the case under all operating conditions. In the aluminum capacitor, allowance must be made for gas evolution on reforming. Even the tantalum

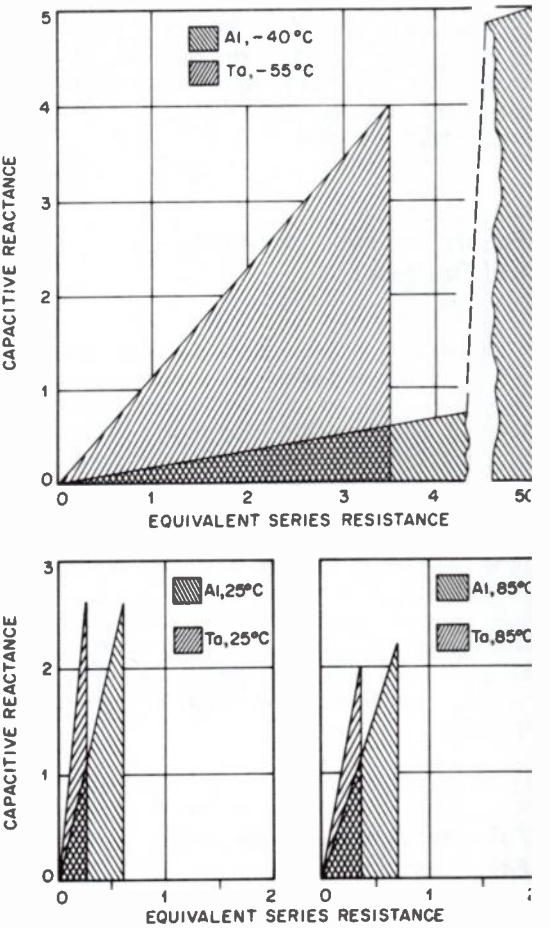

Fig. 12—Typical 120-hertz impedance diagrams for aluminum (Al) and tantalum (Ta) plain-foil polar electrolytic capacitors of 150-volt rating at low, high, and room temperatures. Resistance and reactance are drawn to the same arbitrary scale for all charts.

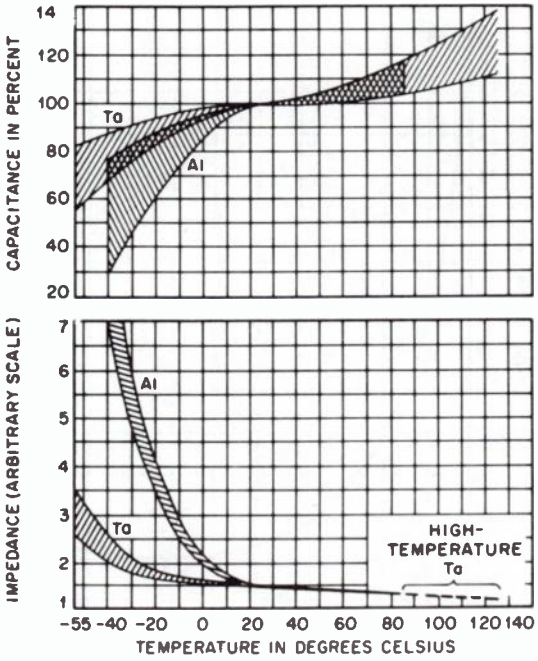

Fig. 13—Capacitance (top) and 120-hertz impedance (below) as a function of temperature for aluminum (Al) and tantalum (Ta) electrolytic capacitors.

capacitor usually must employ only organic materials for sealing, and these do not provide completely hermetic sealing. All organic materials have finite moisture transmission properties and, therefore, at the maximum category temperature the high vapor pressure of the electrolyte results in some diffusion.

An elegant solution to this problem was found by Bell Telephone Laboratories, using a semiconductor instead of an electrolyte. The semiconductor is manganese dioxide in a polycrystalline form and has a higher conductivity than conventional electrolyte systems. This material also provides a limited self-healing feature at a fault, resulting in oxidation of the tantalum and reduction of the manganese dioxide to a nonconducting form.

Electrolytic capacitors take many forms and the anode may be of foil, wire, or a porous sintered body. The foil may be either plain or etched. The porous body may be made with fine or with coarse particles and the body itself may be short and fat or long and thin. The aluminum-foil capacitor has a space factor about 6 times better than that of the equivalent paper capacitor, while tantalum capacitors are even smaller and enjoy a space factor up to 20 times better.

To operate electrolytic capacitors in series–parallel, stabilizing resistors should be used to equalize the voltage distribution. It should also be noted that, even when the case is not connected to one terminal, a low-resistance path exists between it and the electrodes. The case must be insulated from the chassis, particularly if the chassis and the negative terminal are not at the same potential.

Aluminum Electrolytics

This is the most widely known electrolytic capacitor and is used extensively in radio and television equipment. It has a space factor about 6 times better than the equivalent paper capacitor. Types of improved reliability are now available using high-purity (better than 99.99%) aluminum.

Conventional aluminum electrolytic capacitors which have gone 6 months or more without voltage applied may need to be reformed. Rated voltage is applied from a dc source with an internal resistance of 1500 ohms for capacitors with a rated voltage exceeding 100 volts, or 150 ohms for capacitors with a rated voltage equal to or less than 100 volts. The voltage must be applied for one hour after reaching rated value with a tolerance of ±3 percent. The capacitor is then discharged through a resistor of 1 ohm/volt.

Tantalum Foil-Type Electrolytics

This type of capacitor was introduced around 1950 to provide a more reliable type of electrolytic capacitor without shelf-life limitation. It was made possible by the availability of thin high-purity annealed-tantalum foils and wires. Plain-foil types were introduced first, followed by etched types. The purity, and particularly the surface purity, of these materials plays a major part in determining the leakage current and their ability to operate at the higher working voltages.

These capacitors are smaller than their aluminum counterparts and will operate at temperatures up to about 125°C (Figs. 14–16). The plain-foil types usually exhibit less variation of capacitance with temperature or frequency.

Tantalum Electrolytics with Porous Anode and Liquid Electrolyte

This is the first type of tantalum electrolytic capacitor to be introduced and still has the best space factor. Types using sulphuric-acid electrolyte have excellent electrical characteristics up to about 70 working volts. Other types contain neutral electrolytes.

Basically it consists of a sintered porous anode of tantalum powder housed in a silver or silver-

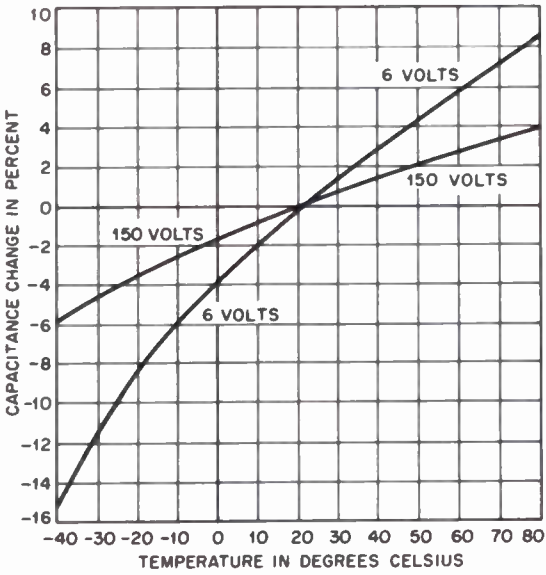

Fig. 14—Variation of capacitance with temperature for plain-tantalum-foil electrolytic capacitors.

plated container. The porous anode is made by pressing a tantalum high-purity powder into a cylindrical body and sintering in vacuum at about 2000°C.

Tantalum Electrolytics with Porous Anode and Solid Electrolyte

This is the so-called solid tantalum capacitor originally developed by Bell Telephone Laboratories. It developed from the porous-anode type with liquid electrolyte by replacing the liquid with a semiconductor. This overcame the problem of sealing common to all other types of electrolytic capacitors. Since there is no liquid electrolyte it is possible to use a conventional hermetic seal.

CERAMIC CAPACITORS

Electrical ceramics have a wide range of electrical characteristics, which makes them the most versatile of capacitor dielectric materials. The low-*K* materials have virtually linear characteristics and their properties are independent of frequency over the normal range. The materials are usually magnesium titanate (which has a positive temperature coefficient of capacitance) and calcium titanate (which has a negative one). By combining these, a range of controlled temperature coefficients can be obtained. These materials, together with other additions, produce a range of ceramics with di-

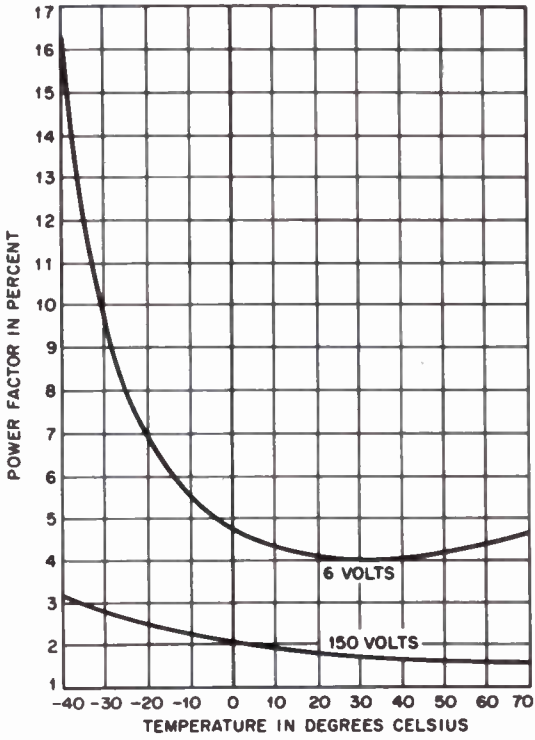

Fig. 15—Variation of power factor with temperature for plain-tantalum-foil electrolytic capacitors.

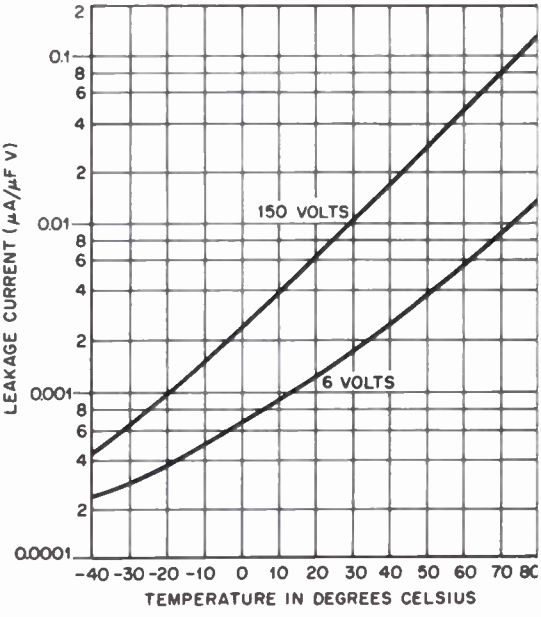

Fig. 16—Variation of leakage current with temperature for plain-tantalum-foil electrolytic capacitors.

electric constant of between 5 and 110 and temperature coefficients from +150 to −4700 ppm/°C with tolerances as small as ±15 ppm/°C. Their properties are largely independent of voltage. For these reasons they are sometimes known as the temperature-compensating ceramics. Glass and porcelain capacitors also have similar characteristics although their temperature coefficients lie in the range 0 to 140 only.

The high-*K* materials are the ferroelectrics. Because of their crystal structure, they sometimes have very high values of internal polarization, giving very high effective dielectric constants. In this way these materials are comparable with ferromagnetic materials. Above the Curie temperature a change of domain structure occurs which results in a change of electrical characteristics. This region is known as the para-electric region. In common with the ferromagnetic materials, a hysteresis effect is apparent and this makes the capacitance voltage-dependent.

The ferroelectrics are based on barium titanate, which has a peak dielectric constant of 6000 at the Curie point of 120°C. Additions of barium stanate, barium zirconate, or magnesium titanate reduce this dielectric constant but make it more uniform over the temperature range. Thus a family of materials can be obtained with a Curie point at about room temperature and with the dielectric constant falling off on either side. The magnitude of this change increases with increasing dielectric constant. These materials exhibit a decrease of capacitance with time and, as a result of the hysteresis effect, with increasing voltage.

Low-*K* ceramics are suitable for resonant-circuit or filter applications, particularly where temperature compensation is a requirement. Disc and tubular types are the best forms for this purpose. Stability of capacitance is good, being next to that of mica and polystyrene capacitors.

High-*K* ceramics are suitable for coupling and decoupling applications where low tangent of loss angle and stable capacitance are not requirements. Inductance in the leads and element causes parallel resonance in the megahertz region. Care is necessary in their application above about 50 megahertz for tubular styles and about 500 megahertz for disc types.

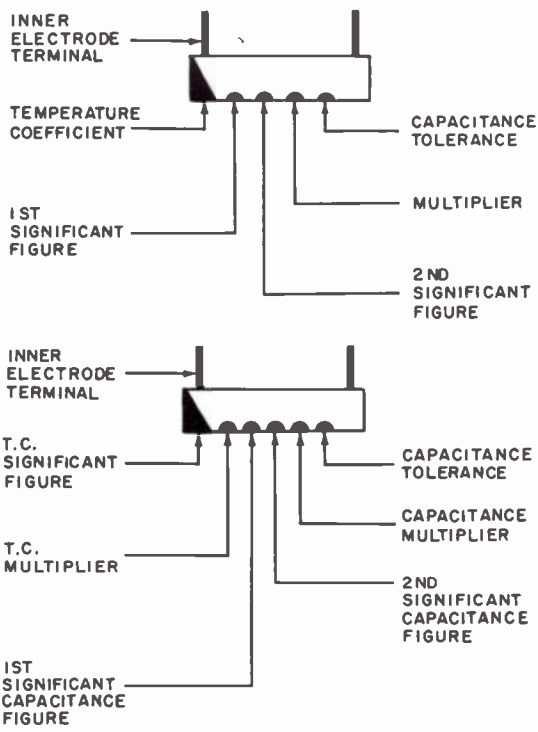

Fig. 17—Color coding of EIA Class-1 ceramic dielectric capacitors. See Table 6 for color code. Tubular style shown to illustrate identification of inner electrode. For disc or plate styles, color code will read from left to right as observed with lead wires downward. Five-dot system at top; six-dot system at bottom.

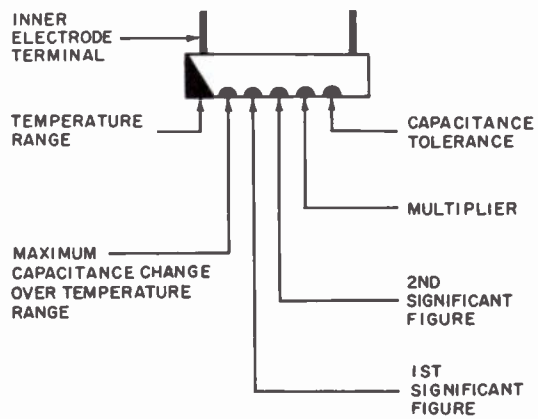

Fig. 18—Color coding of EIA Class-2 ceramic dielectric capacitors. See Table 6 for color code. Tubular style shown to illustrate identification of inner electrode. For disc or plate styles, color code will read from left to right as observed with lead wires downward.

Color Code

The significance of the various colored dots for EIA Standard RS-198-B (ANSI C83.4-1972) fixed ceramic dielectric capacitors is explained by Figs. 17 and 18, and may be interpreted from Table 6.

TABLE 6—COLOR CODE FOR CERAMIC DIELECTRIC CAPACITORS, CLASSES 1 AND 2.*

			Class 1					Class 2		
			Capacitance Tolerance		Temperature Coefficient ppm/°C (5-Dot System)	Temperature Coefficient Significant Figure (6-Dot System)	Temperature Coefficient Multiplier (6-Dot System)	Capacitance Tolerance (%)	Temperature Range (°C)	Maximum Capacitance Change Over Temperature Range (%)
Color	Digit	Multiplier	10 pF or less (pF)	Over 10 pF (%)						
Black	0	1	±2.0	±20	0	0.0	−1	±20	—	±2.2
Brown	1	10	±0.1	±1	−33	—	−10	—	+10 to +85	±3.3
Red	2	100	—	±2	−75	1.0	−100	—	−55 to +125	±4.7
Orange	3	1 000	—	±3	−150	1.5	−1 000	—	+10 to +65	±7.5
Yellow	4	10 000	—	—	−220	2.2	−10 000	GMV	—	±10
Green	5	—	±0.5	±5	−330	3.3	+1	±5	—	±15
Blue	6	—	—	—	−470	4.7	+10	—	—	±22
Violet	7	—	—	—	−750	7.5	+100	—	—	+22, −33
Gray	8	0.01	±0.25	—	+150 to −1500	(−1000 to −5200 ppm/°C, With Black Multiplier)	+1 000	+80, −20	—	+22, −56
White	9	0.1	±1.0	±10	+100 to −750	—	+10 000	±10	—	+22, −82
Silver	—	—	—	—	—	—	—	—	−30 to +85	±1.5
Gold	—	—	—	—	—	—	—	—	−55 to +85	±1

* EIA Standard RS-198-B (ANSI C83.4-1972). This standard classifies ceramic dielectric, fixed capacitors as follows:

Class 1—Temperature compensating ceramics suited for resonant circuit or other applications where high Q and stability of capacitance characteristics are required.

Class 2—Ceramics suited for bypass and coupling applications, or for frequency discriminating circuits where high Q and stability of capacitance characteristics are not of major importance.

Class 3—Low-voltage ceramics specifically suited for transistorized or other electronic circuits for bypass, coupling, or frequency determination where dielectric losses, high insulation resistance, and capacitance stability are not of major importance.

Note: Where size permits, EIA Class-3 ceramics are typographically marked as follows:

(1) Capacitance value in microfarads. (2) Rated voltage. (3) Manufacturer's mark or EIA source code.

(4) Capacitance value tolerance or appropriate code letter; either ±20% (Code M) or +80, −20% (Code Z).

(5) Temperature stability code (see the EIA or ANSI Standard).

Temperature Coefficient

Standard temperature coefficients of capacitance expressed in parts per million per degree Celsius are: +150, +100, +33, 0, −33, −75, −150, −220, −330, −470, −750, −1500, −2200, −3300, and −4700.

PAPER FOIL-TYPE CAPACITORS

General

Paper consists of a network of cellulose fibers, usually produced today from kraft (wood pulp). Very careful control in manufacture is necessary to produce extremely fine tissues with the requisite chemical purity and freedom from unreduced fibers and conducting particles. Paper normally has a moisture content of up to about 10 percent by weight, and this is removed before the capacitor is impregnated with an oil or wax.

Although paper capacitors have been largely replaced by plastic film types in electronic circuits, they are nevertheless still unsurpassed for high-voltage dc and ac power applications. They fall within the category of medium loss and medium stability, and provide an economical solution in this field.

The proper application of paper capacitors is a complex problem requiring consideration of the equipment, duty cycle, desired capacitor life, ambient temperature, applied voltage and waveform, and the capacitor impregnant characteristics.

Construction

The paper capacitor element is manufactured by winding together two aluminum foils interleaved with an appropriate number of layers of capacitor tissue. At least two layers normally are used to avoid the effects of conducting particles in the layer. For higher voltages a large number of layers is preferred.

Contact to the aluminum foils is usually by means of tinned copper tapes, which are preferably welded to the aluminum foil. Circular elements are wound on small-diameter mandrels but, if a large mandrel is used, the element may be flattened to fit conveniently in a rectangular case.

A wide variety of materials is used as impregnants for paper capacitors and these are classified generally as follows.

(A) Waxes. These are normally suitable for dc applications only. Chlorinated naphthalene has a high dielectric constant and therefore gives a cost and space saving. Chlorinated impregnants, however, must be stabilized to avoid electrochemical deterioration. Waxes are not suitable for ac applications because of the formation of gas voids due to shrinkage on cooling.

(B) Mineral oil, polyisobutylene, and silicone oils. These are relatively nonpolar impregnants suitable for either dc or ac applications. Oils have the advantage over waxes of not forming voids, minimizing internal discharges which would otherwise give rise to early failure on ac.

(C) Askarels. The most important of these are the chlorinated diphenyls with trade names such as Aroclor, Diconal, Inertene, and Pyranol. These are polar impregnants having a dielectric constant of about 6, but whose characteristics vary markedly with temperature and frequency. They are used mostly for ac power applications in which the higher dielectric constant gives a cost and space saving as well as an improvement in internal discharge characteristics. Dc operation is satisfactory only if the impregnant is stabilized.

Life Derating

The energy content of a capacitor may be found from

$$W = CE^2/2 \text{ watt-second}$$

where C = capacitance in farads, and E = applied voltage in volts.

In multiple-section capacitors, the sum of the watt-second ratings should be used to determine the proper derating of the unit.

Experiment has shown that the life of paper-dielectric capacitors having the usual oil or wax impregnants is approximately inversely proportional to the 5th power of the applied voltage.

Desired life in years (at ambient≈45°C)	1	2	5	10	20
Applied voltage in percent of rated voltage	100	85	70	60	53

The above life derating is to be applied together with the ambient-temperature derating to determine the adjusted-voltage rating of the paper capacitor for a specific application.

Waveform

Normal filter capacitors are rated for use with direct current. Where alternating voltages are present, the adjusted voltage rating of the capacitor should be calculated as the sum of the direct voltage and the peak value of the alternating voltage. The alternating component must not exceed 20 percent of the rating at 60 hertz, 15 percent at 120 hertz, 6 percent at 1000 hertz, or 1 percent at 10 000 hertz.

Where ac rather than dc conditions govern, this

fact must be included in the capacitor specification, and capacitors specially designed for ac service should be procured.

Where heavy transient or pulse currents are present, standard capacitors may not give satisfactory service unless an allowance is made for the unusual conditions.

Applications

Paper capacitors cover a wide range of applications as follows.

(A) Low-voltage dc. Tubular capacitors for coupling and decoupling in electronics circuits.

(B) High-voltage dc. Capacitors in smoothing filters, power-separating filters, energy-storage capacitors, etc.

(C) Low-voltage ac. Motor start, fluorescent lighting, interference suppression, and power-factor correction.

(D) High-voltage ac. Power-factor correction, power-line coupling, distribution capacitors for high-voltage switchgear, voltage-dividing capacitors for ac voltage measurement, etc.

METALLIZED PAPER CAPACITORS

General

Metallized capacitors use an evaporated metal film as an electrode instead of the conventional aluminum foil, as shown in Fig. 19. The metal film is sufficiently thin so that in the event of breakdown self-healing can occur. This consists of burning away the film in the area of the fault to isolate it. Higher working stresses can thus be tolerated even with single layers of tissue, giving an advantage of space factor in the lower voltage ratings. At 200 volts they are one quarter of the size of conventional paper types.

These capacitors are classified into type 1, which does not normally self-heal in service, and type 2, in which self-healing may occur under working conditions. Healing requires a low-impedance circuit and does not occur unless adequate volt-amperes are supplied for a very short time.

Construction

The capacitors are normally made by winding together two sheets of tissue that have been metallized with an offset electrode pattern. The metallizing in paper capacitors is usually zinc, although aluminum is regarded as superior particularly for plastic film types.

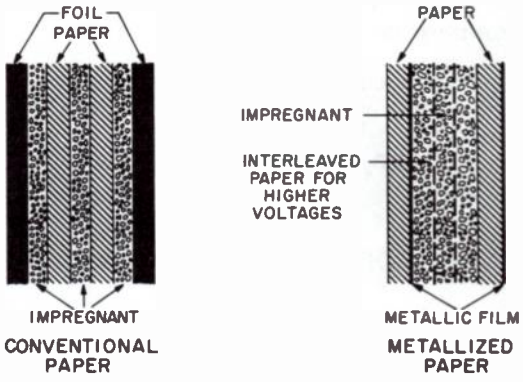

Fig. 19—Construction of conventional and metallized-type paper capacitors.

Connection to the film electrode is by spraying the end of the unit with metal. This is a critical operation which can result in poor contact with the electrodes if not done right. Types of metal vary widely and solder is satisfactory for making connection with zinc. With aluminum it is usually preferable to apply pure copper or zinc and to follow this by solder.

Applications

Direct-Current: Metallized paper capacitors are often used for coupling and decoupling applications in which small size is particularly important. In digital or other circuits where noise is important, it is essential to use a type-1 capacitor. If a type-2 capacitor is operated at 75 percent of rated voltage, self-healing is usually negligible but space advantage is less significant. The lower insulation-resistance performance of type-2 capacitors should be noted.

Alternating-Current: Special designs have been developed for use on ac, particularly for motor-starting and fluorescent-lighting applications.

MICA CAPACITORS

General

Mica capacitors fall within the classification of low loss and good capacitance stability. Mica is one of the earliest dielectric materials used and has an unrivalled combination of physical and electrical characteristics. It is of mineral origin and, because of its monoclinic structure, can be readily slit into thin plates. It has a dielectric

constant of about 6 (largely independent of frequency) together with a very low loss.

Construction

Types of mica capacitors follow.

(A) Clamp type with tin-foil electrodes. This form of construction was used in the manufacture of the earliest filter-type capacitors and is still used today in the construction of standard capacitors. It has been largely superseded for other applications.

(B) Eyelet construction. Silvered mica plates are eyeletted together to form stacks. Because of the possibility of relative movement and bowing of the plates, this construction has poor stability of both capacitance and temperature coefficient.

(C) Bonded silvered mica construction. Mica plates are silvered on both sides with appropriate electrode areas, stacked, and bonded together by firing. The result is dimensionally stable stacks of good stability of capacitance and with characteristics representative of the mica itself.

(D) Button styles. These are circular capacitors with a metal band round the outer periphery forming one terminal, and an eyeletted connection at the center forming the other. They are particularly suitable for high-frequency operation if mounted in a truly coaxial arrangement. These are discussed in detail later in this chapter.

The environmental protection necessary in the mica capacitor depends on the application. For some applications unprotected capacitors can be used, but the adsorption of water on the surface gives rise to relatively poor electrical characteristics. The two main methods of protection are as follows.

(A) *Epoxy resin molding.* Impregnated and wired stacks are molded in an appropriate resin having good moisture-protection properties. The advantage of this construction is that the molding has regular faces with good dimensional control.

(B) *Dipping.* A coating of resin is applied to the capacitor either by dipped or by fluidized-bed methods.

Applications

Because of their low temperature coefficient of capacitance and good capacitance stability both with temperature and frequency, mica capacitors are invaluable for filter applications.

Type Designation

A comprehensive numbering system, the type designation, is used to identify mica capacitors. Type designations are of the form shown in Fig. 20. MIL specifications now require type designation marking. Color coding is now used only for EIA standard capacitors.

Component Designation: Fixed mica-dielectric capacitors are identified by the symbol CM. For EIA, a prefix letter R is always included, and dipped types are identified by the symbol DM.

Case Designation: The case designation is a two-digit symbol that identifies a particular case size and shape.

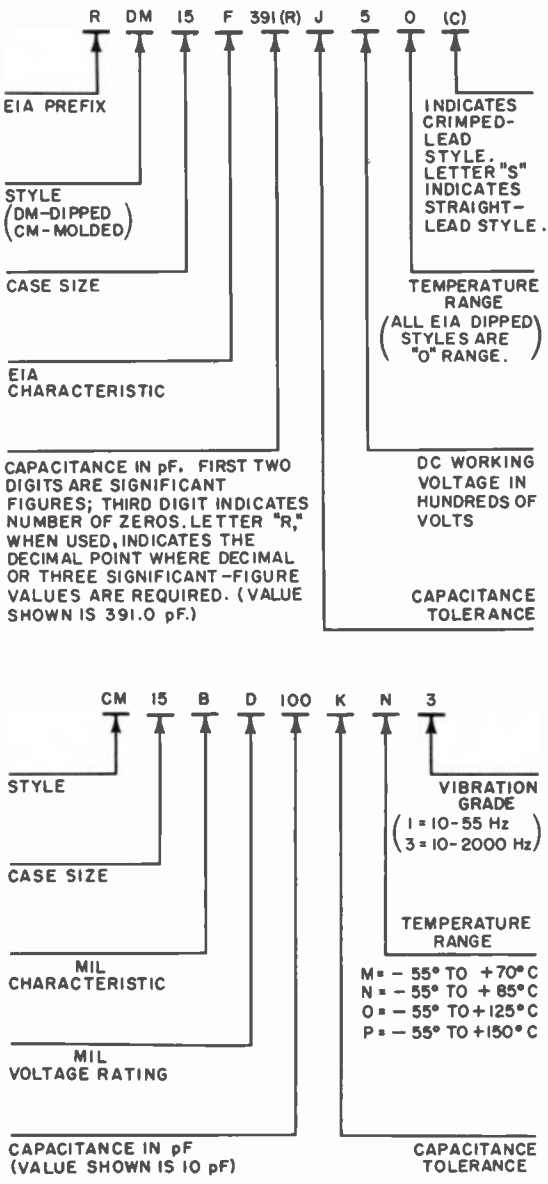

Fig. 20—Type designation for mica-dielectric capacitors. EIA at top; MIL at bottom.

Characteristic: The EIA or MIL characteristic is indicated by a single letter in accordance with Table 7.

Capacitance Value: The nominal capacitance value in picofarads is indicated by a 3-digit number. The first two digits are the first two digits of the capacitance value in picofarads. The final digit specifies the number of zeros that follow the first two digits. For EIA, if more than two significant figures are required, an additional digit is used, and the letter "R" is inserted to designate the decimal position.

Capacitance Tolerance: The symmetrical capacitance tolerance in percent is designated by a letter as shown in Table 1.

Voltage Rating: MIL voltage ratings are designated by a single letter as follows. A=100, B=250, C=300, D=500, E=600, F=1000, G=1200, H=1500, J=2000, K=2500, L=3000, M=4000, N=5000, P=6000, Q=8000, R=10 000, S=12 000, T=15 000, U=20 000, V=25 000, W=30 000, and X=35 000 volts. EIA dc working voltage is a number designating hundreds of volts.

Temperature Range: MIL specifications provide for four temperature ranges all of which have a lower limit of −55° Celsius and upper limits of M=+70, N=+85, O=+125, and P=+150 degrees Celsius. The EIA uses only N and O, which are identical to the MIL standard.

TABLE 7—FIXED-MICA-CAPACITOR REQUIREMENTS BY EIA AND MIL CHARACTERISTIC.

EIA Standard and MIL-Specification Requirements		
EIA or MIL Characteristic	Maximum Capacitance Drift	Maximum Range of Temperature Coefficient (ppm/°C)
B	Not Specified	Not Specified
C	±(0.5%+0.1 pF)	±200
D	±(0.3%+0.1 pF)	±100
E	±(0.1%+0.1 pF)	−20 to +100
F	±(0.05%+0.1 pF)	0 to +70

Vibration Grade: The MIL vibration grade is a number, 1 corresponding to vibration from 10 to 55 hertz at 10g for 4.5 hours and 3 corresponding to 10 to 2000 hertz at 20g for 12 hours.

Color Coding

The significance of the various colored dots for EIA-standard and former MIL-specification mica capacitors is explained by Fig. 21. The meaning of each color may be interpreted from Table 1.

Examples

	Top Row			Bottom Row			
Type	Left	Center	Right	Left	Tolerance Center	Multiplier Right	Description
RCM20B221K	white	red	red	brown	silver	brown	220 pF ±10%, EIA characteristic B.
CM30C681J	black	blue	gray	red	green	brown	680 pF ±5%, MIL characteristic C.

Capacitance

Measured at 1 megahertz for capacitors of 1000 picofarads or smaller; larger capacitors are measured at 1 kilohertz.

Temperature Coefficient

Measurements to determine the temperature coefficient of capacitance and the capacitance drift are based on one cycle over the following temperature values (all in degrees Celsius).

+25, −55, −40, −10, +25, +45, +65, +70, +85, +125, +150, +25.

Measurements at +85, +125, and +150 are not made if these values are not within the applicable temperature range of the capacitor.

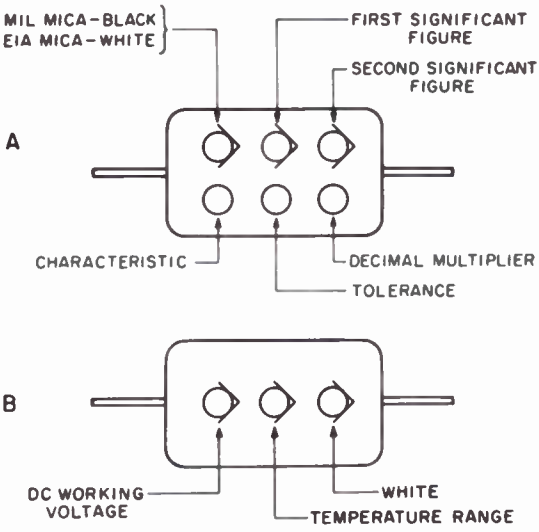

Fig. 21—Standard code for fixed mica capacitors. See color code in Table 1. *A* is the basic 6-dot form. The 9-dot form with *B* on the other side of the capacitor is used if the additional data are required.

Dissipation Factor

EIA and MIL specifications require that for molded and dipped capacitors the dissipation factor not exceed the values shown in Fig. 22. For potted and cast epoxy capacitors, the dissipation factor shall not exceed 0.35 percent from 1 to 1000 picofarads and 0.15 percent above 1000 picofarads.

High-Potential or Withstanding-Voltage Test

Molded or dipped mica capacitors are subjected to a test potential of twice their direct-current voltage rating.

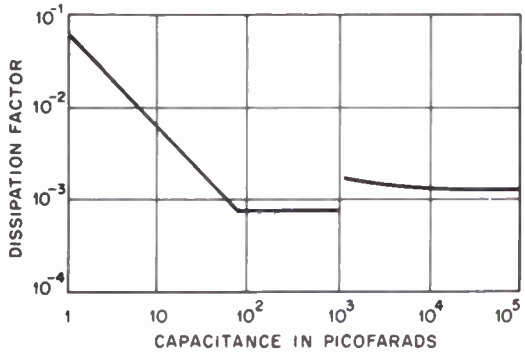

Fig. 22—EIA and MIL maximum dissipation factor at 1 megahertz for capacitance of 1000 picofarads or less and at 1 kilohertz for capacitance greater than 1000 picofarads.

Humidity and Thermal-Shock Tests

EIA Standard RS-153-B capacitors must withstand 5 cycles of −55, +25, +85 or +125 (as applicable), and +25 degrees Celsius thermal shock followed by a humidity test of 10 cycles (each of 24 hours) given for EIA Standard RS-186-D in Fig. 1. Units must pass withstanding-voltage test. Capacitance may not change by more than 1.0 percent or 1.0 picofarad, whichever is greater. Insulation resistance must meet or exceed 30 percent of the initial requirements at 25°C (50 000 megohms for capacitances of 20 000 picofarads or less; 1000 ohm-farads for larger capacitances).

MIL Specification MIL-C-5D capacitors must withstand 5 cycles of −55; +25; +85, +125, or +150 (as applicable); and +25 degrees Celcius thermal shock followed by a humidity test of 10 cycles (each of 24 hours) given for MIL-STD-202E in Fig. 1. Units must pass withstanding-voltage test. Capacitance may not change by more than ±(0.2 percent+0.5 picofarad). Insulation resistance must meet or exceed 30 percent of the initial requirements at 25°C (100 000 megohms for 10 000 picofarads or less; 1000 megohm-microfarads for larger capacitances).

Life

Capacitors are given accelerated life tests at 85 degrees Celsius with 150 percent of rated voltage applied for 2000 hours for MIL specification or 250 hours for EIA standard. If capacitors are rated above +85°C, the test will be at their maximum rated temperature.

BUTTON MICA CAPACITORS

Color Code

Button mica capacitors are color coded in several different ways, of which the two most widely used methods are shown in Fig. 23.

Characteristic

The characteristics for button mica capacitors are given in Table 8. Typical initial *Q* values are approximately 500 for capacitors 5 to 50 picofarads, 700 for capacitors 51 to 100 picofarads, and 1000 for capacitors 101 to 5000 picofarads. Initial insulation resistance shall exceed 7500 megohms for resin-sealed units and 50 gigaohms for hermetically sealed units. Withstanding-voltage tests are made at twice rated voltage.

TABLE 8—REQUIREMENTS FOR BUTTON MICA CAPACITORS.

Characteristic		Max Range of Temp Coeff (ppm/°C)	Maximum Capacitance Drift
MIL	Commercial		
—	C	±200	±0.5%
D	—	±100	±0.3% or 0.3 pF, whichever is greater
—	E	(−20 to +100)+0.05 pF	±(0.1%+0.10 pF)
—	F	(0 to +70)+0.05 pF	±(0.05%+0.10 pF)

Thermal-Shock and Humidity Tests

After 10 cycles of 24 hours each of the cycling for MIL-STD-202E given in Fig. 1, capacitors should have the following properties.

	Resin Seal	Hermetic Seal
Insulation Resistance in megohms (minimum)	500	4000
Q factor, % of initial requirement	50	75
Capacitance change, maximum % of initial capacitance	3	2

Thermal shock and immersion tests are also applied; they have less effect than the cycling humidity test above.

I.F. TRANSFORMER FREQUENCIES

Recognized standard frequencies* for receiver intermediate-frequency transformers are:

Standard broadcast (540 to 1600 kilohertz)	455 and 260 kilohertz
Standard broadcast (vehicular)	262.5 kilohertz
Very-high-frequency broadcast	10.7 megahertz
Very-, ultra-, and super-high-frequency equipment	30, 60, 100 megahertz (common practice)
Television:	
Sound carrier	41.25 megahertz
Picture carrier	45.75 megahertz

* EIA Standard REC-109-C.

COLOR CODES FOR VARIOUS COMPONENTS

*Receiver Leads**

Antenna	Blue
Ground	Black

Intermediate-Frequency Transformers

Primary:	
Plate	Blue
B+	Red
Secondary:	
Grid or diode	Green
Grid return	White
For full-wave transformer:	
Second diode	Violet

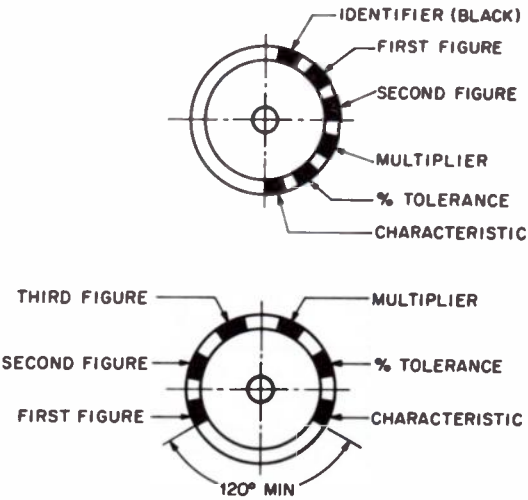

Fig. 23—Color coding of button mica capacitors. See Table 1 for color code. Commercial color code for characteristic not standardized; varies with manufacturer.

* EIA Standard RS-336.

*Traveling-Wave Tubes and Klystrons**

Body (Tracer)	TWT Element		Klystron
Black	Grounds or grounded elements		
Brown†	Heater or filament off ground		
Yellow†	Cathode or common heater–cathode		
Red	Collector		Collector, if isolated
Orange	Helix 1	1st	Reflector, phase modulation element, electrostatic focussing element, etc.
Orange (green)	Helix 2	2nd	
Orange (blue)	Helix 3	3rd	
Orange (gray)	Helix 4	4th	
Orange (black)	—	5th	
Orange (white)	—	6th	
Green	Grid 1		Grid 1
Blue	Grid 2		Grid 2
Gray	Grid 3		Grid 3
White	Grid 4		Grid 4
Green (black)	Grid 5		Grid 5
Blue (black)	Grid 6		Grid 6
Gray (black)	Grid 7		Grid 7
White (black)	Grid 8		Grid 8

† If individual leads are provided for elements having internal connections, the body color will identify the major element and a tracer will identify the internally connected element. For example: Brown (yellow) indicates heater lead internally connected to the cathode.

Note:

No attempt is made to separate anode, control grid, modulating anode, etc. Elements are numbered sequentially according to their relative position starting from the cathode. If two elements are equidistant from the cathode, the lower number indicates the lower-voltage element. Grids or helices not available externally are omitted from the number sequence.

Crossed-Field Devices—Magnetrons, BWO's, etc.*

Color	Magnetron	Voltage-Tunable Magnetron	Backward-Wave Oscillator (M-type)
Black	Body or other grounded elements		
Brown	Heater or filament off ground		
Yellow	Cathode or common heater–cathode		
Red	Anode	Anode	Delay line
Orange	—	—	Sole
Green	—	Injector	Grid
Blue	—	—	Accelerator
White	—	Cold cathode	—
Gray	Turnoff electrode in crossed-field amplifiers		

Electromagnet Leads (When Electromagnet is Integral Part of Microwave-Tube Package)

Orange tracer on black, red, white, or other color body.

* EIA Standard RS-235-C.

*Hall Generator Devices—Wiring**

Black	Control Current–Negative
Red	Control Current–Positive
Yellow	Output–Negative
Blue	Output–Positive

Stereo Pickup Leads†

No. of Leads	Right		Left		Return or Ground
	High	Low	High	Low	
3	red	—	white	—	black
4	red	green	white	blue	—
5	red	green	white	blue	black

* EIA Standard RS-336.
† EIA Standard RS-243.

OTHER MARKING CODES

Single Band or Mark at One End

Semiconductor diode	cathode end
Capacitor, wound-foil type	outside-electrode end
Capacitor, ceramic-tube type	inner electrode

Symbols

Electrolytic capacitor sections—terminal markings.

⌓	□	△	No mark
Highest	Intermediate	Lower	Lowest

The sequence applies first to voltage rating of section. If voltage ratings are the same, the sequence applies to capacitance value. For fewer than 4 terminals any mark may be omitted, but interpretation of marks used follows preceding rules.

Connections

Stereo Headphone 3-Contact Plugs:

Sleeve (barrel)	common
Ring	left phone
Tip	right phone
Polarization	with + on tip or ring, diaphragm moves toward listener's ear (− on barrel).

Phasing of Microphones‡

Terminal or Lead:

In phase	red (or 1)
Out of phase	black (or 2)
Ground	G

‡ EIA Standard RS-221.

PRINTED CIRCUITS

A printed circuit is a conductive circuit pattern applied to one or both sides of an insulating substrate. The conductive pattern can be formed by any of several techniques after which component lead holes are drilled or punched in the substrate and components are installed and soldered in place. Printed-circuit construction is ideal for assembly of circuits which employ miniature solid-state components. Its advantages over conventional chassis and point-to-point wiring include:

(A) Considerable space savings over conventional construction methods is usually a result.

(B) A complex circuit may be modularized by using several small printed circuits instead of a single larger one. Modularization simplifies trouble-shooting, circuit modification, and mechanical assembly in an enclosure.

(C) Soldering of component leads may be accomplished in an orderly sequence by hand or all the leads may be soldered simultaneously by dip or wave soldering.

(D) A more uniform product is produced because wiring errors are eliminated and because distributed capacitances are constant from one production unit to another.

(E) The printed-circuit method of construction lends itself to automatic assembly and testing machinery.

(F) The printed circuit consists of printed wiring but may also include printed components such as capacitors and inductors. Capacitors can

be produced by printing conducting areas on opposite sides of the wiring board, using the board material as the dielectric. Spiral-type inductors can also be printed. Both types of components are illustrated in Fig. 24.

(G) Using appropriate base materials, flexible cables or flexible circuits can be built.

(H) By using several layers of circuits (in proper registry) in a sandwich construction, with the conductors separated by insulating layers, relatively complex wiring can be provided.

Printed-Circuit Base Materials

Rigid printed-circuit base materials are available in thicknesses varying from $\frac{1}{64}$ to $\frac{1}{2}$ inch. The important properties of the usual materials are given in Table 9. For special applications, other rigid or flexible materials are available as follows.

(A) Glass-cloth Teflon (polytetrafluoroethylene, PTFE) laminate.
(B) Kel-F (polymonochlorotrifluoroethylene) laminate.
(C) Silicone rubber (flexible).
(D) Glass-mat–polyester-resin laminate.
(E) Teflon film.
(F) Ceramic.

The most widely used base material is NEMA-XXXP paper-base phenolic.

Conductor Materials

Copper is used almost exclusively as the conductor material, although silver, brass, and aluminum also have been used. The common thicknesses of foil are 0.0014 inch (1 oz/sq ft) and 0.0028 inch (2 oz/sq ft). The current-carrying capacity of a copper conductor may be determined from Fig. 25.

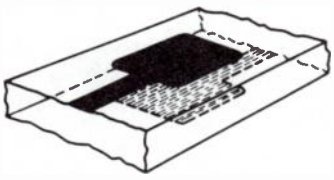

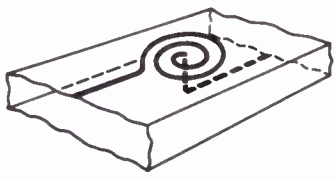

Fig. 24—Formation of reactive elements by printed-circuit methods.

Manufacturing Processes

The most widely used production methods are:

(A) Etching process, wherein the desired circuit is printed on the metal-clad laminate by photographic, silk-screen, photo-offset, or other means, using an ink or lacquer resistant to the etching bath. The board is then placed in an etching bath that removes all of the unprotected metal (ferric chloride is a commonly used mordant for copper-clad laminates). After the etching is completed, the ink or lacquer is removed to leave the conducting pattern exposed.

(B) Plating process, wherein the designed circuit pattern is printed on the unclad base material using an electrically conductive ink and, by electroplating, the conductor is built up to the desired thickness. This method lends itself to plating through punched holes in the board for making connections from one side of the board to the other.

(C) Other processes, including metal spraying and die stamping.

Circuit-Board Finishes

Conductor protective finishes are required on the circuit pattern to improve shelf-storage life of the circuit boards and to facilitate soldering. Some of the most widely used finishes are:

(A) Hot-solder coating (done by dip-soldering in a solder bath) is a low-cost method and gives good results where coating thickness is not critical.

(B) Silver plating is used as a soldering aid but is subject to tarnishing and has a limited shelf life.

(C) Hot-rolled or plated solder coat gives good solderability and uniform coating thickness.

(D) Other finishes for special purposes are gold plate for corrosion resistance and solderability, and electroplated rhodium over nickel for wear resistance. Insulating coatings such as acrylic, polystyrene, epoxy, or silicone resin are sometimes applied to circuit boards to improve circuit performance under high humidity or to improve the anchorage of parts to the board. Conformal coatings are relatively thick and tend to smooth the irregular contour of the mounted items; they add less mass than encapsulation. A protective organic coating (unless excessively thick) will not improve the electrical properties of an insulating base material during long exposure to high humidity. On two-sided circuit boards, where the possibility of components shorting out the circuit patterns exists, a thin sheet of insulating material is sometimes laminated over the circuit before the parts are inserted.

WRH

TABLE 9—PROPERTIES OF TYPICAL PRINTED-CIRCUIT DIELECTRIC BASE MATERIALS.

Material	Comparable MIL Type	Punchability	Mechanical Strength	Moisture Resistance	Insulation	Arc Resistance	Abrasive Action on Tools	Max Temperature (°C)*
NEMA type XXXP paper-base phenolic	—	Good	Good	Good	Good	Poor	No	105
NEMA type XXXPC paper-base phenolic	—	Very good	Good	Very good	Good	Poor	No	105
NEMA type FR-2 paper-base phenolic, flame resistant	—	Very good	Good	Very good	Good	Poor	No	105
NEMA type FR-3 paper-base epoxy, flame resistant	PX	Very good	Very good	Very good	Very good	Good	No	105
NEMA type FR-4 glass-fabric-base epoxy, general purpose, flame resistant	GF	Fair	Excellent	Excellent	Excellent	Very good	Yes	130 (125)
NEMA type FR-5 glass-fabric-base epoxy, temperature and flame resistant	GH	Fair	Excellent	Excellent	Excellent	Very good	Yes	155 (150)
NEMA type G-10 glass-fabric-base epoxy, general purpose	GE	Fair	Excellent	Excellent	Excellent	Very good	Yes	130 (125)
NEMA type G-11 glass-fabric-base epoxy, temperature resistant	GB	Poor	Excellent	Excellent	Excellent	Very good	Yes	155 (150)
Glass-fabric-base polytetrafluoro-ethylene	GT	—	Good	Excellent	Excellent	Excellent	—	(150)
Glass-fabric-base fluorinated ethylene propylene	FEP	—	Good	Excellent	Excellent	Excellent	—	(150)

* MIL-STD-275C rating shown in parentheses if different from industry rating.

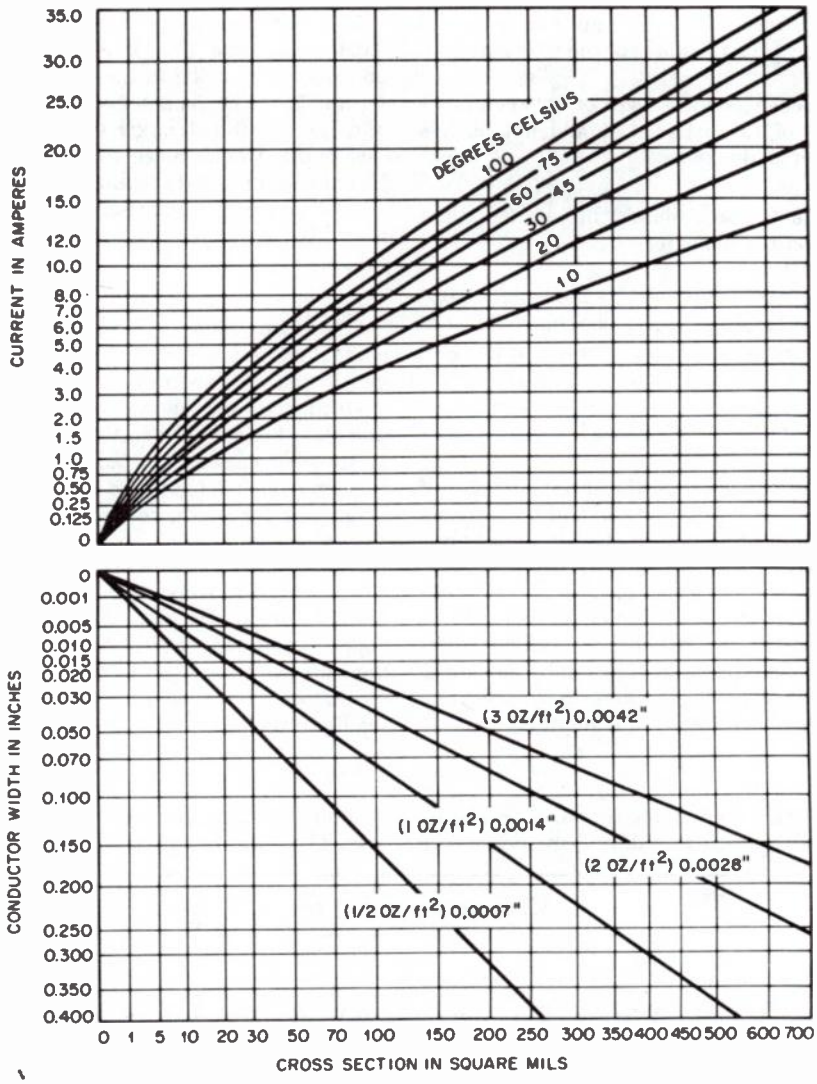

Fig. 25—Current-carrying capacity and sizes of etched copper conductors for various temperature rises above ambient. *From MIL-STD-275C, 9 January 1970.*

Design Considerations

Before a printed-circuit layout is made, the circuit must be breadboarded and tested under the anticipated final operating conditions. This procedure will permit operating deficiencies and quirks to be detected and corrected before the time-consuming process of producing the circuit board is begun. It is important to note that certain circuits may operate differently on a printed-circuit board than on a breadboard and appropriate corrective steps may be necessary. For example, inductive coupling between foil patterns may cause unwanted oscillation in high-frequency or amplifier circuits.

Modular Layout: All features (terminal areas, contacts, board boundaries, holes, etc.) should be arranged to be centered at the intersections of a 0.100-, 0.050-, or 0.025-inch rectangular grid, with preference in the order stated. Many components are available with leads spaced to match the standard grids. Devices with circular lead configurations and a few other multilead devices are exceptions that require special attention and dimensioning. Following this grid-layout principle simplifies drafting and subsequent machine operations in board manufacture and assembly.

Drilled holes must be employed if the stated requirements for punched holes cannot be met, or if the material is not of a punching grade. Drilling is less detrimental to the laminate surrounding the hole; punching may cause crazing or separation of the laminate layers.

Diameter of punched holes in circuit boards should not be less than $\frac{2}{3}$ the thickness of the base material.

Distance between punched holes or between holes and the edge of the material should not be less than the material thickness.

Punched-hole tolerance should not be less than ±0.005 inch on the diameters.

Hole sizes should not exceed by more than 0.020 inch the diameter of the wire to be inserted in the hole. With smaller holes, hand insertion of the wire is difficult. Machine insertion requires the larger allowance. Clinching of the lead is desirable if the clearance is larger.

Tolerances with respect to the true-position-grid location for terminal area centers and for locating edges of boards or other locating features (datums) should not exceed on the board: 0.014 inch diameter for conductor widths and spacings above 0.031 inch; 0.010 inch diameter for conductor widths and spacings 0.010 to 0.031 inch, inclusive. Tolerances on other dimensions (except conductor widths and spacings) may be larger. Closer tolerances may be needed if machine insertion is required.

Terminal area diameters should be at least (A) 0.020 inch larger than the diameter of the flange or projection of the flange on eyelets or standoff terminals, or the diameter of a plated-through hole, and (B) 0.040 inch larger than the diameter of an unsupported hole. Since the terminal area should be unbroken around the finished hole, the diameter should be further increased over the above minimum to allow for the permitted hole-position tolerance.

Conductor widths should be adequate for the current carried. See Fig. 25. For a given conductor-width and copper-thickness intersection, proceed vertically to the allowable temperature-rise line and then horizontally to the left to determine the permissible current. An additional 15% derating is recommended for board thicknesses of $\frac{1}{32}$ inch or less, or for conductors thicker than 0.004 inch (3 oz). The normal ambient temperature surrounding the board plus the allowable temperature rise should not exceed the maximum safe operating temperature of the laminate. For ordinary work copper conductor widths of 0.060 inch are convenient; with high-grade technique (extra cost) conductor widths as small as 0.010 inch can be readily produced.

Conductor spacing requirements are governed by the applied voltage, the maximum altitude, the conductor protective coating used, and the power-source size. The following guide is suggested.*

	Minimum Spacing Between Conductors (inches)		
	Uncoated Boards		Conformal Coated Boards
Voltage Between Conductors	Sea Level to 10 000 Ft	Over 10 000 Ft	All Altitudes
0–30	0.025	0.025	0.010
0–50	0.025	0.025	—
0–150	0.025	—	—
31–50	0.025	0.025	0.015
51–100	0.025	0.060	0.020
101–170	—	0.125	0.030
101–300	—	—	0.030
151–300	0.050	—	0.030
171–250	0.050	0.250	0.030
251–500	—	0.500	—
301–500	0.100	0.500	0.060
Above 500	0.0002 per volt	0.001 per volt	0.00012 per volt

* From MIL-STD-275C.

Preparation of Artwork

Workmanship: In preparing the master artwork for printed circuits, careful workmanship and accuracy are important. When circuits are reproduced by photographic means, much retouching time is saved if care is taken with the original artwork.

Materials: Artwork should be prepared on a dimensionally stable material. Tracing paper and bristol board are now outmoded, and specially treated (toothed) polyethylene terephthalate (Mylar, Cronar) base drafting films are used for most printed-circuit layouts. The layout pattern may be produced using one of the following methods:

1. Hand application of opaque, permanent black ink,
2. Pressure-sensitive tape,
3. Hand-cut stencil made from self-adhesive opaque film, or
4. Preformed self-adhesive layout patterns.

Scale: Artwork should be prepared to a scale that is two to five times oversize. Photographic reduction to final negative size should be possible, however, in one step.

Bends: Avoid the use of sharp corners when laying out the circuit. See Fig. 26.

Holes: The centers of holes to be manually drilled or punched in the circuit board should be indicated by a circle of $\frac{1}{32}$-inch diameter (final size after reduction). See Fig. 27. This feature is not needed on each board if templates or numerically controlled machine tools are used for hole preparation; however, it is still a convenience for checking drawings, master artwork, and photographic negatives.

Registration of Reverse Side: When drawing the second side of a printed-circuit board, corresponding centers should be taken directly from the back of the drawing of the first side.

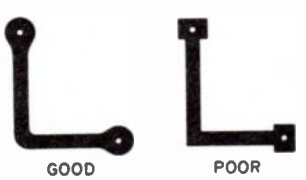

Fig. 26—Proper design of bends for printed-circuit conductors.

Fig. 27—Indication for hole.

Reference Marks: In addition to the illustration of the circuit pattern, the trim line, registration marks, and two scale dimensions at right angles should be shown. Nomenclature, reference designations, operating instructions, and other information may also be added.

Assembly

All components should be inserted on one side of the board if practicable. In the case of boards with the circuit on one side only, the parts should be inserted on the side opposite the circuit. This allows all connections to be soldered simultaneously by dip-soldering.

Dip-soldering consists of applying a flux, usually a rosin–alcohol mixture, to the circuit pattern and then placing the board in contact with molten solder. Slight agitation of the board will insure good fillets around the wire leads. In good present technique, the circuit board with its components assembled (on one side only) has its conductor pattern passed through the crest of a "wave" of molten solder; all junctions are soldered as the board progresses through the wave. The flux, board temperature, solder temperature, and immersion time are interrelated and must be adjusted for best results. Long exposure to hot solder is detrimental to the insulating material and to the adhesive that joins the copper foil to the insulation. For hand dipping, a 5-second dip in a 60/40 tin–lead solder bath maintained at a temperature of 450 degrees Fahrenheit will give satisfactory results.

After solder-dipping, the residual flux should be removed by a suitable solvent. Be sure the solvent is compatible with the materials used in the component parts mounted on the board; solvents frequently dissolve cements or plastics and marking inks, or cause severe stress cracking of plastics.

To secure the advantages of machine assembly:

(A) Components should be of similar size and shape, or separate inserting heads will be required for each different shape of item.

(B) Components of the same size and shape must be mounted using the same terminal lead spacing at all points.

(C) Different values of a part, or even different parts of similar shape and size (if axial-lead style) may be specially sequenced in a lead-taped package for insertion by one programmed insertion head.

(D) A few oddly sized or shaped components may be economically inserted by hand after the machine insertion work is completed.

Reference

An excellent reference on microelectronic printed-circuit techniques is J. A. Scarlett, "Printed Circuit Boards for Microelectronics," Van Nostrand Reinhold Co., New York, 1970.

CHAPTER 6
FUNDAMENTALS OF NETWORKS

INDUCTANCE OF SINGLE-LAYER SOLENOIDS*

The approximate value of the low-frequency inductance of a single-layer solenoid is†

$$L = Fn^2d \text{ microhenries}$$

where F = form factor, a function of the ratio d/l (value of F may be read from Fig. 1), n = number of turns, d = diameter of coil (inches) between centers of conductors, and l = length of coil (inches) = n times the distance between centers of adjacent turns.

The equation is based on the assumption of a uniform current sheet, but the correction due to the use of spaced round wires is usually negligible for practical purposes. For higher frequencies, skin effect alters the inductance slightly. This effect is not readily calculated, but is often negligibly small. However, it must be borne in mind that the equation gives approximately the true value of inductance. In contrast, the apparent value is affected by the shunting effect of the distributed capacitance of the coil.

Example: Required, a coil of 100 microhenries inductance, wound on a form 2 inches in diameter by 2 inches winding length. Then $d/l = 1.00$, and $F = 0.0173$ in Fig. 1.

$$n = (L/Fd)^{1/2}$$
$$= [100/(0.0173 \times 2)]^{1/2}$$
$$= 54 \text{ turns.}$$

Reference to Table 1 will assist in choosing a desirable size of wire, allowing for a suitable spacing between turns according to the application of the coil. A slight correction may then be made for the increased diameter (diameter of form, plus two times radius of wire), if this small correction seems justified.

Approximate Equation

For single-layer solenoids of the proportions normally used in radio work, the inductance is

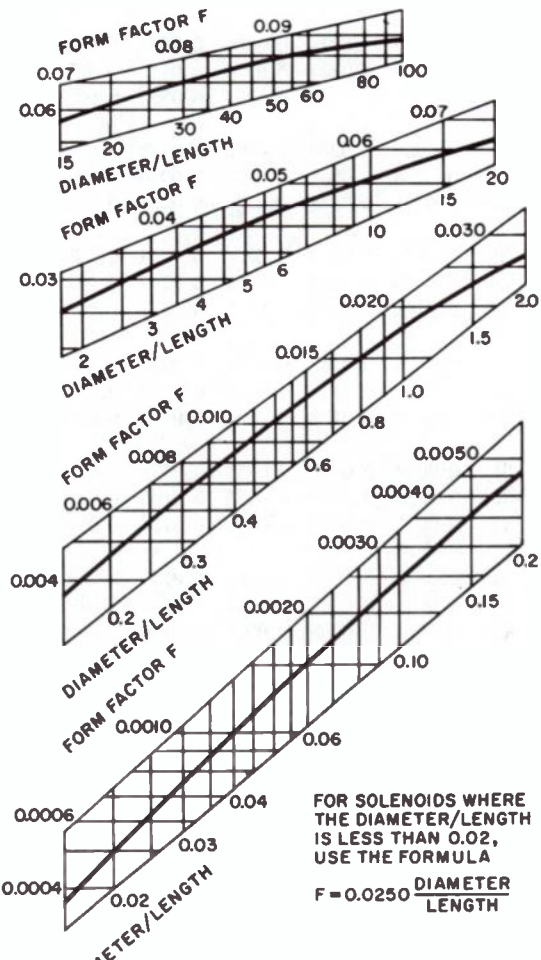

Fig. 1—Inductance of a single-layer solenoid, form factor = F.

* Calculation of copper losses in single-layer solenoids is treated in F. E. Terman, "*Radio Engineers Handbook*," 1st edition, McGraw-Hill Book Company, Inc., New York, N.Y.; 1943: pp. 77–80.

† Equations and Fig. 1 are derived from equations and tables in Bureau of Standards Circular No. C74.

TABLE 1—MAGNET-WIRE DATA.

AWG B & S gauge	Bare nom diam (in.)	Enam nom diam (in.)	SCC* diam (in.)	DCC* diam (in.)	SCE* diam (in.)	SSC* diam (in.)	DSC* diam (in.)	SSE* diam (in.)	Bare min diam (in.)	Bare max diam (in.)	Enameled min diam (in.)	Enameled diam* (in.)
10	0.1019	0.1039	0.1079	0.1129	0.1104	—	—	—	0.1009	0.1029	0.1024	0.1044
11	0.0907	0.0927	0.0957	0.1002	0.0982	—	—	—	0.0898	0.0917	0.0913	0.0932
12	0.0808	0.0827	0.0858	0.0903	0.0882	—	—	—	0.0800	0.0816	0.0814	0.0832
13	0.0720	0.0738	0.0770	0.0815	0.0793	—	—	—	0.0712	0.0727	0.0726	0.0743
14	0.0641	0.0659	0.0691	0.0736	0.0714	—	—	—	0.0634	0.0647	0.0648	0.0664
15	0.0571	0.0588	0.0621	0.0666	0.0643	0.0591	0.0611	0.0613	0.0565	0.0576	0.0578	0.0593
16	0.0508	0.0524	0.0558	0.0603	0.0579	0.0528	0.0548	0.0549	0.0503	0.0513	0.0515	0.0529
17	0.0453	0.0469	0.0503	0.0548	0.0523	0.0473	0.0493	0.0493	0.0448	0.0457	0.0460	0.0473
18	0.0403	0.0418	0.0453	0.0498	0.0472	0.0423	0.0443	0.0442	0.0399	0.0407	0.0410	0.0422
19	0.0359	0.0374	0.0409	0.0454	0.0428	0.0379	0.0399	0.0398	0.0355	0.0363	0.0366	0.0378
20	0.0320	0.0334	0.0370	0.0415	0.0388	0.0340	0.0360	0.0358	0.0316	0.0323	0.0326	0.0338
21	0.0285	0.0299	0.0335	0.0380	0.0353	0.0305	0.0325	0.0323	0.0282	0.0287	0.0292	0.0303
22	0.0253	0.0266	0.0303	0.0343	0.0320	0.0273	0.0293	0.0290	0.0251	0.0256	0.0261	0.0270
23	0.0226	0.0238	0.0276	0.0316	0.0292	0.0246	0.0266	0.0262	0.0223	0.0228	0.0232	0.0242
24	0.0201	0.0213	0.0251	0.0291	0.0266	0.0221	0.0241	0.0236	0.0199	0.0203	0.0208	0.0216
25	0.0179	0.0190	0.0224	0.0264	0.0238	0.0199	0.0219	0.0213	0.0177	0.0181	0.0186	0.0193
26	0.0159	0.0169	0.0204	0.0244	0.0217	0.0179	0.0199	0.0192	0.0158	0.0161	0.0166	0.0172
27	0.0142	0.0152	0.0187	0.0227	0.0200	0.0162	0.0182	0.0175	0.0141	0.0144	0.0149	0.0155
28	0.0126	0.0135	0.0171	0.0211	0.0183	0.0146	0.0166	0.0158	0.0125	0.0128	0.0132	0.0138
29	0.0113	0.0122	0.0158	0.0198	0.0170	0.0133	0.0153	0.0145	0.0112	0.0114	0.0119	0.0125
30	0.0100	0.0108	0.0145	0.0185	0.0156	0.0120	0.0140	0.0131	0.0099	0.0101	0.0105	0.0111
31	0.0089	0.0097	0.0134	0.0174	0.0144	0.0109	0.0129	0.0119	0.0088	0.0090	0.0094	0.0099
32	0.0080	0.0088	0.0125	0.0165	0.0135	0.0100	0.0120	0.0110	0.0079	0.0081	0.0085	0.0090
33	0.0071	0.0078	0.0116	0.0156	0.0125	0.0091	0.0111	0.0100	0.0070	0.0072	0.0075	0.0080
34	0.0063	0.0069	0.0108	0.0148	0.0116	0.0083	0.0103	0.0091	0.0062	0.0064	0.0067	0.0071
35	0.0056	0.0061	0.0101	0.0141	0.0108	0.0076	0.0096	0.0083	0.0055	0.0057	0.0059	0.0063
36	0.0050	0.0055	0.0090	0.0130	0.0097	0.0070	0.0090	0.0077	0.0049	0.0051	0.0053	0.0057
37	0.0045	0.0049	0.0085	0.0125	0.0091	0.0065	0.0085	0.0071	0.0044	0.0046	0.0047	0.0051
38	0.0040	0.0044	0.0080	0.0120	0.0086	0.0060	0.0080	0.0066	0.0039	0.0041	0.0042	0.0046
39	0.0035	0.0038	0.0075	0.0115	0.0080	0.0055	0.0075	0.0060	0.0034	0.0036	0.0036	0.0040
40	0.0031	0.0034	0.0071	0.0111	0.0076	0.0051	0.0071	0.0056	0.0030	0.0032	0.0032	0.0036
41	0.0028	0.0031	—	—	—	—	—	—	0.0027	0.0029	0.0029	0.0032
42	0.0025	0.0028	—	—	—	—	—	—	0.0024	0.0026	0.0026	0.0029
43	0.0022	0.0025	—	—	—	—	—	—	0.0021	0.0023	0.0023	0.0026
44	0.0020	0.0023	—	—	—	—	—	—	0.0019	0.0021	0.0021	0.0024

* Nominal bare diameter plus maximum additions.

For additional data on copper wire, see Chapters 4 and 13.

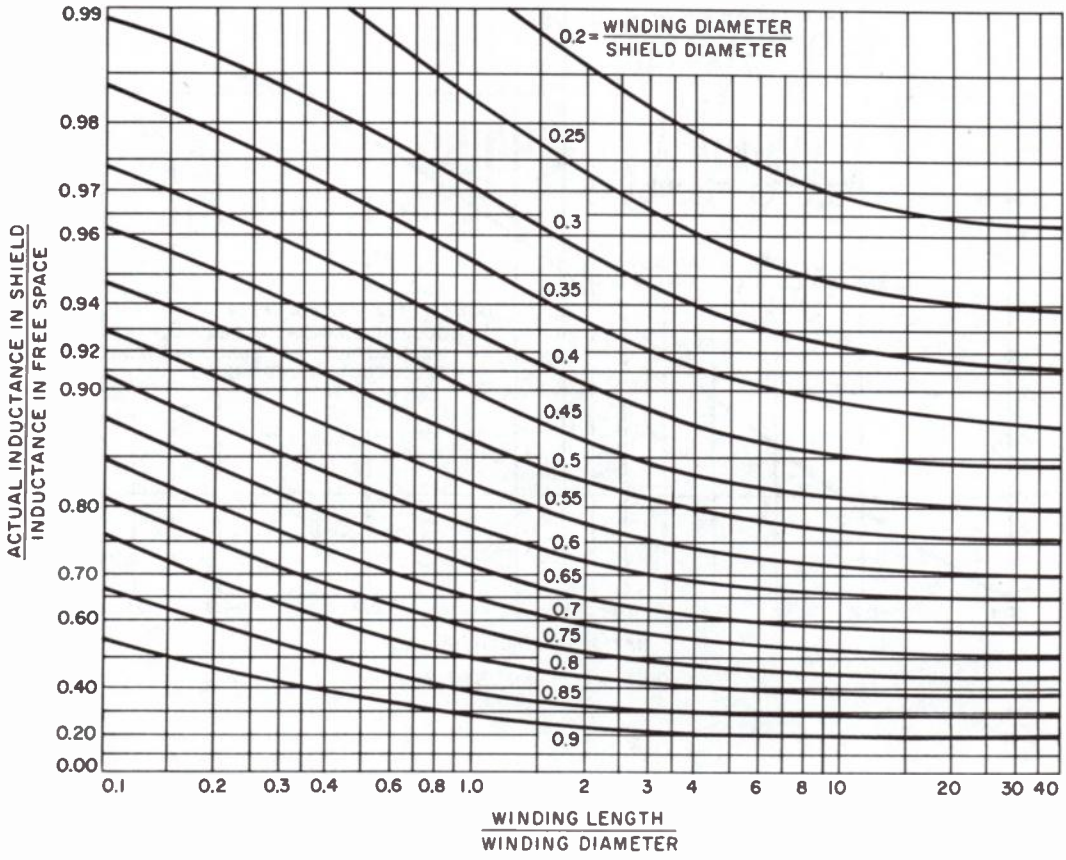

Fig. 2—Curves for determination of inductance decrease when a solenoid is shielded. *By permission of RCA, copyright proprietor.*

given to an accuracy of about 1 percent by

$$L = n^2[r^2/(9r+10l)] \text{ microhenries}$$

where $r = d/2$.

General Remarks

In the use of various charts, tables, and calculators for designing inductors, the following relationships are useful in extending the range of the devices. They apply to coils of any type or design.

(A) If all dimensions are held constant, inductance is proportional to n^2.

(B) If the proportions of the coil remain unchanged, then for a given number of turns the inductance is proportional to the dimensions of the coil. A coil with all dimensions m times those of a given coil (having the same number of turns) has m times the inductance of the given coil. That is, inductance has the dimensions of length.

Decrease of Solenoid Inductance by Shielding*

When a solenoid is enclosed in a cylindrical shield, the inductance is reduced by a factor given in Fig. 2. This effect has been evaluated by considering the shield to be a short-circuited single-turn secondary. The curves in Fig. 2 are reasonably accurate provided the clearance between each end of the coil winding and the corresponding end of the shield is at least equal to the radius of the coil. For square shield cans, take the equivalent shield diameter (for Fig. 2) as being 1.2 times the width of one side of the square.

Example: Let the coil winding length be 1.5 inches and its diameter 0.75 inch, while the shield diameter is 1.25 inches. What is the reduction of inductance due to the shield? The proportions are

$$(\text{winding length})/(\text{winding diameter}) = 2.0$$

$$(\text{winding diameter})/(\text{shield diameter}) = 0.6.$$

* RCA Application Note No. 48; 12 June 1935.

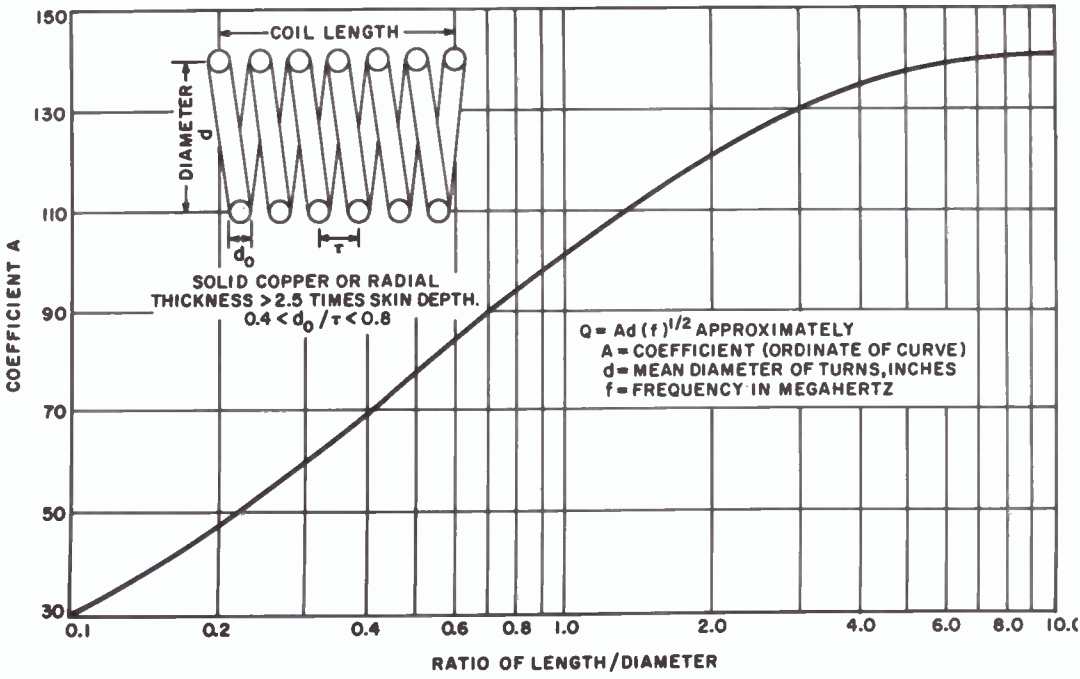

Fig. 3— Q of unshielded coil.

Referring to Fig. 2, the actual inductance in the shield is 72 percent of the inductance of the coil in free space.

Q of Unshielded Solenoid

Figure 3 can be used to obtain the unloaded Q of an unshielded solenoid.

REACTANCE CHARTS

Figures 4, 5, and 6 give the relationships of capacitance, inductance, reactance, and frequency. Any one value may be determined in terms of two others by use of a straightedge laid across the correct chart for the frequency under consideration.

Example: Given a capacitance of 0.001 microfarad, find the reactance at 50 kilohertz and inductance required to resonate. Place a straightedge through these values and read the intersections on the other scales, giving approximately 3200 ohms and 11 millihenries. See Fig. 5.

SKIN EFFECT

Symbols

A = correction coefficient
D = diameter of conductor in inches
f = frequency in hertz
R_{ac} = resistance at frequency f
R_{dc} = direct-current resistance
R_{sq} = resistance per square
T = thickness of tubular conductor in inches
T_1 = depth of penetration of current
δ = skin depth
λ = free-space wavelength in meters
μ_r = relative permeability of conductor materia ($\mu_r = 1$ for copper and other nonmagneti materials)
ρ = resistivity of conductor material at an temperature
ρ_c = resistivity of copper at 20°C = 1.72 microhms-centimeter.

Skin Depth

The skin depth is that distance below the surfac of a conductor where the current density ha diminished to $1/e$ of its value at the surface. Th thickness of the conductor is assumed to be severa (perhaps at least three) times the skin depth Imagine the conductor replaced by a cylindrica shell of the same surface shape but of thickness equal to the skin depth, with uniform current density equal to that which exists at the surface o the actual conductor. Then the total current in

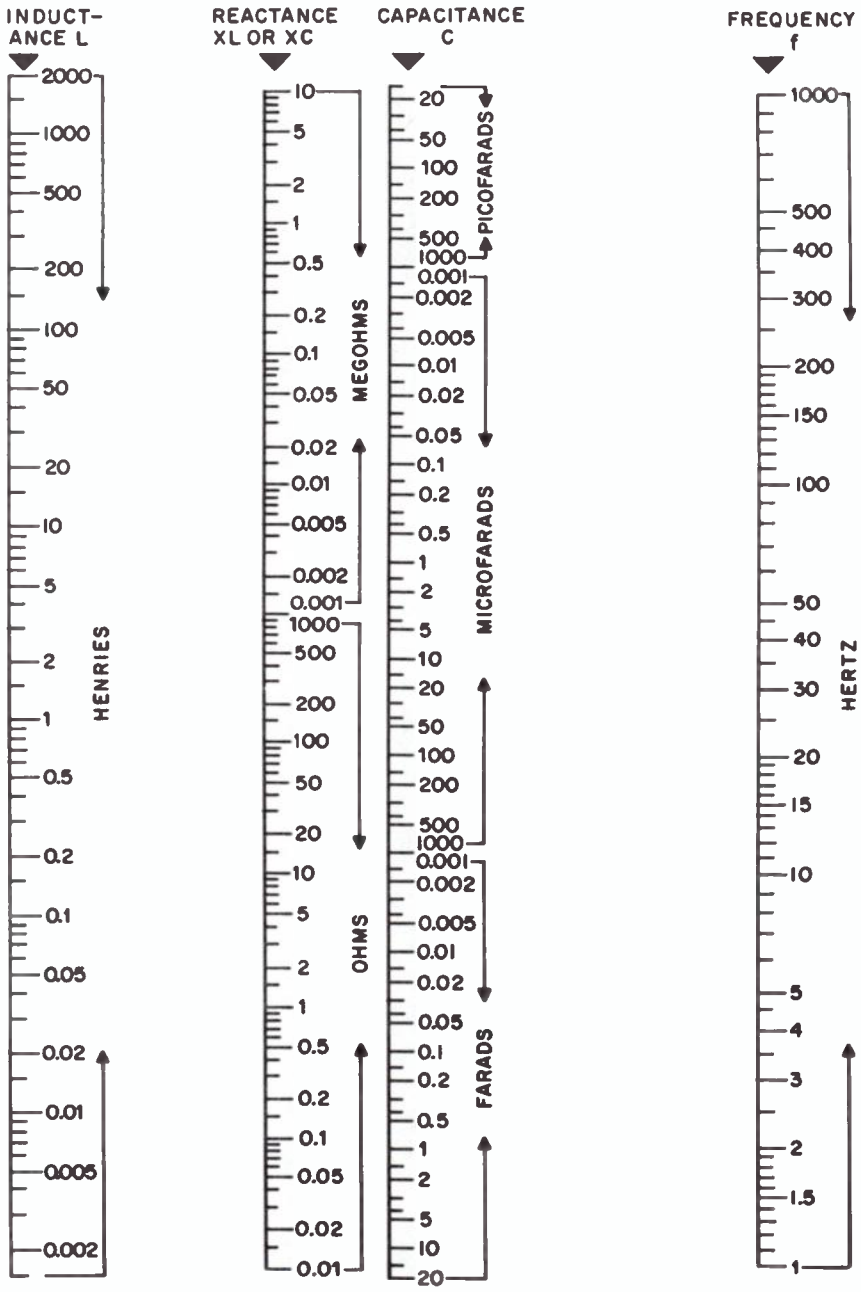

Fig. 4—Chart covering 1 hertz to 1000 hertz.

the shell and its resistance are equal to the corresponding values in the actual conductor.

The skin depth and the resistance per square (of any size), in meter-kilogram-second (rationalized) units, are

$$\delta = (\lambda/\pi\sigma\mu c)^{1/2} \text{ meter}$$

$$R_{sq} = 1/\delta\sigma \text{ ohm}$$

where

c = velocity of light *in vacuo*

$= 2.998 \times 10^8$ meter/second

$\mu = 4\pi \times 10^{-7}\ \mu_r$ henry/meter

$1/\sigma = 1.724 \times 10^{-8}\ \rho/\rho_c$ ohm-meter.

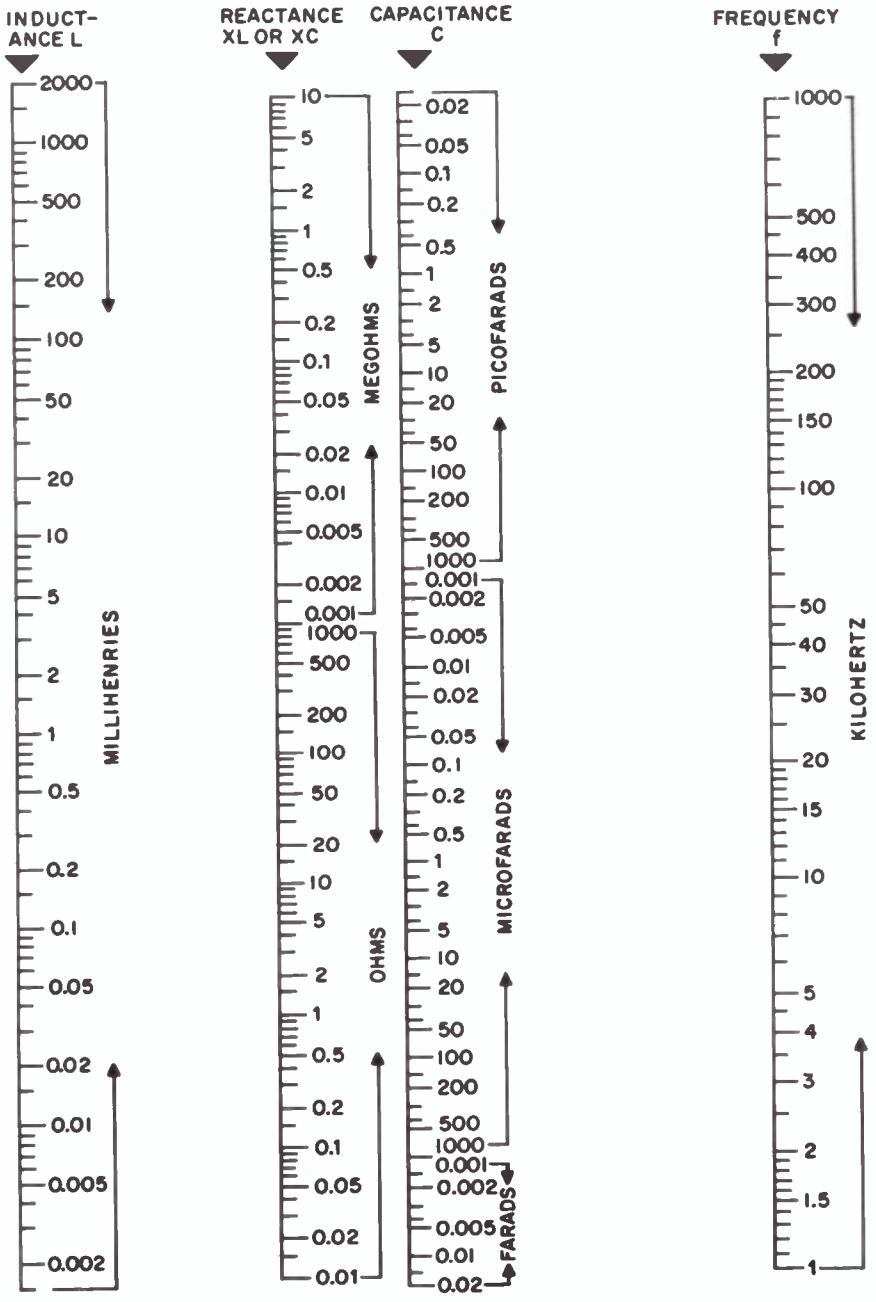

Fig. 5—Chart covering 1 kiloherts to 1000 kiloherts.

For numerical computations

$$\delta = (3.82\times10^{-4}\lambda^{1/2})k_1$$
$$= (6.61/f^{1/2})k_1 \text{ centimeter}$$
$$\delta = (1.50\times10^{-4}\lambda^{1/2})k_1$$
$$= (2.60/f^{1/2})k_1 \text{ inch}$$
$$\delta_m = (2.60/f_{mc}^{1/2})k_1 \text{ mil}$$

$$R_{sq} = (4.52\times10^{-3}/\lambda^{1/2})k_2$$
$$= (2.61\times10^{-7}f^{1/2})k_2 \text{ ohm}$$

where

$$k_1 = [(1/\mu_r)\rho/\rho_c]^{1/2}$$
$$k_2 = (\mu_r\rho/\rho_c)^{1/2}$$

k_1, k_2 = unity for copper.

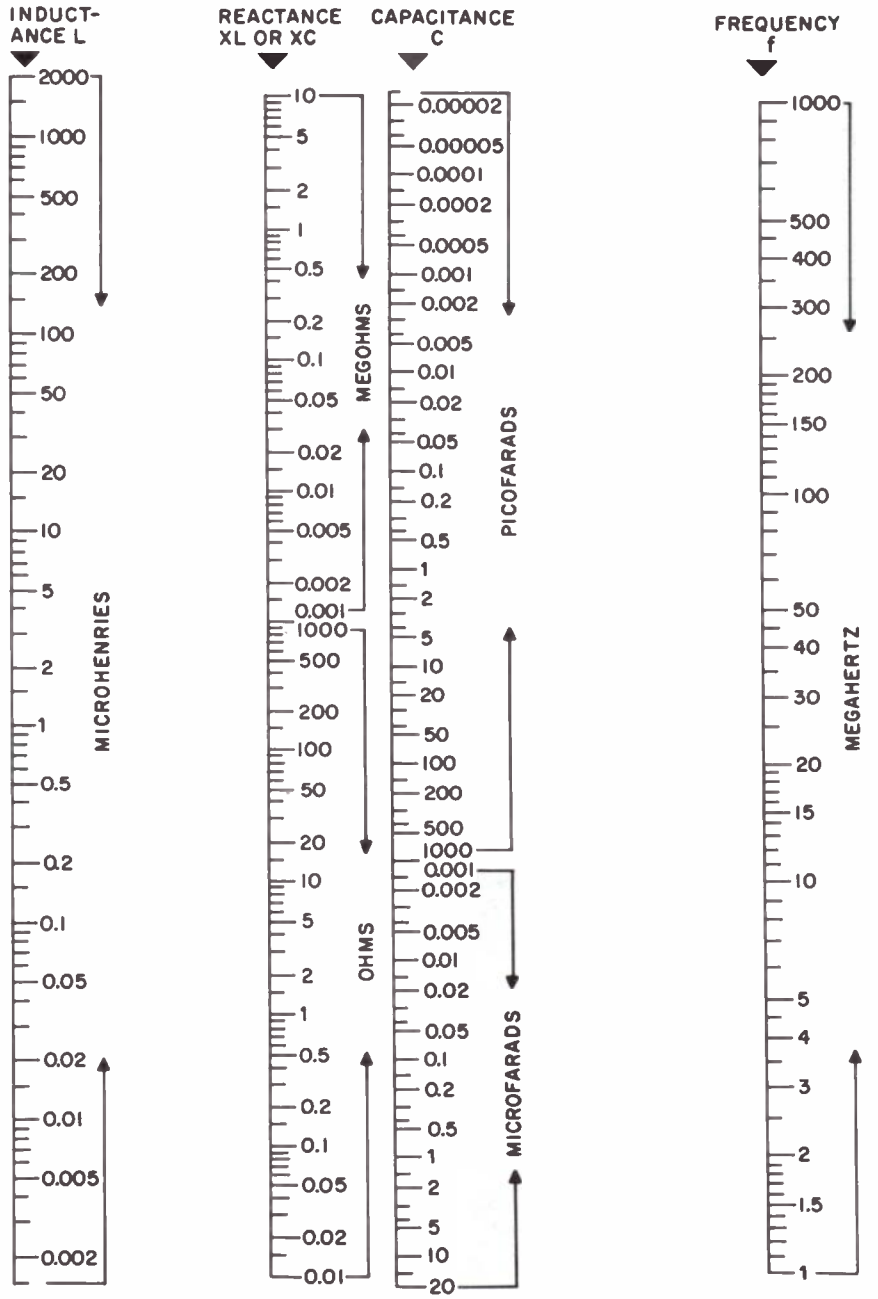

Fig. 6—Chart covering 1 megahertz to 1000 megahertz.

Example: What is the resistance/foot of a cylindrical copper conductor of diameter D inches?

$$R = (12/\pi D)\, R_{sq}$$
$$= (12/\pi D) \times 2.61 \times 10^{-7} (f^{1/2})$$
$$= 0.996 \times 10^{-6} (f^{1/2})/D \text{ ohm/foot.}$$

If $D = 1.00$ inch and $f = 100 \times 10^6$ hertz, then $R = 0.996 \times 10^{-6} \times 10^4 \approx 1 \times 10^{-2}$ ohm/foot.

General Considerations

Figure 7 shows the relationship of R_{ac}/R_{dc} versus $D(f^{1/2})$ for copper, or versus $D(f^{1/2})(\mu_r \rho_c/\rho)^{1/2}$ for any conductor material, for an isolated straight solid conductor of circular cross section. Negligible error in the equations for R_{ac} results when the conductor is spaced at least $10D$ from adjacent conductors. When the spacing between axes of

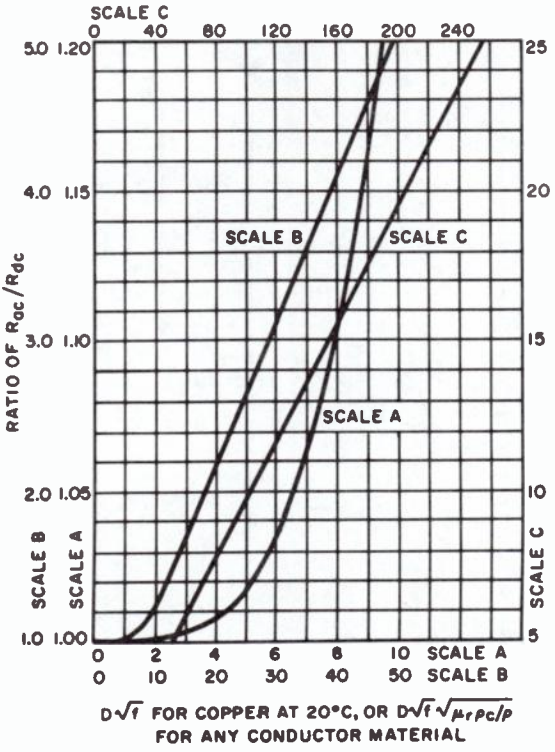

Fig. 7—Resistance ratio for isolated straight solid conductors of circular cross section.

parallel conductors carrying the same current is $4D$, the resistance R_{ac} is increased about 3 percent, when the depth of penetration is small. The equations are accurate for concentric lines due to their circular symmetry.

For values of $D(f^{1/2})(\mu_r\rho_c/\rho)^{1/2}$ greater than 40

$$R_{ac}/R_{dc}=0.0960D(f^{1/2})(\mu_r\rho_c/\rho)^{1/2}+0.26. \quad (1)$$

The high-frequency resistance of an isolated straight conductor (either solid or tubular for $T<D/8$ or $T_1<D/8$) is given in Eq. (2). If the current flow is along the inside surface of a tubular conductor, D is the inside diameter.

$$R_{ac}=A[(f^{1/2})/D][\mu_r(\rho/\rho_c)]^{1/2}\times 10^{-6} \text{ ohm/foot}. \quad (2)$$

The values of the correction coefficient A for solid conductors and for tubular conductors are given in Table 2.

The value of $T(f^{1/2})(\mu_r\rho_c/\rho)^{1/2}$ that just makes $A=1$ indicates the penetration of the currents below the surface of the conductor. Thus, approximately

$$T_1=[3.5/(f^{1/2})](\rho/\mu_r\rho_c)^{1/2} \text{ inch}. \quad (3)$$

When $T_1<D/8$ the value of R_{ac} as given by Eq. (2) (but not the value of R_{ac}/R_{dc} in Table 2, "Tubular Conductors") is correct for any value $T\geq T_1$.

Under the limitation that the radius of curvature of all parts of the cross section is appreciably greater than T_1, Eqs. (2) and (3) hold for isolated straight conductors of any shape. In this case the term $D=$ (perimeter of cross section)$/\pi$.

Examples:

(A) At 100 megahertz, a copper conductor has a depth of penetration $T_1=0.00035$ inch.

(B) A steel shield with 0.005-inch copper plate, which is practically equivalent in R_{ac} to an isolated copper conductor 0.005-inch thick, has a value of $A=1.23$ at 200 kilohertz. This 23-percent increase in resistance over that of a thick copper sheet is satisfactorily low as regards its effect on the losses of the components within the shield. By comparison, a thick aluminum sheet has a resistance $(\rho/\rho_c)^{1/2}=1.28$ times that of copper.

TABLE 2—SKIN-EFFECT CORRECTION COEFFICIENT A FOR SOLID AND TUBULAR CONDUCTORS.

Solid Conductors

$D(f^{1/2})[\mu_r(\rho_c/\rho)]^{1/2}$	A
>370	1.000
220	1.005
160	1.010
98	1.02
48	1.05
26	1.10
13	1.20
9.6	1.30
5.3	2.00
<3.0	$R_{ac}\approx R_{dc}$

$R_{dc}=(10.37/D^2)(\rho/\rho_c)\times 10^{-6}$ ohm/foot

Tubular Conductors

$T(f^{1/2})[\mu_r(\rho_c/\rho)]^{1/2}$	A	R_{ac}/R_{dc}
$=B$ where $B>3.5$	1.00	$0.384B$
3.5	1.00	1.35
3.15	1.01	1.23
2.85	1.05	1.15
2.60	1.10	1.10
2.29	1.20	1.06
2.08	1.30	1.04
1.77	1.50	1.02
1.31	2.00	1.00
$=B$ where $B<1.3$	$2.60/B$	1.00

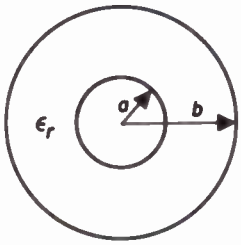

Fig. 8—Coaxial cylindrical capacitor.

EQUATIONS FOR SIMPLE *R*, *L*, AND *C* NETWORKS*

Self-Inductance of Circular Ring of Round Wire at Radio Frequencies, for Nonmagnetic Materials

$$L=(a/100)\times[7.353\log_{10}(16a/d)-6.386]\text{ microhenrys}$$

where a = mean radius of ring in inches, d = diameter of wire in inches, and $a/d>2.5$.

Capacitance

For Parallel-Plate Capacitor:

$$C=0.0885\epsilon_r[(N-1)A]/t$$
$$=0.225\epsilon_r[(N-1)A''/t'']\text{ picofarads}$$

where

A = area of one side of one plate in square centimeters
A'' = area in square inches
N = number of plates
t = thickness of dielectric in centimeters
t'' = thickness in inches
ϵ_r = dielectric constant relative to air.

This equation neglects "fringing" at the edges of the plates.

For Coaxial Cylindrical Capacitor (Fig. 8): Per unit axial length

$$C=2\pi\epsilon_r\epsilon_v/[\log_e(b/a)]$$
$$=\{(5\times10^6\epsilon_r)/[c^2\log_e(b/a)]\}\text{ farads/meter}$$

where

c = velocity of light in vacuo, meters per second $=2.998\times10^8$
ϵ_r = dielectric constant relative to air
ϵ_v = permittivity of free space in farads/meter $=8.85\times10^{-12}$
$C=0.2416\epsilon_r/[\log_{10}(b/a)]$ picofarads/centimeter
$=0.614\epsilon_r/[\log_{10}(b/a)]$ picofarads/inch
$=7.36\epsilon_r/[\log_{10}(b/a)]$ picofarads/foot.

When $1.0<(b/a)<1.4$, then with accuracy of 1 percent or better

$$C=8.50\epsilon_r\frac{(b/a)+1}{(b/a)-1}\text{ picofarads/foot.}$$

T–π or Y–Δ Transformation

The two networks (Fig. 9) are equivalent, as far as conditions at the terminals are concerned, provided the listed equations are satisfied (either the impedance equations or the admittance equations may be used)

$$Y_1=1/Z_1\quad Y_c=1/Z_c,\quad\text{etc.}$$

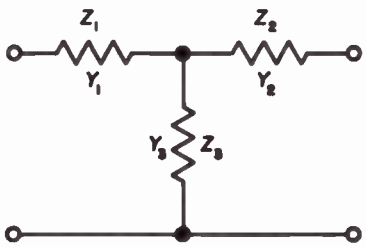

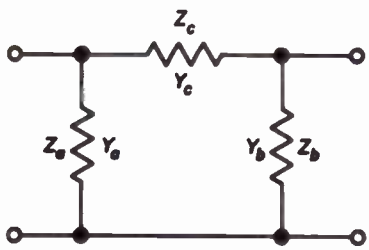

Impedance Equations:

$$Z_c=(Z_1Z_2+Z_1Z_3+Z_2Z_3)/Z_3$$
$$Z_a=(Z_1Z_2+Z_1Z_3+Z_2Z_3)/Z_2$$
$$Z_b=(Z_1Z_2+Z_1Z_3+Z_2Z_3)/Z_1$$

$$Z_1=Z_aZ_c/(Z_a+Z_b+Z_c)$$
$$Z_2=Z_bZ_c/(Z_a+Z_b+Z_c)$$
$$Z_3=Z_aZ_b/(Z_a+Z_b+Z_c)$$

Admittance Equations:

$$Y_c=Y_1Y_2/(Y_1+Y_2+Y_3)$$
$$Y_a=Y_1Y_3/(Y_1+Y_2+Y_3)$$
$$Y_b=Y_2Y_3/(Y_1+Y_2+Y_3)$$

$$Y_1=(Y_aY_b+Y_aY_c+Y_bY_c)/Y_b$$
$$Y_2=(Y_aY_b+Y_aY_c+Y_bY_c)/Y_a$$
$$Y_3=(Y_aY_b+Y_aY_c+Y_bY_c)/Y_c$$

Fig. 9—*T* or *Y* network (left) and π or Δ network.

* Many equations for computing capacitance, inductance, and mutual inductance will be found in Bureau of Standards Circular No. C74, obtainable from the Superintendent of Documents, Government Printing Office, Washington, D.C. 20402.

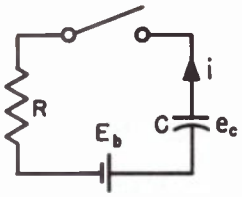

Fig. 10.

TRANSIENTS—ELEMENTARY CASES

The complete transient in a linear network is, by the principle of superposition, the sum of the individual transients due to the store of energy in each inductor and capacitor and to each external source of energy connected to the network. To this is added the steady-state condition due to each external source of energy. The transient may be computed as starting from any arbitrary time $t=0$ when the initial conditions of the energy of the network are known.

Time Constant (Designated T)

The time constant of the discharge of a capacitor through a resistor is the time t_2-t_1 required for the voltage or current to decay to $1/\epsilon$ of its value at time t_1. For the charge of a capacitor the same definition applies, the voltage "decaying" toward its steady-state value. The time constant of discharge or charge of the current in an inductor through a resistor follows an analogous definition.

Energy stored in a capacitor$=\frac{1}{2}CE^2$ joules (watt-seconds)

Energy stored in an inductor$=\frac{1}{2}LI^2$ joules (watt-seconds)

$\epsilon=2.718 \quad 1/\epsilon=0.3679 \quad \log_{10}\epsilon=0.4343$

T and t in seconds, R in ohms, L in henries, C in farads, E in volts, and I in amperes.

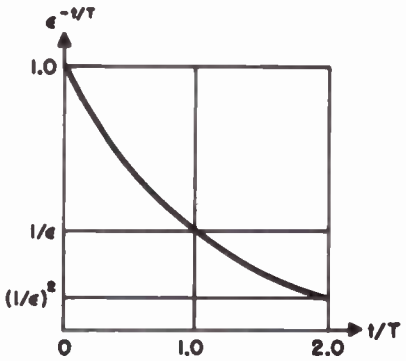

Fig. 11—Capacitor discharge.

Capacitor Charge and Discharge

Closing of switch (Fig. 10) occurs at time $t=0$.
Initial conditions (at $t=0$): Battery$=E_b$; $e_c=E_0$.
Steady state (at $t=\infty$): $i=0$; $e_c=E_b$.

Transient:

$$i=[(E_b-E_0)/R]\exp(-t/RC)$$

$$=I_0\exp(-t/RC)$$

$$\log_{10}(i/I_0)=-(0.4343/RC)t$$

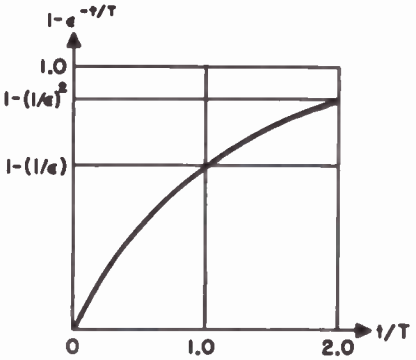

Fig. 12—Capacitor charge.

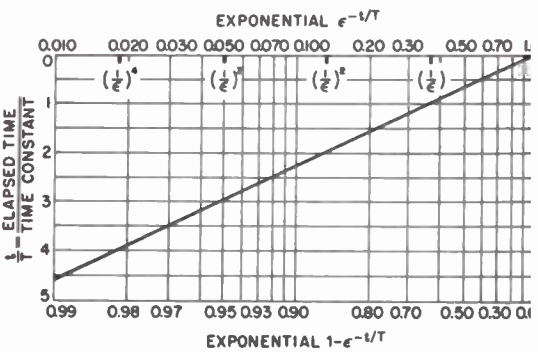

Fig. 13—Exponential functions $\exp(-t/T)$ and $1-\exp(-t/T)$ applied to transients in R–C and L–R circuits. Use exponential $\exp(-t/T)$ for charge or discharge of capacitor or discharge of inductor:

(current at time t)/(initial current).

Discharge of capacitor:

(voltage at time t)/(initial voltage).

Use exponential $1-\exp(-t/T)$ for charge of capacitor:

(voltage at time t)/(battery or final voltage).

Charge of inductor:

(current at time t)/(final current).

$$e_c = E_0 + C^{-1}\int_0^t i\,dt$$

$$= E_0 \exp(-t/RC) + E_b[1-\exp(-t/RC)].$$

Time constant:

$$T = RC.$$

Figure 11 shows current:

$$i/I_0 = \exp(-t/T).$$

Figure 11 shows discharge (for $E_b=0$):

$$e_c/E_0 = \exp(-t/T).$$

Figure 12 shows charge (for $E_0=0$):

$$e_c/E_b = 1-\exp(-t/T).$$

These curves are plotted for a wider range in Fig. 13.

Two Capacitors

Closing of switch (Fig. 14) occurs at time $t=0$. Initial conditions (at $t=0$):

$$e_1 = E_1; \quad e_2 = E_2.$$

Steady state (at $t=\infty$):

$$e_1 = E_f; \quad e_2 = -E_f; \quad i = 0$$

$$E_f = (E_1C_1 - E_2C_2)/(C_1+C_2)$$

$$C' = C_1C_2/(C_1+C_2).$$

Transient:

$$i = [(E_1+E_2)/R] \exp(-t/RC')$$

$$e_1 = E_f + (E_1-E_f)\exp(-t/RC')$$

$$= E_1 - (E_1+E_2)(C'/C_1)[1-\exp(-t/RC')]$$

$$e_2 = -E_f + (E_2+E_f)\exp(-t/RC')$$

$$= E_2 - (E_1+E_2)(C'/C_2)[1-\exp(-t/RC')].$$

Original energy $= \frac{1}{2}(C_1E_1^2 + C_2E_2^2)$ joule

Final energy $= \frac{1}{2}(C_1+C_2)E_f^2$ joule

$$\text{Loss of energy} = \int_0^\infty i^2R\,dt$$

$$= \tfrac{1}{2}C'(E_1+E_2)^2 \text{ joule.}$$

(Loss is independent of the value of R.)

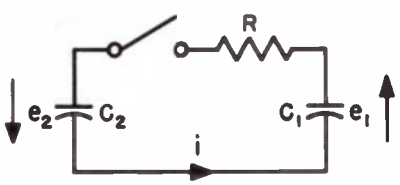

Fig. 14.

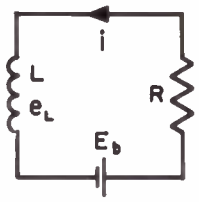

Fig. 15.

Inductor Charge and Discharge (Fig. 15)

Initial conditions (at $t=0$):

$$\text{Battery} = E_b; \quad i = I_0.$$

Steady state (at $t=\infty$):

$$i = I_f = E_b/R.$$

Transient, plus steady state:

$$i = I_f[1-\exp(-Rt/L)] + I_0\exp(-Rt/L)$$

$$e_L = -L\,di/dt$$

$$= -(E_b - RI_0)\exp(-Rt/L).$$

Time constant:

$$T = L/R.$$

Figure 11 shows discharge (for $E_b=0$):

$$i/I_0 = \exp(-t/T).$$

Figure 12 shows charge (for $I_0=0$):

$$i/I_f = [1-\exp(-t/T)].$$

These curves are plotted for a wider range in Fig. 13.

Series R-L-C Circuit Charge and Discharge (Fig. 16)

Initial conditions (at $t=0$):

$$\text{Battery} = E_b; \quad e_c = E_0; \quad i = I_0.$$

Steady state (at $t=\infty$):

$$i = 0; \quad e_c = E_b.$$

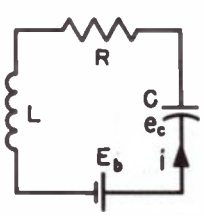

Fig. 16.

Differential equation:

$$E_b - E_0 - C^{-1}\int_0^t i\,dt - Ri - L(di/dt) = 0$$

when

$$L(d^2i/dt^2) + R(di/dt) + (i/C) = 0.$$

Solution of equation:

$$i = \exp(-Rt/2L)\left[\frac{2(E_b-E_0)-RI_0}{R(D^{1/2})}\sinh(Rt/2L) \times (D^{1/2}) + I_0\cosh(Rt/2L)\,(D^{1/2})\right]$$

where $D = 1-(4L/R^2C)$.

Case 1: When L/R^2C is small

$$i = (1-2A-2A^2)^{-1}\left\{\left[\frac{E_b-E_0}{R} - I_0(A+A^2)\right] \times \exp\left(-\frac{t}{RC}(1+A+2A^2)\right) + \left[I_0(1-A-A^2) - \frac{E_b-E_0}{R}\right] \times \exp\left(-\frac{Rt}{L}(1-A-A^2)\right)\right\}$$

where $A = L/R^2C$.

For practical purposes, the terms A^2 can be neglected when $A<0.1$. The terms A may be neglected when $A<0.01$.

Case 2: When $4L/R^2C<1$ for which $D^{1/2}$ is real

$$i = \frac{\exp(-Rt/2L)}{D^{1/2}}\left\{\left[\frac{E_b-E_0}{R} - \tfrac{1}{2}I_0\ (1-D^{1/2})\right] \times \exp\left(\frac{Rt}{2L}D^{1/2}\right) + \left[\tfrac{1}{2}I_0(1+D^{1/2}) - \frac{E_b-E_0}{R}\right]\exp\left(-\frac{Rt}{2L}D^{1/2}\right)\right\}.$$

Case 3: When D is a small positive or negative quantity

$$i = \exp(-Rt/2L)\left\{\frac{2(E_b-E_0)}{R}\left[\frac{Rt}{2L} + \frac{1}{6}\left(\frac{Rt}{2L}\right)^3 D\right] + I_0\left[1 - \frac{Rt}{2L} + \frac{1}{2}\left(\frac{Rt}{2L}\right)^2 D - \frac{1}{6}\left(\frac{Rt}{2L}\right)^3 D\right]\right\}.$$

This equation may be used for values of D up to ± 0.25, at which values the error in the computed current i is approximately 1 percent of I_0 or of $(E_b-E_0)/R$.

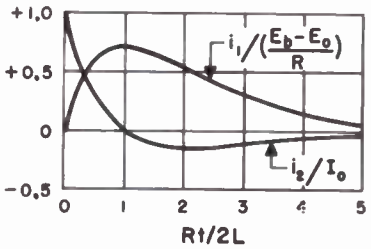

Fig. 17—Transients for $4L/R^2C=1$.

Case 3A: When $4L/R^2C=1$ for which $D=0$, the equation reduces to

$$i = \exp(-Rt/2L)\left[\frac{E_b-E_0}{R}\frac{Rt}{L} + I_0\left(1-\frac{Rt}{2L}\right)\right]$$

or $i=i_1+i_2$, plotted in Fig. 17. For practical purposes, this equation may be used when $4L/R^2C = 1\pm 0.05$ with errors of 1 percent or less.

Case 4: When $4L/R^2C>1$ for which $D^{1/2}$ is imaginary

$$i = \exp(-Rt/2L)\left[\left(\frac{E_b-E_0}{\omega_0 L} - \frac{RI_0}{2\omega_0 L}\right) \times \sin\omega_0 t + I_0\cos\omega_0 t\right] = I_m\exp(-Rt/2L)\sin(\omega_0 t+\psi)$$

where

$$\omega_0 = [(LC)^{-1} - (R^2/4L^2)]^{1/2}$$

$$I_m = (\omega_0 L)^{-1}\{[E_b - E_0 - \tfrac{1}{2}(RI_0)]^2 + \omega_0^2 L^2 I_0^2\}^{1/2}$$

$$\psi = \tan^{-1}\{\omega_0 L I_0/[E_b - E_0 - \tfrac{1}{2}(RI_0)]\}.$$

The envelope of the voltage wave across the inductor is

$$\pm\exp(-Rt/2L)[\omega_0(LC)^{1/2}]^{-1} \times \{[E_b - E_0 - \tfrac{1}{2}(RI_0)]^2 + \omega_0^2 L^2 I_0^2\}^{1/2}.$$

Example: Relay with transient-suppressing capacitor (Fig. 18). The switch is closed until time $t=0$, then opened.

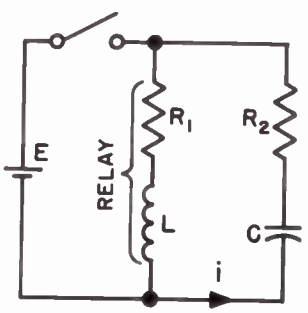

Fig. 18.

Let $L=0.10$ henry, $R_1=100$ ohms, and $E=10$ volts.

Suppose we choose $C=10^{-6}$ farad, and $R_2=100$ ohms.

Then $R=200$ ohms, $I_0=0.10$ ampere, $E_0=10$ volts, $\omega_0=3\times10^3$, and $f_0=480$ hertz.

Maximum peak voltage across L (envelope at $t=0$) is approximately 30 volts. Time constant of decay of envelope is 0.001 second.

Nonoscillating Condition: It is preferable that the circuit be just nonoscillating (Case 3A) and that it present a pure resistance at the switch terminals for any frequency.

$$R_2=R_1=R/2=100 \text{ ohms.}$$

$$4L/R^2C=1$$

$$C=10^{-5} \text{ farad}=10 \text{ microfarads.}$$

At the instant of opening the switch, the voltage across the parallel circuit is $E_0-R_2I_0=0$.

Series R-L-C Circuit with Sinusoidal Applied Voltage

By the principle of superposition, the transient and steady-state conditions are the same for the actual circuit and the equivalent circuit shown in Fig. 19, the closing of the switch occurring at time $t=0$. In the equivalent circuit, the steady state is due to the source e acting continuously from time $t=-\infty$, while the transient is due to short-circuiting the source $-e$ at time $t=0$.

Source:

$$e=E\sin(\omega t+\alpha).$$

Steady state:

$$i=(E/Z)\sin(\omega t+\alpha-\phi)$$

where

$$Z=\{R^2+[\omega L-(1/\omega C)]^2\}^{1/2}$$

$$\tan\phi=(\omega^2LC-1)/\omega CR.$$

The transient is found by determining current $i=I_0$ and capacitor voltage $e_c=E_0$ at time $t=0$, due to the source $-e$. These values of I_0 and E_0 are then substituted in the equations of Case 1, 2, 3, or 4, above, according to the values of R, L, and C.

At time $t=0$, due to the source $-e$

$$i=I_0=-(E/Z)\sin(\alpha-\phi)$$

$$e_c=E_0=(E/\omega CZ)\cos(\alpha-\phi).$$

This form of analysis may be used for any periodic applied voltage e. The steady-state current and the capacitor voltage for an applied voltage

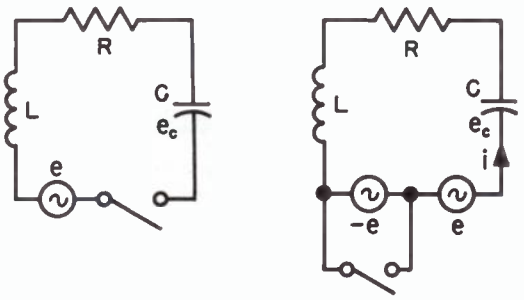

Fig. 19—Actual circuit (left) and equivalent circuit.

$-e$ are determined, the periodic voltage being resolved into its harmonic components for this purpose, if necessary. Then the instantaneous values $i=I_0$ and $e_c=E_0$ at the time of closing the switch are easily found, from which the transient is determined. It is evident, from this method of analysis, that the waveform of the transient need bear no relationship to that of the applied voltage, depending only on the constants of the circuit and the hypothetical initial conditions I_0 and E_0.

TRANSIENTS—OPERATIONAL CALCULUS AND LAPLACE TRANSFORMS

Among the various methods of operational calculus used to solve transient problems, one of the most efficient makes use of the Laplace transform.

If we have a function $v=f(t)$, then by definition the Laplace transform is $\mathcal{L}[f(t)]=F(p)$, where

$$F(p)=\int_0^\infty \exp(-pt)f(t)\,dt. \qquad (4)$$

The inverse transform of $F(p)$ is $f(t)$. Most of the mathematical functions encountered in practical work fall in the class for which Laplace transforms exist. Transforms of functions are given in Chapter 46.

In the following, an abbreviated symbol such as $\mathcal{L}[i]$ is used instead of $\mathcal{L}[i(t)]$ to indicate the Laplace transform of the function $i(t)$.

The electrical (or other) system for which a solution of the differential equation is required, is considered only in the time domain $t\geq0$. Any currents or voltages existing at $t=0$, before the driving force is applied, constitute initial conditions. Driving force is assumed to be 0 when $t<0$.

Example

Take the circuit of Fig. 20, in which the switch is closed at time $t=0$. Before the closing of the

switch, suppose the capacitor is charged; then at $t=0$, we have $v=V_0$. It is required to find the voltage v across capacitor C as a function of time.

Writing the differential equation of the circuit in terms of voltage, and since $i=dq/dt=C(dv/dt)$, the equation is

$$e(t)=v+Ri=v+RC(dv/dt) \tag{5}$$

where $e(t)=E_b$.

Referring to the table of transforms, the applied voltage is E_b multiplied by unit step, or $E_bS_{-1}(t)$; the transform for this is E_b/p. The transform of v is $\mathcal{L}[v]$. That of $RC(dv/dt)$ is $RC[p\mathcal{L}[v]-v(0)]$, where $v(0)=V_0=$ value of v at $t=0$. Then the transform of (5) is

$$E_b/p=\mathcal{L}[v]+RC[p\mathcal{L}[v]-V_0].$$

Rearranging, and resolving into partial fractions

$$\mathcal{L}[v]=\frac{E_b}{p(1+RCp)}+\frac{RCV_0}{1+RCp}$$

$$=E_b[p^{-1}-(p+1/RC)^{-1}]+\frac{V_0}{p+1/RC}. \tag{6}$$

Now we must determine the equation that would transform into (6). The inverse transform of $\mathcal{L}[v]$ is v, and those of the terms on the right-hand side are found in the table of transforms. Then, in the time domain $t\geq 0$

$$v=E_b[1-\exp(-t/RC)]+V_0\exp(-t/RC). \tag{7}$$

This solution is also well known by classical methods. However, the advantages of the Laplace transform method become more and more apparent in reducing the labor of solution as the equations become more involved.

Circuit Response Related to Unit Impulse

Unit impulse (see Laplace transforms) has the dimensions of time^{-1}. For example, suppose a capacitor of 1 microfarad is suddenly connected to a battery of 100 volts, with the circuit inductance and resistance negligibly small. Then the current is 10^{-4} coulomb multiplied by unit impulse.

The general transformed equation of a circuit or system may be written

$$\mathcal{L}[i]=\phi(p)\mathcal{L}[e]+\psi(p). \tag{8}$$

Here $\mathcal{L}[i]$ is the transform of the required current (or other quantity) and $\mathcal{L}[e]$ is the transform of the applied voltage or driving force $e(t)$. The transform of the initial conditions, at $t=0$, is included in $\psi(p)$.

First considering the case when the system is initially at rest, $\psi(p)=0$. Writing i_a for the current in this case

$$\mathcal{L}[i_a]=\phi(p)\mathcal{L}[e]. \tag{9}$$

Now apply unit impulse $S_0(t)$ (multiplied by 1 volt-second), and designate the circuit current in this case by $B(t)$ and its transform by $\mathcal{L}[B]$. The Laplace transform of $S_0(t)$ is 1, so

$$\mathcal{L}[B]=\phi(p). \tag{10}$$

Equation (9) becomes, for any driving force

$$\mathcal{L}[i_a]=\mathcal{L}[B]\mathcal{L}[e]. \tag{11}$$

Applying the convolution function (Laplace transform)

$$i_a=\int_0^t B(t-\lambda)e(\lambda)\,d\lambda$$

$$=\int_0^t B(\lambda)e(t-\lambda)\,d\lambda. \tag{12}$$

To this there must be added the current i_0 due to any initial conditions that exist. From (8)

$$\mathcal{L}[i_0]=\psi(p). \tag{13}$$

Then i_0 is the inverse transform of $\psi(p)$.

Circuit Response Related to Unit Step

Unit step is defined and designated $S_{-1}(t)=0$ for $t<0$ and equals unity for $t>0$. It has no dimensions. Its Laplace transform is $1/p$. Let the circuit current be designated $A(t)$ when the applied voltage is $e=S_{-1}(t)\times(1\text{ volt})$. Then, the current i_a for the case when the system is initially at rest, and for any applied voltage $e(t)$, is given by any of

$$i_a=A(t)e(0)+\int_0^t A(t-\lambda)e'(\lambda)\,d\lambda$$

$$=A(t)e(0)+\int_0^t A(\lambda)e'(t-\lambda)\,d\lambda$$

$$=A(0)e(t)+\int_0^t A'(t-\lambda)e(\lambda)\,d\lambda$$

$$=A(0)e(t)+\int_0^t A'(\lambda)e(t-\lambda)\,d\lambda \tag{14}$$

where A' is the first derivative of A and similarly for e' of e.

As an example, consider the problem of Fig. 20 and Eqs. (5) to (7) above. Suppose $V_0=0$, and that the battery is replaced by a linear source

$$e(t)=Et/T_1$$

where T_1 is the duration of the voltage rise in seconds. By Eq. (7), setting $E_b=1$

$$A(t)=1-\exp(-t/RC).$$

Then using the first equation in (14) and noting that $e(0)=0$, and $e'(t)=E/T_1$ when $0\leq t\leq T_1$, the solution is

$$v=(Et/T_1)-(ERC/T_1)[1-\exp(-t/RC)].$$

This result can, of course, be found readily by direct application of the Laplace transform to Eq. (5) with $e(t)=Et/T_1$.

Heaviside Expansion Theorem

When the system is initially at rest, the transformed equation is given by Eq. (9) and may be written

$$\mathcal{L}[i_a]=[M(p)/G(p)]\mathcal{L}[e]. \qquad (15)$$

$M(p)$ and $G(p)$ are rational functions of p. In the following, $M(p)$ must be of lower degree than $G(p)$, as is usually the case. The roots of $G(p)=0$ are p_r, where $r=1, 2, \cdots, n$, and there must be no repeated roots. The response may be found by application of the Heaviside expansion theorem.

For a force $e=E_{max}\exp(j\omega t)$ applied at time $t=0$

$$\frac{i_a(t)}{E_{max}}=\frac{M(j\omega)}{G(j\omega)}\exp(j\omega t)+\sum_{r=1}^{n}\frac{M(p_r)\exp(p_r t)}{(p_r-j\omega)G'(p_r)} \qquad (16A)$$

$$=\frac{\exp(j\omega t)}{Z(j\omega)}+\sum_{r=1}^{n}\frac{\exp(p_r t)}{(p_r-j\omega)Z'(p_r)}. \qquad (16B)$$

The first term on the right-hand side of either form of (16) gives the steady-state response, and the second term gives the transient. When $e=E_{max}\cos\omega t$, take the real part of (16), and similarly for $\sin\omega t$ take the imaginary part. $Z(p)$ is defined in Eq. (19). If the applied force is the unit step, set $\omega=0$ in Eq. (16).

Application to Linear Networks

The equation for a single mesh is of the form

$$A_n(d^n i/dt^n)+\cdots+A_1(di/dt)+A_0 i+B\int i\,dt=e(t). \qquad (17)$$

System Initially at Rest: Then, Eq. (17) transforms into

$$(A_n p^n+\cdots+A_1 p+A_0+Bp^{-1})\mathcal{L}[i]=\mathcal{L}[e] \qquad (18)$$

where the expression in parentheses is the operational impedance, equal to the alternating-current impedance when we set $p=j\omega$.

If there are m meshes in the system, we get m simultaneous equations like (17) with m unknowns $i_1, i_2, \cdots, i_m$. The m algebraic equations like (18) are solved for $\mathcal{L}[i_1]$, etc., by means of determinants, yielding an equation of the form of (15) for each unknown, with a term on the right-hand side for each mesh in which there is a driving force. Each such driving force may of course be treated separately and the responses added.

Designating any two meshes by the letters h and k, the driving force $e(t)$ being in either mesh and the mesh current $i(t)$ in the other, then the fraction $M(p)/G(p)$ in (15) becomes

$$M_{hk}(p)/G(p)=1/Z_{hk}(p)=Y_{hk}(p) \qquad (19)$$

where $Y_{hk}(p)$ is the operational transfer admittance between the two meshes. The determinant of the system is $G(p)$, and $M_{hk}(p)$ is the cofactor of the row and column that represent $e(t)$ and $i(t)$.

System Not Initially at Rest: The transient due to the initial conditions is solved separately and added to the above solution. The driving force is set equal to zero in (17), $e(t)=0$, and each term is transformed according to

$$\mathcal{L}[d^n i/dt^n]=p^n\mathcal{L}[i]-\sum_{r=1}^{n}p^{n-r}[d^{r-1}i/dt^{r-1}]_{t=0} \qquad (20A)$$

$$\mathcal{L}\left[\int_0^t i\,dt\right]=p^{-1}\mathcal{L}[i]+p^{-1}\left[\int i\,dt\right]_{t=0} \qquad (20B)$$

where the last term in each equation represents the initial conditions. For example, in (20B) the last term would represent, in an electrical circuit, the quantity of electricity existing on a capacitor at time $t=0$, the instant when the driving force $e(t)$ begins to act.

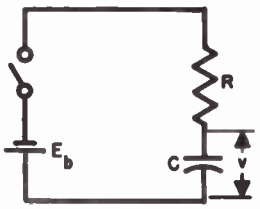

Fig. 20.

Resolution into Partial Fractions: The solution of the operational form of the equations of a system involves rational fractions that must be simplified before finding the inverse transform. Let the fraction be $h(p)/g(p)$ where $h(p)$ is of lower degree than $g(p)$, for example $(3p+2)/(p^2+5p+8)$. If $h(p)$ is of equal or higher degree than $g(p)$, it can be reduced by division.

The reduced fraction can be expanded into partial fractions. Let the factors of the denominator be $(p-p_r)$ for the n nonrepeated roots p_r of the equation $g(p)=0$, and $(p-p_a)$ for a root p_a repeated m times.

$$\frac{h(p)}{g(p)} = \sum_{r=1}^{n} \frac{A_r}{p-p_r} + \sum_{r=1}^{m} \frac{B_r}{(p-p_a)^{m-r+1}}. \quad (21A)$$

There is a summation term for each root that is repeated. The constant coefficients A_r and B_r can be evaluated by reforming the fraction with a common denominator. Then the coefficients of each power of p in $h(p)$ and the reformed numerator are equated and the resulting equations solved for the constants. More formally, they may be evaluated by

$$A_r = \frac{h(p_r)}{g'(p_r)} = \left[\frac{h(p)}{g(p)/(p-p_r)}\right]_{p=p_r} \quad (21B)$$

$$B_r = [1/(r-1)!]f^{(r-1)}(p_a) \quad (21C)$$

where

$$f(p) = (p-p_a)^m[h(p)/g(p)]$$

and $f^{(r-1)}(p_a)$ indicates that the $(r-1)$th derivative of $f(p)$ is to be found, after which we set $p=p_a$.

Fractions of the form $(A_1p+A_2)/(p^2+\omega^2)$ or, more generally

$$\frac{A_1p+A_2}{p^2+2ap+b} = \frac{A(p+a)+B\omega}{(p+a)^2+\omega^2} \quad (22A)$$

where $b>a^2$ and $\omega^2=b-a^2$ need not be reduced further. From the Laplace transforms the inverse transform of (22A) is

$$\exp(-at)\,(A\cos\omega t+B\sin\omega t) \quad (22B)$$

where

$$A = \frac{h(-a+j\omega)}{g'(-a+j\omega)} + \frac{h(-a-j\omega)}{g'(-a-j\omega)} \quad (22C)$$

$$B = j\left[\frac{h(-a+j\omega)}{g'(-a+j\omega)} - \frac{h(-a-j\omega)}{g'(-a-j\omega)}\right]. \quad (22D)$$

Similarly, the inverse transform of the fraction

$$[A(p+a)+B\alpha]/[(p+a)^2-\alpha^2]$$

is $\exp(-at)\,(A\cosh\alpha t+B\sinh\alpha t)$, where A and B are found by (22C) and (22D), except that $j\omega$ is replaced by α and the coefficient j is omitted in the expression for B.

CHAPTER 7
FILTERS, IMAGE-PARAMETER DESIGN

GENERAL

The basic filter half section and the full sections derived from it are shown in Fig. 1. The fundamental filter equations follow, with filter characteristics and design equations next. Also given is the method of building up a composite filter and the effect of the design parameter m on the image-impedance characteristic. An example of the design of a low-pass filter completes the chapter. Note that while the impedance characteristics and design equations are given for the half sections as shown, the attenuation and phase characteristics are for full sections, either T or π.

FUNDAMENTAL FILTER EQUATIONS

Image Impedances Z_T and Z_π

The element-value design equations to be given are derived by assuming that the network is terminated with impedances that change with frequency in accordance with the following image-impedance equations. Unfortunately, this assumption can be only approximately satisfied.

Z_T = mid-series image impedance

= impedance looking into 1–2 (Fig. 1A) with Z_π connected across 3–4.

Z_π = mid-shunt image impedance

= impedance looking into 3–4 (Fig. 1A) with Z_T connected across 1–2.

Equations for the above are

$$Z_T = (Z_1Z_2 + Z_1^2/4)^{1/2}$$

$$= (Z_1Z_2)^{1/2}(1 + Z_1/4Z_2)^{1/2} \text{ ohm}$$

$$Z_\pi = \frac{Z_1Z_2}{(Z_1Z_2 + Z_1^2/4)^{1/2}}$$

$$= \frac{(Z_1Z_2)^{1/2}}{(1 + Z_1/4Z_2)^{1/2}} \text{ ohm}$$

$$Z_TZ_\pi = Z_1Z_2.$$

Image Transfer Constant

The transfer constant $\theta = \alpha + j\beta$ of a network is defined as half the natural logarithm of the complex ratio of the steady-state volt-amperes entering and leaving the network when the latter is terminated in its image impedance. The real part α of the transfer constant is called the image attenuation constant, and the imaginary part β is called the image phase constant.

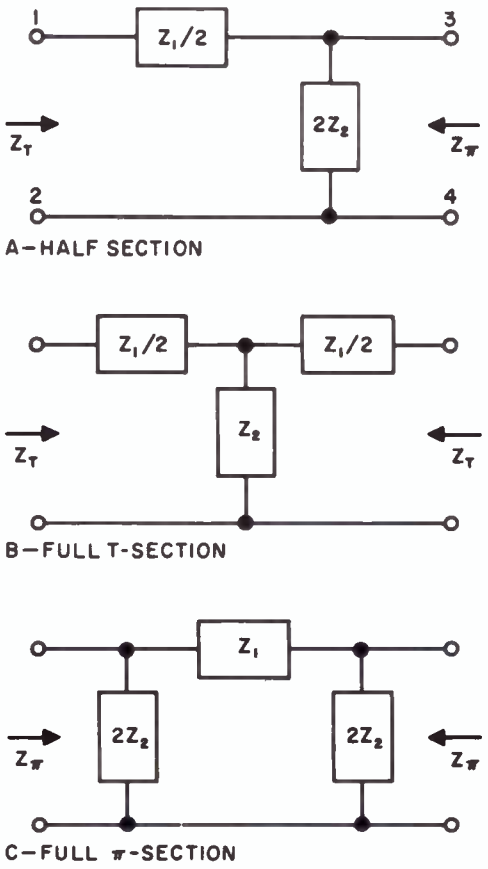

Fig. 1—Basic filter sections.

Equations in terms of full sections are

$$\cosh\theta = 1 + Z_1/2Z_2.$$

Pass Band:

$\alpha = 0$, for frequencies making $-1 \leq Z_1/4Z_2 \leq 0$

$\beta = \cos^{-1}(1 + Z_1/2Z_2)$

$= \pm 2 \sin^{-1}(-Z_1/4Z_2)^{1/2}$ radian

Image impedance = pure resistance.

Stop Band:

$$\begin{cases} \alpha = \cosh^{-1} \mid 1 + Z_1/2Z_2 \mid \\ \quad = 2 \sinh^{-1}(Z_1/4Z_2)^{1/2} \text{ neper} \quad \text{for } Z_1/4Z_2 > 0 \\ \beta = 0 \text{ radian} \end{cases}$$

$$\begin{cases} \alpha = \cosh^{-1} \mid 1 + Z_1/2Z_2 \mid \\ \quad = 2 \cosh^{-1}(-Z_1/4Z_2)^{1/2} \text{ neper} \quad \text{for } Z_1/4Z_2 < -1 \\ \beta = \pm\pi \text{ radian} \end{cases}$$

Image impedance = pure reactance.

The above equations are based on the assumption that the impedance arms are pure reactances with zero loss.

LOW-PASS FILTER DESIGN

Notations

Z in ohms, α in nepers, and β in radians

$\omega_c = 2\pi f_c$ = angular cutoff frequency

$= 1/(L_k C_k)^{1/2}$

$\omega_\infty = 2\pi f_\infty$ = angular frequency of peak attenuation

$m = (1 - \omega_c^2/\omega_\infty^2)^{1/2}$

R = nominal terminating resistance

$= (L_k/C_k)^{1/2}$

$= (Z_{Tk} Z_{\pi k})^{1/2}$

For constant-k type:

$R^2 = Z_{1k} Z_{2k} = k^2$

For m-derived type:

Curves drawn for $m \approx 0.6$

$R^2 = Z_{T2} Z_{\pi 1}$

$= Z_{1(\text{series-}m)} Z_{2(\text{shunt-}m)}$

$= Z_{1(\text{shunt-}m)} Z_{2(\text{series-}m)}$

Constant-k

Half Section

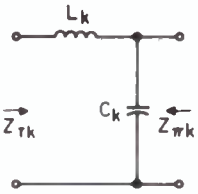

Impedance Characteristics

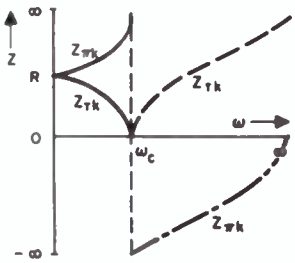

$Z_{Tk} = R(1 - \omega^2/\omega_c^2)^{1/2}$

$Z_{\pi k} = R/(1 - \omega^2/\omega_c^2)^{1/2}$

Full-Section Attenuation α and Phase β Characteristics

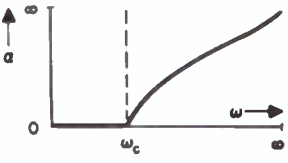

When $0 \leq \omega \leq \omega_c$

$\alpha = 0$

$\beta = 2 \sin^{-1}(\omega/\omega_c)$

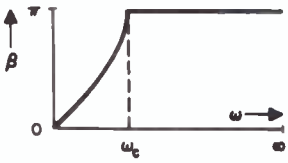

When $\omega_c < \omega < \infty$

$\beta = \pi$

$\alpha = 2 \cosh^{-1}(\omega/\omega_c)$

Design Equations, Half-Section Series Arm

$$L_k = R/\omega_c$$

Design Equations, Half-Section Shunt Arm

$$C_k = 1/\omega_c R$$

Series m-Derived

Half Section

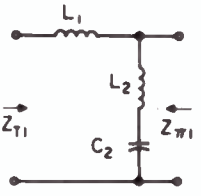

Impedance Characteristics

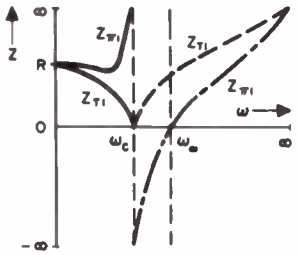

$$Z_{T1}=Z_{Tk}$$

$$Z_{\pi 1}=\frac{R(1-\omega^2/\omega_\infty{}^2)}{(1-\omega^2/\omega_c{}^2)^{1/2}}$$

$$=\frac{R[1-(\omega^2/\omega_c{}^2)(1-m^2)]}{(1-\omega^2/\omega_c{}^2)^{1/2}}$$

Full-Section Attenuation α and Phase β Characteristics

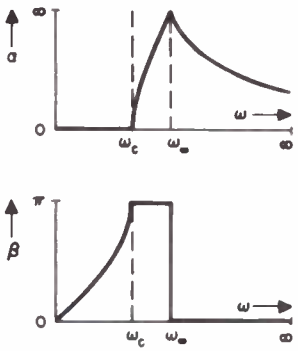

When $\omega_c<\omega<\omega_\infty$, $\beta=\pi$ and

$$\alpha=\cosh^{-1}\left[2\frac{1/\omega_\infty{}^2-1/\omega_c{}^2}{1/\omega_\infty{}^2-1/\omega^2}-1\right]$$

$$=\cosh^{-1}\left[2\frac{m^2}{\omega_c{}^2/\omega^2-(1-m^2)}-1\right]$$

When $0\leq\omega\leq\omega_c$, $\alpha=0$ and

$$\beta=\cos^{-1}\left[1-2\frac{1/\omega_\infty{}^2-1/\omega_c{}^2}{1/\omega_\infty{}^2-1/\omega^2}\right]$$

$$=\cos^{-1}\left[1-2\frac{m^2}{\omega_c{}^2/\omega^2-(1-m^2)}\right]$$

When $\omega_\infty<\omega<\infty$, $\beta=0$ and

$$\alpha=\cosh^{-1}\left[1-2\frac{1/\omega_\infty{}^2-1/\omega_c{}^2}{1/\omega_\infty{}^2-1/\omega^2}\right]$$

$$=\cosh^{-1}\left[1-2\frac{m^2}{\omega_c{}^2/\omega^2-(1-m^2)}\right]$$

Design Equations, Half-Section Series Arm

$$L_1=mL_k$$

Design Equations, Half-Section Shunt Arm

$$L_2=[(1-m^2)/m]L_k$$

$$C_2=mC_k$$

Shunt m-Derived

Half Section

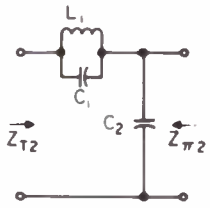

Impedance Characteristics

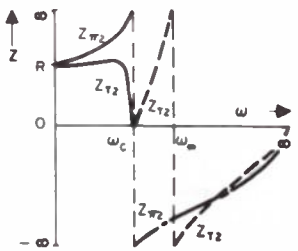

$$Z_{T2}=\frac{R(1-\omega^2/\omega_c{}^2)^{1/2}}{1-\omega^2/\omega_\infty{}^2}$$

$$=\frac{R(1-\omega^2/\omega_c{}^2)^{1/2}}{1-(\omega^2/\omega_c{}^2)(1-m^2)}$$

$$=R^2/Z_{\pi 1}$$

$$Z_{\pi 2}=Z_{\pi k}$$

Full-Section Attenuation α and Phase β Characteristics

Same as for series *m*-derived.

Design Equations, Half-Section Series Arm

$$L_1=mL_k$$

$$C_1=[(1-m^2)/m]C_k$$

Design Equations, Half-Section Shunt Arm

$$C_2=mC_k$$

HIGH-PASS FILTER DESIGN

Notations

Z in ohms, α in nepers, and β in radians

$\omega_c = 2\pi f_c$ = angular cutoff frequency

$= 1/(L_k C_k)^{1/2}$

$\omega_\infty = 2\pi f_\infty$ = angular frequency of peak attenuation

$m = (1-\omega_\infty^2/\omega_c^2)^{1/2}$

R = nominal terminating resistance

$= (L_k/C_k)^{1/2}$

$= (Z_{Tk}Z_{\pi k})^{1/2}$

For constant-k type:

$R^2 = Z_{1k}Z_{2k} = k^2$

For m-derived type:

Curves drawn for $m \approx 0.6$

$R^2 = Z_{T2}Z_{\pi 1}$

$= Z_{1(\text{series}-m)}Z_{2(\text{shunt}-m)}$

$= Z_{1(\text{shunt}-m)}Z_{2(\text{series}-m)}$

Constant-k

Half Section

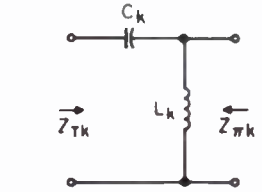

Impedance Characteristics

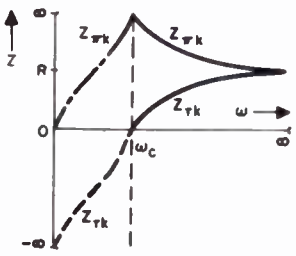

$Z_{Tk} = R[1-(\omega_c^2/\omega^2)]^{1/2}$

$Z_{\pi k} = R/[1-(\omega_c^2/\omega^2)]^{1/2}$

Full-Section Attenuation α and Phase β Characteristics

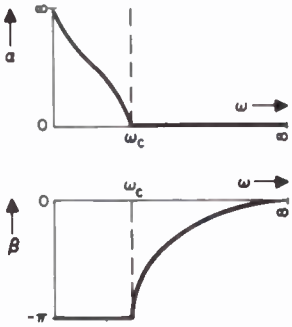

When $0 < \omega < \omega_c$

$\alpha = 2\cosh^{-1}(\omega_c/\omega)$

$\beta = -\pi$

When $\omega_c < \omega < \infty$

$\alpha = 0$

$\beta = -2\sin^{-1}(\omega_c/\omega)$

Design Equations, Half-Section Series Arm

$C_k = 1/\omega_c R$

Design Equations, Half-Section Shunt Arm

$L_k = R/\omega_c$

Series m-Derived

Half Section

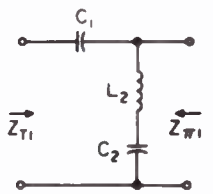

Impedance Characteristics

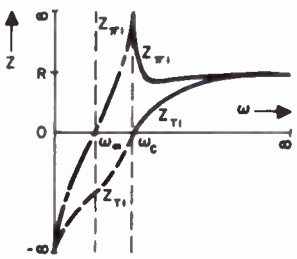

$Z_{T1} = Z_{Tk}$

$$Z_{\pi 1} = \frac{R[1-(\omega_\infty^2/\omega^2)]}{(1-\omega_c^2/\omega^2)^{1/2}}$$

$$= \frac{R[1-(\omega_c^2/\omega^2)(1-m^2)]}{(1-\omega_c^2/\omega^2)^{1/2}}$$

Full-Section Attenuation α and Phase β Characteristics

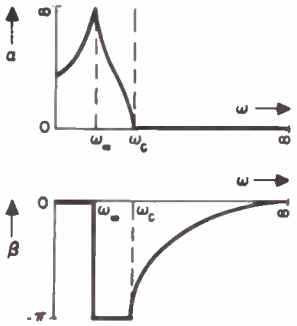

When $\omega_\infty < \omega < \omega_c$, $\beta = -\pi$ and

$$\alpha = \cosh^{-1}\left[2\frac{\omega_c^2-\omega_\infty^2}{\omega^2-\omega_\infty^2}-1\right]$$

$$= \cosh^{-1}\left[2\frac{m^2}{(\omega^2/\omega_c^2)-(1-m^2)}-1\right]$$

When $0 < \omega < \omega_\infty$, $\beta = 0$ and

$$\alpha = \cosh^{-1}\left[1-2\frac{\omega_\infty^2-\omega_c^2}{\omega_\infty^2-\omega^2}\right]$$

$$= \cosh^{-1}\left[1+2\frac{m^2}{(1-m^2)-(\omega^2/\omega_c^2)}\right]$$

When $\omega_c < \omega < \infty$, $\alpha = 0$ and

$$\beta = \cos^{-1}\left[1-2\frac{\omega_\infty^2-\omega_c^2}{\omega_\infty^2-\omega^2}\right]$$

$$= \cos^{-1}\left[1+2\frac{m^2}{(1-m^2)-(\omega^2/\omega_c^2)}\right]$$

Design Equations, Half-Section Series Arm

$$C_1 = C_k/m$$

Design Equations, Half-Section Shunt Arm

$$L_2 = L_k/m$$

$$C_2 = [m/(1-m^2)]C_k$$

Shunt m-Derived

Half Section

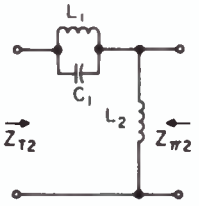

Impedance Characteristics

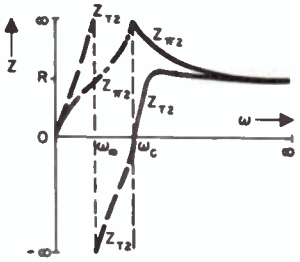

$$Z_{T2} = \frac{R(1-\omega_c^2/\omega^2)^{1/2}}{1-\omega_\infty^2/\omega^2}$$

$$= \frac{R(1-\omega_c^2/\omega^2)^{1/2}}{1-(\omega_c^2/\omega^2)(1-m^2)}$$

$$= R^2/Z_{\pi 1}$$

$$Z_{\pi 2} = Z_{\pi k}$$

Full-Section Attenuation α and Phase β Characteristics

Same as for series m-derived.

Design Equations, Half-Section Series Arm

$$L_1 = [m/(1-m^2)]L_k$$

$$C_1 = C_k/m$$

Design Equations, Half-Section Shunt Arm

$$L_2 = L_k/m$$

BAND-PASS FILTER DESIGN

Notations

The notations apply to the charts on band-pass filter design that appear on the following pages.

Z in ohms, α in nepers, and β in radians

$\omega_1 = 2\pi f_1$ = lower cutoff angular frequency

$\omega_2 = 2\pi f_2$ = upper cutoff angular frequency

$\omega_0 = (\omega_1\omega_2)^{1/2}$ = midband angular frequency

$\omega_2 - \omega_1$ = width of pass band

R = nominal terminating resistance

$\omega_{1\infty} = 2\pi f_{1\infty}$ = lower angular frequency of peak attenuation

$\omega_{2\infty} = 2\pi f_{2\infty}$ = upper angular frequency of peak attenuation

$$m_1 = \frac{(\omega_1\omega_2/\omega^2_{2\infty})\,g + h}{1-(\omega^2_{1\infty}/\omega^2_{2\infty})}$$

$$m_2 = \frac{g + h(\omega^2_{1\infty}/\omega_1\omega_2)}{1-(\omega^2_{1\infty}/\omega^2_{2\infty})}$$

$$g = \{[1-(\omega^2_{1\infty}/\omega_1^2)][1-(\omega^2_{1\infty}/\omega_2^2)]\}^{1/2}$$

$$h = \{[1-(\omega_1^2/\omega^2_{2\infty})][1-(\omega_2^2/\omega^2_{2\infty})]\}^{1/2}$$

$$L_{1k}C_{1k} = L_{2k}C_{2k} = 1/\omega_1\omega_2 = 1/\omega_0^2$$

$$R^2 = L_{1k}/C_{2k} = L_{2k}/C_{1k}$$
$$= Z_{1k}Z_{2k} = k^2$$
$$= Z_{Tk}Z_{\pi k}$$
$$= Z_{1(\text{series}-m)}Z_{2(\text{shunt}-m)}$$
$$= Z_{2(\text{series}-m)}Z_{1(\text{shunt}-m)}$$
$$= Z_{T(\text{shunt}-m)}Z_{\pi(\text{series}-m)}$$

} for any one pair of m-derived half sections.

$$Z_{T(\text{series}-m)} = Z_{Tk}$$

$$Z_{\pi(\text{shunt}-m)} = Z_{\pi k}$$

Constant-k

Half Section

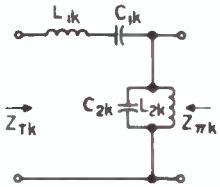

Impedance Characteristics

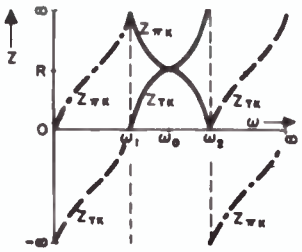

$$Z_{Tk} = \frac{R[(\omega_2^2-\omega^2)(\omega^2-\omega_1^2)]^{1/2}}{\omega(\omega_2-\omega_1)}$$

$$Z_{\pi k} = \frac{R\omega(\omega_2-\omega_1)}{[(\omega_2^2-\omega^2)(\omega^2-\omega_1^2)]^{1/2}}$$

Full-Section Attenuation α and Phase β Characteristics

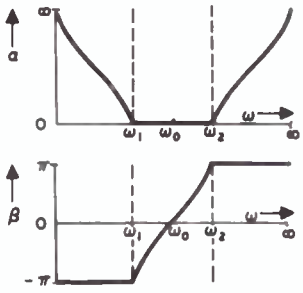

When $\omega_2 < \omega < \infty$, $\beta = \pi$ and

$$\alpha = 2\cosh^{-1}\left[\frac{\omega^2-\omega_0^2}{\omega(\omega_2-\omega_1)}\right]$$

When $0 < \omega < \omega_1$, $\beta = -\pi$ and

$$\alpha = 2\cosh^{-1}\left[\frac{\omega_0^2-\omega^2}{\omega(\omega_2-\omega_1)}\right]$$

When $\omega_1 < \omega < \omega_2$, $\alpha = 0$ and

$$\beta = 2\sin^{-1}\left[\frac{\omega^2-\omega_0^2}{\omega(\omega_2-\omega_1)}\right]$$

Frequencies of Peak α

$$\omega_{1\infty} = 0$$

$$\omega_{2\infty} = \infty$$

Design Equations, Half-Section Series Arm

$$L_{1k} = R/(\omega_2-\omega_1)$$

$$C_{1k} = (\omega_2-\omega_1)/R\omega_0^2$$

Design Equations, Half-Section Shunt Arm

$$L_{2k} = R(\omega_2-\omega_1)/\omega_0^2$$

$$C_{2k} = 1/R(\omega_2-\omega_1)$$

3-Element Series I

Half Section

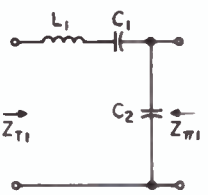

Impedance Characteristics

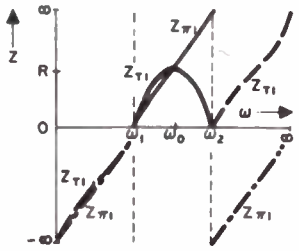

$$Z_{\pi 1}=\frac{R(\omega_2+\omega_1)}{\omega}\left[\frac{\omega^2-\omega_1^2}{\omega_2^2-\omega^2}\right]^{1/2}$$

Full-Section Attenuation α and Phase β Characteristics

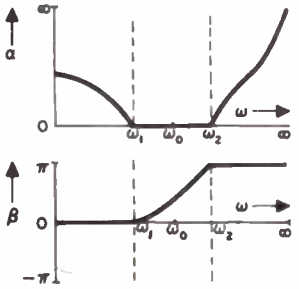

When $0<\omega<\omega_1$, $\beta=0$ and

$$\alpha=\cosh^{-1}\left[1-2\,\frac{\omega^2-\omega_1^2}{\omega_2^2-\omega_1^2}\right]$$

When $\omega_1<\omega<\omega_2$, $\alpha=0$ and

$$\beta=\cos^{-1}\left[1-2\,\frac{\omega^2-\omega_1^2}{\omega_2^2-\omega_1^2}\right]$$

When $\omega_2<\omega<\infty$, $\beta=\pi$ and

$$\alpha=\cosh^{-1}\left[2\,\frac{\omega^2-\omega_1^2}{\omega_2^2-\omega_1^2}-1\right]$$

Conditions

$$m_1=1$$

$$m_2=\omega_1/\omega_2$$

Frequencies of Peak α

$$\omega_{2\infty}=\infty$$

Design Equations, Half-Section Series Arm

$$L_1=L_{1k}$$

$$C_1=C_{1k}/m_2$$

Design Equations, Half-Section Shunt Arm

$$C_2=[(1-m_2)/(1+m_2)]C_{2k}$$

3-Element Shunt I

Half Section

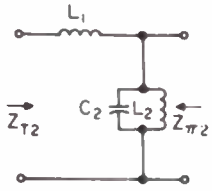

Impedance Characteristics

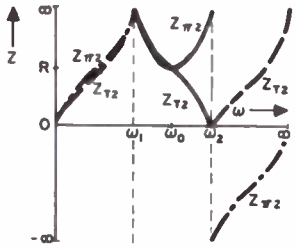

$$Z_{T2}=[R\omega/(\omega_2+\omega_1)][(\omega_2^2-\omega^2)/(\omega^2-\omega_1^2)]^{1/2}$$

$$=R^2/Z_{\pi 1}$$

$$Z_{\pi 2}=Z_{\pi k}$$

Full-Section Attenuation α and Phase β Characteristics

Same as for 3-element series I.

Conditions

Same as for 3-element series I.

Frequencies of Peak α

Same as for 3-element series I.

Design Equations, Half-Section Series Arm

$$L_1=[(1-m_2)/(1+m_2)]L_{1k}$$

Design Equations, Half-Section Shunt Arm

$$L_2=L_{2k}/m_2$$

$$C_2=C_{2k}$$

3-Element Series II

Half Section

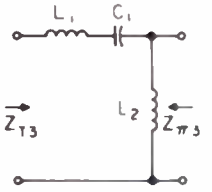

Impedance Characteristics

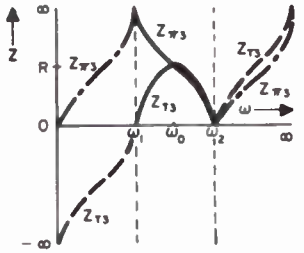

$$Z_{T3}=Z_{Tk}$$

$$Z_{\pi 3}=[R\omega(\omega_2+\omega_1)/\omega_2^2][(\omega_2^2-\omega^2)/(\omega^2-\omega_1^2)]^{1/2}$$

Full-Section Attenuation α and Phase β Characteristics

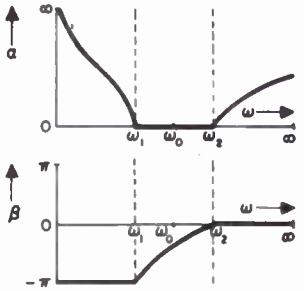

When $0<\omega<\omega_1$, $\beta=-\pi$ and

$$\alpha=\cosh^{-1}\left[2\frac{\omega_1^2(\omega_2^2-\omega^2)}{\omega^2(\omega_2^2-\omega_1^2)}-1\right]$$

When $\omega_1<\omega<\omega_2$, $\alpha=0$ and

$$\beta=\cos^{-1}\left[1-2\frac{\omega_1^2(\omega_2^2-\omega^2)}{\omega^2(\omega_2^2-\omega_1^2)}\right]$$

When $\omega_2<\omega<\infty$, $\beta=0$ and

$$\alpha=\cosh^{-1}\left[1-2\frac{\omega_1^2(\omega_2^2-\omega^2)}{\omega^2(\omega_2^2-\omega_1^2)}\right]$$

Conditions

$$m_1=\omega_1/\omega_2$$

$$m_2=1$$

Frequencies of Peak α

$$\omega_{1\infty}=0$$

Design Equations, Half-Section Series Arm

$$L_1=m_1L_{1k}$$

$$C_1=C_{1k}$$

Design Equations, Half-Section Shunt Arm

$$L_2=[(1+m_1)/(1-m_1)]L_{2k}$$

3-Element Shunt II

Half Section

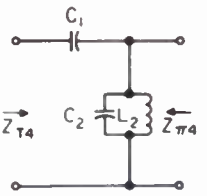

Impedance Characteristics

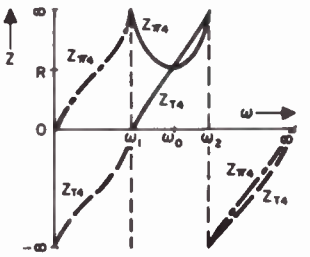

$$Z_{T4}=[R\omega_2^2/\omega(\omega_2+\omega_1)][(\omega^2-\omega_1^2)/(\omega_2^2-\omega^2)]^{1/2}$$

$$=R^2/Z_{\pi 3}$$

$$Z_{\pi 4}=Z_{\pi k}$$

Full-Section Attenuation α and Phase β Characteristics

Same as for 3-element series II.

Conditions

Same as for 3-element series II.

Frequencies of Peak α

Same as for 3-element series II.

Design Equations, Half-Section Series Arm

$$C_1=[(1+m_1)/(1-m_1)]C_{1k}$$

Design Equations, Half-Section Shunt Arm

$$L_2=L_{2k}$$

$$C_2=m_1C_{2k}$$

4-Element Series I

Half Section

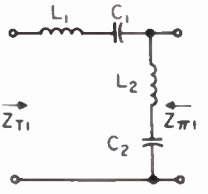

Impedance Characteristics

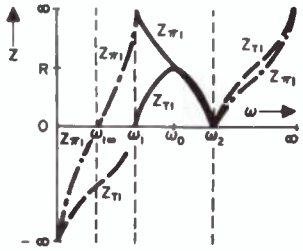

$$Z_{T1}=Z_{Tk}$$

$$Z_{\pi 1}=[R/\omega(\omega_2-\omega_1)]\left[\frac{\omega_2^2-\omega^2}{\omega^2-\omega_1^2}\right]^{1/2}$$

$$\times[(\omega^2-\omega_1^2)+m_1^2(\omega_2^2-\omega^2)]$$

Full-Section Attenuation α and Phase β Characteristics

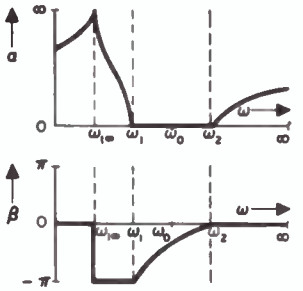

When $\omega_1<\omega<\omega_2$, $\alpha=0$ and

$$\beta=\cos^{-1}A$$

When $0<\omega<\omega_{1\infty}$, $\beta=0$ and

$$\alpha=\cosh^{-1}A$$

When $\omega_{1\infty}<\omega<\omega_1$, $\beta=-\pi$ and

$$\alpha=\cosh^{-1}(-A)$$

When $\omega_2<\omega<\infty$, $\beta=0$ and

$$\alpha=\cosh^{-1}A$$

Conditions

$$A=1-\frac{2}{1+[(\omega^2-\omega_1^2)/m_1^2(\omega_2^2-\omega^2)]}$$

$$m_2=\left[\frac{1-(\omega^2{}_{1\infty}/\omega_1^2)}{1-(\omega^2{}_{1\infty}/\omega_2^2)}\right]^{1/2}$$

$$m_1/m_2=\omega_1/\omega_2$$

Frequencies of Peak α

$$\omega_{1\infty}=\left[\frac{\omega_1^2-\omega_2^2m_1^2}{1-m_1^2}\right]^{1/2}$$

Design Equations, Half-Section Series Arm

$$L_1=m_1L_{1k}$$

$$C_1=C_{1k}/m_2$$

Design Equations, Half-Section Shunt Arm

$$L_2=[(1-m_1^2)/m_1]L_{1k}$$

$$C_2=[m_2/(1-m_2^2)]C_{1k}$$

4-Element Shunt I

Half Section

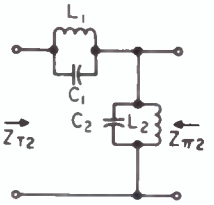

Impedance Characteristics

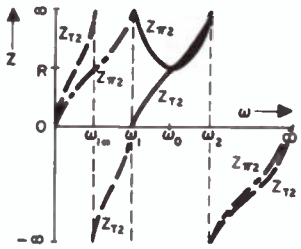

$$Z_{T2}=\frac{R\omega(\omega_2-\omega_1)}{(\omega^2-\omega_1^2)+m_1^2(\omega_2^2-\omega^2)}\left(\frac{\omega^2-\omega_1^2}{\omega_2^2-\omega^2}\right)^{1/2}$$

$$=R^2/Z_{\pi 1}$$

$$Z_{\pi 2}=Z_{\pi k}$$

Full-Section Attenuation α and Phase β Characteristics

Same as for 4-element series I.

Conditions

Same as for 4-element series I.

Frequencies of Peak α

Same as for 4-element series I.

Design Equations, Half-Section Series Arm

$$L_1=[m_2/(1-m_2^2)]L_{2k}$$

$$C_1=[(1-m_1^2)/m_1]C_{2k}$$

Design Equations, Half-Section Shunt Arm

$$L_2 = L_{2k}/m_2$$

$$C_2 = m_1 C_{2k}$$

4-Element Series II

Half Section

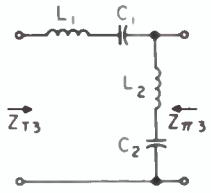

Impedance Characteristics

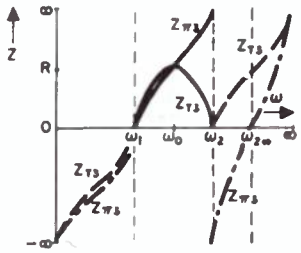

$$Z_{T3} = Z_{Tk}$$

$$Z_{\pi 3} = [R/\omega(\omega_2 - \omega_1)]\left(\frac{\omega^2 - \omega_1^2}{\omega_2^2 - \omega^2}\right)^{1/2} \times [(\omega_2^2 - \omega^2) + m_1^2(\omega^2 - \omega_1^2)]$$

Full-Section Attenuation α and Phase β Characteristics

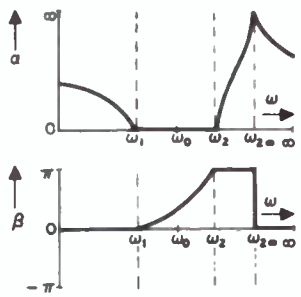

When $\omega_2 < \omega < \omega_{2\infty}$, $\beta = \pi$ and

$$\alpha = \cosh^{-1}(-B)$$

When $0 < \omega < \omega_1$, $\beta = 0$ and

$$\alpha = \cosh^{-1} B$$

When $\omega_1 < \omega < \omega_2$, $\alpha = 0$ and

$$\beta = \cos^{-1} B$$

When $\omega_{2\infty} < \omega < \infty$, $\beta = 0$ and

$$\alpha = \cosh^{-1} B$$

Conditions

$$B = 1 - \frac{2}{1 + [(\omega_2^2 - \omega^2)/m_1^2(\omega^2 - \omega_1^2)]}$$

$$m_1 = \left(\frac{1 - (\omega_2^2/\omega_{2\infty}^2)}{1 - (\omega_1^2/\omega_{2\infty}^2)}\right)^{1/2}$$

$$m_1/m_2 = \omega_2/\omega_1$$

Frequencies of Peak α

$$\omega_{2\infty} = \left(\frac{m_1^2\omega_1^2 - \omega_2^2}{m_1^2 - 1}\right)^{1/2}$$

Design Equations, Half-Section Series Arm

$$L_1 = m_1 L_{1k}$$

$$C_1 = C_{1k}/m_2$$

Design Equations, Half-Section Shunt Arm

$$L_2 = [(1 - m_1^2)/m_1]L_{1k}$$

$$C_2 = [m_2/(1 - m_2^2)]C_{1k}$$

4-Element Shunt II

Half Section

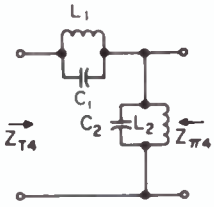

Impedance Characteristics

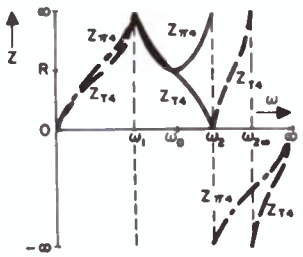

$$Z_{T4} = \frac{R\omega(\omega_2 - \omega_1)}{(\omega_2^2 - \omega^2) + m_1^2(\omega^2 - \omega_1^2)}\left(\frac{\omega_2^2 - \omega^2}{\omega^2 - \omega_1^2}\right)^{1/2} = R^2/Z_{\pi 3}$$

$$Z_{\pi 4} = Z_{\pi k}$$

Full-Section Attenuation α and Phase β Characteristics

Same as for 4-element series II.

Conditions

Same as for 4-element series II.

Frequencies of Peak α

Same as for 4-element series II.

Design Equations, Half-Section Series Arm

$$L_1=[m_2/(1-m_2^2)]L_{2k}$$

$$C_1=[(1-m_1^2)/m_1]C_{2k}$$

Design Equations, Half-Section Shunt Arm

$$L_2=L_{2k}/m_2$$

$$C_2=m_1C_{2k}$$

5-Element Series I

Half Section

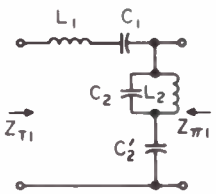

Impedance Characteristics

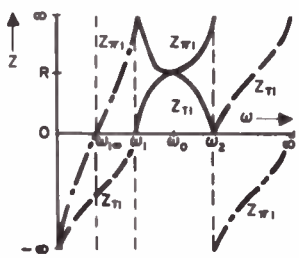

$$Z_{T1}=Z_{Tk}$$

$$Z_{\pi 1}=R\left[\frac{\omega^2(\omega_2^2+\omega_1^2-2\omega_0^2m_2)+\omega_0^4(m_2^2-1)}{\omega(\omega_2-\omega_1)[(\omega_2^2-\omega^2)(\omega^2-\omega_1^2)]^{1/2}}\right]$$

Full-Section Attenuation α and Phase β Characteristics

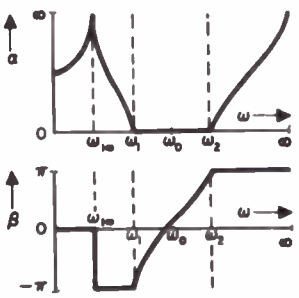

When $\omega_1<\omega<\omega_2$, $\alpha=0$ and

$$\beta=\cos^{-1}\left[1-\frac{2(\omega^2-\omega_0^2m_2)^2}{\omega^2(\omega_2^2+\omega_1^2-2\omega_0^2m_2)+\omega_0^4(m_2^2-1)}\right]$$

When $0<\omega<\omega_{1\infty}$, $\beta=0$ and

$$\alpha=\cosh^{-1}\left[1-\frac{2(\omega^2-\omega_0^2m_2)^2}{\omega^2(\omega_2^2+\omega_1^2-2\omega_0^2m_2)+\omega_0^4(m_2^2-1)}\right]$$

When $\omega_{1\infty}<\omega<\omega_1$, $\beta=-\pi$ and

$$\alpha=\cosh^{-1}\left[\frac{2(\omega^2-\omega_0^2m_2)^2}{\omega^2(\omega_2^2+\omega_1^2-2\omega_0^2m_2)+\omega_0^4(m_2^2-1)}-1\right]$$

When $\omega_2<\omega<\infty$, $\beta=\pi$ and

$\alpha=$ same equation as for $0<\omega<\omega_{1\infty}$

Conditions

$$m_1=1$$

$$m_2=(\omega^2_{1\infty}/\omega_0^2)+[(1-\omega^2_{1\infty}/\omega_1^2)(1-\omega^2_{1\infty}/\omega_2^2)]^{1/2}$$

Frequencies of Peak α

$$\omega_{1\infty}=\omega_0^2\left[\frac{1-m_2^2}{\omega_2^2+\omega_1^2-2\omega_0^2m_2}\right]^{1/2}$$

$$\omega_{2\infty}=\infty$$

Design Equations, Half-Section Series Arm

$$L_1=L_{1k}$$

$$C_1=C_{1k}/m_2$$

Design Equations, Half-Section Shunt Arm

$$L_2=\frac{L_{1k}}{m_2}\left[\frac{(\omega_2-\omega_1)^2}{\omega_0^2}-\frac{(1-m_2)^2}{m_2}\right]$$

$$C_2=C_{1k}\Big/\left[\frac{(\omega_2-\omega_1)^2}{\omega_0^2}-\frac{(1-m_2)^2}{m_2}\right]$$

$$C_2'=[m_2/(1-m_2^2)]C_{1k}$$

5-Element Shunt I

Half Section

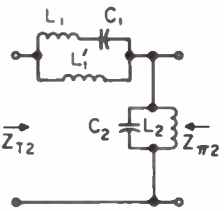

Impedance Characteristics

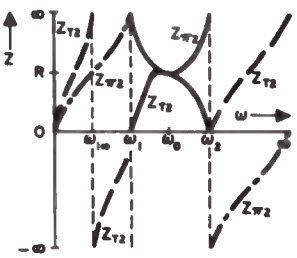

$$Z_{T2}=R^2/Z_{\pi 1}$$

$$Z_{\pi 2}=Z_{\pi k}$$

Full-Section Attenuation α and Phase β Characteristics

Same as for 5-element series I.

Conditions

Same as for 5-element series I.

Frequencies of Peak α

Same as for 5-element series I.

Design Equations, Half-Section Series Arm

$$L_1 = L_{2k} \Big/ \left[\frac{(\omega_2-\omega_1)^2}{\omega_0^2} - \frac{(1-m_2)^2}{m_2}\right]$$

$$C_1 = \frac{C_{2k}}{m_2}\left[\frac{(\omega_2-\omega_1)^2}{\omega_0^2} - \frac{(1-m_2)^2}{m_2}\right]$$

$$L_1' = [m_2/(1-m_2^2)]L_{2k}$$

Design Equations, Half-Section Shunt Arm

$$L_2 = L_{2k}/m_2$$

$$C_2 = C_{2k}$$

5-Element Series II

Half Section

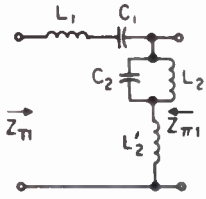

Impedance Characteristics

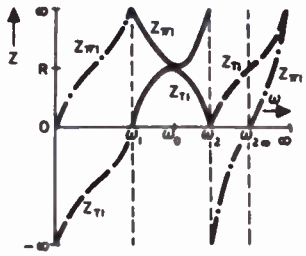

$$Z_{T1} = Z_{Tk}$$

$$Z_{\pi 1} = \frac{\omega R}{(\omega_2-\omega_1)} \frac{\omega_2^2+\omega_1^2-2\omega_0^2 m_1+\omega^2(m_1^2-1)}{[(\omega_2^2-\omega^2)(\omega^2-\omega_1^2)]^{1/2}}$$

Full-Section Attenuation α and Phase β Characteristics

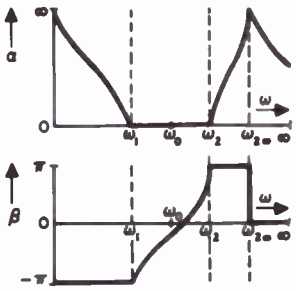

When $\omega_2 < \omega < \omega_{2\infty}$, $\beta = \pi$ and

$$\alpha = \cosh^{-1}\left[1 - \frac{2(\omega^2 m_1-\omega_0^2)^2}{\omega^2[\omega_2^2+\omega_1^2-2\omega_0^2 m_1+\omega^2(m_1^2-1)]}\right]$$

When $0 < \omega < \omega_1$, $\beta = -\pi$ and

$$\alpha = \cosh^{-1}\left[\frac{2(\omega^2 m_1-\omega_0^2)^2}{\omega^2[\omega_2^2+\omega_1^2-2\omega_0^2 m_1+\omega^2(m_1^2-1)]} - 1\right]$$

When $\omega_1 < \omega < \omega_2$, $\alpha = 0$ and

$$\beta = \cos^{-1}\left[1 - \frac{2(\omega^2 m_1-\omega_0^2)^2}{\omega^2[\omega_2^2+\omega_1^2-2\omega_0^2 m_1+\omega^2(m_1^2-1)]}\right]$$

When $\omega_{2\infty} < \omega < \infty$, $\beta = 0$ and

α = same equation as for $0 < \omega < \omega_1$

Conditions

$$m_1 = (\omega_0^2/\omega_{2\infty}^2) + [(1-\omega_1^2/\omega_{2\infty}^2)(1-\omega_2^2/\omega_{2\infty}^2)]^{1/2}$$

$$m_2 = 1$$

Frequencies of Peak α

$$\omega_{1\infty} = 0$$

$$\omega_{2\infty} = \left(\frac{\omega_2^2+\omega_1^2-2\omega_0^2 m_1}{1-m_1^2}\right)^{1/2}$$

Design Equations, Half-Section Series Arm

$$L_1 = m_1 L_{1k}$$

$$C_1 = C_{1k}$$

Design Equations, Half-Section Shunt Arm

$$L_2 = L_{1k}\left[\frac{(\omega_2-\omega_1)^2}{\omega_0^2} - \frac{(m_1-1)^2}{m_1}\right]$$

$$C_2 = m_1 C_{1k} \Big/ \left[\frac{(\omega_2-\omega_1)^2}{\omega_0^2} - \frac{(m_1-1)^2}{m_1}\right]$$

$$L_2' = [(1-m_1^2)/m_1]L_{1k}$$

5-Element Shunt II

Half Section

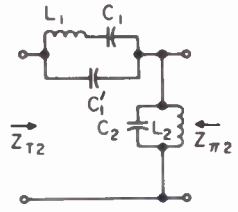

Impedance Characteristics

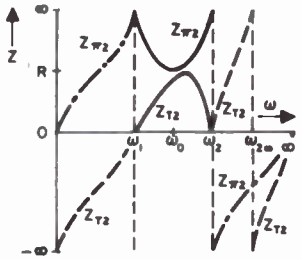

$Z_{T2}=R^2/Z_{\pi 1}$

$Z_{\pi 2}=Z_{\pi k}$

Full-Section Attenuation α and Phase β Characteristics

Same as for 5-element series II.

Conditions

Same as for 5-element series II.

Frequencies of Peak α

Same as for 5-element series II.

Design Equations, Half-Section Series Arm

$$L_1=m_1L_{2k}\Big/\left[\frac{(\omega_2-\omega_1)^2}{\omega_0^2}-\frac{(m_1-1)^2}{m_1}\right]$$

$$C_1=C_{2k}\left[\frac{(\omega_2-\omega_1)^2}{\omega_0^2}-\frac{(m_1-1)^2}{m_1}\right]$$

$$C_1'=[(1-m_1^2)/m_1]C_{2k}$$

Design Equations, Half-Section Shunt Arm

$$L_2=L_{2k}$$

$$C_2=m_1C_{2k}$$

6-Element Series

Half Section

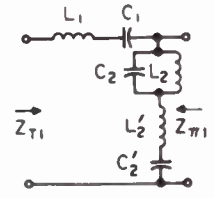

Impedance Characteristics

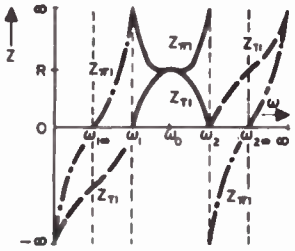

$Z_{T1}=Z_{Tk}$

$$Z_{\pi 1}=\frac{R}{\omega(\omega_2-\omega_1)}$$

$$\times\frac{(\omega_2^2-\omega^2)(\omega^2-\omega_1^2)+(\omega_0^2m_2-\omega^2m_1)^2}{\left[(\omega_2^2-\omega^2)(\omega^2-\omega_1^2)\right]^{1/2}}$$

Full-Section Attenuation α and Phase β Characteristics

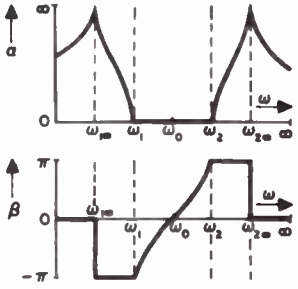

When $\omega_1<\omega<\omega_2$, $\alpha=0$ and

$$\beta=\cos^{-1}\left[1-\frac{2(\omega^2m_1-\omega_0^2m_2)^2}{(\omega^2m_1-\omega_0^2m_2)^2+(\omega_2^2-\omega^2)(\omega^2-\omega_1^2)}\right]$$

When $\omega_2<\omega<\omega_{2\infty}$, $\beta=\pi$ and

$$\alpha=\cosh^{-1}$$

$$\times\left[\frac{2(\omega^2m_1-\omega_0^2m_2)^2}{(\omega^2m_1-\omega_0^2m_2)^2+(\omega_2^2-\omega^2)(\omega^2-\omega_1^2)}+1\right]$$

When $0<\omega<\omega_{1\infty}$, $\beta=0$ and

$$\alpha=\cosh^{-1}$$

$$\times\left[1-\frac{2(\omega^2m_1-\omega_0^2m_2)^2}{(\omega^2m_1-\omega_0^2m_2)^2+(\omega_2^2-\omega^2)(\omega^2-\omega_1^2)}\right]$$

When $\omega_{1\infty}<\omega<\omega_1$, $\beta=-\pi$ and

$$\alpha=\cosh^{-1}$$

$$\times\left[\frac{2(\omega^2m_1-\omega_0^2m_2)^2}{(\omega^2m_1-\omega_0^2m_2)^2+(\omega_2^2-\omega^2)(\omega^2-\omega_1^2)}-1\right]$$

When $\omega_{2\infty}<\omega<\infty$, $\beta=0$ and

$\alpha=$ same equation as for $0<\omega<\omega_{1\infty}$

Conditions

$$m_1=\frac{g(\omega_0^2/\omega^2_{2\infty})+h}{1-(\omega^2_{1\infty}/\omega^2_{2\infty})}$$

$$m_2=\frac{g+h(\omega^2_{1\infty}/\omega_0^2)}{1-(\omega^2_{1\infty}/\omega^2_{2\infty})}$$

Frequencies of Peak α

$$\omega^2_{1\infty}+\omega^2_{2\infty}=\frac{\omega_2^2+\omega_1^2-2\omega_0^2m_1m_2}{1-m_1^2}$$

$$\omega^2_{1\infty}\times\omega^2_{2\infty}=\omega_0^4\left(\frac{1-m_2^2}{1-m_1^2}\right)$$

Design Equations, Half-Section Series Arm

$$L_1=m_1L_{1k}$$

$$C_1=C_{1k}/m_2$$

Design Equations, Half-Section Shunt Arm

$$L_2=\frac{L_{1k}}{m_2}\left[\frac{(\omega_2-\omega_1)^2}{\omega_0^2}-\frac{(m_1-m_2)^2}{m_1m_2}\right]$$

$$L_2'=[(1-m_1^2)/m_1]L_{1k}$$

$$C_2=\frac{m_1C_{1k}}{[(\omega_2-\omega_1)^2/\omega_0^2]-[(m_1-m_2)^2/m_1m_2]}$$

$$C_2'=[m_2/(1-m_2^2)]C_{1k}$$

6-Element Shunt

Half Section

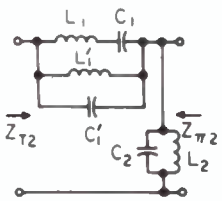

Impedance Characteristics

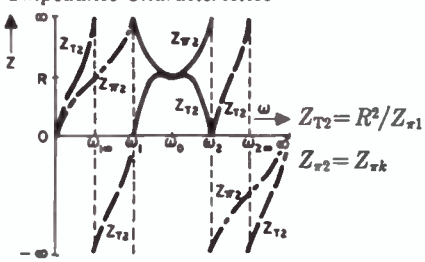

Full-Section Attenuation α and Phase β Characteristics

Same as for 6-element series.

Conditions

Same as for 6-element series.

Frequencies of Peak α

Same as for 6-element series.

Design Equations, Half-Section Series Arm

$$L_1=\frac{m_1L_{2k}}{[(\omega_2-\omega_1)^2/\omega_0^2]-[(m_1-m_2)^2/m_1m_2]}$$

$$C_1=\frac{C_{2k}}{m_2}\left[\frac{(\omega_2-\omega_1)^2}{\omega_0^2}-\frac{(m_1-m_2)^2}{m_1m_2}\right]$$

$$L_1'=[m_2/(1-m_2^2)]L_{2k}$$

$$C_1'=[(1-m_1^2)/m_1]C_{2k}$$

Design Equations, Half-Section Shunt Arm

$$L_2=L_{2k}/m_2$$

$$C_2=m_1C_{2k}$$

BAND-STOP FILTER DESIGN

Notations

Z in ohms, α in nepers, and β in radians

ω_1 = lower cutoff angular frequency

ω_2 = upper cutoff angular frequency

$\omega_0=(\omega_1\omega_2)^{1/2}=1/(L_{1k}C_{1k})^{1/2}$

$=1/(L_{2k}C_{2k})^{1/2}$

$\omega_2-\omega_1$ = width of stop band

$\omega_{1\infty}$ = lower angular frequency of peak attenuation

$\omega_{2\infty}$ = upper angular frequency of peak attenuation

R = nominal terminating resistance

$R^2=L_{1k}/C_{2k}=L_{2k}/C_{1k}$

$=Z_{1k}Z_{2k}=Z_{Tk}Z_{\pi k}=k^2$

$=Z_{1(\text{series}-m)}Z_{2(\text{shunt}-m)}$

$=Z_{2(\text{series}-m)}Z_{1(\text{shunt}-m)}$

$=Z_{T2}Z_{\pi1}$

Constant-k

Half Section

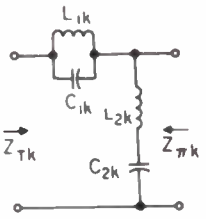

Impedance Characteristics

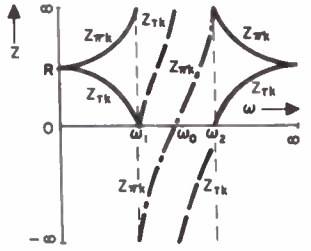

$$Z_{Tk}=\frac{R\left[(\omega^2-\omega_1^2)(\omega^2-\omega_2^2)\right]^{1/2}}{(\omega_0^2-\omega^2)}$$

$$Z_{\pi k}=\frac{R(\omega_0^2-\omega^2)}{\left[(\omega^2-\omega_1^2)(\omega^2-\omega_2^2)\right]^{1/2}}$$

For the pass bands, use $|\omega_0^2-\omega^2|$ in the above equations.

Full-Section Attenuation α and Phase β Characteristics

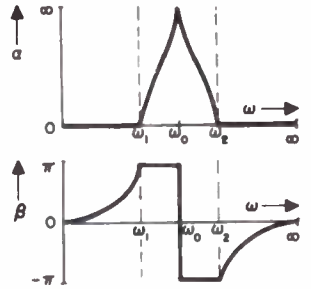

When $\omega=\omega_0$

$$\alpha=\infty$$

When $\omega_0<\omega<\omega_2$

$$\alpha=2\cosh^{-1}\frac{\omega(\omega_2-\omega_1)}{\omega^2-\omega_0^2}$$

$$\beta=-\pi$$

When $\omega_2<\omega<\infty$

$$\alpha=0$$

$$\beta=2\sin^{-1}\frac{\omega(\omega_2-\omega_1)}{\omega_0^2-\omega^2}$$

When $\omega_1<\omega<\omega_0$

$$\alpha=2\cosh^{-1}\frac{\omega(\omega_2-\omega_1)}{\omega_0^2-\omega^2}$$

$$\beta=\pi$$

When $0<\omega<\omega_1$

$$\alpha=0$$

$$\beta=2\sin^{-1}\frac{\omega(\omega_2-\omega_1)}{\omega_0^2-\omega^2}$$

Frequencies of Peak α

$$\omega_\infty=\omega_0$$

Design Equations, Half-Section Series Arm

$$L_{1k}=R(\omega_2-\omega_1)/\omega_1\omega_2$$

$$C_{1k}=1/R(\omega_2-\omega_1)$$

Design Equations, Half-Section Shunt Arm

$$L_{2k}=R/(\omega_2-\omega_1)$$

$$C_{2k}=(\omega_2-\omega_1)/\omega_1\omega_2R$$

Series m-Derived

Half Section

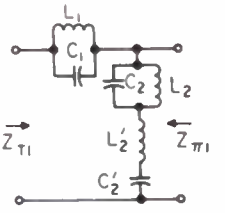

Impedance Characteristics

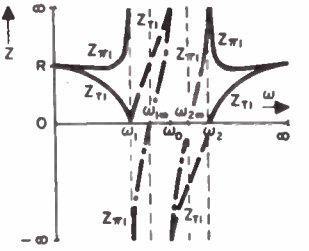

(Curves drawn for $m=0.6$)

$$Z_{T1}=Z_{Tk}$$

$$Z_{\pi 1}=R\left\{\frac{1-(1-m^2)\left[\omega(\omega_2-\omega_1)/(\omega_0^2-\omega^2)\right]^2}{\left\{1-\left[\omega(\omega_2-\omega_1)/(\omega_0^2-\omega^2)\right]^2\right\}^{1/2}}\right\}$$

Full-Section Attenuation α and Phase β Characteristics

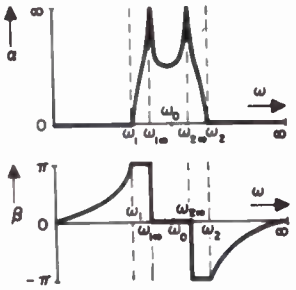

(Curves drawn for $m=0.6$)

When $\omega_2<\omega<\infty$, $\alpha=0$ and

$\beta=$ same equation as for $0<\omega<\omega_1$

When $\omega_{2\infty}<\omega<\omega_2$, $\beta=-\pi$ and

$\alpha=$ same equation as for $\omega_1<\omega<\omega_{1\infty}$

When $0<\omega<\omega_1$, $\alpha=0$ and

$$\beta=\cos^{-1}\left[1-\frac{2\omega^2m^2(\omega_2-\omega_1)^2}{(\omega^2-\omega_1^2)(\omega^2-\omega_2^2)+\omega^2m^2(\omega_2-\omega_1)^2}\right]$$

When $\omega_1<\omega<\omega_{1\infty}$, $\beta=\pi$ and

$$\alpha=\cosh^{-1}\left[\frac{2\omega^2m^2(\omega_2-\omega_1)^2}{(\omega^2-\omega_1^2)(\omega^2-\omega_2^2)+\omega^2m^2(\omega_2-\omega_1)^2}-1\right]$$

When $\omega_{1\infty}<\omega<\omega_{2\infty}$, $\beta=0$ and

$$\alpha=\cosh^{-1}\left[1-\frac{2\omega^2m^2(\omega_2-\omega_1)^2}{(\omega^2-\omega_1^2)(\omega^2-\omega_2^2)+\omega^2m^2(\omega_2-\omega_1)^2}\right]$$

Conditions

$$m=\{1-[(\omega_{2\infty}-\omega_{1\infty})^2/(\omega_2-\omega_1)^2]\}^{1/2}$$

Frequencies of Peak α

$$\omega_{1\infty}\omega_{2\infty}=\omega_0^2$$

Design Equations, Half-Section Series Arm

$$L_1=mL_{1k}$$

$$C_1=C_{1k}/m$$

Design Equations, Half-Section Shunt Arm

$$L_2=[(1-m^2)/m]L_{1k}$$

$$C_2=[m/(1-m^2)]C_{1k}$$

$$L_2'=L_{2k}/m$$

$$C_2'=mC_{2k}$$

Shunt m-Derived

Half Section

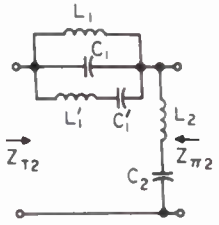

Impedance Characteristics

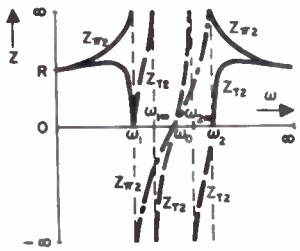

(Curves drawn for $m=0.6$)

$$Z_{T2}=R^2/Z_{\pi 1}$$

$$Z_{\pi 2}=Z_{\pi k}$$

Full-Section Attenuation α and Phase β Characteristics

Same as for series m-derived.

Conditions

Same as for series m-derived.

Frequencies of Peak α

Same as for series m-derived.

Design Equations, Half-Section Series Arm

$$L_1=mL_{1k}$$

$$C_1=C_{1k}/m$$

$$L_1'=[m/(1-m^2)]L_{2k}$$

$$C_1'=[(1-m^2)/m]C_{2k}$$

Design Equations, Half-Section Shunt Arm

$$L_2=L_{2k}/m$$

$$C_2=mC_{2k}$$

BUILDING UP A COMPOSITE FILTER

The intermediate sections (Fig. 2) are matched on an image-impedance basis, but the attenuation characteristics of the sections may be varied by suitably choosing the infinite attenuation frequencies of each section. Thus, the frequencies attenuated only slightly by one section may be strongly attenuated by other sections. However, the image impedance will be far from constant in the pass band and therefore the use of true resistors for terminations will change the attenuation shape.

Some improvement in the uniformity of the image impedance is obtained by using suitably designed terminating half sections. For these terminating sections, a value of $m \approx 0.6$ is usually used (Fig. 3).

EXAMPLE OF LOW-PASS IMAGE-PARAMETER DESIGN

To cut off at 15 kilohertz; to give peak attenuation at 30 kilohertz; with a load resistance of 600 ohms; and using a constant-k midsection and an m-derived midsection. Full T-sections will be used.

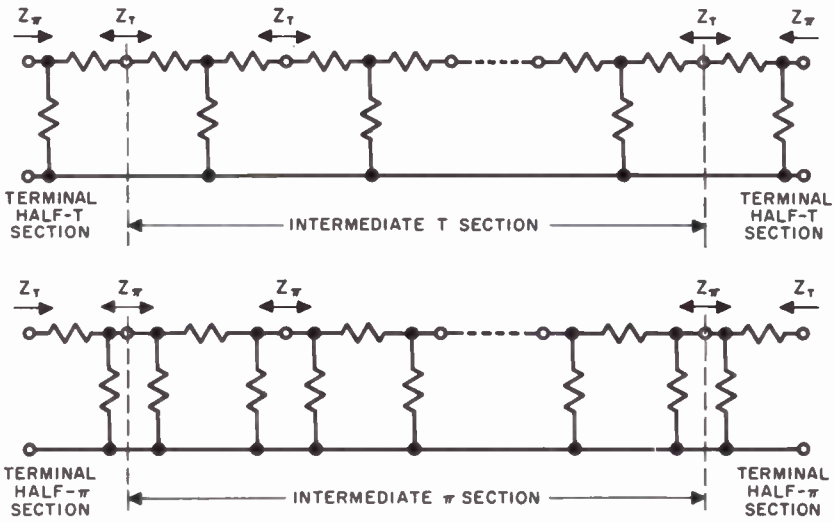

Fig. 2—Method of building up a composite filter.

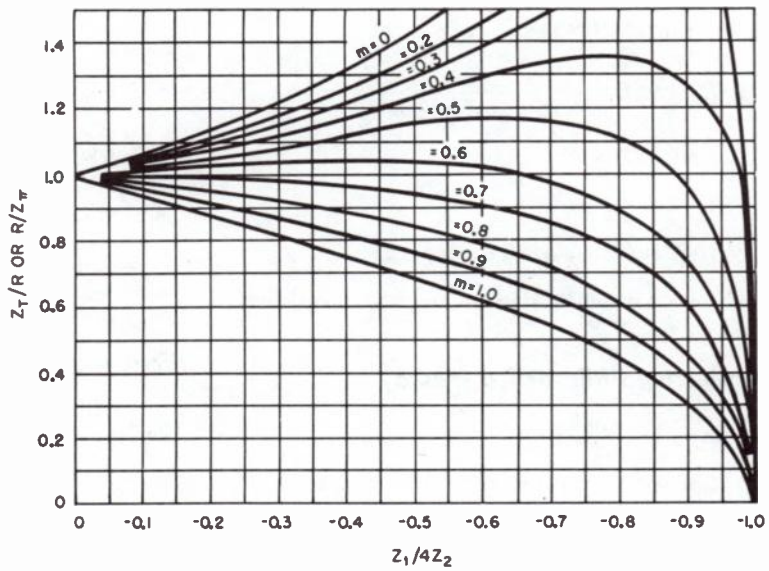

Fig. 3—Effect of design parameter m on the image-impedance characteristics in the pass band.

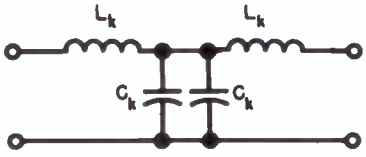

Fig. 4

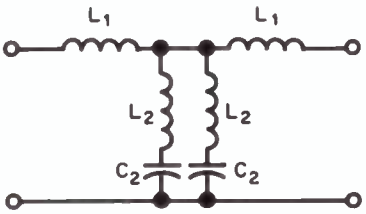

Fig. 5

Fig. 6

Constant-k Midsection (Fig. 4)

$$L_k = R/\omega_c = \frac{600}{(6.28)\,(15\times10^3)}$$

$$= 6.37\times10^{-3} \text{ henry}$$

$$C_k = 1/\omega_c R = \frac{1}{(6.28)\,(15\times10^3)\,(600)}$$

$$= 0.0177\times10^{-6} \text{ farad}$$

$$\alpha = 2\cosh^{-1}(\omega/\omega_c) = 2\cosh^{-1}(f/15)$$

$$\beta = 2\sin^{-1}(\omega/\omega_c) = 2\sin^{-1}(f/15)$$

where α is in nepers, β in radians, and f in kilohertz.

m-Derived Midsection (Fig. 5)

$$m = (1-\omega_c^2/\omega_\infty^2)^{1/2}$$

$$= (1-15^2/30^2)^{1/2}$$

$$= (0.75)^{1/2} = 0.866$$

$$L_1 = mL_k = 0.866(6.37\times10^{-3})$$

$$= 5.52\times10^{-3} \text{ henry}$$

$$L_2 = [(1-m^2)/m]L_k$$

$$= \left[\frac{1-(0.866)^2}{0.866}\right](6.37\times10^{-3})$$

$$= 1.84\times10^{-3} \text{ henry}$$

$$C_2 = mC_k = 0.866(0.0177\times10^{-6})$$

$$= 0.0153\times10^{-6} \text{ farad}$$

$$\alpha = \cosh^{-1}\left[1-\frac{2m^2}{(\omega_c^2/\omega^2)-(1-m^2)}\right]$$

$$= \cosh^{-1}\left[1-\frac{1.5}{(225/f^2)-0.25}\right]$$

$$\beta = \cos^{-1}\left[1-\frac{2m^2}{(\omega_c^2/\omega^2)-(1-m^2)}\right]$$

$$= \cos^{-1}\left[1-\frac{1.5}{(225/f^2)-0.25}\right]$$

End Sections m = 0.6 (Fig. 6)

$$L_1 = mL_k = 0.6(6.37\times10^{-3})$$

$$= 3.82\times10^{-3} \text{ henry}$$

$$L_2 = [(1-m^2)/m]L_k$$

$$= \left[\frac{1-(0.6)^2}{0.6}\right](6.37\times10^{-3})$$

$$= 6.80\times10^{-3} \text{ henry}$$

$$C_2 = mC_k = 0.6(0.0177\times10^{-6})$$

$$= 0.0106\times10^{-6} \text{ farad.}$$

Frequency of Peak Attenuation f_∞

$$f_\infty = [f_c^2/(1-m^2)]^{1/2}$$

$$= \{(15\times10^3)^2/[1-(0.6)^2]\}^{1/2}$$

$$= 18.75 \text{ kilohertz.}$$

Filter Showing Individual Sections (Fig. 7)

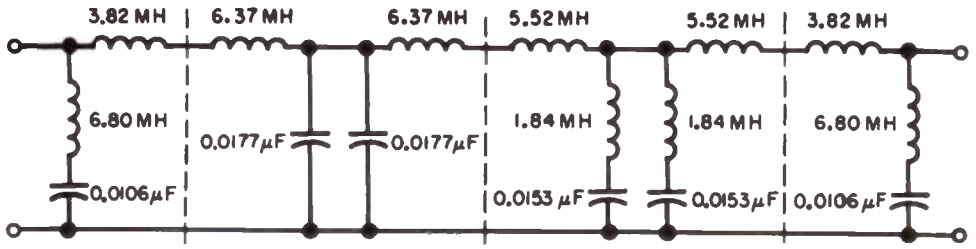

Fig. 7

Filter After Combining Elements (Fig. 8)

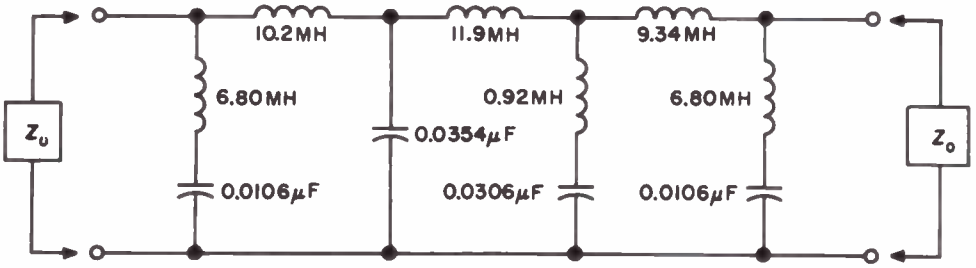

Fig. 8

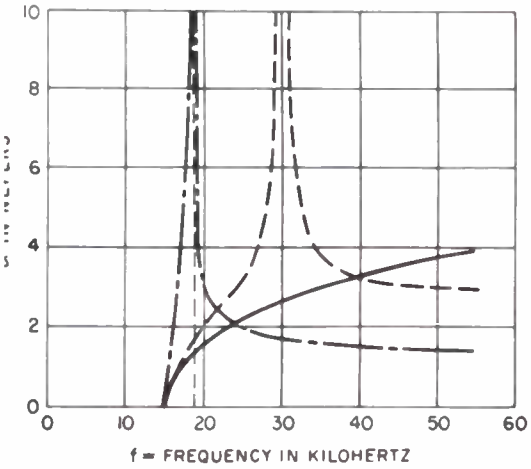

Fig. 9—Image-terminated attenuation of each section. Solid line, constant-k midsection. Dashed, m-derived midsection. Dash-dot, m-derived ends.

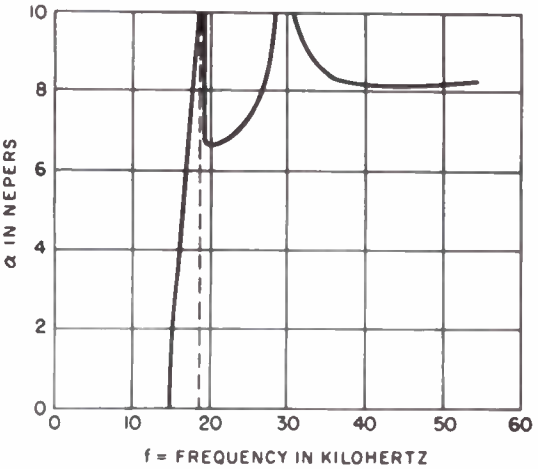

Fig. 10—Image-terminated attenuation of composite filter.

Image Attenuation and Phase Characteristics

Figures 9 through 12 are the image-terminated attenuation and phase characteristics. These shapes are not obtainable when 600-ohm resistors are used in place of the terminating Z_0.

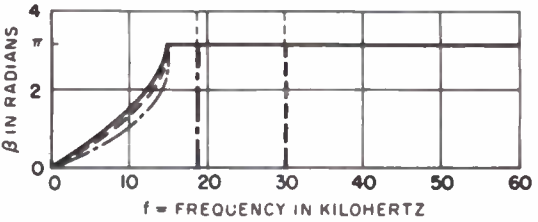

Fig. 11—Image-terminated phase characteristic of each section. Solid line, constant-k midsection. Dashed, m-derived midsection. Dash-dot, m-derived ends.

Impedance required for Proper Termination (Fig. 13)

$$Z_0 = \frac{R[1-(\omega^2/\omega_c^2)(1-m^2)]}{(1-\omega^2/\omega_c^2)^{1/2}}$$

$$= \frac{600[1-0.64(f/15)^2]}{[1-(f/15)^2]^{1/2}}$$

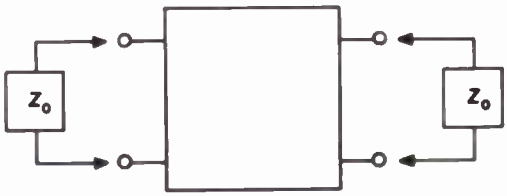

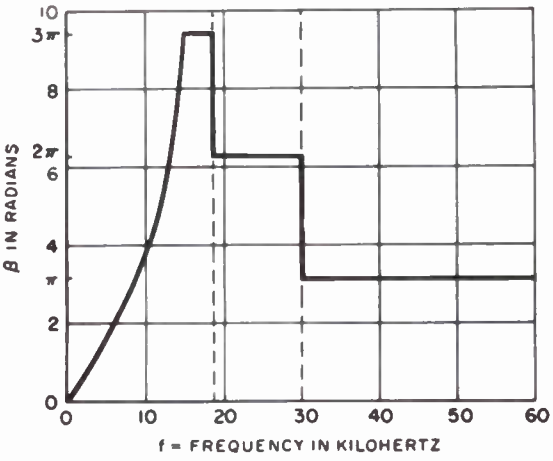

Fig. 12—Image-terminated phase characteristic of composite filter.

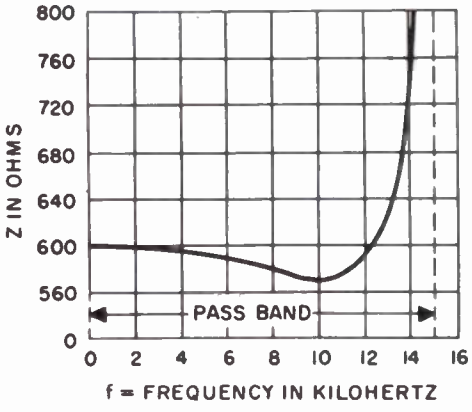

Fig. 13

CHAPTER 8
FILTERS, MODERN-NETWORK-THEORY DESIGN

The design information in this chapter results from the application of modern network theory to electric wave filters. Only design results are supplied, and a careful study of the cited references is required for an understanding of the synthesis procedures that underlie these results.

LIMITATIONS OF IMAGE-PARAMETER THEORY

Consider the simple low-pass ladder network of Fig. 1A. Two simultaneous design equations, (1) and (2), are provided by classical image-parameter theory (refer to Chapter 7).

$$(Z_1/4Z_2)_{f=fc} = -1 \text{ and } 0 \qquad (1)$$

$$Z_{0T} = (Z_1Z_2)^{1/2}[1+(Z_1/4Z_2)]^{1/2}. \qquad (2)$$

Z_1 and Z_2, the full series- and shunt-arm impedances, respectively, must be suitably related to make (1) true at the desired cutoff frequencies, and the generator and load impedance must satisfy (2). Under the image-parameter theory, the resulting attenuation for the low-pass case is

$$\begin{aligned} V_p/V &= 1.0, && (\omega/\omega_c) < 1 \\ &= \exp[(n-1)\cosh^{-1}(\omega/\omega_c)], && (\omega/\omega_c) > 1 \end{aligned} \qquad (3)$$

where n is the number of arms in the network of Fig. 1 and V_p/V and ω are as in Fig. 3. It is this attenuation shape that is plotted in the tabulations of Chapter 7.

Equation (1) offers no problems. The application of (2) to Fig. 1 demands *terminating impedances that are physically impossible with a finite number of elements*. The generator and load impedances for Fig. 1A must be pure resistances of $(L/C)^{1/2}$ ohms at zero frequency. As frequency increases, the value of resistance must decrease to a short-circuit at the cutoff frequency, and with further increase in frequency must behave like a pure inductance starting at zero value at the cutoff frequency and increasing to $L/2$ at infinite frequency.

The physical impracticability of devising such terminating impedances is why element values obtained by (1) cannot simultaneously satisfy (2). The relative attenuation indicated by (3) is similarly incorrect and cannot be realized in practice.

Lattice-configuration filters also require impractical terminating impedances when designed by image-parameter theory. (Constant-resistance lattices are an exception but are seldom used for filtering.) The practical use of resistive terminations automatically makes element values computed on the basis of ideal impedance terminations incorrect.

For more than four decades, filters have been designed according to the image-parameter theory. Their commercial acceptance is due in no small part to the highly approximate requirements for most filters. Where more-exact characteristics are required, shifting of element values in the actual filter has usually resulted in an acceptable design. For precise amplitude and phase response in the pass band, the simple and approximate solutions obtained through image-parameter theory must give way to equations based on modern network theory.

MODERN-NETWORK-THEORY DESIGN

Relative Attenuation

A typical low-pass filter with resistive generator and load is shown in Fig. 1B. It is composed of lumped inductors, capacitors, and the resistive elements unavoidably associated therewith. The circuit equations for the complete network can be written by applying Kirchhoff's laws. Modern network theory does just this and then solves the equations to find the network parameters that will produce optimum performance in some desired respect.

A block diagram of a generalized filter is illustrated in Fig. 2. This may be of low-pass, high-pass, band-pass, band-rejection, phase-compen-

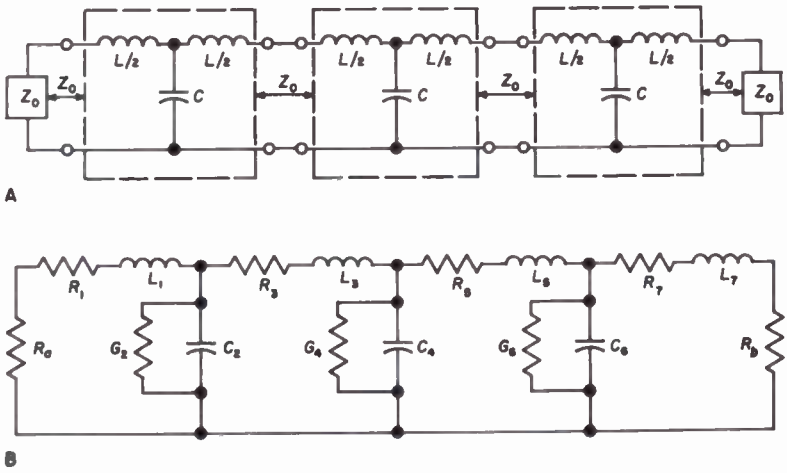

Fig. 1—A 7-element low pass filter considered on the basis of image-parameter theory at A and of modern network theory at B.

sating, or other type. The elements of the filter include resistors, capacitors, self- and mutual-inductors, and possibly coupling elements such as electron tubes or transistors, all according to the design. The terminations shown are a constant-voltage generator (the same voltage at all frequencies) with a series resistor at the input and a resistive load. (Frequently it is preferable to stipulate a constant-current generator with a shunt conductance.) The generator and load resistors need not be equal and they can be assigned any value between zero and infinity. Characteristic impedance plays no part in the modern network theory of filters.

Either or both the generator or load can be reactive, in which case the reactances are absorbed inside the block of Fig. 2 as specified parts of the filter. Either, but not both, R_a or R_b can be zero or infinite.

The term *bandwidth* as used herein has two different meanings, according to the type of filter. For low- or high-pass filters, it is synonymous with the actual frequency of the point in question, or equivalent to the number of hertz in a band terminated on one side by zero frequency and on the other by the actual frequency. The actual frequency can be anywhere in the pass or the reject region. For symmetrical band-pass (Fig. 4) and band-reject filters, it is the difference in hertz between two particular frequencies (anywhere in the pass or reject regions) with the requirement that their geometric mean be equal to the geometric midfrequency f_0 of the pass or reject band.

Typical filter characteristics are plotted in Fig. 3 for a low-pass filter. In Fig. 3A, the magnitude

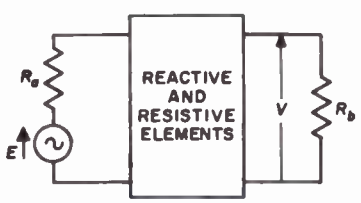

Fig. 2—Block diagram of a filter. The generator and load must be considered part of the filter.

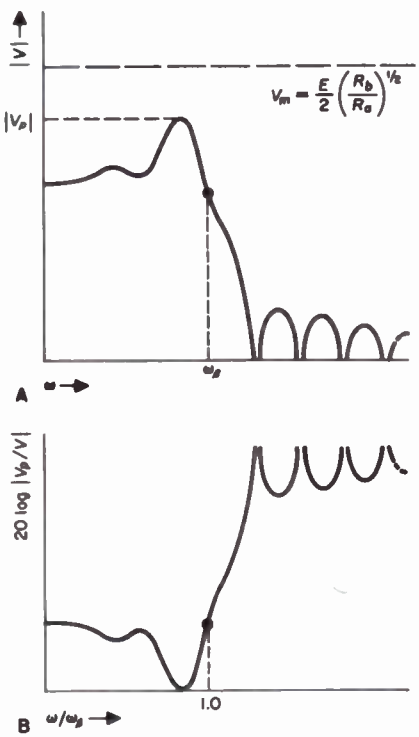

Fig. 3—Low-pass-filter output voltage versus frequency at A; attenuation versus normalized frequency at B. A is the actual voltage across the load as a function of frequency and is for the low-pass case. B uses the information in A to produce a plot of *relative* attenuation against *relative* bandwidth.

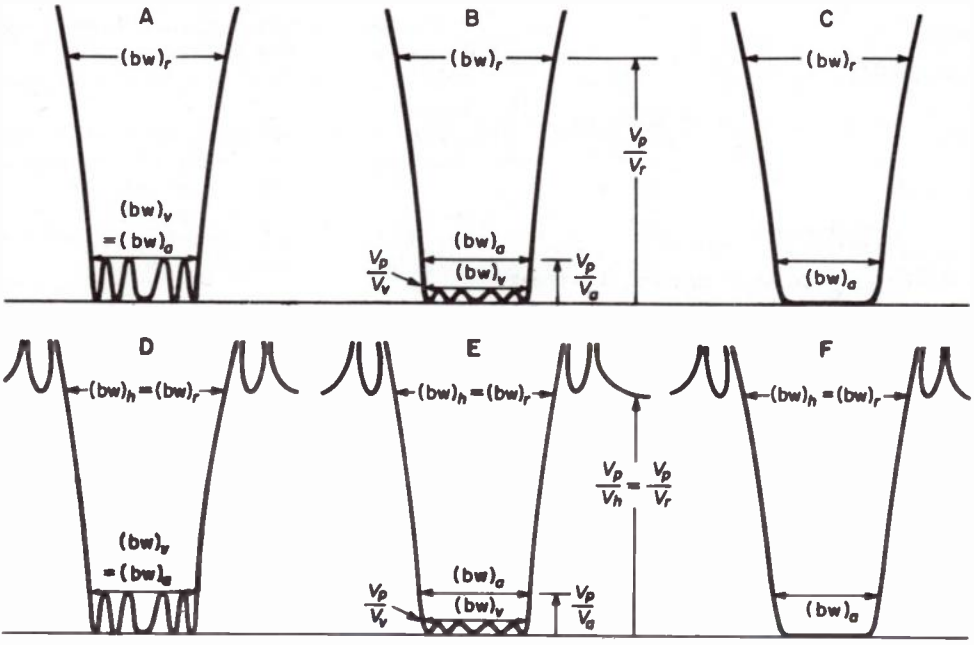

Fig. 4—A, B, C, are the optimum relative attenuation shapes of (4) and (5) that can be produced by networks supplying only transfer-function poles. D, E, F, are the optimum relative attenuation shapes of (8), (12), (13), (16) that can be produced by networks supplying both transfer-function poles and zeros.

of the output voltage V is plotted against radian bandwidth ω. Several specific points are indicated on the diagram. V_p is the peak voltage output, while V_m is the maximum voltage that could be developed across the load were it matched to the generator through an ideal network. Symbol ω_β designates a specified frequency or bandwidth where some particular characteristic is exhibited by the filter, such as the point where the response is 3 decibels down from the peak, for example.

The characteristic of major interest to the filter engineer is the plot, shown in Fig. 3B, of relative attenuation versus relative bandwidth. Relative attenuation is defined as the ratio of the peak output voltage V_p to the voltage output V at the frequency being considered. Relative bandwidth is defined as the ratio of the bandwidth being considered to a clearly specified reference bandwidth (e.g., the 3-decibel-down bandwidth).

It should be noted that the elements of a filter are not uniquely fixed if only a certain relative attenuation shape is specified; in general it is possible also to demand that at one frequency the absolute magnitude of some transfer function be optimized.

The complex relative attenuation of a complete filter (including generator and load) composed of lumped linear passive elements is always equal to a constant multiplied by the ratio of two polynomials in $(j\omega)$. The complex roots of the numerator polynomial are commonly called attenuation poles or transfer-function zeros; the complex roots of the denominator polynomial are commonly called attenuation zeros or transfer-function poles. Modern filter theory has derived various expressions for optimum relative attenuation shapes that can be physically realized from these complex expressions. The shapes are optimum in that they give the maximum possible rate of cutoff between the accept and reject bands for a given number of filter components, with a specified allowable equal ripple in the accept band, and a specified required equal ripple in the reject band. See Fig. 4 for typical shapes of attenuation characteristic for band-pass filters.

CHEBISHEV AND BUTTERWORTH PERFORMANCE WITH FILTERS SUPPLYING ONLY TRANSFER-FUNCTION POLES

The attenuation-curve shapes illustrated in Figs. 4A and 4B are termed Chebishev and that in Fig. 4C is termed Butterworth. The equations for these shapes are (4) and (5), respectively. The Butterworth shape is the same as the limiting case of the Chebishev shape when we set $V_p/V_v = 1.0$.

Chebishev

$$(V_p/V)^2=1+[(V_p/V_v)^2-1]\times\cosh^2[n\cosh^{-1}(x/x_v)]. \quad (4)$$

Butterworth

$$(V_p/V)^2=1+(x/x_{3dB})^{2n} \quad (5)$$

where V = output voltage at point x, V_p = peak output voltage in pass band, V_v = valley output voltage in pass band, and n = number of poles, equal to the number of arms in the ladder network being used. For low-pass and high-pass filters, n = number of reactances in the filter. For band-pass and band-reject, n = total number of resonators in the filter, x = a variable found in the following tabulations, x_v = value of x at point on skirt where attenuation equals valley attenuation, and x_{3dB} = value of x at point on skirt where attenuation is 3 decibels below V_p.

Significance of x

Low-Pass Filters:

$$x=\omega=2\pi f.$$

High-Pass Filters:

$$x=-1/\omega=-1/2\pi f.$$

Symmetrical Band-Pass Filters:

$$x=(\omega/\omega_0-\omega_0/\omega)=(f_2-f_1)/f_0=(\text{bw})/f_0.$$

Symmetrical Band-Reject Filters:

$$x=-1/(\omega/\omega_0-\omega_0/\omega)=-f_0/(\text{bw})$$

where $f_0=(f_1f_2)^{1/2}$ = midfrequency of the pass or reject band and f_1, f_2 = two frequencies where the characteristic exhibits the same attenuation.

Working charts for these filters, derived from (4) and (5), are presented in Figs. 5 through 12 for values of n from 1 through 8, respectively. These curves give

$$(V_p/V)_{dB}=20\log_{10}(V_p/V)$$

versus x/x_{3dB}.

For low-pass and band-pass filters

$$x/x_{3dB}=(\text{bw})/(\text{bw})_{3dB}.$$

For high-pass and band-reject filters, the scale of the abscissa gives $(\text{bw})_{3dB}/(\text{bw})$.

In Figs. 5 through 12, the family of curves toward the right side gives the attenuation shape for points where it is less than 3 decibels, while those toward the left are for the reject band (greater than 3 decibels). Each curve of the former family has been stopped where the attenuation is equal to that of the peak-to-valley ratio.

Thus, in Fig. 6, curve 3 has been stopped at 0.3 decibel, which is the value of $(V_p/V_v)_{dB}$ for which the curve was computed. (See chart on Fig. 6.)

The curves give actual optimum attenuation characteristics based on rigorous computation of the ladder network. In contrast, the commonly used attenuation curves based on "image-parameter theory" are approximations that are actually unattainable in practice.

Time-Delay and Phase-Shift Characteristics of Butterworth Response Shape

The symbols of Figs. 13 and 14 may be applied to low-pass or band-pass responses as follows:

$t_0=d\theta/dw$

= slope of phase characteristic in radians per radian per second at zero frequency for low-pass filters, or at the midfrequency for band-pass filters

t = slope of phase characteristic at a frequency Δf removed from zero frequency for low-pass filters, or from the midfrequency for band-pass filters

Δf_{3dB} = 3-decibel-down bandwidth of the low-pass filter or half the total 3-decibel-down bandwidth of the band-pass filter, in hertz.

Low- and Band-Pass Filters—Required Unloaded Q

Filters supplying only transfer-function poles can be constructed that will actually give the attenuation shapes predicted by modern network theory. To attain this result, it is required that the unloaded Q of each element be greater than a certain minimum value*. The q_{min} column on the charts in Figs. 5 through 12 is used in the following manner to obtain this minimum allowable

* S. Darlington, "Synthesis of Reactance 4-Poles," *Journal of Mathematics and Physics*, vol. *18*, pp. 257-353; September 1939. Also, M. Dishal, "Design of Dissipative Band-Pass Filters Producing Desired Exact Amplitude-Frequency Characteristics," *Proceedings of the IRE*, vol. *37*, pp. 1050–1069; September 1949: also, *Electrical Communication*, vol. *27*, pp. 56–81; March 1950. Also, M. Dishal, "Concerning the Minimum Number of Resonators and the Minimum Unloaded Q Needed in a Filter," *Transactions of the IRE Professional Group on Vehicular Communication*, vol. *PGVC-3*, pp. 85–117; June 1953: also, *Electrical Communication*, vol. *31*, pp. 257–277; December 1954.

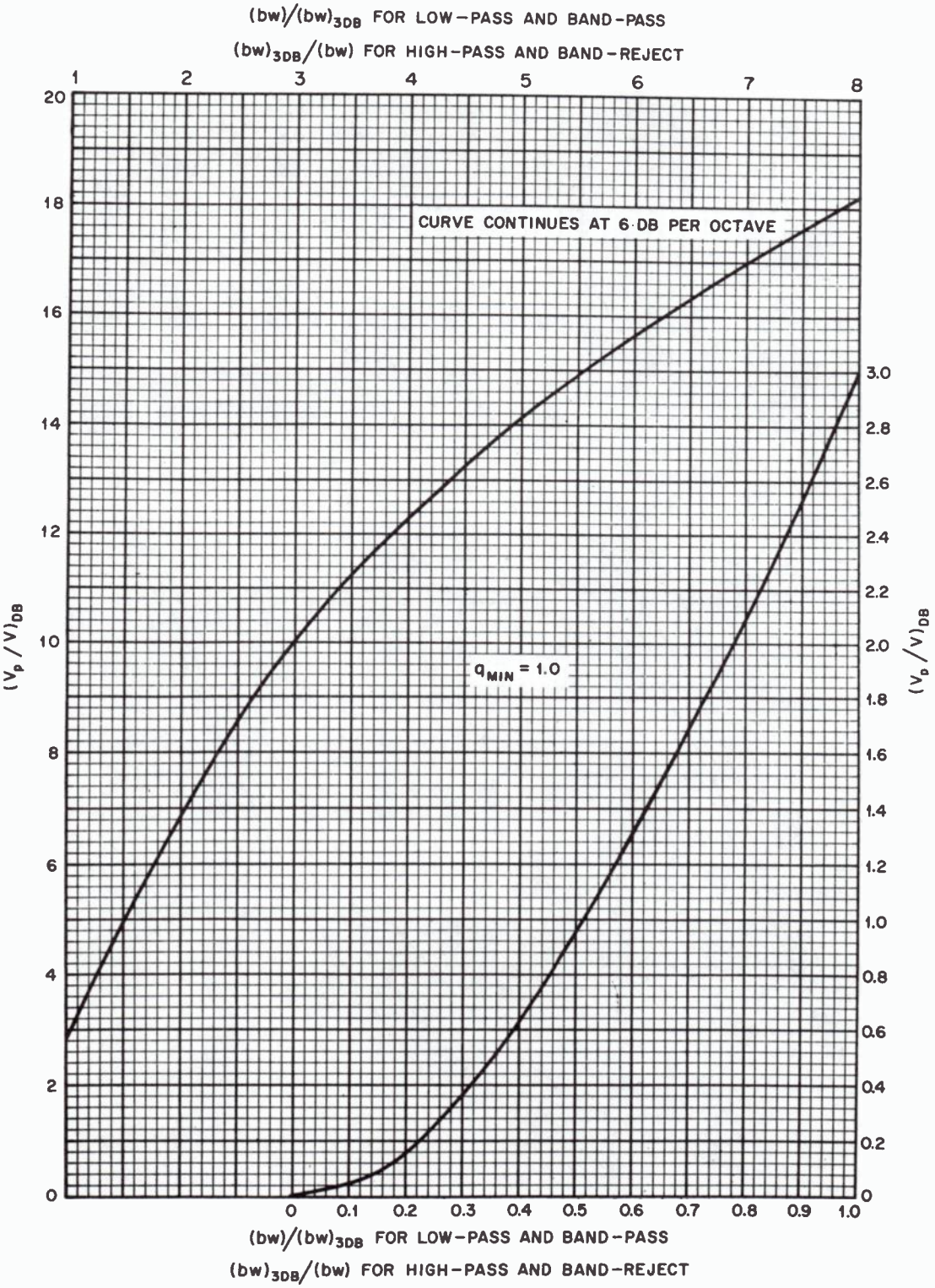

Fig. 5—Relative attenuation for a 1-pole network.

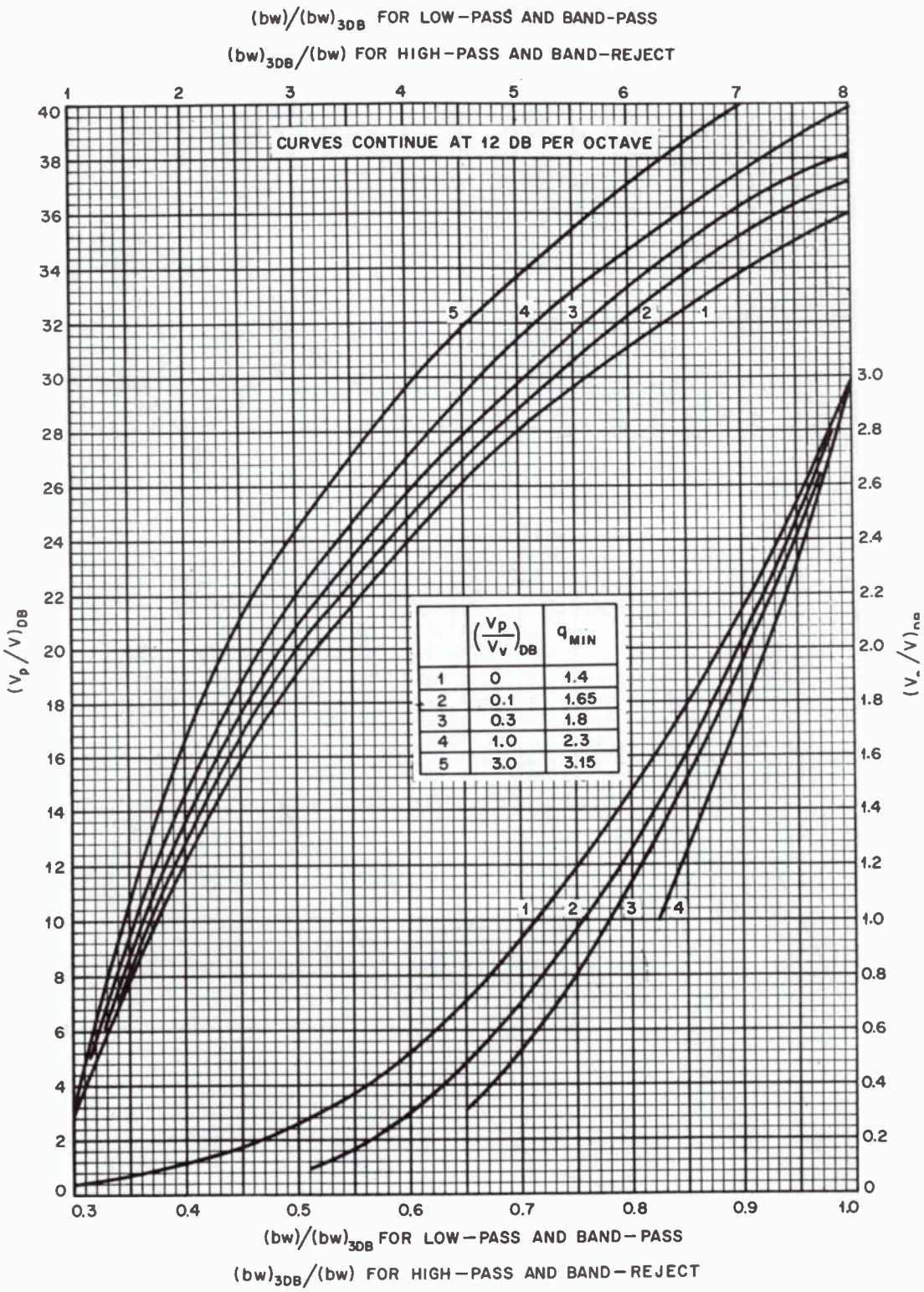

	$\left(\frac{V_p}{V_v}\right)_{DB}$	q_{MIN}
1	0	1.4
2	0.1	1.65
3	0.3	1.8
4	1.0	2.3
5	3.0	3.15

Fig. 6—Relative attenuation for a 2-pole network.

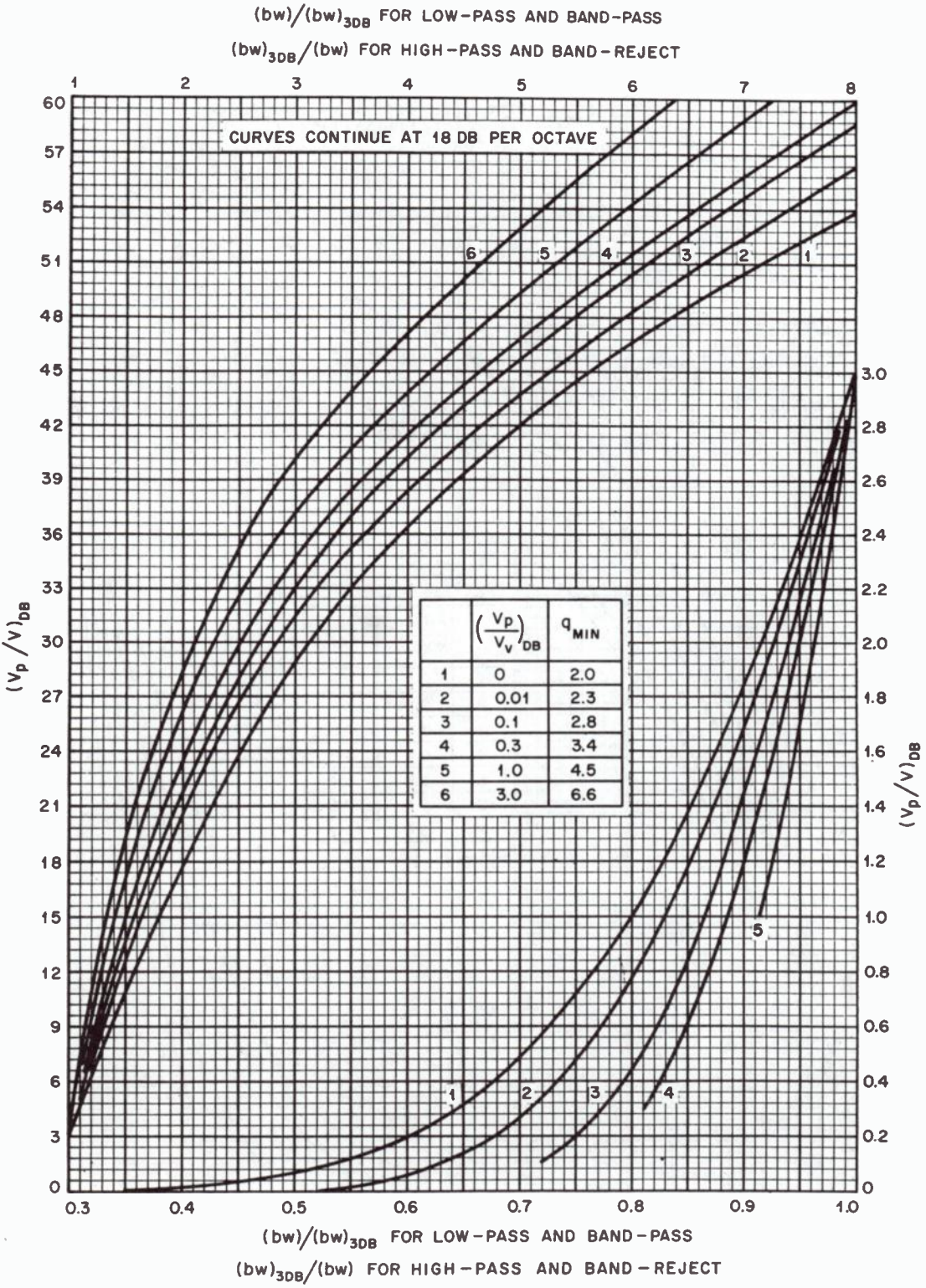

	$\left(\frac{V_p}{V_v}\right)_{DB}$	q_{MIN}
1	0	2.0
2	0.01	2.3
3	0.1	2.8
4	0.3	3.4
5	1.0	4.5
6	3.0	6.6

Fig. 7—Relative attenuation for a 3-pole network.

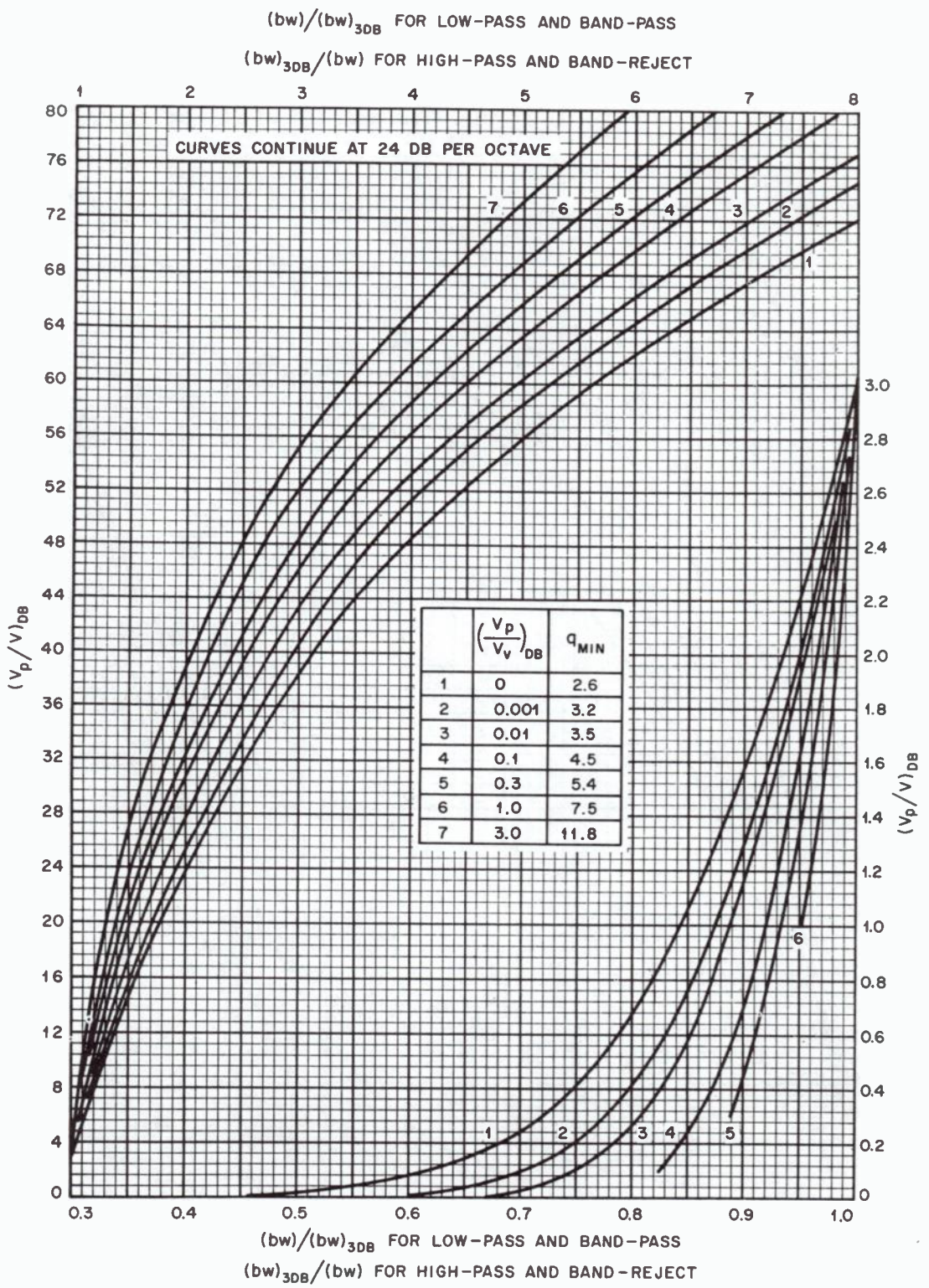

	$\left(\frac{V_p}{V_v}\right)_{DB}$	q_{MIN}
1	0	2.6
2	0.001	3.2
3	0.01	3.5
4	0.1	4.5
5	0.3	5.4
6	1.0	7.5
7	3.0	11.8

Fig. 8—Relative attenuation for a 4-pole network.

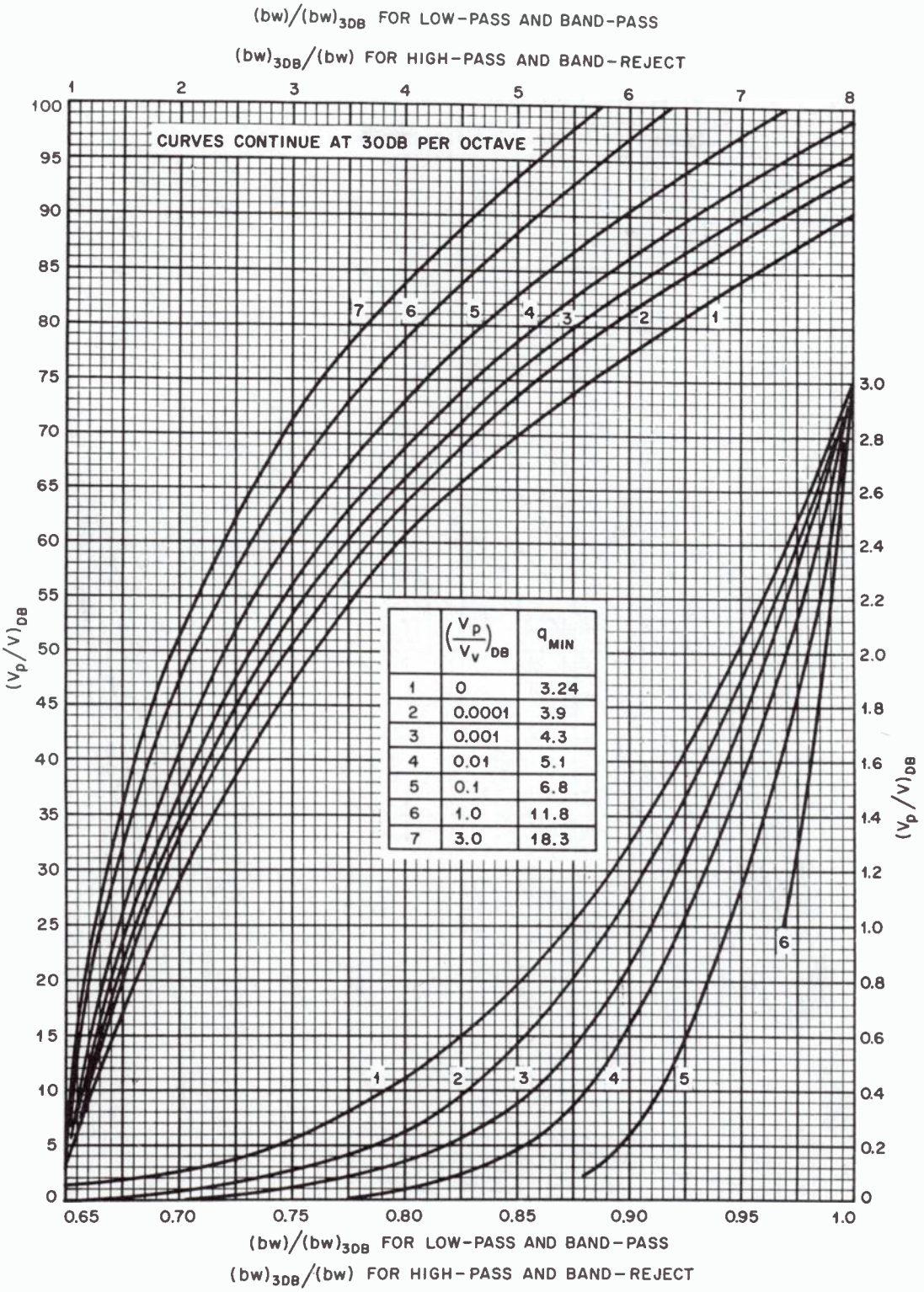

	$\left(\frac{V_p}{V_v}\right)_{DB}$	q_{MIN}
1	0	3.24
2	0.0001	3.9
3	0.001	4.3
4	0.01	5.1
5	0.1	6.8
6	1.0	11.8
7	3.0	18.3

Fig. 9—Relative attenuation for a 5-pole network.

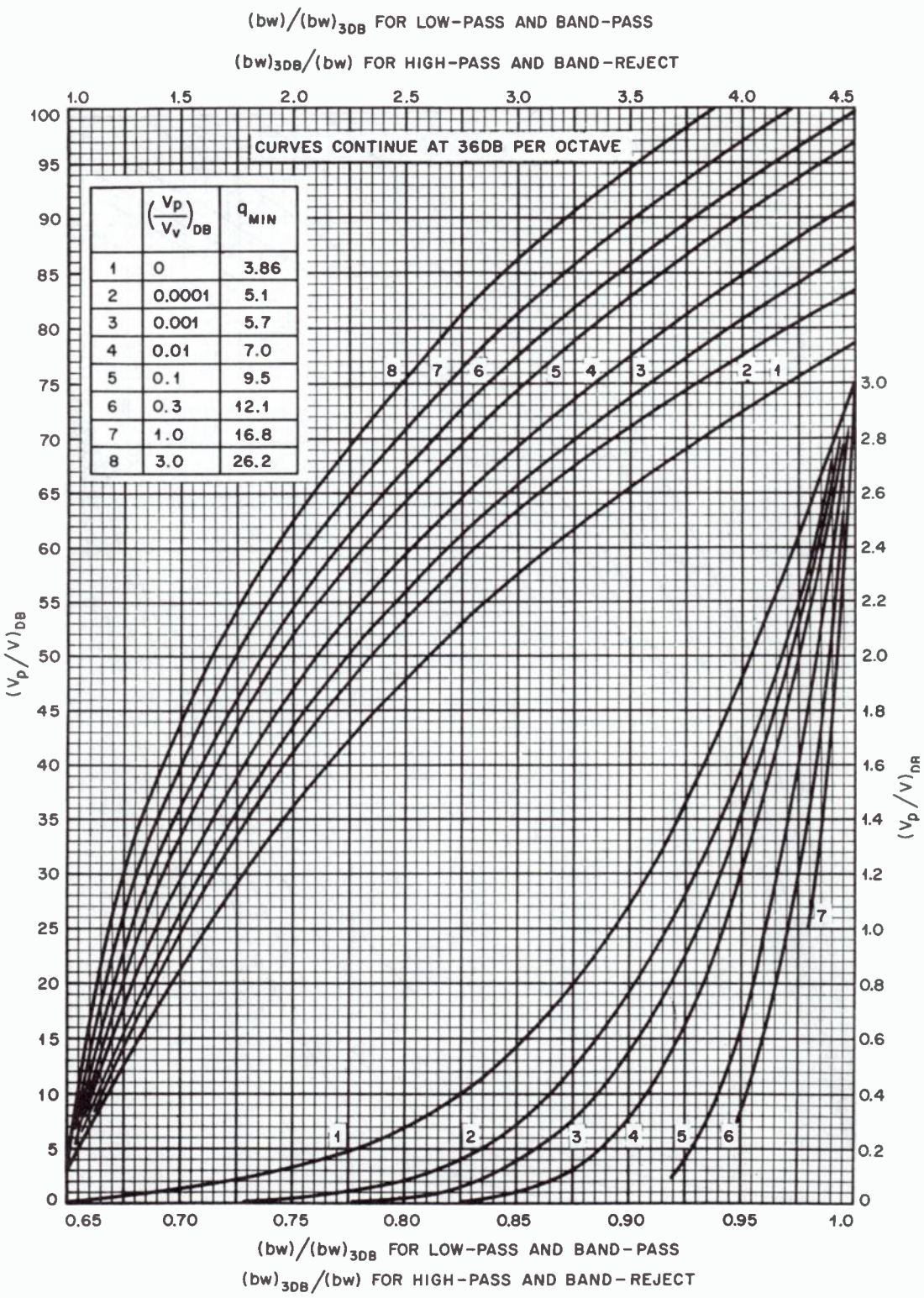

Fig. 10—Relative attenuation for a 6-pole network.

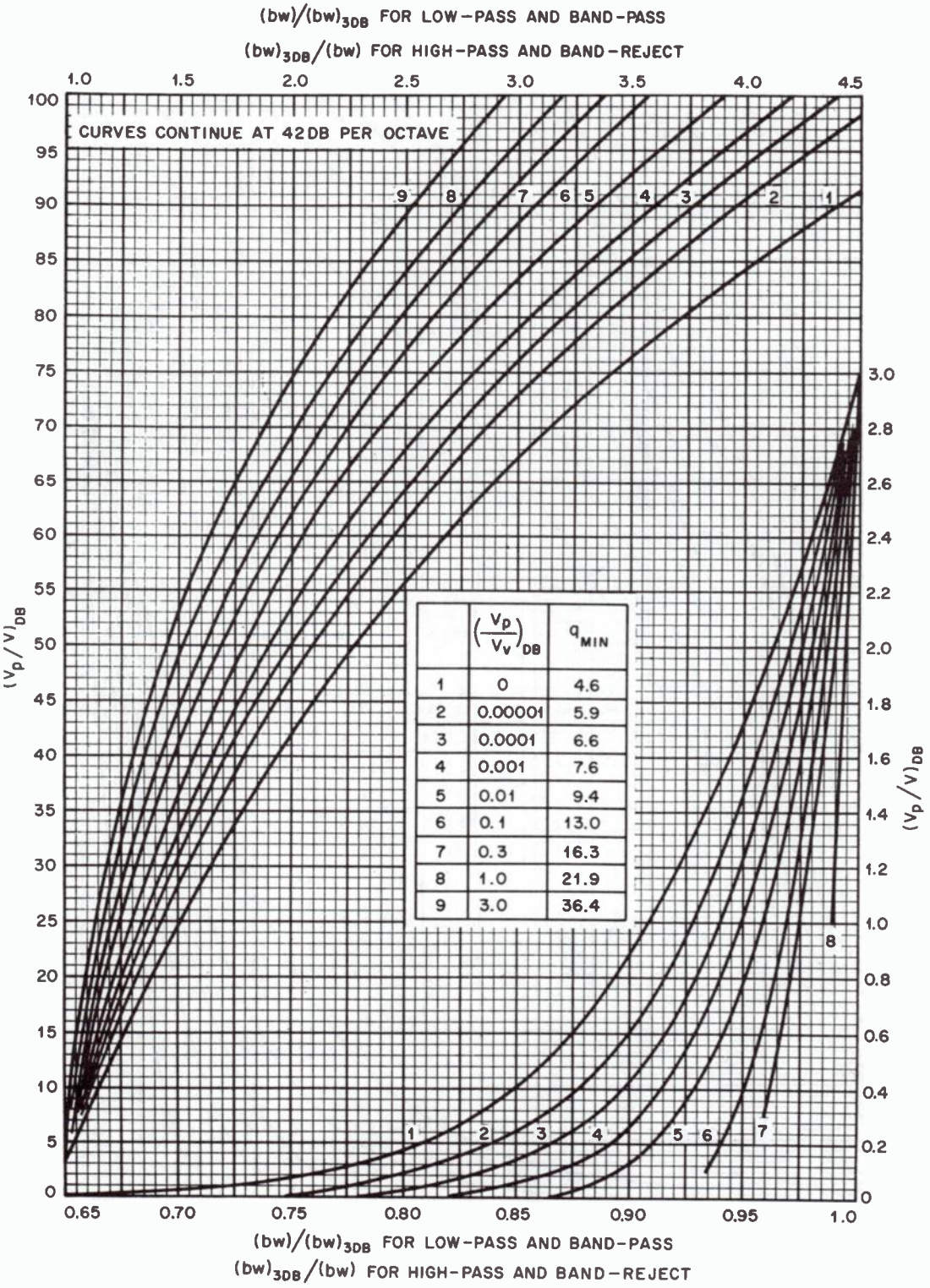

	$\left(\frac{V_p}{V_v}\right)_{DB}$	q_{MIN}
1	0	4.6
2	0.00001	5.9
3	0.0001	6.6
4	0.001	7.6
5	0.01	9.4
6	0.1	13.0
7	0.3	16.3
8	1.0	21.9
9	3.0	36.4

Fig. 11—Relative attenuation for a 7-pole network.

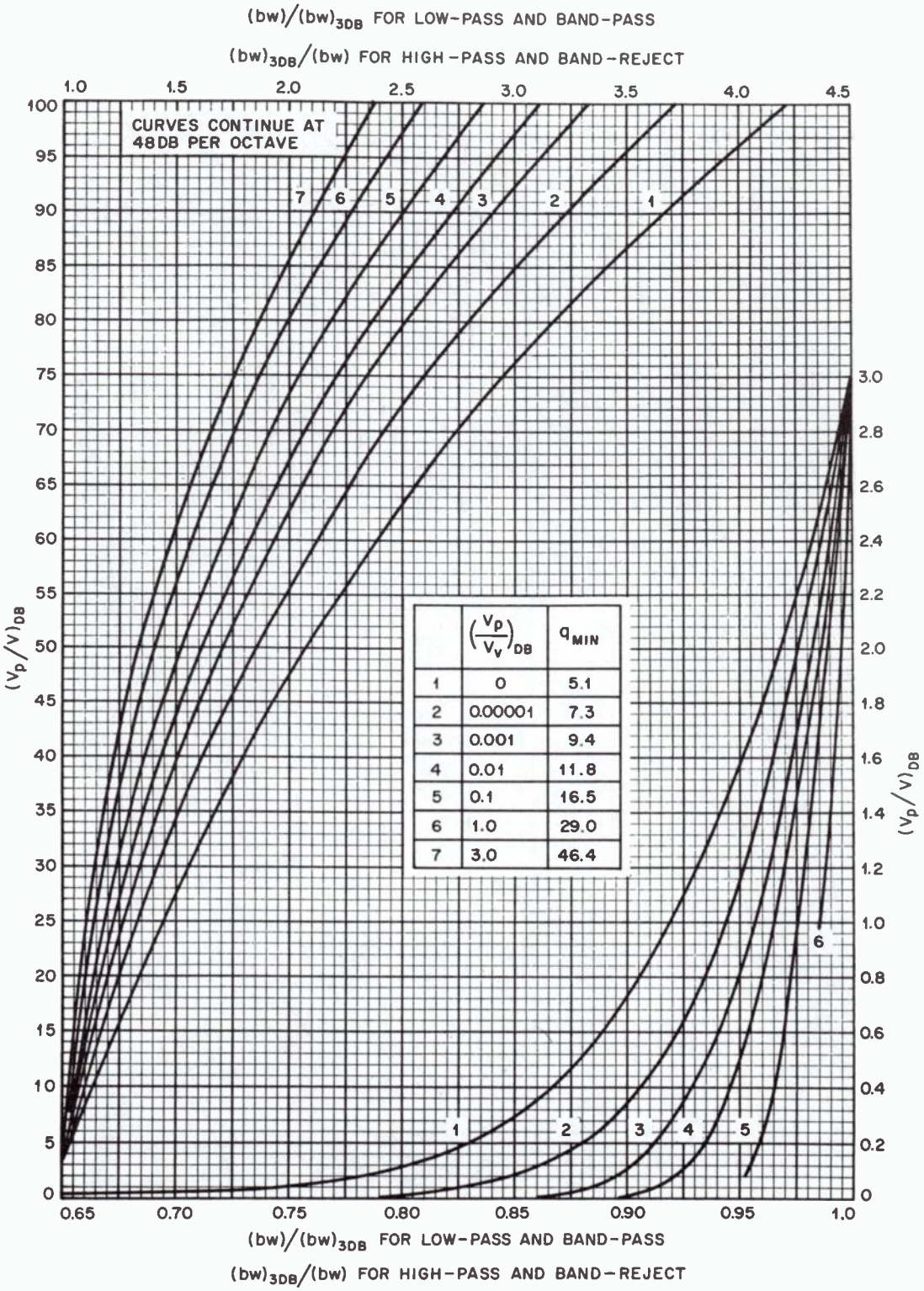

	$\left(\frac{V_p}{V_v}\right)_{DB}$	q_{MIN}
1	0	5.1
2	0.00001	7.3
3	0.001	9.4
4	0.01	11.8
5	0.1	16.5
6	1.0	29.0
7	3.0	46.4

Fig. 12—Relative attenuation for an 8-pole network.

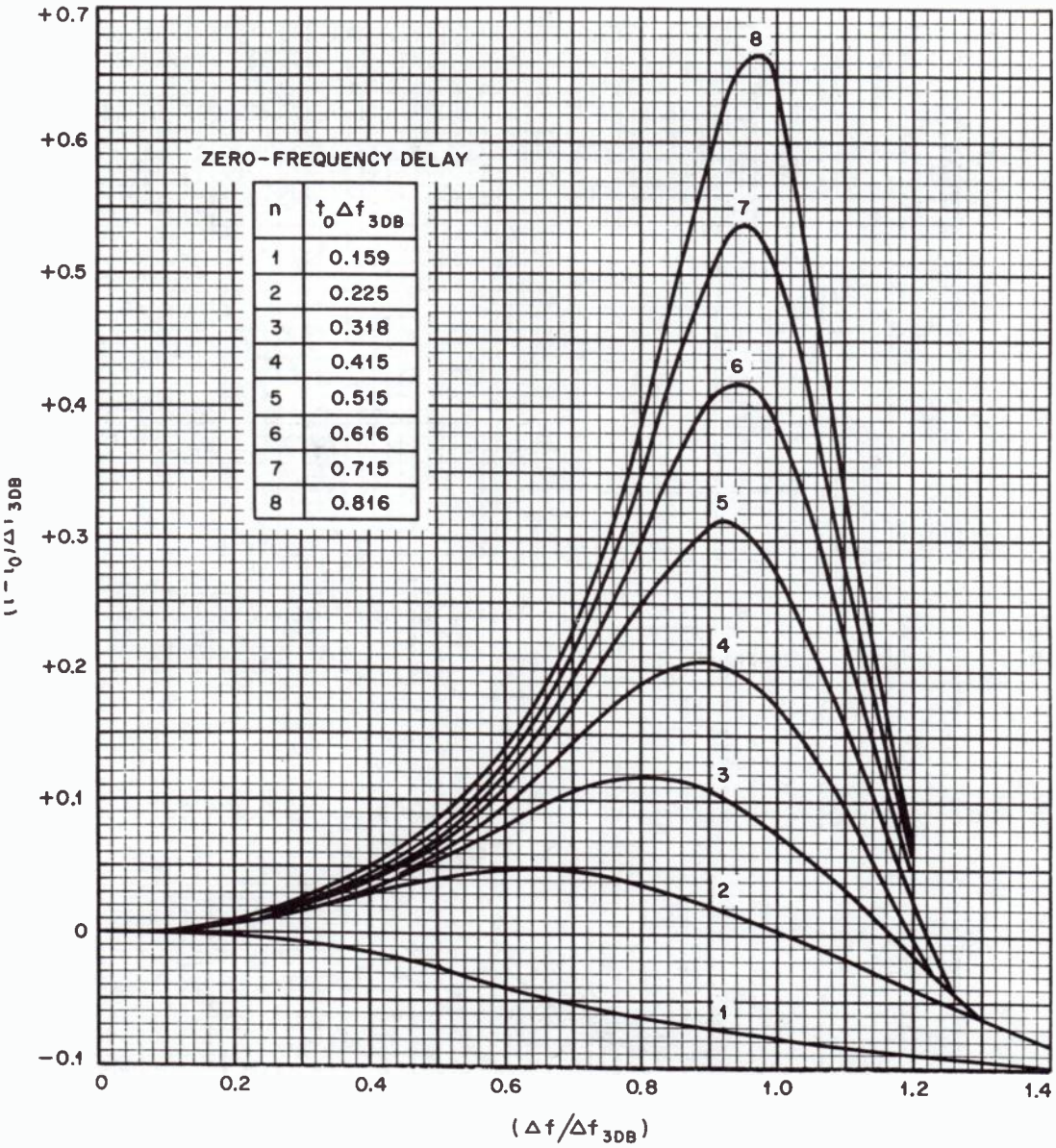

Fig. 13—Delay distortion of Butterworth response shape.

value: For the internal reactances of low-pass circuits

$$Q_{min} = q_{min}.$$

For the internal resonators of band-pass circuits

$$Q_{min} = q_{min}[f_0/(bw)_{3dB}].$$

Examples

(A) In a low-pass filter without any peaks of infinite attenuation at a finite frequency, how few elements are required to satisfy the following specifications, and what minimum Q must they have? Response to be 1 decibel down at 30 kilohertz and 50 decibels down at not more than 75 kilohertz, compared with the peak response.

The allowable ripple is 1 decibel in the pass band. Then

$$(bw)_{50dB}/(bw)_{1dB} < 75/30 = 2.5$$

$$(V_p/V_v)_{dB} \leq 1.0 \text{ decibel.}$$

Since $(bw)_{1dB}$ will be slightly less than $(bw)_{3dB}$,

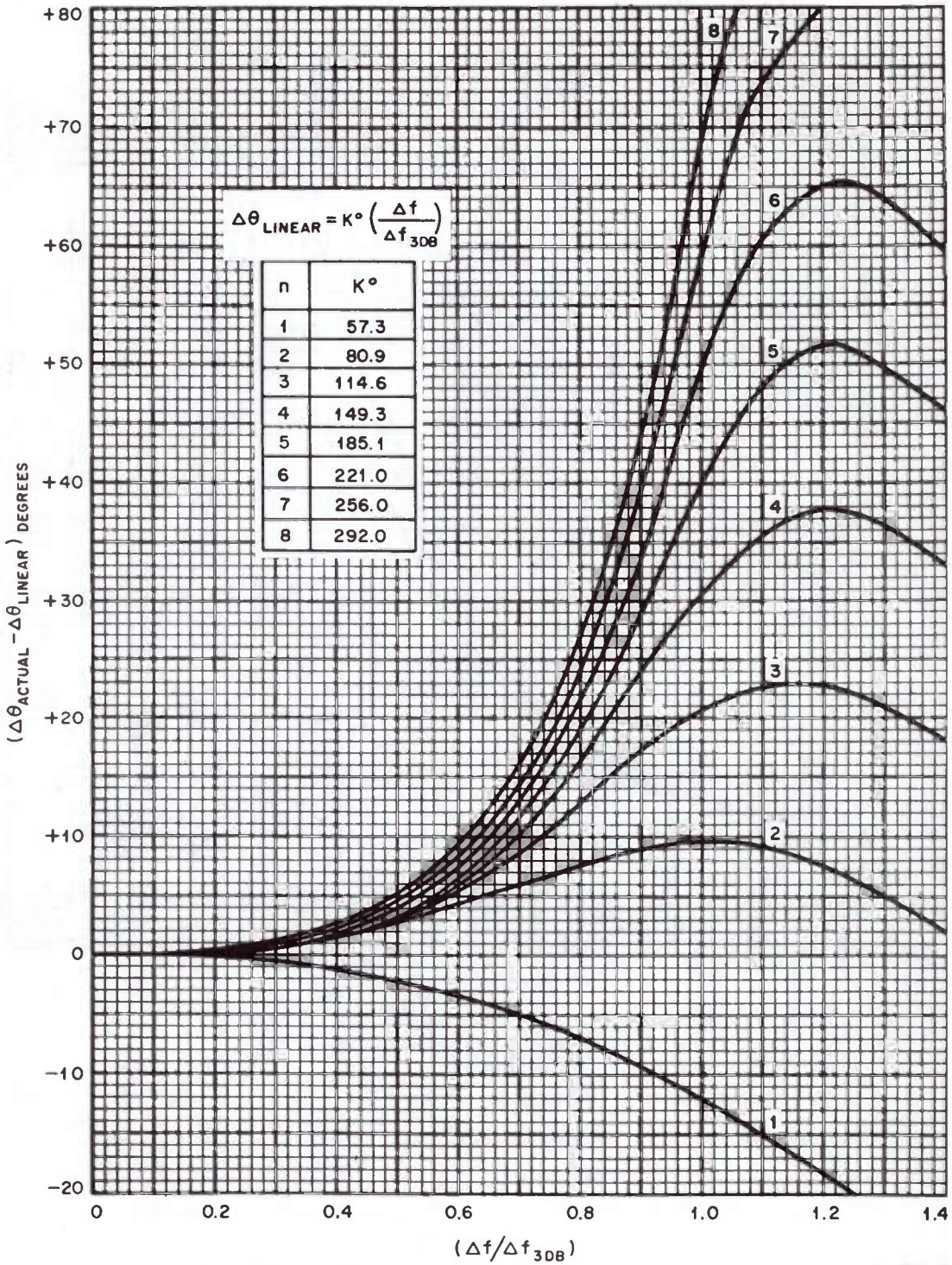

Fig. 14—Phase-shift distortion of Butterworth response shape.

we must have $(bw)_{50dB}/(bw)_{3dB}$ a little less than 2.5 when $(V_p/V)_{dB}=50$ decibels. Consulting Figs. 5 through 12 and examining curves for $(V_p/V_v)_{dB}=1.0$, it is found that a 5-pole network (Fig. 9) is the least that will meet the requirements. Here, curve 6 gives

$$(bw)_{50dB}/(bw)_{3dB}=2.14$$

while

$$(bw)_{1dB}/(bw)_{3dB}=0.97.$$

Then

$$(bw)_{50dB}/(bw)_{1dB}=2.14/0.97=2.20.$$

The 3-decibel frequency will be

$$30(bw)_{3dB}/(bw)_{1dB}=30/0.97=31 \text{ kilohertz.}$$

At this frequency, the Q of each capacitor and inductor must be at least equal to $q_{min}=11.8$ as shown in the table on Fig. 9.

(B) Consider a band-pass filter with requirements similar to the above: bandwidth 1 decibel down to be 30 kilohertz, 50 decibels down at 75-kilohertz bandwidth, and 1-decibel allowable ripple. Further, let the midfrequency be $f_0=500$ kilohertz. The solution at first is the same as above, and a 5-pole network is required.

The 3-decibel bandwidth is 31 kilohertz and the Q of each resonator must be at least

$$11.8\,f_0/(bw)_{3dB}=11.8\times500/31=190$$

where 11.8 is q_{min} as read from the table on Fig. 9. If a Q of 190 is not practical to attain, a greater number of resonators can be used. Suppose 7 resonators or poles are tried, per Fig. 11. Then curve 2 gives

$$(bw)_{50dB}/(bw)_{1dB}=2.10/0.93=2.26.$$

The table shows the peak-to-valley ratio of 10^{-5} decibel and $q_{min}=5.9$. The 3-decibel bandwidth is $30/0.93=32.2$ kilohertz. Then, the minimum Q of each resonator can be $5.9\times500/32.2=92$, which is less than half that required if 5 resonators are used.

(C) In the band-pass filter, suppose the filter is subdivided into N identical stages in cascade, isolated by active devices or decoupling capacitors or resistors. For each stage the response requirements are the original number of decibels divided by N. For $N=2$ stages

$$(bw)_{25dB}/(bw)_{0.5dB}<2.5$$

$$(V_p/V_v)_{dB}\leq0.5 \text{ decibel.}$$

Proceeding as before, it is found that a 3-pole network (Fig. 7) for each stage will just suffice, curve 4 giving

$$(V_p/V_v)_{dB}=0.3$$

and

$$(bw)_{25dB}/(bw)_{0.5dB}=2.1/0.84=2.5.$$

To find the required minimum Q of each of the 6 resonators, the 3-decibel bandwidth of each stage is

$$30/0.84=35.8 \text{ kilohertz.}$$

For curve 4, $q_{min}=3.4$, so the minimum allowable Q for each resonator is

$$3.4\times500/35.8=47.5.$$

Maximally Linear Phase Response

In the design of filters where the linearity of the phase characteristic inside the pass band is important, certain changes in design are necessary compared with the previously considered cases. For filters supplying only transfer-function poles, rate of change of phase with frequency becomes more and more linear as the number of arms is increased, provided the design produces a complex relative attenuation characteristic given by the polynomial of (6)*.

$$\frac{V_p}{V}=\frac{n!}{(2n)!}\sum_{r=0}^{n}\frac{2^r(2n-r)!}{r!(n-r)!}[j(x/x_\beta)^r] \qquad (6)$$

where r is a series of integers. The magnitude of (6) is plotted in Figs. 15 and 16 for several values of n.

The former is for the relative attenuation inside the 3-decibel points and the latter for the response outside these points. The curves for $n=\infty$ are plotted from (7), which is the Gaussian shape that the attenuation characteristic approaches as n approaches infinity.

$$10\log(V_p/V)^2=3(x/x_{3dB})^2. \qquad (7)$$

With a filter supplying only transfer-function poles, a maximally linear phase response can be produced only at the limitation of a rounded attenuation shape in the pass band as illustrated in Figs. 15 and 16.

The column labeled q_{min} on Fig. 15 gives the minimum allowable Q, measured at the 3-decibel-down frequency, of the inductors and capacitors of a low-pass filter. For band-pass filters, the minimum allowable unloaded Q at the midfrequency f_0 is $q_{min}f_0/(bw)_{3dB}$. For the phase response figures on Fig. 15, the symbols are as follows.

* W. E. Thomson, "Networks with Maximally Flat Delay," *Wireless Engineer*, vol. *29*, pp. 256–263; October 1952.

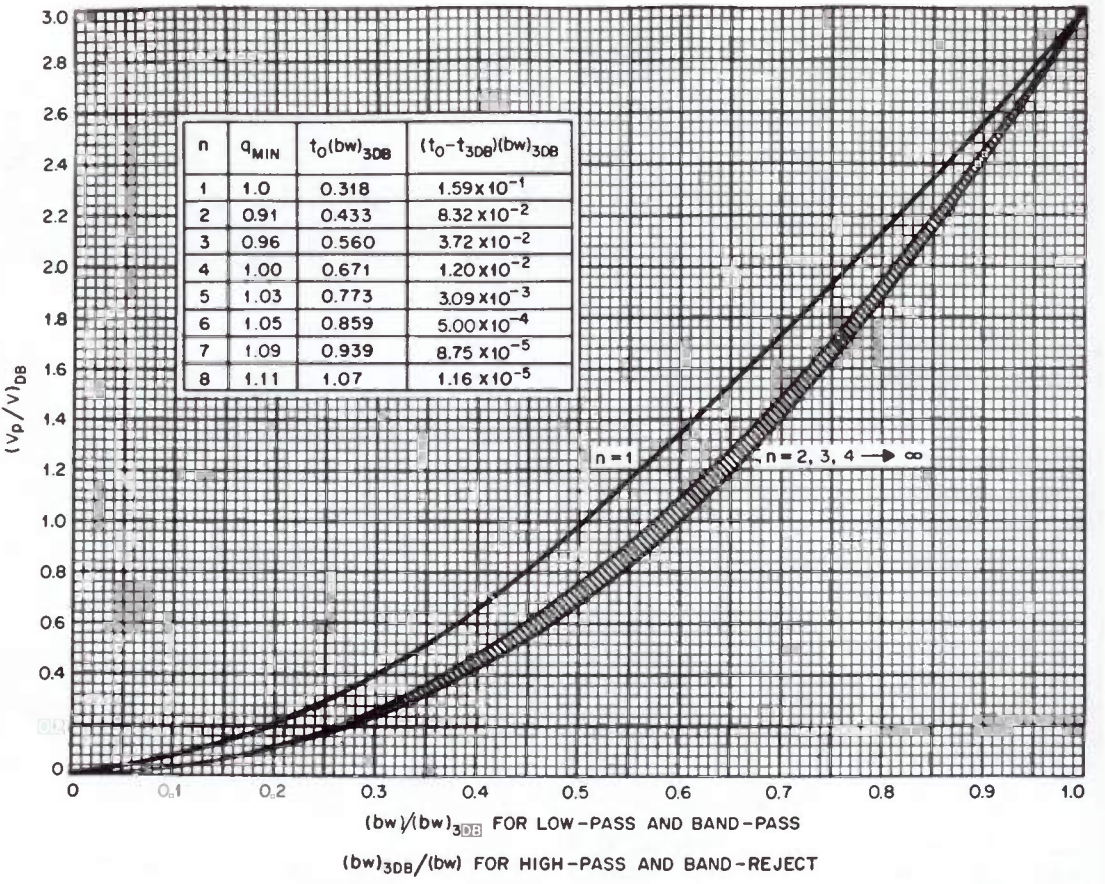

n	q_{MIN}	$t_0(bw)_{3DB}$	$(t_0-t_{3DB})(bw)_{3DB}$
1	1.0	0.318	1.59×10^{-1}
2	0.91	0.433	8.32×10^{-2}
3	0.96	0.560	3.72×10^{-2}
4	1.00	0.671	1.20×10^{-2}
5	1.03	0.773	3.09×10^{-3}
6	1.05	0.859	5.00×10^{-4}
7	1.09	0.939	8.75×10^{-5}
8	1.11	1.07	1.16×10^{-5}

Fig. 15—Attenuation shape within the 3-decibel-down pass band for n-pole maximally flat time-delay filters.

Low-Pass Filter:

$t_0 = d\theta/d\omega$

= slope of phase characteristic at zero frequency in radians per radian per second

t_{3dB} = slope at f_{3dB}

f_{3dB} = frequency of 3-decibel-down response

$(bw)_{3dB} = 2f_{3dB}$.

Band-Pass Filter:

t_0 = slope at midfrequency

t_{3dB} = slope at 3-decibel-down bandwidth

$(bw)_{3dB}$ = total 3-decibel bandwidth.

The column $(t_0 - t_{3dB})(bw)_{3dB}$ shows the *group-delay* distortion over the pass band. It shows numerically that the phase slope becomes much more constant as the number of elements is increased, in a filter designed for this purpose.

FILTERS SUPPLYING BOTH TRANSFER-FUNCTION POLES AND ZEROS

Typical attenuation curves for these filters are shown in Figs. 4D, E, and F. The modern network theory of these filters has been treated by Norton and by Darlington.* The attenuation shapes produced may be called elliptic and inverse-hyperbolic and are optimum in the sense that the rate of cutoff between the accept and reject bands is a maximum. Equation (8) gives the elliptic-function shape.

$$(V_p/V)^2 = 1 + [(V_p/V_v)^2 - 1] \times cd_v^2[n(K_v/K_f)cd_f^{-1}(x/x_v)] \quad (8)$$

where $cd = (cn/dn)$, the ratio of the two elliptic

* S. Darlington, "Synthesis of Reactance 4-Poles," *Journal of Mathematics and Physics*, vol. *18*, pp. 257–353, September 1939.

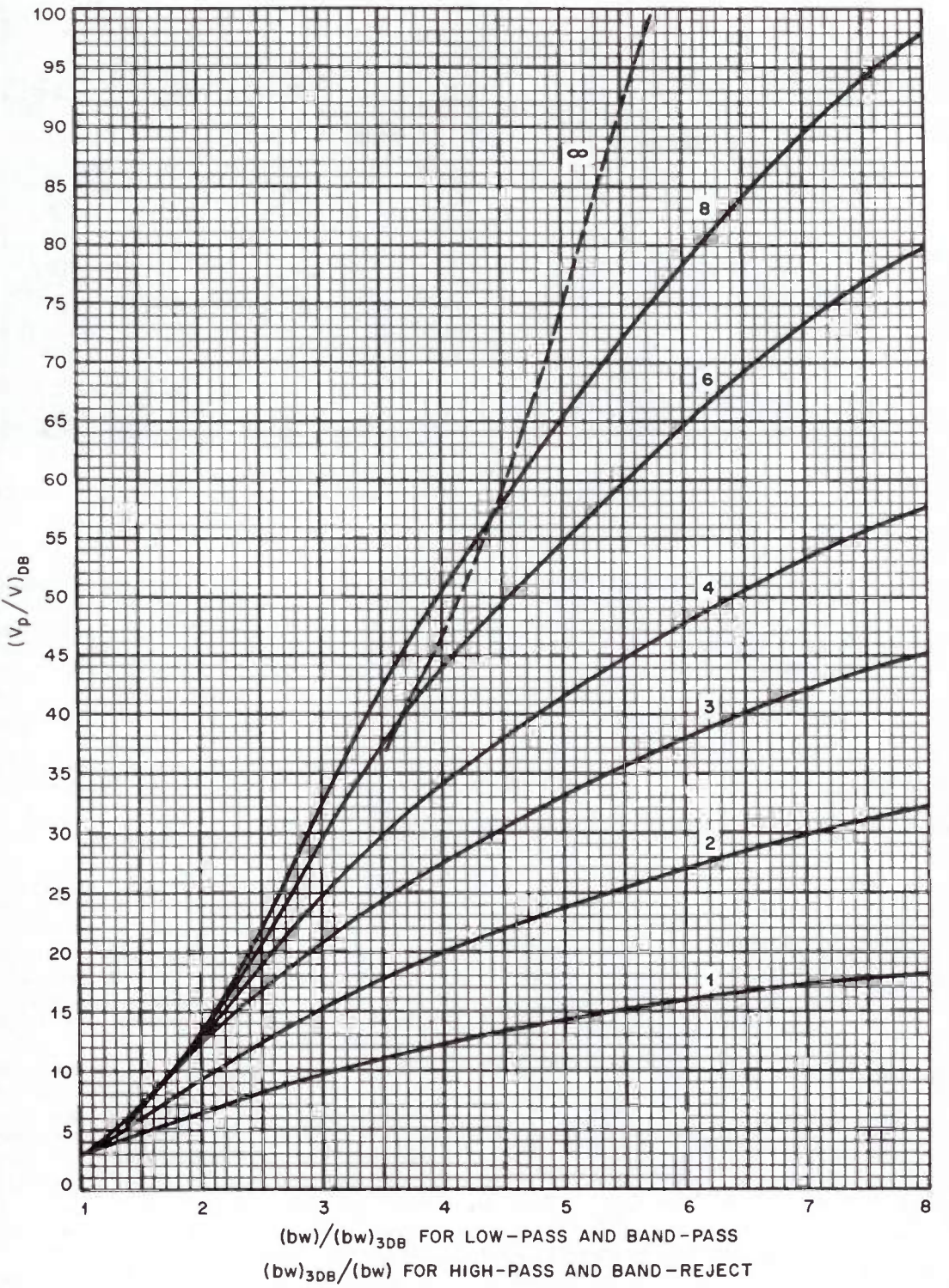

Fig. 16—Attenuation shape beyond 3-decibel-down pass band for n-pole maximally flat time-delay filters.

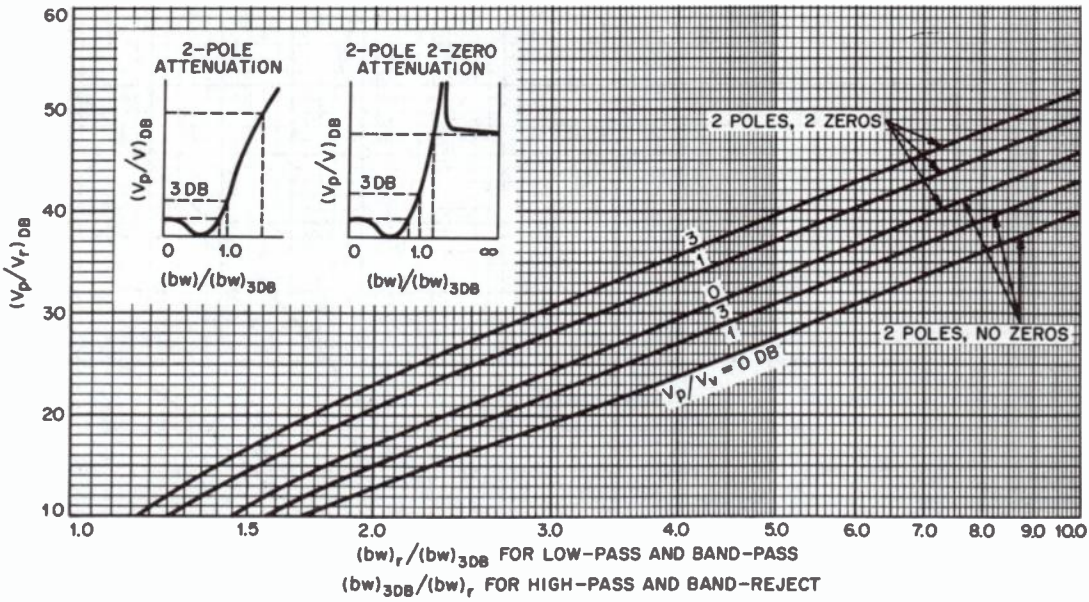

Fig. 17—Maximum rate of cutoff for 2-pole and for 2-pole 2-zero filters.

functions *cn* and *dn**, n= number of poles supplied by the filter, x= a bandwidth variable described under (5), and K_v, K_f= complete elliptic integrals of the first kind, evaluated for the modulus value given by the respective subscript.

Referring to the symbols on Fig. 4, the moduli v and f are given in (9) and (10).

$$v=\{[(V_p/V_v)^2-1]/[(V_p/V_h)^2-1]\}^{1/2} \quad (9)$$

$$f=x_v/x_n=(\text{bw})_v/(\text{bw})_h. \quad (10)$$

These are not independent, but must satisfy the equation

$$\log q_v=n \log q_f \quad (11)$$

where q_k is called the modular constant of the modulus value k, the latter being equal to v or f, respectively. A tabulation of log q is available in the literature.†

In the limit, when $V_p/V_v=1.0$ or zero decibels (Fig. 4F), the ripples in the accept band vanish. Then (8) reduces to the inverse hyperbolic shape of (12).

$$(V_p/V)^2=1+\frac{(V_p/V_h)^2-1}{\cosh^2[n \cosh^{-1}(x_h/x)]}. \quad (12)$$

Curves plotted from (8) and (12) are presented in Figs. 17 to 22. Those labeled $V_p/V_v=0$ decibels, for n poles, m zeros, are plotted from (12) while the others are from (8). For all these shapes, n= the number of poles= the number of arms in the ladder network. When n is an even number, the number of zeros $m=n$. When n is odd, $m=n-1$. The following description of Fig. 17 can be extended to cover the entire group of figures mentioned above.

The maximum rates of cutoff obtainable with 2-pole no-zero and 2-pole 2-zero networks are plotted in Fig. 17 for several ratios of V_p/V_v. Two insert sketches drawn in the figure show typical shapes of the attenuation curves for these two cases. The main curves give the relative coordinates of only two points on the skirt of the attenuation curve. These two points are the 3-decibel-down bandwidth and the "hill bandwidth" (where the response first equals that of the "response hills", where occurs the uniform minimum attenuation in the reject band). Thus each point specifies a different relative attenuation shape.

Comparison of the curves for 2 poles no-zero with those for 2 poles 2 zeros shows the improvement in cutoff rate that is obtainable when zeros are correctly added to the network. More-complete attenuation information on the 2-pole no-zero configuration has been presented on Fig. 6. Again, it is stressed that data of Figs. 6 and 17 represent the actual attenuation shapes and rate of cutoff attainable with filters using finite-Q elements (except for a rounding off of the infinite attenuation peaks). In contrast, the rates of cutoff and the attenuation shapes predicted by the simple "image" theory are unobtainable in physically realizable networks.

* G. W. and R. M. Spencely, "Smithsonian Elliptic Function Tables," (Publication 3863), Smithsonian Institution, Washington, D. C.; 1947.

† E. Jahnke and F. Emde, "Table of Functions with Formulas and Curves," 4th Edition, Dover Publications, New York, 1945: pp. 49–51.

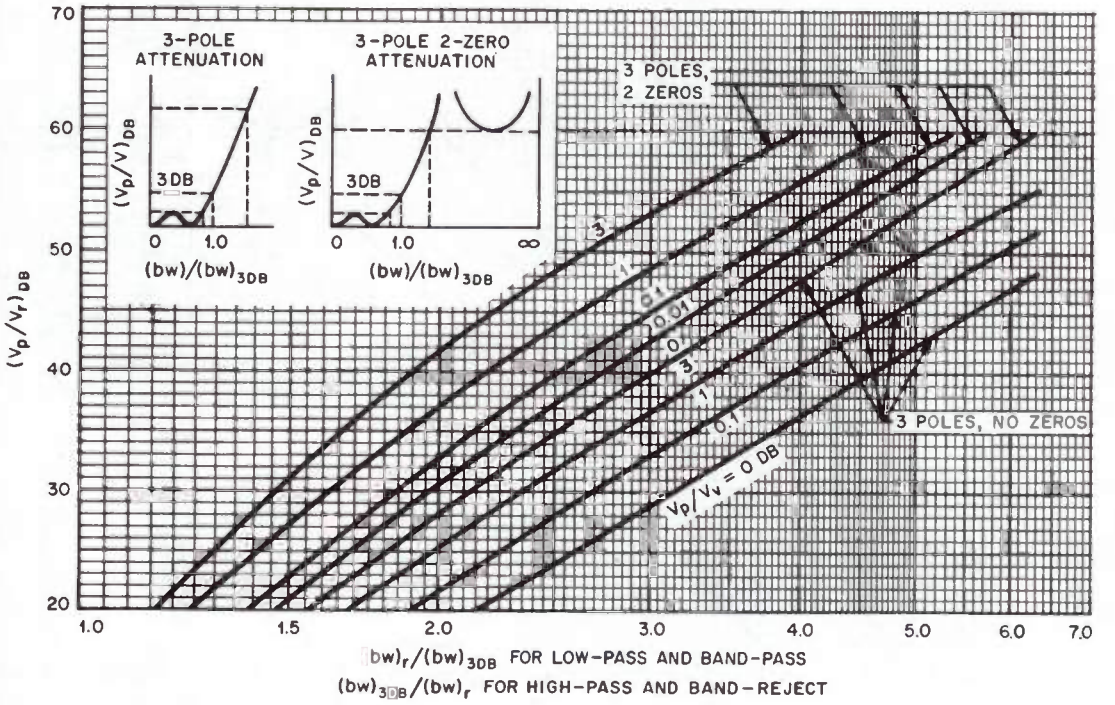

Fig. 18—Maximum rate of cutoff for 3-pole and for 3-pole 2-zero filters.

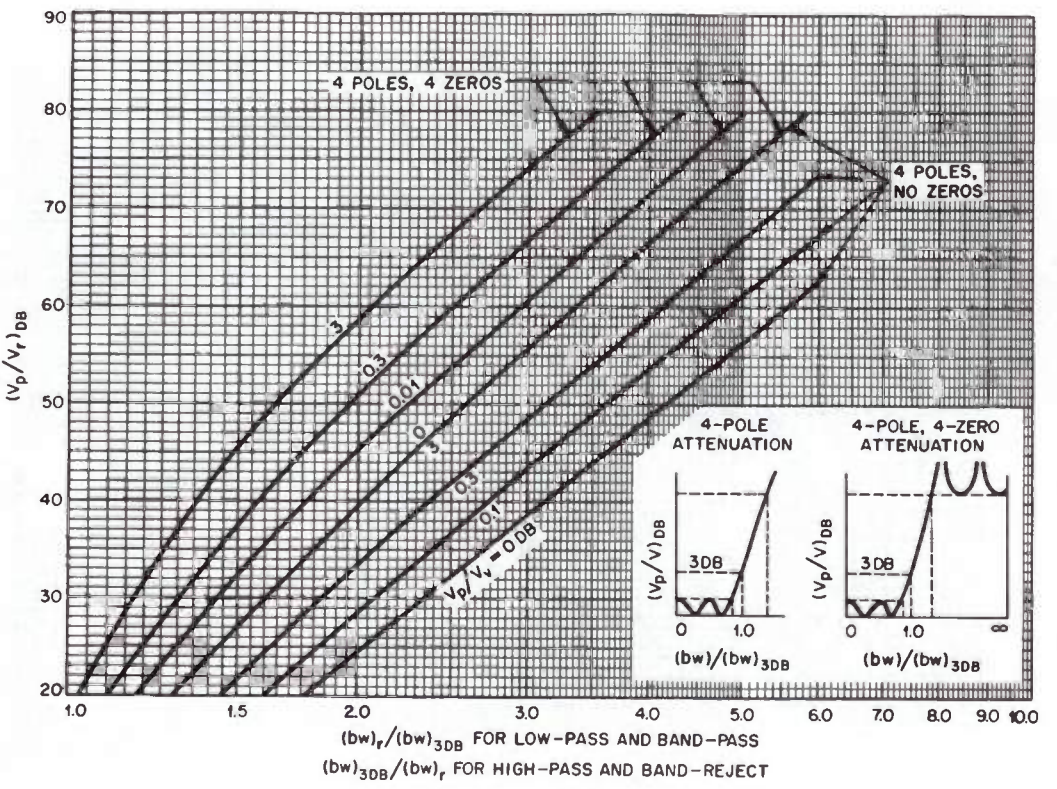

Fig. 19—Maximum rate of cutoff for 4-pole and for 4-pole 4-zero filters.

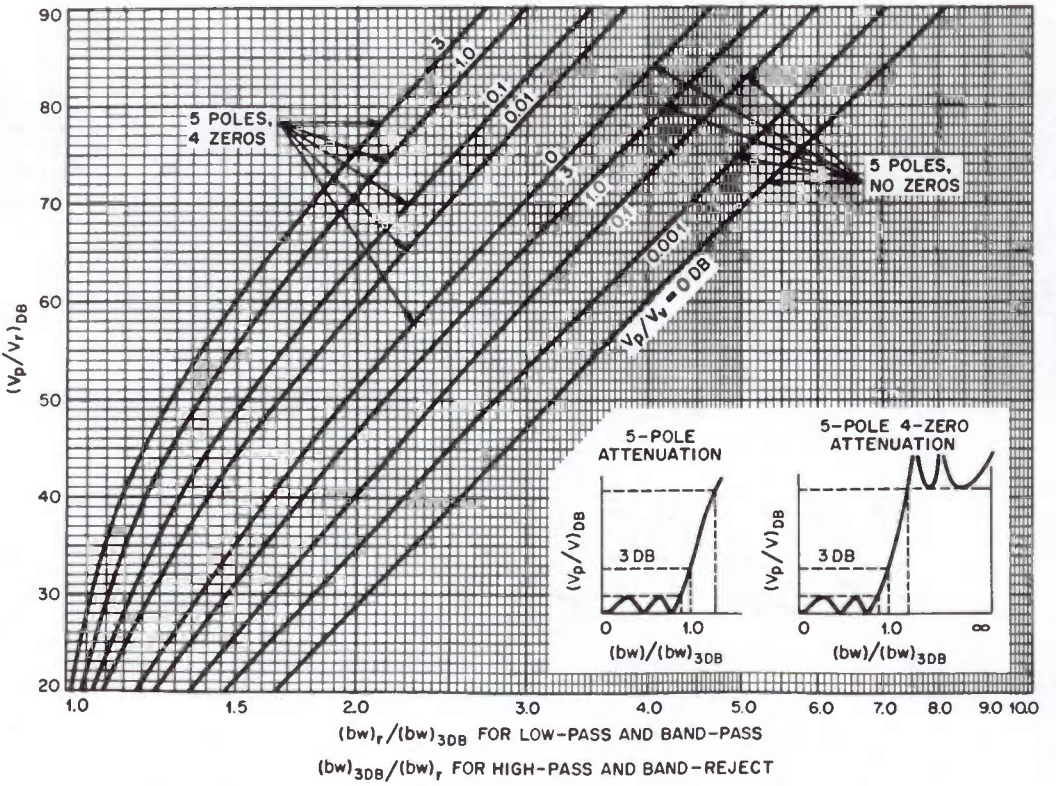

Fig. 20—Maximum rate of cutoff for 5-pole and for 5-pole 4-zero filters.

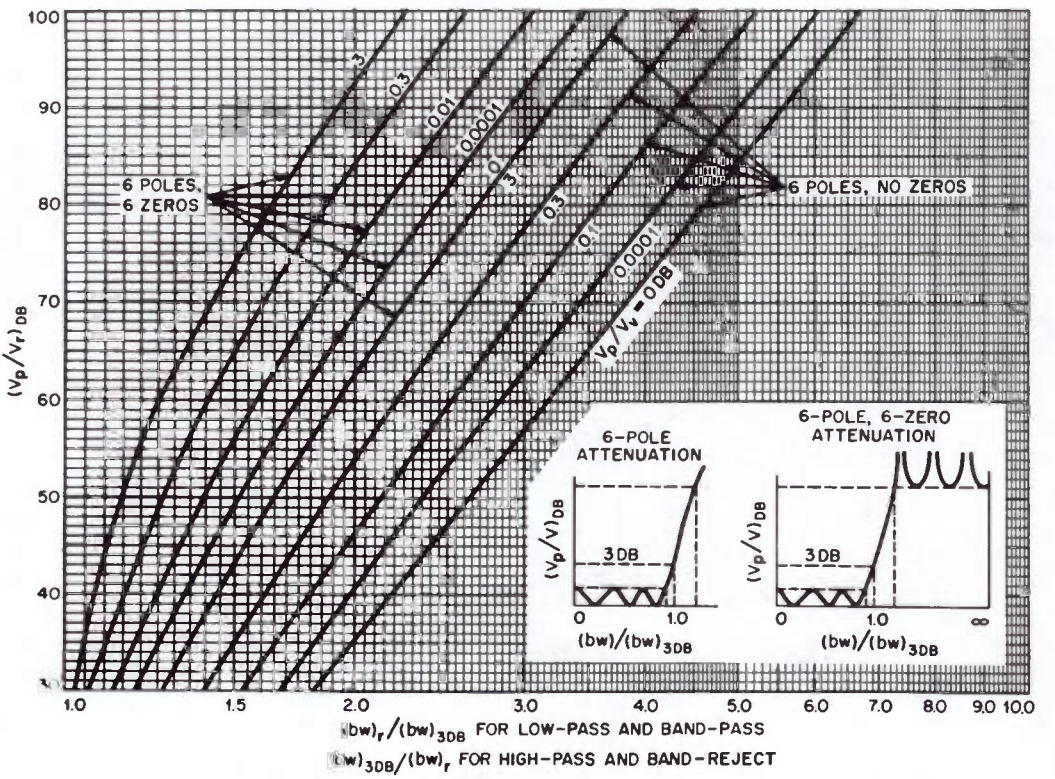

Fig. 21—Maximum rate of cutoff for 6-pole and for 6-pole 6-zero filters.

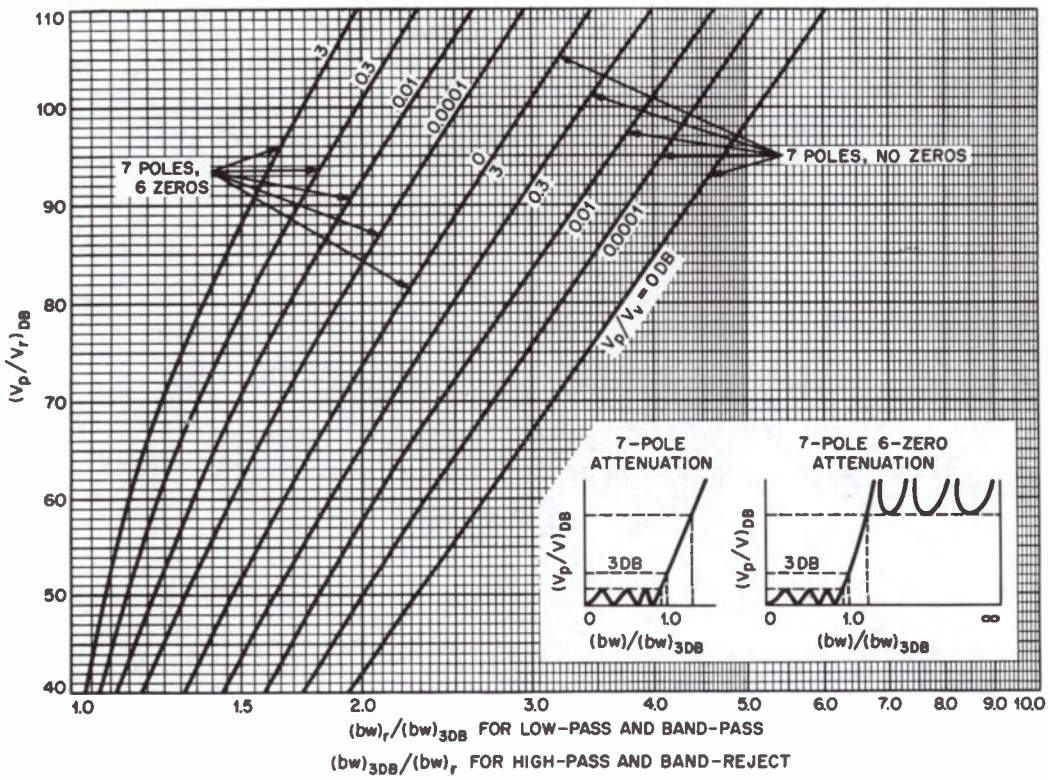

Fig. 22—Maximum rate of cutoff for 7-pole and for 7-pole 6-zero filters.

The rates of cutoff shown are the best that are possible of attainment with the specified number of poles and zeros, and with equal-ripple-type behavior.

Resistive Terminations and n Even

It is evident from the attenuation shapes of Figs. 17, 19, and 21 that for n even, the optimum shape given by (8) produces a finite attenuation at an infinite frequency. This requires a completely reactive termination at one end of the network. If resistive terminations must be used, then the optimum shape that is practically realizable with an even number of arms is given by

$$(V_p/V)^2=1+[(V_p/V_v)^2-1]cd_v^2[n(K_v u/K_f)] \tag{13}$$

where

$$u=sc_f^{-1}\{[(x_v/x)^2-1]^{1/2}[dn_f(K_f/n)]/f'\}. \tag{14}$$

The modulus v is given by (9) and the modulus f by (10). Solving (13) then gives the ratio of hill-to-valley bandwidth as

$$x_h/x_v=[fcd_f(K_f/n)]^{-1}. \tag{15}$$

This optimum attenuation shape (13) produces two fewer points of infinite rejection, or response zeros, than response poles. In contrast, (8) requires an equal number of zeros and poles.

If the ripples in the pass band approach zero decibels ($V_p/V_v=1$) then, as a limit, (13) becomes

$$(V_p/V)^2=1+\frac{(V_p/V_h)^2-1}{\cosh^2(n\cosh^{-1}y)} \tag{16}$$

where

$$y=\left[\left(\frac{x_h}{x}\cos\frac{90}{n}\right)^2+\sin^2\frac{90}{n}\right]^{1/2}.$$

Based on (13) and (16), the rates of cutoff have been plotted in Figs. 23 and 24 for 4-pole 2-zero and for 6-pole 4-zero filters. Figure 6 already has presented the data for a 2-pole no-zero network, the simplest case. An increase in rate of cutoff results when $n-2$ response zeros are suitably added to n response poles as shown by the curves in Figs. 23 and 24.

CIRCUIT-ELEMENT VALUES

This section concerns the values of the circuit elements required to produce the optimum relative-attenuation shapes of ladder-network filters supplying only transfer-function poles. There are two

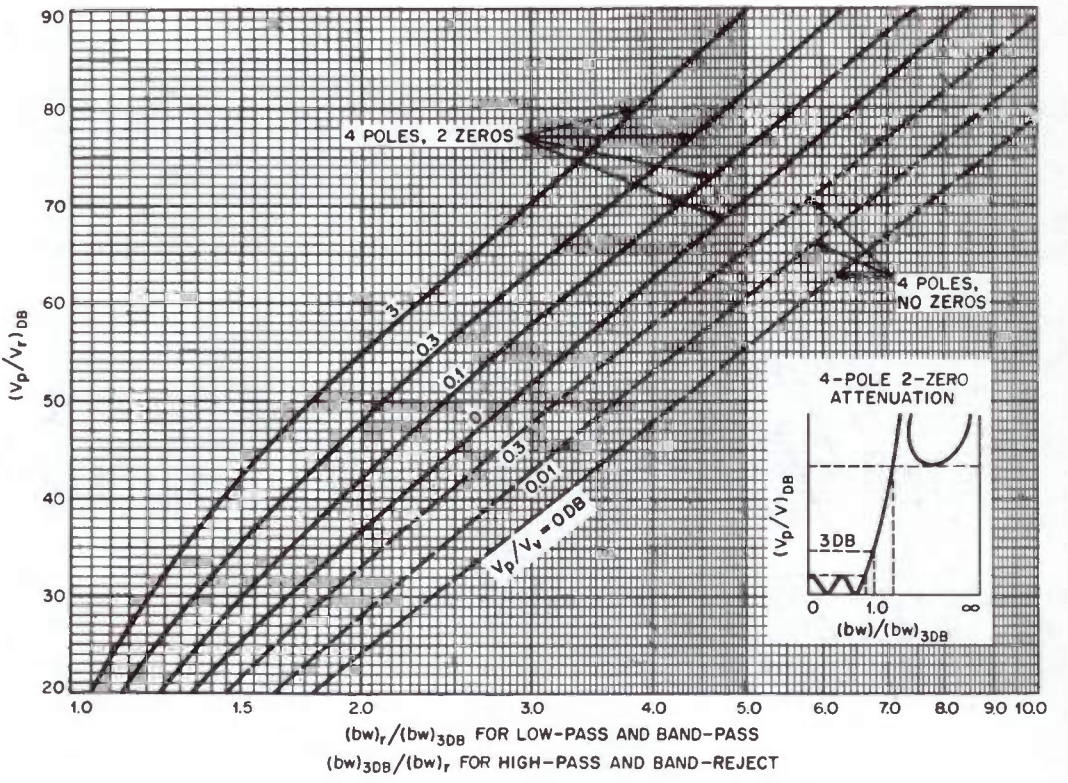

Fig. 23—Maximum rate of cutoff for 4-pole and for 4-pole 2-zero filters.

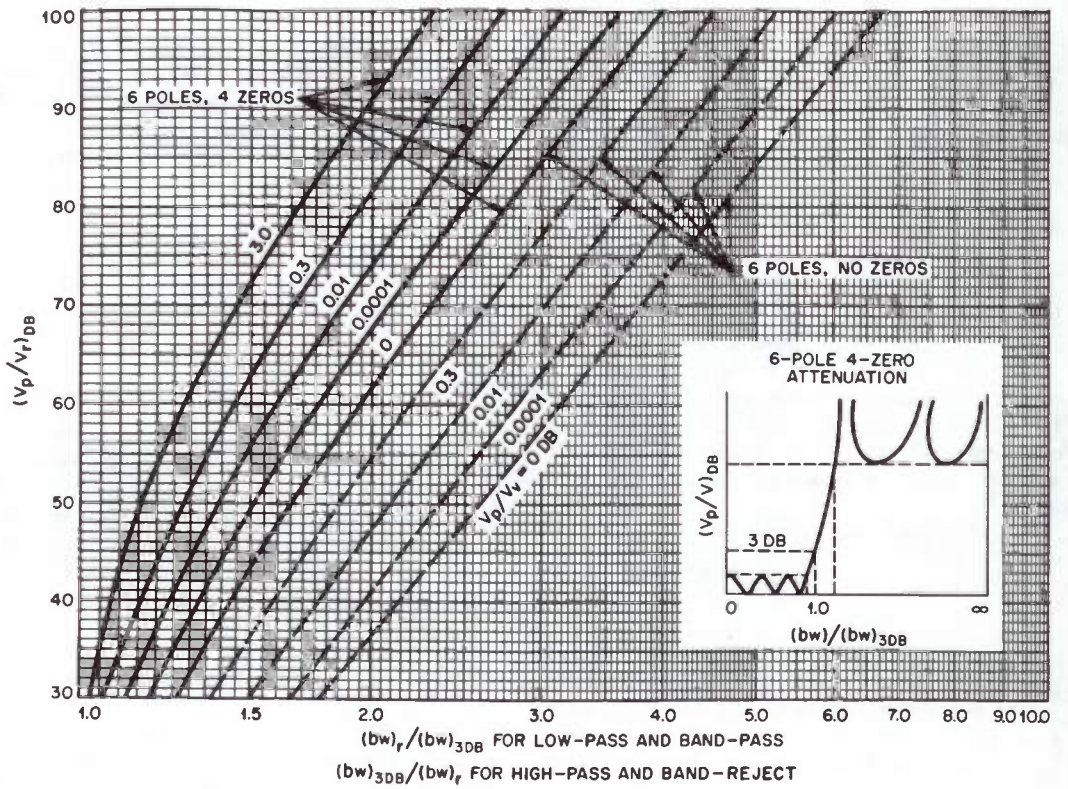

Fig. 24—Maximum rate of cutoff for 6-pole and for 6-pole 4-zero filters.

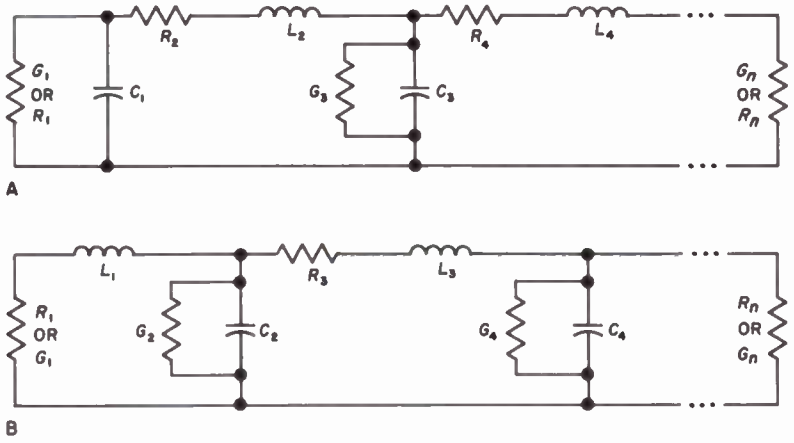

Fig. 25—Relations among normalized k and q and values of inductance, capacitance, and resistance for low-pass and large-percentage-band-pass circuits.

A—Shunt arm at one end. $1/(C_1L_2)^{\frac{1}{2}} = k_{12}\omega_{3\,dB}$, $1/(L_2C_3)^{\frac{1}{2}} = k_{23}\omega_{3\,dB}$, $1/(C_3L_4)^{\frac{1}{2}} = k_{34}\omega_{3\,dB}$, etc.
$G_1/C_1 = (1/q_1)\omega_{3\,dB}$, $q_2 = (\omega_{3\,dB}\ L_2)/R_2$, $q_3 = (\omega_{3\,dB}\ C_3)/G_3$, $q_4 = (\omega_{3\,dB}\ L_4)/R_4$, etc.
B—Series arm at one end. $1/(L_1C_2)^{\frac{1}{2}} = k_{12}\omega_{3\,dB}$, $1/(C_2L_3)^{\frac{1}{2}} = k_{23}\omega_{3\,dB}$, $1/(L_3C_4)^{\frac{1}{2}} = k_{34}\omega_{3\,dB}$, etc.
$R_1/L_1 = (1/q_1)\omega_{3\,dB}$, $q_2 = (\omega_{3\,dB}\ C_2)/G_2$, $q_3 = (\omega_{3\,dB}\ L_3)/R_3$, $q_4 = (\omega_{3\,dB}\ C_4)/G_4$, etc.

To design a band-pass circuit that supplies a frequency response having geometric symmetry, the total required 3-decibel-down bandwidth should replace $\omega_{3\,dB}$, an inductor should be connected across each shunt capacitor, and a capacitor put in series with each series inductor, each such circuit being resonated to the geometric mean frequency $f_0 = (f_1 f_2)^{\frac{1}{2}}$.

convenient ways of expressing the element values for these ladder networks.

(A) The reactive and resistive components of each element may be related to one of the terminating resistances (or to a completely arbitrary normalizing resistance R_0) and also to a definite bandwidth, usually the 3-decibel-down value. The numerical results are called ladder-network coefficients or singly loaded Q's.

(B) The reactive component of each element may be related to the reactive part of the immediately preceding element, and to a definite bandwidth such as the 3-decibel-down value. These numerical results are called the normalized coefficients of coupling. The resistive component of each element is related to its reactive part and the numerical values are called normalized decrements or, when inverted, normalized Q's.

The latter form of normalized coefficients of coupling k and normalized Q's $(=q)$ will be used because the numerical values may be applied directly to the adjustment and checking of actual filters.

Figures 25 through 29 relate the normalized k and q to the inductance, capacitance, and resistance values for various types of filters.

For low-pass filters, Fig. 25 shows that k gives the ratio of resonant frequency of two immediately adjacent elements to the overall 3-decibel-down frequency. The resonant frequency of C_1 and L_2 in this example must be k_{12} times the required overall 3-decibel-down bandwidth.

Figure 25 also gives, as the inverse of q, the ratio of the 3-decibel-down bandwidth of a single element resulting from the resistive load and losses associated with it, to the required 3-decibel-down bandwidth of the overall filter. Thus, $1/R_1C_1$ is the 3-decibel-down radian bandwidth of C_1 and the conductance G_1 that must be shunted across it. If C_1 and G_1 are properly chosen, the measured

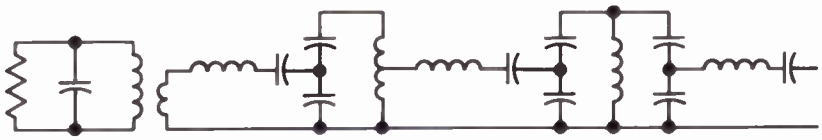

Fig. 26—Band-pass circuit supplying a frequency response having geometric symmetry. Parallel and series circuits must alternate, and Figs. 1 and 2 of Chapter 9 give the relationship between element values and resulting actual coefficient of coupling $K\{=k[(\mathrm{bw})_{3\,dB}/f_0]\}$. Any adjacent pair of resonators may be coupled by any of the methods shown.

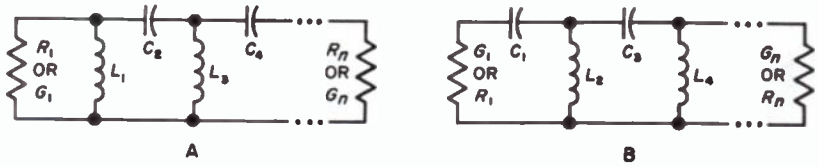

Fig. 27—Relations among normalized k and q and values of inductance, capacitance, and resistance for high-pass and large-percentage-band-reject circuits.

A—Shunt arm at one end. $1/(L_1C_2)^{\frac{1}{2}}=(1/k_{12})\omega_{3dB}$, $1/(C_2L_3)^{\frac{1}{2}}=(1/k_{23})\omega_{3dB}$, $1/(L_3C_4)^{\frac{1}{2}}=(1/k_{34})\omega_{3dB}$, etc. $(R_1/L_1)=q_1\omega_{3dB}$. All reactances are assumed to be lossless.

B—Series arm at one end. $1/(C_1L_2)^{\frac{1}{2}}=(1/k_{12})\omega_{3dB}$, $1/(L_2C_3)^{\frac{1}{2}}=(1/k_{23})\omega_{3dB}$, $1/(C_3L_4)^{\frac{1}{2}}=(1/k_{34})\omega_{3dB}$, etc. $(G_1/C_1)=q_1\omega_{3dB}$. All reactances are assumed to be lossless.

To design a band-reject circuit supplying a frequency response having geometric symmetry, the total required 3-decibel-down bandwidth should replace ω_{3dB}, a capacitor should be placed in series with each shunt inductor, and an inductor in shunt of each series capacitor, each such circuit being resonated to the geometric mean frequency $f_0=(f_1f_2)^{\frac{1}{2}}$.

bandwidth of these elements at their 3-decibel-down point will be $1/q_1$ times the required overall 3-decibel-down bandwidth of the filter.

The legend of Fig. 25 shows how it is applicable also to large-percentage band-pass filters.

When the procedure of Fig. 25 is used to design band-pass circuits of medium- or small-percentage bandwidths, the resulting element value ratios become impractical to obtain. The circuit configuration shown in Fig. 26 gives practical element value ratios for these two cases, while still providing true geometric symmetry.

Figure 27 gives the required information for high-pass and large-percentage band-reject filters.

Similar data are given in Fig. 28 for small-percentage band-pass filters. It should be noted that the required actual coefficient of coupling between resonant circuits, $M_{ab}/(L_aL_b)^{1/2}$ for example, is obtained by multiplying the required overall fractional 3-decibel-down bandwidth by the normalized coefficient of coupling. The required actual resonant-circuit Q results from multiplying the fractional midfrequency by q. An experimental procedure for checking k and q values is available.* Fractional midfrequency $f_0/(\text{bw})_{3dB}$= reciprocal of fractional 3-decibel-down bandwidth.

Figure 29 supplies the data for small-percentage band-reject filters.

TABLE 1—TWO-POLE NO-ZERO FILTER 3-DECIBEL-DOWN k AND q VALUES.

$(V_p/V_v)_{dB}$	q_1	k_{12}	q_2
Maximum-power-transfer terminations			
Linear phase	0.576	0.899	2.15
0	1.414	0.707	1.414
0.3	1.82	0.717	1.82
1.0	2.21	0.739	2.21
3.0	3.13	0.779	3.13
Resistive termination at only one end			
Linear phase	0.455	1.27	∞
0	0.707	1.00	∞
0.3	0.910	0.904	∞
1.0	1.11	0.866	∞
3.0	1.56	0.840	∞

Butterworth, Chebishev, and Maximally Linear Phase Designs

Elegant closed-form equations for k and q values producing optimum Chebishev and Butterworth

TABLE 2—THREE-POLE NO-ZERO FILTER 3-DECIBEL-DOWN k AND q VALUES.

$(V_p/V_v)_{dB}$	q_2	q_1	k_{12}	k_{23}	q_3
Maximum-power-transfer terminations					
Linear phase	∞	0.338	1.74	0.682	2.21
0	∞	1.00	0.707	0.707	1.00
0.1	∞	1.43	0.665	0.665	1.43
1.0	∞	2.21	0.645	0.645	2.21
3.0	∞	3.36	0.647	0.647	3.36
Resistive termination at only one end					
Linear phase	∞	0.293	2.01	0.899	∞
0	∞	0.500	1.22	0.707	∞
0.1	∞	0.714	0.961	0.661	∞
1.0	∞	1.11	0.785	0.645	∞
3.0	∞	1.68	0.714	0.649	∞

* M. Dishal, "Alignment and Adjustment of Synchronously Tuned Multiple-Resonant-Circuit Filters," *Proceedings of the IRE*, vol. 39, pp. 1448–1455; November 1951: Also, *Electrical Communication*, vol. 29, pp. 154–161; June 1952.

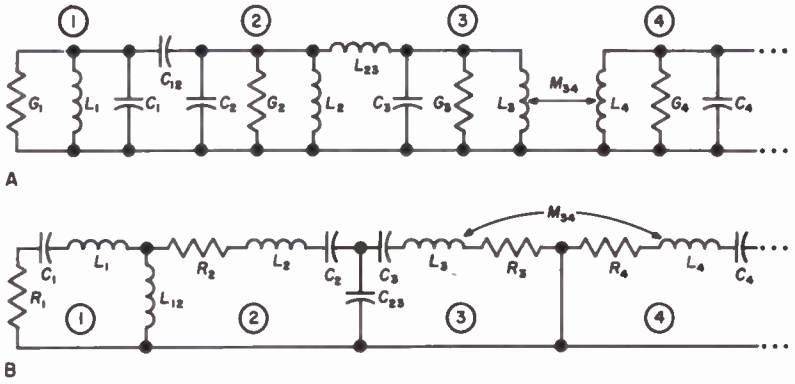

Fig. 28—Relations among normalized k and q and values of inductance, capacitance, and resistance for small-percentage-band-pass circuits.

A—Parallel-resonant circuits. $C_{12}/(C_1C_2)^{\frac{1}{2}} \doteq k_{12}[(\text{bw})_{3\text{dB}}/f_0]$, $(L_2L_3)^{\frac{1}{2}}/L_{23} \doteq k_{23}[(\text{bw})_{3\text{dB}}/f_0]$, $M_{34}/(L_3L_4)^{\frac{1}{2}} \doteq k_{34}[(\text{bw})_{3\text{dB}}/f_0]$, etc. $Q_1 = q_1[f_0/(\text{bw})_{3\text{dB}}]$, $q_2 = Q_2/[f_0/(\text{bw})_{3\text{dB}}]$, $q_3 = Q_3/[f_0/(\text{bw})_{3\text{dB}}]$, $q_4 = Q_4/[f_0/(\text{bw})_{3\text{dB}}]$, etc. Any adjacent pair of resonators may be coupled by any of the three methods shown. Each node must resonate at f_0 with all other nodes short-circuited.

B—Series-resonant circuits. $L_{12}/(L_1L_2)^{\frac{1}{2}} \doteq k_{12}[(\text{bw})_{3\text{dB}}/f_0]$, $(C_2C_3)^{\frac{1}{2}}/C_{23} \doteq k_{23}[(\text{bw})_{3\text{dB}}/f_0]$, $M_{34}/(L_3L_4)^{\frac{1}{2}} \doteq k_{34}[(\text{bw})_{3\text{dB}}/f_0]$, etc. $Q_1 = q_1[f_0/(\text{bw})_{3\text{dB}}]$, $q_2 = Q_2/[f_0/(\text{bw})_{3\text{dB}}]$, $q_3 = Q_3/[f_0/(\text{bw})_{3\text{dB}}]$, $q_4 = Q_4/[f_0/(\text{bw})_{3\text{dB}}]$. Any adjacent pair of resonators may be coupled by any of the three methods shown. Each mesh must resonate at f_0 with all other meshes open-circuited.

response shapes for filters having any number of total arms may be obtained if lossless reactances are used.* The design data in Tables 1 through 7 are based on such equations. The k and q values for the maximally linear phase shape result from the Darlington synthesis procedure applied to (6). The tables provide data for two limiting cases of terminations; maximum-power-transfer loading at the two ends of the filter and resistive loading at only one end.

For Tables 1 through 7, the $(V_p/V_v)_{\text{dB}}$ column gives the ripple in decibels in the pass band, and the corresponding curves on Figs. 5 through 12 give the complete attenuation shape.

For low-pass circuits, $q_{2,3,4,\cdots}$, is the required unloaded Q, measured at the required 3-decibel-down frequency, of the internal inductors and capacitors to be used. For band-pass circuits, the unloaded resonator Q required in the internal resonators is obtained by multiplying the required 3-decibel fractional midfrequency $[f_0/(\text{bw})_{3\text{dB}}]$ by $q_{2,3,4,\cdots}$.

For the detailed way in which the q and k columns fix the required element values, see Figs. 25 through 29 and related discussion.

The first column of each table gives the peak-to-valley ratio within the pass band.

To be exactly correct, the design values given in the tables require that (as shown in the second column of each table except Table 1) infinite unloaded Q's be available for the internal elements of the filter. It should be realized that designs can be made using elements having finite unloaded Q's; these designs are given in Figs. 30 through 56.

Proceeding across each table, figuratively from the left end of the filter, the next column gives q_1 from which, with the aid of Figs. 25 through 29, the relation between the terminating resistance R_1 and the first reactance element is obtained. The next column for k_{12} (with Figs. 25 through 29) provides for the relation between the first and second reactances. Continuing across each table, all relations between adjacent elements are obtained including that of the right-hand terminating resistance.

Example: Reverting to the previous example, a filter is required having $(\text{bw})_{60\text{dB}}/(\text{bw})_{1\text{dB}} = 2.5$, and $V_p/V_v < 1$ decibel. The 5-pole no-zero response with a pass-band peak-to-valley ratio of 1 decibel in Fig. 9 satisfied the requirement.

Table 4 is for 5-pole networks and, if the terminations are to be maximum-power-transfer loads, the upper part of the table should be used. If a shunt capacitance is to appear at one end of the low-pass filter, Fig. 25A will apply.

* V. Belevitch, "Tchebyshev Filters and Amplifier Networks," *Wireless Engineer*, vol. 29, pp. 106–110; April 1952. H. J. Orchard, "Formulas for Ladder Filters," *Wireless Engineer*, vol. 30, pp. 3–5; January 1953. E. Green, "Exact Amplitude–Frequency Characteristics of Ladder Networks," *Marconi Review*, vol. 16, no. 108, pp. 25–68; 1953. M. Dishal, "Two New Equations for the Design of Filters," *Electrical Communication*, vol. 30, pp. 324–337; December 1952.

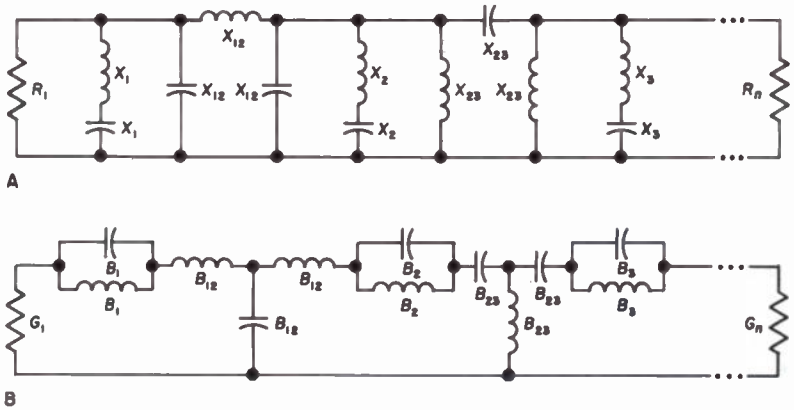

Fig. 29—Relations among normalized k and q and values of inductance, capacitance, and resistance for small-percentage-band-reject circuits.

A—Series-resonant circuits. $X_{12}/(X_1X_2)^{\frac{1}{2}}=(1/k_{12})[(\text{bw})_{3\text{dB}}/f_0]$, $X_{23}/(X_2X_3)^{\frac{1}{2}}=(1/k_{23})[(\text{bw})_{3\text{dB}}/f_0]$, etc. $X_1/R_1=(1/q_1)[f_0(\text{bw})_{3\text{dB}}]$, $X_n/R_n=(1/q_n)[f_0/(\text{bw})_{3\text{dB}}]$. All resonant circuits are assumed to be lossless. Any adjacent pair of resonators may be coupled by either of the two π (or their dual T) couplings shown. The reactances X are measured at the midfrequency of the reject band.

B—Parallel-resonant circuits. $B_{12}/(B_1B_2)^{\frac{1}{2}}=(1/k_{12})[(\text{bw})_{3\text{dB}}/f_0]$, $B_{23}/(B_2B_3)^{\frac{1}{2}}=(1/k_{23})[(\text{bw})_{3\text{dB}}/f_0]$, etc. $B_1/G_1=(1/q_1)[f_0/(\text{bw})_{3\text{dB}}]$, $B_n/G_n=(1/q_n)[f_0/(\text{bw})_{3\text{dB}}]$.

All resonant circuits are assumed to be lossless. Any adjacent pair of resonators may be coupled by either of the two T (or their dual π) couplings shown. The susceptances B are measured at the midfrequency of the reject band.

TABLE 3—FOUR-POLE NO-ZERO FILTER 3-DECIBEL-DOWN k AND q VALUES.

$(V_p/V_v)_{\text{dB}}$	$q_{2,3}$	q_1	k_{12}	k_{23}	k_{34}	q_4
Maximum-power-transfer terminations						
Linear phase	∞	2.24	0.644	1.175	2.53	0.233
0	∞	0.766	0.840	0.542	0.840	0.766
0.01	∞	1.05	0.737	0.541	0.737	1.05
0.1	∞	1.34	0.690	0.542	0.690	1.34
1.0	∞	2.21	0.638	0.546	0.638	2.21
3.0	∞	3.45	0.624	0.555	0.624	3.45
Resistive termination at only one end						
Linear phase	∞	0.211	2.78	1.29	0.828	∞
0	∞	0.383	1.56	0.765	0.644	∞
0.01	∞	0.524	1.20	0.666	0.621	∞
0.1	∞	0.667	1.01	0.626	0.618	∞
1.0	∞	1.10	0.781	0.578	0.614	∞
3.0	∞	1.72	0.692	0.567	0.609	∞

TABLE 4—FIVE-POLE NO-ZERO FILTER 3-DECIBEL-DOWN k AND q VALUES.

$(V_p/V_v)_{dB}$	$q_{2,3,4}$	q_1	k_{12}	k_{23}	k_{34}	k_{45}	q_5
			Maximum-power-transfer terminations				
Linear phase	∞	0.175	3.36	1.56	1.06	0.631	2.26
0	∞	0.618	1.0	0.556	0.556	1.0	0.618
0.001	∞	0.822	0.845	0.545	0.545	0.845	0.822
0.1	∞	1.29	0.703	0.535	0.535	0.703	1.29
1.0	∞	2.21	0.633	0.538	0.538	0.633	2.21
3.0	∞	3.47	0.614	0.538	0.538	0.614	3.47
			Resistive termination at only one end				
Linear phase	∞	0.162	3.62	1.68	1.14	0.804	∞
0	∞	0.309	1.90	0.900	0.655	0.619	∞
0.001	∞	0.412	1.48	0.760	0.603	0.606	∞
0.1	∞	0.649	1.044	0.634	0.560	0.595	∞
1.0	∞	1.105	0.779	0.570	0.544	0.595	∞
3.0	∞	1.74	0.679	0.554	0.542	0.597	∞

TABLE 5—SIX-POLE NO-ZERO FILTER 3-DECIBEL-DOWN k AND q VALUES.

$(V_p/V_v)_{dB}$	$q_{2,3,4,5}$	q_1	k_{12}	k_{23}	k_{34}	k_{45}	k_{56}	q_6
				Maximum-power-transfer terminations				
0	∞	0.518	1.17	0.606	0.518	0.606	1.17	0.518
0.0001	∞	0.679	0.967	0.573	0.518	0.573	0.967	0.679
0.01	∞	0.936	0.810	0.550	0.518	0.550	0.810	0.936
0.1	∞	1.27	0.716	0.539	0.518	0.539	0.716	1.27
1.0	∞	2.21	0.631	0.531	0.520	0.531	0.631	2.21
3.0	∞	3.51	0.610	0.532	0.524	0.532	0.610	3.51
				Resistive termination at only one end				
Linear phase	∞	0.129	4.55	2.09	1.42	1.09	0.803	∞
0	∞	0.259	2.26	1.05	0.732	0.606	0.606	∞
0.0001	∞	0.340	1.76	0.869	0.650	0.573	0.596	∞
0.01	∞	0.468	1.34	0.725	0.591	0.550	0.591	∞
0.1	∞	0.637	1.06	0.642	0.560	0.539	0.589	∞
1.0	∞	1.12	0.771	0.566	0.533	0.531	0.589	∞
3.0	∞	1.75	0.673	0.546	0.529	0.531	0.591	∞

TABLE 6—SEVEN-POLE NO-ZERO FILTER 3-DECIBEL-DOWN k AND q VALUES.

$(V_p/V_v)_{dB}$	$q_{2,3,4,5,6}$	q_1	k_{12}	k_{23}	k_{34}	k_{45}	k_{56}	k_{67}	q_7
				Maximum-power-transfer terminations					
0	∞	0.445	1.34	0.669	0.528	0.528	0.669	1.34	0.445
0.00001	∞	0.580	1.10	0.611	0.521	0.521	0.611	1.10	0.580
0.001	∞	0.741	0.930	0.579	0.519	0.519	0.579	0.930	0.741
0.01	∞	0.912	0.830	0.560	0.519	0.519	0.560	0.830	0.912
0.1	∞	1.26	0.723	0.541	0.517	0.517	0.541	0.723	1.26
1.0	∞	2.25	0.631	0.530	0.517	0.517	0.530	0.631	2.25
3.0	∞	3.52	0.607	0.529	0.519	0.519	0.529	0.607	3.52
				Resistive termination at only one end					
Linear phase	∞	0.105	5.53	2.53	1.72	1.33	1.08	0.804	∞
0	∞	0.223	2.62	1.20	0.824	0.659	0.579	0.598	∞
0.00001	∞	0.290	2.05	0.981	0.710	0.601	0.552	0.589	∞
0.001	∞	0.370	1.64	0.830	0.642	0.570	0.541	0.588	∞
0.01	∞	0.456	1.38	0.744	0.602	0.551	0.538	0.588	∞
0.1	∞	0.629	1.08	0.648	0.560	0.531	0.530	0.587	∞
1.0	∞	1.12	0.770	0.564	0.530	0.521	0.527	0.587	∞
3.0	∞	1.76	0.669	0.542	0.523	0.520	0.528	0.588	∞

TABLE 7—EIGHT-POLE NO-ZERO FILTER 3-DECIBEL-DOWN k AND q VALUES.

$(V_p/V_v)_{dB}$	$q_{2,3,4,5,6,7}$	q_1	k_{12}	k_{23}	k_{34}	k_{45}	k_{56}	k_{67}	k_{78}	q_8
					Maximum-power-transfer terminations					
0	∞	0.391	1.52	0.734	0.551	0.510	0.551	0.734	1.52	0.391
0.00001	∞	0.545	1.16	0.640	0.534	0.510	0.534	0.640	1.16	0.545
0.001	∞	0.717	0.960	0.592	0.524	0.510	0.524	0.592	0.960	0.717
0.01	∞	0.896	0.843	0.567	0.520	0.510	0.520	0.567	0.843	0.896
0.1	∞	1.25	0.727	0.545	0.516	0.510	0.516	0.545	0.727	1.25
1.0	∞	2.20	0.633	0.530	0.514	0.511	0.514	0.530	0.633	2.20
3.0	∞	3.53	0.605	0.527	0.515	0.513	0.515	0.527	0.605	3.53
					Resistive termination at only one end					
0	∞	0.199	2.98	1.36	0.920	0.721	0.615	0.562	0.591	∞
0.00001	∞	0.272	2.17	1.04	0.749	0.627	0.567	0.543	0.587	∞
0.001	∞	0.358	1.69	0.859	0.660	0.580	0.544	0.535	0.584	∞
0.01	∞	0.448	1.40	0.755	0.610	0.556	0.533	0.529	0.583	∞
0.1	∞	0.627	1.08	0.651	0.564	0.534	0.523	0.525	0.582	∞
1.0	∞	1.10	0.779	0.567	0.531	0.519	0.516	0.523	0.583	∞
3.0	∞	1.76	0.668	0.541	0.522	0.516	0.516	0.524	0.585	∞

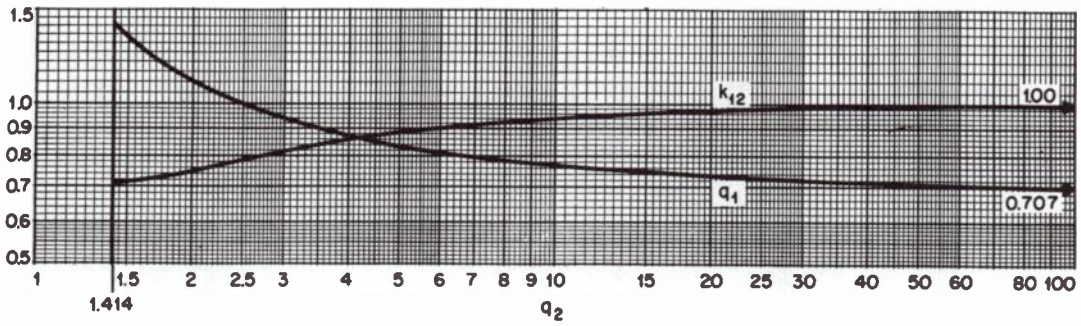

Fig. 30—(Loaded on one side only) 2-pole filter of finite-Q elements producing a maximally flat amplitude shape. See curve 1 of Fig. 6.

Reading along the row for $(V_p/V_v)_{dB}=1$, the second column gives normalized unloaded Q's of infinity at the overall 3-decibel-down frequency, which for this example is 31 kilohertz. Realize that much-lower unloaded-Q designs can be accomplished.

The required value of $q_1=2.21$ is found in the third column. From Fig. 25A, $1/R_1C_1=\omega_{3dB}/2.21=0.451\omega_{3dB}$, from which R_1 or C_1 may be obtained. Experimentally, the 3-decibel-down bandwidth of R_1C_1 must measure 0.451 times the required 3-decibel-down bandwidth or $31\times0.451=14$ kilohertz.

From the table a value of 0.633 is obtained for k_{12} and from Fig. 25A it is found that $1/(C_1L_2)^{1/2}=0.633\omega_{3dB}$. This means that a resonant circuit made

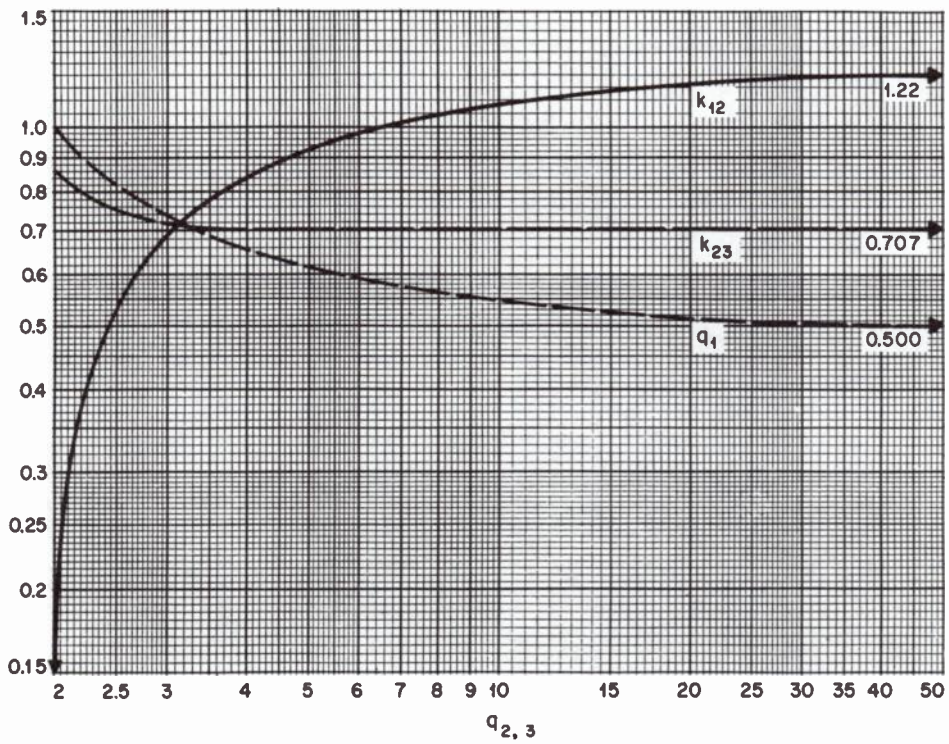

Fig. 31—(Loaded on one side only) 3-pole filter of finite-Q elements producing a maximally flat amplitude shape. See curve 1 of Fig. 7.

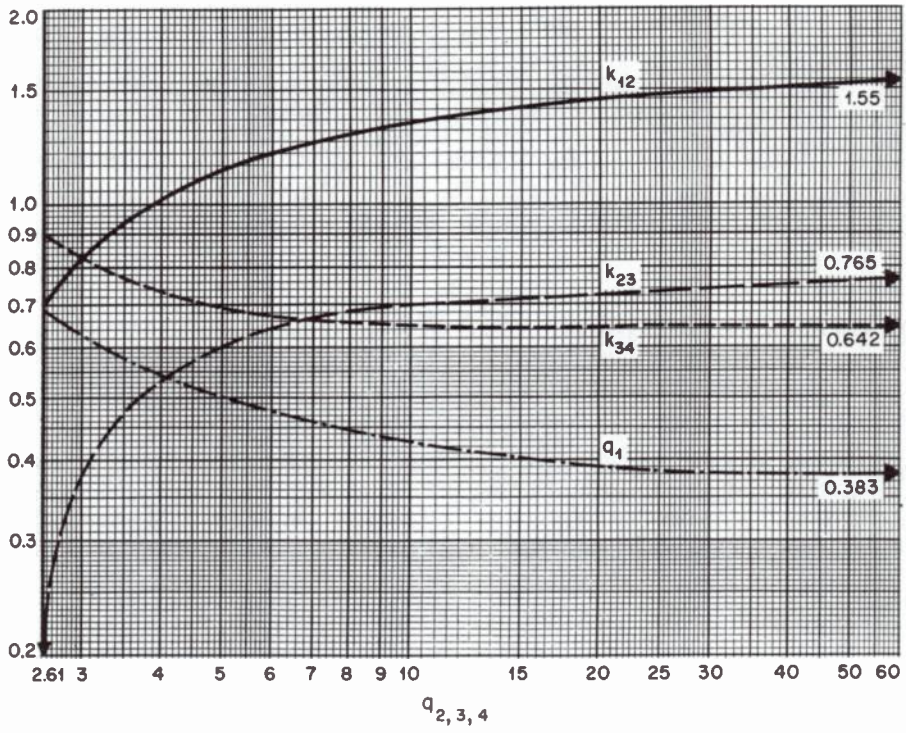

Fig. 32—(Loaded on one side only) 4-pole filter of finite-Q elements producing a maximally flat amplitude shape
See curve 1 of Fig. 8.

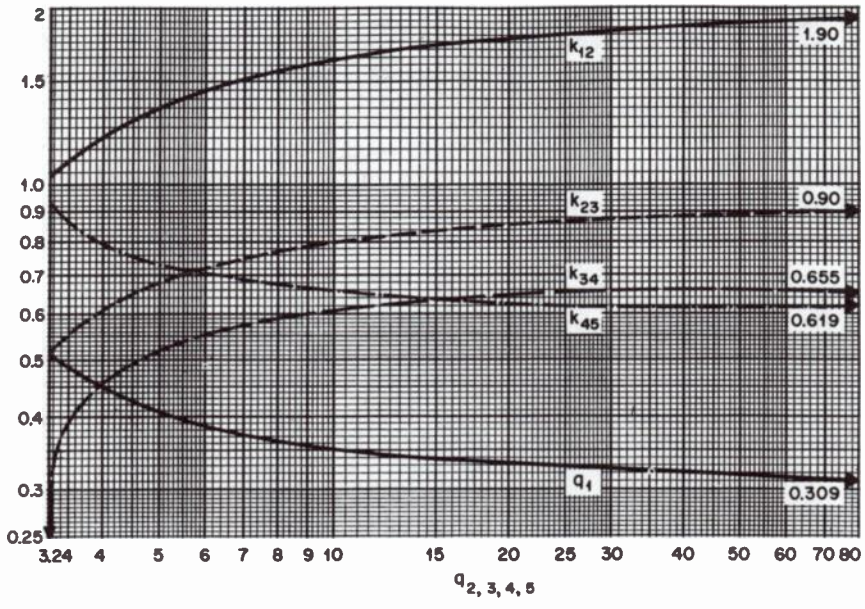

Fig. 33—(Loaded on one side only) 5-pole filter of finite-Q elements producing a maximally flat amplitude shape
See curve 1 of Fig. 9.

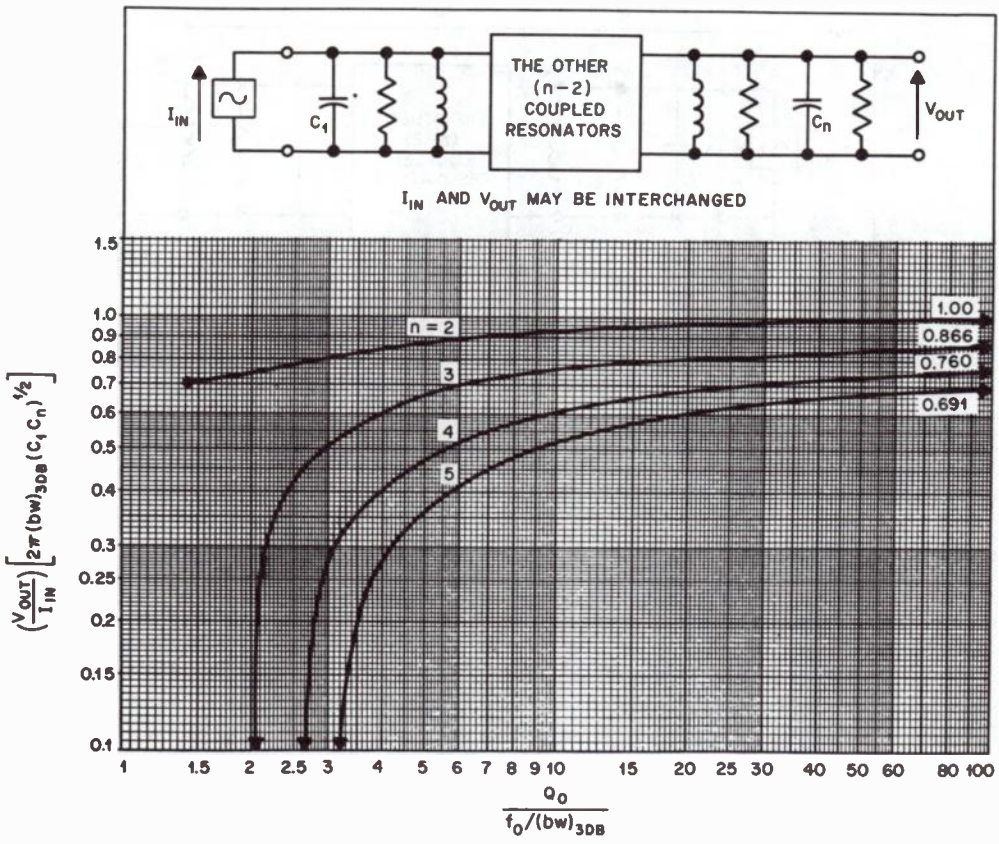

ig. 34—Midfrequency transfer-impedance magnitude for designs of Figs. 30 through 33 with direct resistive loading on one side only.

p of C_1 and L_2 must tune to 0.633 times the equired 3-decibel-down bandwidth or $31 \times 0.633 = 9.7$ kilohertz.

In this fashion, all the remaining elements are etermined. Any one of them may be set arbi-arily (for instance, the input load resistance R_1), ut once it has been set, all other values are rigidly etermined by the k and q factors.

lements of Lower Q

Designs may be accomplished for elements hav-g finite unloaded Q's. These designs are neces-ry for small-percentage band-pass filters. As is ident from Fig. 28, the Q of the internal resona-rs measured at the midfrequency must be the rmalized q multiplied by the fractional mid-equency $f_0/(\mathrm{bw})_{3dB}$. If the bandwidth percentage small, the fractional midfrequency and therefore e actually required Q will be large.

Practical values of end q's and all k's will result if the internal elements have finite q's above the minimum values given in Figs. 5–12. For a required response shape, the resulting data can be expressed as in Figs. 30 through 56. These curves are for zero-decibel ripple (Butterworth) and for the maximally linear phase shape.

There are three possible generator and load conditions.

(A) Resistive generator and resistive load. It is usually desirable to maximize the ratio of the power delivered to the load to that available from the generator. The generator resistance and the load resistance must be transformed onto their associated resonators to obtain the required q_1 and q_n.

(B) Resistive generator and reactive load or vice versa. The function to be considered here is the transfer impedance or admittance. Again, the resistive impedance must be transformed onto the associated resonator.

(C) Reactive generator and load. The transfer impedance or admittance is the significant factor,

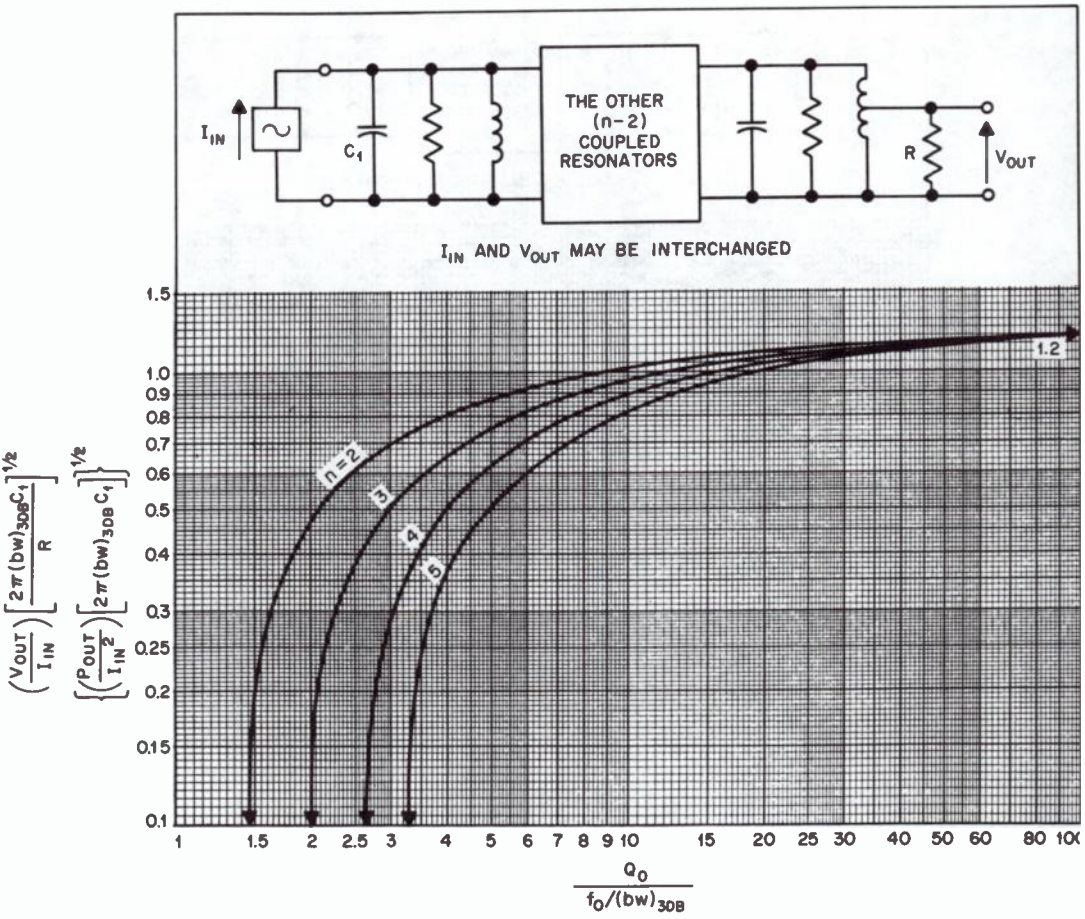

Fig. 35—Midfrequency transfer-impedance magnitude for designs of Figs. 30 through 33 with transformed resistiv loading on one side only.

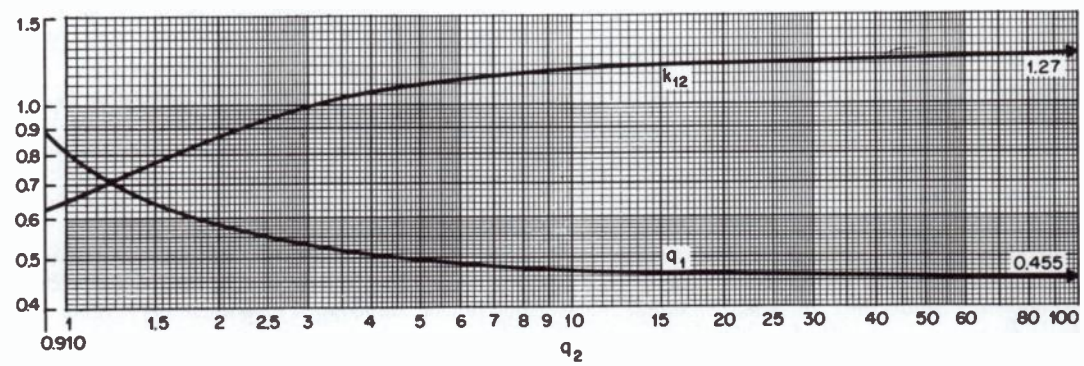

Fig. 36—(Loaded on one side only) 2-pole filter of finite-Q elements producing a maximally linear phase shap See Figs. 15 and 16.

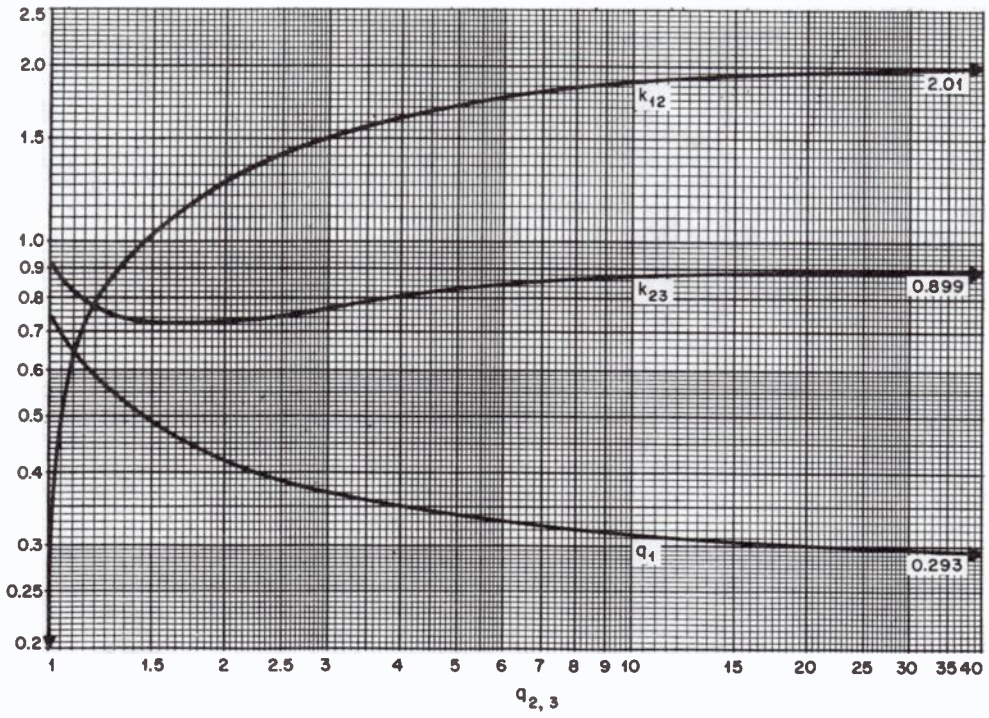

Fig. 37—(Loaded on one side only) 3-pole filter of finite-Q elements producing a maximally linear phase shape. See Figs. 15 and 16.

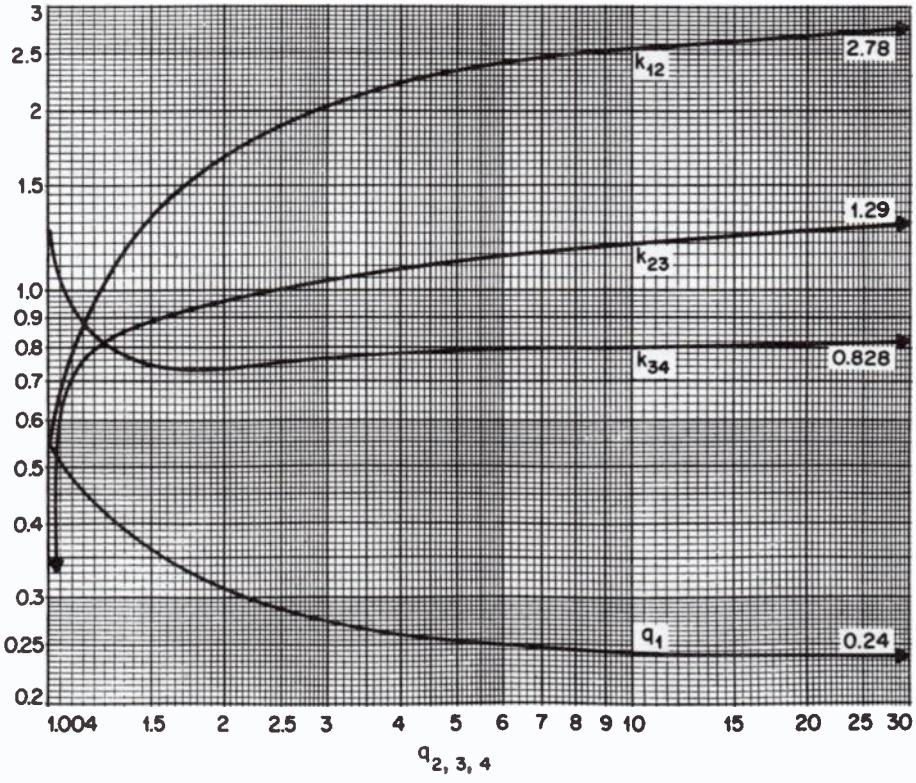

Fig. 38—(Loaded on one side only) 4-pole filter of finite-Q elements producing a maximally linear phase shape. See Figs. 15 and 16.

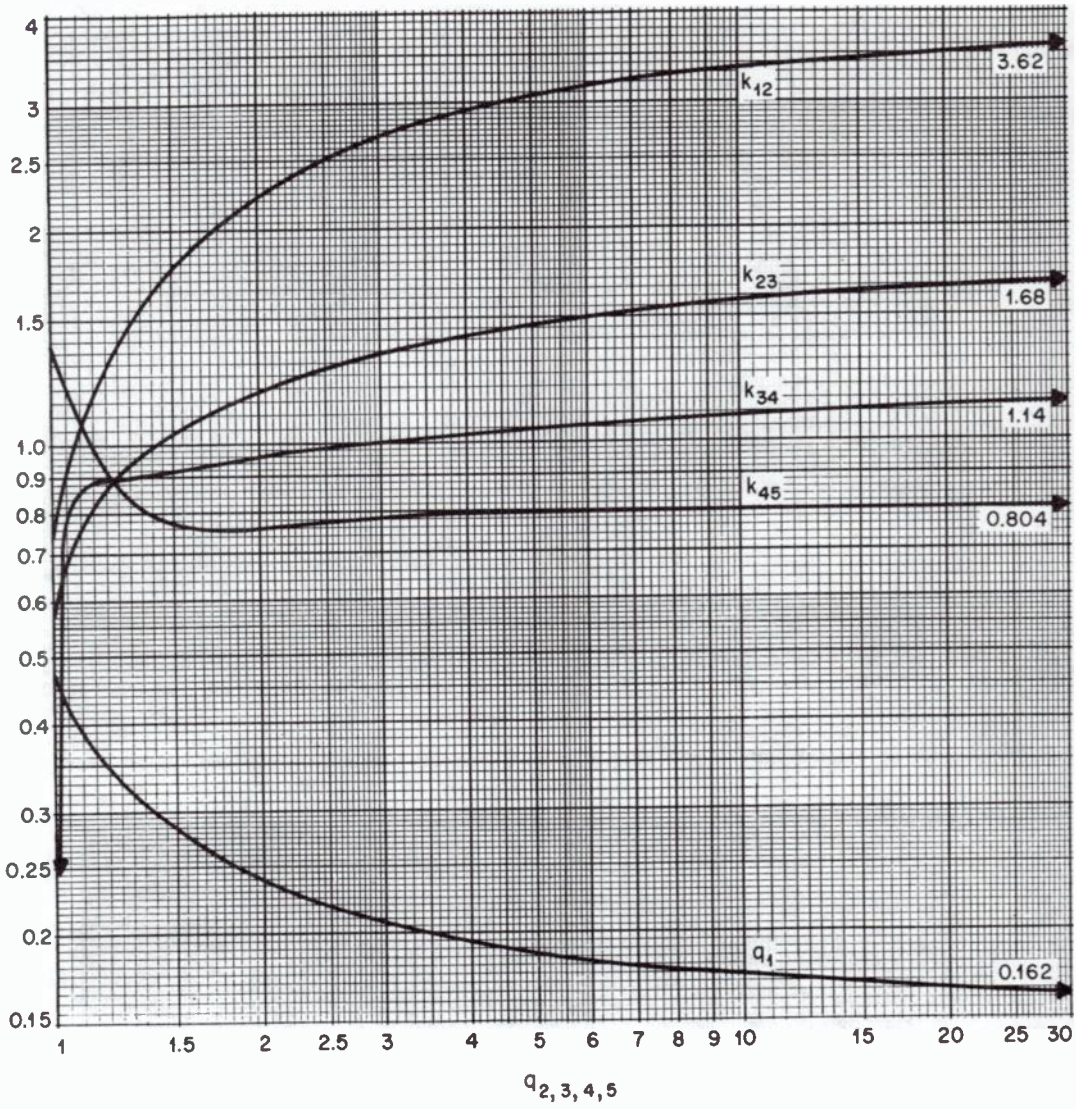

Fig. 39—(Loaded on one side only) 5-pole filter of finite-Q elements producing a maximally linear phase shape See Figs. 15 and 16.

and a loading resistance must be added to either or both end resonators.

Maximum-Transfer Impedance or Admittance Designs

Figures 30 through 41 give optimum design information for cases (B) and (C), above.

Example:

(A) The filter to be designed must have a relative attenuation of $(bw)_{70dB}/(bw)_{3dB}=5$ and ther must be no ripple in the pass band. Curve 1 o Fig. 9 satisfies these conditions and calls for 5-pole network.

(B) The specified fractional midfrequency is 2 (pass band=5 percent of the midfrequency), th Q_{min} from Fig. 9 becomes $3.24\times20=65$. Assum further that resonators with unloaded midfrequenc Q's of 100 are available. As the normalized unloade q is the actual unloaded Q divided by the fractiona midfrequency, the filter must produce a Butter worth shape with 5 resonators having normalize unloaded q's of $100/20=5$.

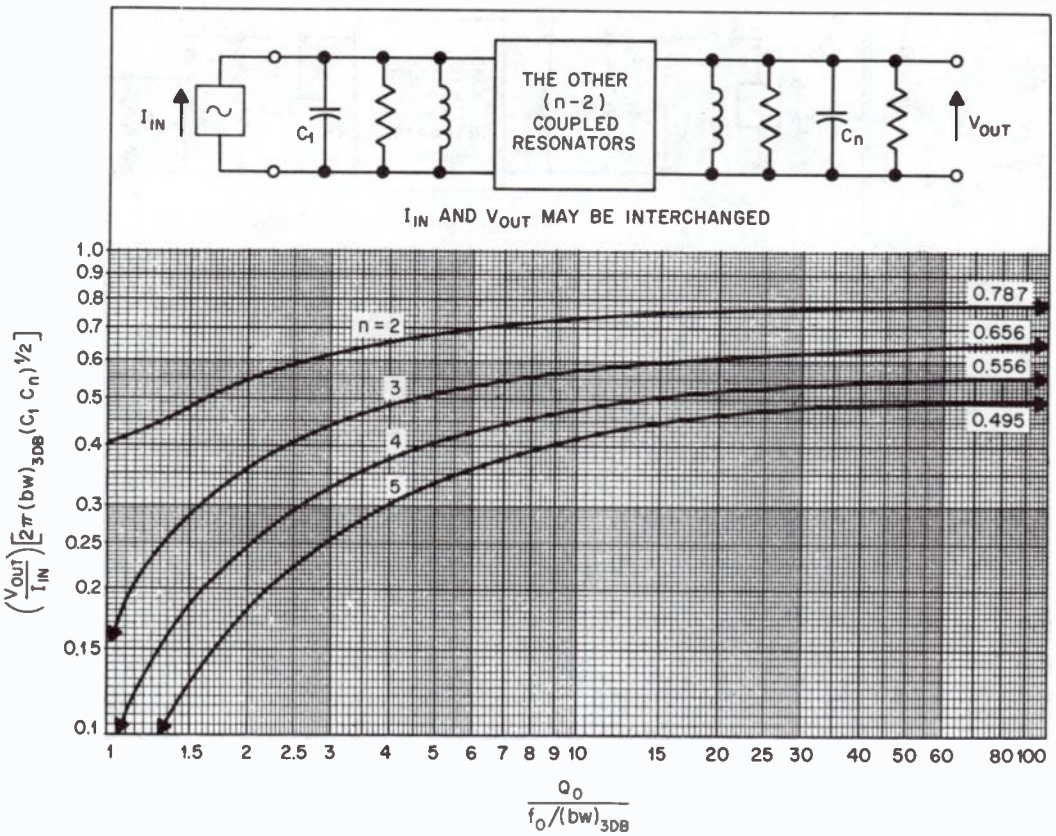

Fig. 40—Midfrequency transfer-impedance magnitude for designs of Figs. 36 through 39 with direct resistive loading on one side only.

Assuming a high-impedance filter to be required, the network of Fig. 42 might well be used. High-side capacitance coupling will be employed and the element values will be obtained from Fig. 33.

(A) The q_1 curve of Fig. 33 intersects the abscissa value of 5 at 0.405. By tapping a resistive generator or load onto it, or placing a resistor across it, the resonator C_1L_1 must be loaded to produce an actual Q of $0.405f_0/(\text{bw})_{3dB}=8.1$ (see Fig. 28A).

(B) As a convenience, the same size of inductor may be used for resonating each node, say 4 millihenries. For a required midfrequency of 80 kilohertz for this example, each node total capacitance will be 1000 picofarads.

(C) Again from Fig. 33, we get k_{12} of 1.35 for an abscissa value of 5. From Fig. 28

$$C_{12}=1.35[(\text{bw})_{3dB}/f_0](C_1C_2)^{1/2}$$
$$=1.35\times0.05\times1000$$
$$=67.5 \text{ picofarads.}$$

At the midfrequency of 80 kilohertz, node 1 must be resonant when all other nodes are short-circuited. To produce the required capacitance in shunt of L_1, C_a must be $1000-67.5=932.5$ picofarads.

(D) From Fig. 33, a value of 0.67 is obtained for k_{23}, and $C_{23}=0.67\times0.05\times1000=33.5$ picofarads. To resonate node 2 at the midfrequency with all other nodes short-circuited, $C_b=1000-33.5-67.5=899$ picofarads.

(E) Additional computations give values for C_{34} of $0.53 \times 0.05 \times 1000 = 26.5$ picofarads

$$C_c=1000-33.5-26.5=940$$

$$C_{45}=0.73\times0.05\times1000=36.5$$

$$C_d=1000-36.5-26.5=937$$

and

$$C_e=1000-36.5=963.5 \text{ picofarads.}$$

All inductances will be identical and of 4 milli-

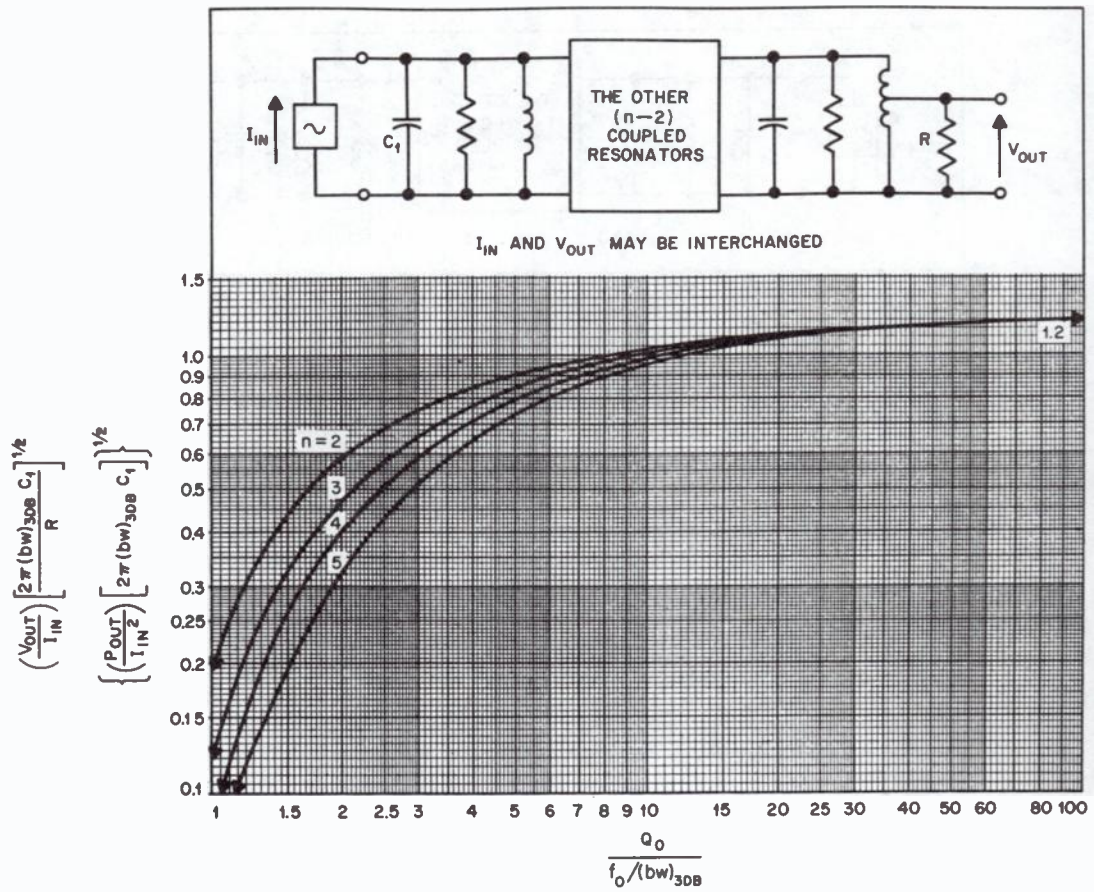

Fig. 41—Midfrequency transfer-impedance magnitude for designs of Figs. 36 through 39 with transformed resistive loading on one side only.

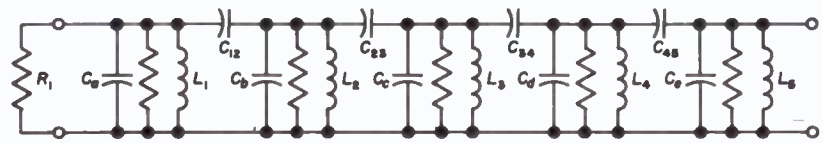

Fig. 42—A 5-resonator filter with high-side capacitance coupling.

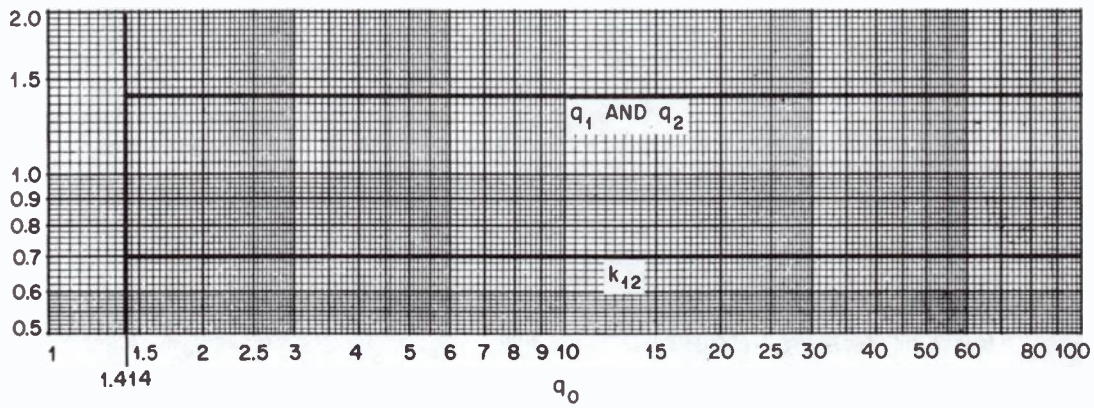

Fig. 43—Resistive generator—resistive load 2-pole filter of finite-Q elements producing a maximally flat amplitude shape. See curve 1 of Fig. 6.

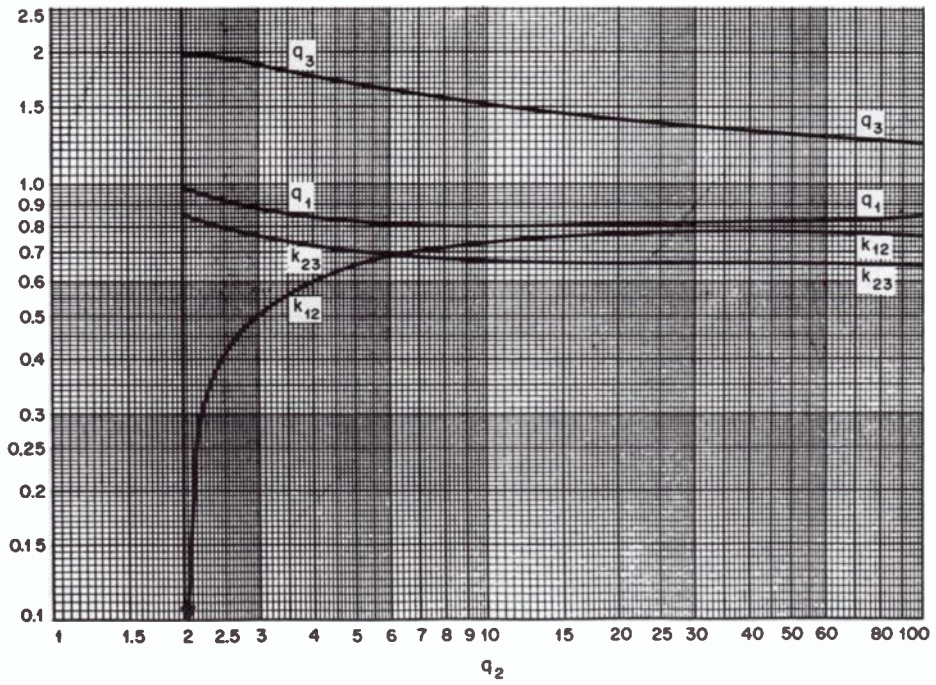

Fig. 44—Resistive generator—resistive load 3-pole filter of finite-Q elements producing a maximally flat amplitude shape. See curve 1 of Fig. 7.

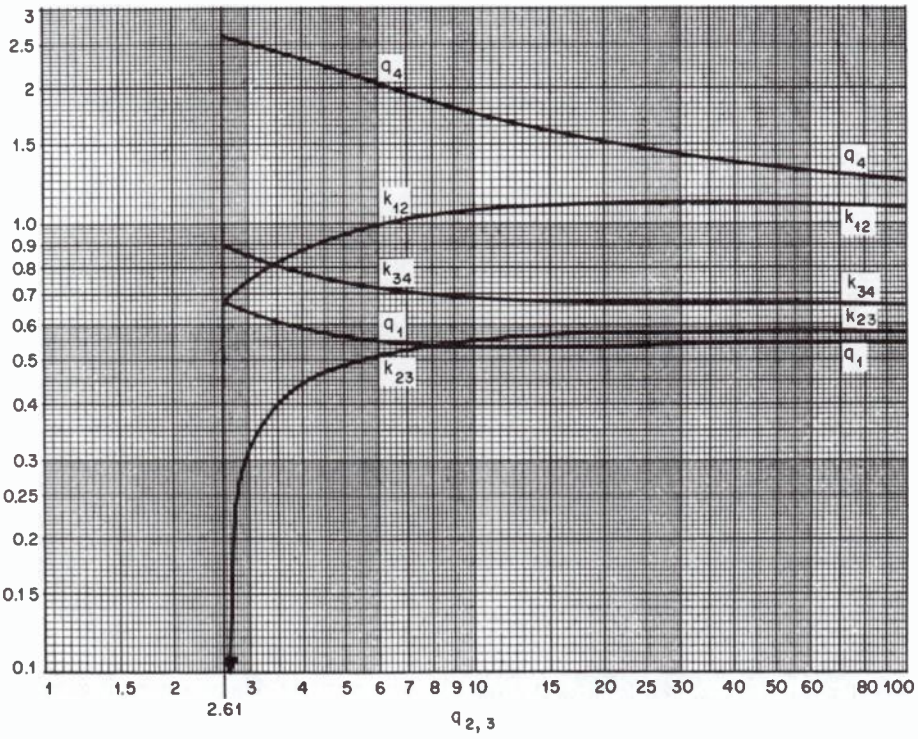

Fig. 45—Resistive generator—resistive load 4-pole filter of finite-Q elements producing a maximally flat amplitude shape. See curve 1 of Fig. 8.

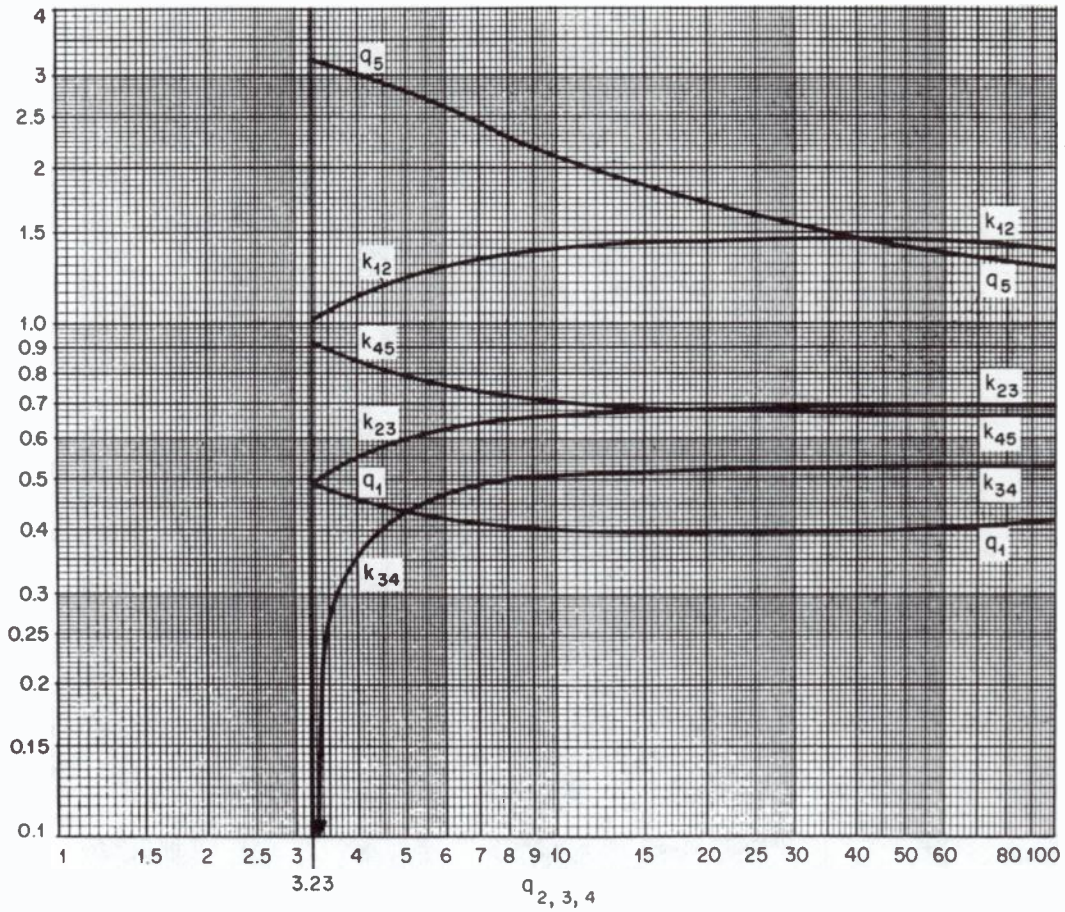

Fig. 46—Resistive generator—resistive load 5-pole filter of finite-Q elements producing a maximally flat amplitude shape. See curve 1 of Fig. 9.

henries, and there will be no inductive coupling among them.

Maximum-Power-Transfer Designs

Maximally Flat Amplitude Shape: When a filter of finite Q is to be placed between a resistive generator and a resistive load, and the Butterworth response shape is desired, Figs. 43 through 49 give the design data that produce maximum possible power transfer between the resistive generator and resistive load.

In Figs. 43 through 49, the abscissa is the normalized unloaded Q of the resonators being used, i.e., $Q_0/[f_0(\mathrm{bw})_{3dB}]$. q_1 and q_n given by the graphs are the required resultant normalized Q's of the end resonators due to their unloaded Q's, plus the coupled loading from the resistive generator and resistive load.

Maximally Linear Phase Shape: Figures 50 through 56 give (loaded on both sides) maximum-power-transfer designs when the maximally linear phase shape is desired.

STAGGER TUNING OF SINGLE-TUNED INTERSTAGES

Butterworth Response (Figs. 4 and 57)

The required Q's are given by

$$Q_m^{-1}=\frac{(\mathrm{bw})_\beta/f_0}{[(V_p/V_\beta)^2-1]^{1/2n}}\sin\left(\frac{2m-1}{n}\,90^\circ\right).$$

The required stagger tuning is given by

$$(f_a-f_b)_m=\frac{(\mathrm{bw})_\beta}{[(V_p/V_\beta)^2-1]^{1/2n}}\cos\left(\frac{2m-1}{n}\,90^\circ\right)$$

$$(f_a+f_b)_m=2f_0.$$

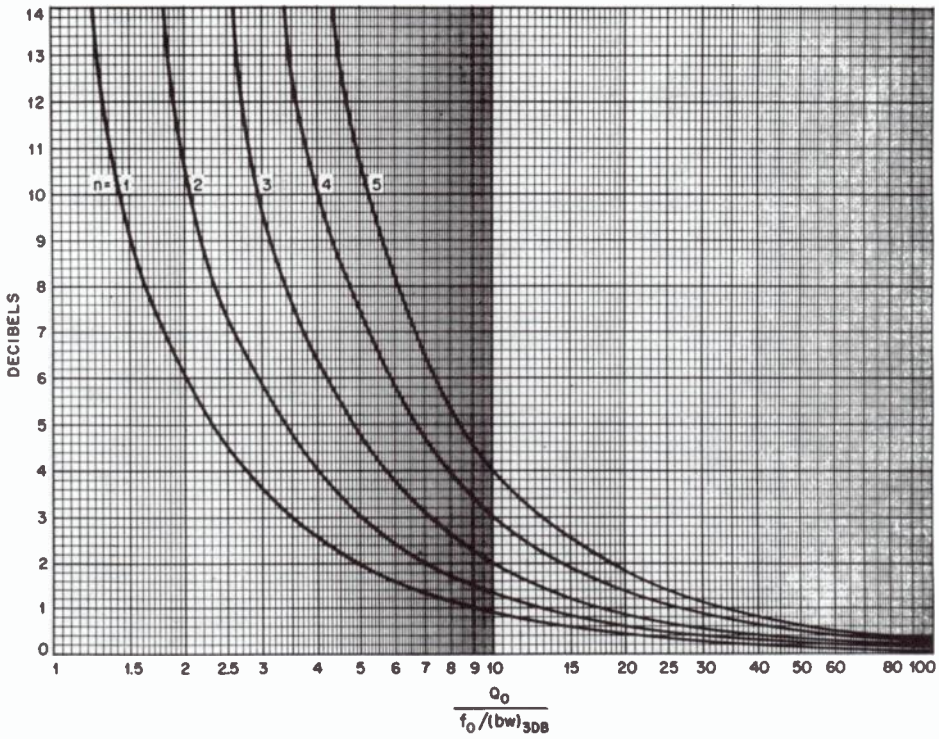

Fig. 47—Ratio of power available from generator to power delivered to load for designs of Figs. 43 through 46.

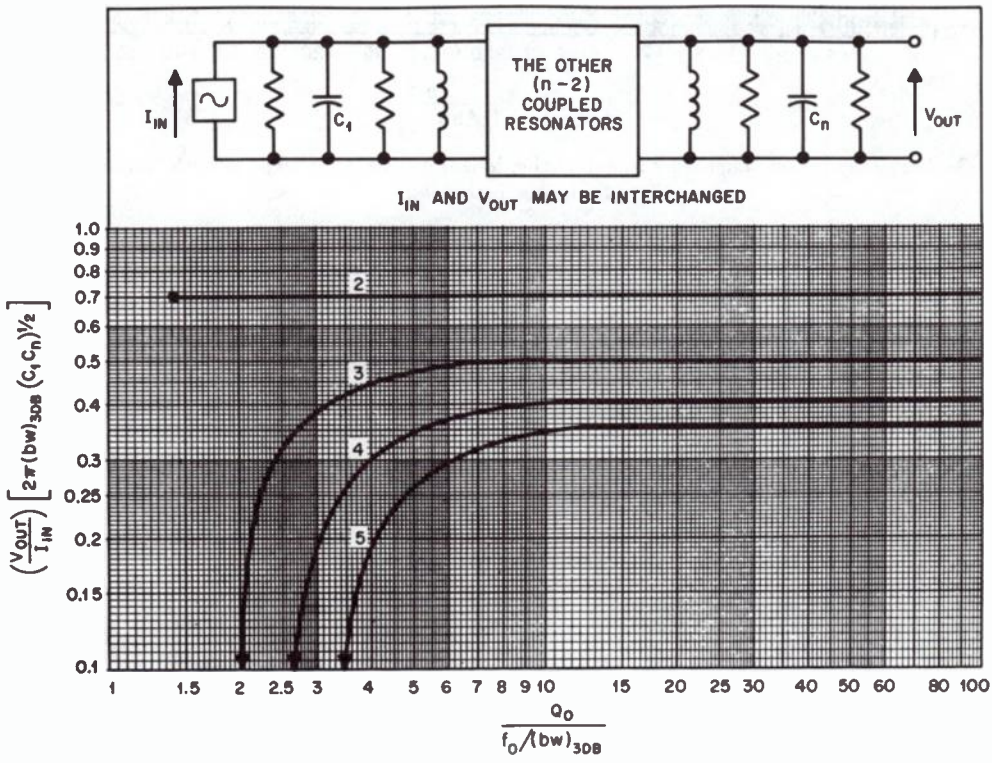

Fig. 48—Midfrequency transfer-impedance magnitude for designs of Figs. 43 through 46 with direct resistive loading on both sides.

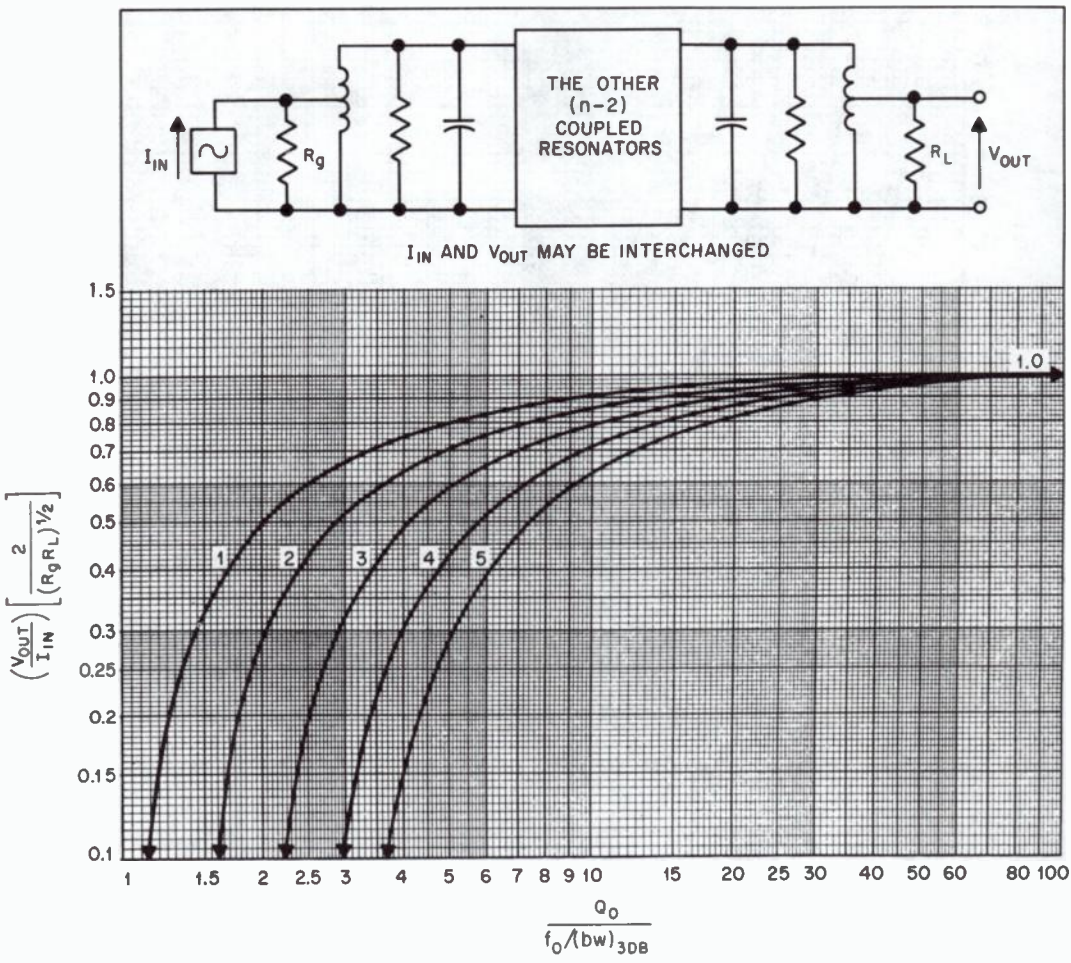

Fig. 49—Midfrequency transfer-impedance magnitude for designs of Figs. 43 through 46 with transformed resistive loading on both sides.

The amplitude response is given by

$$V_p/V = \{1+[(V_p/V_\beta)^2-1][(bw)/(bw)_\beta]^{2n}\}^{1/2}$$

$$\frac{(bw)}{(bw)_\beta} = \left[\frac{(V_p/V)^2-1}{(V_p/V_\beta)^2-1}\right]^{1/2n}$$

$$n = \log\left[\frac{(V_p/V)^2-1}{(V_p/V_\beta)^2-1}\right] \Big/ \left\{2\log\left[\frac{(bw)}{(bw)_\beta}\right]\right\}.$$

$$\text{Stage gain} = \frac{g_m}{2\pi(bw)_\beta C}[(V_p/V_\beta)^2-1]^{1/2n}$$

or

$$n = \log\left\{\frac{(\text{total gain})}{[(V_p/V_\beta)^2-1]^{1/2}}\right\} \Big/ \log\left[\frac{g_m}{2\pi(bw)_\beta C}\right]$$

where g_m = geometric-mean transconductance of n active devices, and C = geometric-mean capacitance.

Chebishev Response (Figs. 4 and 58)

The required Q's are given by

$$Q_m^{-1} = \frac{(bw)_\beta}{f_0} S_n \sin\left(\frac{2m-1}{n}\,90°\right)$$

$$S_n = \sinh\left\{n^{-1}\sinh^{-1}\frac{1}{[(V_p/V_\beta)^2-1]^{1/2}}\right\}.$$

The required stagger tuning is given by

$$(f_a-f_b)_m = (bw)_\beta C_n \cos\left(\frac{2m-1}{n}\,90°\right)$$

$$(f_a+f_b)_m = 2f_0$$

$$C_n = \cosh\left\{n^{-1}\sinh^{-1}\frac{1}{[(V_p/V_\beta)^2-1]^{1/2}}\right\}.$$

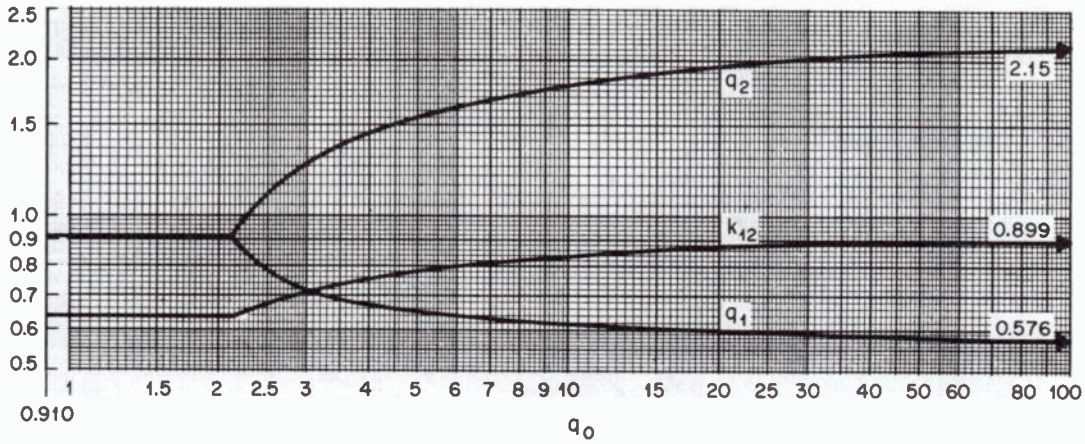

Fig. 50—Resistive generator—resistive load 2-pole filter of finite-Q elements producing a maximally linear phase shape. See Figs. 15 and 16.

Shape outside pass band is

$$\frac{V_p}{V}=\left\{1+\left[\left(\frac{V_p}{V_\beta}\right)^2-1\right]\times\left\{\cosh^2\left[n\cosh^{-1}\frac{(\mathrm{bw})}{(\mathrm{bw})_\beta}\right]\right\}\right\}^{1/2}$$

$$\frac{(\mathrm{bw})}{(\mathrm{bw})_\beta}=\cosh\left\{n^{-1}\cosh^{-1}\left[\frac{(V_p/V)^2-1}{(V_p/V_\beta)^2-1}\right]^{1/2}\right\}$$

$$n=\cosh^{-1}\left[\frac{(V_p/V)^2-1}{(V_p/V_\beta)^2-1}\right]^{1/2}\Big/\cosh^{-1}\left[\frac{(\mathrm{bw})}{(\mathrm{bw})_\beta}\right].$$

Shape inside pass band is

$$\frac{V_p}{V}=\left\{1+\left[\left(\frac{V_p}{V_\beta}\right)^2-1\right]\left\{\cos^2\left[n\cos^{-1}\frac{(\mathrm{bw})}{(\mathrm{bw})_\beta}\right]\right\}\right\}^{1/2}$$

$$\frac{(\mathrm{bw})_{\mathrm{crest}}}{(\mathrm{bw})_\beta}=\cos\left(\frac{2m-1}{n}\,90^\circ\right)$$

$$\frac{(\mathrm{bw})_{\mathrm{trough}}}{(\mathrm{bw})_\beta}=\cos\left(\frac{2m}{n}\,90^\circ\right).$$

$$\text{Stage gain}=\frac{g_m}{2^{1/n}\pi(\mathrm{bw})_\beta C}\left[(V_p/V_\beta)^2-1\right]^{1/2n}$$

$$n=\log\left[\frac{(\text{total gain})}{\frac{1}{2}\left[(V_p/V_\beta)^2-1\right]^{1/2}}\right]\Big/\log\left[\frac{g_m}{\pi(\mathrm{bw})_\beta C}\right]$$

where g_m = geometric-mean transconductance of n active devices, and C = geometric-mean capacitance.

QUARTZ-CRYSTAL BAND-PASS FILTERS FOR $f_0/(bw)_{3dB}$ BETWEEN 10 AND 100

When a filter requires simultaneously a small-percentage bandwidth and a high rate of cutoff, it is usually not practical to obtain sufficiently high unloaded Q in ordinary L-C resonators. When the ultimate attenuation required is no greater than approximately 30 dB, and the percentage bandwidth required is between 10% and 1%, then a single half-lattice filter configuration involving two L-C resonators and $(n-2)$ quartz crystal resonators can be successfully used. It should be realized that piezoelectric crystal resonators often exhibit spurious responses, and the presence of these (usually on the high-frequency side of the response) must be considered. The following sections first give the design procedure for the full-lattice configuration and then present the half-lattice equivalent.

High-Impedance Lattice

An "open-circuited" lattice is shown in Fig. 59. The arrangements of the impedance arms Z_A and Z_B are shown in Fig. 60. In each arm there is an L-C parallel-resonant circuit shunted by $(n/2)-1$ quartz crystals. The number of complex poles in the transfer function is equal to the n. The L-C circuit is loaded by R_p to give the required $Q_p=\omega_0 C_p R_p$. Its capacitance includes those of the crystal holders, and it is resonant to $(f_0+\Delta f_p)$ as shown

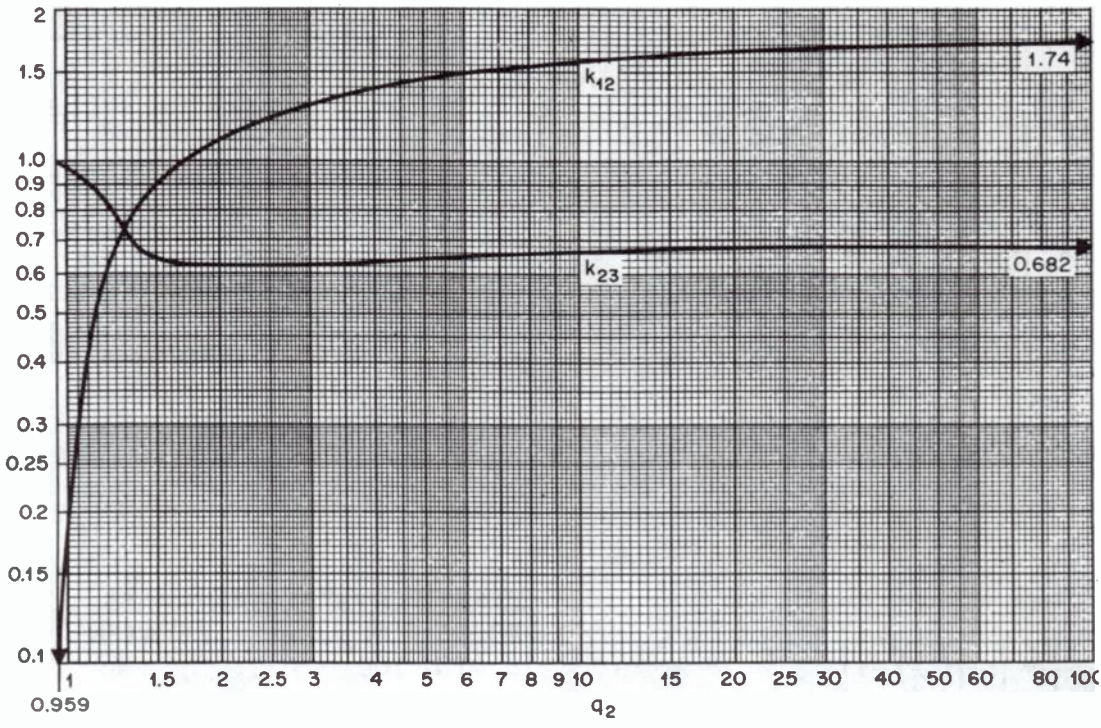

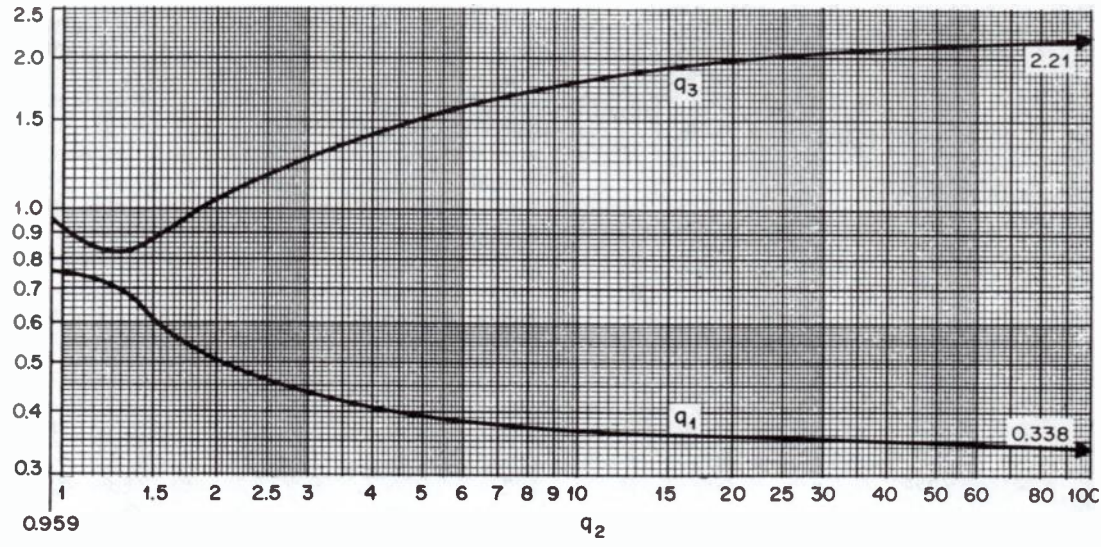

Fig. 51—Resistive generator—resistive load 3-pole filter of finite-Q elements producing a maximally linear phase shape. See Figs. 15 and 16.

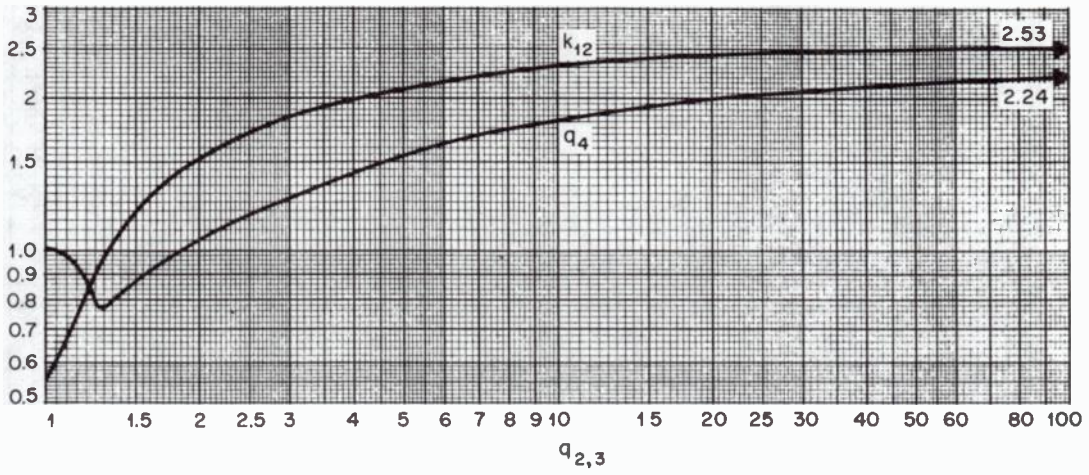

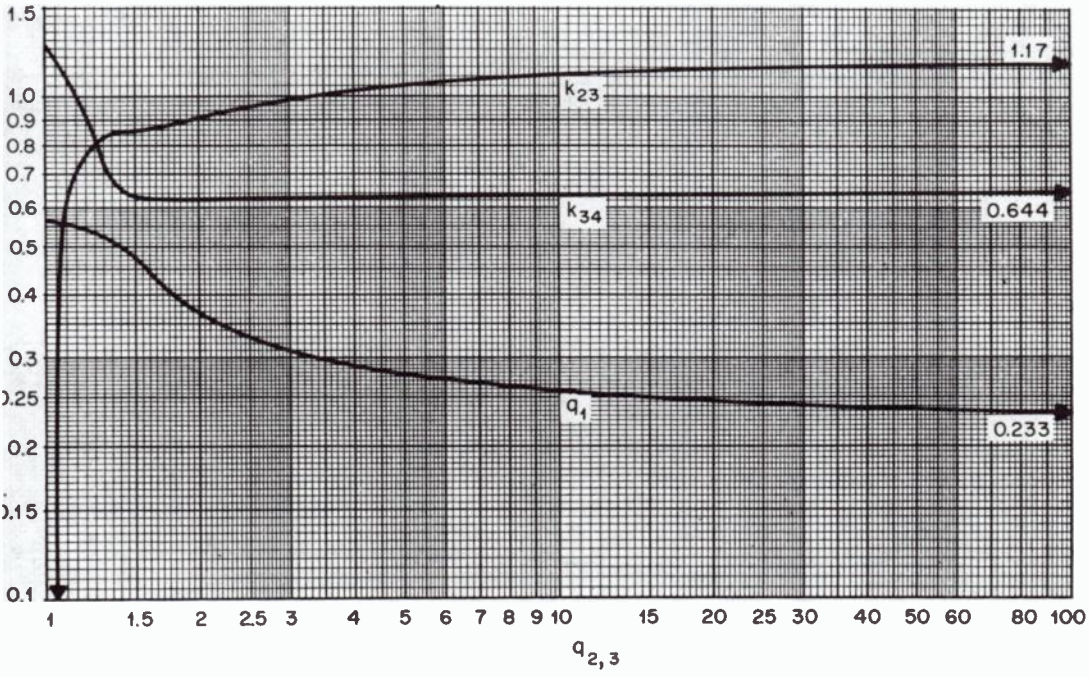

Fig. 52—Resistive generator—resistive load 4-pole filter of finite-Q elements producing a maximally linear phase shape. See Figs. 15 and 16.

in the diagrams. The motional capacitance C_1, C_2, C_3, etc., must have a particular value, and each crystal must be resonant to a particular frequency, $(f_0 \pm \Delta f_1)$, $(f_0 \pm \Delta f_2)$, etc.

Frequently, divided-electrode crystals are used so that one crystal can be used for the identical resonators in the two series arms, and likewise in the lattice arms.

The structure can be modified by converting the lattice to its equivalent in accordance with Fig. 61. The elements Z that are lifted out of the arms and shunted across the terminals consist of L_p, R_p, and most of C_p.

Design Information

The data of Fig. 62 are for the Chebishev and Butterworth response shapes of 4-pole no-zero networks for which the relative attenuation is plotted in Fig. 8. Similarly, Figs. 63 through 65 are for 6-pole, 8-pole, and 10-pole no-zero networks, the

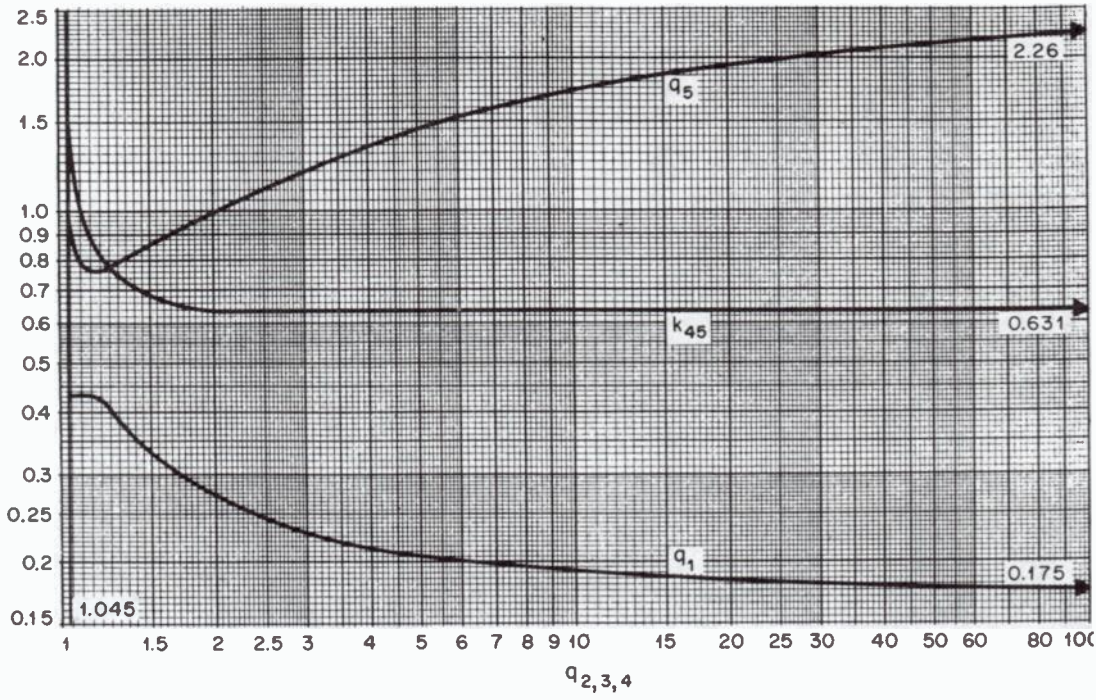

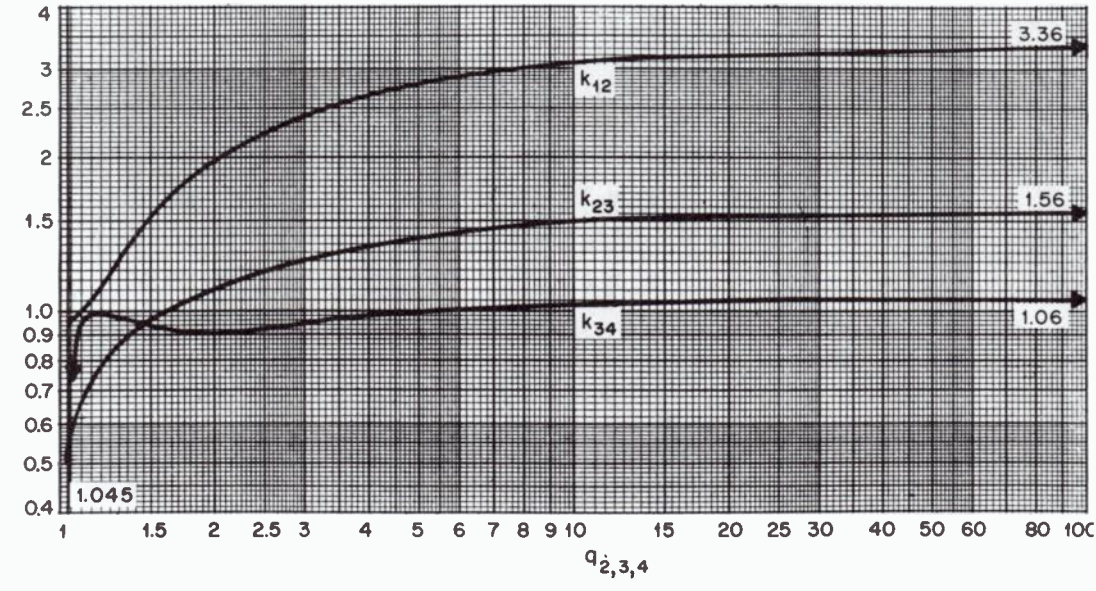

Fig. 53—Resistive generator—resistive load 5-pole filter of finite-Q elements producing a maximally linear phase shape. See Figs. 15 and 16.

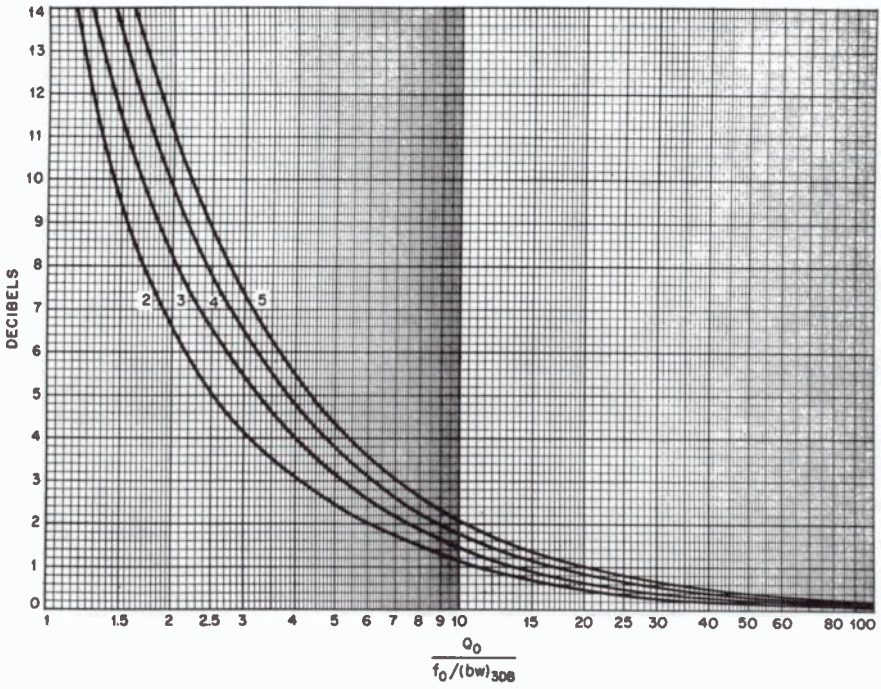

Fig. 54—Ratio of power available from generator to power delivered to load for designs of Figs. 50 through 53.

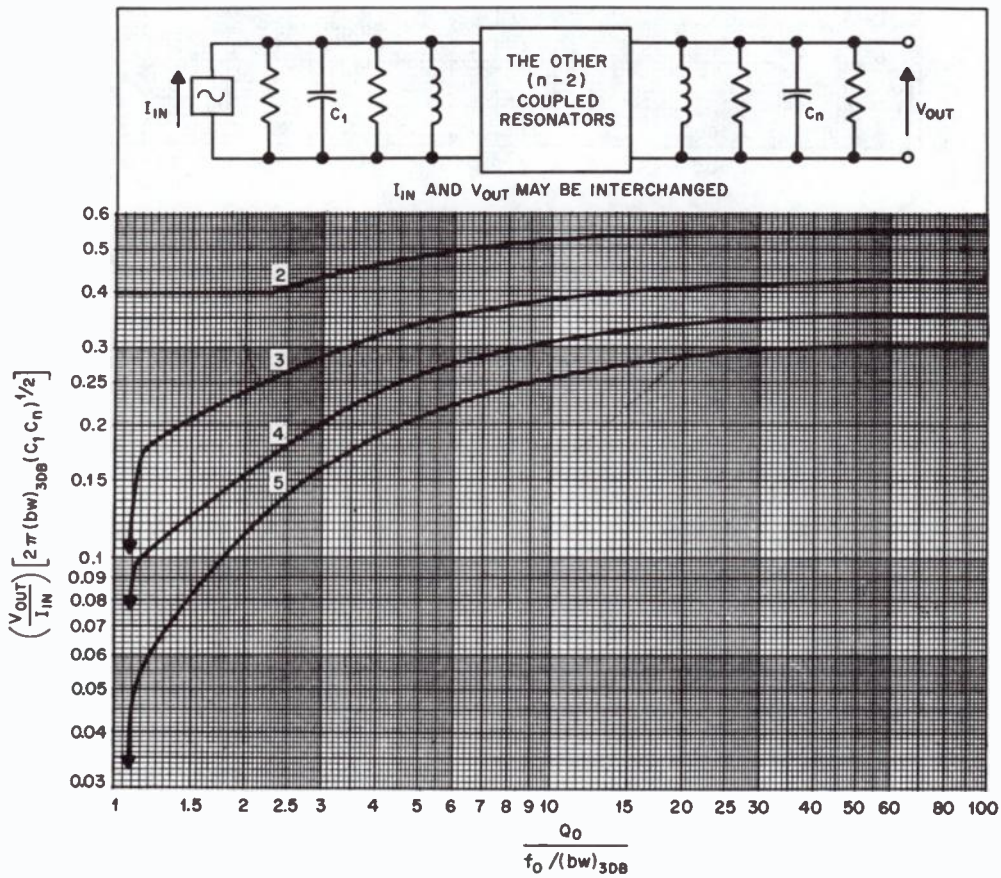

Fig. 55—Midfrequency transfer-impedance magnitude for designs of Figs. 50 through 53 with direct resistive loading on both sides.

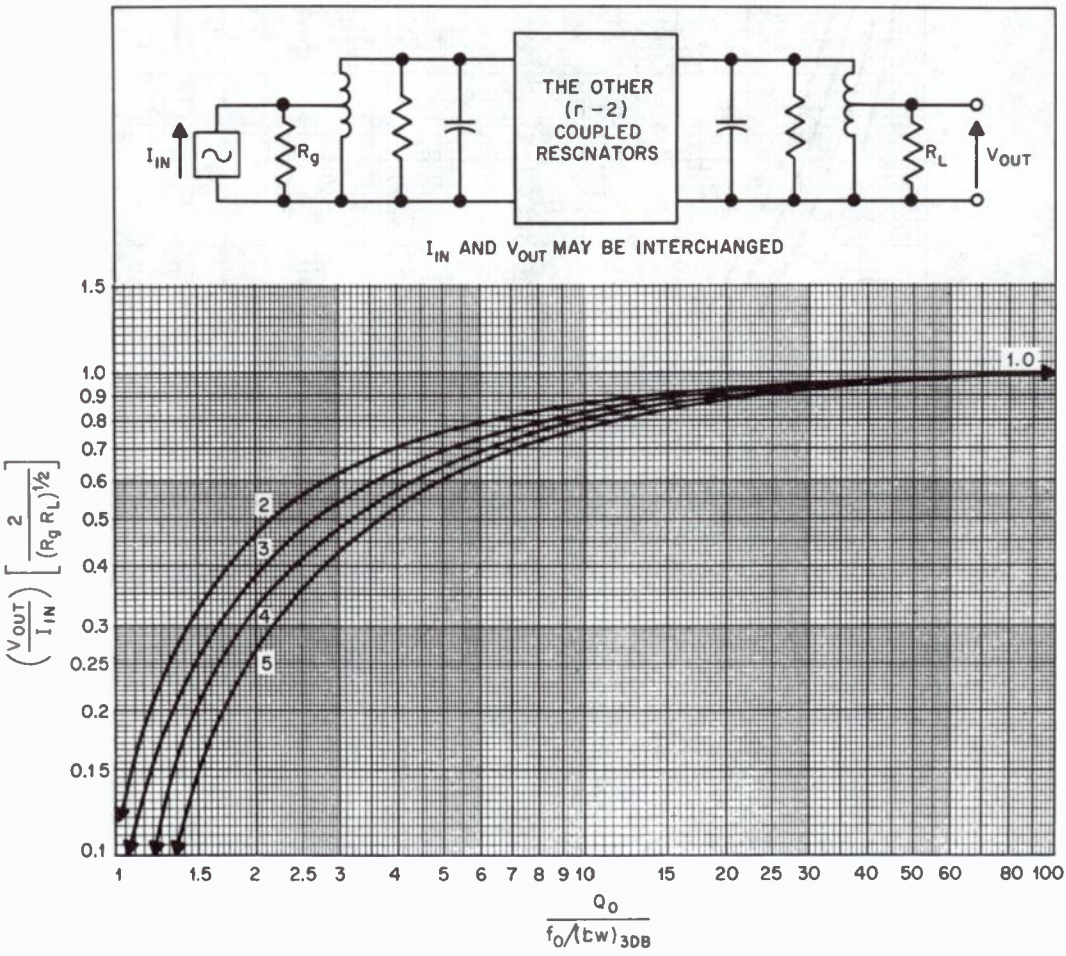

Fig. 56—Midfrequency transfer-impedance magnitude for designs of Figs. 50 through 53 with transformed resistive loading on both sides.

relative attenuation of the former two being plotted in Figs. 10 and 12, respectively.

Examination of the tables shows that the required Q_p of the *L-C* parallel-resonant circuit is roughly the same as the fractional midfrequency. This limits the practical design to $f_0/(\text{bw})_{3dB}$ less than about 250. A lower limit to the $f_0/(\text{bw})_{3dB}$ is of the order of 10 due to the fact that C_p/C_1 is roughly equal to the square of $f_0/(\text{bw})_{3dB}$, and C_p includes the capacitances of the crystal holders and coil and stray distributed capacitances, so it cannot be reduced indefinitely.

The impedance Z in Fig. 61 must include the equivalent-generator and equivalent-load impedances. Since R_p often comes to some hundreds of thousands of ohms, it is obvious that this type of filter requires a very-high-impedance equivalent generator and load.

Example: Required, a filter for $f_0 = 175$ kilohertz, $(\text{bw})_{3dB} = 2.0$ kilohertz, $(\text{bw})_{60dB} < 5.0$ kilohertz, $(V_p/V_v)_{dB} < 0.3$.

Then, $f_0/(\text{bw})_{3dB} = 87.5$ and $(\text{bw})_{60dB}/(\text{bw})_{3dB} < 2.5$. The latter requirement is satisfied by the curve for $(V_p/V_v)_{dB} = 0.1$-decibel ripple on Fig. 10 with a 6-pole, no-zero network. The Q_{min} of the internal resonators must be $q_{min} f_0/(\text{bw})_{3dB} = 9.5 \times 87.5 = 831$. This is far beyond *L-C* possibilities, but crystal unloaded Q usually exceeds 25 000.

In Fig. 63, let $C_1 = 0.020$ picofarad, which can be obtained. Lower values for C_2 can also be realized.

$$C_2 = C_1/2.53 = 0.00800 \text{ picofarad.}$$

$$\Delta f_1 = 0.339 \Delta f_{3dB} = 0.339 \times 1000 = 339 \text{ hertz.}$$

Then the first crystal in arm A is series-resonant at 175 kilohertz minus 339 hertz (in arm B plus 339 hertz).

Similarly, $\Delta f_2 = 0.859 \times 1000 = 859$ hertz. In the parallel-resonant circuits

$$C_p = 2.73 C_1 [f_0/(\text{bw})_{3dB}]^2$$
$$= 2.73 \times 0.020 \times (87.5)^2$$
$$= 422 \text{ picofarads.}$$

Since $F_p = 0$, they are parallel-resonant at 175 kilohertz. The loaded $Q_p = 1.28 \times 87.5 = 112$. The equivalent

$$R_p = Q_p/2\pi f_0 C_p$$
$$= 112/2\pi \times 175 \times 422 \times 10^{-9}$$
$$= 240\,000 \text{ ohms.}$$

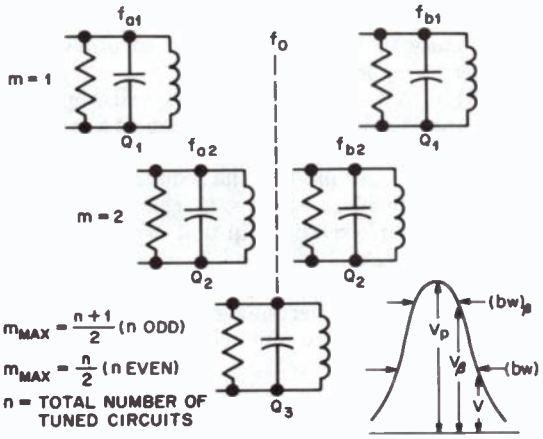

Fig. 57—Stagger-tuned interstages for Butterworth response. Each circuit is coupled to the next only by an isolating active element.

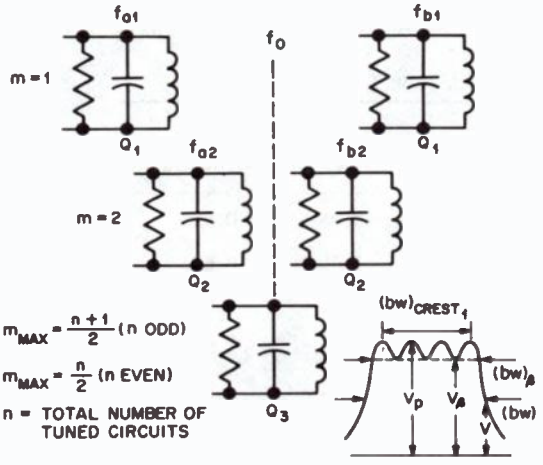

Fig. 58—Stagger-tuned interstages for Chebishev response. Each circuit is coupled to the next only by an isolating active element.

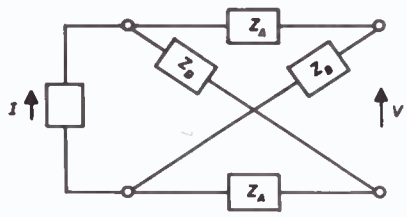

Fig. 59—High-impedance lattice section.

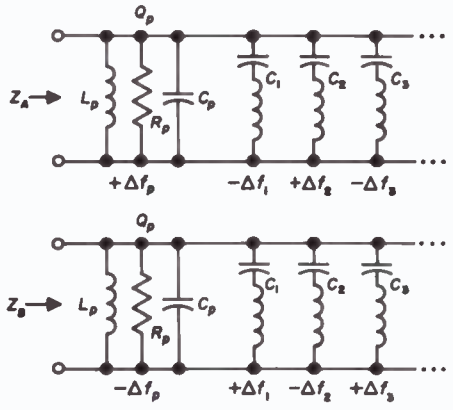

Fig. 60—Detailed structure of the lattice arms indicated in Fig. 59.

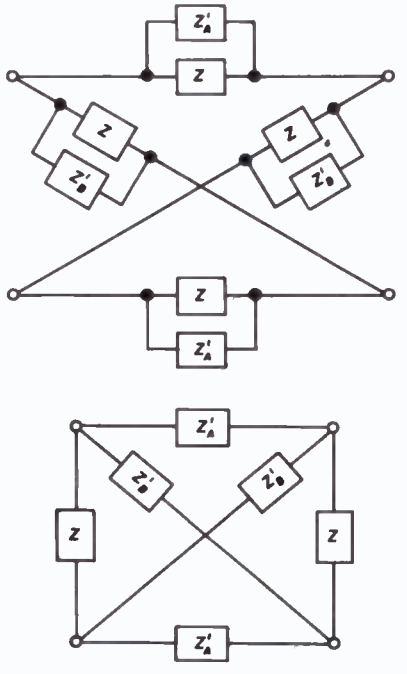

Fig. 61—Equivalent lattices.

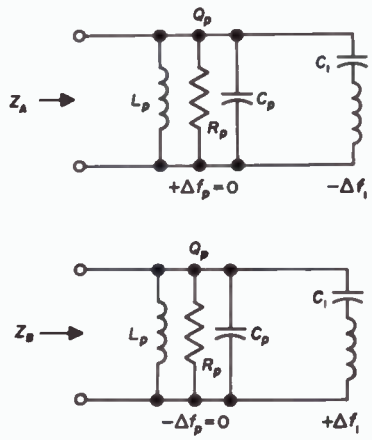

$(V_p/V_t)_{dB}$	$\Delta f_1/\Delta f_{3dB}$	$\frac{C_p/C_1}{[f_0/(bw)_{3dB}]^2}$	$\frac{Q_p}{f_0/(bw)_{3dB}}$
0	0.542	1.414	0.766
0.001	0.541	1.66	0.912
0.01	0.540	1.84	1.05
0.1	0.541	2.10	1.34
1.0	0.546	2.46	2.21
3.0	0.552	2.57	3.44

Fig. 62—Four-pole no-zero lattice-filter design for Chebishev response. Note that Δf_{3dB} is one-half the total 3-decibel bandwidth, or, $2\Delta f_{3dB} = (bw)_{3dB}$.

If the unloaded Q of the inductor L_p is 200, the added loading due to generator or load must be in excess of one-half megohm.

Low-Impedance Generator and Load

A low-impedance generator and/or load may be used with the above filter design by the following procedure: After the arms of Fig. 60 have been designed, convert the resulting lattice of Fig. 59 to the configuration of Fig. 61 so that the Z across each end of the filter consists of L_p, R_p, and most of C_p. Then use either of the following two steps.

(A) Couple the generator to one L_p and the load to the other L_p via mutual inductance, with an effective turns ratio that transforms the low impedance to the value required to produce the proper R_p across each Z.

(B) In each Z, across the filter ends, open the inductor L_p at its midpoint and connect a generator and a load of the proper resistance R_s directly in series with L_p to produce the required Q_p. The required terminal resistances R_s can be calculated from the simple relationship that, with series loading, $Q_p = X_p/R_s$.

With practical crystals, the value of R_s is some tens of ohms for percentage bandwidths around 1 percent, and some hundreds of ohms for bandwidths around 5 percent.

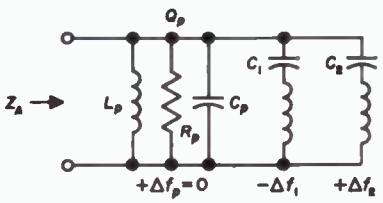

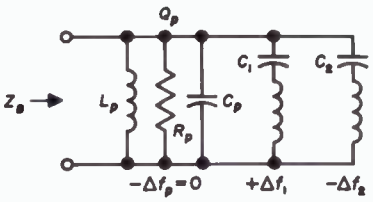

$(V_p/V_v)_{dB}$	$\Delta f_1/\Delta f_{3dB}$	C_1/C_2	$\Delta f_2/\Delta f_{3dB}$	$\frac{C_p/C_1}{[f_0/(bw)_{3dB}]^2}$	$\frac{Q_p}{f_0/(bw)_{3dB}}$
0	0.400	2.30	0.920	1.05	0.518
0.0001	0.370	2.40	0.889	1.51	0.680
0.01	0.350	2.47	0.869	2.14	0.936
0.1	0.339	2.53	0.859	2.73	1.28
1.0	0.330	2.57	0.850	3.49	2.25
3.0	0.332	2.58	0.858	3.72	3.51

Fig. 63—Six-pole no-zero lattice-filter design for Chebishev response. Note that Δf_{3dB} is one-half the total 3-decibel bandwidth, or that $2\Delta f_{3dB} = (bw)_{3dB}$.

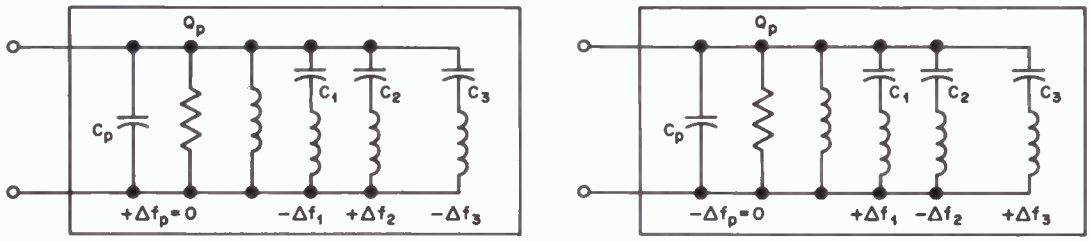

$(V_p/V_v)_{dB}$	$\Delta f_1/\Delta f_{3dB}$	C_1/C_2	$\Delta f_2/\Delta f_{3dB}$	C_1/C_3	$\Delta f_3/\Delta f_{3dB}$	$\frac{C_p/C_1}{[f_0/(bw)_{3dB}]^2}$	$\frac{Q_p}{f_0/(bw)_{3dB}}$
0	0.303	1.08	0.856	2.16	1.063	1.04	0.390
0.00001	0.275	1.24	0.762	2.95	0.996	1.60	0.548
0.001	0.259	1.34	0.715	3.51	0.966	2.20	0.720
0.01	0.249	1.40	0.691	3.93	0.951	2.77	0.900
0.1	0.241	1.46	0.699	4.35	0.938	3.62	1.29
1.0	0.235	1.50	0.655	4.62	0.931	4.70	2.21
3.0	0.234	1.52	0.653	4.75	0.932	5.10	3.53

Fig. 64—Eight-pole no-zero lattice-filter design for Chebishev response.

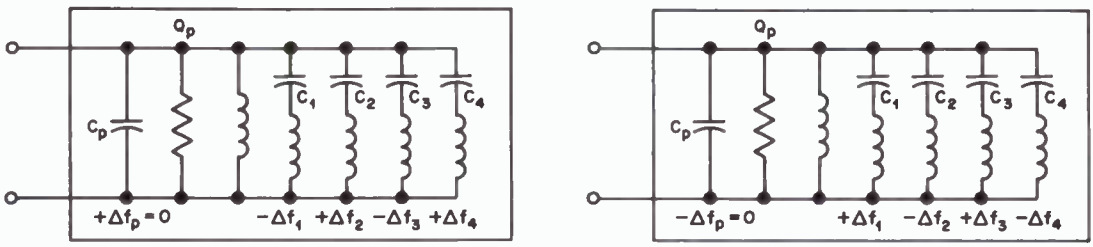

$(V_p/V_v)_{dB}$	$\Delta f_1/\Delta f_{3dB}$	C_1/C_2	$\Delta f_2/\Delta f_{3dB}$	C_1/C_3	$\Delta f_3/\Delta f_{3dB}$	C_1/C_4	$\Delta f_4/\Delta f_{3dB}$	$\frac{C_p/C_1}{[f_0/(bw)_{3dB}]^2}$	$\frac{Q_p}{f_0/(bw)_{3dB}}$
0	0.244	1.27	0.687	0.948	1.118	1.33	1.181	1.021	0.314
0.00001	0.213	1.17	0.608	1.38	0.924	2.85	1.035	1.90	0.509
0.001	0.200	1.19	0.571	1.65	0.862	4.15	0.997	2.72	0.690
0.01	0.193	1.21	0.552	1.83	0.834	5.10	0.981	3.48	0.879
0.1	0.186	1.23	0.534	2.00	0.810	6.18	0.969	4.60	1.24
1.0	0.181	1.26	0.516	2.16	0.793	7.10	0.961	6.07	2.29
3.0	0.180	1.26	0.516	2.22	0.787	7.50	0.958	6.90	6.30

Fig. 65—Ten-pole no-zero lattice-filter design for Chebishev response.

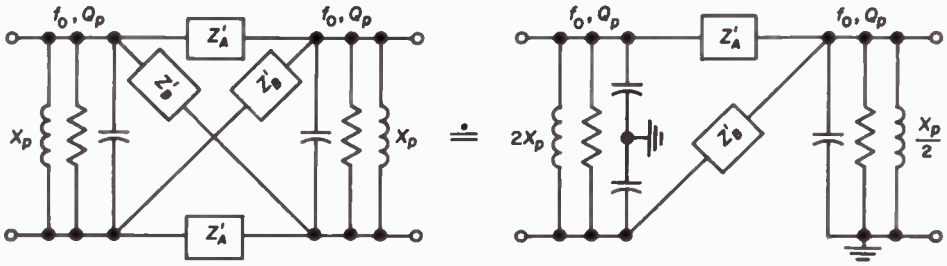

A. FULL-LATTICE CRYSTAL FILTER B. MODIFIED EQUIVALENT CRYSTAL FILTER

Fig. 66—Modification of *L–C* resonators to halve the required number of crystals.

*Lattice Equivalent**

An important lattice equivalent (Fig. 66) halves the number of crystals required for the full-lattice filter. After the full-lattice design is completed, it is merely necessary to double the reactances of one *L–C* resonator and to center-tap it; halve the reactances of the second *L–C* resonator and ground its bottom side; and then, as shown in Fig. 66B, two arms of the full lattice may be omitted. This equivalence is valid when dealing with small-percentage bandwidths and with high *L–C*-resonator loaded *Q*'s (Q_p).

For large-percentage bandwidths and/or low loaded *Q*'s, it is necessary to use an inductive center tap with a coupling coefficient between the two sides of the coil (L_p) approaching unity. The use of a capacitive center tap greatly simplifies the problem of "trimming-in" the tap point, which is always necessary in practice.

* M. Dishal, "Practical Modern Network Theory Design Data for Crystal Filters," *IRE 1957 National Convention Record*, Part 8.

CHAPTER 9
FILTERS, SIMPLE BAND-PASS DESIGN

COEFFICIENT OF COUPLING

Several types of coupled circuits are shown in Table 1 and Figs. 1 and 2, together with equations for the coefficient of coupling. Also shown is the dependence of bandwidth on resonance frequency. This dependence is only a rough approximation to show the trend and may be altered radically if L_m, M, or C_m is adjusted as the circuits are tuned to various frequencies.

K_{12} = coefficient of coupling between resonant circuits
X_{10} = reactance of inductor (or capacitor) of first circuit at f_0
X_{20} = reactance of similar element of second circuit at f_0
$(\text{bw})_C$ = bandwidth with capacitive tuning
$(\text{bw})_L$ = bandwidth with inductive tuning.

GAIN AT RESONANCE

Single Circuit

In Table 1A

$$E_0/E_g = -g_m \mid X_{10} \mid Q$$

where E_0 = output volts at resonance frequency f_0, E_g = input volts to active device, and g_m = transconductance of active device.

Pair of Coupled Circuits (Figs. 3 and 4)

In B through F in Table 1

$$E_0/E_g = jg_m(X_{10}X_{20})^{1/2}Q[K_{12}Q/(1+K_{12}^2Q^2)].$$

This is maximum at critical coupling, where $K_{12}Q = 1$.

$Q = (Q_1Q_2)^{1/2}$ = geometric-mean Q for the two circuits, as loaded with active device input and output impedances.

For circuits with critical coupling and overcoupling, the approximate gain is

$$\mid E_0/E_g \mid \approx 0.1g_m/(C_1C_2)^{1/2}(\text{bw})$$

where (bw) is the useful pass band in megahertz, g_m is in micromhos, and C is in picofarads.

SELECTIVITY FAR FROM RESONANCE

The selectivity curves of Fig. 5 are based on the presence of only a single type of coupling between the circuits. The curves are useful beyond the peak region treated on pp. 9–5 through 9–9.

In the equations for selectivity in Table 1

E = output volts at signal frequency f for same value of E_g as that producing E_0.

For Inductive Coupling

$$A = \frac{Q^2}{1+K_{12}^2Q^2}\left[\left(\frac{f}{f_0}-\frac{f_0}{f}\right)^2 - K_{12}^2\left(\frac{f}{f_0}\right)^2\right]$$

$$\approx \frac{Q^2}{1+K_{12}^2Q^2}\left(\frac{f}{f_0}-\frac{f_0}{f}\right)^2.$$

For Capacitive Coupling

A is defined by a similar equation, except that the neglected term is $-K_{12}^2(f_0/f)^2$. The 180-degree phase shift far from resonance is indicated by the minus sign in the expression for E_0/E.

Example. The use of the curves in Figs. 5, 6, and 7, is indicated by the following example. Given the circuit of Table 1C with input to PB across capacitor C_1. Let $Q = 50$, $K_{12}Q = 1.50$, and $f_0 = 16.0$ megahertz. Required is the response of $f = 8.0$ megahertz.

Here, $f/f_0 = 0.50$ and curve C, Fig. 5, gives -75 decibels. Then applying the corrections from Figs. 6 and 7 for Q and $K_{12}Q$, we find

$$\text{response} = -75+12+4 = -59 \text{ decibels.}$$

TABLE 1—SEVERAL TYPES OF COUPLED CIRCUITS, SHOWING COEFFICIENT OF COUPLING AND SELECTIVITY EQUATIONS.

Diagram	Coefficient of Coupling	Approximate Bandwidth Variation with Frequency	Selectivity Far From Resonance	
			Equation*	Curve in Fig. 5
A 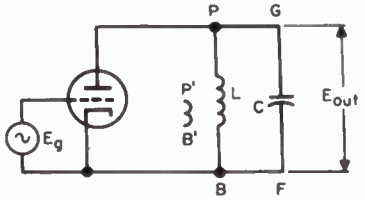			Input to PB or to $P'B'$: $E_0/E = jQ[(f/f_0) - (f_0/f)]$	A
B 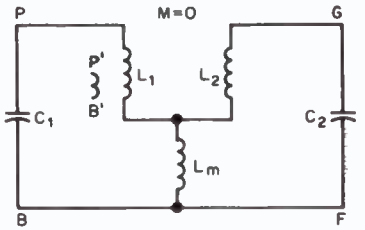	$K_{12} = L_m/[(L_1+L_m)(L_2+L_m)]^{1/2}$ $= \omega_0^2 L_m (C_1 C_2)^{1/2}$ $\approx L_m/(L_1 L_2)^{1/2}$	$(bw)_C \propto f_0$ $(bw)_L \propto f_0^3$	Input to PB: $E_0/E = -A(f/f_0)$ Input to $P'B'$: $E_0/E = -A(f_0/f)$	C D
C 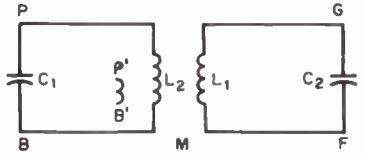	$K_{12} = M/(L_1 L_2)^{1/2}$ $= \omega_0^2 M (C_1 C_2)^{1/2}$ M may be positive or negative	$(bw)_C \propto f_0$ $(bw)_L \propto f_0^3$	Input to PB: $E_0/E = -A(f/f_0)$ Input to $P'B'$: $E_0/E = -A(f_0/f)$	C D

D	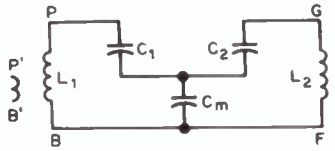	$K_{12} = -\{C_1C_2/[(C_1+C_m)(C_2+C_m)]\}^{1/2}$ $= -1/\omega_0^2 C_m (L_1L_2)^{1/2}$ $\approx -(C_1C_2)^{1/2}/C_m$	$(\text{bw})_C \propto 1/f_0$ $(\text{bw})_L \propto f_0$	Input to PB or to $P'B'$: $E_0/E = -A(f_0/f)$	D
E	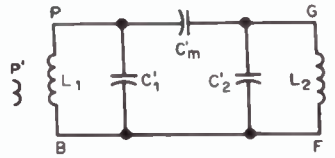	$K_{12} = -C_m'/[(C_1'+C_m')(C_2'+C_m')]^{1/2}$ $= -\omega_0^2 C_m' (L_1L_2)^{1/2}$ $\approx -C_m'/(C_1'C_2')^{1/2}$	$(\text{bw})_C \propto f^2$ $(\text{bw})_L \propto f$	Input to PB or to $P'B'$: $E_0/E = -A(f_0/f)$	D
F	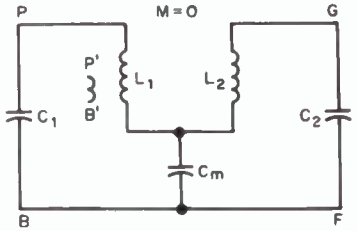	$K_{12} = -\{C_1C_2/[(C_1+C_m)(C_2+C_m)]\}^{1/2}$ $= -1/\omega_0^2 C_m (L_1L_2)^{1/2}$ $\approx -(C_1C_2)^{1/2}/C_m$	$(\text{bw})_C \propto 1/f_0$ $(\text{bw})_L \propto f_0$	Input to PB: $E_0/E = -A(f/f_0)^3$ Input to $P'B'$: $E_0/E = -A(f/f_0)$	B C

*Where $A = [Q^2/(1+K_{12}^2Q^2)][(f/f_0)-(f_0/f)]^2$.

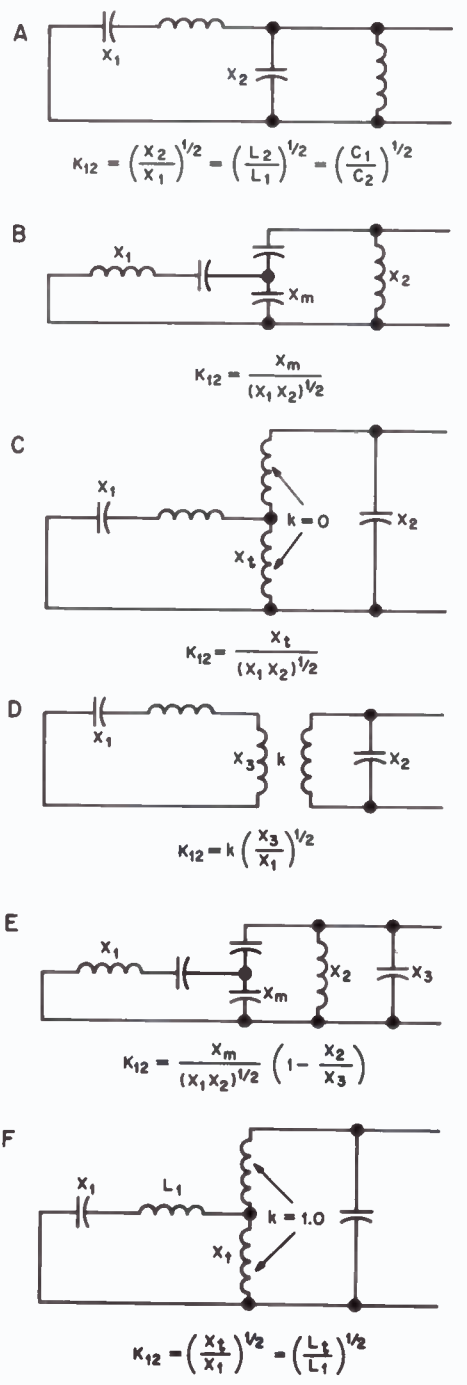

Fig. 1—Additional coefficient-of-coupling configurations (the node resonator is tuned to the desired midfrequency with the mesh resonator open-circuited, or the mesh resonator is tuned to this midfrequency with the node resonator short-circuited).

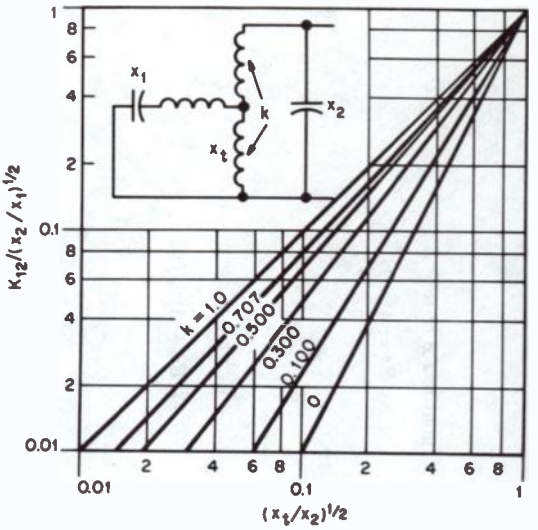

Fig. 2—Coefficient of coupling for configuration shown.

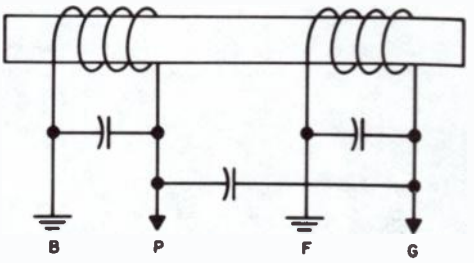

Fig. 3—Connection wherein k_m opposes k_c. (k_c may be due to stray capacitance.) Peak of attenuation is at $f = f_0(-k_m/k_c)^{1/2}$. Reversing connections or winding direction of one coil causes k_m to aid k_c.

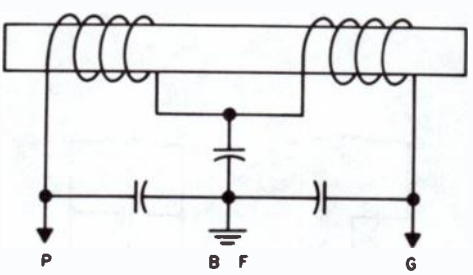

Fig. 4—Connection wherein k_m aids k_c. If mutual-inductance coupling is reversed, k_m will oppose k_c and there will be a transfer minimum at $f = f_0(-k_m/k_c)^{1/2}$.

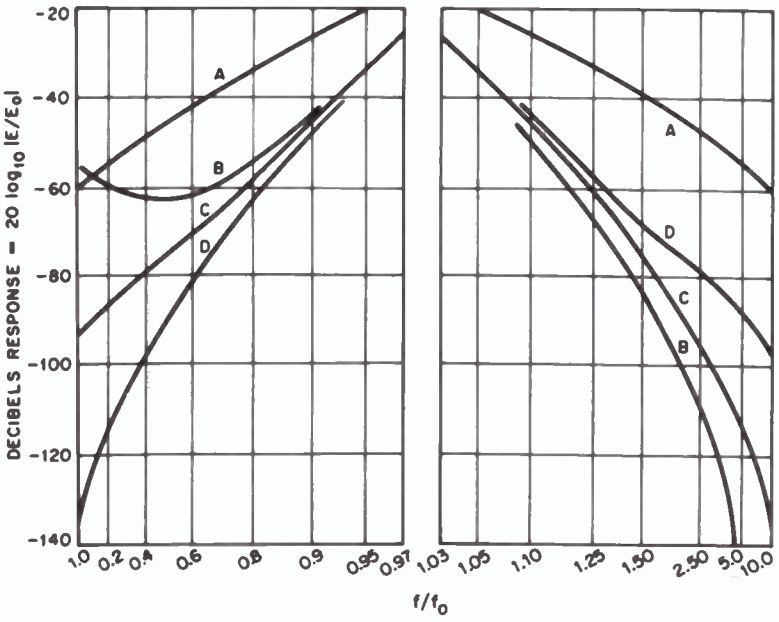

Fig. 5—Selectivity for frequencies far from resonance. $Q=100$ and $|K_{12}|Q=1.0$.

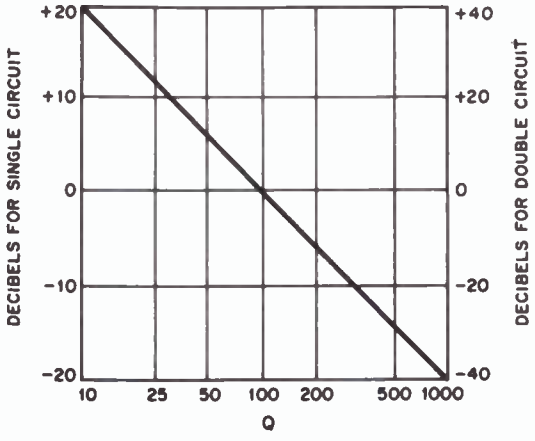

Fig. 6—Correction for $Q \neq 100$.

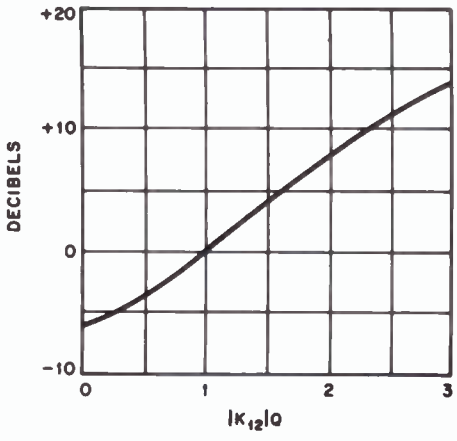

Fig. 7—Correction for $|K_{12}|Q \neq 1.0$.

SELECTIVITY OF SINGLE- AND DOUBLE-TUNED CIRCUITS NEAR RESONANCE

Equations and curves are presented for the selectivity and phase shift:

Of n single-tuned circuits
Of m pairs of coupled tuned circuits.

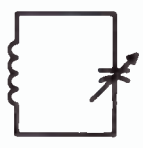

Fig. 8—Single-tuned circuit.

The conditions assumed are

(A) All circuits are tuned to the same frequency f_0.

(B) All circuits have the same Q, or each pair of circuits includes one circuit having Q_1 and the other having Q_2.

(C) Otherwise the circuits need not be identical.

(D) Each successive circuit or pair of circuits is isolated from the preceding and following ones by active devices, with no regeneration around the system.

Certain approximations have been made to simplify the equations. In most actual applications of the types of circuits treated, the error involved is negligible from a practical standpoint. Over the narrow frequency band in question, it is assumed that

(A) The reactance around each circuit is equal to $2X_0\,\Delta f/f_0$.

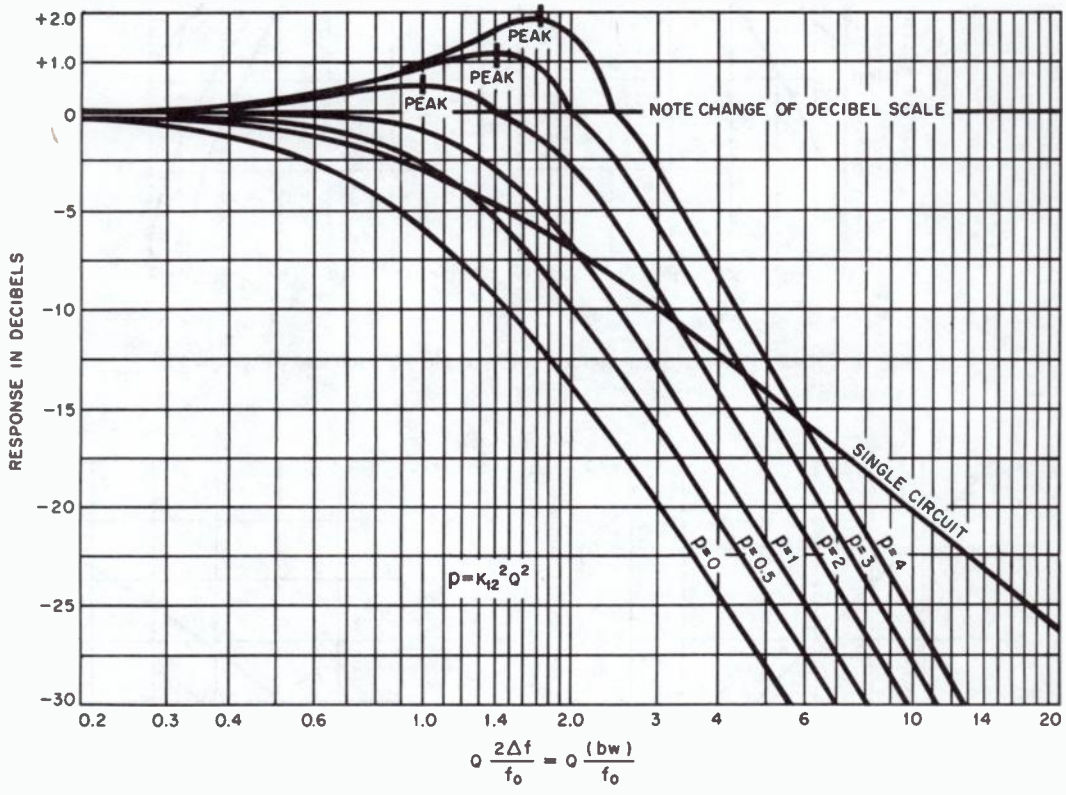

Fig. 9—Selectivity curves showing response of a single circuit $n=1$, and a pair of coupled circuits $m=1$. The selectivity curves are symmetrical about the axis $Q\,\Delta f/f_0=0$ for practical purposes.

Extrapolation beyond lower limits of chart:

Δ Response for Doubling Δf	Circuit	Useful Limit at $(bw)/f_0$	Useful Limit Error Becomes
−6 dB	←single→	0.6	1 to 2 dB
−12 dB	←pair→	0.4	3 to 4 dB

Example of the use of Figs. 9 and 10. Suppose there are three single-tuned circuits ($n=3$). Each circuit has a $Q=200$ and is tuned to 1000 kiloherts. The results are shown in the following table:

Abscissa $Q\,(bw)/f_0$	Bandwidth (kiloherts)	Ordinate dB Response for $n=1$	Decibels Response for $n=3$	ϕ^* for $n=1$	ϕ^* for $n=3$
1.0	5.0	−3.0	−9	∓45°	∓135°
3.0	15	−10.0	−30	∓71½°	∓215°
10.0	50	−20.2	−61	∓84°	∓252°

* ϕ is negative for $f>f_0$, and vice versa.

(B) The resistance of each circuit is constant and equal to X_0/Q.

(C) The coupling between two circuits of a pair is reactive and constant. (When an untuned link is used to couple the two circuits, this condition frequently is far from satisfied, resulting in a lopsided selectivity curve.)

(D) The equivalent input voltage, taken as being in series with the tuned circuit (or the first of a pair), is assumed to bear a constant proportionality to the input voltage of the active device or other driving source, at all frequencies in the band.

(E) Likewise, the output voltage across the circuit (or the final circuit of a pair) is assumed to be proportional only to the current in the circuit.

The following symbols are used in the equations in addition to those defined previously.

$\Delta f/f_0 = (f-f_0)/f_0 =$ (deviation from resonance frequency)/(resonance frequency)

(bw) = bandwidth $= 2\Delta f$

X_0 = reactance at f_0 of inductor in tuned circuit

n = number of single-tuned circuits

m = number of pairs of coupled circuits

ϕ = phase shift of signal at f relative to shift at f_0 as signal passes through cascade of circuits

$p = K_{12}^2Q^2$ or $p = K_{12}^2Q_1Q_2$, a parameter determining the form of the selectivity curve of coupled circuits

$B = p - \frac{1}{2}[(Q_1/Q_2)+(Q_2/Q_1)]$.

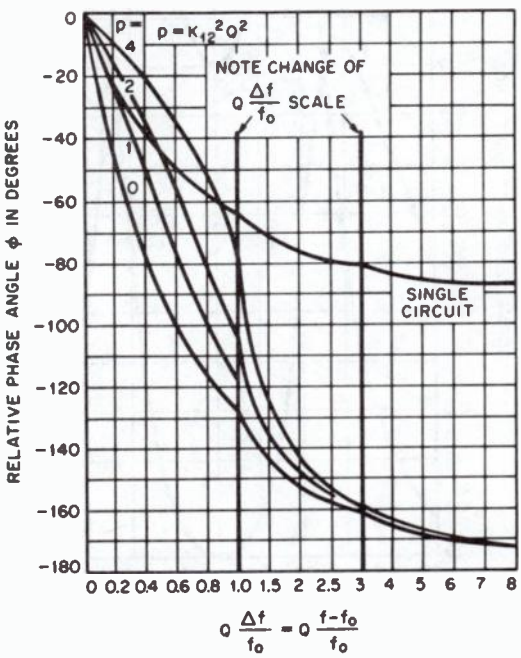

Fig. 10—Phase-shift curves for a single circuit $n=1$ and a pair of coupled circuits $m=1$. For $f>f_0$, ϕ is negative, while for $f<f_0$, ϕ is positive. The numerical value is identical in either case for the same $|f-f_0|$.

Selectivity and Phase Shift of Single-Tuned Circuits (Fig. 8)

$$E/E_0 = \{[1+(2Q\,\Delta f/f_0)^2]^{-1/2}\}^n$$

$$\Delta f/f_0 = \pm(2Q)^{-1}[(E_0/E)^{2/n}-1]^{1/2}$$

Decibel response $= 20\log_{10}(E/E_0)$

(dB response of n circuits) $= n\times$ (dB response of single circuit)

$$\phi = n\tan^{-1}(-2Q\,\Delta f/f_0).$$

These equations are plotted in Figs. 9 and 10.

Q Determination by 3-Decibel Points

For a single-tuned circuit, when

$E/E_0 = 0.707$ (3 decibels down)

$Q = f_0/2\Delta f$

$=$ (resonance frequency)/$(\text{bandwidth})_{3\text{dB}}$.

Selectivity and Phase Shift of Pairs of Coupled Tuned Circuits (Fig. 11)

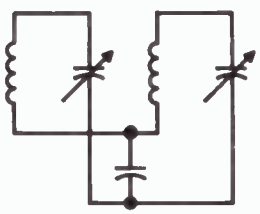

Fig. 11—One of several types of coupling.

Case 1: When $Q_1 = Q_2 = Q$:

These equations can be used with reasonable accuracy when Q_1 and Q_2 differ by ratios up to 1.5 or even 2 to 1. In such cases use the value $Q = (Q_1Q_2)^{1/2}$.

$$E/E_0 = \left[\frac{p+1}{\{[(2Q\,\Delta f/f_0)^2-(p-1)]^2+4p\}^{1/2}}\right]^m$$

$$\Delta f/f_0 = \pm(2Q)^{-1} \times\{(p-1)\pm[(p+1)^2(E_0/E)^{2/m}-4p]^{1/2}\}^{1/2}.$$

For very small values of E/E_0 the equations reduce to

$$E/E_0 = [(p+1)/(2Q\,\Delta f/f_0)^2]^m$$

Decibel response $= 20\log_{10}(E/E_0)$

(dB response of m pairs of circuits) $= m\times$ (dB response of one pair)

$$\phi = m\tan^{-1}\left[\frac{-4Q\,\Delta f/f_0}{(p+1)-(2Q\,\Delta f/f_0)^2}\right].$$

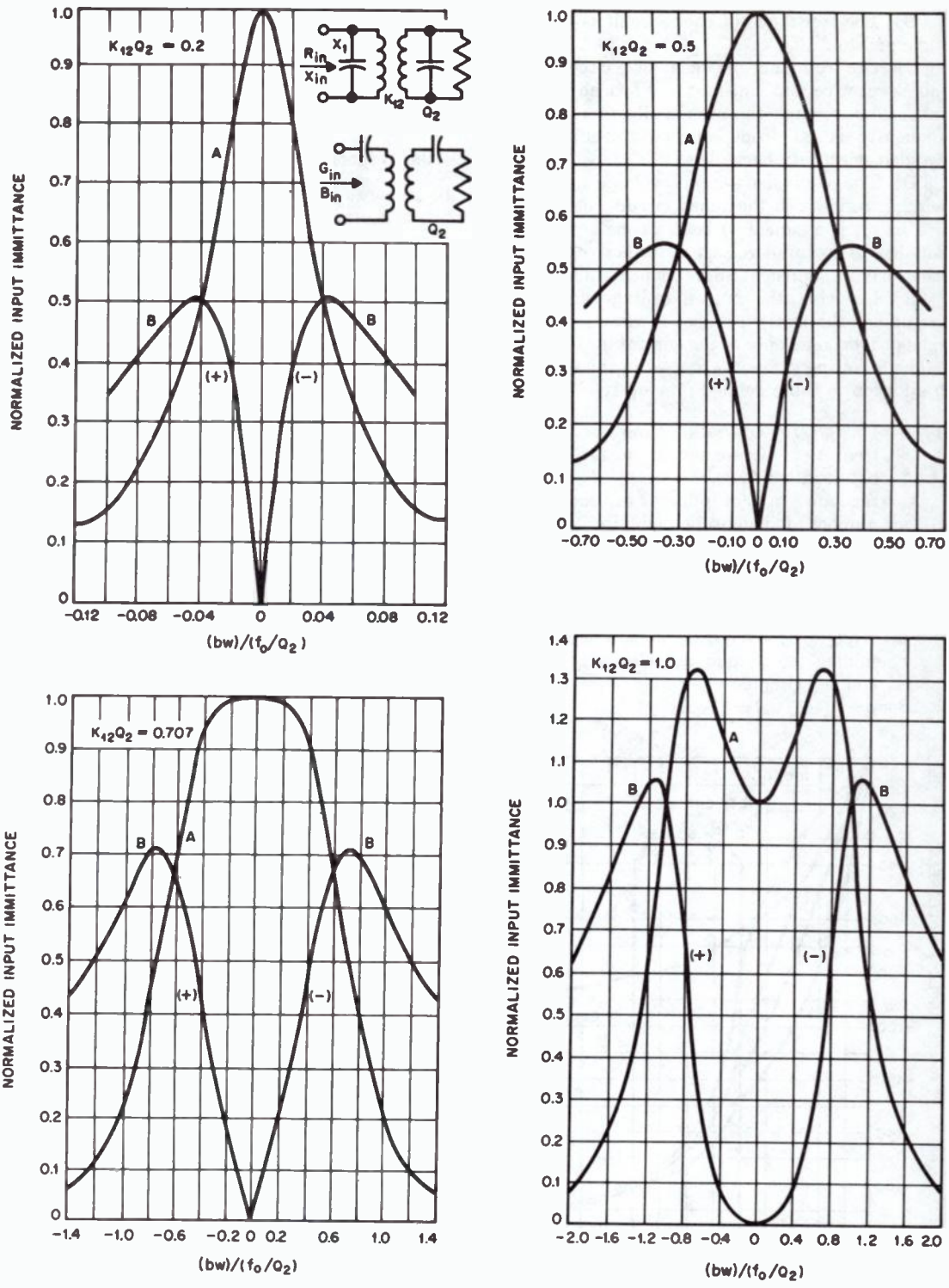

Fig. 12—Normalized input immittance vs. normalized frequency of double-tuned circuits. $A = R_{in}/(X_1/K_{12}^2Q_2)$ or $G_{in}/(B_1/K_{12}^2Q_2)$. $B = X_{in}/(X_1/K_{12}^2Q_2)$ or $B_{in}/(B_1/K_{12}^2Q_2)$.

As p approaches zero, the selectivity and phase shift approach the values for n single circuits, where $n=2m$ (gain also approaches zero).

The above equations are plotted in Figs. 9 and 10.

For Overcoupled Circuits ($p>1$):

Location of peaks:

$$(f_{peak}-f_0)/f_0=\pm(2Q)^{-1}(p-1)^{1/2}.$$

Amplitude of peaks:

$$E_{peak}/E_0=[(p+1)/2(p^{1/2})]^m.$$

Phase shift at peaks:

$$\phi_{peak}=m\tan^{-1}[\mp(p-1)^{1/2}].$$

Approximate pass band (where $E/E_0=1$) is

$$(f_{unity}-f_0)/f_0=\sqrt{2}[(f_{peak}-f_0)/f_0]$$
$$=\pm Q^{-1}[\tfrac{1}{2}(p-1)]^{1/2}.$$

Case 2: *General Equation for Any* Q_1 *and* Q_2:

$$E/E_0=\left[\frac{p+1}{\{[(2Q\,\Delta f_0/f_0)^2-B]^2+(p+1)^2-B^2\}^{1/2}}\right]^m$$

$$B=p-\tfrac{1}{2}[(Q_1/Q_2)+(Q_2/Q_1)]$$

$$\Delta f/f_0=\pm(2Q)^{-1}$$
$$\times\{B\pm[(p+1)^2(E_0/E)^{2/m}-(p+1)^2+B^2]^{1/2}\}^{1/2}$$

$$\phi=m\tan^{-1}$$
$$\times\left(-\frac{2Q\,\Delta f/f_0[(Q_1/Q_2)^{1/2}+(Q_2/Q_1)^{1/2}]}{(p+1)-(2Q\,\Delta f/f_0)^2}\right).$$

For Overcoupled Circuits:

Location of peaks:

$$(f_{peak}-f_0)/f_0=\pm B^{1/2}/2Q$$
$$=\pm\tfrac{1}{2}[K_{12}^2-\tfrac{1}{2}(1/Q_1^2+1/Q_2^2)]^{1/2}.$$

Amplitude of peaks:

$$E_{peak}/E_0=\{(p+1)/[(p+1)^2-B^2]^{1/2}\}^m.$$

Case 3: *Peaks Just Converged to a Single Peak*:

Here $B=0$ or $K_{12}^2=\tfrac{1}{2}(1/Q_1^2+1/Q_2^2)$

$$E/E_0=\{2/[(2Q'\,\Delta f/f_0)^4+4]^{1/2}\}^m$$

where

$$Q'=2Q_1Q_2/(Q_1+Q_2)$$

$$\Delta f/f_0=\pm(\sqrt{2}/4)(1/Q_1+1/Q_2)[(E_0/E)^{2/m}-1]^{1/4}$$

$$\phi=m\tan^{-1}\left[-\frac{4Q'\,\Delta f/f_0}{2-(2Q'\,\Delta f/f_0)^2}\right].$$

The curves of Figs. 9 and 10 may be applied to this case, using the value $p=1$ and substituting Q' for Q.

NODE INPUT IMPEDANCE OR MESH INPUT ADMITTANCE OF A DOUBLE-TUNED CIRCUIT

Figure 12 gives the normalized input immittance versus the normalized frequency of double-tuned circuits.

CHAPTER 10
ACTIVE FILTER DESIGN

The information presented in this chapter may be used by a filter designer to obtain complete designs of a wide variety of types of active filters using standard circuit element values. Only minor computations, such as obtaining a scale factor SF and multiplying the resistances of a given table by SF, are required. For the interested reader, brief descriptions of active filters of various types are given, but to use the results of the chapter it is not necessary to read or understand the textual material, since a self-contained summary follows the discussion of each filter type. Detailed examples of complete designs are provided in the various sections; these examples may be used as guidelines, if desired.

INTRODUCTION

An electric filter is a network which transforms an input signal in some specified manner to produce a desired output signal. In most cases, filters are frequency-selective, phase-shifting, or time-delay devices. These concepts may be more specifically defined by considering the general filter representation of Fig. 1. The transfer function is

$$H(s)=\frac{V_2(s)}{V_1(s)} \tag{1}$$

where V_1 is the input voltage and V_2 is the output voltage.

Fig. 1—A general filter representation.

In the steady-state case, $s=j\omega$, where $\omega=2\pi f$ rad/s and f is the frequency in hertz. The transfer function is then complex, and is given by

$$H(j\omega)=|H(j\omega)|\exp j\phi(\omega) \tag{2}$$

where $|H(j\omega)|$ is the amplitude and $\phi(\omega)$ is the phase. The plots of $|H(j\omega)|$ and $\phi(\omega)$ versus ω are the amplitude and phase responses, respectively.

A frequency-selective filter is one which passes signals of certain frequencies and blocks those of other frequencies. The range, or band, of frequencies which pass is the passband in which the amplitude is relatively large, and ideally a constant. The frequencies which are blocked constitute the stopband in which the amplitude is relatively small, and ideally zero. Of course, a filter may be designed to have more than one passband and/or stopband. Examples of frequency-selective filters are low-pass, high-pass, bandpass, and band-reject filters, which will be described later.

An all-pass filter is one which passes all frequencies equally well. Its amplitude response is constant for all frequencies, and its phase response is a function of frequency. It is thus a phase-shifting filter.

The time delay, $T(\omega)$, of a filter is defined in terms of its phase response by

$$T(\omega)=-\frac{d}{d\omega}\phi(\omega) \tag{3}$$

Ideally, the phase response is linear, say $\phi(\omega)=-\omega T_0$, and thus the time delay is ideally a constant, $T(\omega)=T_0$. Time-delay filters are those designed to have a time delay which is approximately constant over a specified frequency range.

Ideal behavior is impossible to achieve, except in the all-pass case. Therefore, filter design consists of obtaining a transfer function which approximates the ideal response to some prescribed degree and constructing a network which realizes the transfer function. The transfer function is a ratio of two polynomials, and the order of the filter is defined as the degree of the denominator polynomial. In general, the higher the order of the filter, the better the approximation to the ideal case; however, higher order is accompanied by more complexity and higher cost.

Passive filters are those whose components are resistors, inductors, and capacitors and are quite useful for operation in certain frequency ranges. However, for low-frequency operation, say 1 Hz to approximately 0.5 MHz, inductors are undesirable because of their size and considerable departure from ideal behavior. Also, inductors, unlike resistors and capacitors, are not readily adaptable to integrated-circuit techniques, which have become extremely important in recent years.

Active filters are constructed with resistors, capacitors, and one or more active devices, such as transistors, controlled sources, etc. They are extremely useful for operation at the lower fre-

quencies, where they are much to be preferred over passive filters. The active element which is most often used*, and the one exclusively considered in this chapter, is the integrated circuit (IC) operational amplifier.

CIRCUIT ELEMENTS

Operational Amplifiers

The operational amplifier (or "op amp") is a multiterminal device which is often represented in the ideal case by the three-terminal device of Fig. 2. The terminals shown are the inverting input (1), the noninverting input (2), and the output (3) terminals. Ideally, the voltage between the input terminals is zero, and the current into the input terminals is zero. This is a consequence of the ideal op amp's properties of infinite input resistance, zero output resistance, and infinite gain.

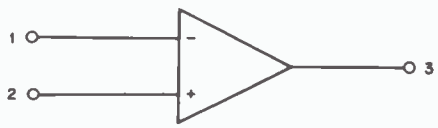

Fig. 2—Symbol for ideal operational amplifier.

Practical op amps approximate the ideal only over a limited frequency range. Typical bipolar op amps, such as the popular 741 type, have open-loop gains of 200 000 at dc, decreasing monotonically to about 1000 at 1 kHz. Input resistances of bipolar devices range from approximately 200 kΩ to 2 MΩ. Typical FET op amps, such as the 536 type, have similar gain characteristics, with input resistances as high as 10^{14} Ω.

Other terminals not shown in Fig. 2 normally include power-supply terminals, compensation terminals, and offset-null terminals. Most op amps have two power-supply terminals which operate from ±5 to ±22 volts. Some (e.g., the 741) are internally compensated and have no compensation terminals. Others (e.g., the 709) require an external compensating network of resistances and capacitances to obtain the desired operating characteristics. Externally compensated op amps generally have performance characteristics at higher frequencies superior to those of internally compensated op amps. Offset null terminals are provided on some op amps, such as the 741, to set the dc output voltage to zero when no signal is applied to the input terminals. The manner in which these additional terminals are connected is generally specified by the manufacturer.

Another important consideration in the selection of an op amp is that of slew rate, which is the maximum rate of change in the output voltage in volts per microsecond. Therefore, in applications requiring large output voltage swings, op amps with high slew rates may be required. Op amps are available with slew rates as high as 320 V/μs.

Resistors

Three commonly used types of resistors are carbon composition, metal film, and wirewound*. Carbon composition resistors are the most common and least expensive. They are generally satisfactory in simpler filter designs if temperature considerations are not critical. Metal film and wirewound resistors are widely used in filter design and have better temperature characteristics. The wirewound resistor generally has the best performance characteristics of the three, but it is also the most expensive.

Capacitors

Capacitors are the most critical elements in active filter design†. Those types commonly used include ceramic disk, Mylar, polystyrene, and teflon. The ceramic disk capacitor is the least expensive and is of the poorest quality. It should be used only in the most noncritical applications. Mylar capacitors are widely available, relatively inexpensive, and suitable in most simpler designs. Polystyrene and teflon capacitors are of the highest quality and yield best results in complex designs.

LOW-PASS FILTERS

A low-pass filter is a frequency-selective filter which passes low frequencies and blocks high frequencies. It has a single passband, $0<\omega<\omega_c$, and a single stopband, $\omega>\omega_c$. The frequency ω_c (or in hertz, $f_c=\omega_c/2\pi$) which separates the two bands is the cutoff frequency.

As an example, the amplitude response of an ideal low-pass filter is represented by the broken line of Fig. 3. The ideal is impossible to realize, since the transfer function of an actual filter is

* J. L. Hilburn and D. E. Johnson, *Manual of Active Filter Design*, McGraw-Hill Book Co., New York, 1973.

* J. G. Graeme, G. E. Tobey, and L. P. Huelsman (eds), *Operational Amplifiers: Design and Applications*, McGraw-Hill Book Co., New York, 1971.

† *Loc. cit.*

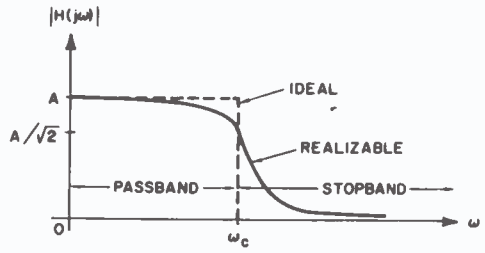

Fig. 3—Ideal and realizable low-pass responses.

a ratio of polynomials and its amplitude cannot possess the sharp corners of the ideal response. A realizable approximation to the ideal is represented by the solid line of Fig. 3. In the realizable case, the division between the passband and stopband is not clearly distinguishable, and the cutoff frequency is defined as the point at which $|H(j\omega)|$ is $1/\sqrt{2}=0.707$ times its maximum value, shown as A in Fig. 3. In decibels, the cutoff frequency is the point at which the amplitude is 3 dB below its maximum value.

The gain of a low-pass filter is the value of its amplitude at zero frequency, or equivalently, gain $=H(0)$, where $H(s)$ is the transfer function.

The simplest transfer function which approximates the ideal low-pass characteristic is the ratio of a constant to a polynomial. It is called an all-pole-function because all its poles, and none of its zeros, are finite.

Second-Order Designs

A second-order all-pole approximation to the ideal low-pass filter with cutoff frequency ω_c is achieved by the transfer function

$$\frac{V_2}{V_1}=\frac{Kb\omega_c^2}{s^2+a\omega_c s+b\omega_c^2} \tag{4}$$

where K, a, and b are appropriately chosen constants. The gain is K, and the coefficients a and b are determined by the type of low-pass filter under consideration, such as Butterworth or Chebishev, to be considered later.

One of the simplest active filters which realizes the second-order low-pass filter is the multiple-feedback (MFB) network* of Fig. 4. This circuit realizes (4) with an inverting gain $-K$ $(K>0)$ for

$$R_2=\frac{2(K+1)}{\{aC+[a^2C^2-4bCC_1(K+1)]^{1/2}\}\omega_c}$$
$$R_1=R_2/K$$
$$R_3=1/bCC_1\omega_c^2R_2 \tag{5}$$

* J. G. Graeme, G. E. Tobey, and L. P. Huelsman (eds), *ibid.*

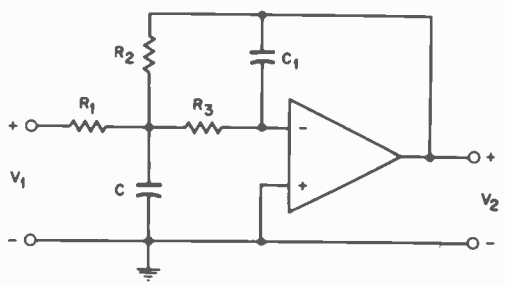

Fig. 4—A second-order MFB low-pass filter.

Thus for a given K, a, b, and ω_c, one may select C and C_1 (with C_1 sufficiently small to make the denominator of R_2 real) and determine the resistances.

The MFB filter is one of the most commonly used filters with inverting gain, because of its minimal number of circuit elements. Other advantages are its low output resistance, which makes it convenient for cascading with other stages, and its good stability characteristics. A disadvantage, however, is that relatively high gains are not possible.

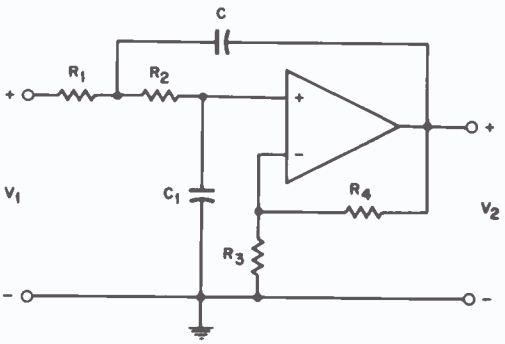

Fig. 5—A second-order VCVS low-pass filter.

Another commonly used circuit which realizes the second-order low-pass filter is the voltage-controlled voltage source (VCVS) network* of Fig. 5. This circuit yields a noninverting gain $K>0$, realizing (4) with

$$R_1=\frac{2}{(aC+\{[a^2+4b(K-1)]C^2-4bCC_1\}^{1/2})\omega_c}$$
$$R_2=1/bCC_1R_1\omega_c^2$$
$$R_3=K(R_1+R_2)/(K-1), \qquad K\neq 1$$
$$R_4=K(R_1+R_2) \tag{6}$$

The latter two equations give $K=1+R_4/R_3$ in a way which minimizes the dc offset of the op amp.

* R. P. Sallen and E. L. Key, "A Practical Method of Designing RC Active Filters," *IRE Trans. on Circuit Theory*, CT-2, pp. 74–85, March 1955.

If $K=1$, they may be taken as $R_3=\infty$ (open circuit) and $R_4=0$ (short circuit). For minimum dc offset, $R_4=R_1+R_2$ in this case.

For a given K, a, b and ω_c, one may select C and C_1 to make R_1 real, and determine the resistances.

The VCVS filter is perhaps the most popular of the noninverting gain types. Its advantages include a minimal number of elements, a low output resistance, a capability of relatively high gains, and a relative ease of adjustment of characteristics. For example, the gain may be set precisely by adjusting R_3 and R_4. This circuit, however, is not as stable as the MFB filter.

Fourth-Order Designs

A fourth-order all-pole low-pass filter transfer function is a ratio of a constant to a fourth-degree polynomial. One method of realizing the function is to factor it into two second-order factors like (4), given by

$$\frac{V_2}{V_1}=\frac{K_1 b_1\omega_c^2}{s^2+a_1\omega_c s+b_1\omega_c^2}\cdot\frac{K_2 b_2\omega_c^2}{s^2+a_2\omega_c s+b_2\omega_c^2} \qquad (7)$$

Each factor is then realized by a network, or stage, like Fig. 4 or Fig. 5, and the two stages are cascaded as shown in Fig. 6. The small output resistance of

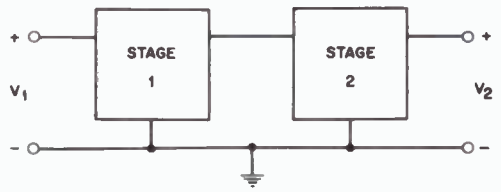

Fig. 6—Cascading of two second-order stages to realize a fourth-order filter.

practical op amps prevents one stage from loading down the other.

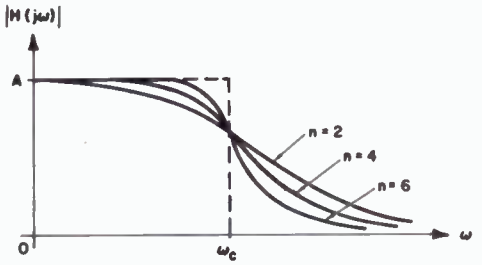

Fig. 7—Butterworth low-pass amplitude responses.

The gains of the stages are K_1 and K_2, respectively, and the overall gain is $K=K_1K_2$.

Butterworth Filters

One method of approximating the ideal low-pass response of Fig. 3 is with the amplitude function

$$|H(j\omega)|=\frac{A}{[1+(\omega/\omega_c)^{2n}]^{1/2}}; \qquad n=1,2,3,\cdots \qquad (8)$$

This is the amplitude response of the Butterworth low-pass filter of order n, which is exceedingly flat (so-called maximally flat) in the passband $0<\omega<\omega_c$. As n increases, (8) better approximates the ideal response, as may be seen in Fig. 7 for $n=2$, 4, and 6.

For low-pass Butterworth designs, the coefficients of (4) for the second-order case ($n=2$) and (7) for the fourth-order case ($n=4$) are given in Table 1.

To obtain a practical design of a second-order Butterworth filter, one may select standard values of C and C_1, and substitute the appropriate values of a and b given by Table 1 and the desired values of ω_c and K into (5) for the MFB realization of Fig. 4, or into (6) for the VCVS realization of Fig. 5.

TABLE 1—LOW-PASS COEFFICIENTS FOR SECOND- AND FOURTH-ORDER DESIGNS.

		Butterworth	Chebishev		
n			0.1 dB	0.5 dB	1 dB
2	a	1.41421	2.37209	1.42562	1.09773
	b	1.00000	3.31329	1.51620	1.10251
4	a_1	0.76537	0.52827	0.35071	0.27907
	b_1	1.00000	1.32981	1.06352	0.98650
	a_2	1.84776	1.27536	0.84668	0.67374
	b_2	1.00000	0.62282	0.35641	0.27940

TABLE 2—SECOND-ORDER MFB LOW-PASS BUTTERWORTH DESIGNS.

Gain	C_1	R_1	R_2	R_3
2	0.150C	1.612	3.223	2.068
10	0.033C	1.021	10.211	2.968

TABLE 3—SECOND-ORDER VCVS LOW-PASS BUTTERWORTH DESIGNS.

Gain	C_1	R_1	R_2	R_3	R_4
2	1C	0.707	1.414	4.242	4.242
10	2C	0.290	1.723	2.237	20.131

To facilitate the design procedure and eliminate most of the calculations, one may use Table 2 for the MFB filter and Table 3 for the VCVS filter. The procedure is as follows: Select a standard value of the capacitance C. Determine a scale factor SF from

$$SF=\frac{500}{\pi f_c C'} \tag{9}$$

where f_c is the desired cutoff frequency in hertz and C' is C in microfarads. For example, if $C=0.01$ μF, then $C'=0.01$. For a gain of 2 or 10, multiply the resistances in Table 2 or Table 3 by SF. The results are the filter elements in kilohms. Capacitance C_1 is given by the table in terms of C. The filter should be constructed in accordance with Fig. 4 or Fig. 5, using the indicated capacitances and standard values of resistances as close as possible to the calculated values.

For fourth-order designs, the Butterworth coefficients a_1, b_1, a_2, and b_2 of Table 1 should be used along with the gains K_1 and K_2 of each stage. (The filter gain, it will be recalled, is $K=K_1K_2$.) Each stage should then be determined as in the second-order case and the two stages cascaded as in Fig. 6. The process may be considerably shortened for a gain of 4 (2 per stage) by the use of Tables 4 and 5 for the MFB and VCVS filters, respectively. The procedure for each stage is identical to that of the second-order design, described earlier. That is, for each stage, select C, determine SF from (9), and obtain C_1 and the unscaled resistances for the stage from Table 4 or 5, as appropriate. The unscaled resistances multiplied by SF are the filter resistances in kilohms.

A detailed example, illustrating both the direct calculation method and the use of the tables, is given in a later section.

Chebishev Filters

Another method of approximating the ideal low-pass response of Fig. 3 is by means of the Chebishev low-pass filter. Its amplitude function is given by

$$|H(j\omega)|=\frac{A}{[1+\epsilon^2 C_n^2(\omega/\omega_c)]^{1/2}}; \qquad n=1,2,3,\cdots \tag{10}$$

TABLE 4—FOURTH-ORDER MFB LOW-PASS BUTTERWORTH DESIGNS.

Stage	Gain	C_1	R_1	R_2	R_3
1	2	0.047C	3.286	6.572	3.238
2	2	0.220C	1.100	2.200	2.066

TABLE 5—FOURTH-ORDER VCVS LOW-PASS BUTTERWORTH DESIGNS.

Stage	Gain	C_1	R_1	R_2	R_3	R_4
1	2	1C	1.307	0.765	4.144	4.144
2	2	1C	0.541	1.848	4.778	4.778

where A and ϵ are constants and C_n is the Chebishev polynomial of degree n given by

$$C_n(x) = \cos(n \cos^{-1} x) \qquad (11)$$

The amplitude response is characterized by ripples (which are equal in magnitude) in the channel $0<\omega<\omega_c$, and a monotonically decreasing response in the band $\omega>\omega_c$. This is shown in Fig. 8 for $n=2$, 3, and 4. The Chebishev filter has a much sharper cutoff than the Butterworth filter for a given allowable deviation in the band $0<\omega<\omega_c$. In this respect, it is the best of the all-pole filters.*

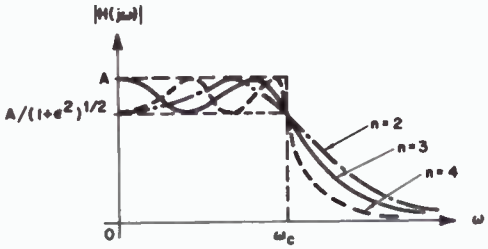

Fig. 8—Chebishev low-pass amplitude responses.

TABLE 6—RATIO OF CONVENTIONAL CUTOFF $f_{3\,db}$ TO RIPPLE CHANNEL TERMINAL f_c FOR LOW-PASS CHEBISHEV FILTERS.

	$f_{3\,db}/f_c$	
dB	$n=2$	$n=4$
0.1	1.943	1.213
0.5	1.390	1.093
1	1.218	1.053

As is clear from Fig. 8, if $\epsilon=1$, ω_c is the cutoff frequency in the conventional sense, because the amplitude is $A/\sqrt{2}$ at ω_c. However, if $0<\epsilon<1$, the cutoff frequency is greater than ω_c. In any case ω_c is the terminal frequency of the ripple channel and will be used in lieu of the cutoff frequency. Table 6 gives the conventional cutoff frequency in terms of $f_c=\omega_c/2\pi$ for various ripple widths so that a designer may find from the desired cutoff frequency the appropriate ω_c to be used in (10).

The bottom of the ripple channel is $10 \log_{10}(1+\epsilon^2)$ decibels below the top, since

$$\text{dB} = 20 \log_{10} A - 20 \log_{10}[A/(1+\epsilon^2)^{1/2}]$$

or

$$\text{dB} = 10 \log_{10}(1+\epsilon^2) \qquad (12$$

The ripple width may be used to characterize the Chebishev filter, as was done in Table 6. For example, a 1-dB filter is one for which dB = 1 in (12), or $\epsilon=0.50885$.

The coefficients in (4) and (7) for second- and fourth-order Chebishev functions are given, for the 0.1-, 0.5-, and 1-dB cases, in Table 1.

To obtain second- or fourth-order Chebishev low-pass filter designs, one may use the same procedure as in the Butterworth case. The only difference is in the values of the coefficients in Table 1. Also, as in the Butterworth case, the procedure is greatly simplified by the use of tables. Tables 7 and 8 apply for the second-order MFB and VCVS Chebishev filters, respectively, and Tables 9 and 10 apply for the fourth-order cases. Capacitor C is selected for the second-order case or for a stage of the fourth-order case, SF is calculated from (9), and the unscaled resistances in the appropriate table are multiplied by SF to obtain the filter resistances. Capacitance C_1 is determined from the table.

TABLE 7—SECOND-ORDER MFB LOW-PASS CHEBISHEV DESIGNS.

Gain	C_1	R_1	R_2	R_3	dB
2	0.100C	0.820	1.641	1.840	0.1
10	0.033C	0.672	6.717	1.362	
2	0.100C	1.590	3.180	2.074	0.5
10	0.022C	1.011	10.105	2.967	
2	0.050C	1.635	3.270	5.548	1
10	0.020C	1.390	13.904	3.262	

* P. I. Richards, "Universal Optimum-Response Curve for Arbitrarily Selected Coupled Resonators," *Proc. IRE*, vol. 34, pp. 624–629, September 1946.

TABLE 8—SECOND-ORDER VCVS LOW-PASS CHEBISHEV DESIGNS.

Gain	C_1	R_1	R_2	R_3	R_4	dB
2	1C	0.422	0.716	2.275	2.275	0.1
10	2C	0.163	0.927	1.211	10.902	
2	1C	0.701	0.940	3.283	3.283	0.5
10	2C	0.247	1.335	1.758	15.819	
2	1C	0.911	0.996	3.813	3.813	1
10	2C	0.296	1.533	2.032	18.289	

TABLE 9—FOURTH-ORDER MFB LOW-PASS CHEBISHEV DESIGNS.

Stage	Gain	C_1	R_1	R_2	R_3	dB
1	2	0.015C	4.124	8.247	6.079	0.1
2	2	0.200C	1.831	3.662	2.192	
1	2	0.0082C	6.171	12.342	9.291	0.5
2	2	0.100C	2.167	4.334	6.474	
1	2	0.005C	7.215	14.431	14.049	1
2	2	0.100C	2.946	5.893	6.074	

TABLE 10—FOURTH-ORDER VCVS LOW-PASS CHEBISHEV DESIGNS.

Stage	Gain	C_1	R_1	R_2	R_3	R_4	dB
1	2	1C	1.893	0.397	4.580	4.580	0.1
2	2	1C	0.784	2.048	5.664	5.664	
1	2	1C	2.851	0.330	6.362	6.362	0.5
2	2	1C	1.181	2.376	7.113	7.113	
1	2	1C	3.583	0.283	7.732	7.732	1
2	2	1C	1.484	2.411	7.791	7.791	

Practical Design Example

As an example, suppose it is desired to construct a low-pass VCVS Butterworth filter of second order having a gain of $K=2$ and a cutoff frequency of 1000 Hz. Assume capacitance values of $C=C_1=0.01\,\mu\text{F}=10^{-8}$ F. From Table 1, $a=1.41421=\sqrt{2}$ and $b=1$, so that by (6),

$$R_1 = 2/(\sqrt{2}(10^{-8}) + \{[(\sqrt{2})^2 + 4(1)(2-1)](10^{-16}) - 4(1)(10^{-16})\}^{1/2})(2\pi)(10^3)\Omega$$

$$= 11.254\ \text{k}\Omega$$

$$R_2 = 1/[(1)(10^{-16})(11.254)(10^3)(2\pi)^2(10^6)]\Omega$$

$$= 22.508\ \text{k}\Omega$$

$$R_3 = \frac{2(11.254+22.508)}{2-1} = 67.524\ \text{k}\Omega$$

$$R_4 = 2(11.254+22.508) = 67.524\ \text{k}\Omega$$

To use the tables to obtain the design, note that $C' = 0.01$ so that (9) yields

$$SF = \frac{500}{\pi(1000)(0.01)} = 15.915$$

By Table 3 for a gain of 2, $C_1 = C = 0.01\ \mu\text{F}$, and the resistances are

$$R_1 = 0.707SF = 11.252\ \text{k}\Omega$$

$$R_2 = 1.414SF = 22.504\ \text{k}\Omega$$

$$R_3 = R_4 = 4.242SF = 67.511\ \text{k}\Omega$$

Standard values of resistance as close as possible to the calculated values should be used in constructing the circuit in accordance with Fig. 5.

Design Summary of Low-Pass Filters

For the desired filter type (Butterworth or Chebishev) with gain K and cutoff frequency f_c (hertz), select the circuit (Fig. 4 for the MFB filter or Fig. 5 for the VCVS filter) and the capacitance C to be used. In the Chebishev case, the design formulas and tables are given with f_c as the terminal frequency of the ripple channel. If the conventional cutoff frequency $f_{3\,\text{db}}$ is specified, then the proper value of f_c to be used is found from Table 6. A good choice of C is a standard value approximately equal to $10/f_c\ \mu\text{F}$.

Method 1:

(A) Obtain coefficients a and b in the second-order case, or a_1, a_2, b_1, and b_2 in the fourth-order case, from Table 1.

(B) Select a standard value of C_1 so that

$$C_1 < \frac{a^2C}{4b(K+1)} \qquad \text{(MFB)}$$

$$C_1 < \frac{[a^2+4b(K-1)]C}{4b} \qquad \text{(VCVS)}$$

for the second-order case, or for each stage in the fourth-order case.

(C) Obtain the resistances from (5) for the MFB filter and from (6) for the VCVS filter.

Method 2:

(A) Find SF from (9).

(B) From the appropriate one of Tables 2 through 5 and 7 through 10, find C_1. Determine the resistances in kilohms by multiplying the table values by SF.

In either method, the filter should be constructed from standard values of resistances as close as possible to the calculated values. Generally, Mylar capacitors and 5% carbon composition resistors yield suitable designs. In all designs, a dc return to ground is required for each input terminal of the op amp. In the selection of an op amp, the open-loop gain should be at least 50 times the gain of the filter, and the peak-to-peak output voltage should not exceed $10^6/\pi f_a$ times the slew rate of the op amp, where f_a is the highest frequency of interest in the passband. A specific example of a low-pass design, given earlier, may be used as a guideline.

HIGH-PASS FILTERS

A high-pass filter passes high frequencies and blocks low frequencies. Thus it has $0 < \omega < \omega_c$ as the stopband and $\omega > \omega_c$ as the passband, where, as in the low-pass case, ω_c is the cutoff frequency. An ideal response, along with a realizable approximation, is shown in Fig. 9.

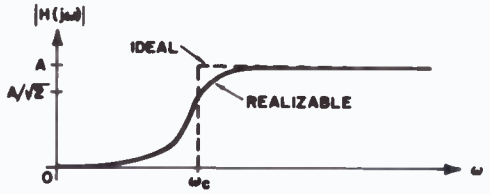

Fig. 9—Ideal and realizable high-pass responses.

The transfer function of a high-pass filter may be obtained from that of a low-pass filter by replacing s by $1/s$. This has the effect of interchanging the low and high frequencies, and thus the stopband and passband. In the second-order case, effecting the transformation $s \rightarrow 1/s$ in the low-pass function (4) results in the second-order high-pass function,

$$\frac{V_2}{V_1} = \frac{Ks^2}{s^2 + \frac{a\omega_c}{b}s + \frac{\omega_c^2}{b}} \qquad (13)$$

In the fourth-order case the transformation is applied to (7), resulting in

$$\frac{V_2}{V_1}=\frac{K_1 s^2}{s^2+\frac{a_1\omega_c}{b_1}s+\frac{\omega_c^2}{b_1}}\cdot\frac{K_2 s^2}{s^2+\frac{a_2\omega_c}{b_2}s+\frac{\omega_c^2}{b_2}} \qquad (14)$$

In (13) and (14), the a's and b's are the low-pass coefficients of (4) and (7).

For a Butterworth or Chebishev high-pass filter, (13) and (14) are obtained in the second- and fourth-order cases by using the appropriate coefficients from Table 1. The Butterworth response is maximally flat, and the Chebishev response has ripples in the passband ($\omega>\omega_c$). In the Chebishev case, ω_c is the beginning of the ripple channel rather than the conventional 3-dB cutoff frequency. To relate the two, one may use the reciprocals of the values in Table 6, since $\omega_{3\,db}<\omega_c$ in the high-pass case.

The gain of a high-pass filter is defined as the value of its transfer function as $s\longrightarrow\infty$. From (13) and (14) it may be seen that the gain of the second-order filter is K and that of the fourth-order filter is $K=K_1K_2$, which is precisely that of its low-pass counterpart.

Second-Order Designs

Like its low-pass counterpart, the second-order high-pass filter may be realized by an MFB circuit or a VCVS circuit. The MFB circuit* is shown in Fig. 10 and realizes (13) if

$$R_1=\frac{aK}{C(2K+1)\omega_c}$$

$$R_2=\frac{b(2K+1)}{aC\omega_c}$$

$$C_1=C/K \qquad (15)$$

where the gain is $-K$ (inverting).

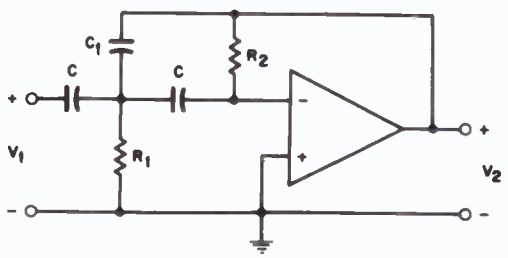

Fig. 10—A second-order MFB high-pass filter.

* J. G. Graeme, G. E. Tobey, and L. P. Huelsman (eds), *op cit.*

Since $K=C/C_1$, C may be selected arbitrarily, and for given values of a, b, and ω_c, values of C_1, R_1, and R_2 may be calculated. It should be noted that the gain K is restricted to a ratio of standard capacitances.

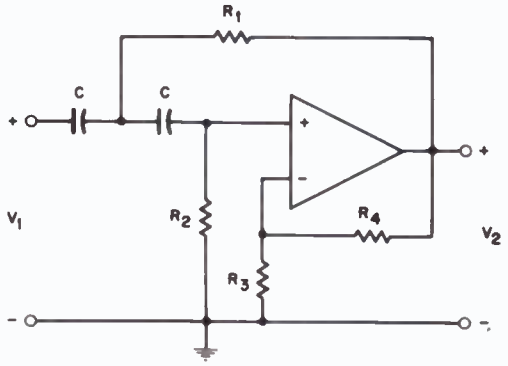

Fig. 11—A VCVS second-order high-pass filter.

A VCVS realization* of (13) is shown in Fig. 11, where

$$R_2=\frac{4b}{C\{a+[a^2+8b(K-1)]^{1/2}\}\omega_c}$$

$$R_1=b/C^2R_2\omega_c^2$$

$$R_3=\frac{KR_2}{K-1}, \qquad K\neq 1$$

$$R_4=KR_2 \qquad (16)$$

The gain is given by

$$K=1+R_4/R_3$$

and R_3 and R_4 are selected to minimize the dc offset of the op amp. If $K=1$, then R_3 is infinite (open circuit) and $R_4=0$. For minimum dc offset, let $R_4=R_2$.

Second-order high-pass Butterworth and Chebishev filters may be constructed in exactly the same manner as their low-pass counterparts described in the previous section. Eq. (15) or (16) may be used directly for chosen practical values of C and/or C_1. A shortcut procedure, using tables, is also provided for certain gains. The procedure and the tables are given later in this section.

Fourth-Order Designs

Fourth-order MFB and VCVS high-pass filters may be constructed by realizing each factor of the transfer function (14) by a section such as Fig. 10

* R. P. Sallen and E. L. Key, *op cit.*

TABLE 11—SECOND-ORDER MFB HIGH-PASS BUTTERWORTH DESIGNS.

Gain	C_1	R_1	R_2
2	$0.5C$	0.566	3.536
10	$0.1C$	0.673	14.849

TABLE 12—SECOND-ORDER VCVS HIGH-PASS BUTTERWORTH DESIGNS.

Gain	R_1	R_2	R_3	R_4
2	1.144	0.874	1.748	1.748
10	2.504	0.399	0.444	3.993

TABLE 13—FOURTH-ORDER MFB HIGH-PASS BUTTERWORTH DESIGNS.

Stage	Gain	C_1	R_1	R_2
1	2	$0.5C$	0.306	6.533
2	2	$0.5C$	0.739	2.706

or 11, as described previously. Cascading the two sections then results in the desired fourth-order filter. A shortcut procedure, using Tables 13, 14, 17, and 18, is described at the end of this section, for certain gains in the case of Butterworth and Chebishev filters.

TABLE 15—SECOND-ORDER MFB HIGH-PASS CHEBISHEV DESIGNS.

Gain	C_1	R_1	R_2	dB
2	$0.5C$	0.949	6.984	0.1
10	$0.1C$	1.130	29.332	
2	$0.5C$	0.570	5.318	0.5
10	$0.1C$	0.679	22.334	
2	$0.5C$	0.439	5.022	1
10	$0.1C$	0.523	21.091	

Design Summary of High-Pass Filters

For the desired filter type (Butterworth or Chebishev) with gain K and cutoff frequency f_c (hertz), select the circuit (Fig. 10 for the MFB filter or Fig. 11 for the VCVS filter) and the capacitance C to be used. In the Chebishev case, the design formulas and tables are given with f_c as the beginning frequency of the ripple channel. If the conventional cutoff $f_{3\,db}$ is specified, then the

TABLE 14—FOURTH-ORDER VCVS HIGH-PASS BUTTERWORTH DESIGNS.

Stage	Gain	R_1	R_2	R_3	R_4
1	2	0.924	1.082	2.165	2.165
2	2	1.307	0.765	1.531	1.531

TABLE 16—SECOND-ORDER VCVS HIGH-PASS CHEBISHEV DESIGNS.

Gain	R_1	R_2	R_3	R_4	dB
2	2.010	1.648	3.297	3.297	0.1
10	4.500	0.736	0.818	7.363	
2	1.297	1.169	2.338	2.338	0.5
10	2.993	0.507	0.563	5.066	
2	1.066	1.034	2.069	2.069	1
10	2.519	0.438	0.486	4.377	

TABLE 17—FOURTH-ORDER MFB HIGH-PASS CHEBISHEV DESIGNS.

Stage	Gain	C_1	R_1	R_2	dB
1	2	0.5C	0.211	12.586	0.1
2	2	0.5C	0.510	2.442	
1	2	0.5C	0.140	15.162	0.5
2	2	0.5C	0.339	2.105	
1	2	0.5C	0.112	17.675	1
2	2	0.5C	0.269	2.074	

TABLE 18—FOURTH-ORDER VCVS HIGH-PASS CHEBISHEV DESIGNS.

Stage	Gain	R_1	R_2	R_3	R_4	dB
1	2	0.958	1.388	2.776	2.776	0.1
2	2	0.962	0.648	1.295	1.295	
1	2	0.822	1.294	2.587	2.587	0.5
2	2	0.684	0.521	1.042	1.042	
1	2	0.776	1.272	2.544	2.544	1
2	2	0.578	0.483	0.966	0.966	

proper value of f_c to be used is found by using the *reciprocal* of the figures in Table 6. A good choice of C is a standard value approximately equal to $10/f_c\ \mu$F.

Method 1:

(A) Obtain coefficients a and b in the second-order case, or a_1, a_2, b_1, and b_2 in the fourth-order case, from Table 1.

(B) Obtain the resistances from (15) for the MFB filter and from (16) for the VCVS filter. Note: For the MFB filter, the gain K and the selection of C must be such that $C_1 = C/K$ is a standard value of capacitance.

Method 2:

(A) Find SF from (9).

(B) From the appropriate one of Tables 11 through 18, find the resistances in kilohms by multiplying the table resistance values by SF. In the MFB case, C_1 is also found in the tables.

In either method, the filter should be constructed with standard values of resistances as close as possible to the calculated values. The suggestions in the low-pass design summary apply except that the dc return to ground is already satisfied by R_2 in both circuits.

BANDPASS FILTERS

A bandpass filter is one with a single passband, $\omega_1 < \omega < \omega_2$, and two stopbands, $0 < \omega < \omega_1$ and $\omega > \omega_2$. An ideal and a realizable bandpass response are shown in Fig. 12. The frequencies ω_1 and ω_2 are the cutoff frequencies, and in the nonideal case

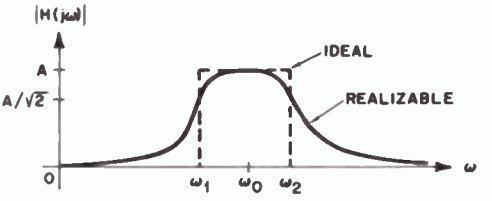

Fig. 12—Ideal and realizable bandpass responses.

TABLE 19—SECOND-ORDER MFB BANDPASS DESIGNS.

Q	Gain	C_1	R_1	R_2	R_3
2	2	$1C$	1.000	0.333	4.000
2	10	$2C$	0.200	1.000	3.000
4	2	$1C$	2.000	0.133	8.000
4	10	$2C$	0.400	0.105	6.000
6	2	$1C$	3.000	0.086	12.000
6	10	$2C$	0.600	0.061	9.000
8	2	$1C$	4.000	0.063	16.000
8	10	$2C$	0.800	0.044	12.000
10	2	$1C$	5.000	0.051	20.000
10	10	$2C$	1.000	0.034	15.000

they are the points at which the amplitude equals $1/\sqrt{2}$ times its maximum value.

The frequency ω_0, about which the passband is approximately centered, is the center frequency, and the bandwidth B is defined by $B=\omega_2-\omega_1$. The quality factor Q is defined by $Q=\omega_0/B$, so that large Q implies small bandwidth and vice-versa. The gain of a bandpass filter is the value of its amplitude at the center frequency. That is, $K=|H(j\omega_0)|$.

Bandpass transfer functions may be obtained from low-pass functions by replacing s in the low-pass function for $\omega_c=1$ by

$$S=\frac{s^2+\omega_0^2}{Bs} \tag{17}$$

Thus applying (17) to the first-order low-pass function,

$$\frac{V_2}{V_1}=\frac{K}{s+1}$$

results in the second-order bandpass function,

$$\frac{V_2}{V_1}=\frac{KBs}{s^2+Bs+\omega_0^2}=\frac{\frac{K\omega_0}{Q}s}{s^2+\frac{\omega_0}{Q}s+\omega_0^2} \tag{18}$$

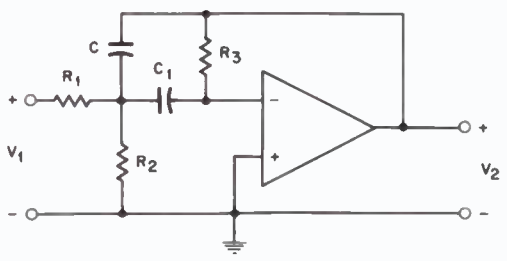

Fig. 13—A second-order MFB bandpass filter.

with center frequency $\omega_0=(\omega_1\omega_2)^{1/2}$, quality factor Q (or bandwidth $B=\omega_0/Q$), and gain K. A fourth-order bandpass function results when (17) is applied to the second-order function (4) with $\omega_c=1$, as given later.

Second-Order Designs

An MFB second-order bandpass filter* which realizes (18) is shown in Fig. 13. For a given ω_0, Q, and K, the resistances are

$$R_1=\frac{Q}{C\omega_0K}$$

$$R_2=\frac{Q}{\omega_0[C(Q^2-K)+C_1Q^2]}$$

$$R_3=\frac{Q}{\omega_0}\left(\frac{1}{C}+\frac{1}{C_1}\right) \tag{19}$$

Capacitances C and C_1 are arbitrary and may be given standard values so that R_2 is positive. The filter yields an inverting gain of $-K$ $(K>0)$.

For certain values of Q and K, Table 19 is provided for rapid designs. A scale factor SF is calculated from

$$SF=\frac{500}{\pi f_0C'} \tag{20}$$

where $f_0=\omega_0/2\pi$ and C' is the value of C in microfarads. Capacitance C_1 is then as shown in the table, and the circuit resistances are those of the table multiplied by SF. A complete design example is given later in the section.

The MFB bandpass filter has a minimal number of elements, has an inverting gain, and is capable of values of Q up to about 10 for moderate gains.

* L. P. Huelsman, *Theory and Design of Active RC Circuits*, McGraw-Hill Book Co., New York, 1968.

Another popular second-order bandpass filter is the VCVS circuit* of Fig. 14. It realizes (18) for

$$R_1=\frac{2Q}{C\omega_0 K}$$

$$R_2=\frac{2Q}{C\omega_0\{-1+[(K-1)^2+8Q^2]^{1/2}\}}$$

$$R_3=\frac{1}{C^2\omega_0^2}\left(\frac{1}{R_1}+\frac{1}{R_2}\right)$$

$$R_4=2R_3 \qquad (21)$$

For given values of K, ω_0, and Q and a selected value of C, one may calculate the required resistances. The resistance of R_4 is chosen to minimize the dc offset of the op amp.

* W. J. Kerwin and L. P. Huelsman, "The Design of High Performance Active RC Band-Pass Filter," *IEEE International Convention Record*, vol. 14, pt. 10, pp. 74–80, 1960.

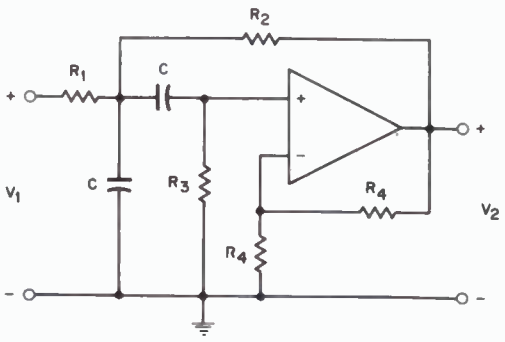

Fig. 14—A second-order VCVS bandpass filter.

Advantages of the VCVS bandpass filter are in general the same as those of the VCVS low-pass filter, discussed previously. It yields a noninverting gain, and for moderate gains, it can easily achieve a value of Q up to 10. Table 20 may be used with (20) to obtain a shortcut practical design for certain values of Q and gain.

TABLE 20—SECOND-ORDER VCVS BANDPASS DESIGNS.

Q	Gain	R_1	R_2	R_3	R_4
2	2	2.000	0.843	1.686	3.372
2	10	0.400	0.415	4.908	9.815
4	2	4.000	0.772	1.545	3.089
4	10	0.800	0.594	2.932	5.864
6	2	6.000	0.750	1.500	3.000
6	10	1.200	0.659	2.351	4.702
8	2	8.000	0.739	1.478	2.956
8	10	1.600	0.685	2.084	4.169
10	2	10.000	0.733	1.465	2.930
10	10	2.000	0.697	1.934	3.868

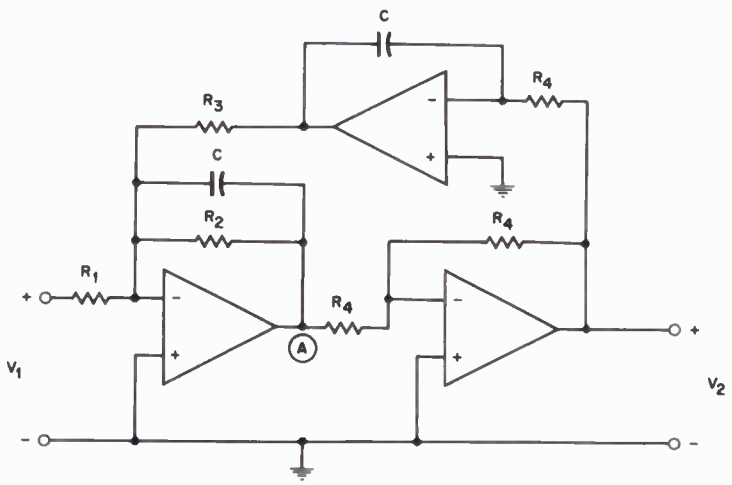

Fig. 15—A second-order biquad bandpass filter.

Another popular second-order bandpass filter is the biquad circuit* of Fig. 15. The general second-order bandpass function (18) is realized for arbitrary values of R_4 and C with

$$R_1 = Q/K\omega_0 C$$
$$R_2 = Q/\omega_0 C = KR_1$$
$$R_3 = 1/\omega_0^2 C^2 R_4 \qquad (22)$$

The gain is noninverting, but an inverting gain of the same magnitude may be obtained by taking the output at point A in Fig. 15.

The biquad circuit requires more elements than the MFB or VCVS circuits, but it is capable of achieving values of Q up to 100. Also, it has very low sensitivity to element changes and is very easy to tune. The center frequency can be adjusted by varying R_3, Q can be adjusted by varying R_2, and the gain can be adjusted by varying R_1.

A shortcut design procedure is provided by means of Table 21 and (20).

TABLE 21—SECOND-ORDER BIQUAD BANDPASS DESIGNS†

R_1	R_2	R_3, R_4
Q/K	Q	1

† K = gain, Q = quality factor

Fourth-Order Designs

Applying transformation (17) to the second-order low-pass function (4) with $\omega_c = 1$ results in the fourth-order bandpass function,

$$\frac{V_2}{V_1} = \frac{\omega_0^2 bKs^2/Q^2}{s^4 + \frac{a\omega_0}{Q}s^3 + \left(2 + \frac{b}{Q^2}\right)\omega_0^2 s^2 + \frac{a\omega_0^3}{Q}s + \omega_0^4} \qquad (23)$$

Thus Butterworth (with flat passband) and Chebishev (with passband ripples) designs may be obtained by properly selecting the low-pass coefficients a and b of Table 1.

As in the low- and high-pass cases, fourth-order bandpass filters may be constructed by factoring the transfer function (23) into two second-order bandpass functions, realizing each with a second-order section, and cascading the two sections.

A shortcut procedure, using two biquad sections, is given at the end of the section.

* J. Tow, "Design Formulas for Active RC Filters Using Operational Amplifier Biquad," *Electron. Letters*, pp. 339–341, July 24, 1969.

Practical Design Example

Suppose it is desired to obtain a second-order bandpass VCVS filter with a center frequency of $f_0 = 1000$ Hz, a gain of $K = 10$, and $Q = 10$, with $C = 0.1\ \mu\text{F} = 10^{-7}$ F. By (21) the resistances are

$$R_1 = \frac{2(10)}{(10^{-7})(2\pi)(10^3)(10)}\Omega = 3.183\ \text{k}\Omega$$

$$R_2 = \frac{2(10)}{(10^{-7})(2\pi)(10^3)\{-1+[(10-1)^2+8(10)^2]^{1/2}\}}$$
$$= 1.110\ \text{k}\Omega$$

$$R_3 = \frac{1}{(10^{-14})(2\pi)^2(10^6)}\left[\frac{1}{3.183}+\frac{1}{1.110}\right](10^{-3})\Omega$$
$$= 3.078\ \text{k}\Omega$$

$$R_4 = 2R_3 = 6.156\ \text{k}\Omega$$

Alternately, to use Table 20, it is necessary to find SF from (20):

$$SF = \frac{500}{\pi(10^3)(0.1)} = 1.5915$$

Multiplying the appropriate resistances from Table 20 by SF results in the network resistances, in kilohms.

$$R_1 = 2.000SF = 3.183$$
$$R_2 = 0.697SF = 1.109$$
$$R_3 = 1.934SF = 3.078$$
$$R_4 = 3.868SF = 6.156$$

Design Summary of Bandpass Filters

For the desired gain K, quality factor Q, and center frequency f_0 (hertz), select the circuit (Fig. 13 for the MFB filter, Fig. 14 for the VCVS filter, or Fig. 15 for the biquad filter) and the capacitance C to be used. A good choice of C is a standard value approximately equal to $10/f_0\ \mu\text{F}$.

Method 1 (second-order cases only):

(A) If the MFB filter is used, select a standard value of C_1 so that

$$C_1 > C(K-Q^2)/Q^2$$

(B) Obtain the resistances from (19) for the MFB filter, from (21) for the VCVS filter, or from (22) for the biquad filter.

Method 2:

(A) Find SF from (20).

(B) From the appropriate one of Tables 19 through 25, determine the resistances in kilohms

TABLE 22—FOURTH-ORDER BIQUAD BANDPASS BUTTERWORTH DESIGNS.*

Q	Stage	R_1	R_2	R_3, R_4
2	1	2.000/K	2.404	0.700
	2	2.000/K	3.436	1.429
4	1	4.000/K	5.197	0.838
	2	4.000/K	6.205	1.194
6	1	6.000/K	8.013	0.888
	2	6.000/K	9.016	1.125
10	1	10.000/K	13.659	0.932
	2	10.000/K	14.661	1.073
20	1	20.000/K	27.793	0.965
	2	20.000/K	28.793	1.036
50	1	50.000/K	70.215	0.986
	2	50.000/K	71.214	1.014

* K = gain per stage

TABLE 23—FOURTH-ORDER BIQUAD BANDPASS CHEBISHEV DESIGNS (0.1 dB).*

Q	Stage	R_1	R_2	R_3, R_4
2	1	1.099/K	1.260	0.494
	2	1.099/K	2.548	2.023
4	1	2.197/K	2.878	0.707
	2	2.197/K	4.073	1.415
6	1	3.296/K	4.538	0.794
	2	3.296/K	5.715	1.260
10	1	5.494/K	7.887	0.871
	2	5.494/K	9.056	1.148
20	1	10.987/K	16.300	0.933
	2	10.987/K	17.465	1.071
50	1	27.469/K	41.583	0.973
	2	27.469/K	42.747	1.028

* K = gain per stage.

TABLE 24—FOURTH-ORDER BIQUAD BANDPASS CHEBISHEV DESIGNS (0.5 dB).*

Q	Stage	R_1	R_2	R_3, R_4
2	1	1.624/K	2.250	0.604
	2	1.624/K	3.726	1.656
4	1	3.248/K	4.988	0.778
	2	3.248/K	6.413	1.286
6	1	4.873/K	7.769	0.846
	2	4.873/K	9.185	1.182
10	1	8.121/K	13.359	0.904
	2	8.121/K	14.770	1.106
20	1	16.243/K	27.371	0.951
	2	16.243/K	28.780	1.051
50	1	40.606/K	69.448	0.980
	2	40.606/K	70.855	1.020

* K = gain per stage

by multiplying the table values by SF. In the MFB case, C_1 is found in the table also. Tables 19 through 21 are second-order designs, and Tables 22 through 25 are cascaded fourth-order designs.

In either method, the filter should be constructed with standard values of resistances as close as possible to the calculated values. The suggestions for the low-pass design summary apply except that the dc return to ground is already satisfied in every case.

The example of a practical design, given earlier, may be used as a guideline.

BAND-REJECT FILTERS

A band-reject, or notch, filter is one with a single stopband, $\omega_1<\omega<\omega_2$, and two passbands, $0<\omega<\omega_1$ and $\omega>\omega_2$. An ideal and a physically realizable band-reject response are shown in Fig. 16. The cutoff frequencies are ω_1 and ω_2, defined in the nonideal case as the points at which the amplitude equals $1/\sqrt{2}$ times its maximum value.

The frequency ω_0, about which the stopband is approximately centered, is the center frequency.

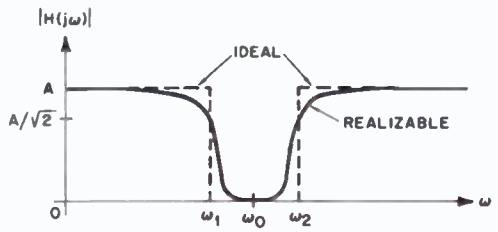

Fig. 16—Ideal and realizable band-reject responses.

The bandwidth is $B=\omega_2-\omega_1$, and the quality factor is $Q=\omega_0/B$. The gain of the band-reject filter is the value of its amplitude at zero frequency or at infinite frequency, shown in Fig. 16 as A.

Band-reject transfer functions may be obtained from low-pass functions by replacing s in the low-pass function for $\omega_0=1$ by

$$S=\frac{Bs}{s^2+\omega_0^2} \qquad (24)$$

Applying (24) to the first-order function

$$\frac{V_2}{V_1}=\frac{K}{s+1}$$

TABLE 25—FOURTH-ORDER BIQUAD BANDPASS CHEBISHEV DESIGNS (1 dB).*

Q	Stage	R_1	R_2	R_3, R_4
2	1	1.905/K	2.986	0.639
	2	1.905/K	4.673	1.565
4	1	3.809/K	6.557	0.799
	2	3.809/K	8.202	1.251
6	1	5.715/K	10.174	0.861
	2	5.715/K	11.811	1.161
10	1	9.524/K	17.440	0.914
	2	9.524/K	19.073	1.094
20	1	19.047/K	35.641	0.956
	2	19.047/K	37.272	1.046
50	1	47.619/K	90.289	0.982
	2	47.619/K	91.920	1.018

* K = gain per stage

results in the second-order band-reject function

$$\frac{V_2}{V_1}=\frac{K(s^2+\omega_0^2)}{s^2+Bs+\omega_0^2}=\frac{K(s^2+\omega_0^2)}{s^2+(\omega_0/Q)s+\omega_0^2} \qquad (25)$$

having center frequency ω_0, quality factor Q (or bandwidth $B=\omega_0/Q$), and gain K.

Second-Order Designs

A VCVS second-order band-reject filter* which realizes (25) is shown in Fig. 17. The gain is $K=1$, and for specified ω_0 and Q and an arbitrary value of C, the resistances are given by

$$R_1=1/(2\omega_0 QC)$$
$$R_2=2Q/(\omega_0 C)$$
$$R_3=2Q/[\omega_0 C(4Q^2+1)] \qquad (26)$$

Values of Q up to 10 may be readily obtained.

Equations (26) may be used, for a specified value of C, to obtain a band-reject filter design.

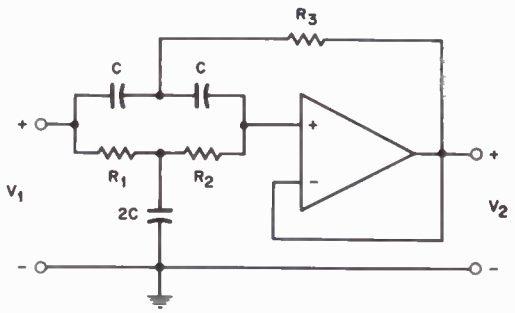

Fig. 17—A second-order VCVS band-reject filter.

For certain values of Q, Table 26 may be used in a shortcut procedure. A value of SF is found from (20), where C' is the value of C in microfarads, and the resistances are those of the table multiplied by SF.

An MFB circuit which also realizes (25) is shown in Fig. 18.* For given K, ω_0, and Q, there

* R. M. Inigo, "Active Filter Realization Using Finite-Gain Voltage Amplifiers," *IEEE Transactions on Circuit Theory*, vol. CT-17, pp. 445–448, Aug. 1970.

* L. P. Huelsman, *Active Filters: Lumped, Distributed, Integrated, Digital, and Parametric*, McGraw-Hill Book Co., New York, 1970.

are many ways to solve for the circuit elements. One way is to choose C and R_6 arbitrarily, with the remaining resistances given by

$$R_1 = Q/(2\omega_0 C)$$
$$R_2 = Q/[2\omega_0 C(Q^2-1)] = R_1/(Q^2-1), \qquad Q>1$$
$$R_3 = 2Q/(\omega_0 C) = 4R_1$$
$$R_4 = KR_6$$
$$R_5 = 2R_6 \qquad (27)$$

The gain for the circuit is $-K$ (inverting).

The MFB filter requires more elements than the VCVS band-reject filter, but it has the advantage that the gain can be specified. For moderate gains, the filter may easily achieve values of Q up to 25. Instead of using the equations, a shortcut design procedure, using (20) and Table 27 as described for the VCVS filter, is available.

Practical Design Example

Suppose it is desired to construct a second-order band-reject MFB filter with $f_0=\omega_0/2\pi=1000$ Hz, $Q=6$, and an inverting gain of $K=10$, using 0.01-μF capacitances. By (27), the resistances are

$$R_1 = \frac{6}{2(2\pi)(10^3)(10^{-8})}\Omega = 47.747\ \text{k}\Omega$$
$$R_2 = 47.747/35 = 1.364\ \text{k}\Omega$$
$$R_3 = 4(47.747) = 190.988\ \text{k}\Omega$$
$$R_4 = 10R_6, \qquad R_5 = 2R_6$$

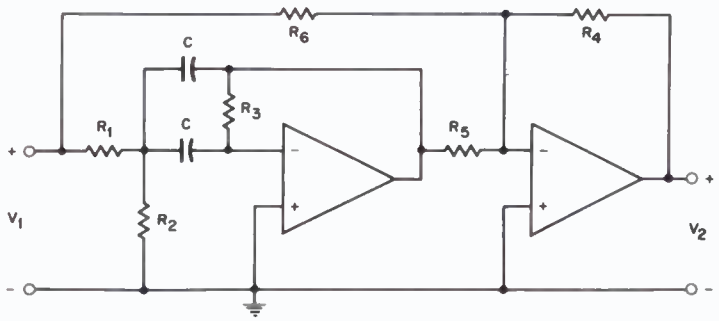

Fig. 18—A second-order MFB band-reject filter

TABLE 26—SECOND-ORDER VCVS BAND-REJECT DESIGNS.*

Q	R_1	R_2	R_3
1	0.500	2.000	0.400
2	0.250	4.000	0.235
3	0.167	6.000	0.162
4	0.125	8.000	0.123
5	0.100	10.000	0.099
6	0.083	12.000	0.083
7	0.071	14.000	0.071
8	0.063	16.000	0.062
9	0.056	18.000	0.055
10	0.050	20.000	0.050

* Gain=1 in all cases.

TABLE 27—SECOND-ORDER MFB BAND-REJECT DESIGNS.*

Q	Gain	R_1	R_2	R_3	R_4
2	2	1.000	0.333	4.000	2.000
2	10	1.000	0.333	4.000	10.000
4	2	2.000	0.133	8.000	2.000
4	10	2.000	0.133	8.000	10.000
6	2	3.000	0.086	12.000	2.000
6	10	3.000	0.086	12.000	10.000
8	2	4.000	0.063	16.000	2.000
8	10	4.000	0.063	16.000	10.000
10	2	5.000	0.051	20.000	2.000
10	10	5.000	0.051	20.000	10.000
12	2	6.000	0.042	24.000	2.000
12	10	6.000	0.042	24.000	10.000

* In all cases, $R_5=2$ and $R_6=1$.

Selecting $R_6 = 10$ kΩ yields $R_4 = 100$ kΩ and $R_5 = 20$ kΩ.

For the shortcut method using Table 27, it is necessary first to find SF, given by (20) as

$$SF = 500/[\pi(10^3)(0.01)] = 15.915$$

Multiplying the appropriate resistances of the table by SF yields the network resistances in kilohms:

$$R_1 = 3SF = 47.745$$

$$R_2 = 0.086SF = 1.369$$

$$R_3 = 12SF = 190.98$$

$$R_4 = 10SF = 159.15$$

$$R_5 = 2SF = 31.83$$

$$R_6 = 1SF = 15.92$$

If R_6 had been selected as 15.92 kΩ instead of 10 kΩ in the first method, the values of R_4, R_5, and R_6 obtained by the two methods would agree.

Design Summary of Band-Reject Filters

For the desired gain K, quality factor Q, and center frequency f_0 (hertz), select the circuit (Fig. 17 for the VCVS filter or Fig. 18 for the MFB filter) and the capacitance C to be used. A good choice of C is a standard value approximately equal to $10/f_0$ μF.

Method 1:

Obtain the resistances from (26) for the VCVS filter or from (27) for the MFB filter. Note: The gain of the VCVS filter is restricted to 1 and that of the MFB filter is inverting.

Method 2:

(A) Find SF from (20).

(B) From the appropriate one of Tables 26 and 27, determine the resistances in kilohms by multiplying the table values by SF.

In either method, the filter should be constructed with standard values of resistances as close as possible to the calculated values. The suggestions for the low-pass design summary apply except that the dc return to ground is already satisfied in the MFB circuit.

The example of a practical design, given earlier, may be used as a guideline.

ALL-PASS FILTERS

An all-pass, or phase-shifting, filter has a constant amplitude response and a phase response that varies with frequency. A second-order all-pass filter has a transfer function

$$\frac{V_2}{V_1} = \frac{K(s^2 - a\omega_0 s + b\omega_0^2)}{s^2 + a\omega_0 s + b\omega_0^2} \qquad (28)$$

which has a constant amplitude or gain K, and a phase given by

$$\phi(\omega) = -2\tan^{-1}[a\omega_0\omega/(b\omega_0^2 - \omega^2)] \qquad (29)$$

The numbers a and b are constants and are the transfer-function coefficients when $\omega_0 = 1$.

From (29), the phase shift at $\omega_0 = 2\pi f_0$ is given by

$$\phi_0 = \phi(\omega_0) = -2\tan^{-1}[a/(b-1)] \qquad (30)$$

Thus for a given ϕ_0, parameters a and b may be determined. Since a may be expressed in terms of b, an additional constraint, such as gain, dc offset minimization, or damping factor, may be satisfied.

Second-Order Design

An MFB filter which realizes (28) is shown in Fig. 19.* For a specified gain K $(0 < K < 1)$, phase

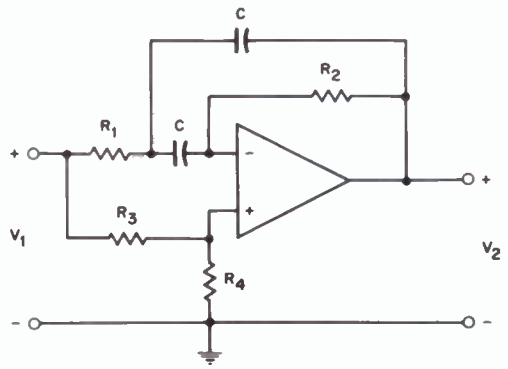

Fig. 19—A second-order MFB all-pass filter.

shift $\phi_0 = \phi(\omega_0)$ at a given frequency ω_0, and arbitrary value of C, the resistances are given by

$$R_2 = \frac{2}{a\omega_0 C}$$

$$R_1 = \frac{(1-K)}{4K} R_2$$

$$R_3 = R_2/K$$

$$R_4 = R_2/(1-K) \qquad (31)$$

where for $0 < \phi_0 < 180°$,

* T. Deliyannis, "RC Active Allpass Sections," *Electron. Letters*, vol. 5, pp. 59–60, February 1969.

$$a=\frac{1-K}{2K\tan(\phi_0/2)}\left[-1+\left(1+\frac{4K}{1-K}\cdot\tan^2(\phi_0/2)\right)^{1/2}\right], \quad (32)$$

and for $-180°<\phi_0<0$,

$$a=\frac{1-K}{2K\tan(\phi_0/2)}\left[-1-\left(1+\frac{4K}{1-K}\cdot\tan^2(\phi_0/2)\right)^{1/2}\right] \quad (33)$$

The resistances have been calculated to minimize the dc offset of the op amp.

A shortcut design using equation (20) and Table 28 is available for certain cases of phase shift and gain. The procedure is identical to that of the band-reject filter case considered in the previous section.

Practical Design Example

Suppose an all-pass filter is desired with a phase shift $\phi_0=-90°$ at $f_0=1000$ Hz, a gain of 3/4, and capacitances of 0.01 μF. By (33), it is found that

$$a=\frac{0.25}{2(0.75)(-1)}\left[-1-\left(1+\frac{4(0.75)}{0.25}(1)\right)^{1/2}\right]$$
$$=0.76759$$

By (31) the resistances are

$$R_2=\frac{2}{(0.76759)(2\pi)(10^3)(10^{-8})}\Omega=41.469\text{ k}\Omega$$

$$R_1=\frac{0.25}{4(0.75)}(41.469)=3.456\text{ k}\Omega$$

$$R_3=\frac{41.469}{0.75}=55.292\text{ k}\Omega$$

$$R_4=\frac{41.469}{0.25}=165.875\text{ k}\Omega$$

To use Table 28, SF is given from (20) to be

$$SF=\frac{500}{\pi(10^3)(0.01)}=15.915$$

and the resistances, in kilohms, are

$$R_1=0.217SF=3.454$$
$$R_2=2.606SF=41.474$$
$$R_3=3.474SF=55.290$$
$$R_4=10.422SF=165.866$$

Design Summary of All-Pass Filters

For the gain K and phase shift ϕ_0 desired at the frequency f_0 (hertz), select the capacitance C to be used in the MFB filter of Fig. 19. A good choice of C is a standard value approximately equal to $10/f_0\,\mu$F.

Method 1:

(**A**) Obtain a from (32) or (33).

(**B**) Obtain the resistances from (31).

TABLE 28—SECOND-ORDER MFB ALL-PASS DESIGNS.*

Phase Shift	R_1	R_2	R_3	R_4
10°	1.948	23.374	31.165	93.495
20	1.026	12.317	16.423	49.268
30	0.735	8.824	11.765	35.296
40	0.597	7.169	9.558	28.675
50	0 518	6.219	8.292	24.875
60	0.467	5.605	7.473	22.420
70	0.431	5.175	6.900	20.700
80	0.405	4.855	6.474	19.421
90	0.384	4.606	6.141	18.422
−10	0.043	0.513	0.685	2.054
−20	0.081	0.974	1.299	3.897
−30	0.113	1.360	1.813	5.440
−40	0.139	1.674	2.232	6.696
−50	0.161	1.930	2.573	7.719
−60	0.178	2.141	2.855	8.564
−70	0.193	2.319	3.092	9.275
−80	0.206	2.472	3.295	9.886
−90	0.217	2.606	3.474	10.422

* Gain = 0.75 in all cases.

Method 2:

(A) Find SF from (20).

(B) Determine the resistances in kilohms by multiplying the appropriate values in Table 28 by SF. Note: The gain using the table is restricted to 0.75.

In either method, the filter should be constructed with standard values of resistances as close as possible to the calculated values. The suggestions for the low-pass design summary apply except that the dc return to ground is already satisfied by R_2 and R_4.

The practical design example, given earlier, may be used as a guideline.

CONSTANT-TIME-DELAY FILTERS

A filter which achieves an approximately constant time delay over the range $0<\omega<\omega_0$ is the Bessel filter*, with a second-order transfer function given by

$$\frac{V_2}{V_1}=\frac{3K\omega_0^2}{s^2+3\omega_0 s+3\omega_0^2} \qquad (34)$$

The gain is K, and the time delay at $\omega_0=2\pi f_0$ is given by

$$T_0=T(\omega_0)=12/(13\omega_0) \text{ seconds} \qquad (35)$$

Equation (34) is a low-pass function with the same form as (4) where $a=b=3$ and ω_c is replaced by ω_0. Therefore the MFB low-pass circuit of Fig. 4, using (5), or the VCVS low-pass circuit of Fig. 5, using (6), may be used to obtain a realization. The frequency ω_0 may be found from a given time delay T_0 by using (35). Conversely, if ω_0 is specified, the constant delay which results is then T_0.

TABLE 29—SECOND-ORDER MFB CONSTANT-TIME-DELAY DESIGNS.

Gain	C_1	R_1	R_2	R_3
2	$0.200C$	0.691	1.382	1.206
10	$0.047C$	0.471	4.709	1.506

Tables 29 and 30 are available for shortcut designs. For a given T_0, $\omega_0=2\pi f_0$ is found from (35), and the result is then used to find SF from (20). The resistances are then those of the table multiplied by SF.

Practical Design Example

Suppose it is desired to construct an MFB constant-time-delay filter which has $T_0=100$ μs and a gain of 2; the capacitances are to be $C=0.01$ μF and $C_1=0.002$ μF. From (35), ω_0 is

$$\omega_0=\frac{12}{13(10^{-4})}=9231=2\pi f_0 \qquad (36)$$

The pertinent design equations are (5) with $\omega_c=\omega_0$ and $a=b=3$, resulting in

$$R_2=2(3)/\{3(10^{-8})+[9(10^{-16})-4(3)(2)(10^{-17})(3)]^{1/2}\}(9231)\,\Omega$$

$$=14.971 \text{ k}\Omega$$

$$R_1=14.971/2=7.486 \text{ k}\Omega$$

$$R_3=\frac{1}{3(2)(10^{-17})(9231)^2(14.971)(10^3)}\Omega=13.065 \text{ k}\Omega$$

In the shortcut procedure, SF is given by (20) and (36) to be

$$SF=\frac{500}{(9231/2)(0.01)}=10.833$$

The resistances (in kilohms) are the appropriate ones of Table 29 multiplied by SF, or

$$R_1=0.691SF=7.486$$

$$R_2=1.382SF=14.971$$

$$R_3=1.206SF=13.065$$

Design Summary of Constant-Time-Delay Filters

For the desired gain K and time delay T_0, select the circuit (Fig. 4 for the MFB filter or

TABLE 30—SECOND-ORDER VCVS CONSTANT-TIME-DELAY DESIGNS.

Gain	C_1	R_1	R_2	R_3	R_4
2	$1C$	0.333	1.000	2.667	2.667
10	$2C$	0.158	1.054	1.346	12.118

* L. Storch, "Synthesis of Constant-Time-Delay Ladder Networks Using Bessel Polynomials," *Proc. of the IRE*, vol. 42, no. 11, pp. 1666–1675. November 1954.

Fig. 5 for the VCVS filter) and the capacitance C to be used. A good choice of C is a standard value approximately equal to $10/f_0$ μF. Calculate $f_0 = \omega_0/2\pi$ Hz from (35). (Alternately, ω_0 may be specified and T_0 calculated.)

Method 1:

This method is identical to that given earlier in the low-pass design summary, except that only second-order cases are considered, and $a = b = 3$.

Method 2:

(A) Find SF from (20).

(B) From the appropriate one of Tables 29 or 30, find C_1. Determine the resistances in kilohms by multiplying the table values by SF.

In either method, the filter should be constructed with standard values of resistances as close as possible to the calculated values. The suggestions for the low-pass design summary apply directly.

The practical time-delay design example, given earlier, may be used as a guideline.

CHAPTER 11
ATTENUATORS

DEFINITIONS

An attenuator is a network designed to introduce a known loss when working between resistive impedances Z_1 and Z_2 to which the input and output impedances of the attenuator are matched. Either Z_1 or Z_2 may be the source and the other the load. The attenuation of such networks expressed as a power ratio is the same regardless of the direction of working.

Three forms of resistance network that may be conveniently used to realize these conditions are shown on page 11-4. These are the T section, the π section, and the bridged-T section. Equivalent balanced sections also are shown. Methods are given for the computation of attenuator networks, the hyperbolic expressions giving rapid solutions with the aid of tables of hyperbolic functions in Chapter 47. Tables of the various types of attenuators are given on pages 11-6 through 11-9.

LADDER ATTENUATOR

Ladder attenuator, Fig. 1, input switch points P_0, P_1, P_2, P_3 at shunt arms. Also intermediate point P_m tapped on series arm. May be either unbalanced, as shown, or balanced.

Ladder, for design purposes, Fig. 2, is resolved into a cascade of π sections by imagining each shunt arm split into two resistors. Last section matches Z_2 to $2Z_1$. All other sections are symmetrical, matching impedances $2Z_1$, with a terminating resistor $2Z_1$ on the first section. Each section is designed for the loss required between the switch points at the ends of that section.

Input to P_0:

$$\text{Loss in decibels} = 10 \log_{10}[(2Z_1+Z_2)^2/4Z_1Z_2]$$

$$\text{Input impedance} = Z_2/2$$

$$\text{Output impedance} = Z_1Z_2/(Z_1+Z_2).$$

Input to P_1, P_2, *or* P_3: Loss in decibels = 3+ (sum of losses of π sections between input and output). Input impedance = Z_1.

Input to P_m (on a symmetrical π section):

$$e_0/e_m = \frac{1}{2}\,\frac{m(1-m)(K-1)^2+2K}{K-m(K-1)}$$

where e_0 = output voltage when $m=0$ (switch on P_1), e_m = output voltage with switch on P_m, and K = current ratio of the section (from P_1 to P_2) $(K>1)$.

Input impedance

$$Z_1' = Z_1\{m(1-m)[(K-1)^2/K]+1\}$$

maximum $Z_1' = Z_1\{[(K-1)^2/4K]+1\}$ for $m=0.5$.

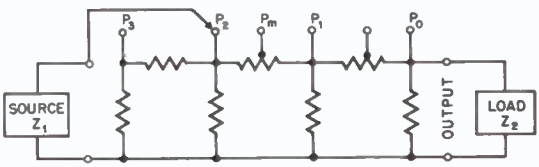

Fig. 1—Ladder attenuator.

The unsymmetrical last section may be treated as a system of voltage-dividing resistors. Solve for the resistance R from P_0 to the tap, for each value of

$$\left(\frac{\text{output voltage with input on } P_0}{\text{output voltage with input on tap}}\right).$$

A Useful Case

When $Z_1 = Z_2 = 500$ ohms.

Then loss on P_0 is 3.52 decibels.

Let the last section be designed for loss of 12.51 decibels. Then from Attenuator Network Design table, page 11-4.

$$R_{13} = 2444 \text{ ohms}$$

$$R_{23} = 654 \text{ ohms}$$

$$R_{12} = 1409 \text{ ohms}.$$

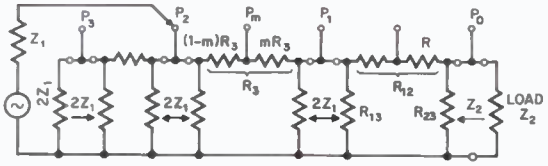

Fig. 2—Ladder attenuator resolved into a cascade of π sections.

The table shows the location of the tap and the input and output impedances for several values of loss, relative to the loss on P_0.

Relative Loss (dB)	Tap R (ohms)	Input Impedance (ohms)	Output Impedance (ohms)
0	0	250	250
2	170	368	304
4	375	478	353
6	615	562	394
8	882	600	428
10	1157	577	454
12	1409	500	473

Input to P_0: Output impedance$=0.6Z$. (See Fig. 3.)

Input to P_0, P_1, P_2, *or* P_3: Loss in decibels$=6+$(sum of losses of π sections between input and output). Input impedance$=Z$.

Input to P_m:

$$\frac{e_0}{e_m}=\frac{1}{4}\,\frac{m(1-m)(K-1)^2+4K}{K-m(K-1)}$$

Input impedance:

$$Z'=Z\left[\frac{m(1-m)(K-1)^2}{2K}+1\right]$$

$$\text{maximum } Z'=Z\left[\frac{(K-1)^2}{8K}+1\right] \text{ for } m=0.5.$$

LOAD IMPEDANCE

Effect of Incorrect Load Impedance on Operation of an Attenuator

In the applications of attenuators, the question frequently arises as to the effect on the input impedance and the attenuation by the use of a load impedance different from that for which the network was designed. The following results apply to all resistive networks that, when operated between resistive impedances Z_1 and Z_2, present matching terminal impedances Z_1 and Z_2, respectively. The results may be derived in the general case by the application of the network theorems and may be readily confirmed mathematically for simple specific cases such as the T section.

For the designed use of the network, let

Z_1 = input impedance of properly terminated network
Z_2 = load impedance that properly terminates the network
N = power ratio from input to output
K = current ratio from input to output
$K=i_1/i_2=(NZ_2/Z_1)^{1/2}$ (different in the two directions except when $Z_2=Z_1$).

For the actual conditions of operation, let

$$(Z_2+\Delta Z_2)=Z_2(1+\Delta Z_2/Z_2)$$
$$=\text{actual load impedance}$$
$$(Z_1+\Delta Z_1)=Z_1(1+\Delta Z_1/Z_1)$$
$$=\text{resulting input impedance}$$
$$(K+\Delta K)=K(1+\Delta K/K)$$
$$=\text{resulting current ratio.}$$

While Z_1, Z_2, and K are restricted to real quantities by the assumed nature of the network, ΔZ_2 is not so restricted, for example,

$$\Delta Z_2=\Delta R_2+j\Delta X_2.$$

As a consequence, ΔZ_1 and ΔK can become imaginary or complex. Furthermore, ΔZ_2 is not restricted to small values.

The results for the actual conditions are

$$\frac{\Delta Z_1}{Z_1}=\frac{2\Delta Z_2/Z_2}{2N+(N-1)(\Delta Z_2/Z_2)}$$

and

$$\frac{\Delta K}{K}=\left(\frac{N-1}{2N}\right)\frac{\Delta Z_2}{Z_2}.$$

Certain Special Cases May Be Cited

Case 1: For small $\Delta Z_2/Z_2$

$$\Delta Z_1/Z_1=(1/N)(\Delta Z_2/Z_2) \quad \text{or} \quad \Delta Z_1=(1/K^2)\Delta Z_2$$
$$\Delta i_2/i_2=-\tfrac{1}{2}(\Delta Z_2/Z_2)$$

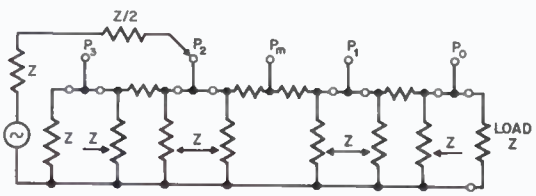

Fig. 3—A variation of the ladder attenuator, useful when $Z_1=Z_2=Z$. Simpler in design, with improved impedance characteristics, but having minimum insertion loss 2.5 decibels higher than attenuator of Fig. 2. All π sections are symmetrical.

but the error in insertion power loss of the attenuator is negligibly small.

Case 2: Short-circuited output

$$\Delta Z_1/Z_1 = -2/(N+1)$$

or

$$\text{input impedance} = \left(\frac{N-1}{N+1}\right) Z_1 = Z_1 \tanh\theta$$

where θ is the designed attenuation in nepers.

Case 3: Open-circuited output

$$\Delta Z_1/Z_1 = 2/(N-1)$$

or

$$\text{input impedance} = \left(\frac{N+1}{N-1}\right) Z_1 = Z_1 \coth\theta.$$

Case 4: For $N=1$ (possible only when $Z_1=Z_2$ and directly connected)

$$\Delta Z_1/Z_1 = \Delta Z_2/Z_2$$

$$\Delta K/K = 0.$$

Case 5: For large N

$$\Delta K/K = \tfrac{1}{2}(\Delta Z_2/Z_2).$$

ATTENUATOR NETWORK DESIGN (See table on pages 11-4—11-5)

Symbols

Z_1 and Z_2 are the terminal impedances (resistive) to which the attenuator is matched.

N is the ratio of the power absorbed by the attenuator from the source to the power delivered to the load.

K is the ratio of the attenuator input current to the output current into the load. When $Z_1=Z_2$, $K=N^{1/2}$. Otherwise K is different in the two directions.

Attenuation in decibels $= 10 \log_{10} N$.
Attenuation in nepers $= \theta = \frac{1}{2} \log_e N$.

For a table of decibels versus power and voltage or current ratio, see Chapter 3. Factors for converting decibels to nepers, and nepers to decibels, are given at the foot of that table.

Notes on Error Equations

The equations and figures for errors, given in Tables 1 through 5, are based on the assumption that the attenuator is terminated approximately by its proper terminal impedances Z_1 and Z_2. They hold for deviations of the attenuator arms and load impedances up to ± 20 percent or somewhat more.

The error due to each element is proportional to the deviation of the element, and the total error of the attenuator is the sum of the errors due to each of the several elements.

When any element or arm R has a reactive component ΔX in addition to a resistive error ΔR, the errors in input impedance and output current are

$$\Delta Z = A(\Delta R + j\Delta X)$$

$$\Delta i/i = B[(\Delta R + j\Delta X)/R]$$

where A and B are constants of proportionality for the elements in question. These constants can be determined in each case from the figures given for errors due to a resistive deviation ΔR.

The reactive component ΔX produces a quadrature component in the output current, resulting in a phase shift. However, for small values of ΔX, the error in insertion loss is negligibly small.

For the errors produced by mismatched terminal load impedance, refer to Case 1, page 11-2.

SYMMETRICAL *T* OR *H* ATTENUATORS

Interpolation of Symmetrical T or H Attenuators (Table 1)

Column R_1 may be interpolated linearly. Do not interpolate R_3 column. For 0 to 6 decibels interpolate the $1000/R_3$ column. Above 6 decibels, interpolate the column $\log_{10} R_3$ and determine R_3 from the result.

Errors in Symmetrical T or H Attenuators (Fig. 4)

Series Arms R_1 and R_2 in Error: Error in input impedances:

$$\Delta Z_1 = \Delta R_1 + (1/K^2)\Delta R_2$$

and

$$\Delta Z_2 = \Delta R_2 + (1/K^2)\Delta R_1.$$

Error in insertion loss, in decibels:

$$\text{decibels} = 4[(\Delta R_1/Z_1) + (\Delta R_2/Z_2)] \text{ approximately.}$$

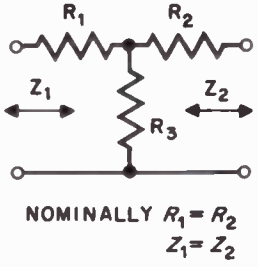

Fig. 4.

ATTENUATOR NETWORK DESIGN *(See page 11-3 for symbols)*

Description	Unbalanced Configuration	Balanced Configuration	Hyperbolic Equations*
Unbalanced T and balanced H (refer to Table 5)	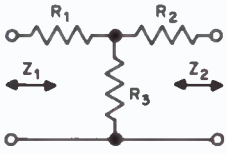	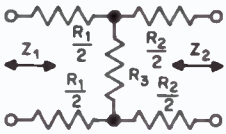	$R_3=(Z_1Z_2)^{1/2}/\sinh\theta$ $R_1=(Z_1/\tanh\theta)-R_3$ $R_2=(Z_2/\tanh\theta)-R_3$
Symmetrical T and H ($Z_1=Z_2=Z$) (refer to Table 1)	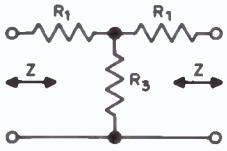		$R_3=Z/\sinh\theta$ $R_1=Z\tanh(\theta/2)$
Minimum-loss pad matching Z_1 and Z_2 ($Z_1>Z_2$) (refer to Table 4)	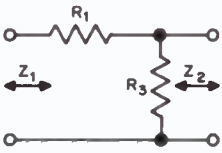	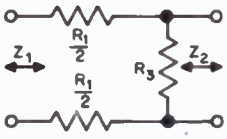	$\cosh\theta=(Z_1/Z_2)^{1/2}$ $\cosh 2\theta=2(Z_1/Z_2)-1$
Unbalanced π and balanced O	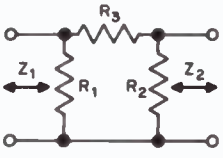	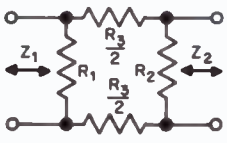	$R_3=(Z_1Z_2)^{1/2}\sinh\theta$ $1/R_1=(1/Z_1\tanh\theta)-(1/R_3)$ $1/R_2=(1/Z_2\tanh\theta)-(1/R_3)$
Symmetrical π and O ($Z_1=Z_2=Z$) (refer to Table 2)	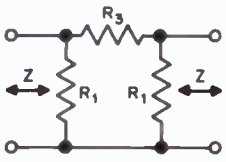	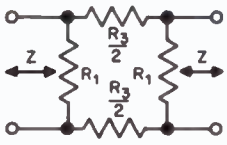	$R_3=Z\sinh\theta$ $R_1=Z/\tanh(\theta/2)$
Bridged T and bridged H (refer to Table 3)	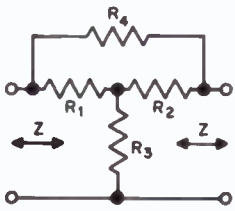	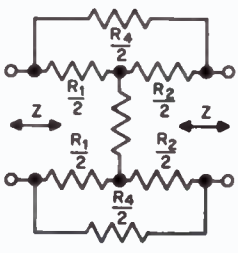	

* *Four-terminal networks*: The hyperbolic equations above are valid for passive linear 4-terminal networks in general, working between input and output impedances matching the respective image impedances. In this case: Z_1 and Z_2

Arithmetic Equations	Checking Equations
$R_3=2(NZ_1Z_2)^{1/2}/(N-1)$	
$R_1=Z_1[(N+1)/(N-1)]-R_3$	
$R_2=Z_2[(N+1)/(N-1)]-R_3$	
$R_3=\dfrac{2Z(N)^{1/2}}{N-1}=\dfrac{2ZK}{K^2-1}$	$R_1R_3=\dfrac{Z^2}{1+\cosh\theta}=Z^2\dfrac{2K}{(K+1)^2}$
$=\dfrac{2Z}{K-1/K}$	$R_1/R_3=\cosh\theta-1=2\sinh^2(\theta/2)$
	$=(K-1)^2/2K$
	$Z=R_1[1+2(R_3/R_1)]^{1/2}$
$R_1=Z[(N^{1/2}-1)/(N^{1/2}+1)]=Z[(K-1)/(K+1)]$	
$=Z[1-2/(K+1)]$	
$R_1=Z_1[1-(Z_2/Z_1)]^{1/2}$	$R_1R_2=Z_1Z_2$
$R_2=Z_2/[1-(Z_2/Z_1)]^{1/2}$	$R_1/R_2=(Z_1/Z_2)-1$
	$N=\{(Z_1/Z_2)^{1/2}+[(Z_1/Z_2)-1]^{1/2}\}^2$
$R_3=\frac{1}{2}(N-1)(Z_1Z_2/N)^{1/2}$	
$1/R_1=(1/Z_1)[(N+1)/(N-1)]-(1/R_3)$	
$1/R_2=(1/Z_2)[(N+1)/(N-1)]-(1/R_3)$	
$R_3=Z[(N-1)/2(N)^{1/2}]=Z[(K^2-1)/2K]$	$R_1R_2=Z^2(1+\cosh\theta)=Z^2[(K+1)^2/2K]$
$=Z(K-1/K)/2$	$R_3/R_1=\cosh\theta-1=(K-1)^2/2K$
$R_1=Z[(N^{1/2}+1)/(N^{1/2}-1)]=Z[(K+1)/(K-1)]$	$Z=R_1/[1+2(R_1/R_3)]^{1/2}$
$=Z[1+2/(K-1)]$	
$R_1=R_2=Z$	$R_3R_4=Z^2$
$R_4=Z(K-1)$	$R_4/R_3=(K-1)^2$
$R_3=Z/(K-1)$	

are the image impedances; R_1, R_2, and R_3 become complex impedances; and θ is the image transfer constant. $\theta=\alpha+j\beta$, where α is the image attenuation constant and β is the image phase constant.

TABLE 1—SYMMETRICAL T AND H ATTENUATOR VALUES. $Z=500$ OHMS RESISTIVE (DIAGRAM ON PAGE 11-4).

Attenuation (dB)	Series Arm R_1 (ohms)	Shunt Arm R_2 (ohms)	$1000/R_2$	$\log_{10} R_2$
0.0	0.0	∞	0.0000	—
0.2	5.8	21 700	0.0461	—
0.4	11.5	10 850	0.0921	—
0.6	17.3	7 230	0.1383	—
0.8	23.0	5 420	0.1845	—
1.0	28.8	4 330	0.2308	—
2.0	57.3	2 152	0.465	—
3.0	85.5	1 419	0.705	—
4.0	113.1	1 048	0.954	—
5.0	140.1	822	1.216	—
6.0	166.1	669	1.494	2.826
7.0	191.2	558	—	2.747
8.0	215.3	473.1	—	2.675
9.0	238.1	405.9	—	2.608
10.0	259.7	351.4	—	2.546
12.0	299.2	268.1	—	2.428
14.0	333.7	207.8	—	2.318
16.0	363.2	162.6	—	2.211
18.0	388.2	127.9	—	2.107
20.0	409.1	101.0	—	2.004
22.0	426.4	79.94	—	1.903
24.0	440.7	63.35	—	1.802
26.0	452.3	50.24	—	1.701
28.0	461.8	39.87	—	1.601
30.0	469.3	31.65	—	1.500
35.0	482.5	17.79	—	1.250
40.0	490.1	10.00	—	1.000
50.0	496.8	3.162	—	0.500
60.0	499.0	1.000	—	0.000
80.0	499.9	0.1000	—	−1.000
100.0	500.0	0.01000	—	−2.000

Shunt Arm R_2 in Error (10 *Percent High*):

Designed Loss (dB)	Error in Insertion Loss (dB)	Error in Input Impedance $100(\Delta Z/Z)$ Percent
0.2	−0.01	0.2
1	−0.05	1.0
6	−0.3	3.3
12	−0.5	3.0
20	−0.7	1.6
40	−0.8	0.2
100	−0.8	0.0

Error in input impedance:

$$\frac{\Delta Z}{Z}=2\,\frac{K-1}{K(K+1)}\,\frac{\Delta R_2}{R_2}.$$

Error in output current:

$$\frac{\Delta i}{i}=\frac{K-1}{K+1}\,\frac{\Delta R_2}{R_2}.$$

See notes on page 11-3.

SYMMETRICAL π AND O ATTENUATORS

Interpolation of Symmetrical π and O Attenuators (Table 2)

Column R_1 may be interpolated linearly above 16 decibels, and R_2 up to 20 decibels. Otherwise interpolate the $1000/R_1$ and $\log_{10}R_2$ columns respectively.

TABLE 2—SYMMETRICAL π AND O ATTENUATORS $Z=500$ OHMS RESISTIVE (DIAGRAM ON PAGE 11-4)

Attenuation (dB)	Shunt Arm R_1 (ohms)	$1000/R_1$	Series Arm R_2 (ohms)	$\log_{10} R_2$
0.0	∞	0.000	0.0	—
0.2	43 400	0.023	11.5	—
0.4	21 700	0.046	23.0	—
0.6	14 500	0.069	34.6	—
0.8	10 870	0.092	46.1	—
1.0	8 700	0.115	57.7	—
2.0	4 362	0.229	116.1	—
3.0	2 924	0.342	176.1	—
4.0	2 210	0.453	238.5	—
5.0	1 785	0.560	304.0	—
6.0	1 505	0.665	373.5	—
7.0	1 307	0.765	448.0	—
8.0	1 161.4	0.861	528.4	—
9.0	1 049.9	0.952	615.9	—
10.0	962.5	1.039	711.5	—
12.0	835.4	1.197	932.5	—
14.0	749.3	1.335	1 203.1	—
16.0	688.3	1.453	1 538	—
18.0	644.0	—	1 954	—
20.0	611.1	—	2 475	3.394
22.0	586.3	—	3 127	3.495
24.0	567.3	—	3 946	3.596
26.0	552.8	—	4 976	3.697
28.0	541.5	—	6 270	3.797
30.0	532.7	—	7 900	3.898
35.0	518.1	—	14 050	4.148
40.0	510.1	—	25 000	4.398
50.0	503.2	—	79 100	4.898
60.0	501.0	—	2.50×10^5	5.398
80.0	500.1	—	2.50×10^6	6.398
100.0	500.0	—	2.50×10^7	7.398

Errors in Symmetrical π and O Attenuators (Fig. 5)

Error in input impedance:

$$\frac{\Delta Z'}{Z'} = \frac{K-1}{K+1}\left(\frac{\Delta R_1}{R_1} + \frac{1}{K^2}\frac{\Delta R_2}{R_2} + \frac{2}{K}\frac{\Delta R_3}{R_3}\right).$$

Error in insertion loss, in decibels:

decibels $= -8(\Delta i_2/i_2)$ (approximately)

$$= 4\frac{K-1}{K+1}\left(-\frac{\Delta R_1}{R_1} - \frac{\Delta R_2}{R_2} + 2\frac{\Delta R_3}{R_3}\right).$$

See notes on page 11-3.

BRIDGED *T* OR *H* ATTENUATORS

Interpolation of Bridged T or H Attenuators (Table 3)

Bridge Arm R_4: Use the formula $\log_{10}(R_4+500) = 2.699 + \text{decibels}/20$ for $Z = 500$ ohms. However, if preferred, the tabular values of R_4 may be interpolated linearly, between 0 and 10 decibels only.

Shunt Arm R_3: Do not interpolate R_3 column. Compute R_3 by $R_3 = 10^6/4R_4$, for $Z = 500$ ohms.

Note: For attenuators of 60 decibels and over, the bridge arm R_4 may be omitted provided a shunt arm is used having twice the resistance tabulated in the R_3 column. (This makes the input impedance 0.1 of 1 percent high at 60 decibels.)

TABLE 3—VALUES FOR BRIDGED *T* OR *H* ATTENUATORS. $Z = 500$ OHMS RESISTIVE, $R_1 = R_2 = 500$ OHMS (DIAGRAM ON PAGE 11-4).

Attenuation (decibels)	Bridge Arm R_4 (ohms)	Shunt Arm R_3 (ohms)
0.0	0.0	∞
0.2	11.6	21 500
0.4	23.6	10 610
0.6	35.8	6 990
0.8	48.2	5 180
1.0	61.0	4 100
2.0	129.5	1 931
3.0	206.3	1 212
4.0	292.4	855
5.0	389.1	642
6.0	498	502
7.0	619	404
8.0	756	331
9.0	909	275.0
10.0	1 081	231.2
12.0	1 491	167.7
14.0	2 006	124.6
16.0	2 655	94.2
18.0	3 472	72.0
20.0	4 500	55.6
25.0	8 390	29.8
30.0	15 310	16.33
40.0	49 500	5.05
50.0	157 600	1.586
60.0	499 500	0.501
80.0	5.00×10^6	0.0500
100.0	50.0×10^6	0.00500

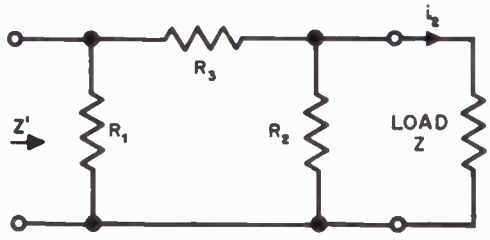

NOMINALLY $R_1 = R_2$ AND $Z' = Z$

Fig. 5.

Errors in Bridged T or H Attenuators

Resistance of any one arm 10 percent higher than correct value:

Designed Loss (decibels)	*A* (decibels)	*B* (percent)	*C* (percent)
0.2	0.01	0.005	0.2
1	0.05	0.1	1.0
6	0.2	2.5	2.5
12	0.3	5.6	1.9
20	0.4	8.1	0.9
40	0.4	10	0.1
100	0.4	10	0.0

Element in Error (10 percent high)	Error in Loss	Error in Terminal Impedance
Series arm R_1 (analogous for arm R_2)	Zero	*B*, for adjacent terminals*
Shunt arm R_3	$-A$†	*C*
Bridge arm R_4	*A*‡	*C*

Notes:

* Error in impedance at opposite terminals is zero.

† Loss is lower than designed loss.

‡ Loss is higher than designed loss.

Error in input impedance:

$$\frac{\Delta Z_1}{Z_1} = \left(\frac{K-1}{K}\right)^2\frac{\Delta R_1}{R_1} + \frac{K-1}{K^2}\left(\frac{\Delta R_3}{R_3} + \frac{\Delta R_4}{R_4}\right).$$

For $\Delta Z_2/Z_2$ use subscript 2 in equation in place of subscript 1.

TABLE 4—VALUES FOR MINIMUM-LOSS PADS MATCHING Z_1 AND Z_2, BOTH RESISTIVE (DIAGRAM ON PAGE 11-4).

Z_1 (ohms)	Z_2 (ohms)	Z_1/Z_2	Loss (decibels)	Series Arm R_1 (ohms)	Shunt Arm R_3 (ohms)
10 000	500	20.00	18.92	9 747	513.0
8 000	500	16.00	17.92	7 746	516.4
6 000	500	12.00	16.63	5 745	522.2
5 000	500	10.00	15.79	4 743	527.0
4 000	500	8.00	14.77	3 742	534.5
3 000	500	6.00	13.42	2 739	547.7
2 500	500	5.00	12.54	2 236	559.0
2 000	500	4.00	11.44	1 732	577.4
1 500	500	3.00	9.96	1 224.7	612.4
1 200	500	2.40	8.73	916.5	654.7
1 000	500	2.00	7.66	707.1	707.1
800	500	1.60	6.19	489.9	816.5
600	500	1.20	3.77	244.9	1224.7
500	400	1.25	4.18	223.6	894.4
500	300	1.667	6.48	316.2	474.3
500	250	2.00	7.66	353.6	353.6
500	200	2.50	8.96	387.3	258.2
500	160	3.125	10.17	412.3	194.0
500	125	4.00	11.44	433.0	144.3
500	100	5.00	12.54	447.2	111.80
500	80	6.25	13.61	458.3	87.29
500	65	7.692	14.58	466.4	69.69
500	50	10.00	15.79	474.3	52.70
500	40	12.50	16.81	479.6	41.70
500	30	16.67	18.11	484.8	30.94
500	25	20.00	18.92	487.3	25.65

Error in output current:

$$\frac{\Delta i}{i} = \frac{K-1}{2K}\left(\frac{\Delta R_3}{R_3} - \frac{\Delta R_4}{R_4}\right).$$

See notes on page 11-3.

MINIMUM-LOSS PADS

Interpolation of Minimum-Loss Pads (Table 4)

Table 4 may be interpolated linearly with respect to Z_1, Z_2, or Z_1/Z_2 except when Z_1/Z_2 is between 2.0 and 1.2. The accuracy of the interpolated value becomes poorer as Z_1/Z_2 passes below 2.0 toward 1.2, especially for R_3.

For Other Terminations

If the terminating resistances are to be Z_A and Z_B instead of Z_1 and Z_2, respectively, the procedure is as follows. Enter the table at $Z_1/Z_2 = Z_A/Z_B$ and read the loss and the tabular values of R_1 and R_3. Then the series and shunt arms are, respectively, MR_1 and MR_3, where $M = Z_A/Z_1 = Z_B/Z_2$.

Errors in Minimum-Loss Pads

Impedance Ratio Z_1/Z_2	D Decibels*	E Percent*	F Percent*
1.2	0.2	+4.1	+1.7
2.0	0.3	7.1	1.2
4.0	0.35	8.6	0.6
10.0	0.4	9.5	0.25
20.0	0.4	9.7	0.12

* *Notes*:

Series arm R_1 10 percent high: Loss is increased by D decibels from above table. Input impedance Z_1 is increased by E percent. Input impedance Z_2 is increased by F percent.

Shunt arm R_3 10 percent high: Loss is decreased by D decibels from above table. Input impedance Z_2 is increased by E percent. Input impedance Z_1 is increased by F percent.

TABLE 5—VALUES FOR MISCELLANEOUS *T* AND *H* PADS (DIAGRAM ON PAGE 11-4).

Resistive Terminations			Attenuator Arms		
Z_1 (ohms)	Z_2 (ohms)	Loss (decibels)	Series R_1 (ohms)	Series R_2 (ohms)	Shunt R_3 (ohms)
5000	2000	10	3889	222	2222
5000	2000	15	4165	969	1161
5000	2000	20	4462	1402	639
5000	500	20	4782	190.7	319.4
2000	500	15	1763	165.4	367.3
2000	500	20	1838	308.1	202.0
2000	200	20	1913	76.3	127.8
500	200	10	388.9	22.2	222.2
500	200	15	416.5	96.9	116.1
500	200	20	446.2	140.2	63.9
500	50	20	478.2	19.07	31.94
200	50	15	176.3	16.54	36.73
200	50	20	183.8	30.81	20.20

Errors in input impedance:

$$\Delta Z_1/Z_1 = (1-Z_2/Z_1)^{1/2}(\Delta R_1/R_1 + N^{-1}\,\Delta R_3/R_3)$$

$$\Delta Z_2/Z_2 = (1-Z_2/Z_1)^{1/2}(\Delta R_3/R_3 + N^{-1}\,\Delta R_1/R_1).$$

Error in output current, working either direction:

$$\Delta i/i = \tfrac{1}{2}(1-Z_2/Z_1)^{1/2}(\Delta R_3/R_3 - \Delta R_1/R_1).$$

See notes on page 11-3.

MISCELLANEOUS *T* AND *H* PADS (*Table 5*)

Errors in T and H Pads

Series Arms R_1 and R_2 in Error: Errors in input impedances are

$$\Delta Z_1 = \Delta R_1 + N^{-1}(Z_1/Z_2)\Delta R_2$$

and

$$\Delta Z_2 = \Delta R_2 + N^{-1}(Z_2/Z_1)\Delta R_1.$$

Error in insertion loss, in decibels

$$= 4(\Delta R_1/Z_1 + \Delta R_2/Z_2) \text{ approximately.}$$

Shunt Arm R_3 in Error (10 *Percent High*):

Z_1/Z_2	Designed Loss (decibels)	Error in Insertion Loss (decibels)	Error in Input Impedance $100(\Delta Z_1/Z_1)$	Error in Input Impedance $100(\Delta Z_2/Z_2)$
2.5	10	−0.4	1.1%	7.1%
2.5	15	−0.6	1.2	4.6
2.5	20	−0.7	0.9	2.8
4.0	15	−0.5	0.8	6.0
4.0	20	−0.65	0.6	3.6
10	20	−0.6	0.3	6.1

$$\frac{\Delta Z_1}{Z_1} = \frac{2}{N-1}\left[\left(\frac{NZ_2}{Z_1}\right)^{1/2} + \left(\frac{Z_1}{NZ_2}\right)^{1/2} - 2\right]\frac{\Delta R_3}{R_3}$$

(for $\Delta Z_2/Z_2$ interchange subscripts 1 and 2)

$$\frac{\Delta i}{i} = \frac{N+1-(N^{1/2})[(Z_1/Z_2)^{1/2}+(Z_2/Z_1)^{1/2}]}{N-1}\frac{\Delta R_3}{R_3}$$

where i is the output current.

CHAPTER 12
BRIDGES AND IMPEDANCE MEASUREMENTS

In the diagrams of bridges below, the source is shown as a generator, and the detector as a pair of headphones. The positions of these two elements may be interchanged as dictated by detailed requirements in any individual case, such as location of grounds. For all but the lowest frequencies, a shielded transformer is required at either the input or output (but not usually at both) terminals of the bridge. This is shown in some of the diagrams. The detector is chosen according to the frequency of the source. When insensitivity of the ear makes direct use of headphones impractical, a simple radio receiver or its equivalent is essential. Some selectivity is desirable to discriminate against harmonics, for the bridge is often frequency sensitive. The source may be modulated to obtain an audible signal, but greater sensitivity and discrimination against interference are obtained by the use of a continuous-wave source and a heterodyne detector. An amplifier and oscilloscope or an output meter are sometimes preferred for observing nulls. In this case it is convenient to have an audible output signal available for the preliminary setup and for locating trouble, since much can be deduced from the quality of the audible signal that would not be apparent from observation of amplitude only.

FUNDAMENTAL ALTERNATING-CURRENT OR WHEATSTONE BRIDGE

Balance condition is $Z_x = Z_s Z_a / Z_b$. Maximum sensitivity exists when Z_d is the conjugate of the bridge output impedance and Z_g the conjugate of its input impedance. Greatest sensitivity exists when bridge arms are equal, for example, for resistive arms

$$Z_d = Z_a = Z_b = Z_x = Z_s = Z_g.$$

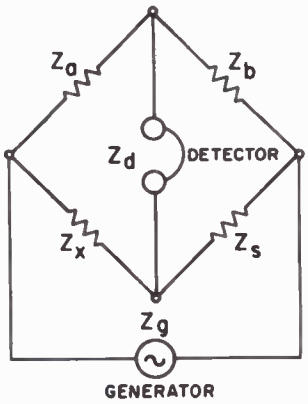

BRIDGE WITH DOUBLE-SHIELDED TRANSFORMER

Shield on secondary may be floating, connected to either end, or to center of secondary winding. It may be in two equal parts and connected to opposite ends of the winding. In any case, its capacitance to ground must be kept to a minimum.

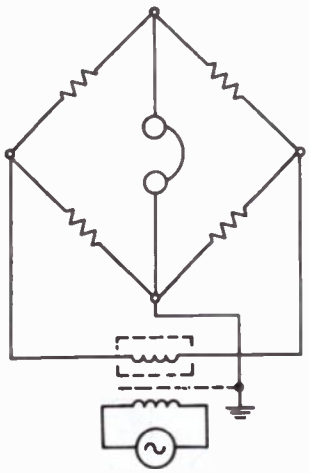

WAGNER EARTH CONNECTION

None of the bridge elements are grounded directly. First balance bridge with switch to B. Throw switch to G and rebalance by means of R and C. Recheck bridge balance and repeat as required. The capacitor balance C is necessary only when the frequency is above the audio range. The transformer may have only a single shield as

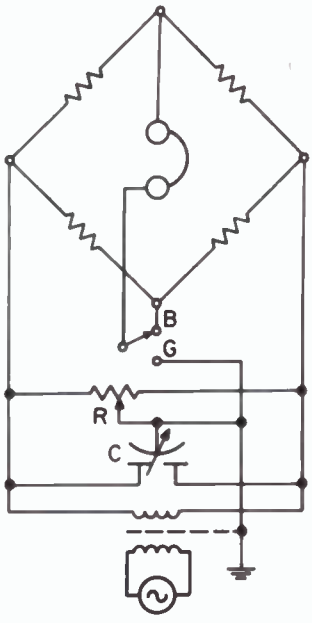

shown, with the capacitance of the secondary to the shield kept to a minimum.

CAPACITOR BALANCE

Useful when one point of bridge must be grounded directly and only a simple shielded transformer is used. Balance bridge, then open the two arms at P and Q. Rebalance by auxiliary capacitor C. Close P and Q and check balance.

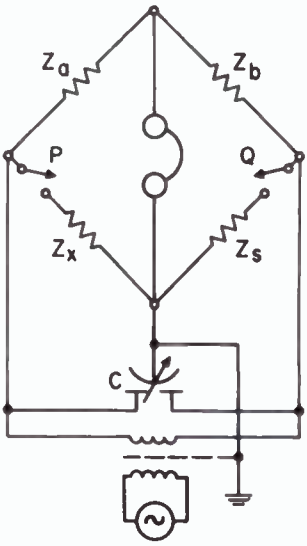

SERIES-RESISTANCE-CAPACITANCE BRIDGE

$$C_x = C_s R_b / R_a$$

$$R_x = R_s R_a / R_b.$$

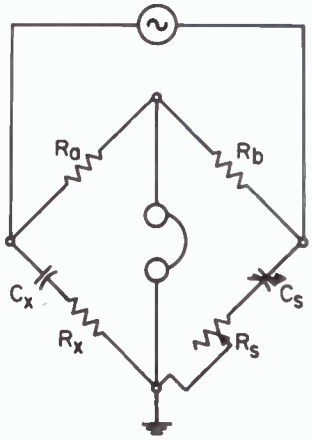

WIEN BRIDGE

$$C_x/C_s = (R_b/R_a) - (R_s/R_x)$$

$$C_s/C_x = 1/\omega^2 R_s R_x.$$

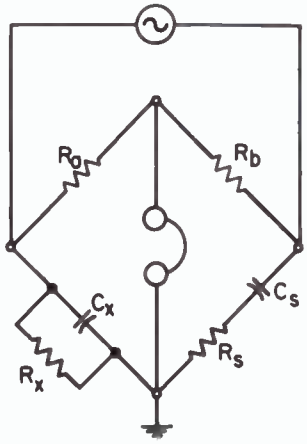

For measurement of frequency, or in a frequency-selective application, if we make $C_x = C_s$, $R_x = R_s$, and $R_b = 2R_a$, then

$$f = (2\pi C_s R_s)^{-1}.$$

OWEN BRIDGE

$$L_x = C_b R_a R_d$$

$$R_x = (C_b R_a / C_d) - R_c.$$

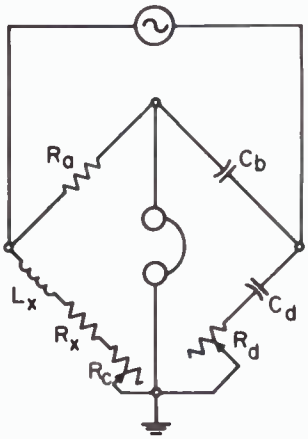

RESONANCE BRIDGE

$$\omega^2 LC = 1$$

$$R_x = R_s R_a / R_b.$$

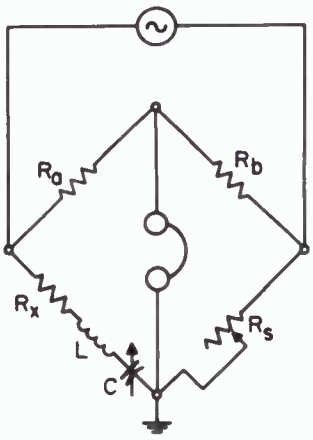

MAXWELL BRIDGE

$$L_x = R_a R_b C_s$$

$$R_x = R_a R_b / R_s$$

$$Q_x = \omega (L_x/R_x) = \omega C_s R_s.$$

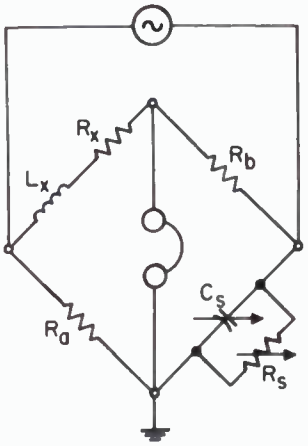

HAY BRIDGE

For measurement of large inductance.

$$L_x = R_a R_b C_s / (1 + \omega^2 C_s^2 R_s^2)$$

$$Q_x = \omega L_x / R_x = (\omega C_s R_s)^{-1}.$$

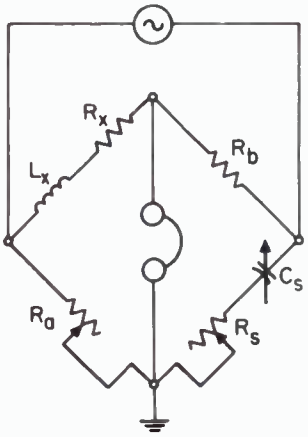

SCHERING BRIDGE

$$C_x = C_s R_b / R_a$$

$$1/Q_x = \omega C_x R_x = \omega C_b R_b.$$

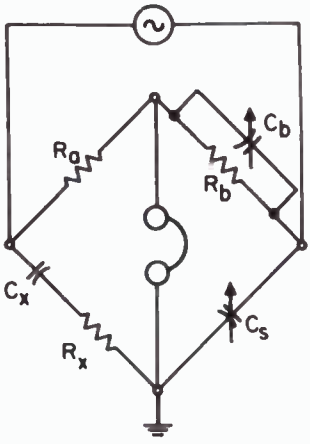

SUBSTITUTION METHOD FOR HIGH IMPEDANCES

Initial balance (unknown terminals x–x open):

C_s' and R_s'.

Final balance (unknown connected to x–x):

C_s'' and R_s''.

Then when $R_x > 10/\omega C_s'$, there results, with error < 1 percent

$$C_x = C_s' - C_s''.$$

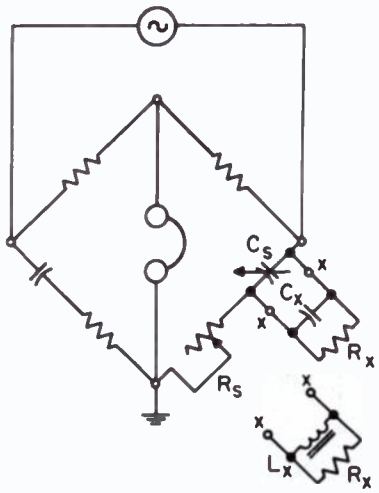

The parallel resistance is

$$R_x = [\omega^2 C_s'^2 (R_s' - R_s'')]^{-1}.$$

If unknown is an inductor

$$L_x = -(\omega^2 C_x)^{-1} = [\omega^2 (C_s'' - C_s')]^{-1}.$$

MEASUREMENT WITH CAPACITOR IN SERIES WITH UNKNOWN

Initial balance (unknown terminals x–x short-circuited):

C_s' and R_s'.

Final balance (x–x unshorted):

C_s'' and R_s''.

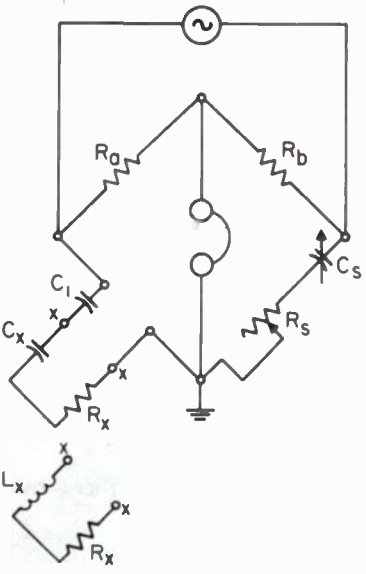

Then the series resistance is

$$R_x = (R_s'' - R_s') R_a / R_b$$

$$C_x = \frac{R_b C_s' C_s''}{R_a (C_s' - C_s'')}$$

$$= \frac{R_b}{R_a} C_s' \left(\frac{C_s'}{C_s' - C_s''} - 1 \right).$$

When $C_s'' > C_s'$

$$L_x = \frac{1}{\omega^2} \frac{R_a}{R_b C_s'} \left(1 - \frac{C_s'}{C_s''} \right).$$

MEASUREMENT OF DIRECT CAPACITANCE

Connection of N to N' places C_{nq} across phone and C_{np} across R_b which requires only a sma readjustment of R_s.

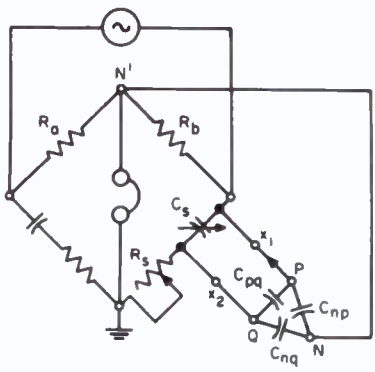

Initial balance: Lead from P disconnected fro X_1 but lying as close to the connected position a practical.

Final balance: Lead connected to X_1.

By the substitution method above

$$C_{pq} = C_s' - C_s''.$$

FELICI MUTUAL-INDUCTANCE BALANCE

At the null

$$M_x = -M_s.$$

This is useful at lower frequencies where capaci tive reactances associated with windings ar negligibly small.

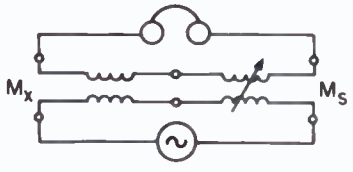

MUTUAL-INDUCTANCE CAPACITANCE BALANCE

Using low-loss capacitor, at the null

$$M_x = 1/\omega^2 C_s.$$

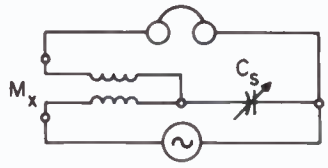

HYBRID-COIL METHOD

At the null

$$Z_1 = Z_2.$$

The transformer secondaries must be accurately matched and balanced to ground. This is useful at audio and carrier frequencies.

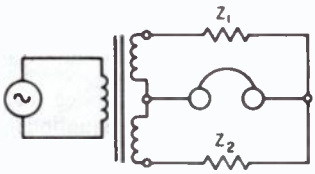

Q OF RESONANT CIRCUIT BY BANDWIDTH

For 3-decibel or half-power points. Source loosely coupled to circuit. Adjust frequency to each side of resonance, noting bandwidth when

$v = 0.71 \times$ (v at resonance)
$Q =$ (resonance frequency)/(bandwidth).

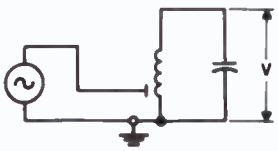

Q-METER *(Boonton Radio Type 160A)*

$R_1 = 0.04$ ohm
$R_2 = 100$ megohms
$V =$ vacuum-tube voltmeter
$I =$ thermal milliammeter
$L_x R_x C_0 =$ unknown coil plugged into COIL terminals for measurement.

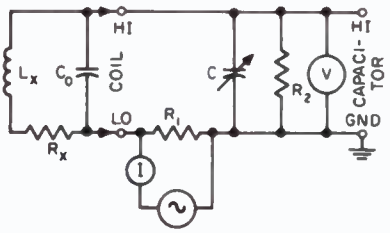

Correction of Q Reading

For distributed capacitance C_0 of coil

$$Q_{true} = Q[(C + C_0)/C]$$

where Q = reading of Q-meter (corrected for internal resistors R_1 and R_2 if necessary), and C = capacitance reading of Q-meter.

Measurement of C_0 and True L_x

C plotted against $1/f^2$ is a straight line.

L_x = true inductance

$$= \frac{1/f_2^2 - 1/f_1^2}{4\pi^2(C_2 - C_1)}$$

C_0 = negative intercept
f_0 = natural frequency of coil.

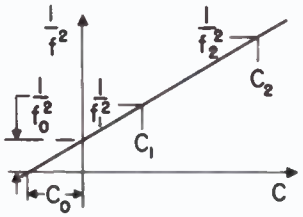

When only two readings are taken and $f_1/f_2 = 2.00$

$$C_0 = (C_2 - 4C_1)/3.$$

Using microhenries, megahertz, and picofarads

$$L_x = 19\,000/f_2^2(C_2 - C_1).$$

Measurement of Admittance

Initial reading $C'Q'$ (LR_p is any suitable coil):

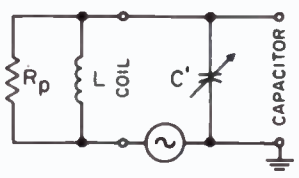

Final reading $C'''Q''$:

$$1/Z = Y = G + jB = 1/R_p + j\omega C.$$

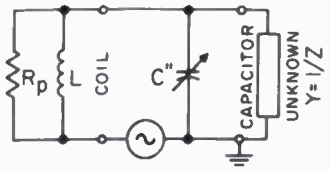

Then

$$C = C' - C''$$

$$1/Q = G/\omega C$$

$$= C'/C(1000/Q'' - 1000/Q') \times 10^{-3}.$$

If Z is inductive

$$C'' > C'.$$

Measurement of Impedances Lower Than Those Directly Measurable

For the initial reading $C'Q'$, CAPACITOR terminals are open.

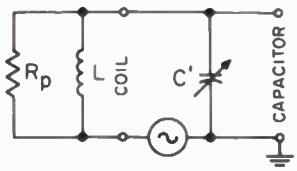

On second reading $C''Q''$, a capacitive divider C_aC_b is connected to the CAPACITOR terminals.

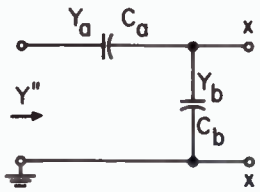

Final reading $C'''Q'''$, unknown connected to x–x.

$$Y_a = G_a + j\omega C_a \qquad Y_b = G_b + j\omega C_b$$

with G_a and G_b not shown in diagrams.

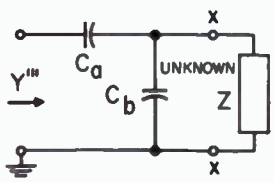

Then the unknown impedance is

$$Z = [Y_a/(Y_a + Y_b)]^2 (Y''' - Y'')^{-1} - (Y_a + Y_b)^{-1} \text{ ohm}$$

where, with capacitance in picofarads and $\omega = 2\pi \times$ frequency in megahertz

$$(Y''' - Y'')^{-1} = \frac{10^6/\omega}{C'(1000/Q''' - 1000/Q'') \times 10^{-3} + j(C'' - C''')}$$

Usually G_a and G_b may be neglected, then the results

$$Z = \left(\frac{1}{1 + C_b/C_a}\right)^2 (Y''' - Y'')^{-1} + j\frac{10^6}{\omega(C_a + C_b)} \text{ ohms}$$

For many measurements, C_a may be 100 picofarads. $C_b = 0$ for very low values of Z and for highly reactive values of Z. For unknowns that are principally resistive and of low or medium value, C_b may take sizes up to 300 to 500 picofarads. When $C_b = 0$

$$Z = (Y''' - Y'')^{-1} + j(10^6/\omega C_a) \text{ ohms}$$

and the "second" reading above becomes the "initial," with $C' = C''$ in the equations.

Measurement of Coupling Coefficient of Loosely Coupled Coils

The coefficient of coupling

$$k = M/(L_1L_2)^{1/2}$$

between two high-Q coils can be obtained by measuring the inductance L with S_1 closed and again with S_1 open. From these two measurements

$$k = (1 - L_{closed}/L_{open})^{1/2}.$$

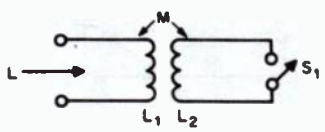

When the coil self-inductances are known, a measurement of L_a and L_b yields

$$k = (L_a - L_b)/4(L_1L_2)^{1/2}.$$

If $L_1 = L_2$

$$k = (L_a - L_b)/(L_a + L_b).$$

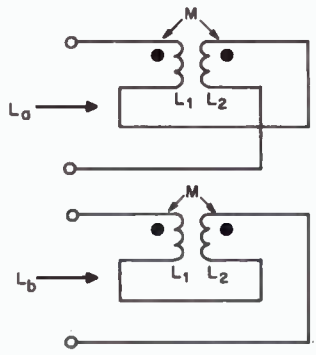

Neither of the above methods provides adequate precision when two high-Q coils are only about critically coupled. In that case, the Q of each coil is measured with the other coil open-circuited. Then the coupled coils (L_1R_1 and L_2R_2) and a low-loss adjustable capacitor (C_2) are connected to the Q-meter as shown, C_2 is disconnected, and C is adjusted to maximize the Q-meter reading; C_2 is then connected and adjusted to minimize the reading. If the final reading is Q_0

$$K=[1/Q_2(1/Q_0-1/Q_1)]^{1/2}.$$

If the final reading is too small to be read accurately, Q_2 may be reduced by inserting a small resistance in series with L_2R_2.

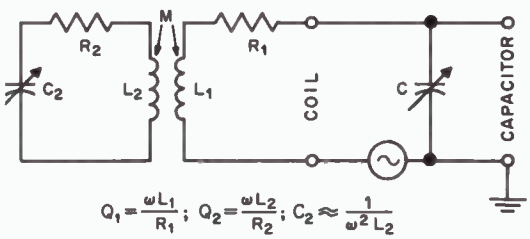

PARALLEL-T (SYMMETRICAL)

Conditions for zero transfer are

$$\omega^2C_1C_2=2/R_2^2$$

$$\omega^2C_1^2=1/2R_1R_2$$

$$C_2R_2=4C_1R_1.$$

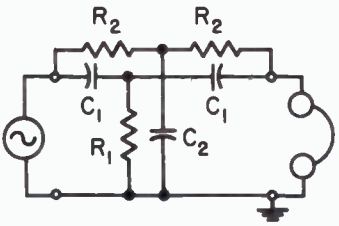

When used as a frequency-selective network, if we make $R_2=2R_1$ and $C_2=2C_1$, then

$$f=1/2\pi C_1R_2=1/2\pi C_2R_1.$$

For additional information, see G. E. Valley, Jr. and H. Wallman, "Vacuum Tube Amplifiers," McGraw-Hill Book Company, Inc., New York, N.Y.; 1948; pp. 387–389.

TWIN-T ADMITTANCE-MEASURING CIRCUIT *(General Radio Type 821-A)*

This circuit may be used for measuring admittances in the range somewhat exceeding 400 kilohertz to 40 megahertz. It is applicable to the special measuring techniques described above for the Q-meter.

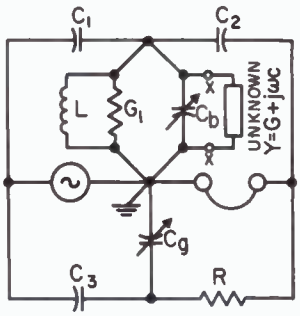

Conditions for null in output

$$G+G_l=R\omega^2C_1C_2(1+C_g/C_3)$$

$$C+C_b=1/\omega^2L-C_1C_2(1/C_1+1/C_2+1/C_3).$$

With the unknown disconnected, call the initial balance C_b' and C_g'. With unknown connected, final balance is C_b'' and C_g''. Then the components of the unknown $Y=G+j\omega C$ are

$$C=C_b'-C_b''$$

$$G=(R\omega^2C_1C_2/C_3)(C_g''-C_g').$$

CHAPTER 13
MAGNETIC-CORE TRANSFORMERS AND REACTORS

MAGNETIC-CORE TRANSFORMERS

Magnetic-core transformers, with few exceptions, are closely coupled circuits for transmitting alternating-current energy and for matching impedances between the generator and the load. The major types of transformers follow.

Power transformers (25, 50, 60, 400 Hz): plate, filament, isolation, vibrator, auto.
Audio-frequency transformers (20–20 000 Hz): input, output, interstage, matching, driver, modulation
High-frequency transformers (2–1000 kHz): input, output, matching, modulation
Pulse transformers (repetition rates up to 4 MHz): isolation, step-up, step-down, blocking oscillator

The equivalent circuit of a generalized transformer is shown in Fig. 1.

POWER TRANSFORMERS

Power transformers operate from a nearly zero source impedance at a single low frequency, primarily to transfer power at convenient voltages.

The magnetic cores used for these types of transformers are usually Type E and I laminations of 4% silicon steel. Grain-oriented silicon-steel Type C cores are also used. They are wound in tape form on a rectangular mandrel, impregnated, and cut into halves. These halves are then banded around the wound transformer coil. Table 1 gives typical operating conditions for these types of cores.

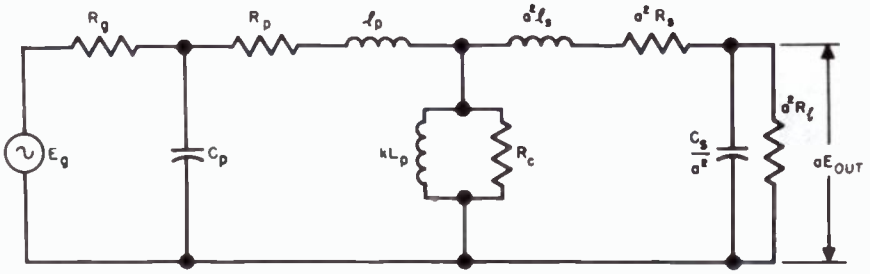

Fig. 1—Equivalent network of a transformer.

a = turns ratio = N_p/N_s
C_p = primary equivalent shunt capacitance
C_s = secondary equivalent shunt capacitance
E_g = root-mean-square generator voltage
E_{out} = root-mean-square output voltage
k = coefficient of coupling
L_p = primary inductance
l_p = primary leakage inductance
l_s = secondary leakage inductance
R_c = core-loss equivalent shunt resistance
R_g = generator impedance
R_l = load impedance
R_p = primary-winding resistance
R_s = secondary-winding resistance

TABLE 1—TYPICAL OPERATING CONDITIONS FOR CORE MATERIALS AT VARIOUS FREQUENCIES.

Frequency in Hertz	Lamination Thickness in Inches	Core Material	Core Flux Density B_m in Gauss	Approximate Core Loss in Watts/Lb	Approximate Exciting (VA)/Lb
25	0.025	2.5-percent silicon	14 000	0.65	4.0
60	0.014	4-percent silicon	12 000	1.0	6.0
60	0.014	Grain-oriented silicon	15 000	1.0	6.0
400	0.004	Grain-oriented silicon	10 000	4.5	10.0
800	0.004	Grain-oriented silicon	6 000	4.5	10.0

DESIGN OF POWER TRANSFORMERS FOR RECTIFIERS USING E AND I LAMINATIONS

The equivalent circuit of a power transformer for a vacuum-tube circuit is shown in Fig. 2.

(A) Determine total output volt-amperes and compute the primary and secondary currents from

$$E_pI_p \times 0.9 = (1/\eta)[(E_sI_{dc})_{pl}K + (EI)_{fil}]$$

$$I_s = K'I_{dc}$$

where the numeric 0.9 is the power factor, and the efficiency η and the K, K' factors are listed in Tables 2 and 3. E_pI_p is the input volt-amperes, I_{dc} refers to the total direct-current component drawn by the supply, and the subscripts pl and fil refer to the volt-amperes drawn from the plate-supply and filament-supply (if present) windings, respectively. E_s is the total voltage across the secondary of the transformer.

$$E_s = 2.35E_{dc}$$

for a single-phase full-wave rectifier. E_{dc} is the direct-current output voltage of the rectifier. Factor 2.35 is twice the ratio of root-mean-square to average values plus an allowance for 5-percent regulation.

(B) Compute the size of wire of each winding on the basis of current densities given by the following.

For 60-hertz sealed units

$$\text{amperes/inch}^2 = 2470 - 585 \log W_{out}$$

or

$$\text{inches diameter} \approx 1.13 \left[\frac{I \text{ (in amperes)}}{2470 - 585 \log W_{out}}\right]^{1/2}.$$

For 60-hertz open units (uncased)

$$\text{amperes/inch}^2 = 2920 - 610 \log W_{out}$$

or

$$\text{inches diameter} \approx 1.13 \left[\frac{I \text{ (in amperes)}}{2920 - 610 \log W_{out}}\right]^{1/2}.$$

(C) Compute roughly, the net core area

$$A_c = \frac{(W_{out})^{1/2}}{5.58} (60/f)^{1/2} \text{ inches}^2$$

where f is in hertz (refer to Table 4). Select a

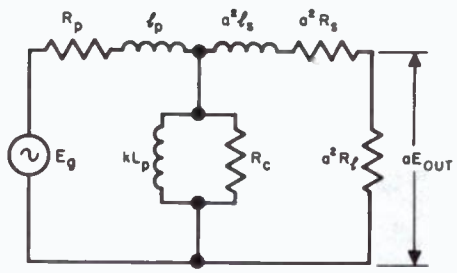

Fig. 2—Equivalent network of a power transformer. l_p and l_s may be neglected when there are no strict requirements on voltage regulation.

TABLE 2—FACTORS K AND K' FOR SINGLE-PHASE-RECTIFIER SUPPLIES.

Filter	K	K'
Full-wave:		
Capacitor input	0.707	1.06
Reactor input	0.5	0.707
Half-wave:		
Capacitor input	1.4	2.2
Reactor input	1.06	1.4

TABLE 3—EFFICIENCY OF VARIOUS SIZES OF POWER SUPPLIES.*

Output in Watts	Approximate Efficiency in Percent
20	70
30	75
40	80
80	85
100	86
200	90

* From "Radio Components Handbook," Technical Advertising Associates, Cheltenham, Pa.; May 1948: p. 92.

TABLE 4—EQUIVALENT *EI* RATINGS OF POWER TRANSFORMERS. B_m = flux density in gauss. *EI* rating = volt-ampere capability at 60 and 400 hertz for various core sizes. Ratings are based on a rise above ambient of 50° C. These values should be reduced to obtain lower temperature rise when more than two windings are required or when extra-high-voltage operation is required. *Adapted from "Radio Components Handbook," Technical Advertising Associates, Cheltenham, Pa.; May 1948: p. 92.*

At 60 Hertz		At 400 Hertz		Current Density	EI-Type	Tongue Width of Lamination	Stack Height	Average Copper Mean Length per Turn	Core Weight
EI	B_m*	*EI*	B_m*	(amps/sq m)	Lamination†	*g* (in.)	*p* (in.)	(MLT) (in.)	(lb)
3.9	14 000	9.5	5 000	3 200	EI-21	0.5	0.5	3.12	0.199
5.8	14 000	15.0	4 900	2 700	EI-625	0.625	0.625	3.62	0.361
13.0	14 000	30.0	4 700	2 560	EI-75	0.75	0.75	4.33	0.609
17.0	14 000	38.0	4 600	2 560	EI-75	0.75	1.00	4.83	0.812
24.0	13 500	50.0	4 500	2 330	EI-11	0.875	0.875	5.04	0.966
37.0	13 000	80.0	4 200	2 130	EI-12	1.00	1.00	5.71	1.43
54.0	13 000	110	4 000	2 030	EI-12	1.00	1.50	6.71	2.14
82.0	12 500	180	3 900	1 800	EI-125	1.25	1.25	7.21	2.83
110	12 000	230	3 900	1 770	EI-125	1.25	1.75	8.21	3.97
145	12 000	325	3 700	1 600	EI-13	1.50	1.50	8.63	4.92
195	11 000	420	3 500	1 500	EI-13	1.50	2.00	9.63	6.56
525	10 500	1 100	3 200	1 220	EI-19	1.75	1.75	12.8	9.75

* Refers to silicon steel 0.014 inch thick.
† Lamination designation and constants per Allegheny Ludlum Corp., Pittsburgh, Pa.

TABLE 5—DATA ON METALLIC CORE MATERIALS.

Metal or Alloy	Material or Trade Name	Composition in Percent (remainder is iron)	Characteristic Property or Application	Permeability		Direct-Current Saturation in Kilogauss	Residual Induction in Kilogauss	Coercive Force in Oersteds	Resistivity in $\mu\Omega$-Centimeters	Curie Temperature in Degrees Celsius
				Initial	Maximum					
Silicon–iron*	Silicon–Iron	4 Si	Transformer	400	7 000	20	12	0.5	60	690
	Hypersil Trancor 3*X* Silectron	3.5 Si	Grain oriented	1 500	35 000	20	13.7	0.1 to 0.3	50	750
	Sendust	9.5 Si, 5.5 Al	High frequency, powder	30 000	120 000	10	5	0.05	80	—
Cobalt–iron*	Hyperco	35 Co, 0.5 Cr	High saturation	650	10 000	24	>13	>1	28	970
	Permendur 2*V*	49 Co, 2 V		800	4 500	24	14	2	25	980
Nickel–iron*	Perminvar 45–25	45 Ni, 25 Co		400	2 000	15.5	3.3	1.2	20	715
	Perminvar 7–70	70 Ni, 7 Co	"Constant"	850	4 000	12.5	2.4	0.6	15	650
	Conpernik	50 Ni	permeability	1 500	2 000	16	—	—	45	—
	Isoperm 36	36 Ni, 9 Cu		60	65	—	—	—	70	300
	Isoperm 50	50 Ni	High frequency	90	100	16	—	—	40	500
	Permalloy 45	45 Ni		2 700	23 000	16.5	8	0.3	45	440
	Allegheny 4750	47 to 50 Ni		9 000	50 000	16	6.2†	0.08†	52	430
	Armco 48	48 Ni	Combine good	—	—	16	—	—	—	—
	Nicaloi	49 Ni	permeability	—	—	16	—	—	—	—
	High Perm 49	49 Ni	and flux	5 000	50 000	16	6.5	0.03	43	475
	Hipernik	50 Ni, Si, Mn	density	4 000	100 000	16	8†	0.03†	45	500
	Monimax	47 Ni, 3 Mo		2 000	38 000	15	—	0.06	80	390
	Sinimax	42 Ni, 3 Si	High resistivity	3 500	30 000	11	—	0.1	90	290

	Permenorm 5000Z Permenite Deltamax Hypernik *V* Orthonik Orthonol	45 to 50 Ni		400 to 1 700	40 000 to 100 000	15.5 to 16	13 to 15	0.2 to 0.4	40 to 50	450 to 500
	Permalloy 65	65 to 68 Ni	Rectangular hysteresis loop	1 500	250 000 to 600 000	13	13	0.03	20	600
	Alloy 1040	72 Ni, 14 Cu, 3 Mo		40 000	100 000	6	2.5	0.02	55	290
	Mumetal	77 Ni, 5 Cu, 2 Cr		20 000	100 000	8	6	0.05	60	400
	Permalloy 78	78 Ni, 0.6 Mn		9 000	100 000	10.7	6	0.05	16	580
	Mo-Permalloy 4–79	79 Ni, 4 Mo		20 000	75 000	8	5.5	0.05	55	—
	Supermalloy	79 Ni, 5 Mo	Highest permeability, low saturation	55 000 to 150 000	500 000 to 1 000 000	6.8 to 7.8	—	0.002 to 0.05	65	400
	Hymu 80	80 Ni		10 000	100 000	8	—	0.06	58	460
Ferrites‡	3C3	MnZi	High-frequency transformers	2 200±20%		4.6	3.5	0.1	60×10^6	150
	3B7 and 3B9	MnZi	High-*Q* coils	2 300±20%		4.6	3.0	0.2	100×10^6	170
	3D3	NiZi	High-frequency	750±20%		4.7	3.0	0.5	150×10^6	150
	4C4	NiZi	High-*Q* coils	125±20%		4.1	2.0	4.5	10×10^9	300

* Reprinted by permission from S. R. Hoh, "Evaluation of High-Performance Core Materials (Part 1)," *Tele-Tech and Electronic Industries*, vol. 12, pp. 86–89, 154–156; October 1953.

† $B_m = 10\,000$ gauss.

‡ Data furnished by Ferroxcube Corporation of America, Saugerties, N.Y.

Note 1—The table shows characteristics as listed by the manufacturers. The parameters of different lots of material may vary considerably from the above values. In the cases of residual induction and coercive force, the difference may amount to 50 percent.

Note 2—For information on ferrite materials, see Table 23 in Chapter 4, Properties of Materials.

lamination and core size from the manufacturer's data book that will nearly meet the space requirements, and provide core area for a flux density B_m not to exceed the values shown in Table 1. Further information on available core materials is given in Table 5.

(D) Compute the primary turns N_p from the transformer equation

$$N_p = \frac{3.49E_p \times 10^6}{fA_cB_m}$$

with A_c in square inches and B_m in gauss. Then the secondary turns

$$N_s = 1.05(E_s/E_p)N_p$$

(this allows 5 percent for IR drop of windings).

(E) Calculate the number of turns per layer that can be placed in the lamination window space deducting from the latter the margin space given in Table 6 (see also Fig. 3).

(F) From (D) and (E) compute the number of layers n_l for each winding. Use interlayer insu

TABLE 6—WIRE TABLE FOR TRANSFORMER DESIGN. The resistance R_T at any temperature T is given by $R_T = (234.5+T)/(234.5+t) \times r$, where t = reference temperature of winding, and r = resistance of winding at temperature t, all in degrees Celsius. Additional data on wire will be found in Chapter 4, Properties of Materials, and Chapter 6, Fundamentals of Networks.

AWG B & S Gauge	Diameter in Inches			Turns per Inch (Formvar)	Space Factor	Ohms per 1000 Ft†	Pounds per 1000 Ft	Margin m in Inches	Interlayer Insulation Thickness t(in.)‡
	Bare	Single Formvar*	Double Formvar						
10	0.1019	0.1039	0.1055	8	90	0.9989	31.43	0.25	0.010K
11	0.0907	0.0927	0.0942	9	90	1.260	24.92	0.25	0.010K
12	0.0808	0.0827	0.0842	10	90	1.588	19.77	0.25	0.010K
13	0.0719	0.0738	0.0753	12	90	2.003	15.68	0.25	0.010K
14	0.0641	0.0659	0.0673	13	90	2.525	12.43	0.25	0.010K
15	0.0571	0.0588	0.0602	15	90	3.184	9.858	0.25	0.010K
16	0.0508	0.0524	0.0538	17	90	4.016	7.818	0.1875	0.010K
17	0.0453	0.0469	0.0482	19	90	5.064	6.200	0.1875	0.007K
18	0.0403	0.0418	0.0431	21	90	6.385	4.917	0.1875	0.007K
19	0.0359	0.0374	0.0386	23	90	8.051	3.899	0.1562	0.007K
20	0.0320	0.0334	0.0346	26	90	10.15	3.092	0.1562	0.005K
21	0.0285	0.0299	0.0310	30	90	12.80	2.452	0.1562	0.005K
22	0.0253	0.0266	0.0277	33	90	16.14	1.945	0.125	0.003K
23	0.0226	0.0239	0.0249	37	90	20.36	1.542	0.125	0.003K
24	0.0201	0.0213	0.0223	42	90	25.67	1.223	0.125	0.002G
25	0.0179	0.0190	0.0200	47	90	32.37	0.9699	0.125	0.002G
26	0.0159	0.0169	0.0179	52	89	40.81	0.7692	0.125	0.002G
27	0.0142	0.0152	0.0161	57	89	51.47	0.6100	0.125	0.002G
28	0.0126	0.0135	0.0145	64	89	64.90	0.4837	0.125	0.0015G
29	0.0113	0.0122	0.0131	71	89	81.83	0.3836	0.125	0.0015G
30	0.0100	0.0109	0.0116	80	89	103.2	0.3042	0.125	0.0015G
31	0.0089	0.0097	0.0104	88	88	130.1	0.2413	0.125	0.0015G
32	0.0080	0.0088	0.0094	98	88	164.1	0.1913	0.0937	0.0013G
33	0.0071	0.0079	0.0084	110	88	206.9	0.1517	0.0937	0.0013G
34	0.0063	0.0070	0.0075	124	88	260.9	0.1203	0.0937	0.001G
35	0.0056	0.0062	0.0067	140	88	329.0	0.0954	0.0937	0.001G
36	0.0050	0.0056	0.0060	155	87	414.8	0.0757	0.0937	0.001G
37	0.0045	0.0050	0.0054	170	87	523.1	0.0600	0.0937	0.001G
38	0.0040	0.0045	0.0048	193	87	659.6	0.0476	0.0625	0.001G
39	0.0035	0.0040	0.0042	215	86	831.8	0.0377	0.0625	0.0007G
40	0.0031	0.0036	0.0038	239	86	1049	0.0299	0.0625	0.0007G

* Dimensions very nearly the same as for enamelled wire.

† Values are at 20 degrees Celsius.

‡ K = kraft paper, G = glassine.

lation of thickness t as given in Table 6, except that the voltage stress should be limited to 40 volts/mil.

(G) Calculate the coil-build a

$$a=1.1[n_l(D+t)-t+t_c]$$

for each winding from (B) and (F), where D= diameter of insulated wire, and t_c= thickness of insulation under and over the winding; the numeric 1.1 allows for a 10-percent bulge factor. The total coil-build should not exceed 85–90 percent of the window width. (Note: Insulation over the core may vary from 0.025 to 0.050 inch for core-builds of $\frac{1}{2}$ to 2 inches.)

(H) Compute the mean length per turn (MLT), of each winding, from the geometry of core and windings as shown in Fig. 4. Compute length of each winding N(MLT).

$$(\text{MLT})_1=2(r+J)+2(s+J)+\pi a_1$$

$$(\text{MLT})_2=2(r+J)+2(s+J)+\pi(2a_1+a_2)$$

where a_1= build of first winding, a_2= build of second winding, J= thickness of winding form, and r,s= winding-form dimensions.

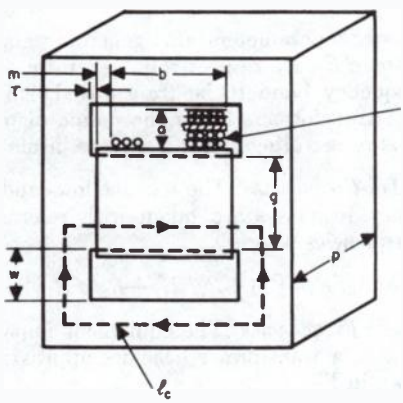

Fig. 3—Dimensions relating to the design of a transformer coil-build and core.

A_c = core area = $(gp)k$
a = height of coil
= coil-build
b = coil width
g = width of lamination tongue
l_c = average length of magnetic-flux path
k = stacking factor
≈0.90 for 14-mil lamination
≈0.80 for 2-mil lamination or ribbon-wound core
m = marginal space given in Table 6
p = height of lamination stack
t = thickness of interlayer insulation
w = width of core window
τ = window length tolerance
= 1/16 inch, total.

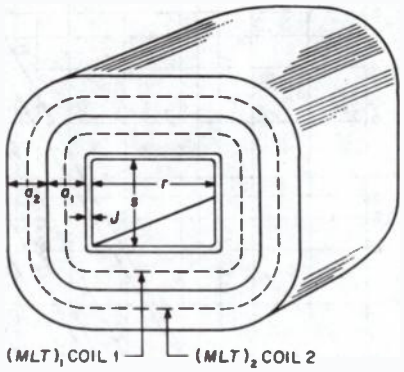

Fig. 4—Dimensions relating to coil mean length of turn (MLT).

(I) Calculate the resistance of each winding from (H) and Table 6 and determine IR drop and I^2R loss for each winding.

(J) Make corrections, if required, in the number of turns of the windings to allow for the IR drops, so as to have the required E_s.

$$E_s=(E_p-I_pR_p)N_s/N_p-I_sR_s.$$

(K) Compute core losses from weight of core and Table 1 or Fig. 5.

(L) Determine the percent efficiency η and voltage regulation (vr) from

$$\eta=\frac{W_{\text{out}}\times 100}{W_{\text{out}}+(\text{core loss})+(\text{copper loss})}$$

$$(\text{vr})=\frac{I_s[R_s+(N_s/N_p)^2R_p]}{E_s}.$$

(M) For a more accurate evaluation of voltage regulation, determine leakage-reactance drop= $I_{dc}\omega l_{sc}/2\pi$, and add to the above (vr) the value of $(I_{dc}\omega l_{sc})/2\pi E_{dc}$. Here, l_{sc}= leakage inductance viewed from the secondary; see "Methods of Winding Transformers" (in this chapter) to evaluate l_{sc}.

(N) Bring out all terminal leads using the wire of the coil, insulated with suitable sleevings, for all sizes of wire heavier than 21; and by using 7-30 stranded and insulated wire for smaller sizes.

Effect of Power Frequency on Design

Design procedure is similar to that described above for 60-hertz transformers except for the flux density at which the core is operated. Operation at lower frequencies requires a larger core (see equation in paragraph (C) above) although reduction of core loss partly compensates the size

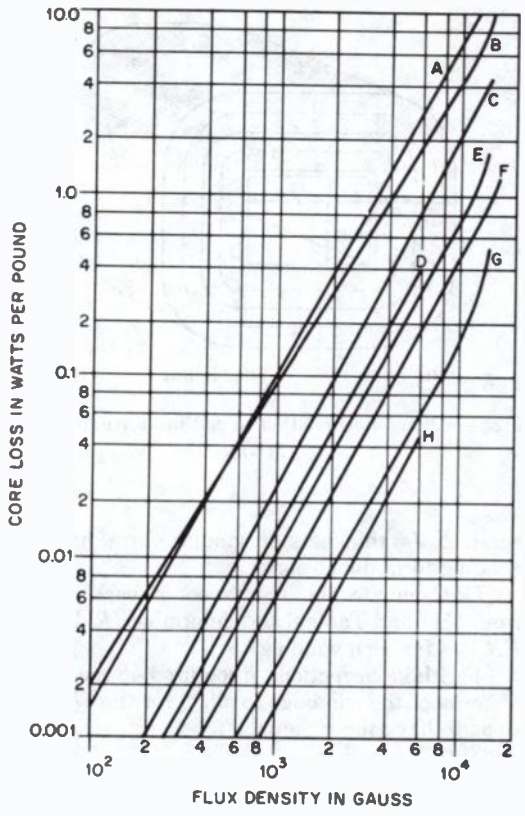

Fig. 5—Core loss characteristics.

A–400-hertz 0.014-inch grain-oriented silicon.
B–400-hertz 0.004-inch grain-oriented silicon.
C–400-hertz 0.006-inch low nickel.
D–400-hertz 0.006-inch high nickel.
E–60-hertz 0.014-inch 4% silicon.
F–60-hertz 0.012-inch grain-oriented silicon.
G–60-hertz 0.014-inch low nickel.
H–60-hertz 0.014-inch high nickel.

increase. As an example, a 25-hertz transformer is approximately twice as large as its 60-hertz equivalent.

Effect of Duty Cycle on Design

If a transformer is operated at different loads according to a regular duty cycle, the equivalent volt-ampere (VA) rating is

$$(\mathrm{VA})_{eq} = \left[\frac{(\mathrm{VA})_1^2 t_1 + (\mathrm{VA})_2^2 t_2 + (\mathrm{VA})_3^2 t_3 + \cdots (\mathrm{VA})_n^2 t_n}{t_1 + t_2 + t_3 + \cdots t_n}\right]^{1/2}$$

where $(\mathrm{VA})_1$ = output during time (t_1), etc.

Example: 5 kilovolt-ampere output, 1 minute on, 1 minute off.

$$(\mathrm{VA})_{eq} = \left[\frac{(5000)^2(1)+(0)^2(1)}{1+1}\right]^{1/2} = \left[\frac{(5000)^2}{2}\right]^{1/2}$$

$$= 5000/(2)^{1/2} = 3535 \text{ volt-amperes.}$$

AUDIO-FREQUENCY TRANSFORMERS

Audio-frequency transformers are used mainly for matching impedances and transmitting audio frequencies. They also provide isolation from direct currents and present balanced impedances to lines or circuits.

The magnetic core for this type of transformer is usually an E–I type using either audio-grade silicon steel or nickel-alloy steel (refer to Table 5). High-permeability nickel-alloy tape cores in toroidal form are used for extreme bandwidths.

DESIGN OF AUDIO-FREQUENCY TRANSFORMERS

Important parameters are: generator and load impedances R_g, R_l, respectively, generator voltage E_g, frequency band to be transmitted, efficiency (output transformers only), harmonic distortion, and operating voltages (for adequate insulation).

At Mid-Frequencies: The relative low- and high-frequency responses are taken with reference to mid-frequencies where

$$aE_{out}/E_g = [(1+R_s/R_l)+R_l/a^2R_l]^{-1}.$$

At Low Frequencies: The equivalent unity-ratio network of a transformer becomes approximately as shown in Fig. 6.

$$\text{Amplitude} = 1/[1+(R'_{par}/X_m)^2]^{1/2}$$

$$\text{Phase angle} = \tan^{-1}(R'_{par}/X_m)$$

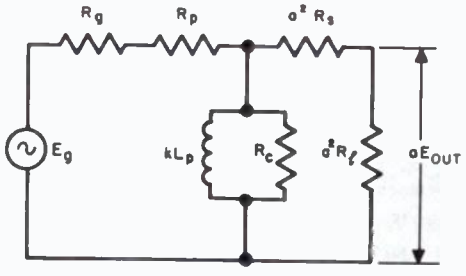

Fig. 6—Equivalent network of an audio-frequency transformer at low frequencies. $R_1 = R_g + R_p$, and $R_2 = R_s + R_l$. In a good output transformer, R_p, R_s, and R_c may be neglected. In input or interstage transformers, R_c may be omitted.

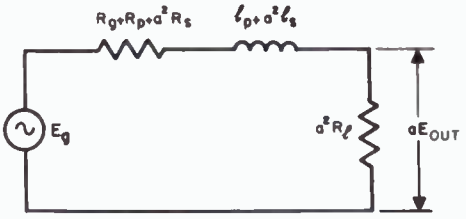

Fig. 7—Equivalent network of an audio-frequency transformer at high frequencies, neglecting the effect of the winding shunt capacitances.

where

$$R'_{par}=(R_1R_2a^2)/(R_1+R_2a^2), \quad R_1=R_g+R_p,$$

$$R_2=R_l+R_s, \quad X_m=2\pi fL_p.$$

At High Frequencies: Neglecting the effect of winding and other capacitances (as in low-impedance-level output transformers), the equivalent unity-ratio network becomes approximately as in Fig. 7.

$$\text{Amplitude}=[1+(X_l/R'_{se})^2]^{-1/2}$$

$$\text{Phase angle}=\tan^{-1}(X_l/R'_{se})$$

where

$$R'_{se}=R_1+R_2a^2, \qquad X_l=2\pi fl_{scp},$$

and l_{scp} = inductance measured across primary with secondary short-circuited $=l_p+a^2l_s$.

These low- and high-frequency responses are shown on the curves of Fig. 8.

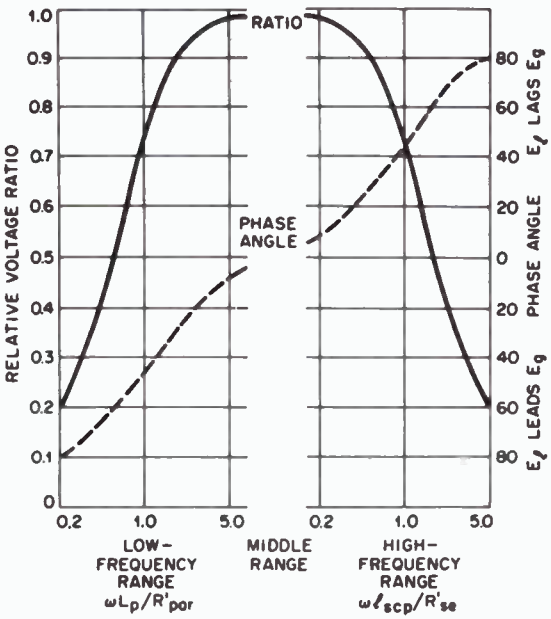

Fig. 8—Universal frequency and phase response of output transformers. *Courtesy McGraw-Hill Publishing Co.*

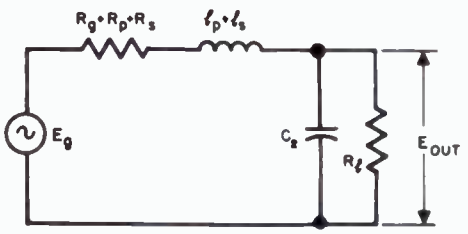

Fig. 9—Equivalent network of a 1:1-turns-ratio audio-frequency transformer at high frequencies when effect of winding shunt capacitances is appreciable. In a step-up transformer, C_2 = equivalent shunt capacitances of both windings. In a step-down transformer, C_2 shunts both leakage inductances and R_2.

If at high frequencies the effect of winding and other capacitances is appreciable, the equivalent network on a 1:1-turns-ratio basis becomes as shown in Fig. 9. The relative high-frequency response of this network is given by

$$\frac{(R_1+R_2)/R_2}{[(R_1/X_c+X_l/R_l)^2+(X_l/X_c-R_g/R_l-1)^2]^{1/2}}.$$

This high-frequency response is plotted in Figs. 10 and 11 for $R_1=R_2$ (matched impedances), and $R_2=\infty$ (input and interstage transformers) based on simplified equivalent networks as indicated.

Harmonic distortion requirements may constitute a deciding factor in the design of transformers. Such distortion is caused by either variations in load impedance or nonlinearity of magnetizing current. The percent harmonic voltage appearing in the output of a loaded transformer is given by

$$\text{(percent harmonics)} = E_h/E_f=I_h/I_f(R'_{par}/X_m)[1-(R'_{par}/4X_m)]$$

where $100I_h/I_f$ = percent of harmonic current measured with zero-impedance source (values in Table 7 are for 4-percent silicon-steel core).*

TABLE 7—HARMONICS PRODUCED BY VARIOUS FLUX DENSITIES B_m IN A 4-PERCENT SILICON-STEEL-CORE AUDIO TRANSFORMER.

B_m	Percent 3rd Harmonic	Percent 5th Harmonic
100	4	1.0
500	7	1.5
1 000	9	2.0
3 000	15	2.5
5 000	20	3.0
10 000	30	5.0

* N. Partridge, "Harmonic Distortion in Audio-Frequency Transformers," *Wireless Engineer*, vol. 19; September, October, and November, 1942.

Insertion Loss: Loss introduced in circuit by addition of transformer. At midband, loss is caused by winding resistance and core loss. Frequency discrimination adds to this at low and high frequencies. Insertion loss is input divided by output expressed in decibels or (in terms of measured voltages and impedance)

$$(\text{dB insertion loss}) = 10 \log[(E_g^2 R_l)/(4E_0^2 R_g)].$$

Impedance Match: For maximum power transfer, the reflected load impedance should equal the generator impedance. Winding resistance should be included in this calculation: For matching

$$R_g = a^2(R_l + R_e) + R_p.$$

Also, in a properly matched transformer

$$R_g = a^2 R_l = (Z_{oc} \times Z_{sc})^{1/2}$$

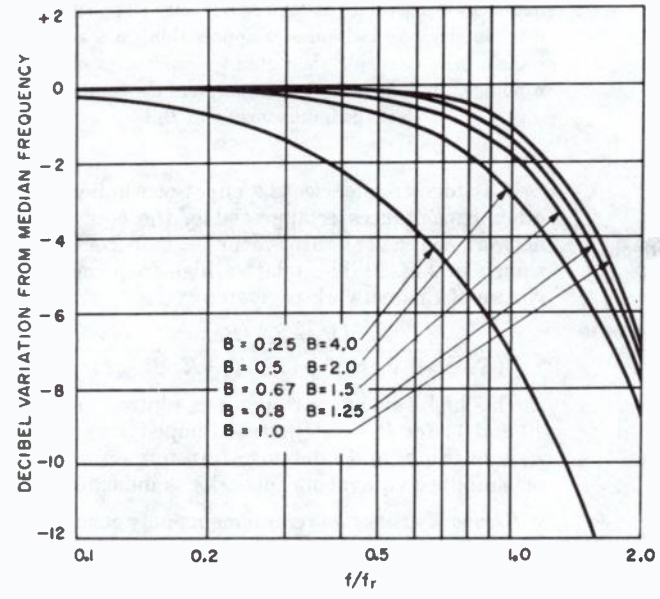

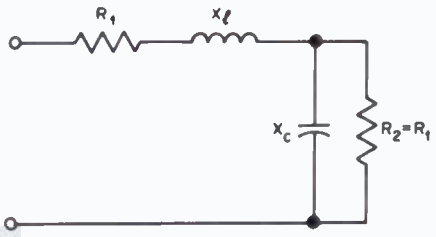

Fig. 10—Transformer characteristics at high frequencies for matched impedances. At frequency f_r, $X_l = X_c$ and $B = X_c/R_1$. *Reprinted from "Electronic Transformers and Circuits," by R. Lee, 2nd ed., p. 151, 1955; by permission, John Wiley & Sons, New York.*

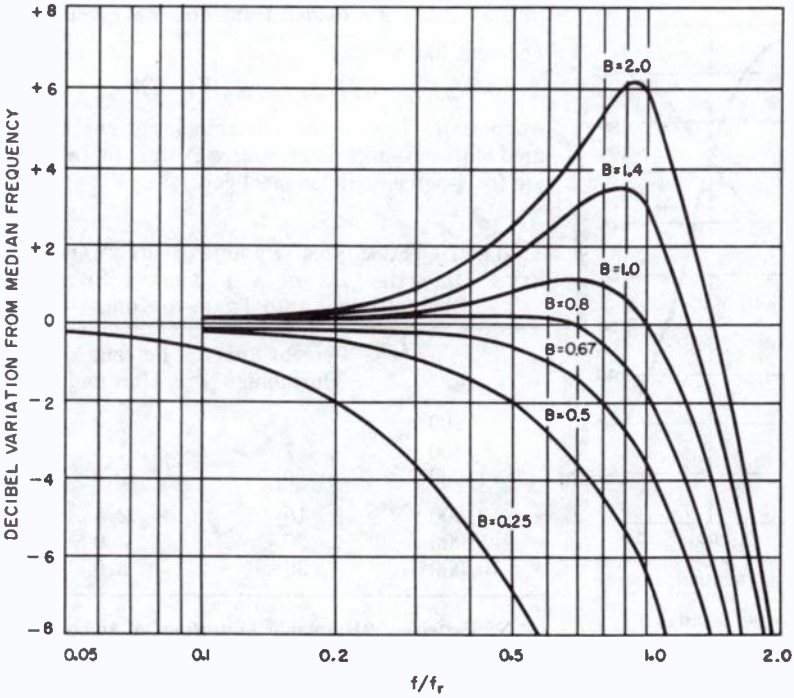

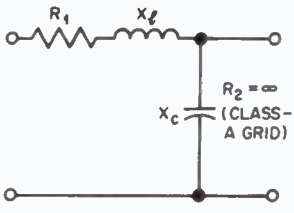

Fig. 11—Input- or interstage-transformer characteristics at high frequencies. At f_r, $X_l = X_c$ and $B = X_c/R_1$. *Reprinted from "Electronic Transformers and Circuits," by R. Lee, 2nd ed., p. 153, 1955; by permission, John Wiley & Sons, New York.*

where Z_{oc} = transformer primary open-circuit impedance, and Z_{sc} = transformer primary impedance with secondary winding short-circuited.

If more than one secondary is used, the turns ratio to match impedances properly depends on the power delivered from each winding.

$$N_s/N_p = (R_n/R_g \times W_n/W_p)^{1/2}.$$

Example: Using Fig. 12

$$N_2/N_p = (10/600 \times 10/16)^{1/2} = 0.102$$

$$N_3/N_p = (50/600 \times 5/16)^{1/2} = 0.161$$

$$N_4/N_p = (100/600 \times 1/16)^{1/2} = 0.102.$$

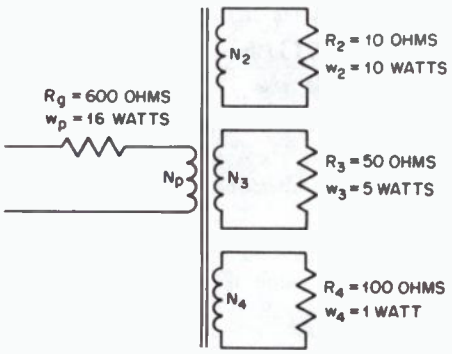

Fig. 12—Multisecondary audio transformer.

Example of Audio-Output-Transformer Design

This transformer is to operate from a 4000-ohm impedance; to deliver 5 watts to a matched load of 10 ohms; to transmit frequencies of 60 to 15 000 hertz with a V_{out}/V_{in} ratio of 71 percent of that at mid-frequencies (400 hertz); and the harmonic distortion is to be less than 2 percent. (See Figs. 6 and 7.)

(A) We have

$$E_s = (W_{out}R_l)^{1/2} = 7.1 \text{ volts}$$

$$I_s = W_{out}/E_s = 0.7 \text{ ampere}$$

$$a = (R_g/R_l)^{1/2} = 20.$$

Then

$I_p \approx 1.1 I_s/a = 0.039$ ampere, and $E_p \approx 1.1 a E_s = 156$.

(B) To evaluate the required primary inductance to transmit the lowest frequency of 60 hertz, determine

$$R'_{se} = R_1 + a^2R_2 \text{ and } R'_{par} = (R_1R_2a^2)/(R_1+R_2a^2)$$

where $R_1 = R_g + R_p$, and $R_2 = R_l + R_s$. We choose winding resistances $R_s = R_p/a^2 \approx 0.05R_l = 0.5$ (for a copper efficiency $= R_l a^2 \times 100/[(R_l+R_s)a^2+R_p] =$ 91 percent). Then $R'_{se} = 2R_1 = 8400$ ohms, and $R'_{par} = R_1/2 = 2100$ ohms.

(C) To meet the frequency-response requirements, we must have according to Fig. 8

$$\omega_{low}L_p/R'_{par} = 1 = \omega_{high}l_{scp}/R'_{se}$$

which yield $L_p \approx 5.6$ henries and $l_{scp} = 0.089$ henry.

(D) Harmonic distortion is usually a more important factor in determining the minimum inductance of output transformers than is the attenuation requirement at low frequencies. Compute now the number of turns and inductance for an assumed $B_m = 5000$ for 4-percent silicon-steel core with type EI-12 punchings in square stack. From manufacturer's catalog, A_c(net) = 0.90 inch^2, and $l_c = 6.0$ inches. From Fig. 13, $\mu_{ac} \approx 5000$.

$$N_p = \frac{3.49E_p \times 10^6}{fA_cB_m} = 2020$$

$$N_s = 1.1N_p/a = 111$$

$$L_p \approx \frac{3.19N_p^2\mu_{ac}A_c}{l_c} \times 10^{-8} = 97 \text{ henries.}$$

At 60 hertz, $X_m = \omega L_p = 36\,600$, and $R'_{par}/X_m \approx 0.06$. From values of I_h/I_f for 4-percent silicon steel (Table 7)

$$E_h/E_f = (I_h/I_f)(R'_{par}/X_m)[1-(R'_{par}/4X_m)]$$

$$\approx 0.012 \text{ or } 1.2 \text{ percent.}$$

(E) Now see if core window is large enough to fit windings. Assuming a simple method of winding (secondary over the primary), compute from

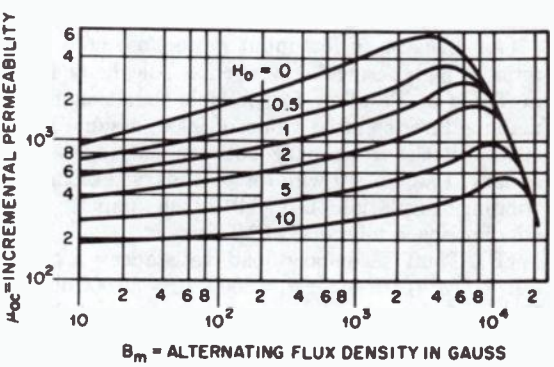

Fig. 13—Incremental permeability μ_{ac} characteristics of Allegheny audio-transformer "A" sheet steel at 60 hertz. No. 29 US gauge, L-7 standard laminations stacked 100 percent, interleaved. This is 4-percent silicon-steel core material. H_0 = magnetizing field in oersteds. *Courtesy of Allegheny-Ludlum Corp., Pittsburgh, Pa.*

geometry of core the approximate (MLT) for each winding (Fig. 4).

For the primary, (MLT)≈0.42 foot and

$$N_p(\text{MLT})\approx 850 \text{ feet.}$$

For the secondary, (MLT)≈0.58 foot and

$$N_s(\text{MLT})\approx 65 \text{ feet.}$$

For the primary, then, the size of wire is obtained from $R_p/N_p(\text{MLT})=0.236$ ohm/foot; and from Table 6, use No. 33. For the secondary, $R_s/N_s(\text{MLT})\approx 0.008$, and size of wire is No. 18.

(F) Compute the turns/layer, number of layers, and total coil-build, as for power transformers. For an efficient design, (total coil-build)≈(0.85 to 0.90)×(window width).

(G) To determine if leakage inductance is within the required limit of (C) above, evaluate

$$l_{\text{scp}}=\frac{10.6N_p^2(\text{MLT})\,(2nc+a)}{n^2b\times 10^9}=0.036 \text{ henry}$$

which is less than the limit 0.089 henry of (C). The symbols of this equation are defined in Fig. 17. If leakage inductance is high, interleave windings as indicated in the section on methods of winding transformers.

Example of Audio-Input-Transformer Design

This transformer must couple a 500-ohm line to the grids of 2 tubes in class-A push–pull. Attenuation to be flat to 0.5 decibel over 100 to 15 000 hertz; step-up = 1:10; and input to primary is 2 volts.

(A) Because of low input power, use core material of high permeability, such as Allegheny 4750 in Table 5. To allow for possible variation from manufacturer's stated value of 9000, assume $\mu_0=4000$. Interleave primary between halves of secondary. Use No. 40 wire for secondary. For interwinding insulation use 0.010-inch paper. Use winding-space tolerance of 10 percent.

(B) Total secondary load resistance $=R'_{\text{par}}=a^2R_1R_2/(a^2R_1+R_2)\approx a^2R_1=500\times 10^2=50\,000$ ohms. From universal-frequency-response curves of Fig. 8 for 0.5-decibel down at 100 hertz (voltage ratio = 0.95)

$$(\omega_{\text{low}}L_s)/R'_{\text{par}}=3, \text{ or } L_s\approx 240 \text{ henries.}$$

(C) Try Allegheny type EI-68 punchings, square stack. From manufacturer's catalog, $A_c=0.473$ inch^2, $l_c=4.13$ inches, and window dimensions = $1\frac{1}{32}\times 1\frac{1}{32}$ inches, interleaved singly; $l_g=0.0002$ inch. From

$$L=\frac{3.19N^2A_c}{l_g+l_c/\mu_0}\times 10^{-8}$$

and above constants, compute

$$N_s=4400$$

$$N_p=N_s/a=440.$$

(D) Choose size of wire for primary winding, so that $R_p\approx 0.1R_g=50$ ohms. From geometry of core, (MLT)≈0.29 foot; also, $R_p/N_p(\text{MLT})=0.392$, or No. 35 wire ($D=0.0062$ for No. 35F).

(E) Turns per layer of primary $=0.9b/d=110$; number of layers $n_p=N_p/110=4$; turns per layer of secondary $0.9b/d=200$; number of layers $n_s=N_s/200=22$.

(F) Secondary leakage inductance

$$l_{\text{scs}}=\frac{10.6N_s^2(\text{MLT})\,(2nc+a)\times 10^{-9}}{n^2b}=0.35 \text{ henry.}$$

(G) Secondary effective layer-to-layer capacitance

$$C_e=(4C_l/3n_l)\,(1-n_l^{-1})$$

where $C_l=0.225A\epsilon/t=1770$ picofarads (refer to section on methods of winding transformers). Substituting this value of C_l into above expression of C_e, we find

$$C_e=107 \text{ picofarads.}$$

(H) Winding-to-core capacitance $=0.225A\epsilon/t\approx 63$ picofarads (using 0.030-inch insulation between winding and core). Assuming tube and stray capacitances total 30 picofarads, total secondary capacitance $C_s\approx 200$ picofarads.

(I) Series-resonance frequency of l_{sc} and C_s is

$$f_r=1/2\pi(l_{\text{sc}}C_s)^{1/2}=19\,200 \text{ hertz.}$$

At f_r, $B=X_c/R_1=1/2\pi f_rC_sR_1=0.83$; at 15 000 hertz, $f/f_r=0.78$. From Fig. 10, decibel variation from median frequency is seen to be less than 0.5.

If it is required to extend the frequency range, use Mumetal core material for its higher μ_0 (20 000). This will reduce the primary turns, the leakage inductance, and the winding shunt capacitance.

Considerations in Audio-Frequency-Transformer Design

Using modifications of the design procedures just described, it is possible to design the following types of transformers:

Modulation
Driver
Class-A output
Class-B output
Push–pull output

For further information consult R. Lee, "Electronic Transformers and Circuits," 2nd edition, John Wiley & Sons, New York; 1955.

HIGH-FREQUENCY TRANSFORMERS

High-frequency transformers are categorized by continuous-wave excitation over a broad band of frequencies to differentiate them from tuned transformers and pulse transformers. Their application is principally in the telephone carrier range limited to 1 megahertz. Their function is primarily the same as for audio-frequency transformers.

The principles discussed in the section on audio-frequency transformers can be used for designing high-frequency transformers, but the core materials, leakage inductance, and winding capacitance become more critical. Generally the smaller a transformer can be made and still meet the low-frequency requirements, the better the transformer will operate at high frequency.

Because of the high resistivity and permeability of ferrites, E-I or pot cores of this material (Table 5) are generally used.

For more-detailed information consult R. Lee, "Electronic Transformers and Circuits." 2nd edition, John Wiley & Sons, New York; 1955.

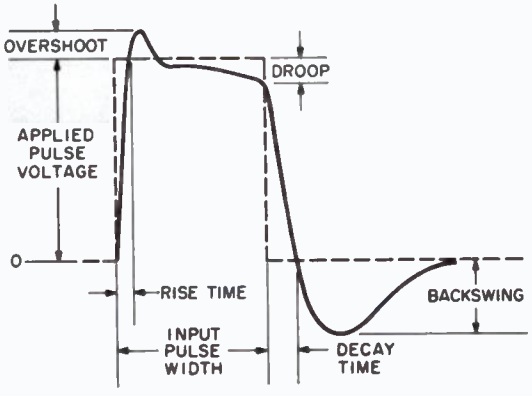

Fig. 14—Output pulse shape. In the strictest sense, pulse rise and decay times are measured between the 10- and 90-percent values; width is measured between the 50-percent values.

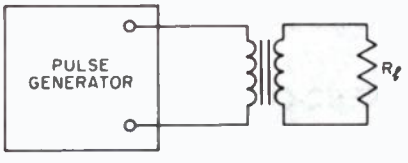

Fig. 15—Pulse-transformer circuit.

PULSE TRANSFORMERS

Pulse transformers are designed to transmit square waves or trains of pulses while maintaining as closely as possible the original shape (refer to the section on pulse modulation in Chapter 23). Fourier analysis shows that such pulse waveforms consist of a wide range of frequency components. Thus the transformer must have suitable bandwidth to maintain fidelity.

Pulse transformers can be analyzed by considering the leading edge, top, and trailing edge of the pulse separately. Figure 14 portrays a typical transformer output pulse compared with input pulse. Figure 15 shows the fundamental circuit, and Fig. 16 illustrates equivalent circuits for the various transient conditions.

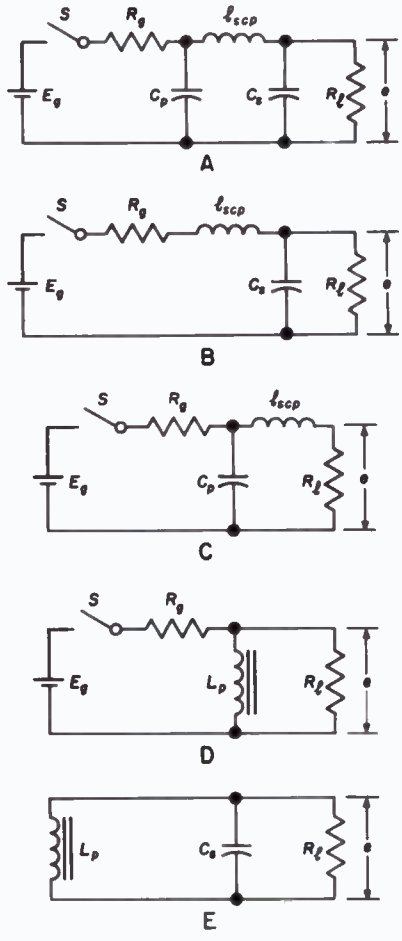

Fig. 16—Pulse-transformer equivalent circuits. A–Leading-edge equivalent circuit. B–Leading-edge equivalent circuit for step-up-ratio transformer. C–Leading-edge equivalent circuit for step-down-ratio transformer. D–Top-of-pulse equivalent circuit. E–Trailing-edge equivalent circuit.

Leading-edge reproduction requires transmission of a wide band of frequencies and is controlled by leakage inductance l_{scp} and winding capacitances C_p and C_s as indicated in Fig. 16A, B, and C. Analysis for step-up and step-down transformers varies slightly as shown. Leakage inductance and winding capacitance must be minimized to achieve a sharp rise; however, output voltage may overshoot input voltage and oscillation may be encountered where very abrupt rise times are involved.

Pulse-top response depends on the magnitude of the open-circuit inductance of the transformer, as indicated in Fig. 16D. The greater the inductance L_p, the smaller the droop from input voltage level.

Control of the trailing edge of the pulse depends on the open-circuit inductance and secondary winding capacitance, as shown in Fig. 16E. The lower the capacitance, the faster the rate of voltage decay. Negative backswing depends on the magnitude of the transformer magnetizing current. The greater the magnetizing current, the greater the backswing.

Pulse-transformer design involves analysis of transient effects and thus direct solution is complex. Empirical or graphical solution* is usually used.

Low-loss core materials such as grain-oriented silicon-steel loop cores or nickel-iron alloys in 2-mil thickness are normally used. Small air gaps are commonly used to reduce remanent magnetism in core due to unidirectional pulses. Windings are normally interleaved to reduce leakage reactance. If load impedance is high, single-layer primary and secondary windings are best; if low, interleaved windings are best.

METHODS OF WINDING TRANSFORMERS

The most common methods of winding transformers are shown in Fig. 17. Leakage inductance is reduced by interleaving, i.e., by dividing the primary or secondary coil into two sections and placing the other winding between the two sections. Interleaving may be accomplished by concentric and by coaxial windings, as shown in Fig. 17B and C; reduction of leakage inductance is computed from

$$l_{sc} = \frac{10.6N^2(\mathrm{MLT})(2nc+a)}{n^2b\times 10^9} \text{ henries}$$

with dimensions in inches to be the same for Fig. 17B and C.

* R. Lee, "Electronic Transformers and Circuits," 2nd edition, John Wiley & Sons, New York; 1955: chapter 10, p. 292.

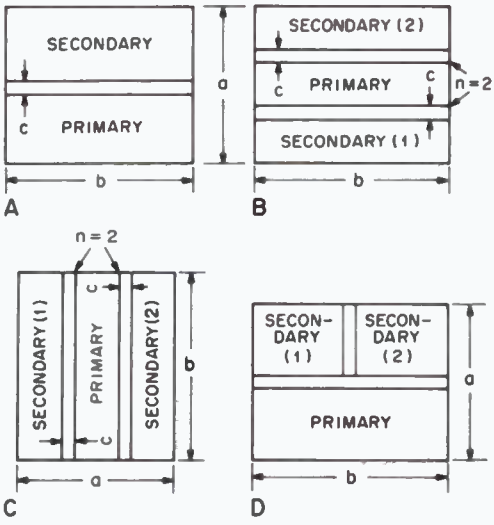

Fig. 17—Methods of winding transformers.

Means of reducing leakage inductance are:

(A) Minimize turns by using high-permeability core.
(B) Reduce build of coil.
(C) Increase winding width.
(D) Minimize spacing between windings.
(E) Use bifilar windings.

Means of minimizing capacitance are:

(A) Increase dielectric thickness t.
(B) Reduce winding width b and thus area A.
(C) Increase number of layers.
(D) Avoid large potential differences between winding sections, as the effect of capacitance is proportional to applied potential squared.

Note: Leakage inductance and capacitance requirements must be compromised in practice since corrective measures are opposites.

Effective interlayer capacitance of a winding may be reduced by sectionalizing it as shown in Fig. 17D. This can be seen from

$$C_e = (4C_l/3n_l)(1-1/n_l) \text{ picofarads}$$

where n_l = number of layers, C_l = capacitance of one layer to another = $0.225A\epsilon/t$ picofarads, A = area of winding layer = $(\mathrm{MLT})b$ inches^2, t = thickness of interlayer insulation in inches and ϵ = dielectric constant ≈ 3 for paper.

MAGNETIC-CORE REACTORS

Magnetic-core reactors basically fall into two categories: rectifier filter reactors and audio filter reactors. The rectifier filter reactor is used mainly

in direct-current power supplies to smooth the output ripple voltage. (Refer to Chapter 14.) It carries all the direct current of the rectifier filter and must be designed not to saturate with direct current in the reactor winding. Audio filter reactors (sometimes called coils) are used principally in audio filters to provide the necessary inductance with relatively high quality factor Q. (Refer to Chapter 8.) The term "audio" filter reactor is used to differentiate it from "rectifier" filter reactor; its applications are not restricted to audio frequencies but extend into the megahertz range.

Rectifier Filter Reactors

This type of reactor must be made relatively large, depending on the inductance and direct current. Consequently the core is usually either E-I laminations using 4% silicon steel or type "C" tape core loops using grain-oriented silicon steel.

Design of Rectifier Filter Reactors

These reactors carry direct current and are provided with suitable air gaps. Optimum design data may be obtained from Hanna curves, Fig. 18. These curves relate direct-current energy stored in the core per unit volume, LI_{dc}^2/V to magnetizing field NI_{dc}/l_c (where l_c = average length of flux path in core), for an appropriate air gap. Heating is seldom a factor, but direct-current-resistance requirements affect the design; however, the transformer equivalent volt-ampere ratings of chokes given in Table 8 should be useful in determining

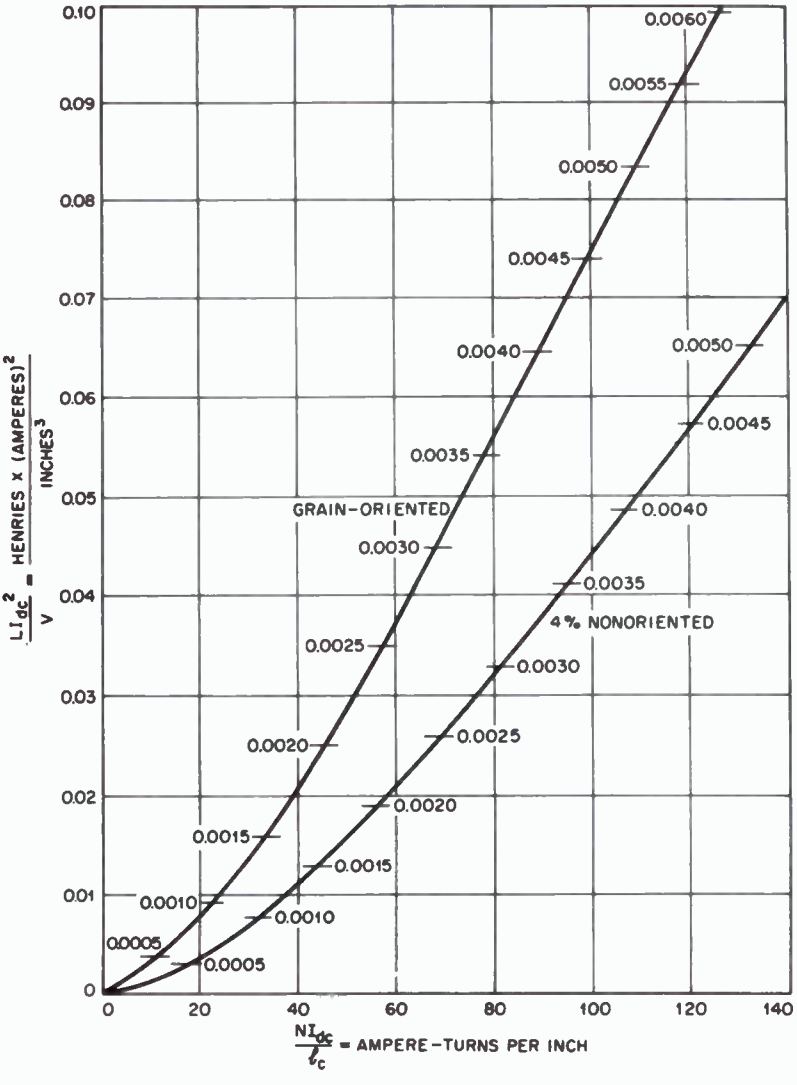

Fig. 18—Hanna curves for silicon steel. The numbers on the curves represent length of air gap l_g/length of flux path l_c, in inches.

TABLE 8—EQUIVALENT LI^2 RATING OF FILTER REACTOR FOR RECTIFIERS. L = inductance in henries, I = direct current in amperes. The rating is based on power supply frequencies up to 400 hertz and 50° C temperature rise above ambient. The LI^2 values should be reduced for lower temperature rises and high-voltage operation.

LI^2*	Current Density* (amps/sq in.)	EI-Type Lamination†	Stack Height p (in.)	Core Volume V (cu in.)	Magnetic Path Length l_c (in.)	Average Copper Mean Length per Turn (MLT) (in.)
0.0195	3200	EI-21	0.5	0.80	3.25	3.12
0.0288	2700	EI-625	0.625	1.45	3.75	3.62
0.067	2560	EI-75	0.75	2.51	4.50	4.33
0.088	2560	EI-75	1.00	3.35	4.50	4.83
0.111	2330	EI-11	0.875	3.88	5.25	5.04
0.200	2130	EI-12	1.00	5.74	6.00	5.71
0.300	2030	EI-12	1.50	8.61	6.00	6.71
0.480	1800	EI-125	1.25	11.4	7.50	7.21
0.675	1770	EI-125	1.75	16.0	7.50	8.21
0.850	1600	EI-13	1.50	19.8	9.00	8.63
1.37	1500	EI-13	2.00	26.4	9.00	9.63
3.70	1200	EI-19	1.75	39.4	13.0	12.8

* From "Radio Components Handbook," Technical Advertising Associates, Cheltenham, Pa.; May 1948: page 92.

† Lamination designation and constants per Allegheny Ludlum Corp., Pittsburgh, Pa.

their sizes. This is based on the empirical relationship $(VA)_{eq} = 188LI_{dc}^2$.

As an example, take the design of a choke that is to have an inductance of 10 henries with a superimposed direct current of 0.225 ampere and a direct-current resistance $\leq$ 125 ohms. This reactor shall be used for suppressing harmonics of 60 hertz, where the alternating-current ripple voltage (2nd harmonic) is about 35 volts.

(A) $LI^2 = 0.51$. Based on data of Table 8, try 4% silicon-steel core, type EI-125 lamination, with a core buildup of 1.5 inches.

(B) From Table 8, $V = (11.4/1.25) \times 1.5 = 13.7$ in.^{3}, $l_c = 7.50$, $LI^2/V = 0.51/13.7 = 0.037$. From Fig. 18, $NI/l_c = 88$ ampere-turns per inch, $N = 88l_c/I = (88 \times 7.5)/0.225 = 2930$ turns. $l_g/l_c = 0.0032$, the length of air gap $l_g = 0.0032 \times 7.5 = 0.024$ inch.

(C) From Table 8, coil (MLT) = (7.21 + 0.5)/12 = 0.643 foot, and length of coil = $N \times$ (MLT) = $2930 \times 0.643 = 1884$ feet. Since the maximum resistance is 125 ohms, the maximum ohms/ft = 125/1884 = 0.0663 or 66.3 ohms/1000 ft. From Table 6, the nearest size of wire is No. 28.

(D) Now see if 2930 turns of No. 28 single-Formex wire will fit in the window space of the core. (Determine turns per layer, number of layers, and coil-build, as explained in the design of power transformers.)

(E) This is an actual coil design; in case lamination window space is too small (or too large), change stack of laminations, or size of laminations, so that the coil meets the electrical requirements, and the total coil-build $\approx$ 0.85 to 0.90 $\times$ (window width).

Note: To allow for manufacturing variations in permeability of cores and resistance of wires, use at least 10-percent tolerance.

Swinging reactors are used where direct current in the rectifier circuit varies. These reactors are designed to saturate under full-load current while providing adequate inductance for filtering. At light-load current, higher inductance is available to perform proper filtering and prevent "capacitor effect."

Equivalent Reactor Size:

$$LI^2 = (L_{max} \times L_{min})^{1/2} I_{dc(max)}^2.$$

The design is similar to that of a normal reactor and is based on meeting both L and I_{dc} extremes. Typical swing in inductance is 4:1 for a current swing of 10:1.

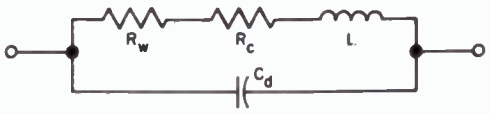

Fig. 19—Equivalent network of an audio filter coil.

L = calculated inductance based on turns and magnetic-core constant
C_d = distributed capacitance of winding
R_w = copper losses in winding
R_c = magnetic-core losses reflected in series with winding
Q = quality factor = $\omega L/(R_w+R_c)$, $\omega = 2\pi f$.

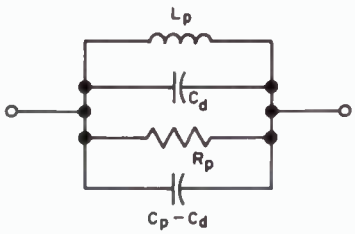

Fig. 20—Parallel tuned mesh.

L_p = equivalent parallel inductance
R_p = equivalent parallel resistance
C_d = distributed capacitance of winding
C_p = parallel tuning capacitance
Q_p = effective parallel Q
$L_p = L$, for $Q > 10$
$R_p = (R_w+R_c)(Q^2+1)$, for $Q_p = Q$.

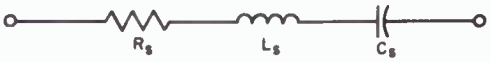

Fig. 21—Series tuned mesh.

L_s = equivalent series inductance
R_s = equivalent series resistance
C_s = series tuning capacitance
Q_s = effective series Q.

For $Q > 10$
$L_s = L/(1-\omega^2 LC_d)$
$R_s = (R_w+R_c)/(1-\omega^2 LC_d)^2$
$Q_s = Q(1-\omega^2 LC_d)$
$L = L_s/(1+\omega^2 L_s C_d)$.

Audio Filter Reactors (Coils)

Audio filter reactors, hereafter referred to as coils, are inductances that have the following qualities:

(A) High quality factor Q.
(B) Stable inductance with variations in frequency, operating level, and temperature.

To design coils having these qualities, it is necessary to understand the equivalent circuit of a coil (Fig. 19) and its application to the parallel tuned mesh (Fig. 20) and series tuned mesh (Fig. 21). The distributed capacitance C_d is very important in series tuned meshes, as it affects both the inductance and the Q. If possible, it is desirable to keep the distributed capacitance C_d to one-tenth of the tuning capacitance C_s. Means of minimizing C_d are discussed in succeeding sections.

R_w represents the copper loss in the coil winding. It is made up of the dc resistance of the wire and the eddy-current losses generated in the winding by stray flux from the core cutting the winding. This eddy-current loss can be minimized at high frequencies by dividing the wire into many small wires. This type of wire is called Litz wire.

R_c represents the loss due to the magnetic core reflected in series with the coil winding. The calculation of this factor is discussed in succeeding sections.

There are three principal types of audio filter coils. Their use is usually dictated by the frequency range of interest and the desired Q. At frequencies below 300 hertz, laminated punchings of nickel–steel alloy usually are used. For frequencies between 300 and 5000 hertz, toroidal permalloy-dust cores are usually used. For frequencies above 5000 hertz, ferrite pot cores are usually used. (Refer to Table 9.)

Audio Filter Coils with Punching Laminated Cores

Externally this coil resembles a transformer. The punchings are usually "F" in shape to create an air gap in the center leg of the core. For high Q, nickel–steel laminations either 14 or 6 mils thick are used (Table 9). An air gap is placed in the core to reduce the effective permeability μ_e, which reduces the effective core losses and stabilizes the inductance.

The winding is usually layer wound as described in the section on methods of winding transformers. The techniques for reducing capacitance described

TABLE 9—CHARACTERISTICS OF SOME CORE MATERIALS FOR AUDIO FILTER COILS.

$R_e/(\mu_0 Lt) = aB_m + c + ef$, where R_e = series resistance in ohms due to core loss.*

Material or Alloy	Initial Permeability (μ_0)	Resistivity (ohm-cm)	Hysteresis Coefficient ($a\times10^6$)	Residual Coefficient ($c\times10^6$)	Eddy-Current Coefficient ($e\times10^9$)	Gauge (mils)	Application and Frequency Range (kilohertz)
4% silicon steel	400	60×10^{-6}	120	75	870	14	Rectifier filters
Low nickel	3 500 to 10 000	44×10^{-6}	0.4	14	1 550	14	Audio filters up to 0.2
					284	6	Audio filters up to 10
High nickel	10 000 to 20 000	57×10^{-6}	0.05	0.05	950	14	Audio filters up to 0.2
					175	6	Audio filters up to 10
Molybdenum permalloy dust	200†	1.0	1.3	40	40	—	Audio filters 0.1–7
	160†	1.0	1.5	38	25	—	Audio filters 0.1–10
	125†	1.0	1.6	30	19	—	Audio filters 0.2–20
	60*	1.0	3.2	50	10	—	Audio filters 5–50
	26*	1.0	6.9	96	7.7	—	Audio filters 15–60
	14*	1.0	11.4	143	7.1	—	Audio filters 40–150
Carbonyl types:							
C	55	—	9	80	7	—	High-frequency filters
P	26	—	3.4	220	27	—	High-frequency filters
Th	16	—	2.5	80	8	—	High-frequency filters
Ferrites‡:							
3B7	2 300	100	§	§	§	—	Audio filters 0.2–300
3B9	1 800	100	§	§	§	—	Audio filters 0.2–300
3D3	750	10^5	§	§	§	—	HF filters 200–2 500
4C4	125	10^5	§	§	§	—	HF filters 1 000–20 000

* Data and coefficients a, c, and e are from V. E. Legg and F. J. Given, "Compressed Powdered Molybdenum Permalloy for High Quality Inductance Coils," *Bell System Technical Journal*, vol. 19, no. 3, pp. 385–406; July 1940.

† Data from Catalog PC-303, Magnetics, Inc., Butler, Pa.

‡ Data from Bulletin 220-C, Ferroxcube Corporation of America, Saugerties, N.Y.

§ See Fig. 27.

in that section can be used to reduce the distributed capacitance of the winding.

A detailed method for designing this type of coil can be found in "High Q Reactors for Low Frequencies," Bulletin A10, Magnetic Metals Co.. Camden, N.J.

Toroidal Audio Filter Coils

Toroidal coils are doughnut shaped, with the winding covering the entire core. The core is usually made of pressed molybdenum-permalloy dust, although some cores are made of carbonyl powdered iron for very-high-frequency applications (Table 9).

Permalloy-dust toroidal cores are made in various sizes with several material compositions to change the effective permeability μ_e for different frequency ranges. Figure 22 gives the Q-vs-frequency characteristics of four sizes of toroids with four different effective permeabilities. In addition, the inductance in millihenries per 1000 turns, A_L, is given for each size of core.

Figure 23 gives the number of turns of various sizes of heavy Formvar wire which can be placed

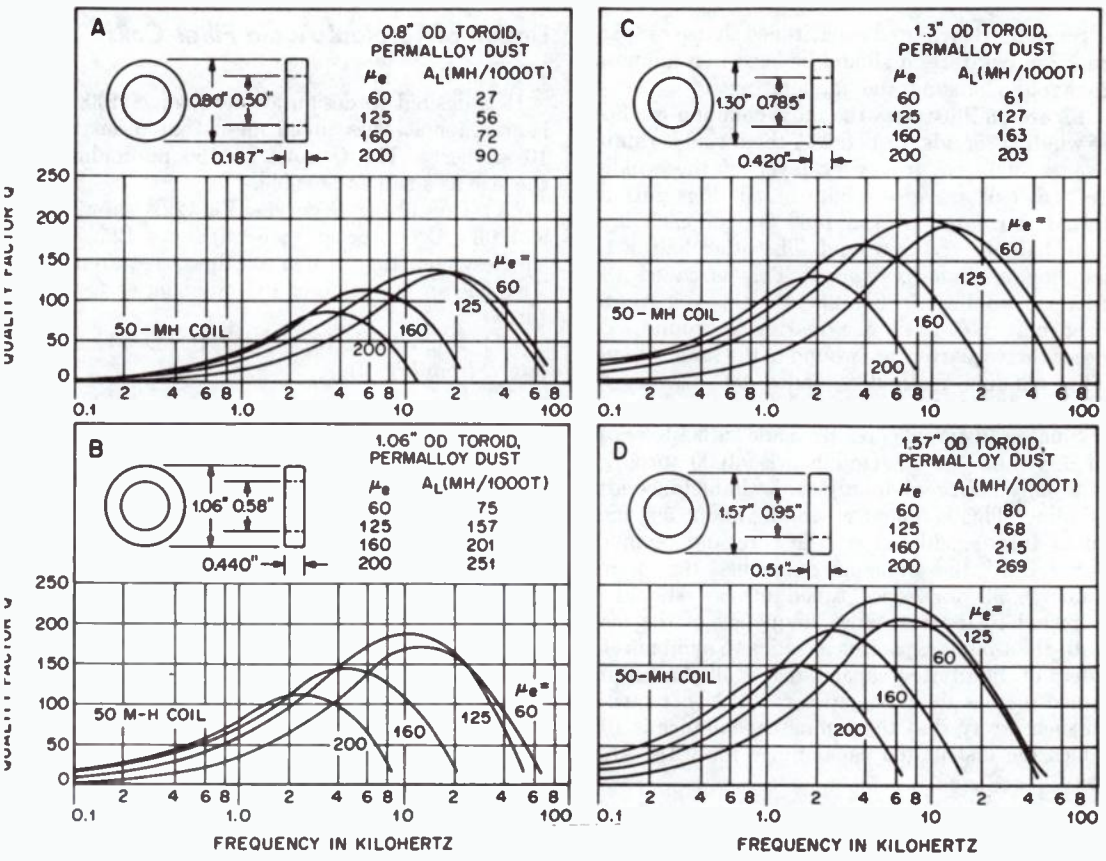

Fig. 22—Quality factor Q as a function of frequency for several sizes of permalloy-dust toroids. The data have been replotted from "Permalloy Powder Cores," Catalog PC-303, Magnetics, Inc., Butler, Pa.

on the toroid as well as the mean length of turn (MLT) for the respective toroidal cores of Fig. 22. These curves are based on a single winding wound with 180° traverse using commercially available toroidal winding machines.

Figure 24 gives the core loss factor in ohms per millihenry for various effective permeabilities and frequencies. This factor is multiplied by the inductance in millihenries to determine R_c. The curves are based on a low magnetic induction of 20 gauss. For higher levels, R_c can be calculated from the Legg coefficients given in Table 9.

Table 10 gives an approximate value of distributed capacitance C_d that can be expected for the different sizes of cores and winding methods.

When maximum temperature stability of inductance is required, most manufacturers of permalloy toroidal cores can provide various types of stabilized cores. The stabilizations most used follow.

TABLE 10—ESTIMATION OF DISTRIBUTED CAPACITANCE FOR CORE SIZE AND WINDING METHOD.

Toroid Core Size	Distributed Capacitance C_d (picofarads) 360° Traverse	180° Traverse	90° Traverse
0.8″ O.D.	120	60	30
1.06″ O.D.	200	100	50
1.30″ O.D.	300	150	75
1.57″ O.D.	360	180	90

Identification	Inductance Temperature Stability (%)	Temperature Range (°C)
B	±0.1	+13 to +35
D	±0.1	0 to +55
W	±0.25	−55 to +85

Since the distributed capacitance changes rapidly with temperature, it should be kept to a minimum to avoid changing the inductance.

Figure 25 illustrates the most common methods of winding toroids. In Fig. 25A the toroid is rotated over a 360° arc for every layer of the winding (called 360° traverse winding). In Fig. 25B the toroid is rotated over a 180° arc for each layer until half the coil is wound. The other half of the winding is similarly wound. This is called 180° traverse winding. In Fig. 25C the toroid is rotated over only 90° until one-quarter is wound. The other three-quarters are wound in the same manner. This winding method is called 90° traverse or quadrature winding.

Since most toroid cores are made with a tolerance of ±8% on the A_L (millihenries/1000 turns), it is usually necessary to adjust the inductance after winding. This is done by winding about 5% more turns than calculated on the core and removing turns until the inductance reaches the desired value. Coils for series tuned meshes should be adjusted to the resonance frequency of the mesh with the tuning capacitor in series to eliminate the effect of distributed capacitance. Coils for parallel tuned meshes should be adjusted at low frequency in such a way that the tuning capacitance is 1000 times the distributed capacitance for 0.1% accuracy.

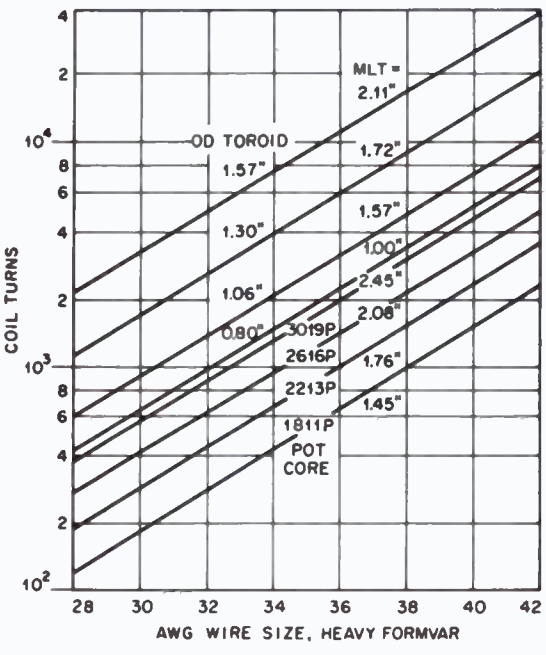

Fig. 23—Coil turns as a function of wire gauge for various core sizes and types.

*Design of Toroidal Audio Filter Coils**

It is desired to design an inductor of 100 millihenries for a series tuned mesh that resonates at 10 kilohertz. The Q must be 150 minimum and the size as small as possible.

(A) Consulting Q curves, Fig. 22B shows that a 1.06″ O.D. toroid core with $\mu_e = 125$ is the smallest core that will meet the Q requirements. This has an A_L value of 157 millihenries per 1000 turns.

(B) From Table 10, $C_d \approx 200$ picofarads. Calculate L from Fig. 21.

$$L = \frac{L_s}{1+\omega^2 L_s C_d}$$

$$= \frac{100}{1+(2\pi 10\ 000)^2 \times 0.1 \times 200 \times 10^{-12}}$$

$$= 92.68 \text{ millihenries.}$$

(C) Compute the number of turns required from

$$N = 1000(L_{\text{millihenries}}/A_L)^{1/2}$$

$$= 1000(92.68/157)^{1/2}$$

$$= 768 \text{ turns.}$$

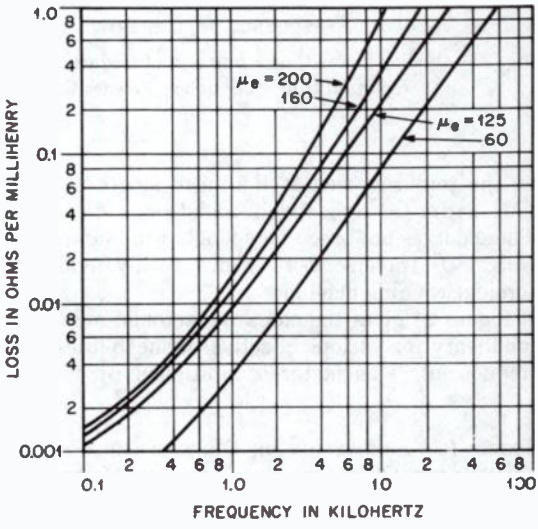

Fig. 24—Molybdenum permalloy-dust-core loss characteristics. $B_m = 20$ gauss. The data have been replotted from "Permalloy Powder Cores," Catalog PC-303, Magnetics, Inc., Butler, Pa.

* For more-detailed data on designing toroid coils, consult "Permalloy Powder Cores," Catalog PC-303, Magnetics, Inc., Butler, Pa.

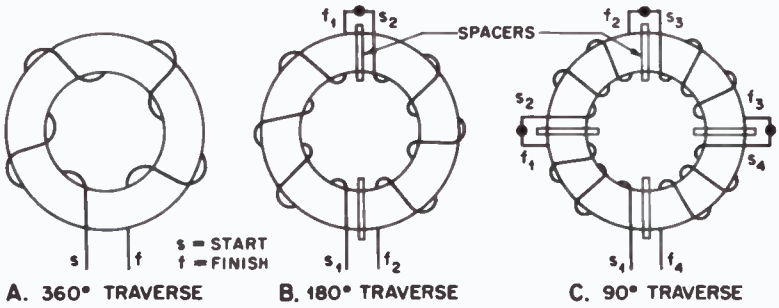

Fig. 25—Methods of winding toroid cores.

(D) Figure 23 gives the maximum size of wire and mean length of turn. Use No. 30 heavy Formvar for 768 turns. On a 1.06″ O.D. core the (MLT) = 1.57″.

(E) Calculate R_w from (MLT), N, and Table 6.

$$R_w = \frac{(\text{MLT}) \times N \times \text{ohms/1000 ft}}{12\ 000}$$

$$= \frac{1.57 \times 768 \times 103.2}{12\ 000}$$

$$= 10.36 \text{ ohms.}$$

(F) Calculate R_c from R/L values of Fig. 24 for $\mu_e = 125$ and $f = 10$ kilohertz. $R/L = 0.23$ ohm/millihenry. $R_c = (R/L)L = 0.23 \times 92.68 = 21.32$ ohms.

(G) Calculate Q per Fig. 19.

$$Q = \frac{\omega L}{R_w + R_c} = \frac{2\pi 10 \times 92.68}{10.36 + 21.32} = 183.8.$$

(H) Calculate Q_s per Fig. 21.

$$Q_s = Q(1 - \omega^2 L C_d)$$

$$= 183.8[1 - (2\pi 10\ 000)^2 \times 0.09268 \times 200 \times 10^{-12}]$$

$$= 170.4.$$

This should approximate the measured Q.

(I) The coil is wound using 360° traverse winding and, since no special temperature stability is required, a standard unstabilized core is used.

Ferrite-Pot-Core Audio Filter Coils

A ferrite-pot-core coil resembles a thin cylinder with the core entirely surrounding the winding except where the leads protrude. The core is pressed in two halves of green ferrite material and is fired like a ceramic. Each half has a recessed ring where the coil is placed after being wound. (See Fig. 26.) The cores are made of different compositions of ferrite to obtain different permeabilities, loss characteristics, and temperature coefficients. (See Table 9 and Fig. 27.)

To reduce the effective permeability μ_e, an air gap is machined into the center leg of the core. The larger the air gap the smaller the μ_e. Lowering the μ_e reduces the core losses, A_L (millihenries per 1000 turns), and temperature coefficient. Figure 28 gives Q-vs-frequency characteristics of four sizes of pot cores, each with three different effective

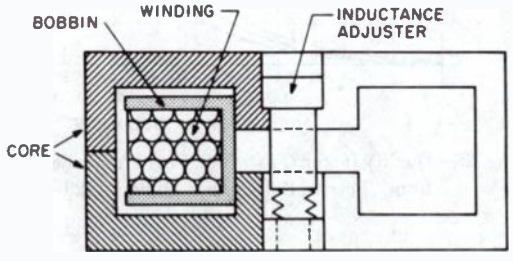

Fig. 26—Typical pot-core coil.

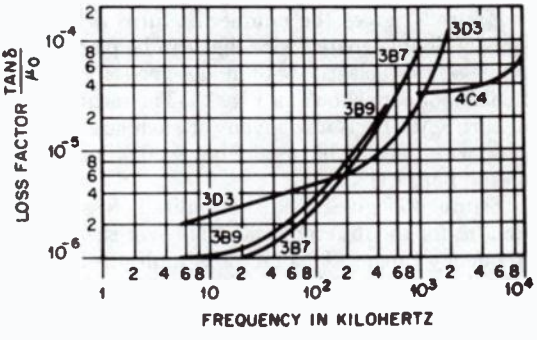

Fig. 27—Loss factor as a function of frequency. From "Ferrite Pot Cores," Bulletin 220-C, Ferroxcube Corporation of America, Saugerties, N.Y.

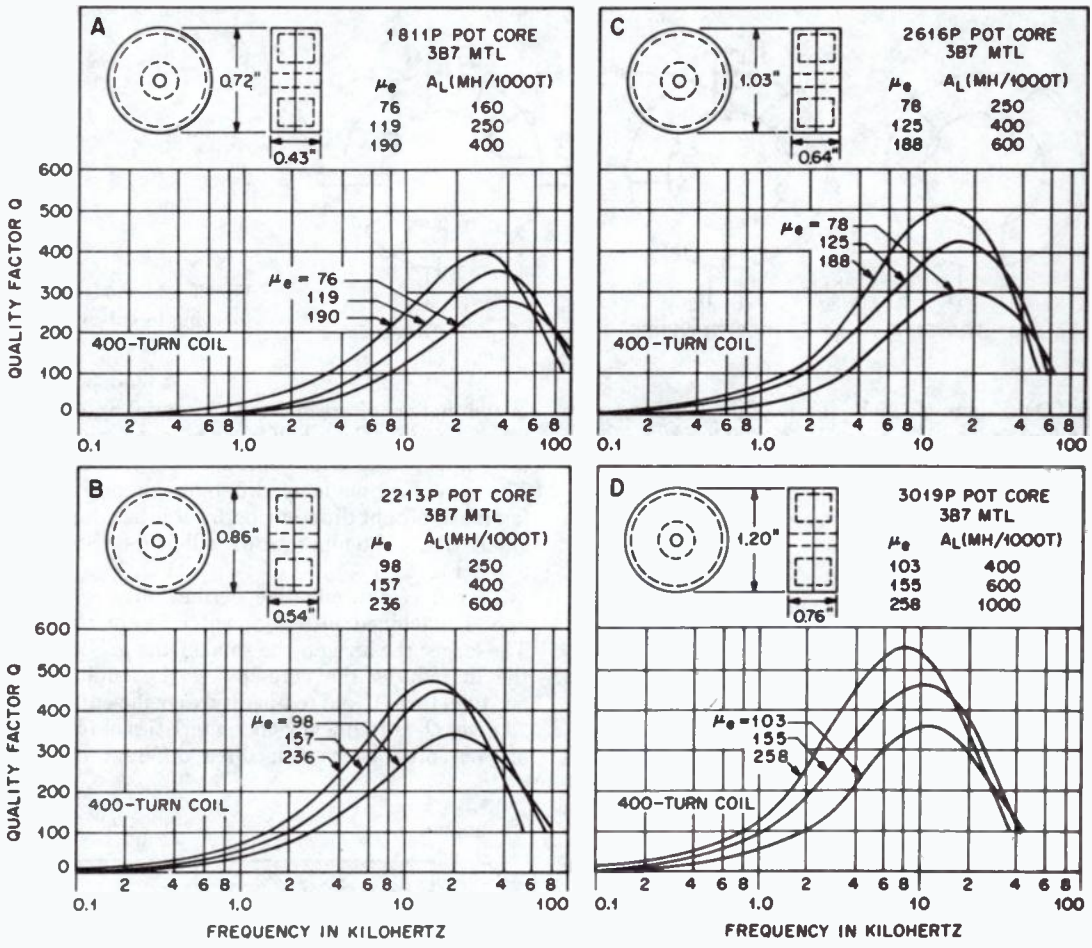

Fig. 28—Quality factor Q as a function of frequency for several types of ferrite pot cores. The data have been replotted from "Ferrite Pot Cores," Bulletin 220–C, Ferroxcube Corporation of America, Saugerties, N. Y.

permeabilities and A_L values. Q values are based on a single section winding using 400 turns of solid wire.

Figure 23 gives the number of turns of various sizes of double-coated wire that can be placed on a single-section plastic bobbin designed for a particular pot core shown in Fig. 28. The mean length of turn (MLT) is also given for each size of core. Litz wire should be used above 20 kilohertz to obtain better Q's.

Figure 27 gives the normalized loss factor $\tan\delta/\mu_0$ for the different materials over their useful frequency ranges. This factor is multiplied by the effective permeability μ_e and the inductive reactance $(2\pi fL)$ to determine R_c. This loss factor is based on low-level excitation, and losses will be greater for high-excitation applications.

Table 11 gives approximate values of distributed

TABLE 11—ESTIMATION OF DISTRIBUTED CAPACITANCE FOR CORE SIZE AND TYPE OF BOBBIN USED.

Ferrite Pot Core No.	Distributed Capacitance C_d (picofarads)		
	1-Section Bobbin	2-Section Bobbin	3-Section Bobbin
3019P	75	31	21
2616P	64	29	19
2213P	48	20	14
1811P	35	16	11

capacitance C_d that can be expected for different core sizes and numbers of sections in a bobbin. Since the core is external to the winding, grounding the core will increase these values.

The temperature stability is roughly proportional to the effective permeability μ_e. Ferroxcube 3B7 material has a flat temperature coefficient. Its temperature factor ($\pm 0.6\times10^{-6}$) multiplied by μ_e gives the temperature-coefficient limits of inductance from +20 to +70°C. For a positive temperature coefficient, 3B9 material is used. This material has a temperature factor of +1.4 to $+2.2\times10^{-6}$ from −30 to +70°C. Care must be taken to clamp and process these ferrite coils properly to realize these temperature coefficients. Distributed capacitance should also be minimized because of its effect on the inductance (Fig. 21).

Generally it is possible to obtain from the core manufacturer winding bobbins that have 1, 2, or 3 sections. Table 11 shows that the use of more than 1 section reduces the distributed capacitance but requires a smaller-diameter wire. Figure 29 illustrates the three bobbins mentioned. The sections are wound one at a time from start to finish without breaking the wire.

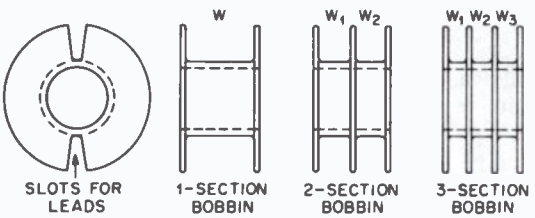

Fig. 29—Ferrite-pot-core bobbins available.

Because the ferrite pot core comes in two halves, it is necessary to clamp or cement them together in assembly. Clamping is preferred, as cement on the mating surfaces will decrease the A_L value and affect the temperature coefficient. Manufacturers of ferrite pot cores can furnish clamping hardware.

It is possible to vary the inductance of a pot core by threading a ferrite slug into the center hole of the core. As this slug bridges the air gap in the center leg of the core (Fig. 26), μ_e is increased and hence the inductance increases. In most applications the adjustment range is +13% with a sensitivity of better than 0.1%.

Most ferrite pot cores for this application have preadjusted air gaps to guarantee an A_L value within limits of ±3%. If an inductance adjuster is used (Fig. 26), it is possible to adjust the coil to within 0.1%. Also, if a ±2% mesh tuning capacitor is used, the mesh can be tuned using the inductance adjuster alone, thus eliminating the need for padding capacitors.

*Design of Ferrite-Pot-Core Audio Filter Coils**

It is desired to design an inductor of 1000 millihenries for a series tuned mesh that resonates at 5 kilohertz. The Q should be near 200, the temperature coefficient less than ±100 ppm/°C, and the coil adjustable to tune the mesh, with a fixed capacitor of ±2% tolerance.

(A) To obtain a flat temperature coefficient, 3B7 material should be used; for ±100 ppm/°C, the effective permeability μ_e should be less than 100/0.6, or 167.

(B) Consulting the Q curves, Fig. 28B shows that a 2213P pot core with $\mu_e=157$ and $A_L=400$ should meet the Q requirements.

(C) From Table 11, C_d is 48 picofarads for a 1-section coil. From Fig. 21

$$L=\frac{L_s}{1+\omega^2 L_s C_d}$$

$$=\frac{1000}{1+(2\pi 5000)^2\times 1.0\times 48\times 10^{-12}}$$

$$=954.8 \text{ millihenries.}$$

(D) Since we must use an inductance adjuster that increases the inductance by 13% maximum, the coil without adjuster should have an inductance of 954.8/1.06=900.7 millihenries. This allows an inductance adjustment of ±6%.

(E) Compute the number of turns required from

$$N=1000(L_{\text{millihenries}}/A_L)^{1/2}$$

$$=1000(900.7/400)^{1/2}$$

$$=1500 \text{ turns.}$$

(F) Consult Fig. 23 to determine maximum wire size and mean length of turn: Use No. 38 heavy Formvar for 1500 turns. On a 2213P pot core, the (MLT)=1.76″.

(G) Calculate R_w from (MLT), N, and Table 6.

$$R_w=\frac{1.76\times 1500\times 659.6}{12\ 000}=145.1 \text{ ohms.}$$

(H) Effective permeability μ_e with adjuster= $157\times1.06=166.4$. From Fig. 27, estimate loss

* For more details about designing ferrite-pot-core coils, consult Bulletin 220-C, Ferroxcube Corporation of America, Saugerties, N. Y.

TABLE 12—CLASSIFICATION OF ELECTRICAL INSULATING MATERIALS. *Abridged from "General Principles Upon Which Temperature Limits are Based in the Rating of Electrical Equipment," AIEE Standard No. 1; Dec. 1962.*

Class	Insulating Material	Limiting Insulation Temperature (Hottest Spot) in °C
O	Materials or combinations of materials such as cotton, silk, and paper without impregnation*	90
A	Materials or combinations of materials such as cotton, silk, and paper when suitably impregnated or coated or when immersed in a dielectric liquid*	105
B	Materials or combinations of materials such as mica, glass fiber, asbestos, etc., with suitable bonding substances*	130
F	Same as for Class B	155
H	Materials or combinations of materials such as silicone elastomer, mica, glass fiber, asbestos, etc., with suitable bonding substances such as appropriate silicone resins*	180
C	*	220
Over C	Materials consisting entirely of mica, porcelain, glass, quartz, and similar inorganic materials*	Over 220

* (Other) materials or combinations of materials may be included in this class if by experience or accepted tests they can be shown to have comparable thermal life at the temperature given in the right-hand column.

These temperatures are, and have been in most cases over a long period of time, benchmarks descriptive of the various classes of insulating materials, and various accepted test procedures have been or are being developed for use in their identification. They should not be confused with the actual temperatures at which these same classes of insulating materials may be used in the various specific types of equipment nor with the temperatures on which specified temperature rise in equipment standards are based.

In the above definitions the words "accepted tests" are intended to refer to recognized test procedures established for the thermal evaluation of materials by themselves or in simple combinations. Experience or test data, used in classifying insulating materials, are distinct from the experience or test data derived for the use of materials in complete insulation systems. The thermal endurance of complete systems may be determined by suitable test procedures.

A material that is classified as suitable for a given temperature may be found suitable for a different temperature, either higher or lower, by an insulation system test procedure. For example, it has been found that some materials suitable for operation at one temperature in air may be suitable for a higher temperature when used in a system operated in an inert gas atmosphere. Likewise some insulating materials when operated in dielectric liquids will have lower or higher thermal endurance than in air.

It is important to recognize that other characteristics (in addition to thermal endurance) such as mechanical strength, moisture resistance, and corona endurance, are required in varying degrees in different applications for the successful use of insulating materials.

factor $\tan\delta/\mu_0$ for 5 kilohertz $=0.5\times10^{-6}$. (This requires extrapolation of the curve for 3B7 material.) Calculate R_c from

$$R_c = 2\pi f L \mu_e (\tan\delta/\mu_0)$$
$$= 2\pi 5000 \times 0.9548 \times 166.4 \times 0.5 \times 10^{-6}$$
$$= 2.50 \text{ ohms.}$$

(J) Calculate Q per Fig. 19.

$$Q = \frac{2\pi fL}{R_w + R_c} = \frac{2\pi 5000 \times 0.9548}{145.1 + 2.5} = 203.2.$$

(K) Calculate Q_s per Fig. 21.

$$Q_s = Q(1-\omega^2 LC_d)$$
$$= 203.2[1-(2\pi 5000)^2 \times 0.9548 \times 48 \times 10^{-12}]$$
$$= 194.0.$$

(L) Temperature coefficient

$$= \mu_e \times \pm 0.6 \times 10^{-6} = 166.4 \times 0.6 \times 10^{-6}$$

or ± 99.8 ppm/°C from +20 to +70°C.

(M) The coil is wound on a 1-section bobbin for a 2213P core and is assembled with a 2213P $A_L = 400$ core and proper clamping assembly. The adjuster is screwed into the core and the inductance is checked to be sure there is a $\pm 3\%$ tuning range of about 1000 millihenries at 5 kilohertz. Some adjustment of turns may be necessary to allow for the winding method, processing, and estimated C_d.

TEMPERATURE AND HUMIDITY

Table 12 lists the standard classes of insulating materials and their limiting operating temperatures. Table 13 compares the properties of five high-temperature wire-insulating coatings.

Open-type constructions generally permit greater

TABLE 13—COMPARISON OF FIVE HIGH-TEMPERATURE WIRE-INSULATING MATERIALS. *From J. Holland, "Choosing Wire Insulation For High Temperatures," Electronic Design, vol. 2, p. 14; July 1954.*

Characteristic	Modified Teflon	Teflon	Silicone Enamel DC1360	Formvar (vinyl acetal)	Plain Enamel
Upper temp limit	+250°C	+250°C	+180°C	+105°C	+80°C
Lower temp limit	−100°C	−100°C	−40°C	−40°C	−40°C
Dielectric strength	Excellent	Very good	Very good	Good	Good
Dielectric constant (60 Hz–30 000 MHz)	2.0–2.05*	2.0–2.05*	Inferior	Inferior	Inferior
Power factor (60 Hz–10 000 MHz)	0.0002*	0.0002*	Inferior, about 0.006–0.007	Inferior	Inferior
Space factor	Excellent	Excellent	Excellent	Excellent	Excellent
Solvent resistance	Excellent	Excellent	Fair	Fair	Poor
Abrasion resistance	Good	Fair	Very good	Excellent	Good
Thermoplastic flow	Good	Fair	Excellent	Excellent	Good
Crazing resistance	Excellent	Very good	Fair	Fair	Fair
Flame resistance	Excellent	Excellent	Fair	Poor	Poor
Fungus resistance	Excellent	Excellent	Good	Good	Poor
Moisture resistance	Excellent	Excellent	Good	Good	Good
Continuity of insulation	Excellent	Excellent	Good	Good	Good
Arc resistance	Excellent	Excellent	Good	Good	Good
Flexibility	Excellent	Very good	Good	Good	Good

* Stable at temperatures up to 250°C.

cooling than enclosed types, thus allowing smaller sizes for the same power ratings. Moderate humidity protection may be obtained by impregnating and dip-coating or molding transformers in polyester or epoxy resins; these units provide good heat dissipation but are not as good in this respect as completely open transformers.

Protection against the detrimental effects of humidity is commonly obtained by enclosing transformers in hermetically sealed metal cases. This is particularly important if very fine wire, high output voltage, or direct-current potentials are involved. Heat conductivity to the case exterior may be improved by the use of asphalt or thermosetting resins as filling materials. Best conductivity is obtained with high-melting-point silica-filled asphalts or resins of the polyester or epoxy types. Coils impregnated with these resins dissipate heat best since voids in the heat path may be eliminated.

Immersion in oil is an excellent means of removing heat from transformers. An air space or bellows must be provided to accommodate expansion of oil when heated.

DIELECTRIC INSULATION AND CORONA

For class A (Table 12), a maximum dielectric strength of 40 volts/mil is considered safe for small thicknesses of insulation. At high operating voltages, due regard must be paid to corona that occurs before dielectric breakdown and will in time deteriorate insulation and cause dielectric failure. Best practice is to operate insulation at least 25 percent below the corona starting voltage. Approximate 60-hertz root-mean-square corona voltage V is

$$\log \frac{V \text{ (in volts)}}{800} = \tfrac{2}{3} \log(100t)$$

where t = total insulation thickness in inches. This may be used as a guide in determining the thickness of insulation. With the use of varnishes that require no solvents, but solidify by polymerization, the bubbles present in the usual varnishes are eliminated, and much higher operating voltages and, hence, reduction in the size of high-voltage units may be obtained. Epoxy resins and some polyesters belong in this group. In the design of high-voltage transformers, the creepage distance required between wire and core may necessitate the use of insulating channels covering the high-voltage coil, or taping of the latter. For units operating at 10 kilovolts or higher, oil insulation will greatly reduce creepage and, hence, the size of the transformer.

CHAPTER 14
RECTIFIERS AND FILTERS

BASIC RECTIFIER CHARACTERISTICS

All rectifiers exhibit relatively low resistance (forward resistance) when the anode is positive with respect to its cathode, and high resistance (reverse resistance—typically at least 10^3 times the forward resistance) when the anode is negative with respect to the cathode. Since semiconductors have replaced electron tubes in most rectifier applications, the discussion of electron-tube rectifiers is brief and most of the material deals with semiconductor rectifiers.

COMPARISON OF RECTIFIER TYPES

Electron-tube rectifiers have one advantage over semiconductors. The reverse resistance of a tube rectifier is essentially infinite (neglecting insulation leakage, etc.) while that of a semiconductor is finite (although considerably higher than the forward resistance). Semiconductors have the advantages of requiring no filament power and, for a given power rating, are much smaller in size. For many high-power applications, semiconductor rectifiers must be mounted on heat sinks. However, the combination of rectifier and heat sink generally occupies less space than an equivalent electron-tube device.

Table 1 compares the characteristics of silicon, germanium, selenium, and copper-oxide semiconductor rectifiers.

TYPICAL RECTIFIER CIRCUITS

Table 2 shows seven of the most commonly used power-rectifier circuits and general design information for each type. Their advantages, disadvantages, and common applications follow.

Single-Phase Half-Wave Rectifier: Since only half of the input wave is used, the efficiency is low and the regulation is relatively poor. Capacitors are commonly used in half-wave circuits to increase the output voltage and decrease the ripple. The output voltage and degree of filtering are determined by the value of capacity used in relation to the load current. Transformer design is complicated, and the unidirectional secondary current flow causes core saturation and poor regulation. Most half-wave circuits operate either directly from ac lines, or at a high voltage with a relatively low current.

Single-Phase Full-Wave Center-Tap Rectifier: The efficiency is good but the transformer ac voltage is approximately 2.2 times the dc output voltage. The circuit requires a larger transformer than an equivalent bridge rectifier, with the added complication of a center tap. Each arm of the center-tap circuit must block the full terminal voltage of the transformer. Because of this, center-tap connections are economical only in voltage ranges where not more than one rectifier per arm is required. If series units must be used to obtain the required output voltage, a bridge circuit is preferable.

Single-Phase Full-Wave Bridge Rectifier: If single-phase full-wave output is required, a bridge circuit is commonly used. Efficiency is good and transformer design is easy. Filtering is simplified because the ripple frequency is twice the input frequency.

Three-Phase Wye (or Star) Half-Wave Rectifier: Commonly used if dc output-voltage requirements are relatively low and current requirements are moderately large. The dc output voltage is approximately equal to the phase voltage. However, each of the three arms must block the line-to-line voltage, which is approximately 2.5 times the phase voltage. For this reason, it is desirable to use a 3-phase half-wave connection only where one series unit per arm will provide the required dc output. The transformer design and utilization are somewhat complicated because there is a tendency to saturate the core with unidirectional current flow in each winding.

Three-Phase Full-Wave Bridge Rectifier: Commonly used if high dc power is required and if efficiency must be considered. The ripple component in the load is 4.2% at a frequency 6 times the input frequency, so additional filtering is required in most applications. The dc output voltage is approximately 25% higher than the phase voltage, and each arm must block only the phase voltage. Transformer utilization is good.

TABLE 1—COMPARISON OF SEMICONDUCTOR RECTIFIERS.

	Silicon	Germanium	Selenium	Copper Oxide
Size	Very small	Very small	Large	Large
Weight	Very light	Very light	Light	Heavy
Cooling	Natural or forced	Natural or forced	Natural or forced	Natural or forced
Life	Very long	Very long	60 000 to 100 000 hrs. normal; can vary according to rating and cooling means	Long
Aging (forward resistance)	None	None	Increases	Stabilizes
Forward loss at same current density	Good	Excellent (lowest)	Fair (highest)	Good
Approx. dc forward voltage drop per cell	0.9 volt	0.65 volt	1.0 volt	0.5 volt
Leakage (reverse) current	Excellent	Excellent	Good	Fair
Ability to recover from voltage transients	None	None	Excellent	Good
Unforming (loss of rectifier characteristic)	None	None	Some	None
Series operation of cells	Good	Good	Excellent	Excellent
Parallel operation of cells	Good	Good	Excellent	Excellent
Present cell operating temperature limit	200°C	105°C	130°C	75°C
Thermal capacity	Poor	Poor	Fair	Best
Efficiency at low voltage	Good	Excellent	Fair	Good
Humidity effects	Hermetically sealed	Hermetically sealed	Negligible	Negligible
Frequency response	Good	Good	Poor	Fair

Three-Phase Diametric Half-Wave Rectifier: The characteristics of this circuit approximate those of the 3-phase double-wye circuit without an interphase transformer. Popular applications include requirements for very high dc load currents in low- to medium-voltage ranges (approximately 6 to 125 volts dc).

Three-Phase Double-Wye Half-Wave Rectifier: A 3-phase double-wye connection is recommended if a very high direct current is required at a relatively low dc voltage. Each arm is required to block the full phase voltage of the secondary windings. The dc output current rating is double that of a three-phase bridge or half-wave connection. However, the output voltage is only 75% of the phase voltage. The transformer design is complicated by additional connections and extra insulation, and an interphase transformer (or balance coil) is required.

CIRCUIT DESIGN FOR SEMICONDUCTOR POWER RECTIFIERS

Tables 3 and 4 show the theoretical values of direct and alternating voltages, current, and power for the basic rectifier and transformer elements of single-phase and polyphase conversion circuits, based on perfect rectifiers and transformers. The equations and the values of the constants K and I_{ac} are approximate, but they are sufficiently accurate for practical design of small rectifier circuits.

Symbols for Tables 3 and 4

I_{ac} = transformer secondary current in root-mean-square amperes

I_{dc} = average load direct current in amperes

K = circuit form factor

n = number of cells in series in each arm of rectifier

V_{ac} = alternating root-mean-square input voltage per secondary winding (see diagrams)

$V_{ac\Delta}$ = phase-to-phase alternating input voltage for 3-phase full-wave bridge

V_{dc} = average value of direct-current output voltage

V_p = reverse root-mean-square voltage per cell (rating of rectifier cell)

ΔV = root-mean-square voltage drop per cell at I_{dc}.

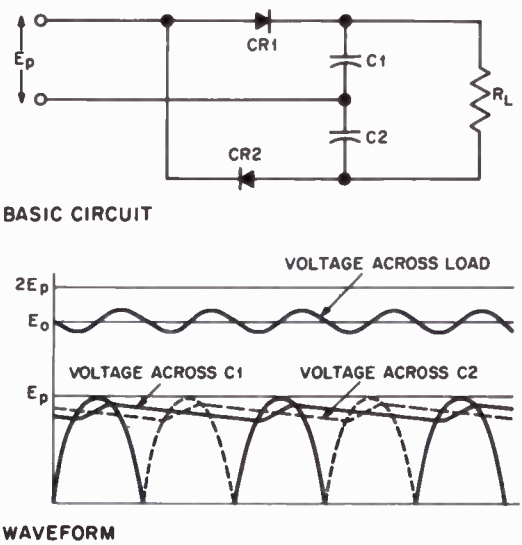

Fig. 1—Conventional voltage doubler.

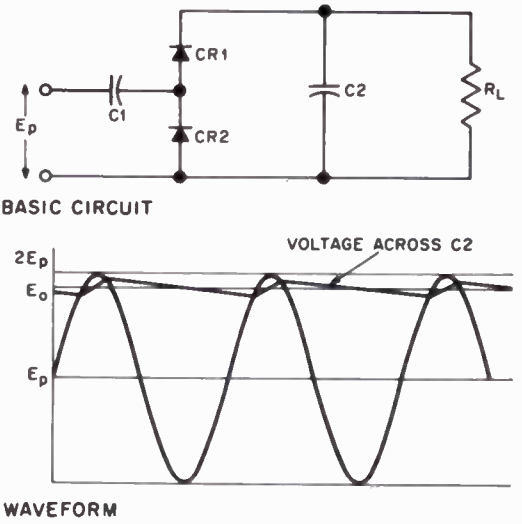

Fig. 2—Cascade voltage doubler.

More-rigorous equations, to be found in textbooks and technical papers, should be used in designing rectifiers with outputs in excess of about 10 kW and for accurate computations of regulation, efficiency, power factor, and overload characteristics of even small rectifiers.

VOLTAGE-MULTIPLIER RECTIFIER CIRCUITS

These circuits use the principle of charging capacitors in parallel from the ac input and adding the voltages across them in series to obtain dc voltages higher than the source voltage. Filtering must be of the capacitor-input type.

Conventional and Cascade Voltage Doublers: In the conventional circuit (Fig. 1), capacitors C1 and C2 are each charged, during alternate half-cycles, to the peak value of the alternating input voltage. The capacitors are discharged in series into load R_L, thus producing an output across the load of approximately twice the ac peak voltage.

In the cascade circuit (Fig. 2), C1 is charged to the peak value of the ac input voltage through rectifier CR2 during one half-cycle, and during the other half-cycle it discharges in series with the ac source through CR1 to charge C2 to twice the ac peak voltage.

The "conventional" circuit has slightly better regulation and, since the ripple frequency is twice the supply frequency, the output is easier to filter, the percentage ripple being approximately the same in both circuits. In addition, both capacitors are rated at the ac peak voltage, whereas C2 in the cascade circuit must be rated at twice this value. With both circuits, the peak inverse voltage across each rectifier is twice the ac peak. The cascade

TABLE 2—RECTIFIER CIRCUIT CHART. THE DATA ASSUME ZERO FORWARD DROP AND ZERO

Type of Circuit→		Single-Phase Half Wave	Single-Phase Center Tap	Single-Phase Bridge	Three-Phase Star (Wye)
Primary→		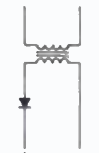	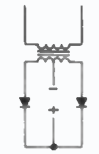	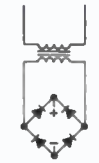	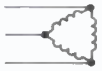
Secondary→					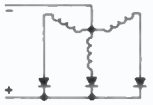
One Cycle Wave of Rectifier Output Voltage (No Overlap)					
Number of rectifier elements	=	1	2	4	3
RMS dc volts output	=	1.57	1.11	1.11	1.02
Peak dc volts output	=	3.14	1.57	1.57	1.21
Peak reverse volts per rectifier element	=	3.14	3.14	1.57	2.09
	=	1.41	2.82	1.41	2.45
	=	1.41	1.41	1.41	1.41
Average dc output current	=	1.00	1.00	1.00	1.00
Average dc output current per rectifier element	=	1.00	0.500	0.500	0.333
RMS current per rectifier element:					
Resistive load	=	1.57	0.785	0.785	0.587
Inductive load	=	—	0.707	0.707	0.578
Peak current per rectifier element:					
Resistive load	=	3.14	1.57	1.57	1.21
Inductive load	=	—	1.00	1.00	1.00
Ratio of peak to average current per element:					
Resistive load	=	3.14	3.14	3.14	3.63
Inductive load	=	—	2.00	2.00	3.00
% Ripple (rms of ripple/ average output voltage)	=	121%	48%	48%	18.3%
Ripple frequency	=	1	2	2	3
		Resistive Load		Inductive Load or Large Choke Input Filter	
Transformer secondary rms volts per leg	=	2.22	1.11 (to center-tap)	1.11 (total)	0.855 (to neutral)
Transformer secondary rms volts line-to-line	=	2.22	2.22	1.11	1.48
Secondary line current	=	1.57	0.707	1.00	0.578
Transformer secondary volt-amperes	=	3.49	1.57	1.11	1.48
Transformer primary rms amperes per leg	=	1.57	1.00	1.00	0.471
Transformer primary volt-amperes	=	3.49	1.11	1.11	1.21
Average of primary and secondary volt-amperes	=	3.49	1.34	1.11	1.35
Primary line current	=	1.57	1.00	1.00	0.817
Line power factor	=	—	0.900	0.900	0.826

REVERSE CURRENT IN RECTIFIERS AND NO ALTERNATING-CURRENT LINE OR SOURCE REACTANCE.

Three-Phase Bridge	Six-Phase Star (Three-Phase Diametric)	Three-Phase Double Wye with Interphase Transformer	Note: Assumes perfect rectifiers and zero reactance of ac line and source / To Determine Actual Value of Parameter in Any Column, Multiply Factor Shown By Value of:
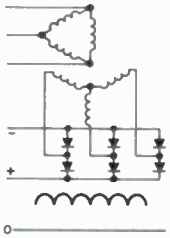	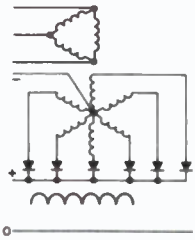	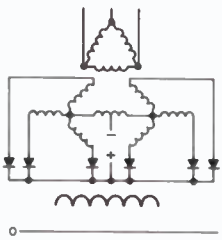	
6	6	6	
1.00	1.00	1.00	× Average dc voltage output
1.05	1.05	1.05	× Average dc voltage output
1.05	2.09	2.42	× Average dc voltage output
2.45	2.83	2.83	× RMS secondary volts per transformer leg
1.41	1.41	1.41 (diametric)	× RMS secondary volts line-to-line
1.00	1.00	1.00	× Average dc output current
0.333	0.167	0.167	× Average dc output current
0.579	0.409	0.293	× Average dc output current
0.578	0.408	0.289	× Average dc output current
1.05	1.05	0.525	× Average dc output current
1.00	1.00	0.500	× Average dc output current
3.15	6.30	3.15	
3.00	6.00	3.00	
4.2%	4.2%	4.2%	
6	6	6	× Line frequency f
Inductive Load or Large Choke Input Filter			
0.428 (to neutral)	0.740 (to neutral)	0.855 (to neutral)	× Average dc voltage output
0.740	1.48 (max)	1.71 (max-no load)	× Average dc voltage output
0.816	0.408	0.289	× Average dc output current
1.05	1.81	1.48	× DC watts output
0.816	0.577	0.408	× Average dc output current
1.05	1.28	1.05	× DC watts output
1.05	1.55	1.26	× DC watts output
1.41	0.817	0.707	× (Avg. load current × sec. leg voltage)/ primary line voltage
0.955	0.955	0.955	

TABLE 3—SINGLE-PHASE-RECTIFIER CIRCUITS, EQUATIONS, AND DESIGN CONSTANTS.

Constant	Half-Wave	Full-Wave Center Tap	Full-Wave Bridge
Circuit	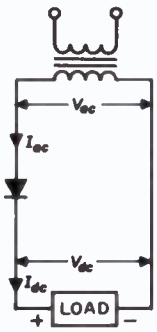	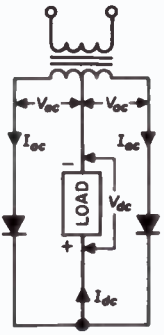	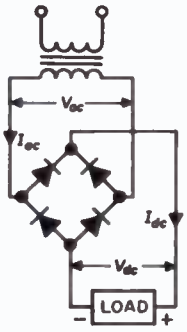
V_{ac}	$KV_{dc}+n\Delta V$	$KV_{dc}+n\Delta V$	$KV_{dc}+2n\Delta V$
Resistive and inductive loads:			
n	$KV_{dc}/(V_p-\Delta V)$	$2KV_{dc}/(V_p-2\Delta V)$	$KV_{dc}/(V_p-2\Delta V)$
V_p	V_{ac}/n	$2V_{ac}/n$	V_{ac}/n
K	2.26	1.13	1.13
$I_{ac,rms}$	$1.57I_{dc,Av}$	$0.785I_{dc,Av}$	$1.11I_{dc,Av}$
Battery and capacitive loads:			
n	$2KV_{dc}/(V_p-2\Delta V)$	$2KV_{dc}/(V_p-2\Delta V)$	$KV_{dc}/(V_p-2\Delta V)$
V_p	$2V_{ac}/n$	$2V_{ac}/n$	V_{ac}/n
K	1.0	0.85	0.85
$I_{ac,rms}$	$2.3I_{dc,Av}$	$1.15I_{dc,Av}$	$1.65I_{dc,Av}$

circuit, however, has the advantage of a common input and output terminal and, therefore, permits the combination of units to give higher-order voltage multiplications. The regulation of both circuits is poor, so that only small load currents can be drawn.

Bridge Voltage Doubler: This circuit (Fig. 3) is a combination of the conventional voltage doubler and the bridge rectifier circuit. If CR3 and CR4 are removed, the circuit becomes a "conventional" voltage doubler. If the two capacitors and the connection from their midpoint to the junction of CR3 and CR4 are removed, the circuit becomes a standard bridge rectifier.

Further Voltage Multiplication: The cascade voltage doubler shown in Fig. 2 can be combined several times to obtain higher dc voltages, as shown in Fig. 4. The voltage ratings of all the capacitors and rectifiers are twice the ac peak voltage, but the capacitors must have the values shown. The value of C will be the same as that for the cascade voltage doubler (Fig. 2), which is the basic unit for the circuit in Fig. 4. The load current must be small. The increasing size of capacitors and the deterioration in regulation limit the voltages that can be obtained from this type of circuit.

SILICON RECTIFIERS

Ratings

Silicon-rectifier ratings* are generally expressed in terms of reverse-voltage ratings and of mean-

* For a complete list of silicon-rectifier ratings, refer to the EIA—JEDEC Recommendations for Letter Symbols, Abbreviations, Terms and Definitions for Semiconductor Device Data Sheets and Specifications, published by Electronics Industries Association, 2001 Eye Street, N.W., Washington, D.C. 20006.

TABLE 4—THREE-PHASE-RECTIFIER CIRCUITS, EQUATIONS, AND DESIGN CONSTANTS. USED FOR ALL LOADS.

Constant	Half-Wave	Full-Wave-Bridge
Circuit	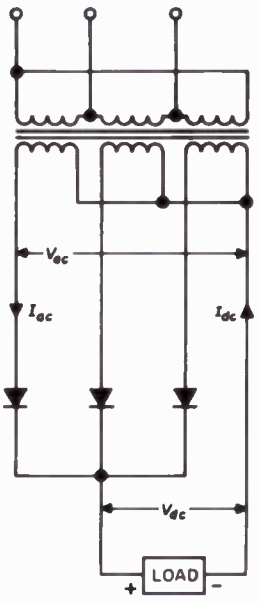	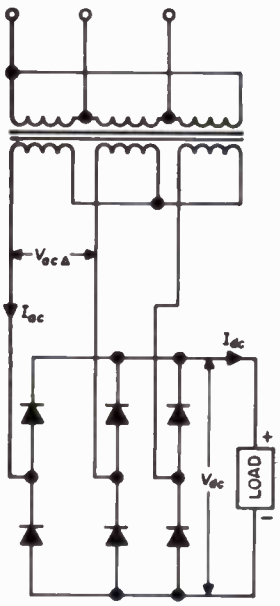
Input	$V_{ac}=KV_{dc}+n\Delta V$	$V_{ac\Delta}=KV_{dc}+2n\Delta V$
n	$1.73KV_{dc}/(V_p-1.73\Delta V)$	$KV_{dc}/(V_p-2\Delta V)$
V_p	$1.73V_{ac}/n$	$V_{ac\Delta}/n$
K	0.855	0.74
$I_{ac,rms}$	$0.577I_{dc,Av}$	$0.816I_{dc,Av}$

forward-current ratings in a half-wave circuit operating from a 60-hertz sinusoidal supply and into a purely resistive load.

There are three reverse-voltage ratings of importance.

Peak transient reverse voltage	V_{RM}
Maximum repetitive reverse voltage	$V_{RM(rep)}$
Working peak reverse voltage	$V_{RM(wkg)}$

V_{RM} is the rated maximum value of any nonrecurrent surge voltage, and this value must not be exceeded under any circumstances, even for a microsecond.

$V_{RM(rep)}$ is the maximum value of reverse voltage that may be applied recurrently, e.g., in every cycle, and will include any circuit oscillatory voltage that may appear on the sinusoidal supply voltage.

$V_{RM(wkg)}$ is the crest value of the sinusoidal voltage of the supply at its maximum limit. The manufacturer generally recommends a $V_{RM(wkg)}$ that has an appreciable safety margin in relation to the V_{RM} to allow for the commonly experienced transient overvoltages on power mains.

Three forward-current ratings are similarly of importance.

Nonrecurrent surge current	$I_{FM(surge)}$
Repetitive peak forward current	$I_{FM(rep)}$
Average forward current	$I_{F(av)}$

Silicon diodes have comparatively small thermal mass, and care must be taken to ensure that short-term overload currents are limited. The nonrecurrent surge current is sometimes given as a single value which must not at any time be exceeded, but it is more generally given in the form of a graph of permissible surge current versus time.

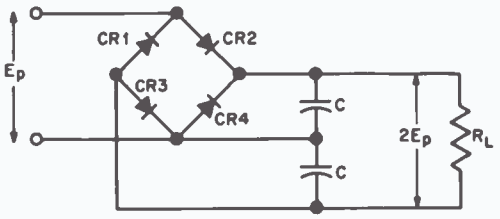

Fig. 3—Bridge voltage doubler.

It is important to observe whether the surge current scale is marked in peak, rms, or average value in order that the data be correctly interpreted.

The repetitive peak forward current is the peak value of the forward current reached in every cycle and excludes random peaks due to transients. Its relation to the average forward current depends on the circuit used and on the load that is applied. For example, the repetitive peak is about three times the average for a half-wave or bridge circuit working into a resistive load; it may be many times greater when the same circuits work into capacitive loads.

Forward Characteristics

The manufacturer generally supplies curves of instantaneous forward voltage versus instantaneous forward current at one or more operating temperatures; a typical characteristic is shown by the solid curve in Fig. 5.

Such curves are not exact for all rectifiers of a given type but are subject to normal production spreads. They are of particular importance in determining the power dissipated by the rectifier under given working conditions.

Calculation of power dissipation from the voltage/current curves need not be done in every instance since the manufacturer gives curves of power dissipation versus forward current for a limited number of commonly used circuits. However, cases do arise for which the particular form of circuit or load is not covered, and it is then necessary to calculate the dissipation for these particular conditions. The calculation can be greatly simplified, with little loss of accuracy in most cases, by approximating the actual V/I characteristic curve to a straight line, as shown by the broken line in Fig. 5. The approximate characteristic corresponds to that of a fixed voltage (the *threshold* voltage) plus a fixed resistance (the *slope* resistance). For any shape of current waveform, the power dissipated at constant voltage is the product of the average current and this fixed voltage, while the power dissipated at constant resistance is the product of the square of the rms current and this fixed resistance. Thus, the following simple equation can be used.

$$P = I_{F(av)} \times V_T + I_{F(rms)}^2 \times R_s$$

where P is the forward power dissipation, $I_{F(av)}$ is the average forward current through the rectifier, averaged over one complete cycle, $I_{F(rms)}$ is the rms value of the forward current through the rectifier, V_T is the threshold voltage, and R_s is the slope resistance.

For the best accuracy, the straight-line approximation should be drawn through points on the current curve corresponding to 50% and 150% of the peak current at which the rectifier is to be used. Thus, in Fig. 5 the dotted line would correspond to a peak working current of 200 amperes.

Carrier Storage

On switching from forward conduction to reverse blocking, a silicon diode cannot immediately revert to its blocking state because of the presence of stored carriers at the junction. These have the effect of allowing current to flow in reverse, as through a forward-biased junction, when reverse voltage is applied. The current is limited only by the external voltage and circuit. However, the carriers are rapidly removed from the junction, both by internal recombination and by the sweeping effect of the reverse current, and when this has happened the diode reverts to its blocking condition in which only a low leakage current flows. This sudden cessation of a large reverse current can cause objectionable voltage transients if there is appreciable circuit inductance and surge suppression has not been included. The reverse current due to carrier storage is not excessive in normal operation of power rectifier circuits and

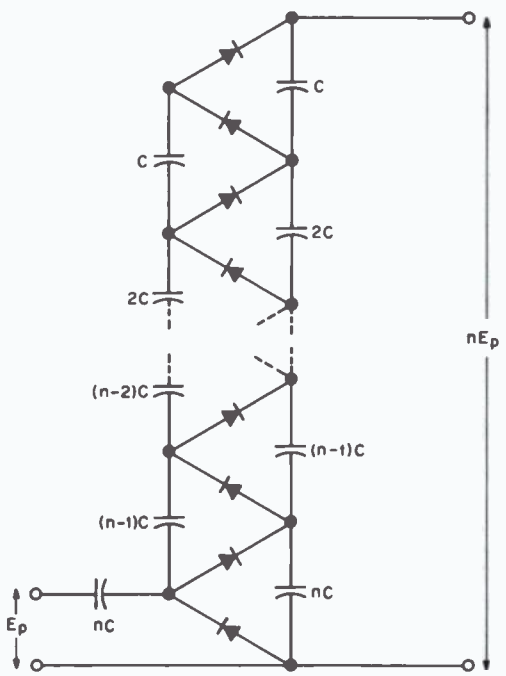

Fig. 4—Circuit for high-order voltage multiplication.

does not in itself constitute a hazard; however, its effect can sometimes lead to complications in switching arrangements. For example, in an inductively loaded circuit, the current will "free-wheel" through the diodes after the supply has been removed until the inductive energy has been discharged. Should the supply be reapplied while this process is going on, some of the diodes will be required to conduct in a forward direction but others will be required to block; while the latter are recovering from the carrier storage injected by the free-wheeling current, the short-circuit across the supply can cause a damaging surge current to flow.

Parallel Operation

Silicon diodes are frequently used in parallel assemblies to provide large outputs of rectified current. However, diodes of any one type do not necessarily have exactly the same forward characteristic, and this leads to problems of current sharing.

When the manufacturer divides the production output of a particular type of diode into several grades according to their measured forward characteristics, it is important to use diodes all of one grade in a parallel assembly. It may still be necessary to apply a current derating factor, as recommended by the manufacturer, to determine the number of diodes that will be required to carry a given current.

In addition, care should be taken that the electrical connections to the individual diodes are in a reasonably symmetrical arrangement so that no extra unbalance is introduced by unequal external resistance. It is an advantage to mount as many of the diodes as possible on a common heat sink to facilitate heat transfer between them.

Individual resistances or reactances may be used in the connections to each diode to assist in forced sharing of current. However, these can be difficult to mount in association with normal air-cooled assemblies, and their expense may outweigh the cost of the additional diodes that would otherwise be necessary for safe rating.

Series Operation

When higher voltage outputs are required than are normally possible with existing ratings of single diodes, series assemblies of diodes are used. The problem here is to assure equal sharing of reverse voltage so that the voltage across any one diode does not exceed its rated value. One factor which tends to prevent equal voltage sharing is the dissimilarity between the reverse-leakage-current characteristics of several diodes of the same nominal type. This problem is generally overcome by applying shunt resistance across each rectifier in the chain such that the current they take when the diodes are reverse-biased is several times greater than the leakage current of the diodes.

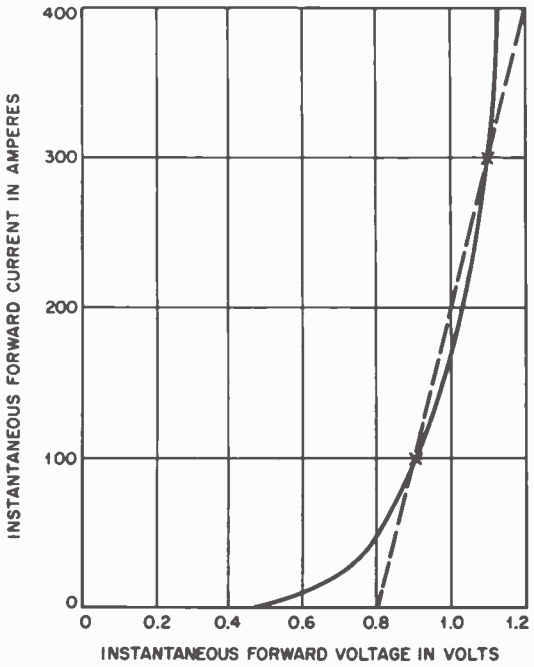

Fig. 5—Instantaneous forward voltage–current characteristic for a typical 100-ampere diode operated at 100°C junction temperature. The ideal threshold forward voltage V_T is the value where the broken line intercepts zero current.

Another factor is the difference between the extent of carrier storage present in the diodes after they have been carrying the same forward current. If no precautions are taken, the effect of the different recovery time of each diode (when reverse voltage is applied) will be to apply the full voltage across the first diode in the chain to recover. To overcome this problem, capacitors are connected across each diode in the chain to equalize the transient reverse voltage during the recovery period.

If very long chains of diodes are used to achieve very high voltage rectification, or if a high-frequency supply is used, the effect of stray capacitance to earth must be taken into account. The stray capacitance from each diode interconnection to earth, coupled with the diode junction capacitances, effectively form a capacitive ladder attenuator the effect of which is to apply an unfair share of the total reverse voltage across the early diodes in the chain (at the ac input end). The solution is to keep the ratio of shunt-to-stray-capacitance large, either by minimizing stray capacitance in the layout or by adding effective quantities of capacitance across each diode.

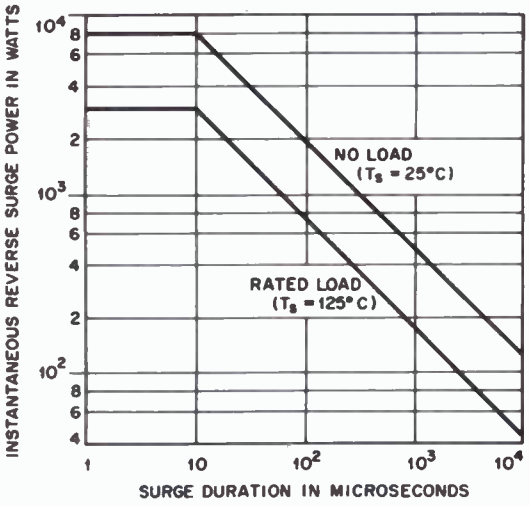

Fig. 6—Reverse surge-power rating of 10-ampere avalanche rectifier with stud temperatures corresponding to the no-load and rated-load conditions.

Heat Sinks

Heat-sink data are generally provided in the diode data sheets to enable the user to select a suitable size of heat sink in relation to the operating current, ambient temperature, and cooling medium (air, convection, or forced air). If the data are applicable to a number of different semiconductor devices, the information is generally set out in the form of graphs of temperature drop in the heat sink versus power dissipation in the device. It is then necessary to note from the silicon-diode data the maximum *case* (or *stud*) temperature that is permissible for a given flow of current. This temperature, less the temperature drop in the sink, is the maximum permissible ambient temperature for the particular working conditions.

Silicon junctions have a very low thermal mass, generally much lower than that of their associated heat sinks, and therefore the heat-sink calculations are only relevant to steady-state operating data. The heat sink will play little part in preventing a sudden burnout due to a heavy overcurrent transient, for example. The junction mass is so small, in fact, that its temperature will actually follow the cyclic variations of current at the supply frequency. This factor is taken into account by the manufacturer in arriving at a rated (mean) operating junction temperature at normal supply frequencies. At lower frequencies, the junction will more nearly reach its steady-state temperature corresponding to the peak of the alternating current; therefore care should be taken to derate appropriately if working at frequencies much lower than that of the normal supply.

SILICON AVALANCHE RECTIFIERS

The avalanche rectifier can withstand high reverse power dissipation without damage. As an example, an avalanche diode with normal forward rating of 10 amperes can dissipate a reverse transient power of 8 kilowatts for 10 microseconds without damage. Even for 10 milliseconds it can withstand a reverse power of 125 watts. Figure 6 illustrates the reverse power rating of such a diode when operated at no load (stud temperature= 25°C) and at rated load (stud temperature= 125°C).

The advantages of the avalanche diode follow.

(A) The elimination of surge absorption devices and networks required for conventional diodes.

(B) The elimination of voltage dividing networks from series-operated high-voltage diode chains.

(C) Fewer diodes are needed in series for a given voltage since there is no need to underrate them on reverse voltage to allow for transient peaks.

In very long chains of diodes designed for extra-high-voltage operation, or where a high supply frequency is used, it may still be advisable to use shunt dividing capacitors (but *not* resistors) even with avalanche rectifiers; this is because of the effects of carrier storage and stray capacitance.

ZENER DIODES

Zener is the name given to a class of silicon diodes having a sharp turnover characteristic at a particular reverse voltage, as shown in Fig. 7. If such a diode is operated in this part of its characteristic, no breakdown (in the sense of dielectric

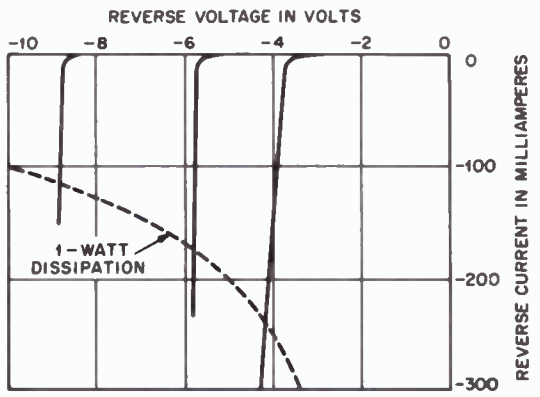

Fig. 7—Typical reverse characteristics for three low-voltage zener diodes of 1-watt rating. *From J. M. Waddell and D. R. Coleman, "Zener Diodes—Their Properties and Applications," Wireless World, vol. 66, no. 1, p. 18, fig. 2; January 1960.* *©1959, Iliffe Electrical Publications, Ltd., London, England.*

breakdown) occurs and the process is reversible without damage. The steepness of the reverse part of the current–voltage characteristic in the turnover region makes these diodes excellent elements for voltage reference and voltage regulation.

A factor of importance in circuit design is the slope resistance, which is the change of reverse voltage per unit change of current in the breakdown region. It is usual to distinguish between ac and dc slope resistance. The former is the dynamic resistance as measured at constant junction temperature. Under dc conditions, however, the junction temperature will stabilize at a new value for each different value of reverse current. The dc slope resistance will therefore be higher than the ac when the diode temperature coefficient is positive and lower when the coefficient is negative. Figure 8 shows typical ac slope resistances for diodes of different breakdown voltages, when run at various mean reverse currents. The temperature coefficient for a typical range of zener diodes is shown in Fig. 9. It will be seen that the coefficient changes from negative to positive in the region of 5 volts. Use is sometimes made of this phenomenon to match diodes of opposite coefficient to produce a series pair having a low effective temperature coefficient in combination.

The capacitance of a zener diode in its breakdown region is usually of no practical significance, since it is effectively shunted by the slope resistance of the diode in this region. At reverse voltages below breakdown, capacitance changes with voltage in a manner similar to that of a conventional diode, i.e., capacitance decreases with increase of voltage. Figure 10 illustrates typical values of capacitance for 1-watt zener diodes operated below their breakdown voltage.

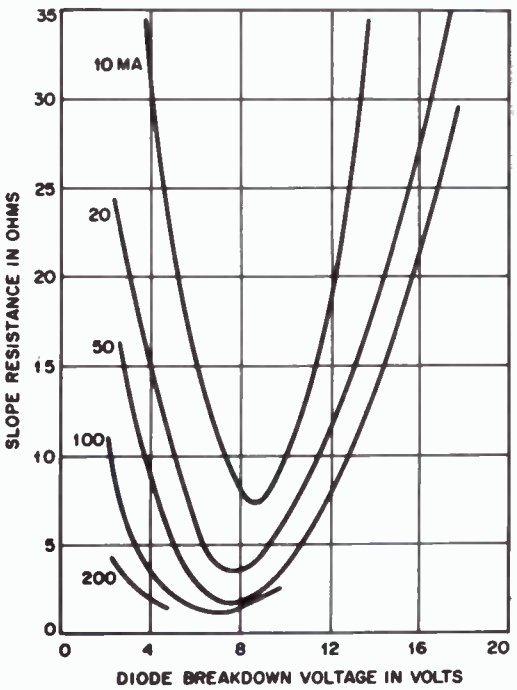

Fig. 8—Slope resistance for zener diodes of various breakdown voltages, at various operating currents. *From J. M. Waddell and D. R. Coleman, "Zener Diodes—Their Properties and Applications," Wireless World, vol. 66, no. 1, p. 18, fig. 3; January 1960. ©1959, Iliffe Electrical Publications, Ltd., London, England.*

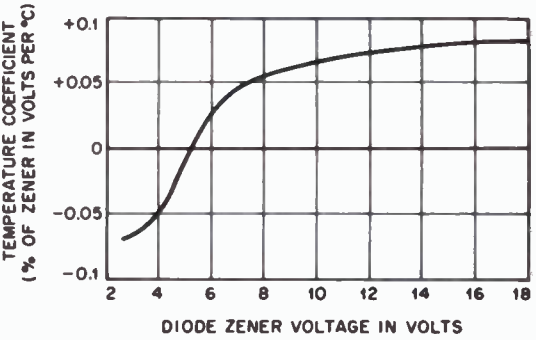

Fig. 9—Temperature coefficient for a typical range of low-voltage zener diodes. *From J. M. Waddell and D. R. Coleman, "Zener Diodes—Their Properties and Applications," Wireless World, vol. 66, no. 1, p. 18, fig. 4; January 1960. ©1959, Iliffe Electrical Publications, Ltd., London, England.*

Zener diodes have found a variety of low-voltage applications. In addition to voltage references and regulators, they are used as waveform clippers, voltage quantizers, and as coupling elements in dc logic circuits. Figures 11, 12, and 13 illustrate three simple applications of the zener diode.

THYRISTORS (SILICON CONTROLLED RECTIFIERS)

The thyristor* is much like a normal rectifier which has been modified to "block" in the forward direction until a small signal is applied to the control (gate) electrode. After the signal is applied, the device conducts in the forward direction with a forward characteristic very similar to that of a normal silicon rectifier and continues to conduct even after the control signal has been removed. The characteristics are similar to those of a gas thyratron except that the forward drop is about one tenth of that of a thyratron and the deionization time is shorter by several orders of magnitude. The maximum voltage that the thyristor will block is lower, in the present state of the art,

* This term, which indicates a general class of solid-state controlled rectifiers, is used throughout this section instead of the term "silicon controlled rectifier" (a 4-layer *pnpn* device that is the most common member of the class).

than can be achieved with thyratrons, but is considerably higher than normally obtainable with transistors.

A small pulse is required at the gate electrode to switch a thyristor on, and the anode supply must be removed, reduced, or reversed to switch it off. If proportional control is required, means must be provided for adjusting the phase of the trigger pulse with respect to the supply to control the proportion of the cycle during which the thyristor is permitted to conduct. In ac circuit applications, the switchoff is obtained by the natural reversal of the supply voltage every half-cycle; in dc circuits it is usual to charge a "commutating" capacitor during the "on" period and to apply this charge in negative polarity between the anode and cathode when it is desired to switch off.

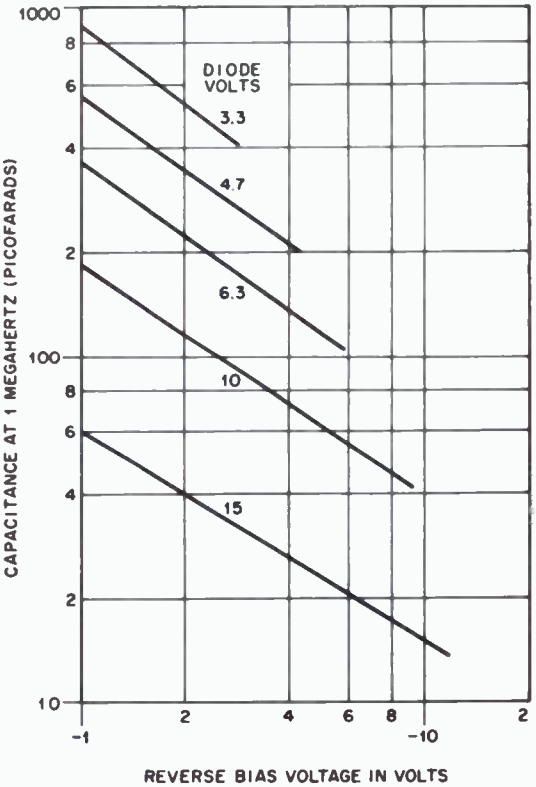

Fig. 10—Typical values of capacitance for 1-watt zener diodes of various voltages, operated below breakdown. *From J. M. Waddell and D. R. Coleman, "Zener Diodes—Their Properties and Applications," Wireless World, vol. 66, no. 1, p. 21, fig. 15; January 1960. ©1959, Iliffe Electrical Publications, Ltd., London, England.*

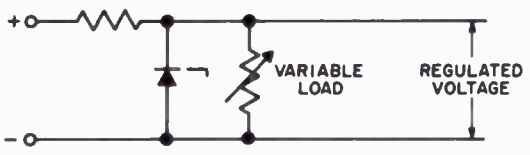

Fig. 11—Simple voltage regulator using a zener diode. *From J. M. Waddell and D. R. Coleman, "Zener Diodes—Their Properties and Applications," Wireless World, vol. 66, no. 1, p. 20, fig. 8; January 1960. ©1959, Iliffe Electrical Publications, Ltd., London, England.*

Ratings

Voltage and current ratings are generally expressed in similar terms to those for silicon rectifiers, as discussed in a previous section. It is necessary, however, to add the following ratings.

Peak Forward Blocking Voltage is the maximum safe value that may be applied, under recurrent or nonrecurrent transient conditions, while the thyristor is in the blocking state. The thyristor will break over into a conducting state regardless of gate drive if either (A) too high a positive voltage is applied between anode and cathode or (B) a positive anode–cathode voltage is applied too quickly (*dv/dt* firing). Even small voltage pulses, if their leading edges are sufficiently steep at the anode, can turn the thyristor on. Firing by condition (A) is avoided by making the peak forward blocking voltage lower than the breakover voltage of any thyristor of a particular type and by seeing that this voltage is not exceeded in practice. Trouble from *dv/dt* effects may be minimized by locating the gate wires to avoid stray coupling between anode and gate, by use of negative bias on the gate during blocking, and by use of *C–R*

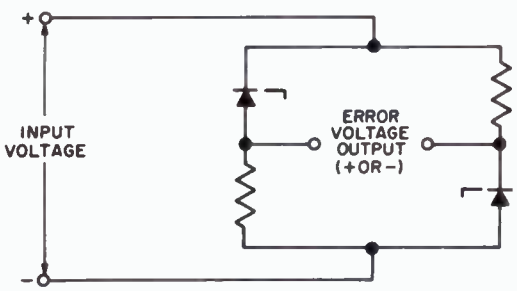

Fig. 12—Voltage reference or comparator circuit using zener diodes.

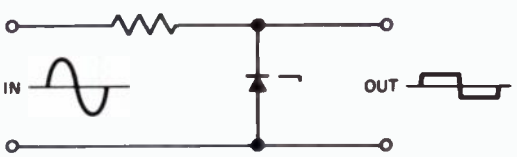

Fig. 13—Waveform clipper or surge limiter using a zener diode. *From J. M. Waddell and D. R. Coleman, "Zener Diodes—Their Properties and Applications," Wireless World, vol. 66, no. 1, p. 20, fig. 9; January 1960. ©1959, Iliffe Electrical Publications, Ltd., London, England.*

damping circuits between anode and cathode to slow down the rate of change of applied voltage.

Continuous Forward Blocking Voltage covers operation under dc conditions.

Peak Forward Gate Voltage is quoted for anode positive with respect to cathode and for anode negative with respect to cathode. The voltage rating is quite low in the latter case (typically 0.25 V) since reverse voltage rating is reduced by forward gate current.

Peak Reverse Gate Voltage is generally the same whether the anode is positive or negative with respect to the cathode.

Peak Forward Gate Current. Forward gate impedance is a finite value subject to quite large variations between samples and over a temperature range. It is usually necessary to plot a load line on gate current–voltage characteristics to determine the gate current that may flow due to a given external gate voltage and source resistance. Care must be taken that the rating is not exceeded with all known spreads of gate–cathode characteristic and temperature.

Gate Dissipation is generally given in terms both of average rating and of peak rating.

Characteristics

Characteristics of the thyristor important for circuit design are as follows.

Leakage Currents are specified for both forward and reverse blocking, at maximum applied voltage and at maximum rated temperature. Although these are low in comparison with forward conducting currents and can be neglected in assessing power losses, they must be taken into account in certain circumstances. An example would be a circuit in which a capacitor is slowly charged from

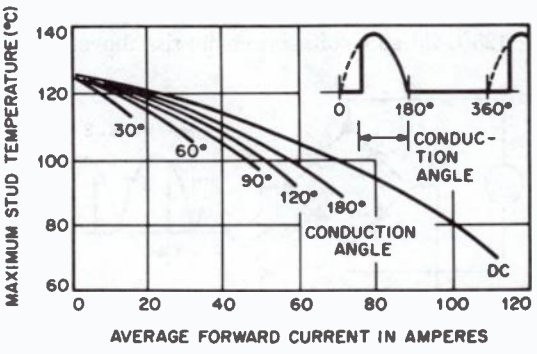

Fig. 14—Maximum permitted stud temperature vs average thyristor forward current in single-phase half-wave or bridge circuit feeding a resistive load. (70-ampere average rated thyristor.)

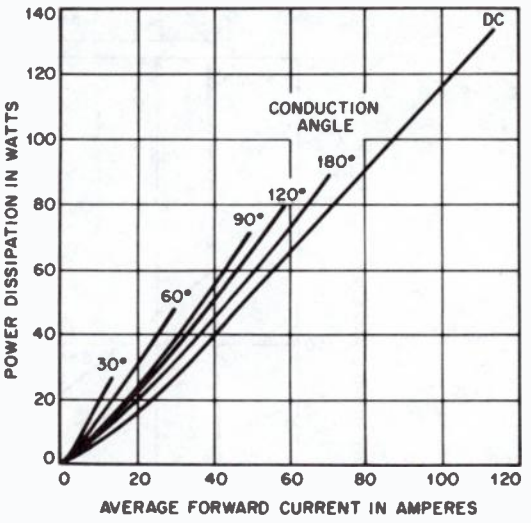

Fig. 15—Power dissipation vs average thyristor forward current in single-phase half-wave or bridge circuit feeding a resistive load. (70-ampere average rated thyristor.)

an external source and then suddenly discharged through a thyristor into a second circuit (as in pulse modulators); the capacitor charging operation may be affected by the amount of forward leakage current conducted by the thyristor in its blocking state.

Holding Current is the minimum anode–cathode current that will keep the thyristor conducting after it has been switched on. In some applications a thyristor with a high holding current is wanted so that it can be turned off easily without the need of reducing the anode current to a very low level. In other applications, where a low load current is normal, it might be desirable to have a low holding current to ensure that the thyristor latches on reliably with light loading.

Forward Voltage Drop is important in assessing power loss. The same methods of assessing power loss in terms of the forward current–voltage characteristic apply as in the case of silicon rectifiers. It is impracticable to measure the junction temperature under working conditions, and therefore the manufacturers list maximum values of stud or case temperature related to the forward current. This is expressed in the form of a graph, as shown in Fig. 14. Note that since the ratio of rms to average forward current varies with the angle of conduction, the power dissipation for any average current also varies with this angle. Figure 14 is drawn for fractional sine waves, as would apply to the cases of single-phase half-wave or bridge rectifier circuits working into a resistive load.

Figure 15 shows a typical relationship between power dissipation and average current for a 70-

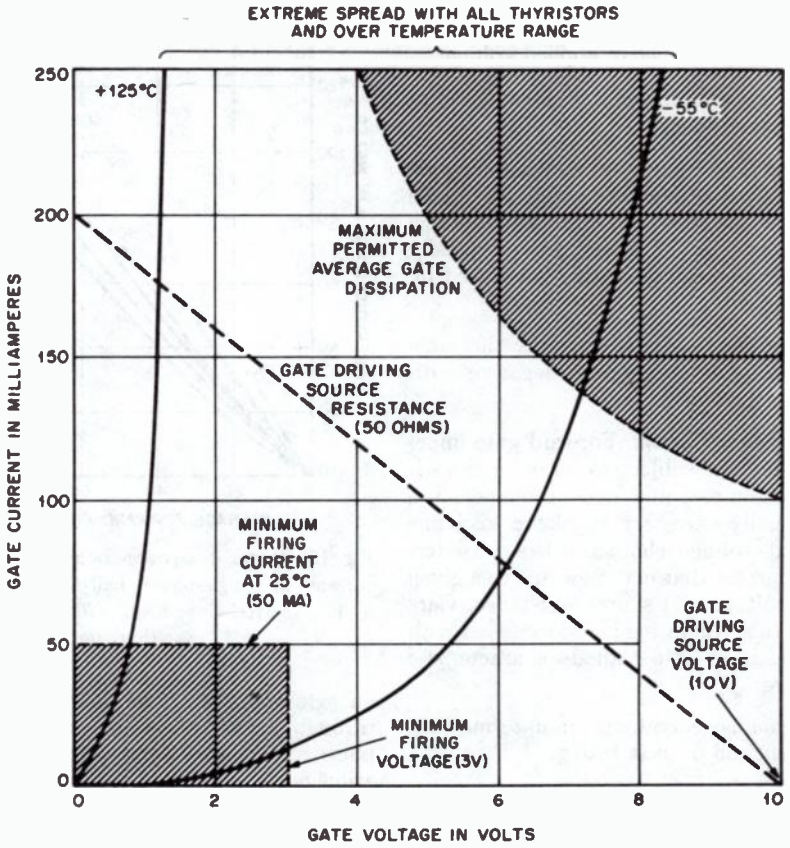

Fig. 16—Gate current–voltage characteristics for all samples of one type of thyristor (70-ampere rating) and for an extreme range of temperature. The maximum rated average gate dissipation is shown and a load line is drawn for typical values of gate driving source voltage and resistance.

ampere thyristor under the same circuit conditions. The two types of graphs illustrated by Figs. 14 and 15 together enable one to calculate the thermal resistance of heat sink required to keep the thyristor below its maximum temperature ratings under given working conditions of current and ambient temperature.

Gate Trigger Sensitivity is specified in terms of a minimum voltage and/or current that must be applied to ensure that all samples of a particular type of thyristor will be triggered into conduction. The minimum voltage is not temperature sensitive but the minimum trigger current varies considerably with temperature, more current being required to turn on at low temperature than at high. The basic requirements of a gate drive circuit are therefore that the driving voltage and source resistance must be such that either the minimum voltage or the minimum current (or both) are exceeded but that the rated gate dissipation is not exceeded. These points are illustrated in Fig. 16, which shows a portion of the gate current–voltage characteristics for a 70-ampere range of thyristors.

In Fig. 16 the two thyristor gate curves represent extremes of characteristics for all thyristors of this type operated over a wide temperature range. The shaded areas must be avoided because of the danger of excess gate dissipation or the danger of inadequate triggering level applied. Any driver load line which avoids these areas, such as the line illustrated, will be satisfactory. Note that in the case of the high-conductance thyristor operated at +125°C the gate voltage does not rise above 1.25 V.

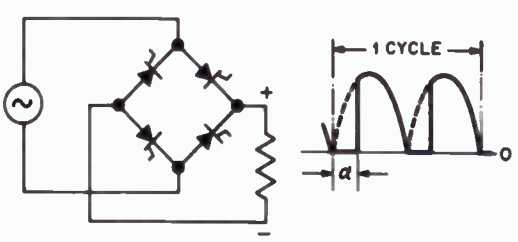

Fig. 17—Full-controlled single-phase thyristor bridge. The broken lines indicate the path of the normal waveform at full conduction, i.e., where $\alpha = 0°$ and the circuit behaves like a diode rectifier. α is the firing angle delay. Delay range required for this circuit is 0° to 180°.

Although this is less than the minimum 3 V specified, the thyristor will fire satisfactorily because the gate current is 175 mA, which is considerably greater than the 50 mA minimum specified. In Fig. 16 the power-dissipation curve corresponds to the average rated value. In practice one very rarely applies steady dc to the gate and, in the cases of pulses or half-sine waves, it is perfectly in order for the load line to cut into the area shown *provided that the peak gate dissipation is not exceeded* (a separate curve may be plotted for this) and so long as the average dissipation (averaged over a complete cycle) is within the limit given.

Switching Times of importance are the turnon and turnoff times, the latter generally being at least one order greater than the former. When a gate signal is applied to the thyristor, there is a finite delay time during which the anode current remains at its normal blocking level; this is followed by a "rise time" during which the anode current increases from its blocking level to a value determined by the external load circuit. Turnon time is the sum of these two times. For a given thyristor the turnon time is influenced by the magnitude of gate drive, the load current to be achieved, and, to a lesser extent, the applied anode supply voltage. The time is reduced by high gate drive, low load current, and high anode supply voltage. Turnoff time is similarly composed of two individual periods; the first is a storage time, analogous to that obtained with a saturated transistor, and the second is a recovery time. Forward voltage may not be reapplied before the completion of both phases of the turnoff process or the thyristor will conduct again. After this period, however, forward voltage may be applied and the thyristor will remain in its blocking state so long as the rate of rise of anode voltage is not allowed to exceed the specified maximum dv/dt, as already discussed.

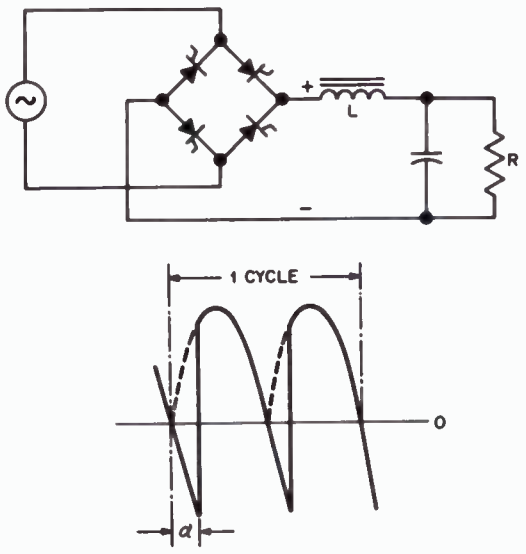

Fig. 18—Full-controlled single-phase thyristor bridge working into an inductive load where $\omega L \gg R$. Delay range required is 0° to 90°.

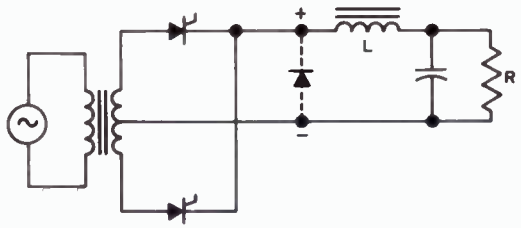

Fig. 19—Half-controlled single-phase thyristor bridge working into inductive load. Common-anode thyristor connection. Waveform and delay range as for Fig. 17.

THYRISTOR CONTROLLED RECTIFIER CIRCUITS

Figures 17 to 22 are basic circuits of thyristors used as controlled rectifiers. In many applications it is not necessary for all rectifier elements to be controllable, and it is common to find bridges composed of thyristors and ordinary diodes in equal numbers; such circuits are called *half-controlled*, whereas those containing only thyristors are termed *full-controlled*.

Figures 17 and 18 show a full-controlled single-phase thyristor bridge, the thyristor circuit being the same whether a resistive or inductive load is being driven. The voltage waveforms are different, however, in the two cases. The principal difference of practical importance is that the range of firing-pulse phase control is required to be different in the two cases. For the resistive load, phase control over the range 0° to 180° is necessary to obtain

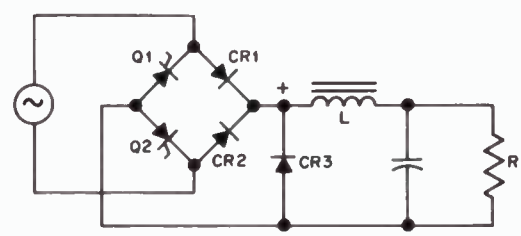

Fig. 20—Full-controlled single-phase push-pull thyristor rectifier working into inductive load. With diode connected, waveform and delay range are as for Fig. 17. Without diode, waveform and delay range are as for Fig. 18 (if $\omega L \gg R$). Addition of diode reduces critical inductance of L for continuous current.

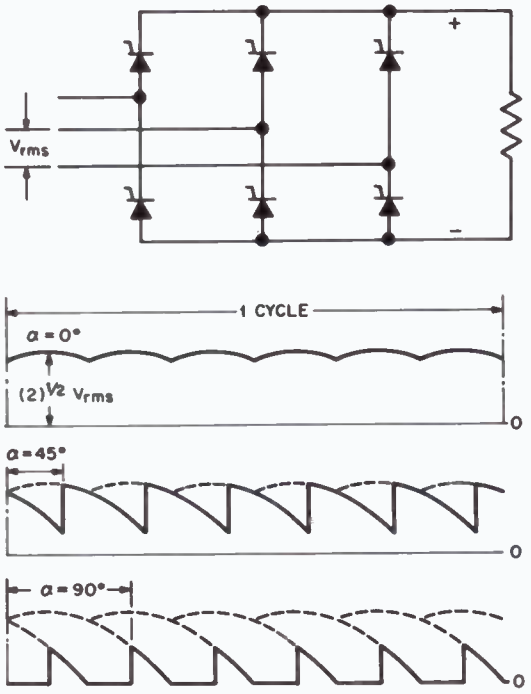

Fig. 21—Full-controlled three-phase thyristor bridge working into resistive load; waveforms of voltage output are shown for three values of α. Waveform develops characteristic flat portion when $\alpha \geq 60°$. Delay range required is 0° to 120°.

full control from maximum output voltage down to zero; for an almost pure inductive load (i.e., a very high $\omega L/R$ ratio) full-phase control is obtained with a range of only 0° to 90°.

Figure 19 shows a half-controlled single-phase rectifier driving an inductive load. For such loads a bypass diode*, CR3, must be added at the output; at the end of a voltage half-cycle, current still flows in the choke, but in this circuit the current is transferred at the end of the voltage half-cycle to the bypass diode. The two important effects of this diode are (A) that the output voltage is clamped to zero while this inductively maintained current flows, so that the output waveform is the same as with Fig. 17 (having the characteristic flat portion) and (B) the transfer of load current from the thyristor to the diode turns the thyristor off. If CR3 were not present, the waveform would still be the same since a zero voltage clamp would exist through a series combination CR1–Q1 or CR2–Q2, depending on which thyristor was conducting the previous half-cycle. However, this flow of uncontrolled current through the thyristor, bypassing the supply, is undesirable; for example, should it be required that the output voltage be turned off by removal of gate pulses, this action may prove to be impossible. The thyristor can be held on continuously through the negative half-cycle by inductive circulating current and is then ready to conduct the next positive half-cycle. Thus the gate has lost control and a continuous half-wave output is produced. The bypass diode overcomes these difficulties by ensuring thyristor turnoff at the end of each voltage half-cycle.

Figure 20 is a push–pull controlled rectifier circuit. Figure 21 is a three-phase full-controlled rectifier circuit. Figure 22 shows the circuit of a three-phase half-controlled rectifier, the bypass diode being necessary only for inductive loads.

In all the cases illustrated in which a bypass diode is used, this diode must be rated continuously for a maximum average current equal to the load current if the full load current is to be drawn when

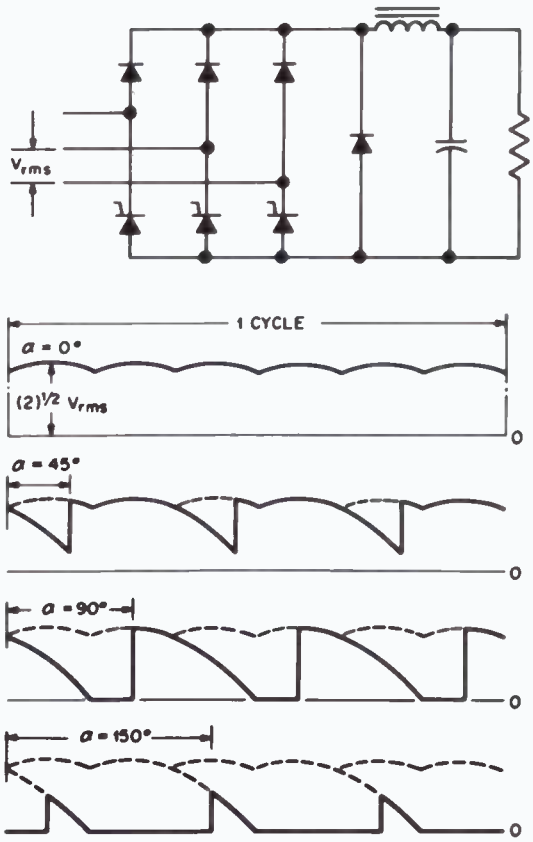

Fig. 22—Half-controlled three-phase thyristor bridge. The bypass diode is necessary only when feeding an inductive load. The waveforms are the same for resistive or inductive load. Delay range required is 0° to 180°. Note that the three thyristors could have been put in the positive bridge arms; it is more usual to put them in the negative arms because a common anode connection permits the use of a common heat sink when thyristors with anode studs are used.

* Sometimes called a "commutating," "freewheel," or "flywheel" diode.

TABLE 5—MEAN DC OUTPUT VOLTAGE FOR THYRISTOR CONTROLLED RECTIFIERS.

Circuit	V_{do}	$V_{d\alpha}$
Fig. 17	$2E_p/\pi$	$V_{do}\frac{1}{2}(1+\cos\alpha)$
Fig. 18	$2E_p/\pi$	$V_{do}\cos\alpha$
Fig. 19	$2E_p/\pi$	$V_{do}\frac{1}{2}(1+\cos\alpha)$
Fig. 20, no diode and inductive load	$2E_p/\pi$	$V_{do}\cos\alpha$
Fig. 20, all other cases	$2E_p/\pi$	$V_{do}\frac{1}{2}(1+\cos\alpha)$
Fig. 21	$3E_p/\pi$	$V_{do}\cos\alpha$, for $\alpha=0°$ to $60°$ $V_{do}[1+\cos(\alpha+60°)]$, for $\alpha=60°$ to $120°$
Fig. 22	$3E_p/\pi$	$V_{do}\frac{1}{2}(1+\cos\alpha)$

the average output voltage is reduced almost to zero. In practice, a larger diode is often used in this position than in the bridge arms, or several diodes may be used in parallel.

For each of the circuits illustrated in Figs. 17 through 22, Table 5 gives equations for the average dc output voltage, $V_{d\alpha}$, at any angle α in terms of the maximum average dc output voltage, V_{do}, obtained at $\alpha=0°$. The table also shows the value of V_{do} for each circuit in terms of the peak sinusoidal input voltage, E_p. For the single-phase push–pull circuit, the peak input voltage is E_p—0—E_p, and for all the three-phase circuits E_p means the peak value of the line-to-line voltage.

THYRISTOR AC POWER CONTROL CIRCUITS

Figures 23, 24, and 25 show three basic circuits for single-phase ac control, and Figs. 26, 27, and 28 show the load voltage and current waveforms applicable to all three when driving purely resistive and inductive loads.

The load rms current I_{rms} at any phase delay angle α is given in terms of the normal full-load rms current at $\alpha=0°$, I_{rms-0}, by

$$I_{rms}=I_{rms-0}[1-(\alpha/\pi)+(2\pi)^{-1}\sin 2\alpha]^{1/2}.$$

The load rms voltage bears the same relation to the full-load rms load voltage. This equation shows that, although the theoretical delay range for complete control is 0° to 180°, a practical range of 20° to 160° gives a power control of approximately 99% to 1% of maximum.

Figure 23 requires a trigger pulse source having a pair of isolated outputs, insulated from each other by at least the peak value of the supply voltage; the two pulse trains must be phased 180° with respect to each other and must shift together, with respect to the supply voltage phase, when the power throughput is adjusted. Provided that two separate pulse trains are used, it is permissible for the two trains to be identical, operating at twice the supply frequency; the thyristor whose anode–cathode is forward-biased will fire when pulses are applied to both. Normally it is not considered safe to drive a thyristor gate positive while its anode is reverse-biased; however, in this circuit it is permissible since the thyristor that is fired immediately removes the reverse voltage from the other.

Figure 24 is a variation of the basic circuit and removes the necessity for isolation of the two pulse

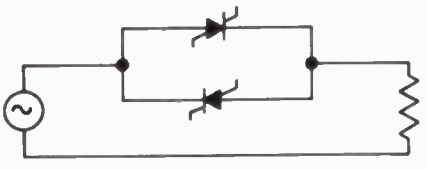

Fig. 23—Inverse-parallel ac control circuit.

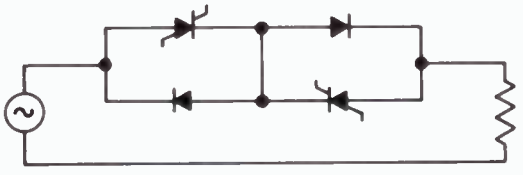

Fig. 24—Inverse-parallel bridge ac control circuit.

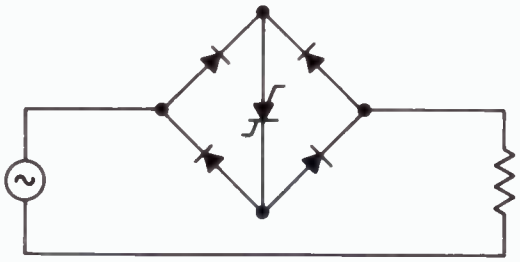

Fig. 25—Single thyristor ac control circuit.

trains from each other; the common thyristor cathode connection permits the use of a simple three-terminal push–pull pulse source. The advantage is gained, however, at the expense of two extra diodes, each of which must be rated for the same current and voltage as the thyristors; there will be twice the heat dissipation compared with the simpler circuit and it is therefore generally used only in low-power circuits (up to about 5 amperes rms load current). Since no reverse voltage, or at least not more than 1 or 2 volts, can be applied to the thyristors in the circuit of Fig. 24, this circuit may be preferred if transient spike voltages are likely to be present on the supply. In Fig. 24 the only resulting breakdown in the thyristors must be in the forward direction, which is not as dangerous as reverse breakdown because the thyristor is automatically turned on by the overvoltage and the voltage across it rapidly drops to zero.

Figure 25 is another variation that is used in low-power control systems. Its main advantage is the use of a single thyristor, with the consequent simplification of trigger circuits. Its main disadvantage is that the conducting path in each direction contains three devices, two diodes and a thyristor in series, with relatively high power dissipation.

With inductive loads, as shown in Fig. 28, there is a sharp transient change of load voltage at the end of each current loop. This may not be important to the load but it does stress the thyristors. Thus at the end of the first positive loop of current, as shown by the dotted waveform in the upper diagram of Fig. 28, the conducting thyristor turns off, thereby disconnecting the load from the supply;

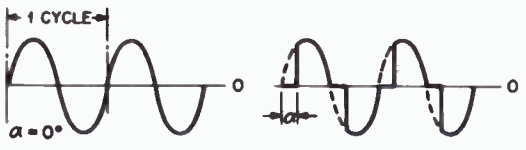

Fig. 26—Load voltage and current waveforms for full and reduced conduction angles (purely resistive load). Delay range required is 0° to 180°.

the voltage at the load therefore rapidly returns to ground. The effect of this transient voltage in the circuits of Figs. 23 and 24 is to apply a sharply rising positive anode voltage to the thyristor opposing the one which has been conducting. If the rated dv/dt is exceeded, this thyristor will then turn on and conduction will take place independent of the gate drive. The rate of rise of voltage may, however, be controlled by adding a resistor in shunt with the load; the rate of rise of voltage will then be determined by the time constant L/R where L is the load inductance and R is the series sum of the load resistance and the added resistor. This resistor has the further advantage of providing a direct resistive path for thyristor current so that

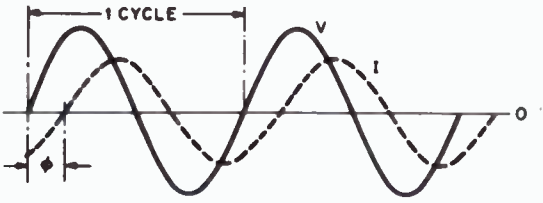

Fig. 27—Voltage and current with full conduction into inductive load.

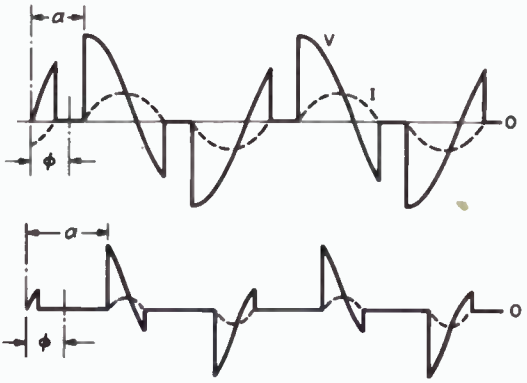

Fig. 28—Voltage and current with reduced conduction, $\alpha > \phi$.

the holding current is established quickly after turnon instead of at a time determined by the rate of rise of load current, which is fixed by the applied voltage and load inductance.

When an intervening transformer couples the load to the thyristor control circuit, it is particularly important to ensure that the two thyristors are fired exactly at 180° relative to each other. If this is not achieved, the positive and negative current loops will differ in magnitude and a resultant dc will flow through the primary of the transformer. For this reason it is unsatisfactory to determine the firing phases by independent trigger circuits using, for example, separate trigger diodes which may differ in breakdown voltage.

The above ac control circuits may be used, via transformers, to drive ordinary diode rectifier circuits; this is done where it is inconvenient to use thyristors in the rectifier circuit itself, because either the rectifier current or the voltage level is too high for existing thyristors.

There are similarly several basic methods of three-phase ac power control, as illustrated by Figs. 29 and 30. Figure 30 is used more frequently for its economy in parts. When driving a transformer–rectifier load, care must be taken to ensure that the phase of thyristor gate pulses bears the correct relationship with the commutation phases of the diode rectifier.

In Figs. 29 and 30 the required delay range of pulses is 0° to 210° with respect to the supply phase-to-neutral voltages. When driving a transformer–rectifier, the necessary delay range is reduced to 120° for Fig. 29 and to 180° for Fig. 30. For star–star or delta–delta transformer connection the zero firing phase corresponds to 30° lag behind the supply phase-to-neutral zero phase. For a delta–star connection the zero firing phase corresponds to the supply phase-to-neutral phase.

THYRISTOR SERVO SYSTEMS

Closed-loop feedback servo systems may be constructed using thyristors as the control element. Figure 31 illustrates three typical systems. Figure 31A represents a voltage-regulated power supply system, for either single- or three-phase inputs. A line transformer feeds a thyristor controlled rectifier of one of the types described, and the output passes through a smoothing filter to the dc load. A portion of the load voltage is compared with a zener diode (or similar) voltage reference and the difference is used to control the phase of trigger pulses applied to the thyristor gates. The usual feedback stability criteria apply. Assuming the use of a trigger phase-shift circuit having a reasonably linear phase-vs-input-voltage characteristic, the low-frequency gain of the system is greatest at the steepest part of the $V_{d\alpha}$–α curve, as defined for various circuits by Table 5. The greatest value of the slope $dV_{d\alpha}/d\alpha$ occurs at $\alpha = 90°$ for all the equations shown in Table 5 except those for Fig. 21; here the maximum slope occurs at $\alpha = 60°$. The choke critical inductance and the input ripple to the smoothing filter are both much greater for controlled rectifier circuits than for conventional diode rectifiers. The normal single-stage choke-input filter will have a 12-dB-per-octave response slope at quite a low frequency. It is therefore necessary for stability to ensure that the feedback control circuit has a low cutoff frequency sufficient to reduce the loop gain well below unity at the smoothing-filter cutoff frequency.

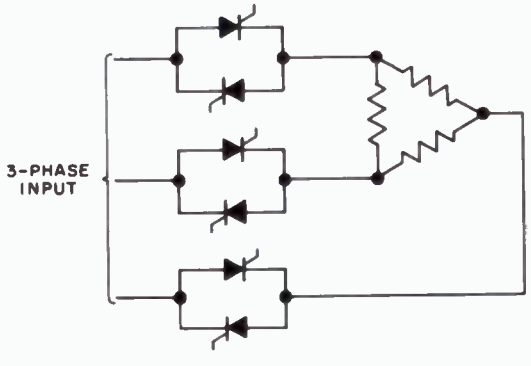

Fig. 29—Full-thyristor three-phase ac control.

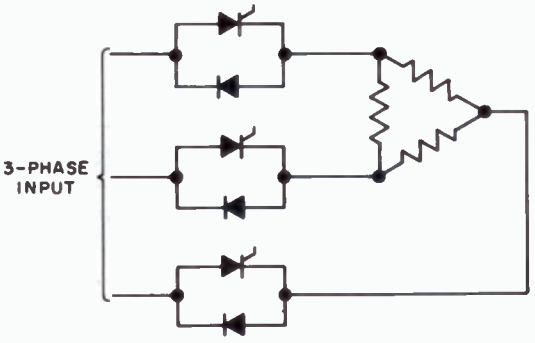

Fig. 30—Half-thyristor three-phase ac control.

Figure 31B illustrates thyristor ac control on the primary side of the rectifier transformer, with ordinary diode rectification on the secondary. With this arrangement it is important to protect the thyristors from the rapid dv/dt transient that can occur on actuating the circuit on the supply side. The solution is to apply capacitance on the mains side of the thyristor stack, between line and neutral or from line to line, which in conjunction with normal mains reactance will slow the rate of rise of thyristor anode voltage sufficiently.

Figure 31C involves no rectification. This is a simple oven temperature control in which a thermistor is used for temperature sensing.

THYRISTOR INVERTERS AND CHOPPERS

Application in pure dc circuits and in dc-to-ac conversion is more complex than in ac circuits because the means of turning the thyristors off cyclically is not automatically present in supply reversals. Inverters generally use a separate oscillator to provide timing for the gate circuits. Industrial sequence switching applications often charge a capacitor during the on period of a thyristor and discharge it in reverse through the

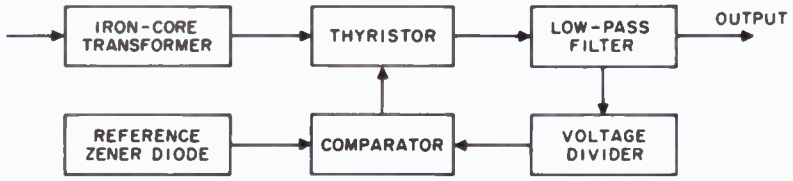

A. VOLTAGE-REGULATED DC POWER SUPPLY SYSTEM.

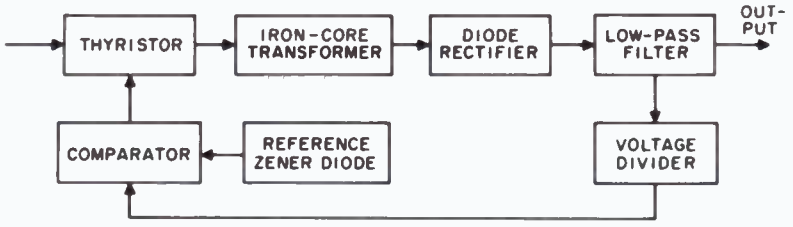

B. VOLTAGE-REGULATED DC POWER SUPPLY SYSTEM, USING THYRISTOR AC CONTROL ON THE TRANSFORMER PRIMARY.

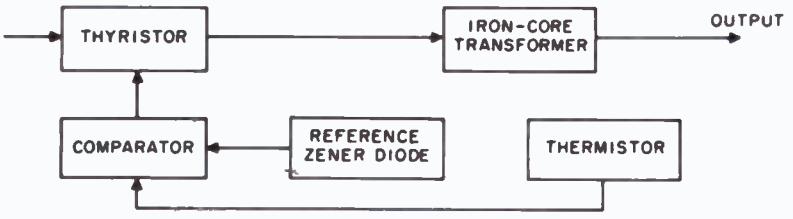

C. TEMPERATURE-CONTROLLED AC POWER SUPPLY SYSTEM, USING THERMISTOR SENSING.

Fig. 31—Three examples of closed-loop thyristor control systems.

thyristor when it is to be turned off. Monostable switching is also achievable by using *L–C* circuits in which reverse oscillatory current is used to turn off the thyristor at a predetermined time after turnon.

High-power inverters use thyristors designed as gate-controlled switches or for turnoff type of operation. Conventional thyristors may be operated successfully from dc in ring counters and other low-power applications.

Direct-current chopper circuits for power control or for small servos have an advantage over conventional dc power circuits by being able to operate at higher frequencies. This improves the response time of control systems and enables smaller iron-core parts to be used. The upper frequency limit of operation is determined by thyristor turnoff time and the drop in efficiency created by switching times that are an appreciable fraction of the overall cycle.

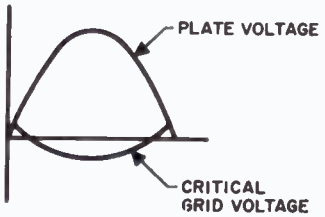

Fig. 32—Critical grid voltage versus plate voltage.

GRID-CONTROLLED GAS RECTIFIERS

Grid-controlled rectifiers are used to obtain closely controlled voltages and currents. They are commonly used in the power supplies of high-power radio transmitters. For low voltages, gas-filled tubes such as argon (those that are unaffected by temperature changes) are used. For higher voltages, mercury-vapor tubes are used to avoid flashback (conduction of current when plate is

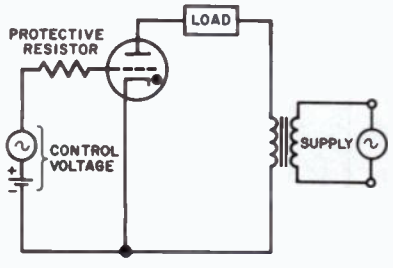

Fig. 33—Basic thyratron circuit. The grid voltage has dc and ac components.

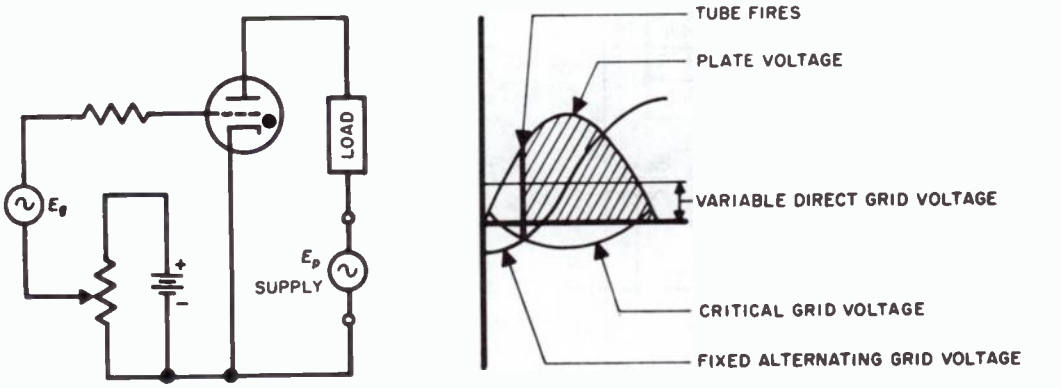

Fig. 34—Control of plate-current conduction period by means of adjustable direct grid voltage. E_g lags E_p by 90°.

negative). These circuits permit large power to be handled, with smooth and stable control of voltage, and permit the control of short-circuit currents through the load by automatic interruption of the rectifier output long enough to permit short-circuit arcs to clear, followed by immediate reapplication of voltage.

In a thyratron, the grid has a one-way control of conduction, and serves to fire the tube at the instant that it acquires a critical voltage. Relationship of the critical voltage to the plate voltage is shown in Fig. 32. Once the tube is fired, current flow is generally determined by the external circuit conditions; the grid then has no control, and plate current can be stopped only when the plate voltage drops to zero.

Basic Circuit

The basic circuit of a thyratron with ac plate and grid excitation is shown in Fig. 33. The average plate current may be controlled by maintaining the following.

(A) An adjustable direct grid voltage plus a fixed alternating grid voltage that lags the plate voltage by 90 degrees (Fig. 34).

(B) A fixed direct grid voltage plus an alternating grid voltage of adjustable phase (Fig. 35).

Phase Shifting

The phase of the grid voltage may be shifted with respect to the plate voltage as follows.

(A) Adjusting the indicated resistor in Fig. 35.

(B) Adjusting the inductance of the saturable reactor in Fig. 35.

(C) Adjusting the capacitor in Fig. 36.

On multiphase circuits, a phase-shifting transformer can be used.

For a stable output with good voltage regulation, it is necessary to use an inductor-input filter in the load circuit. The value of the inductance is critical, increasing with the firing angle. The design of the plate-supply transformer of a full-wave circuit (Fig. 36) is the same as that of an ordinary full-wave rectifier, to which the circuit of Fig. 36 is closely similar. Grid-controlled rectifiers yield larger harmonic output than ordinary rectifier circuits.

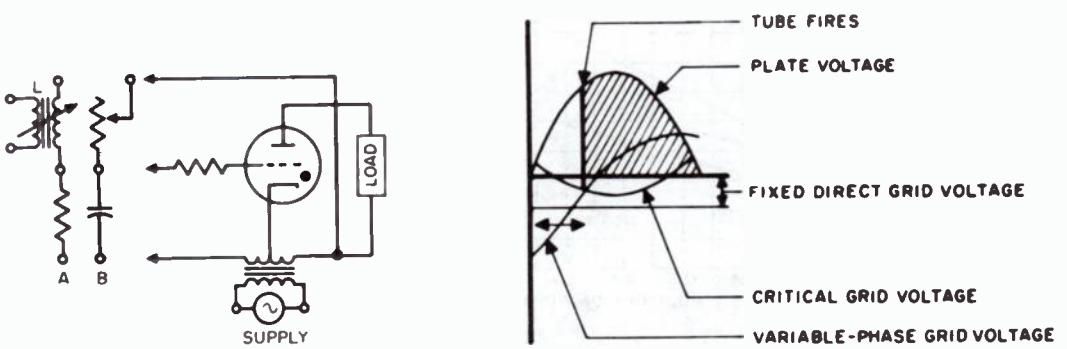

Fig. 35—Control of plate-current conduction period by fixed direct grid voltage (not indicated in schematic) and alternating grid voltage of adjustable phase. Either inductance–resistance (A) or capacitance–resistance (B) phase-shift networks may be used. L may be an adjustable inductor of the saturable-reactor type.

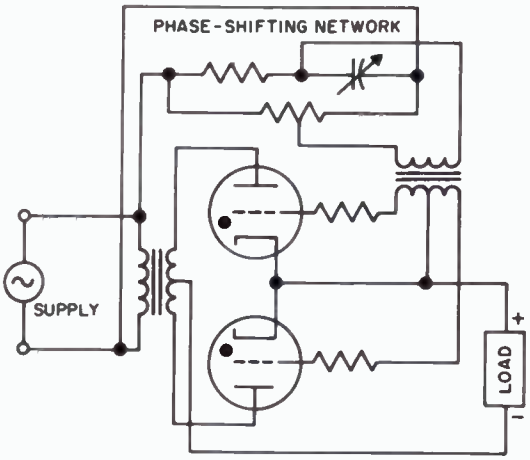

Fig. 36—Full-wave thyratron rectifier. The capacitor is the adjustable element in the phase-shift network and hence gives control of output voltage.

SELENIUM RECTIFIERS

Ratings

It is common practice to rate a selenium rectifier cell on the basis of the root-mean-square sinusoidal voltage that it can withstand in the reverse direction and on the average forward current that it will pass at a certain current density. Typical ratings at 35°C ambient temperature are: 26 volts rms per cell, and 600 milliamperes dc per square inch of active rectifying area. High-current-density selenium plates can operate continuously at up to 1950 milliamperes per square inch of active area.

Forward Characteristics

Typical dynamic forward voltage-drop characteristics for selenium rectifiers are shown in Fig. 37. The forward voltage drop per rectifying element or plate is highest for battery-charging and capacitive load applications, due to the high ratio of root-mean-square current to average direct current.

Rating of a Selenium Rectifier Stack

Stacks are operated at a temperature that is a safe value with allowance for aging. Catalog rating is in most cases based on an ambient temperature of 35 degrees Celsius. Ratings for higher temperatures (Fig. 38) are based on reduction in forward current to reduce forward-current losses, reduction in reverse voltage to reduce reverse-current losses, or a combination of both forward-current and reverse-voltage reductions to obtain the desired operating temperature with good electrical efficiency. The forward voltage drop and consequent heating depend to a small degree on the temperature of the rectifier cell, as does also the reverse current.

The 35°C rating of a rectifier is based typically on a current density for a cell of 600 milliamperes

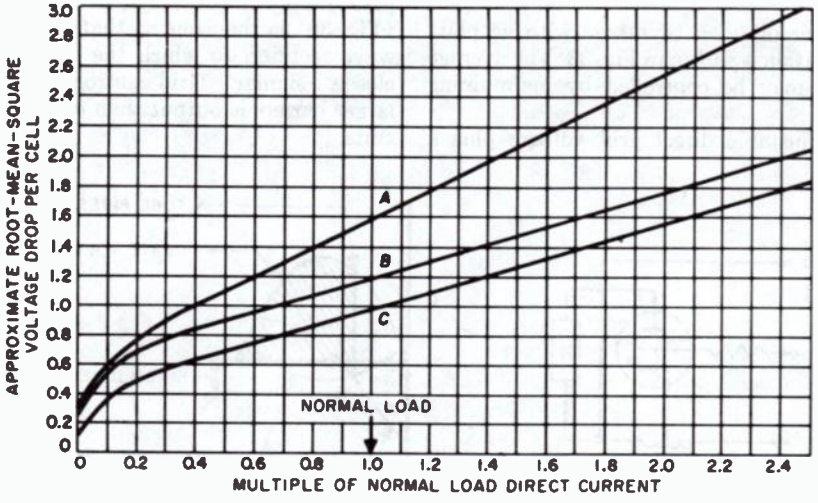

Fig. 37—Typical dynamic forward-voltage-drop curves for selenium-rectifier cells, at 65°C cell temperature. A—Battery or capacitive loads: single-phase half-wave, bridge, or center-tap. B—Resistive or inductive loads: single-phase half-wave, bridge, or center-tap; and 3-phase half-wave. C—All types of loads: 3-phase bridge or center-tap.

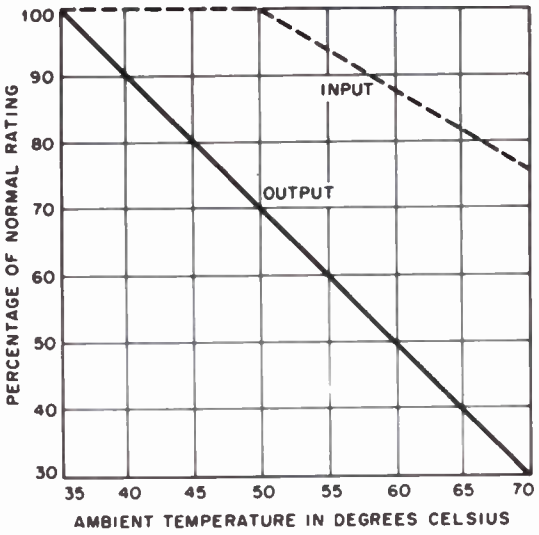

Fig. 38—Selenium-rectifier temperature derating curves (approximate), for root-mean-square alternating input voltage and average direct output current based on 35-degree-Celsius ambient.

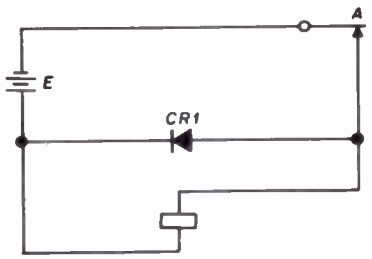

Fig. 39—Conventional method of using the selenium rectifier as a spark suppressor.

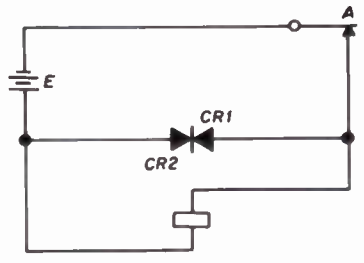

Fig. 40—Method of improving the release time by adding a second rectifier.

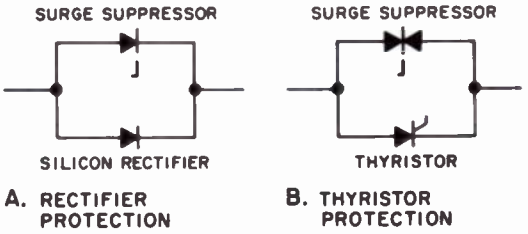

Fig. 41—Basic surge-suppressor configurations.

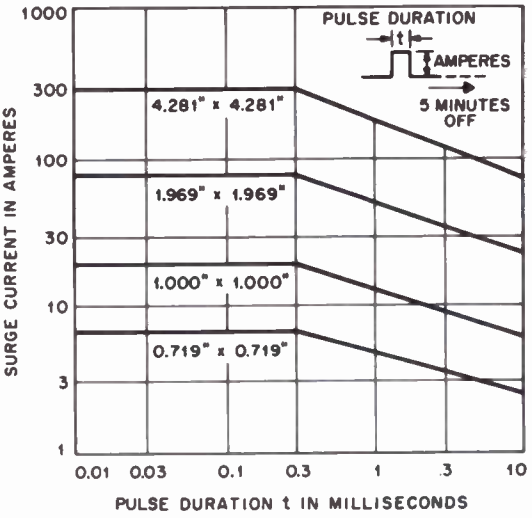

Fig. 42—Surge current vs duration for several sizes of selenium surge-suppressor plates.

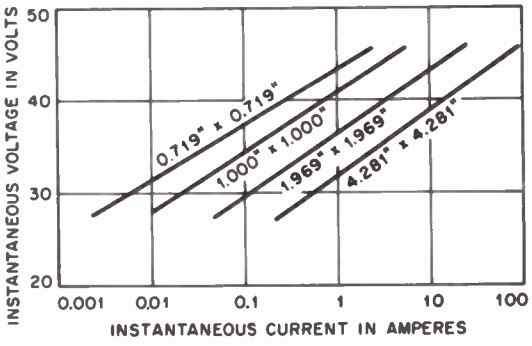

Fig. 43—Instantaneous reverse voltage vs instantaneous reverse current for several sizes of surge-suppressor plates.

TABLE 6—PEAK VOLTAGES AND RELEASE TIMES FOR ELECTROMAGNETS WITH DIFFERENT CONTACT PROTECTIONS. *Courtesy of Transactions of the AIEE.*

Contact Protection	Telephone Clutch Magnet $L=0.485$ henry $R=164$ ohms $I=0.293$ ampere		Telephone Relay $L=3.45$ henries $R=1650$ ohms $I=0.029$ ampere	
	Release Time in Milliseconds	Peak Voltage at Contact	Release Time in Milliseconds	Peak Voltage at Contact
Three 9/32-inch-diameter selenium cells (Fig. 39)	4.0	83	55.0	57
Two 9/32-inch-diameter selenium cells (Fig. 40)*	1.3	180	12.0	150
Three 1-inch square selenium cells (Fig. 40)*	1.3	192	10.9	169
Silicon-carbide varistor	1.3	210	12.8	140
0.5 microfarad+510 ohms	—	arcing	10.9	160
0.1 microfarad+510 ohms	—	arcing	7.9	259
Unprotected	1.0	400 to 900	7.6	450 to 750

* For each rectifier, CR1 and CR2.

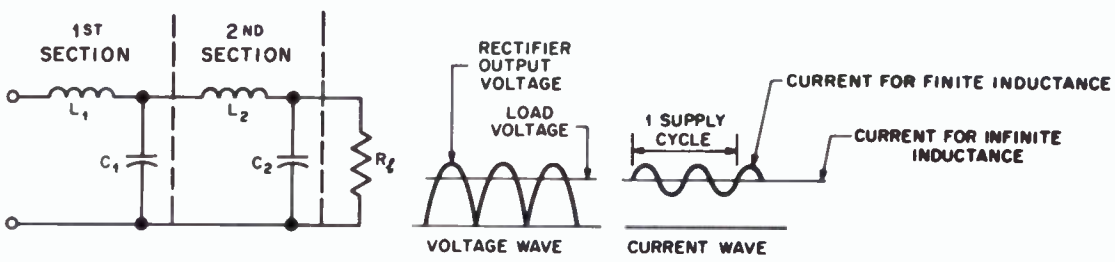

Fig. 44—Inductor-input filter.

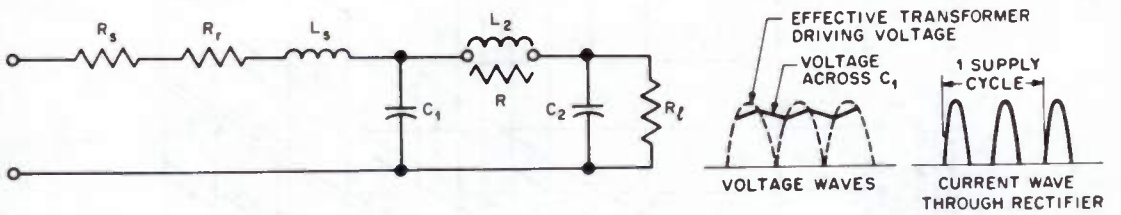

Fig. 45—Capacitor-input filter. C_1 is the input capacitor. $R_s = \frac{1}{2} \times$ (secondary-winding resistance). L_s = leakage inductance viewed from $\frac{1}{2}$ secondary winding. R_r = equivalent resistance of IR drop in rectifier element.

per square inch of active rectifying area. While each cell has this basic rating, it is common practice to increase the current density for the same temperature rise by increasing the space between cells or by using forced-air or oil cooling. The increase in spacing allows for current-density increases from 20 to 50 percent; the higher percentage applies to smaller cells. This causes some reduction in efficiency due to higher voltage drop.

The cells at each end of a stack have the lowest temperature due to greatest cooling there. Cell temperatures rise successively from each end toward the center of the stack. In a long stack, the temperatures of a number of the central cells are practically identical. As a consequence, some manufacturers raise the rating of stacks of 1 to 8 cells as much as 50 percent, and of stacks of 9 to 16 cells as much as 25 percent. These increases apply only to the normal-spaced convection-cooled ratings and not to the wide-spaced or forced-air-cooled or oil-cooled ratings.

For forced-air-cooled or oil-cooled rectifiers, experience shows that up to twice the normal rating is a good design figure to use when long life, good efficiency, and good voltage regulation are emphasized.

RECTIFIERS FOR MAGNETIC AMPLIFIERS

Rectifiers used in conjunction with magnetic amplifiers must have low reverse leakage currents to obtain as high a gain as possible with a given set of components. Rectifier leakage current behaves like negative feedback, thus reducing amplification. Changes in the rectifier operating temperature which result in changes in the reverse leakage current may also result in objectionable unbalances between associated amplifiers. For best amplifier performance, the reverse leakage of rectifiers for magnetic-amplifier applications should be held to approximately 0.2 percent of the required forward current.

RECTIFIERS FOR SPARK QUENCHING

If the current in an inductive circuit is suddenly interrupted, the resulting surge can have several undesirable effects.

(A) Contact arcing, producing deterioration that eventually results in circuit failure due to mechanical locking or snagging, or to high contact resistance.

(B) High-voltage transients resulting in insulation breakdown.

(C) Wide-band electrical interference.

One method of suppressing surges is to shunt a selenium rectifier across the inductor as shown in Figs. 39 and 40.

The rectifier in Fig. 39 appreciably lengthens the release time (as when the electromagnet is a relay coil). By connecting the rectifier across contact A instead of across the coil, a release time only slightly lengthened is secured. This, however, is usually a less desirable connection, especially when there are several contacts controlling the same coil. Also, when contact A is open a small reverse current flows, of the order of 0.5 milliampere. The system of Fig. 39 is applicable to dc circuits only.

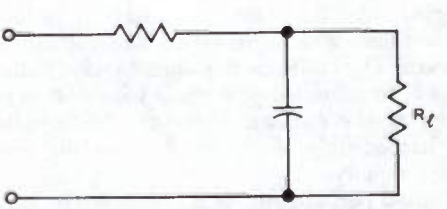

Fig. 46—Resistor-input filter.

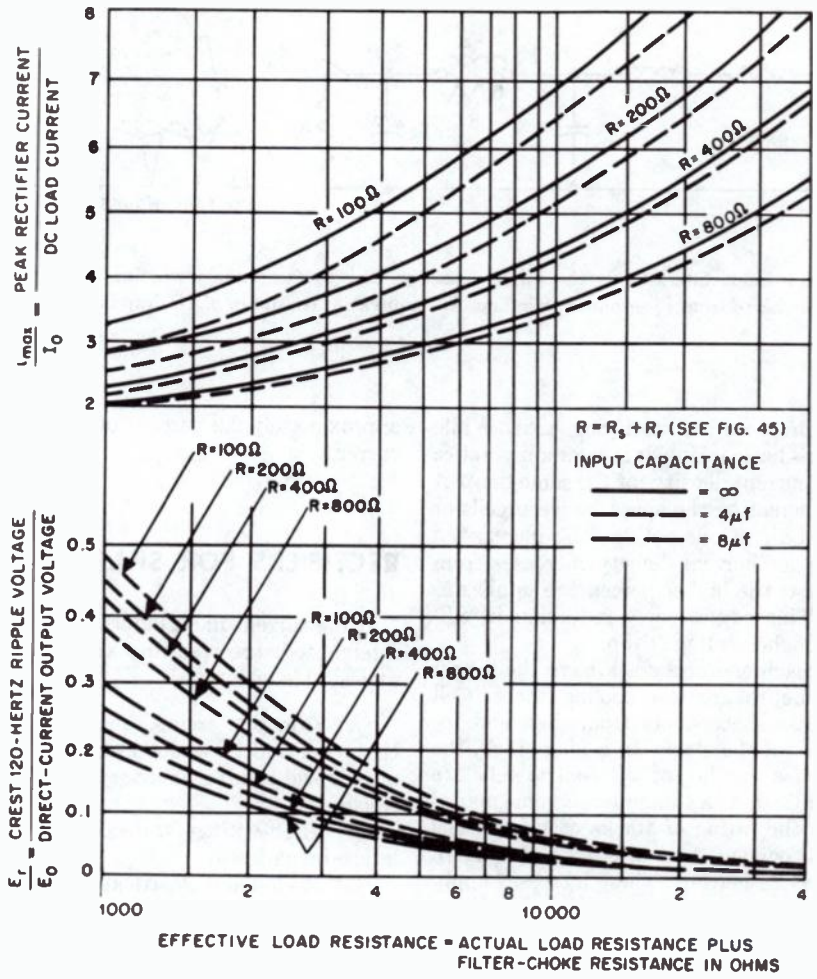

Fig. 47—Performance of capacitor-input filter for 60-hertz full-wave rectifier, assuming negligible leakage-inductance effect. *Adapted from "Radio Engineers Handbook," by F. E. Terman, 1st ed., p. 603; 1943. By permission McGraw-Hill Book Co., New York, N. Y.*

The system of Fig. 40 gives good protection with only a small lengthening of the release time over that when no protection is used. It is applicable to both ac and dc circuits. When contact A is closed, CR1 blocks current flow from the battery. On opening contact A, the reverse-resistance characteristic of CR2 comes into play. It is high at low voltages and decreases as the voltage is increased. The voltage rise due to the inductive surge is thus limited to a value too small to cause arcing at the contact. However, the inductor is not immediately short-circuited, so the current decays rapidly.

Typical performance data are shown in Table 6. For comparison, data are included for cases where a capacitor with series resistor is shunted across the coil; also for a silicon–carbide varistor in place of the rectifier shown in Fig. 39.

RECTIFIERS FOR SURGE SUPPRESSION

The arrangement shown in Fig. 40 that uses the reverse-resistance characteristic of a selenium rectifier for surge suppression has led to specially designed selenium stacks. Their application extends to the protection of silicon rectifiers and thyristors, which are more susceptible than selenium to the effects of overvoltage. The surge suppressor has a

well-defined knee in its reverse voltage–current characteristic and a steep slope beyond the knee. The transient energy is dissipated as a reverse current in the selenium stack, and the transient voltage is limited to a value determined by the turnover of the reverse characteristic of the stack.

The basic configurations for rectifier and thyristor protection are shown in Fig. 41, and it is possible to build combinations of these on a single spindle for composite duty.

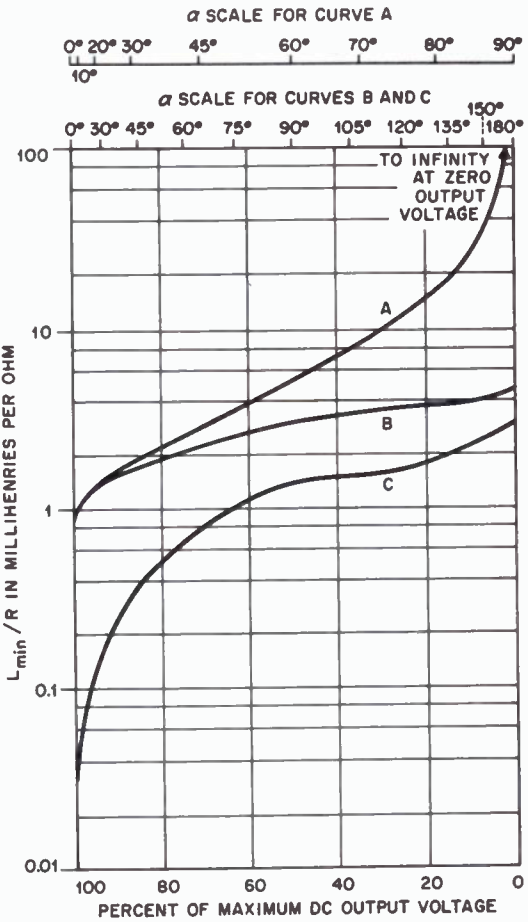

Fig. 48—L_{min}/R as a function of the percentage of maximum dc output voltage for thyristor rectifiers. The values of L_{min}/R given by the curves apply to a supply frequency of 60 hertz. Curve A is for full-controlled single-phase rectifiers such as those in Fig. 18 and in Fig. 20 with the bypass diode omitted. Curve B is for half-controlled single-phase rectifiers such as those in Fig. 19 and in Fig. 20 with the bypass diode included. Curve C is for a half-controlled three-phase rectifier such as that in Fig. 22. It could also apply to Fig. 30, feeding a transformer and three-phase diode bridge rectifier.

In Fig. 41A the suppressor is built with a sufficient number of plates to ensure that the power dissipated by reverse leakage current is low when the normal rms voltage is applied. Negligible forward current is taken by the suppressor, since a single silicon rectifier junction has a much lower forward voltage drop per unit of current than the corresponding series assembly of selenium plates that is necessary to produce a similar reverse-voltage rating. A figure of between 2 and 2.5 is normally obtainable for the ratio of peak limited transient reverse voltage to normal rms working

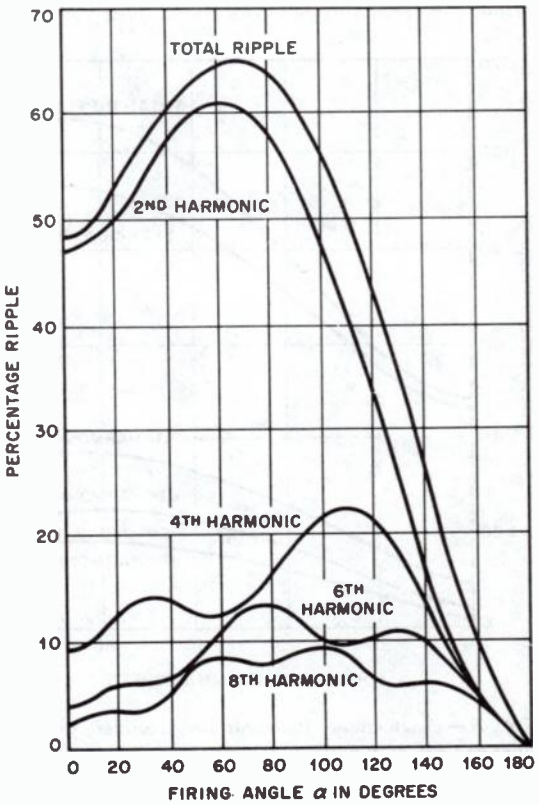

Fig. 49—Single-phase full-controlled rectifiers with bypass diode on resistive or inductive loads, or without bypass diode on resistive load; also applies to half-controlled rectifiers with or without bypass diode on resistive or inductive loads. The waveform is as illustrated by the example of Fig. 17 and typical circuits are Figs. 17, 19, and 20 with the diode inserted. *From R. Smith, "Harmonic Voltages in the Outputs of Controlled Rectifier Circuits," Electronic Engineering, vol. 36, no. 442, p. 833, fig. 1;* *© December 1964, Morgan Brothers (Publishers) Ltd., London, England.*

voltage, and lower ratios can be obtained by selection of selenium plates of particular voltage grades.

In Fig. 41B two suppressor sections are connected in opposition so that a voltage-limiting characteristic is obtained for both polarities of applied voltage; forward current cannot flow in either direction through this stack. This configuration is necessary for thyristor protection to ensure that both the reverse and the forward blocking voltages are limited.

Figure 42 shows typical surge-current ratings versus surge duration for several sizes of plates. Figure 43 shows the instantaneous reverse voltage developed at various reverse currents for the same range of plate sizes.

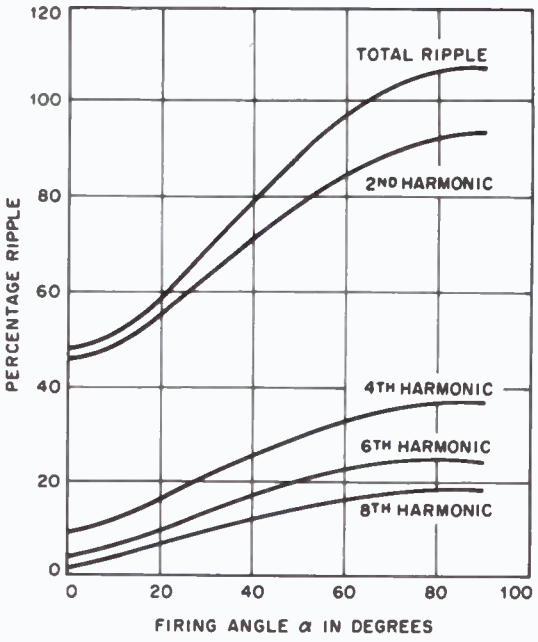

Fig. 50—Single-phase full-controlled rectifier without bypass diode on infinitely inductive load. The waveform is as illustrated by the example of Fig. 18 and typical circuits are Fig. 18, and Fig. 20 with the diode omitted. *From R. Smith, "Harmonic Voltages in the Outputs of Controlled Rectifier Circuits," Electronic Engineering, vol. 36, no. 442, p. 833, fig. 2;* © *December 1964, Morgan Brothers (Publishers) Ltd., London, England.*

FILTERS FOR RECTIFIER CIRCUITS

Rectifier filters may be classified into three types:

Inductor Input (*Fig.* 44): Have good voltage regulation, high transformer utilization factor, and low rectifier peak currents, but also give relatively low output voltage.

Capacitor Input (*Fig.* 45): Have high output voltage, but poor regulation, poor transformer utilization factor, and high peak currents. Used mostly in television and radio receivers.

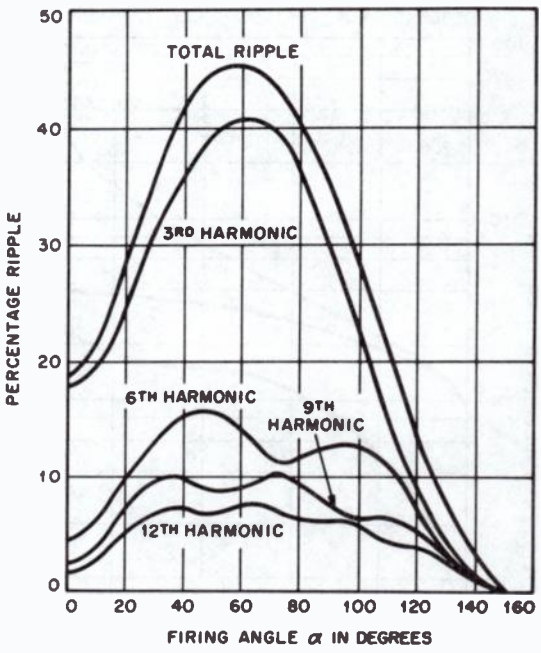

Fig. 51—Three-phase half-wave full-controlled rectifier with bypass diode on resistive or inductive loads, or without bypass diode on resistive load. *From R. Smith, "Harmonic Voltages in the Outputs of Controlled Rectifier Circuits," Electronic Engineering, vol. 36, no. 442, p. 833, fig. 3;* © *December 1964, Morgan Brothers (Publishers) Ltd., London, England.*

Resistor Input (*Fig.* 46): Used for low-current applications.

DESIGN OF INDUCTOR-INPUT FILTERS

The constants of Fig. 44 are determined from the following considerations:

(A) There must be sufficient inductance to ensure continuous operation of rectifiers and good voltage regulation. Increasing this critical value of inductance by a 25-percent safety factor, the

minimum value becomes

$$L_{min} = (K/f_s) R_l \text{ henry} \quad (1)$$

where

f_s = frequency of source in hertz
R_l = maximum value of total load resistance in ohms
K = 0.060 for full-wave single-phase circuits
= 0.0057 for full-wave two-phase circuits
= 0.0017 for full-wave three-phase circuits.

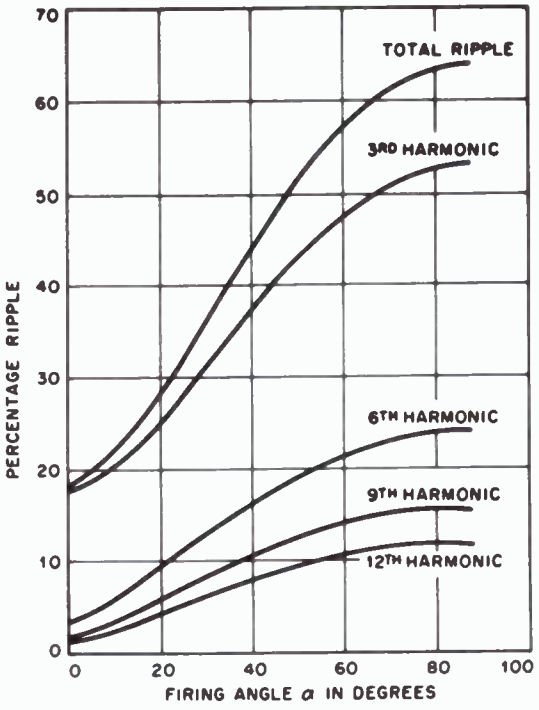

Fig. 52—Three-phase half-wave full-controlled rectifier without bypass diode on infinitely inductive load. *From R. Smith, "Harmonic Voltages in the Outputs of Controlled Rectifier Circuits," Electronic Engineering, vol. 36, no. 442, p. 833, fig. 4; © December 1964, Morgan Brothers (Publishers) Ltd., London, England.*

At 60 hertz, single-phase full-wave

$$L_{min} = R_l/1000 \text{ henry.} \quad (1A)$$

(B) The LC product must exceed a certain minimum, to ensure a required ripple factor

$$r = E_r/E_{dc}$$
$$= [\sqrt{2}/(p^2-1)][10^6/(2\pi f_s p)^2 L_1 C_1]$$
$$= K'/L_1 C_1 \quad (2)$$

where, except for single-phase half-wave, p = effective number of phases of rectifier, E_r = root-mean-square ripple voltage appearing across C_1, E_{dc} = direct-current voltage on C_1, and L_1 is in henries and C_1 in microfarads.

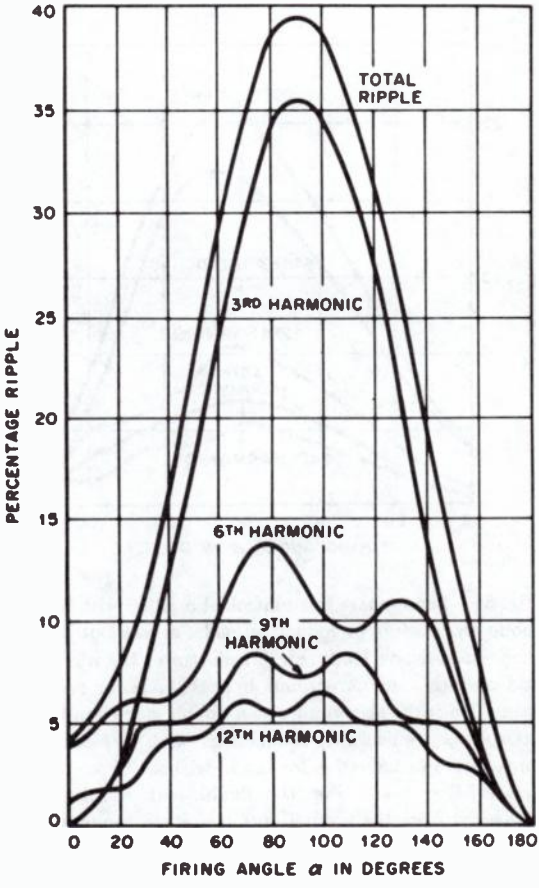

Fig. 53—Three-phase half-controlled rectifier with or without bypass diode on resistive or inductive loads. The waveform and the circuit are as shown by the example of Fig. 22. *From R. Smith, "Harmonic Voltages in the Outputs of Controlled Rectifier Circuits," Electronic Engineering, vol. 36, no. 442, p. 834, fig. 5; © December 1964, Morgan Brothers (Publishers) Ltd., London, England.*

For single-phase full-wave, $p = 2$ and

$$r = (0.83/L_1 C_1)(60/f_s)^2. \quad (2A)$$

For three-phase full-wave, $p = 6$ and

$$r = (0.0079/L_1 C_1)(60/f_s)^2. \quad (2B)$$

Equations (1) and (2) define the constants L_1 and C_1 of the filter, in terms of the load resistor R_l and allowable ripple factor r.

Swinging Chokes: Swinging chokes have inductances that vary with the load current. When the load resistance varies through a wide range, a swinging choke, with a bleeder resistor R_b (10 000 to 20 000 ohms) connected across the filter output, is used to guarantee efficient operation; i.e., $L_{min}=$

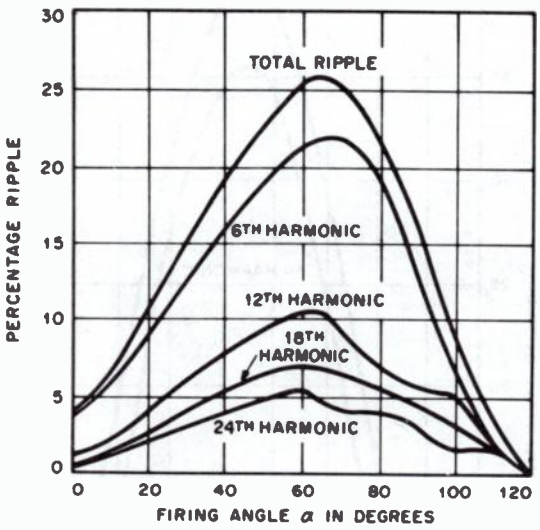

Fig. 54—Three-phase full-controlled rectifier with bypass diode on resistive or inductive loads, or without bypass diode on resistive loads. Fig. 21 illustrates the waveform and also the circuit without bypass diode for resistive load. The curve also applies to a double-star circuit with interphase transformer connections with bypass diode on resistive or inductive loads and without bypass diode on resistive loads. For the double-star circuit, α is measured from the normal output-voltage commutation point, not from the commutation point of the individual three-phase half-wave rectifiers. *From R. Smith, "Harmonic Voltages in the Outputs of Controlled Rectifier Circuits," Electronic Engineering, vol. 36, no. 442, p. 834, fig. 6; © December 1964, Morgan Brothers (Publishers) Ltd., London, England.*

$R_l'/1000$ for all loads, where $R_l'=(R_lR_b)/(R_l+R_b)$. Swinging chokes are economical because of their smaller relative size and result in adequate filtering in many cases.

Second Section: For further reduction of ripple voltage E_{r1}, a smoothing section (Fig. 44) may be added and will result in output ripple voltage E_{r2}.

$$E_{r2}/E_{r1}=10^6/(2\pi f_r)^2L_2C_2 \qquad (3)$$

where $f_r=$ ripple frequency.

DESIGN OF CAPACITOR-INPUT FILTERS

The constants of the input capacitor (Fig. 45) are determined from the following.

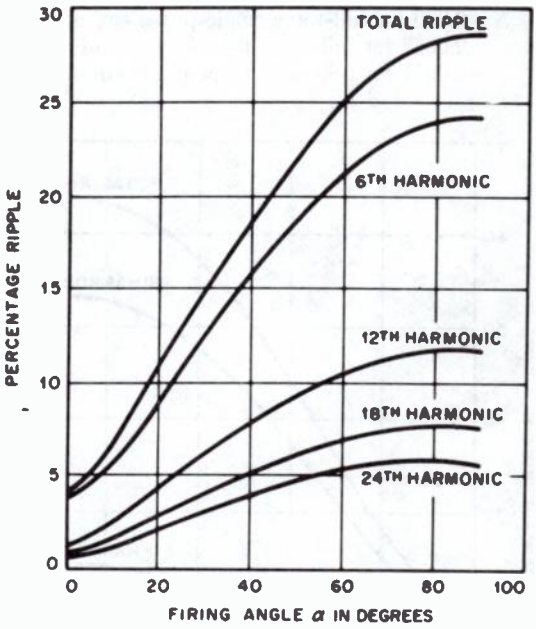

Fig. 55—Three-phase full-controlled rectifier without bypass diode on infinitely inductive load. The curve applies to the double-star circuit with interphase transformer when there is no bypass diode and the load is infinitely inductive. The same remarks as in Fig. 54 apply to the measurement of α. *From R. Smith, "Harmonic Voltages in the Outputs of Controlled Rectifier Circuits," Electronic Engineering, vol. 36, no. 442, p. 834, fig. 7; © December 1964, Morgan Brothers (Publishers) Ltd., London, England.*

(A) Degree of filtering required.

$$r=E_r/E_{dc}$$

$$=\sqrt{2}/2\pi f_rC_1R_l$$

$$=(0.00188/C_1R_l)\,(120/f_r) \qquad (4)$$

where C_1R_l is in microfarads×megohms, or farads×ohms.

(B) A maximum allowable C_1 (so as not to exceed the maximum allowable peak-current rating of the rectifier).

Unlike the inductor-input filter, the source impedance (transformer and rectifier) affects output dc and ripple voltages and the peak currents. The equivalent network is shown in Fig. 45.

Neglecting leakage inductance, the peak output ripple voltage E_{r1} (across the capacitor) and the peak rectifier current for varying effective load resistance are given in Fig. 47. If the load current is small, there may be no need to add the L-section consisting of an inductor and a second capacitor. Otherwise, with the completion of an L_2C_2 or RC_2 section (Fig. 45), greater filtering is obtained, the peak output-ripple voltage E_{r2} being given by (3) or by

$$E_{r2}/E_{r1} = 1/2\pi f_r RC_2. \quad (5)$$

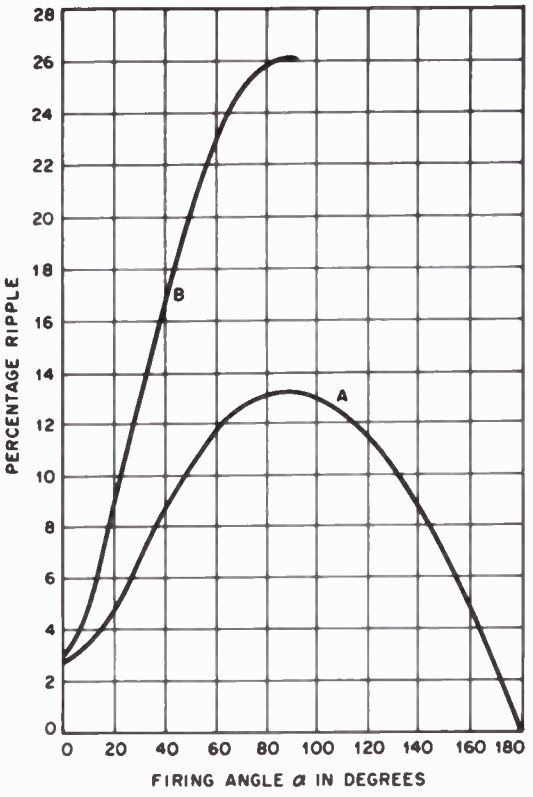

Fig. 56—Curve A is a weighted ripple curve, including all harmonics up to the 24th, weighted with respect to 800 hertz. This curve applies to the same circuits as for Fig. 49. Curve B is produced on the same basis but refers to the circuits as for Fig. 50. *From R. Smith, "Harmonic Voltages in the Outputs of Controlled Rectifier Circuits," Electronic Engineering, vol. 36, no. 442, p. 834, fig. 8; © December 1964, Morgan Brothers (Publishers) Ltd., London, England.*

FILTERS FOR CONTROLLED RECTIFIERS

The same general principles apply to filters for controlled rectifier circuits as to those for ordinary rectifier circuits. Capacitive-input filters, however, are rarely used since a capacitive load restricts the range of conduction angle control that it is possible to obtain with thyristors.

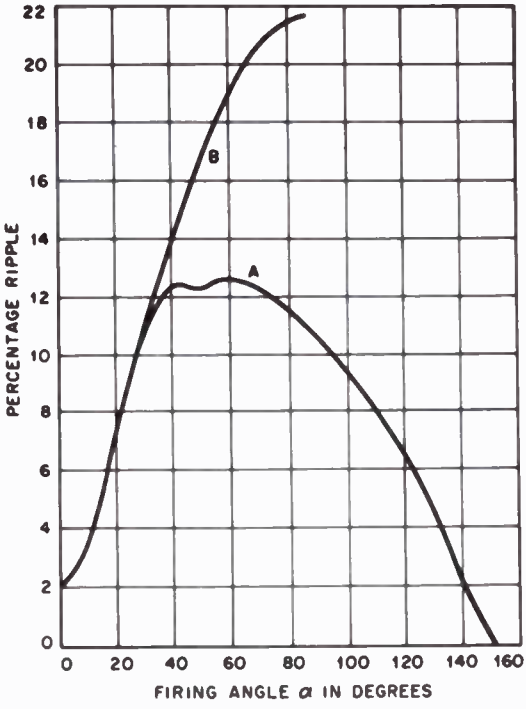

Fig. 57—These curves are weighted as in Fig. 56. Curve A applies to the same circuits as for Fig. 51 and curve B applies to the same circuits as for Fig. 52. *From R. Smith, "Harmonic Voltages in the Outputs of Controlled Rectifier Circuits," Electronic Engineering, vol. 36, no. 442, p. 835, fig. 9; © December 1964, Morgan Brothers (Publishers) Ltd., London, England.*

The two main differences to consider in filter design for controlled rectifiers, compared with that for ordinary rectifiers, are (A) the greatly increased values of critical inductance for the input choke and (B) the larger input ripples.

Empirical equations for the critical inductance L_{min} were given that apply to various configurations of diode rectifiers. In controlled rectifiers, L_{min} rises as the conduction angle is decreased by trigger control, i.e., as the firing angle delay α is increased. Figure 48 shows the ratio L_{min}/R as

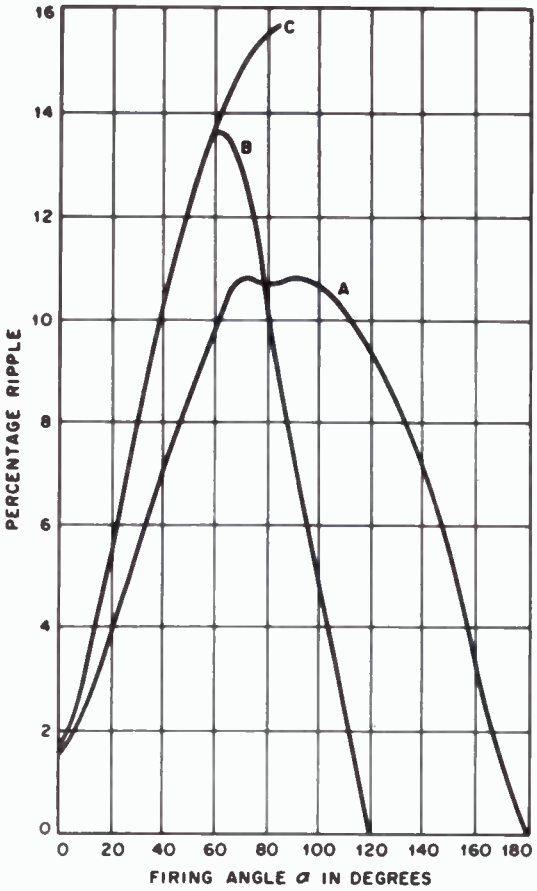

Fig. 58—These curves are weighted as in Fig. 56. Curve A applies to the same circuits as for Fig. 53, curve B applies to the same circuits as for Fig. 54, and curve C applies to the same circuits as for Fig. 55. *From R. Smith, "Harmonic Voltages in the Outputs of Controlled Rectifier Circuits," Electronic Engineering, vol. 36, no. 442, p. 835, fig. 10;* © *December 1964, Morgan Brothers (Publishers) Ltd., London, England.*

a function of the percentage of maximum output voltage obtained from three-phase half-controlled and from single-phase half- and full-controlled rectifier types discussed in the section on thyristors. Scales are included to show the corresponding values of α for various percentage outputs.

Ripple

The ripple from a controlled rectifier is generally larger than that obtained from a conventional diode rectifier, and its value varies with the firing angle α. Two sets of ripple curves are reproduced here, and in every case the ripple is expressed as a percentage of the maximum output voltage of the rectifier, i.e., at $\alpha = 0°$.

Set 1: Normal ripple (Figs. 49–55).
Set 2: Ripple weighted to 800 hertz (Figs. 56–58).

The ripple figures in Set 1 include all harmonics up to the 24th. Each graph shows the total ripple in the particular circuit and the amplitudes of the first four significant harmonics.

The weighted curves in Set 2 have been calculated for a supply frequency of 50 hertz but they also apply approximately at 60 hertz. The weighting uses a CCITT* table of factors by which harmonics occurring in the output of rectifiers should be multiplied to yield interfering noise on a telephone circuit equivalent to that produced by an 800-hertz tone. In practice the equivalent weighted ripple is evaluated by using noise measuring sets in the United States and psophometers in Europe.

* Refer to Directives of the Comité Consultatif International Téléphonique et Télégraphique (CCIF and CCIT), Geneva; 1952.

CHAPTER 15
MAGNETIC AMPLIFIERS

INTRODUCTION

The magnetic amplifier enjoyed its maximum prominence in power control and low-frequency signal-processing electronics from about 1947 to 1957. By 1957 junction transistors were readily available. Development rapidly shifted away from magnetic amplifiers toward transistor and semiconductor switch equivalents, combined magnetic/transistor amplifiers, and the host of new devices made possible by the joint use of square-loop cores and transistors. Complex magnetic-amplifier designs developed in this period must be looked on as an interim technology. Many magnetic amplifiers in present use and manufacture are the result of early design commitments which have not yet been replaced.

There are a few areas, however, in which magnetic amplifiers continue to excel. In power control, they tolerate extreme environmental and overload conditions that would be fatal to semiconductors. They may also generate less noise because of the slower switching saturable reactors. Perhaps most important, they permit the summing of a number of input signals that must remain electrically isolated. In instrumentation amplifiers, magnetic-amplifier circuits still offer high, drift-free gain with this summing feature. The development of magnetic-core transistor oscillators makes it possible to supply ac power of practically any desired frequency for these amplifiers, making them much smaller than they would be with power-frequency excitation. Similar circuits have come into increasing use in magnetometry where the unique direct transducing capability of the magnetic amplifier puts it in a class by itself.

The magnetic-core transistor oscillator, which is capable of inverting dc to ac up to about 100 kilohertz and by rectification can convert a single primary dc power source at high efficiency to several independent conductively isolated dc voltage supplies, today has all of the engineering prominence that magnetic amplifiers once enjoyed. Many of these newer circuits are, in fact, regulated and timed by magnetic-amplifier principles.

The history and present state of the art in magnetic amplifiers is documented in the proceedings of the Conference on Nonlinear Magnetics and Magnetic Amplifiers [1], and the more recent *IEEE Transactions on Magnetics* [2]. Several books ranging between texts and advanced treatments of design principles are also available [3–7]. The development of soft magnetic materials used in magnetic-amplifier circuits can be traced in the proceedings of the Annual Conferences on Magnetism and Magnetic Materials [8]. Most of the material to be found in these references deals with basic principles and the physical properties of materials. For the circuit engineer who wishes to capitalize quickly and effectively on the design rules that have emerged from this effort, the design manuals available from the manufacturers of magnetic-amplifier core materials tabulate the available material types and related design information such as wire holding capacity, insulation, and temperature characteristics. Having made the basic selection of the core windings and circuit configuration, the designer should expect to spend some time tailoring the circuit to meet design specifications.

PRINCIPLE OF THE MAGNETIC AMPLIFIER

The elementary principle of magnetic amplification can be conveniently represented in terms of a flux-actuated switch in series with a load. The magnetic material is characterized by the nearly rectangular hysteresis loop of Fig. 1. In this figure, the narrow hysteresis loop corresponds to the loop measured at dc and the wider loop is that measured at the power supply frequency. It should be noted that this dynamic loop widens with increasing frequency. Figure 2 shows the dc hysteresis loops corresponding to three of the materials listed in Table 1.

Figure 3 shows a winding on a core in series with a resistor representing the load. At the beginning of a positive half-cycle of the supply voltage, the

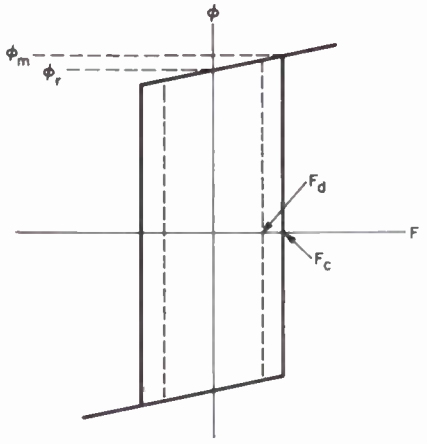

Fig. 1—Schematic representation of dynamic and dc (dotted lines) hysteresis loops.

core is in some initial flux state ϕ_0. Essentially all of the supply voltage is impressed on the core winding until the flux in the core reaches saturation. In saturation, the core becomes a very low impedance and practically all of the supply voltage appears across the resistor. This situation is diagrammed in Fig. 4A for a sinusoidal supply voltage and in Fig. 4B for a square-wave supply voltage. The lower portions of the diagrams show that the switching of the supply voltage from the core to the resistor becomes perfect when the width of the hysteresis loop is zero. In practical designs, the choice of power supply voltage and frequency, core size, winding, and load impedance is subject to the constraints of the problem. To approximate the above-mentioned ideal conditions is often the main object of the design.

Figure 5 shows integrals of portions of the supply-voltage integral in analytical form. It is clear from this figure that the average voltage applied to the load is a function of the switching angle α, which in turn depends on the initial flux ϕ_0. The half-cycle average of the load voltage is expressed in terms of ϕ_0 for the sine-wave and square-wave cases as follows.

Sine Wave	Square Wave
$\bar{v}_r=(2/T)(E_s/\omega)\times(1+\cos\alpha)$	$\bar{v}_r=E_s[1-(\alpha/\pi)]$
$(E_s/\omega)(1-\cos\alpha)=(E_s/\omega)-N\phi_0$	$(T/2)E_s(\alpha/\pi)=N(\phi_m-\phi_0)$
$\cos\alpha=\phi_0/\phi_m$	$\alpha/\pi=\frac{1}{2}[1-(\phi_0/\phi_m)]$
$\bar{v}_r=(2/T)(E_s/\omega)\times[1+(\phi_0/\phi_m)]$	$\bar{v}_r=E_s/2[1+(\phi_0/\phi_m)]$

It is further obvious that in order for there to be no output, and no excess flux capacity in the core (normal excitation), the flux linkage capacity of the core must be set equal to the volt-second capacity of the power supply. This results in the simple equations

$$E_s=B_mA\omega N \qquad \text{(sine wave)}$$

$$E_s=(2/\pi)B_mA\omega N \qquad \text{(square wave)}$$

relating the peak value of the supply voltage, the maximum flux density of the core (in webers/meter^2), the material cross-section (in meters^2), the angular frequency, and the number of turns.

Correspondingly, the exciting current for a given coercive force F_c in ampere-turns is $i_x=F_c/N=H_cl/N$, where H_c is in ampere-turns/meter and l is the mean length of the magnetic path in the core in meters. These equations in CGS units become

$$E_s=B_mA\omega N\times10^{-8} \qquad \text{(sine wave)}$$

$$E_s=(2/\pi)B_mA\omega N\times10^{-8} \qquad \text{(square wave)}$$

where B_m=gauss, A=cm^2, E_s=volts (peak), and N=turns.

$$I_m=0.794H_cl/N$$

where H_c=oersteds, l=cm, and I=amperes.

Although the above discussion contains most of the ideas basic to magnetic amplifiers, no mention has been made of how ϕ_0 is related to the control

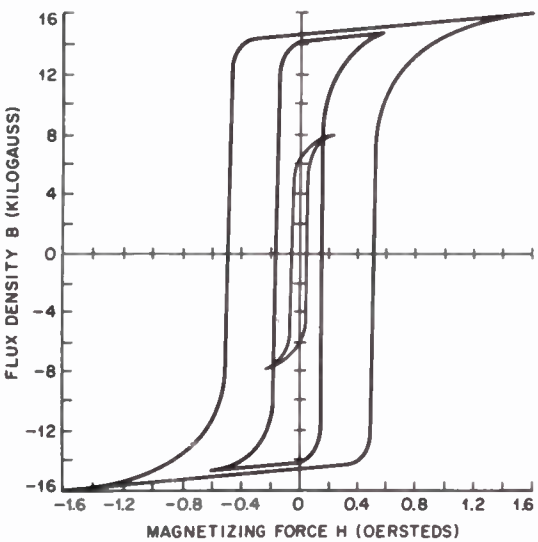

Fig. 2—Comparison of dc loops of three materials listed in Table 1.

TABLE 1—MATERIALS AND APPLICATIONS.

Material Letter Code	Trade Name	Cost/Core* Relative to Material A	Principal Use
A	Square Orthonol, Hipernik V, Orthonik, 49 Square Mu, Deltamax	1.00	High-gain amplifiers, oscillators, integrators, timers, memory devices.
N	Round Orthonol	1.00	Amplifier applications with slightly less gain, but less liability to triggering instability, than material A.
H	48 Alloy, Carpenter 49	1.00	Material A and N applications with lower sensitivity, lower losses, and less triggering instability. High-quality transformers.
D	Square Permalloy 80, Square Mu 79, Super Square Mu 79, Hy Ra 80, 4-79 Permalloy, Square Permalloy	1.14	High-gain amplifiers at low signal levels and low losses, low-power-consumption inverters and converters.
R	Round Permalloy 80, Hy Mu 80	1.14	High-quality low-loss inductors and transformers.
F	Supermalloy	1.63	Material D and R applications in which the lowest possible exciting currents and losses are required.
K	Magnesil, Selectron, Microsil, Hypersil, Supersil	0.70	Power amplifiers requiring lower gain and lower cost than material A applications. High-quality power transformers.
S	Supermendur	3.4	Material A and K applications where minimum size and weight and maximum operating temperatures are required.

* Based on 2-mil tape-wound core of about 3-inch diameter.

signal. Further, note that at the end of the half-cycle, ϕ is at saturation. Thus the core must be reset to ϕ_0 in the second half-cycle. If a similar voltage is to be applied to the load in the second half-cycle, a second core must be included in the circuit. Such resetting and output problems are responsible for the variety of amplifier circuit configurations that have been used.

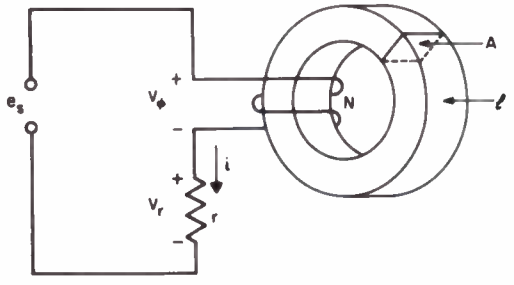

Fig. 3—Saturable reactor in series with a resistor.

AMPLIFIER CONFIGURATIONS

The amplifier configuration is arranged with two considerations in mind. One is the method of control, and the other is the type of output desired. As seen from the discussion above, a core that is brought to saturation and is gating power to a load on a positive half-cycle must be reset to its initial state if it is to repeat this function on the next positive half-cycle. On the other hand it is usually desirable to deliver power to the load on both half-cycles. Thus a second core will be gating power to the load during the half-cycle in which

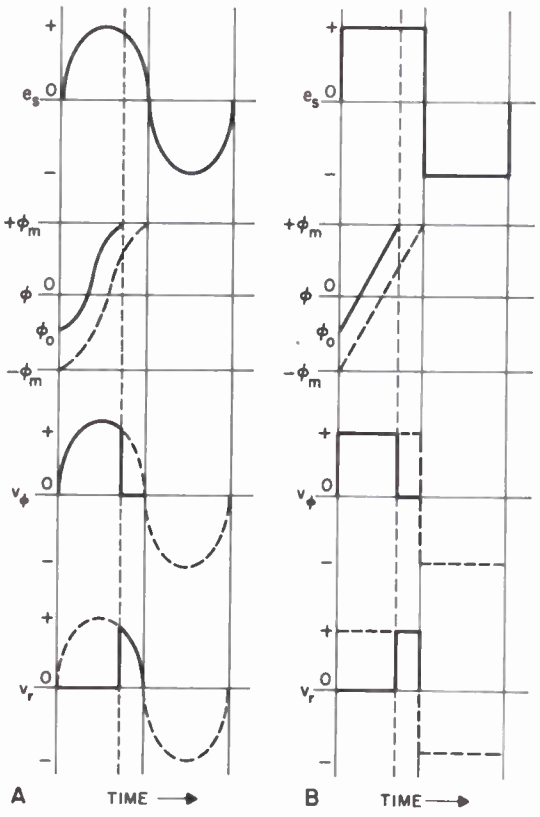

Fig. 4—Voltage and flux waveforms for the circuit of Fig. 3 for (A) sine-wave and (B) square-wave excitation.

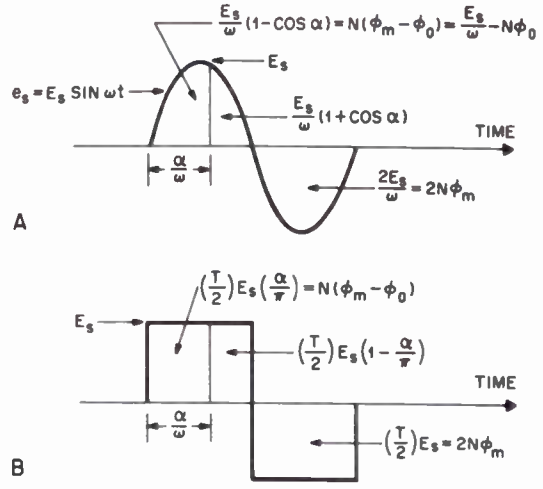

Fig. 5—Components of integrals of (A) sine-wave and (B) square-wave half-cycles.

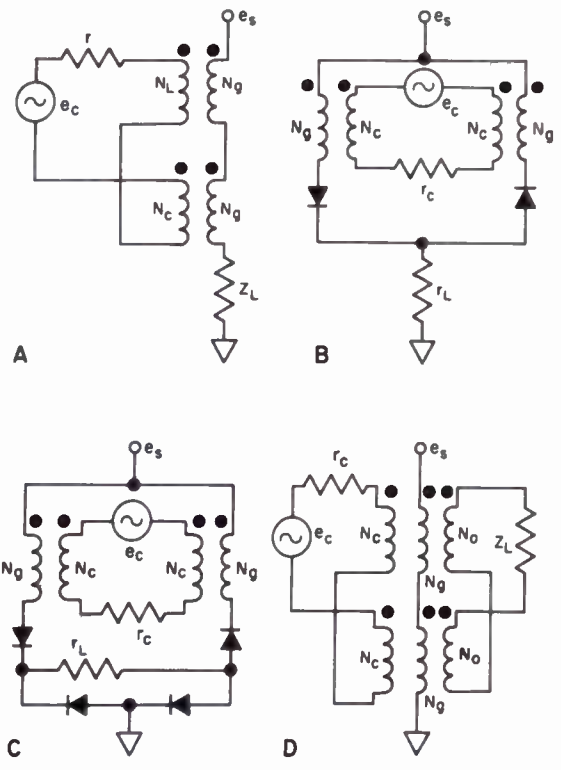

Fig. 6—Circuits for (A) the series-connected amplifier or transductor, (B) self-saturating amplifier with ac output, (C) self-saturating amplifier with dc output, and (D) second-harmonic modulator. N_c = control turns, N_g = gating turns, and N_o = output turns.

the first core is being reset. Since the increment in flux linkage in the two cores is equal in the steady state, the core driven from the power supply can be used to reset the second core by transformer action through the control circuit. In single-phase circuits the roles of the cores interchange during alternate half-cycles. The use of one core to reset the other is fundamental to most amplifier configurations.

Several of the most common configurations are shown in Fig. 6. Figure 6A is the series-connected amplifier, sometimes called the transductor. It has been extensively analyzed [3, 9, 10] and is commonly used to measure large direct currents in electrochemical and power applications [11]. The details of the circuit operation are complicated but, in essence, at most one core is saturated at a time, gating power to the load. During this interval, the second (unsaturated) core, which has a very small coercive force, must therefore maintain the condition $N_L i_L - N_c i_c = F_c$, the dynamic coercive force of the unsaturated core. The control current i_c has the same waveform as the load current i_L

but has the same polarity on each half-cycle. Thus, the rectified average values of the load current and the control current, I_L and I_c, are related by the turns ratio.

$$I_L = (N_c/N_L)\,I_c + (1/N_L)\,F_c$$

a linear function with a constant offset as shown in Fig. 7A. In practice, the linearity of this function can be kept within about 0.1 percent, which makes it very useful for instrumentation.

The circuit in Fig. 6B is characterized by parallel-connected saturable reactors, so that the load current does not have to flow through an unsaturated core. Thus, since the resetting core is primarily transformer driven through the control circuit by the power-gating core, only the exciting current for the resetting core must be carried in the control circuit. In the steady state, the flux linkages coming from the winding on the gating core must equal the flux linkages delivered to the resetting core. With zero control voltage, the two flux linkages will differ by the integral of $i_c r_c$ over the half-cycle. The function of the control voltage is to offset this voltage drop to make the two flux linkages equal at the desired output level. The diodes decouple the cores from the power supply during their resetting half-cycles.

When the amplifier is delivering full output, there is essentially no flux excursion in the gating core. It therefore does not drive the resetting core. Since the resetting core must not be reset under these conditions, the control current must be just below the coercive direct current for the core. At zero output, the gating core drives the resetting core at normal power voltage, resulting in a control current equal to the normal power-frequency coercive current. Full control of the amplifier is obtained over a control-current range equal to the widening of the hysteresis loop from dc to the power-frequency loop, divided of course by the control-winding turns. The resulting control characteristic is shown in Fig. 7B, with reference to Fig. 1. Again, there is a minimum output corresponding to the exciting current for the gating core. Also, the control current and voltage are automatically rectified because of the half-cycle symmetry of the circuit as seen from the control terminals. The modification shown in Fig. 6C delivers dc to the load.

A fourth configuration (Fig. 6D) used for very-small-signal amplifiers and magnetometers [12, 13] takes advantage of transformer coupling of the output to eliminate the residual exciting-current component found in the other circuits. The fundamental component of the induced voltage is canceled out and, at input currents other than zero, there is a second-harmonic component in the output proportional to the input current. The

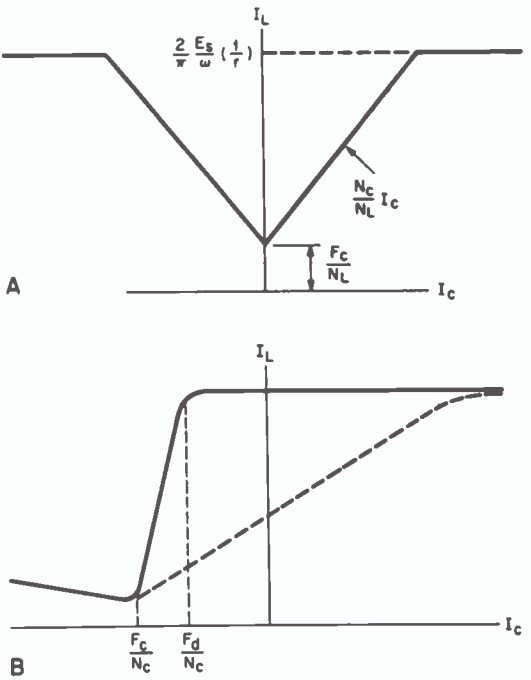

Fig. 7—Control characteristics for (A) the amplifier of Fig. 6A; and (B) for the amplifier of Fig. 6B and 6C. The dotted characteristic corresponds to nonsquare hysteresis loop, resistively shunted rectifiers, or negative feedback.

phase of this output reverses with the input-current polarity. Other examples of high-sensitivity amplifiers can be found in the literature [14]. For many power applications, 3-phase amplifiers are preferred for the usual reasons. The output is much easier to filter when dc is required [15].

Examples of parametric amplifiers and microwave magnetic amplifiers can be found in the literature.

MULTISTAGE AMPLIFIERS

Because of the bilateral characteristics of magnetic amplifiers, multistage amplifiers are difficult to analyze. In addition, their properties as measured experimentally are technically unattractive and they are difficult to design even by empirical techniques except when the coupling-circuit impedance isolates the circuits. In this case, gain and frequency response are usually sacrificed. With the advent of a highly developed transistor technology, it is rarely necessary to design multistage amplifiers. Where it is necessary, the problem is treated as though the first stage were driving any other *R–L* or *R–L–C* isolated dc load. If this

approach does not yield adequate performance, the designer must resort to less well documented techniques or initiate a new approach to solving the problem.

BIAS AND FEEDBACK

Bias and feedback windings look and act exactly like the control windings shown in Fig. 6. Problems in design arise because these windings couple induced voltages from the cores into the bias and feedback circuits. Thus, the circuits are not simply unilateral and passive [16]. If these circuits are isolated by suitable R–L networks, then the currents can be treated as though they were additive. In that case, the bias winding simply translates the origin of the control current in the direction of the bias.

The output current or voltage can be rectified and passed through simple R, R–L, or R–L–C networks and the derived current put into a feedback winding. In such a case, feedback is treated as it is in any other amplifier. It can linearize the amplifier successfully if the range of output is lowered. If the amplifier is used as a power device and its range of output is fixed by performance specifications, feedback is of no help unless compensating nonlinearity can be inserted in other amplifying stages. Feedback in such cases is useful primarily to lower output or impedance of the amplifier.

FREQUENCY RESPONSE

Analysis has shown that the voltage-gain bandwidth product [17] is

$G_v \times (\text{bw}) = 4f/N$ (series-connected amplifier, Fig. 6A)

$G_v \times (\text{bw}) = 2f/N$ (self-saturating amplifier, Fig. 6B)

where f is the frequency and N is the turns ratio N_c/N_g. These relations show again the advantage of high-frequency power supplies. They also suggest that if a design is adjusted to increase gain, the bandwidth (frequency response) will be reduced unless the turns ratios are adjusted to raise the gain–bandwidth product. High-gain amplifiers can be expected to have a bandwidth of about one-tenth the carrier frequency, which is frequently sufficient in instrumentation applications. In signal-processing applications, it is preferable to use several stages of low-gain wide-band amplification since the gains multiply and the bandwidths go down more or less additively. It is in this area that magnetic amplifiers have been largely replaced by semiconductor circuits.

CHOICE OF CORE MATERIALS

A variety of core materials can be chosen for magnetic amplifiers. They can be obtained in the form of tape-wound cores, laminations, and encapsulated tape cores cut into two mating C-shaped pieces. The latter configurations permit the use of simple inexpensive lathe-wound windings which can be assembled on the core. The cut-C core configuration maintains the rolling direction of the tape along the primary magnetic path. The laminations are stamped out of continuous strip such that part of the magnetic path is along the direction of rolling and part is perpendicular to it. Since most good-quality strip is anisotropic, the resulting characteristics of the cores are not as good as they would be in the tape-wound configuration, which has the best magnetic qualities. As a result, only the lower-cost lower-quality magnetic materials are widely used in other than the tape-wound configuration. In addition to differences in processing and in the cost of raw materials, the above manufacturing considerations significantly contribute to the economic basis for choosing core materials. Cost is the dominant consideration in most amplifier designs. There are, however, extreme cases where only the highest-quality material can meet the technical specifications.

In general, the large, heavy, power-control applications make use of the least expensive materials in the least expensive configuration. In one important sense, they are sometimes technically superior as well. First, because of low remanence of the core, using these materials in a self-saturating configuration (Fig. 6B, 6C) results in a control characteristic which crosses the control-current axis as shown dotted in Fig. 7B. This automatically biases the amplifier near the desired operating point. In addition, the lack of squareness also causes fairly slow switching at the firing time of the power-gating core. The result is much less noise than found in the more objectionable gas tubes, semiconductors, and square-loop core circuits.

Table 1 lists the core materials available in tape-wound cores from most of the core manufacturers, plus a guide to their principal applications. An approximate cost ratio is given for 2-mil tape in a core of about 3 inches in diameter. This indicates the economic advantage of using materials no better than necessary. In lamination form, the cost per pound of the material is lower by about a factor of 5.

TABLE 2—TECHNICAL PROPERTIES OF MATERIALS.

Material Letter Code	Flux Density (kilogauss)	Squareness (B_r/B_m) (400 Hz) ccfr*	Coercive Force (oersted) (dc)	Coercive Force (oersted) (400 Hz) ccfr*	Gain (kG/oe) (400 Hz) ccfr*	Curie Temp (°C)	Core Loss (mW/lb) (at +1 kG, 400 Hz)
A	14.2–15.8	0.94 up	0.1–0.2	0.45–0.65	310–715	500	56
N	14.0–15.6	0.85–0.95	0.07–0.17	0.10–0.20	260–500	500	42
H	11.5–14.0	0.80–0.92	0.05–0.15	0.08–0.15	280–550	500	19
D	6.6–8.2	0.80 up	0.02–0.04	0.022–0.044	550–1650	460	6.5
R	6.6–8.2	0.45–0.75	0.008–0.02	0.008–0.026	250–715	460	4.5
F	6.5–8.2	0.40–0.70	0.003–0.008	0.004–0.015	250–715	460	3.7
K	15.0–18.0	0.85 up	0.40–0.60	0.45–0.65	130–220	750	42
S	19.0–22.0	0.90 up	0.15–0.35	0.50–0.70	85–135	940	230

* The values are typical of cores with ID/OD ratio of about 0.80 and tape thickness of 0.002 in. Tests made are in accordance with AIEE Standards paper II-432. (ccfr = constant-current-flux reset.)

Table 2 summarizes the technical properties of these materials. Note that many of their properties are given in terms of the IEEE standard referenced in AIEE Standards paper II-432 [18]. The use of these standards in circuit design and component specification is highly recommended.

The control-current range for self-saturating amplifiers, as indicated in Fig. 7B, can be estimated by referring to the difference between the dc and 400-hertz coercive-force columns in Table 2. This value must be multiplied by about 0.8 times the mean magnetic path length of the core in centimeters to obtain control ampere-turns. The values are for 400 hertz and must be corrected experimentally for other frequencies. Studies of the properties of materials and their influence on circuits covering a wide range of frequencies, temperatures, and materials can be found in the published literature [19, 20].

For more-specific and detailed design information, the designer should use the referenced literature. Also, several core-materials manufacturers have prepared excellent booklets containing all the essential tables and nomograms for designing magnetic-core circuits.

OTHER DESIGN CONSIDERATIONS

The basic design calculations, as discussed above, pick the core size and number of turns to fit the frequency and voltage. For a given magnetic material, a larger core requires fewer turns to support a given voltage at a given frequency. The number of turns varies as the inverse of the cross-section. From this fact alone, exciting current rises linearly with cross-section. There is also a linear relation between the exciting current and the mean magnetic path length for a fixed H. Thus, the exciting current is proportional to the volume of the core, as indicated by the energy dissipated in the material.

As the frequency rises, it is possible to use a smaller core for a fixed voltage. Comparing a 400-hertz design with a 60-hertz design, for example, the cores in the 400-hertz unit would be smaller by about a factor of 7. Since this is true for transformers and inductors as well, high-frequency power supplies are commonly found on aircraft where space and weight are important. The higher supply frequency also puts the carrier farther above the modulation-signal frequency spectrum, making it easier to recover the signal.

Since in many small-signal applications it is not necessary to have a large supply voltage, it is common to change available dc signals to square-wave ac voltages in the range from 5 to 25 kHz and higher. This means very small cores and very compact, sensitive amplifiers, a combination that often yields better performance in low-noise low-signal applications than semiconductor circuits.

REFERENCES

1. Institute of Electrical and Electronics Engineers, 345 East 47th Street, New York, New York 10017, before 1965. Many papers published in *Communication and Electronics* as well.
2. *IEEE Transactions on Magnetics*, Vol. MAG-1, No. 1; March 1965.
3. H. F. Storm, "Magnetic Amplifiers," John Wiley & Sons, Inc., New York; 1955.

4. G. E. Lynn, T. J. Pula, J. F. Ringelman, and F. G. Timmel, "Self-Saturating Magnetic Amplifiers," McGraw-Hill Book Co., Inc., New York; 1960.
5. D. L. Lafuze, "Magnetic Amplifier Analysis," John Wiley & Sons, Inc., New York; 1962.
6. W. A. Geyger, "Magnetic Amplifier Circuits," McGraw-Hill Book Co., Inc., New York; 1957.
7. R. C. Barker, "Nonlinear Magnetics," *Electro-Technology*, Science and Engineering Series 51; March 1963.
8. Each proceedings is published as a special issue of the Journal of Applied Physics in the spring of each year.
9. R. C. Barker, "The Series Magnetic Amplifier, Parts I and II," *Communication and Electronics*, pp. 819–831; January 1957.
10. A. G. Milnes, "Transductors and Magnetic Amplifiers," Macmillan Co. Ltd., London; 1957.
11. A. B. Rosenstein, "160 000-Ampere High-Speed Magnetic-Amplifier Design," *AIEE Transactions*, Vol. 74, Part I, pp. 90–97; 1955.
12. D. I. Gordon, R. H. Lundsten, and R. A. Chiarodo, "Factors Affecting the Sensitivity of Gamma-Level Ring-Core Magnetometers," *IEEE Transactions on Magnetics*, Vol. MAG-1, No. 4, pp. 330–337; December 1965.
13. R. C. Barker, "On the Analysis of Second-Harmonic Modulators," *IEEE Transactions on Magnetics*, Vol. MAG-1, No. 4, pp. 337–341; December 1965. See also S. Ohteru and H. Kobayashi, "A New Type Magnetic Modulator," *IEEE Transactions on Magnetics*, Vol. MAG-1, No. 1, pp. 56–62; March 1965.
14. H. E. Darling, "New Magnetic Amplifier Improves EMF to Current Converter," *IEEE Transactions on Magnetics*, Vol. MAG-3, No. 3, pp. 365–369; September 1967.
15. H. C. Bourne, Jr., and T. Kusuda, "A Three-Phase Magnetic Amplifier: Part II—Experimental Results," *IEEE Transactions on Magnetics*, Vol. MAG-3, No. 1, pp. 17–22; March 1967.
16. L. A. Finzi and J. J. Suozzi, "On the Feedback in Magnetic Amplifiers: Part II—Combined Magnetic and Electric Feedbacks," *AIEE Transactions*, Vol. 78, Part I, pp. 136–141; 1959.
17. R. C. Barker and G. M. Northrop, "Some Frequency Response Measurements on Magnetic Amplifiers," *Proceedings of the National Electronics Conference*, Vol. 12, pp. 444–453; 1956.
18. AIEE Standards Paper No. 432, obtainable from IEEE Headquarters [1].
19. M. Pasnak and R. Lundsten, "Effects of Ultrahigh Temperature on Magnetic Properties of Core Materials," *AIEE Transactions*, Vol. 78, Part I, pp. 1033–1039; 1959.
20. C. E. Ward and M. F. Littman, "Relation of D-C Magnetic Properties of Oriented 48-Per-Cent Nickel-Iron to Magnetic-Amplifier Performance," *AIEE Transactions*, Vol. 74, Part I, pp. 422–427; 1955.

CHAPTER 16
FEEDBACK CONTROL SYSTEMS

INTRODUCTION

A feedback control system (Fig. 1) is one in which the difference between a reference input and some function of the controlled variable is used to supply an actuating error to the control elements in the control system. The amplified actuating error signal is fed back to the system, thus tending to reduce the difference to zero. Supplemental power for signal amplification is available in such systems.

The two most common types of feedback control systems are regulators and servomechanisms. Fundamentally, the systems are similar but the choice of systems depends on the nature of reference inputs, the disturbance to which the control is subjected, and the number of integrating elements in the control. Thus, regulators are designed primarily to maintain the controlled variable or system output very nearly equal to a desired value in the presence of output disturbances. Generally, a regulator does not contain any integrating elements.

A servomechanism is a feedback control system in which the controlled variable is a position (or velocity). Ordinarily in a servomechanism the reference input is the input signal of primary importance; load disturbances, while they may be present, are of secondary importance. Generally, one or more integrating elements are contained in the forward transfer function of the servomechanism.

Control system problems may generally be classified into two types, linear and nonlinear. All physical systems are nonlinear and have time-varying parameters to some degree. Where the effect of the nonlinearity is very small or the time-varying parameters are slow with respect to time, linear fixed-parameter analysis of the system is adequate for engineering purposes.

The most important property of a linear system is that the principle of superposition applies. Thus, in a linear system the shape of the time response is independent of the size of the input or initial condition. A linear system, described by a linear constant coefficient differential equation, can be analyzed in a uniform fashion using a general technique.

In a control system where the control elements possess such properties as saturation, limiting, backlash, or hysteresis, the system exhibits nonlinear characteristics and the principle of superposition does not hold. The response of the system becomes dependent on the size of the input and initial condition. Exact analytical solutions to a nonlinear system (nonlinear differential equation) are very rare, and the analysis of the system must be by other means such as numerical or graphical methods.

In the following sections both the linear (Part 1) and nonlinear (Part 2) systems are discussed.

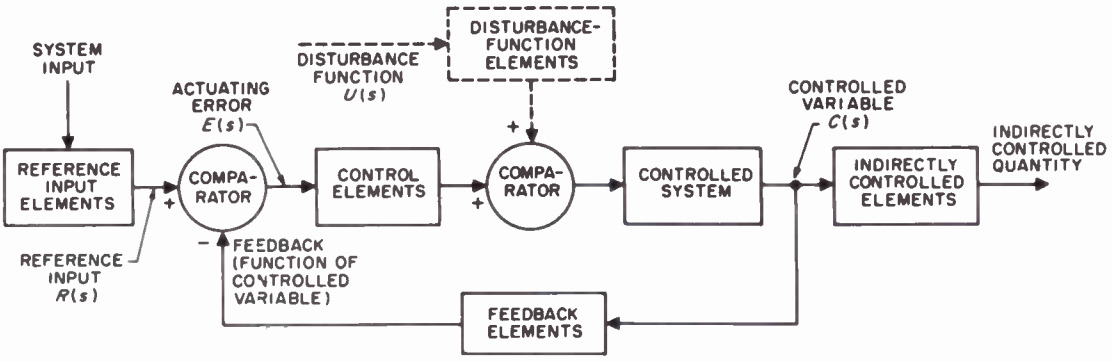

Fig. 1—Block diagram of feedback control system.

PART 1—LINEAR SYSTEMS

TYPES OF LINEAR SYSTEMS

The various types of feedback control systems can be described most effectively in terms of the simple closed-loop direct feedback system. Figure 2 shows such a system. $R(s)$, $C(s)$, and $E(s)$ are the Laplace transforms of the reference input, controlled variable, and error signal, respectively.

Note: The complex variable s instead of p will be employed in this chapter to conform with the general practice in the literature on feedback control systems.

For a typical linear system, $G(s)$ might appear as

$$C(s)/E(s)=G(s)=\frac{K(T_1s+1)(T_3s+1)}{s^n(T_2s+1)(T_4s+1)}.$$

The value of the exponent n, an integer, designates the type of the system. This in turn reveals the nature of the steady-state performance of the system as outlined below.

Type-0 System: A constant value of the controlled variable requires a constant error signal under steady-state conditions. A feedback control system of this type is generally referred to as a regulator system.

Type-1 System: A constant rate of change of the controlled variable requires a constant error signal under steady-state conditions. A type-1 feedback control system is generally referred to as a servomechanism system. For reference inputs that change with time at a constant rate, a constant error is required to produce the same steady-state rate of the controlled variable. When applied to position control, type-1 systems may also be referred to as "zero-displacement-error" systems. Under steady-state conditions, it is possible for the reference signal to have any desired constant position or displacement and the feedback signal or controlled variable to have the same displacement.

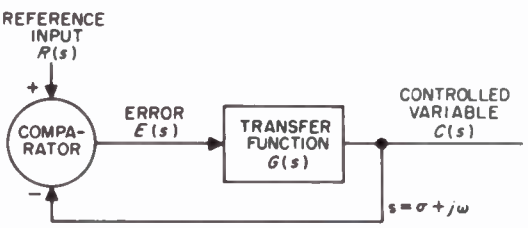

Fig. 2—Single-loop system.

Type-2 System: A constant acceleration of the controlled variable requires a constant error under steady-state conditions for a type-2 system. Since these systems can maintain a constant value of controlled variable and a constant controlled variable speed with no actuating error, they are sometimes referred to as "zero-velocity-error" systems.

STABILITY OF LINEAR SYSTEMS

A linear control system is unstable when its response to any aperiodic bounded signal increases without bound. Mathematically, instability may be investigated by analysis of the closed-loop response of the system shown in Fig. 2.

$$(C/R)(s)=G(s)/[1+G(s)]$$

$$s=\sigma+j\omega.$$

The stability of the system depends upon the location of the poles of $C(s)/R(s)$ or the zeros of $[1+G(s)]$ in the complex s plane. Several methods of stability determination can be employed.

Routh's Criterion

A method due to Routh is constructed as follows. Let D = numerator polynomial of $1+G(s)$. Then form

$$D=\sum_{i=0}^{i=n}a_is^i$$

where $a_n>0$.

(A) Construct the table shown below, with the first two rows formed directly from the coefficients and succeeding rows found as indicated.

a_n	a_{n-2}	a_{n-4}	a_{n-6}	·	·	·
a_{n-1}	a_{n-3}	a_{n-5}	a_{n-7}	·	·	·
b_1	b_2	b_3	b_4	·	·	·
c_1	c_2	c_3	c_4	·	·	·
d_1	d_2	d_3	·	·	·	·
e_1	e_2	·	·	·	·	·
f_1	·	·	·	·	·	·
·	·	·	·	·	·	·
·	·	·	·	·	·	·
·	·	·	·	·	·	·

where

$$b_1 = (a_{n-1}a_{n-2} - a_{n-3}a_n)/a_{n-1}$$

$$b_2 = (a_{n-1}a_{n-4} - a_{n-5}a_n)/a_{n-1}$$

$$b_3 = (a_{n-1}a_{n-6} - a_{n-7}a_n)/a_{n-1}$$

$$c_1 = (b_1a_{n-3} - b_2a_{n-1})/b_1$$

$$c_2 = (b_1a_{n-5} - b_3a_{n-1})/b_1$$

$$c_3 = (b_1a_{n-7} - b_4a_{n-1})/b_1$$

$$d_1 = (c_1b_2 - b_1c_2)/c_1$$

$$d_2 = (c_1b_3 - b_1c_3)/c_1$$

$$d_3 = (c_1b_4 - b_1c_4)/c_1$$

$$\vdots$$

The table will consist of n rows.

(B) The system is stable; i.e., the polynomial has no right-half-plane zeros if every entry in the first column of the table is positive. If any complete row is zero, the rest of the table cannot be formed. In such a case the polynomial always has zeros in the right-half plane or on the imaginary axis.

Nyquist Stability Criterion

A second method for determining stability is known as Nyquist stability criterion. This method consists in obtaining the locus of the transfer function $G(s)$ in the complex G plane for values of $s=j\omega$ for ω from $-\infty$ to $+\infty$. For single-loop systems, if the locus thus described encloses the point $-1+j0$, the system is unstable; otherwise it is stable. Since the locus is always symmetrical about the real axis, it is sufficient to draw the locus for positive values of ω only. Figure 3 shows loci for several simple systems. Curves A and C represent stable systems and are typical of the

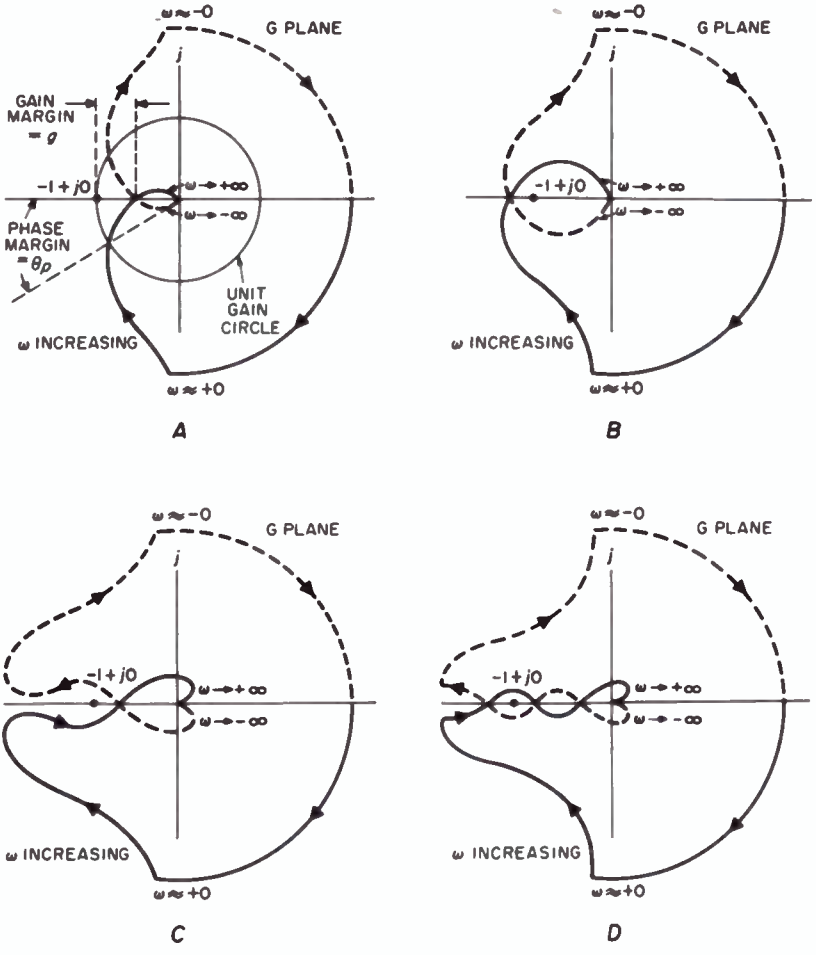

Fig. 3—Typical Nyquist loci.

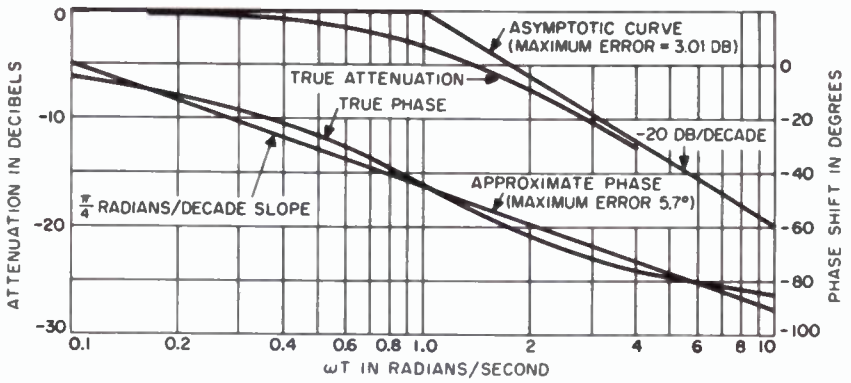

Fig. 4—Transfer-function plot. $G(j\omega) = 1/(1+j\omega T)$.

type-1 system; curve B is an unstable system. Curve D is conditionally stable; that is, for a particular range of values of gain K it is unstable. The system is stable both for larger and smaller values of gain. *Note*: It is unstable as shown.

Phase margin θ_p and gain margin g are also illustrated in Fig. 3A. The former is the angle between the negative real axis and $G(j\omega)$ at the point where the locus intersects the unit-gain circle. It is positive when measured as shown.

Gain margin g is the negative dB value of $G(j\omega)$ corresponding to the frequency at which the phase angle is 180 degrees (i.e., where $G(j\omega)$ intersects the negative real axis). The gain margin is often expressed in decibels, so that $g = -20 \times \log_{10} G(j\omega)$. Typical satisfactory values are -10 dB for g and an angle of 30° for θ_p. These values are selected on the basis of a good compromise between speed of response and reasonable overshoot. Note that for conditionally stable systems, the terms gain margin and phase margin are without their usual significance.

Logarithmic Plots

The transfer function of a feedback control system can be described by separate plots of attenuation and phase versus frequency. This provides a very simple method for constructing a Nyquist diagram from a given transfer function. Use of logarithmic frequency scale permits simple straight-line (asymptotic) approximations for each curve. Figure 4 illustrates the method for a transfer function with a single time constant. A comparison between approximate and actual values is included.

Transfer functions of the form $G = (1+j\omega T)$ have similar approximations except that the attenuation curve slope is inverted upward (+20 dB/decade) and the values of phase shift are positive.

The transfer function of feedback control systems can often be expressed as a fraction with the numerator and denominator each composed of linear factors of the form $(Ts+1)$. Certain types of control systems, such as hydraulic motors where compressibility of the oil in the pipes is appreciable or some steering problems where the viscous damping is small, give rise to transfer functions in which quadratic factors occur in addition to the linear factors. The process of taking logarithms (as in making a dB plot) facilitates computation because only the addition of product terms is involved. The associated phase angles are directly additive.

For example,

$$G(j\omega) = \frac{K(1+j\omega T_2)}{[T^2(j\omega)^2+2\zeta T(j\omega)+1](1+j\omega T_1)(1+j\omega T_3)}$$

where $s = j\omega$. The exact magnitude of G in decibels is

$$20 \log_{10} |G| = 20 \log_{10} K + 20 \log_{10} |1+j\omega T_2| - 20 \log_{10} |1+j\omega T_1| - 20 \log_{10} |1+j\omega T_3| - 20 \log_{10} |T^2(j\omega)^2+2\zeta T(j\omega)+1|.$$

Plots of attenuation and phase for quadratic factors as a function of the relative damping ratio ζ are given in Figs. 5 and 6. The low-frequency asymptote is 0 dB, but the high-frequency asymptote has a slope of ±40 dB/decade (the positive slope applies to zero quadratic factors), twice the slope of the simple pole or zero case. The two asymptotes intersect at

$$\omega = 1/T.$$

The difference between the asymptotic plot and the actual curves depends on the value of ζ with a variety of shapes realizable for the actual curve. Regardless of the value of ζ, the actual curve approaches the asymptotes at both low and high

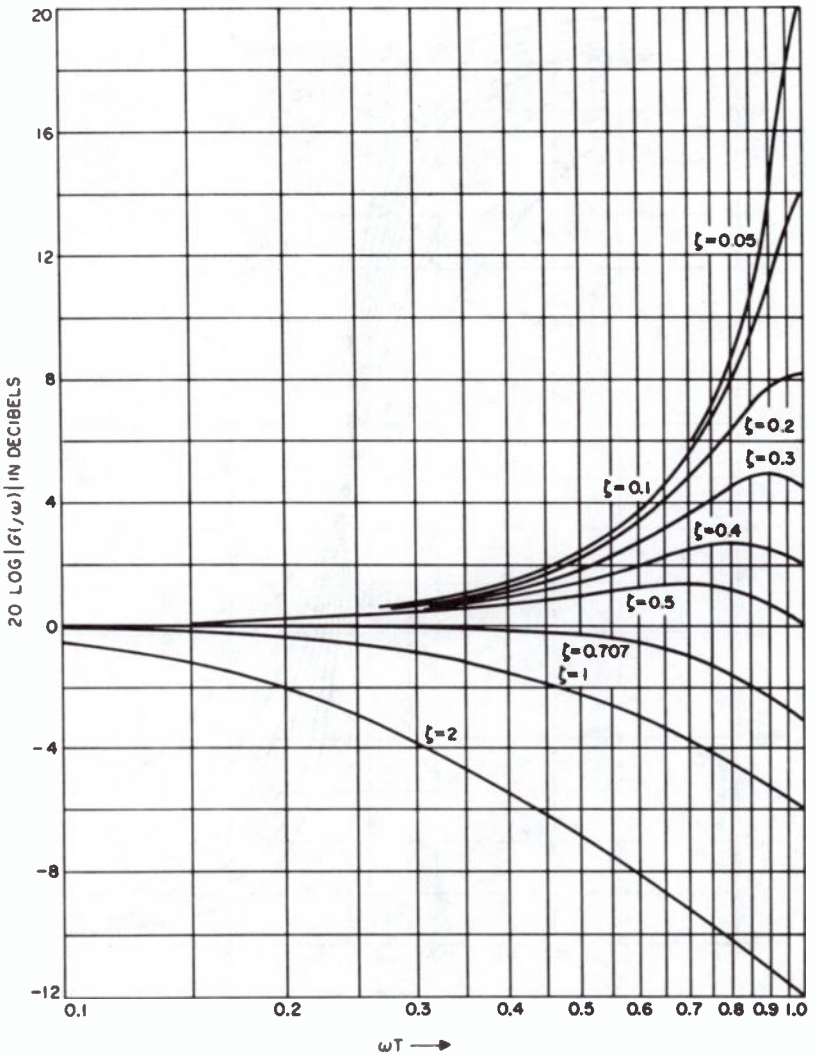

Fig. 5—Attenuation curve for quadratic factor. $G(j\omega)=1/[T^2(j\omega^2)+2\zeta T(j\omega)+1]$. *By permission from "Automatic Feedback Control System Synthesis," by J. G. Truxal. Copyright 1955, McGraw-Hill Book Company, Inc.*

frequencies. In addition, the error between the asymptotic plot and the actual curve is geometrically symmetrical about the break frequency $\omega=1/T$. As a result of this symmetry, the curves of Fig. 5 are plotted only for $\omega T \leq 1$. The error for $\omega=\alpha/T$ is identical with the error at $\omega=1/\alpha T$.

Log Plots Applied to Transfer Functions

Nyquist's method, although yielding satisfactory results, has undesirable limitations when applied to system synthesis because the quantitative effect of parameter changes is not readily apparent. The use of attenuation–phase plots yields a more direct approach to the problem. The method* is based on the relation between phase and the rate of change of gain with frequency of networks. As a first approximation, which is valid for simple systems, a gain rate of change of 20 dB/decade corresponds to a phase shift of 90°. Since the stability of a system can be determined from its phase margin at unity gain (0 dB), simple criteria for the slope of the attenuation curve can be established. Thus it is obvious that to avoid insta-

* A theorem due to Bode shows that the phase angle of a network at any desired frequency is dependent on the rate of change of gain with frequency, where the rate of change of gain at the desired frequency has the major influence on the value of the phase angle at that frequency.

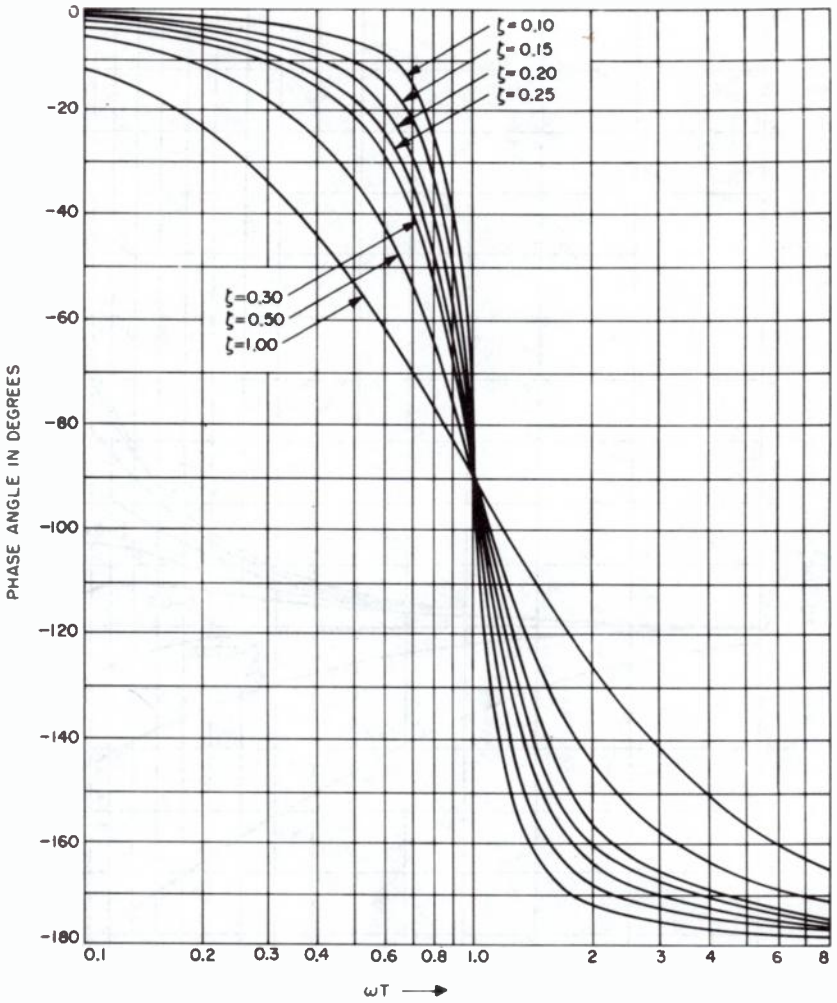

Fig. 6—Phase characteristic. *By permission from "Theory of Servomechanisms," by H. M. James, N. B. Nichols, and R. S. Phillips. Copyright 1947, McGraw-Hill Book Company, Inc.*

bility, the slope of the attenuation curve at unity gain must be appreciably less than −40 dB/decade (commonly about −33 dB/decade).

The design procedure is to construct asymptotic attenuation–phase curves as a first approximation. From this it can be determined whether the stability requirements are met. Refinements can be made by using the actual instead of asymptotic values for the curve as outlined in Fig. 4.

Figures 7 and 8 are examples of transfer functions plotted in this manner. In Fig. 7 a positive phase margin exists and the system is stable. Associated with the first-order pole at the origin is a uniform (low-frequency) slope of −20 dB/decade and −90° phase shift. This may be considered characteristic of the integrating action of a type-1 control system. Figure 8 is an unstable system. It has a negative phase margin (as a result of the steep slope of the attenuation curve). The former is stable, the latter is unstable.

Root-Locus Method

Root locus is a method of design due to Evans, based on the relation between the poles and zeros of the closed-loop system function and those of the open-loop transfer function. The rapidity and ease with which the loci can be constructed form the basis for the success of root-locus design methods, in much the same way that the simplicity of the gain and phase plots (Bode diagrams) makes design in the frequency domain so attractive. The root-locus plots can be used to adjust system gain, guide the design of compensation networks, or study the effects of changes in system parameters.

In the usual feedback control system, $G(s)$ is a rational algebraic function, the ratio of two polynomials in s; thus

$$G(s) = m(s)/n(s).$$

From Fig. 2

$$(C/R)(s) = G(s)/[1+G(s)]$$

$$= \frac{m(s)/n(s)}{1+[m(s)/n(s)]}$$

$$= m(s)/[m(s)+n(s)].$$

The zeros of the closed-loop system are identical with those of the open-loop system function.

The closed-loop poles are the values of s at which $m(s)/n(s) = -1$. The root-locus method is a graphic technique for determination of the zeros of $m(s)+n(s)$ from the zeros of $m(s)$ and $n(s)$. Root loci are plots in the complex s plane of the variations of the poles of the closed-loop system

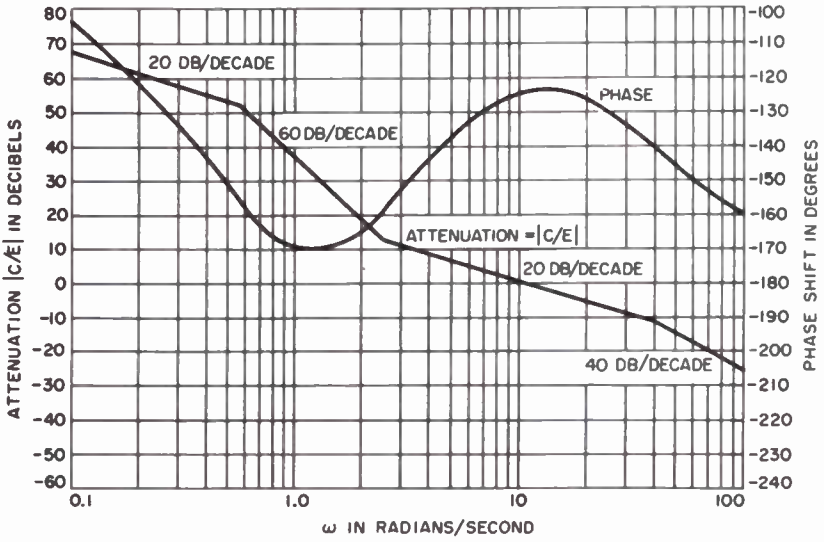

$$G = \frac{C}{E} = \frac{200(1+j0.4\omega)^2}{j\omega(1+j1.789\omega)^2(1+j0.25\omega)}$$

Fig. 7—Attenuation and phase shift for a stable system.

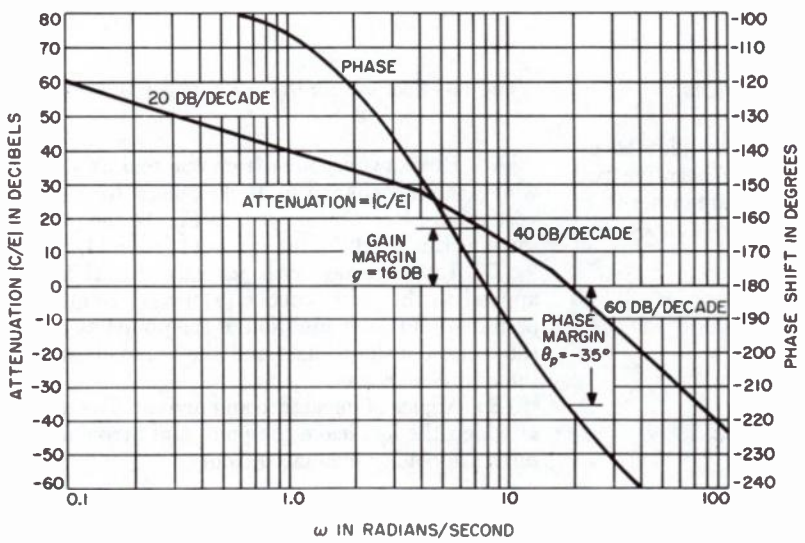

$$G = \frac{C}{E} = \frac{100}{j\omega(1+j0.25\omega)(1+j0.0625\omega)}$$

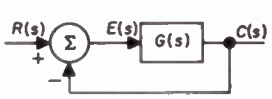

Fig. 8—Attenuation and phase shift for an unstable system.

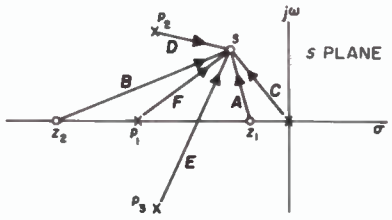

$$G(s)=K(AB/CDEF)$$
$$=\angle A+\angle B-\angle C-\angle D-\angle E-\angle F$$

Fig. 9—Graphic interpretation of $G(s)$.

function with changes in the open-loop gain. For the single-loop system of Fig. 2, the root loci constitute all s-plane points at which

$$\angle \mathbf{G(s)}=180°+n\,360°$$

where n is any integer including zero. For a type-1 feedback control system

$$\mathbf{G(s)}=\frac{K(s+z_1)(s+z_2)}{s(s+p_1)(s+p_2)(s+p_3)}.$$

A graphic interpretation is given in Fig. 9. Examples are given in Figs. 10 and 11.

Gain K_1, Fig. 11, produces the case of critical damping. An increase in gain somewhat beyond this value causes a damped oscillation to appear. The latter increases in frequency (and decreases in damping) with further increase in gain. At gain K_3 a sustained oscillation will result. Instability exists for gain greater than K_3, as at K_4. This corresponds to poles in the right half of the s plane for the closed-loop transfer function.

Aids in Sketching Root-Locus Plots

(A) The simplest portions of the plot to establish are the intervals along the negative real ($-\sigma$) axis, because then all angles are either 0° or 180°.

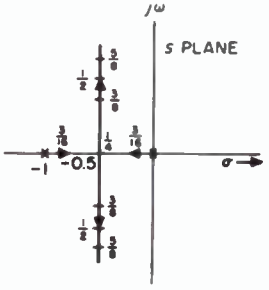

Fig. 10—Root loci for $G(s)=K/[s(s+1)]$. Values of K as indicated by fractions.

Complex pairs of zeros or poles contribute no net angle for points along the real axis.

Along the real axis, the locus will exist for intervals that have an *odd* number of zeros and poles to the right of the interval (Fig. 12).

(B) For very large values of s, all angles are essentially equal. The locus will thus finally approach asymptotes at the angles (Fig. 13) given by

$$\frac{180+n\,360°}{(\text{poles})-(\text{zeros})}.$$

These asymptotes meet at a point s_1 (on the negative real axis) given by

$$s_1=\frac{\sum(\text{poles})-\sum(\text{zeros})}{(\text{finite poles})-(\text{finite zeros})}.$$

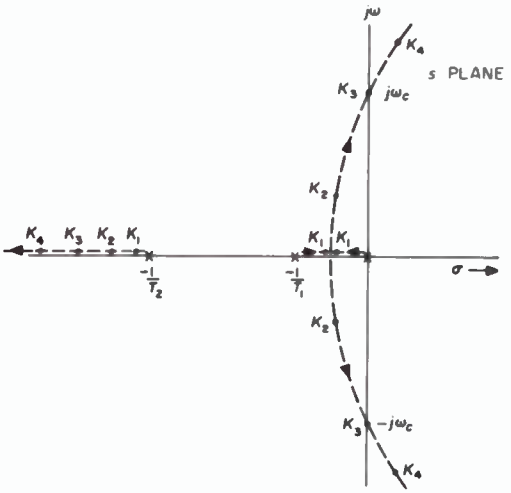

Fig. 11—Root loci for $G(s)=K/[s(T_1s+1)(T_2s+1)]$.

(C) Breakaway points from the real axis occur where the net change in angle caused by a small vertical displacement is zero. In Fig. 14 the point p satisfies this condition at $1/x_0=(1/x_1)+(1/x_2)$.

(D) Intersections with $j\omega$ axis. Routh's test applied to the polynomial $m(s)+n(s)$ frequently permits rapid determination of the points at which the loci cross the $j\omega$ axis and the value of gain at these intersections.

(E) Angles of departure and arrival. The angles at which the loci leave the poles and arrive at the zeros are readily evaluated from

$$\sum\angle\text{vectors from zeros to } s$$
$$-\sum\angle\text{vectors from poles to } s=180°+n\,360°.$$

For example, consider Fig. 15. The angle of departure of the locus from the pole at $(-1+j1)$ is

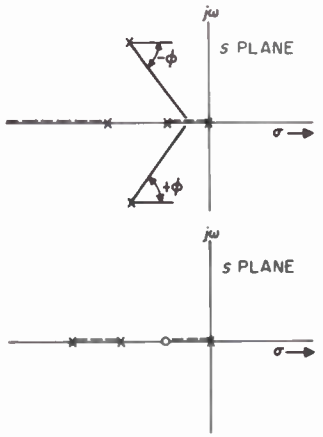

Fig. 12—Root-locus intervals along the real axis.

desired. If a test point is assumed only slightly displaced from the pole, the angles contributed by all critical frequencies (except the pole in question) are determined approximately by the vectors from these poles and zeros to $(-1+j1)$. The angle contributed by the pole at $(-1+j1)$ is then just sufficient to make the total angle 180°. In the example shown in the figure the departure angle is found from the relation

$$\overbrace{+45°}^{s+2} - (\overbrace{135°}^{s} + \overbrace{90°}^{s+1+j1} + \overbrace{26.6°}^{s+3} + \overbrace{\theta}^{s+1-j1}) = 180° + n\,360°.$$

Hence, $\theta = -26.6°$, the angle at which the locus leaves $(-1+j1)$.

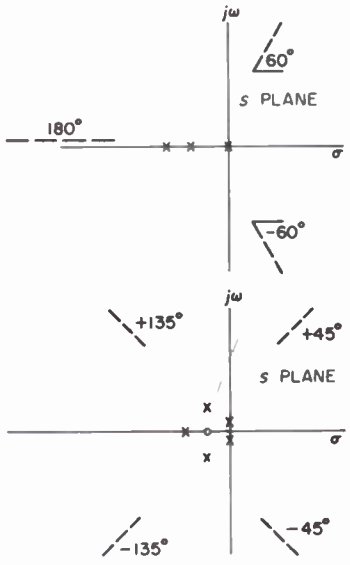

Fig. 13—Final asymptotes for root loci. Top, 60° asymptotes for system having 3 poles. Bottom, 45° asymptotes for system having an excess of 4 poles over zeros.

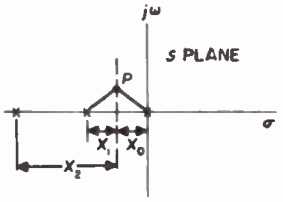

Fig. 14—Breakaway point.

METHODS OF STABILIZATION

Methods of stabilization for improving feedback-control-system response fall into the following basic categories:

(A) Series (cascade) compensation.
(B) Feedback (parallel) compensation.
(C) Load compensation.

In many cases any one of the above methods may be used to advantage and it is largely a question of practical considerations as to which is selected. Figure 16 illustrates the three methods.

Networks for Series Stabilization

Common networks for stabilization are shown in Fig. 17 with the transfer functions. The bridged-T network can be used for stabilization of ac systems although it has the disadvantage of requiring close control of the carrier frequency. Asymptotic attenuation and phase curves for the first three networks are shown in Figs. 18 and 19. The positive values of phase angle are to be associated with the phase-lead network whereas the negative values are to be applied to the phase-lag network. Figure 20 is a plot of the maximum phase shift for lag and

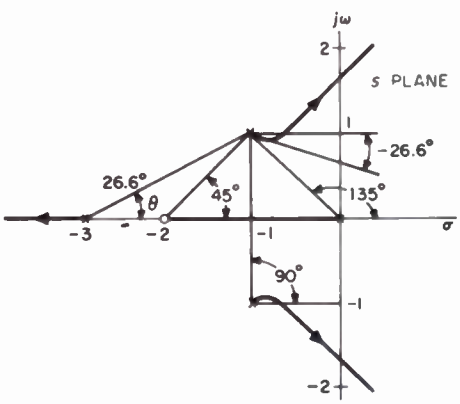

Fig. 15—Loci for
$G(s) = K(s+2)/[s(s+3)(s^2+2s+2)]$.

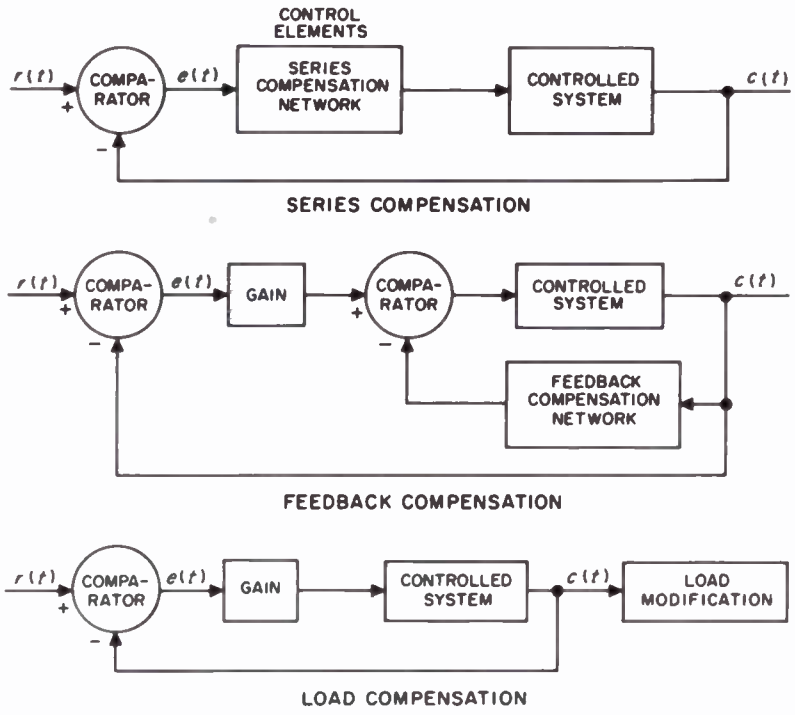

Fig. 16—Simple schemes for compensation.

lead networks as a function of the time-constant ratio.

Instead of direct feedback, the feedback connection may contain frequency-sensitive elements. Typical of such frequency-sensitive elements are tachometers or other rate- or acceleration-sensitive devices that may be fed back directly or through suitable stabilizing means.

Load Stabilization

The commonest form of load stabilization involves the addition of an oscillation damper (tuned or untuned) to change the apparent characteristics of the load. Oscillation dampers can be used to obtain the equivalent of tachometric feedback. The primary advantages of load stabilization are the simplicity of instrumentation and the fact that the compensating action is independent of drift of the carrier frequency in ac systems.

Error Coefficients

Of major importance in feedback control systems, along with stability, is system accuracy. *Static accuracy* refers to the accuracy of a system after the steady state is reached and is ordinarily measured with the system input constant or slowly varying. *Dynamic accuracy* refers to the ability of the system to follow rapid changes of the input. The following refers to a system such as Fig. 2.

Static-Error Coefficients

Position Error Constant:

$$K_p = \lim_{s\to 0}[C(s)/E(s)] = \lim_{s\to 0} G(s)$$

$$= (\text{controlled variable})/(\text{actuating error})$$

for a constant value of controlled variable.

Velocity Error Constant:

$$K_v = \lim_{s\to 0}[sC(s)/E(s)] = \lim_{s\to 0} sG(s)$$

$$= \frac{(\text{velocity of controlled variable})}{(\text{actuating error})}$$

for a constant velocity of controlled variable.

Acceleration Error Constant:

$$K_a = \lim_{s\to 0}[s^2C(s)/E(s)] = \lim_{s\to 0} s^2G(s)$$

$$= \frac{(\text{acceleration of controlled variable})}{(\text{actuating error})}$$

for constant acceleration of the controlled variable.

Phase-Lag Network:

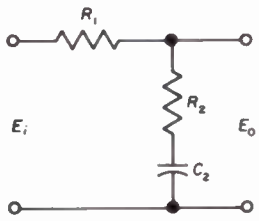

$$E_o/E_i=(T_2s+1)/(T_1s+1)$$

where

$$T_2=R_2C_2$$

$$T_1=(R_1+R_2)C_2.$$

Lead-Lag Network:

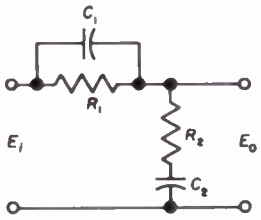

$$E_o/E_i=\frac{(T_1s+1)(T_2s+1)}{T_1T_2s^2+(T_1+T_2+T_{12})s+1}$$

where

$$T_1=R_1C_1$$

$$T_2=R_2C_2$$

$$T_{12}=R_1C_2$$

$$G_1=(T_1+T_2)/(T_1+T_2+T_{12}).$$

Phase-Lead Network:

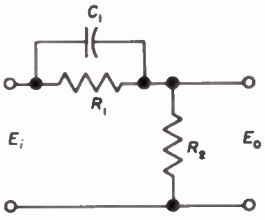

$$E_o/E_i=(T_2/T_1)[(T_1s+1)/(T_2s+1)]$$

where

$$T_1=R_1C_1$$

$$T_2=R_2R_1C_1/(R_1+R_2).$$

Bridged-T Network:

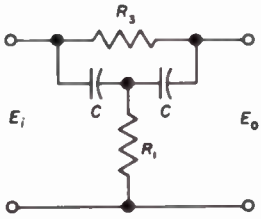

$$E_o/E_i=\frac{T_1T_2s^2+2T_1s+1}{T_1T_2s^2+(2T_1+T_2)s+1}$$

where

$$T_1=R_1C$$

$$T_2=R_2C.$$

Fig. 17—Networks for series stabilization.

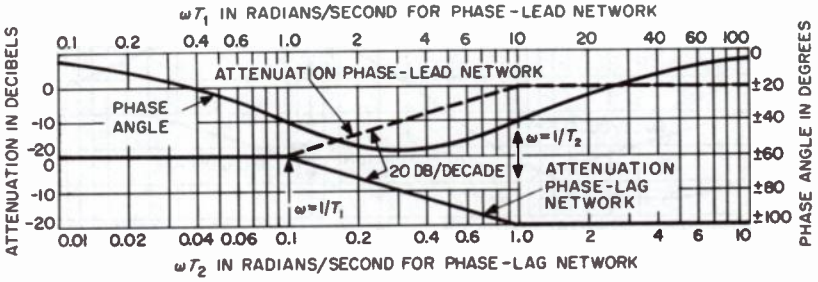

Fig. 18—Phase and attenuation for phase-lead and phase-lag networks. $T_1=10T_2$.

MULTIPLE INPUTS AND LOAD DISTURBANCES

Frequently systems are subjected to unwanted signals entering the system at points other than the input. Examples are load-torque disturbances, noise generated at a point within the system, etc. These may be represented as additional inputs to the system. Figure 21 is a block diagram of such a condition.

For linear operation

(A) $C/R = G_1G_2/(1+HG_1G_2)$

(B) $C/U = G_2/(1+HG_1G_2)$.

Combining (A) and (B)

$$C/U = (1/G_1)(C/R).$$

If it is desired that the sum of R and U be reproduced in the output (controlled variable), then G_1 should be equal to unity. If U is a disturbance to be minimized, then G_1 should be as large as possible. An example of such a disturbance is the torque produced on a radar antenna by wind forces.

Practical Application

An example of a common application is the positioning-type servomechanism shown in Fig. 22. Such a system ordinarily includes the following components: a comparator to measure the error, an amplifier, a second comparator or mixer to measure (E_1-B), a motor, and a tachometer.

For this system

$$C(s)/E(s) = G_1(s)G_2(s)/[1+H(s)G_2(s)]$$

$$C(s)/R(s) = \frac{G_1(s)G_2(s)}{[1+H(s)G_2(s)+G_1(s)G_2(s)]}.$$

CONTROL-SYSTEM COMPONENTS

Error-Measuring Systems: Potentiometers, Synchros

Commonly used error-measuring systems or comparators are shown in Fig. 23.

For synchros whose primary excitation is 115 volts, the error sensitivity is approximately 1 volt/degree for a load resistance of 10 000 ohms across the control-transformer rotor.

The static error of a synchro transmitter and control transformer combination is of the order of 18 minutes maximum and is a function of the rotor position. In some precision units, this error may be reduced to a few minutes of arc. In synchro-control transformers, a very undesirable characteristic is the presence of residual voltages at the null position. In well-designed units this voltage will be less than 30 millivolts.

Synchro errors can be materially reduced by the use of double-speed systems. Such systems consist of a dual set of synchro units whose shafts are geared in such a manner as to provide a "fine" and a "coarse" control. The synchro error can be effectively reduced by the factor of the gear ratio employed. Synchronizing networks are employed to provide for proper switching between the two sets of synchros.

Linear Motor and Load Characteristics

In the following, subscript m refers to motor, l refers to load, and 0 refers to combined motor and load.

θ = angular position in radians
r = angular velocity in radians/sec $= d\theta/dt$
T_m = motor-developed torque in pound-feet
J_m = motor moment of inertia in slug-feet^2
E_m = impressed volts
k_t = motor stalled-torque constant in pound-feet/volt $= [\Delta T_m/\Delta E_m]_{r_m}$
f_m = motor internal-damping characteristic in pound-feet-seconds/radian $= -[\Delta T_m/\Delta_{rm}]_{E_m}$
r_m = motor torque-inertia constant in 1/second $= T_m/J_m$
J_l = load inertia in slug-feet^2
f_l = load viscous-friction coefficient in pound-feet-seconds/radian

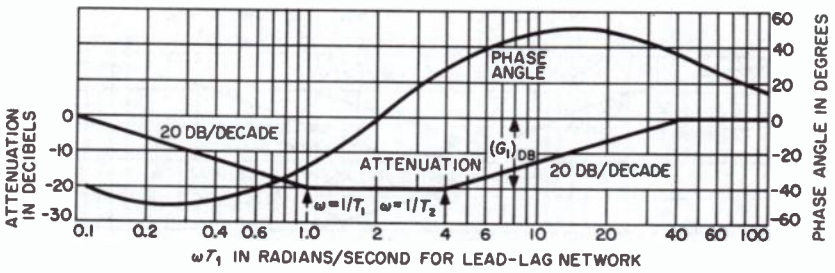

Fig. 19—Phase and attenuation for lead-lag network.

$G_1 = (T_1+T_2)/(T_1+T_2+T_{12})$. $T_2 = T_1/4$ and $T_{12} = 11.25T_1$.

F_l = load coulomb friction in pound-feet
N = motor-to-load gear ratio
$= \theta_m/\theta_l$
f_0 = overall viscous-friction coefficient referred to load shaft
$= f_l + N^2 f_m$
J_0 = overall inertia referred to load shaft
$= J_l + N^2 J_m$
T_0 = overall time constant in seconds
$= J_0/f_0$.

The ideal motor characteristics of Fig. 24 are quite representative of dc shunt motors. For alternating-current two-phase servomotors, one phase of which is excited from a constant-voltage source (the reference winding), the curves are approximately valid up to about 40 percent of synchronous speed.

The speed and load-transfer characteristics are given by

$$\theta_0(s) = [k_t N E_m(s) - F_l(s)]/(J_0 s^2 + f_0 s).$$

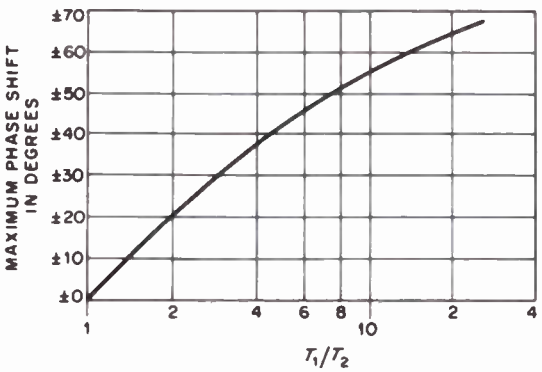

Fig. 20—Maximum phase shift for phase-lead (use positive angles) and phase-lag (negative angles) networks.

When the coulomb friction F_l can be neglected

$$G(s) = \theta_0(s)/E_m(s)$$
$$= k_t N/[f_0 s(T_0 s + 1)].$$

Rate Generators

A rate generator (or tachometer generator) is a precision electromechanical component resembling a small motor and having an output voltage proportional to its shaft rotational speed. Rate generators have extensive applications both as computing instruments and as stabilizing components of feedback control systems. An example of the latter is illustrated in Fig. 22. The use of the rate generator produces an effective viscous damping and also tends to linearize the servomechanism by inserting damping of a linear nature and of such magnitude that it swamps out the rather large nonlinear damping of the motor. To eliminate the backlash between rate generators and servomotors, they are often constructed as integral units having a common shaft. These units are available for dc or ac (either 400- or 60-hertz) operation.

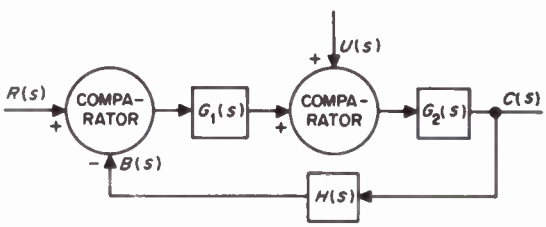

Fig. 21—Multiple-input control system.

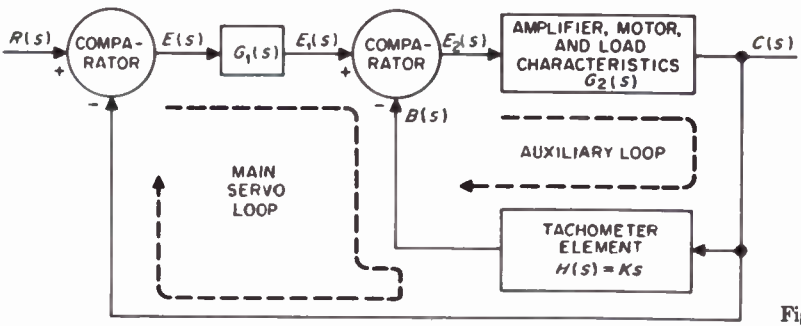

Fig. 22—Positioning-type servo.

PART 2—NONLINEAR SYSTEMS

SCOPE

All physical systems have nonlinearities and time-varying parameters to some degree. This is justified by the fact that any element may physically break down or exhibit deterioration as a result of time.

Linear systems, as described in the preceding sections, have a linear relationship between the variables described by a linear differential equation; the theory of superposition also applies. Analysis and synthesis techniques applicable to any linear system have been thoroughly investigated and developed.

Nonlinear systems have no general methods of analysis and synthesis. Therefore, for reasons of simplicity, they are often treated with linear approximations and, in many cases of small nonlinear effects, satisfactory results have been obtained. In general, however, linear methods become restrictive in their application and quite often unrealistic.

There are many different ways of solving nonlinear systems that may be applicable to a certain type of system but not to all. Among these methods, two techniques have proved useful in the study of nonlinear systems.

The describing-function technique was first applied to the analysis of nonlinear feedback control systems by Kochenburger.* It is the object of the describing-function method of analysis to reduce the representation of the nonlinearity to an equivalent linear gain and phase angle. The representation of the nonlinearity is described in terms of the fundamental component of the distorted output waveform in response to a sinusoidal input. The result of the describing-function analysis is a representation of the system in the frequency domain; however, the correlation between the time and frequency domains in comparison with linear system analysis is much less precise in nonlinear system analysis. The synthesis of nonlinear systems can be carried out with the describing-function technique in much the same way as is done with linear systems. The describing-function technique is therefore most useful in complex systems of relatively high order and where the effect of the nonlinearity is small but significant.

The phase-plane method, on the other hand, is a representation of the behavior of the first- and second-order systems portrayed on the phase plane. The phase-plane diagrams can be interpreted directly in terms of time domain; they thus are a useful tool in the study of transient response to any initial condition and in some cases to step and ramp inputs. The phase-plane method does not readily indicate the steps required to correct system performance, and synthesis is carried out by trial-and-error procedures.

This method can be extended to higher-order systems in the so-called phase space. However, an nth-order system in the nth-dimensional phase space compared with the phase plane is difficult to envision and interpret and may be less effective

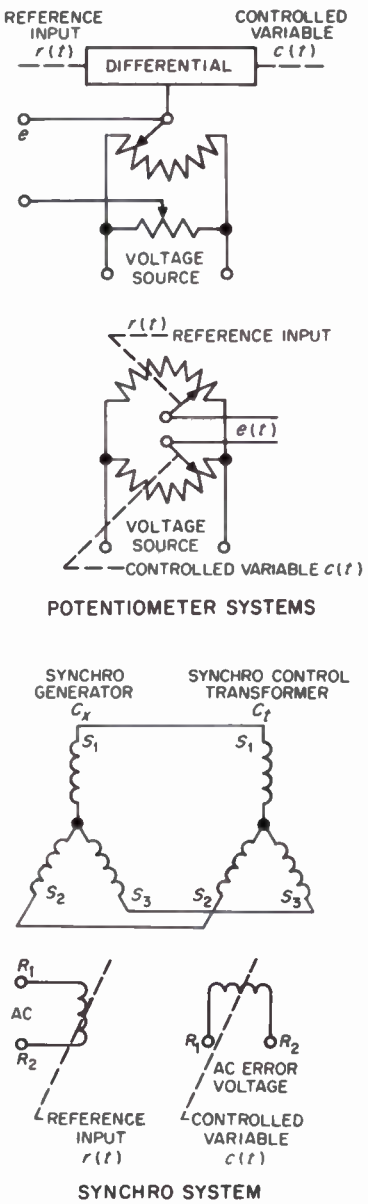

Fig. 23—Error-measuring systems.

* R. J. Kochenburger, "A Frequency Response Method For Analyzing and Synthesizing Contractor Servomechanisms," *AIEE Transactions*, vol. 69, pp. 270–284; 1950.

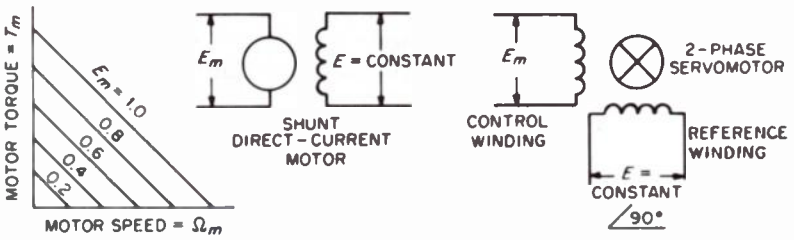

Fig. 24—Ideal motor curves.

in its usefulness. In summary, this method is useful for large nonlinearities of the second-order systems.

The two methods are in a sense complementary and constitute the principal tools for the study of nonlinear control problems.

CHARACTERISTICS OF NONLINEAR SYSTEMS

A comparison of linear and nonlinear systems yields the following representative characteristics.

Principle of Superposition Does Not Apply

In nonlinear systems, the response to a combination of individual signals at the input will not be the same as the response to the sum of those same signals. The impulse response (weighting function) describing the frequency response is therefore not applicable. The familiar Laplace transform operation ($s=\sigma+j\omega$) and the transfer-function concept used extensively in linear systems cannot be directly applied without some modification. In fact, transfer functions are noncommutative in nonlinear systems. That is, in a linear system transfer, functions $G_1(s)$ and $G_2(s)$ can be cascaded as $G_1(s)\cdot G_2(s)$ or $G_2(s)\cdot G_1(s)$, whereas in nonlinear systems $N_1\cdot N_2$ is not the same as $N_2\cdot N_1$.

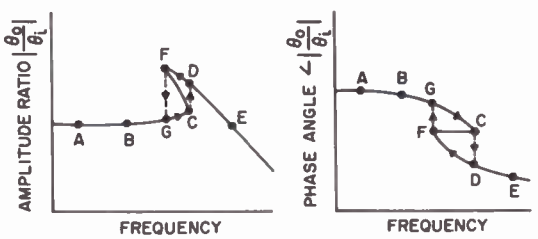

Fig. 25—Jump resonance.

Nonlinear Response Is Dependent On Input Signal

In linear systems, the system response is strictly a function of the system parameters. A system proved to possess a good stable response to one type of input will behave similarly to any other type of input. Nonlinear systems, on the other hand, are dependent on the input-signal size and initial conditions as well as the system parameter. A stable response for one input signal may be unstable for another.

In nonlinear systems, phenomena which are ordinarily unexplainable by linear analytical methods (generation of new frequencies, jump resonance, limit cycles, etc.) exist. The following are examples of such unique nonlinear phenomena.

Jump Resonance

The phenomenon called jump resonance is observed in certain closed-loop systems with saturation, where the input–output amplitude ratio and phase angle as a function of frequency exhibit sudden discontinuities. The typical closed-loop gain characteristics of a saturating system with jump resonance are shown in Fig. 25. $|\theta_o/\theta_i|$ is plotted as a function of frequency for a fixed amplitude θ_i. As the frequency is increased from zero, the frequency response follows the curve along points A, B, and C. At point C a sudden discontinuous jump to D is observed with an incremental increase in frequency. Further increase in frequency leads to point E along the curve. If the frequency is reversed, the response retraces the path E, D and continues to point F at which a sudden jump to point G occurs and continues on through B and A of the gain curve. The phase-angle response behaves similarly. The overall response curve exhibits a hysteresis-type property or jump resonance. The system response dependent on the input-signal size is illustrated in Fig. 26. $|\theta_o/\theta_i|$ is plotted for different values of θ_i. For small-signal values of θ_i,

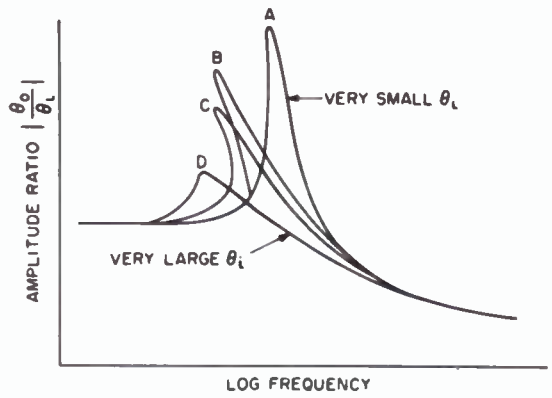

Fig. 26—Closed-loop frequency response of a saturating amplifier. *D. Graham and D. McRuer, "Analysis of Nonlinear Control Systems," fig. 1–18, ©1961, John Wiley & Sons, Inc., New York.*

the system behaves linearly, corresponding to curve A. As the input-signal value is increased, jump resonance is observed as shown in curves B and C.

Limit Cycle

Limit cycle is a phenomenon of oscillation peculiar to nonlinear systems. The oscillatory behavior, unexplainable in terms of linear theory, is characterized by a constant amplitude and frequency determined by the nonlinear properties of the system. Limit cycles are distinguishable from linear oscillation in that their amplitude of oscillation is independent of initial conditions. For instance, if a system has a stable limit cycle, the system will tend to fall into the limit cycle, with the output approaching the amplitude of that limit cycle regardless of the initial condition and forcing function. A limit cycle is easily recognized in the phase plane as an isolated closed path as shown in Fig. 27.

Often the system falls into a limit cycle in the presence of very small excitation or disturbances. This behavior is termed *soft self-excitation*. Conversely, for systems requiring forced excitation above a certain minimum amplitude or appropriate initial condition before entering a limit cycle, the term *hard self-excitation* is used. In any event, the presence of limit cycles in control systems is undesirable and makes isolation of these limit cycles important to the analysis of nonlinear systems. The phase-plane method described on p. 15-28 provides techniques for investigating limit cycles.

Generation of New Frequencies

In a nonlinear system the output of the nonlinear device contains harmonic and subharmonic frequencies of the input signal. For instance, application of two sine waves of different frequencies f_1 and f_2 to the input will produce components corresponding to the input frequencies f_1, f_2, their sum and difference $f_1 \pm f_2$, their higher harmonics mf_1, nf_2, and their various combinations of sums and differences $mf_1 \pm nf_2$. In a linear system only the components of the input frequencies f_1, f_2 will be reflected in the output. This exemplifies why the frequency-response concept pertaining to linear systems must be modified for nonlinear applications.

Hysteresis

Multivalued functions exist when two or more function values correspond to the value of the variable. Multivalued functions are intrinsically nonlinear. Some examples of this are the hysteresis curves of magnetic materials and the backlash of a gear train.

TYPES OF NONLINEAR ELEMENTS

Because of the infinite variety of nonlinearities, specific classification becomes impossible. Two generally accepted classifications do exist; they are the *incidental* and *intentional* nonlinearities.

Incidental nonlinearities are extraneous to system design and are usually undesirable. Saturation, dead zone, and backlash are examples of nonlinearities that may lead to inaccurate and poor response or even instability. There are cases, however, where incidental nonlinearities aid and improve the system response.

Intentional nonlinearities are functions purposely introduced into the system to compensate and improve performance. The relay servo system is typical of this type. Other classifications are the *single-valued* function and *multivalued* function. These functions are transfer characteristics describing the input-to-output relationship of the

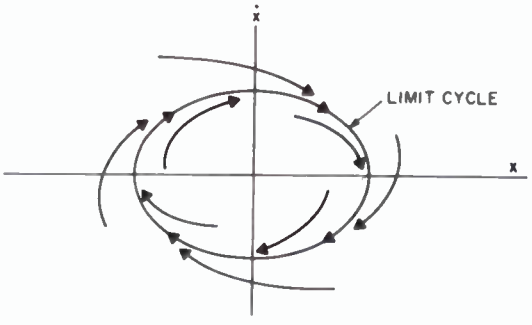

Fig. 27—Limit cycle.

nonlinear element. Single-valued functions have only one output value corresponding to the input value, while the multivalued functions have two or more output values. Several typical nonlinear characteristics commonly encountered in control systems are presented in Fig. 28.

In addition to the classifications described above, other functions to be found may include large and small values of continuous and discontinuous types of nonlinearities. More than one classification may apply to any nonlinear function.

ANALYTICAL METHODS FOR SOLVING NONLINEAR SYSTEMS

The analytical methods for solving nonlinear systems described in this section will be concentrated mainly on graphical methods for describing-function techniques and phase-plane methods. Other methods of analysis are:

(A) Direct Solution to the Nonlinear Differential Equation. There are certain nonlinear differential equations of lower order that are analytically solvable or integrable; however, they are very rare.

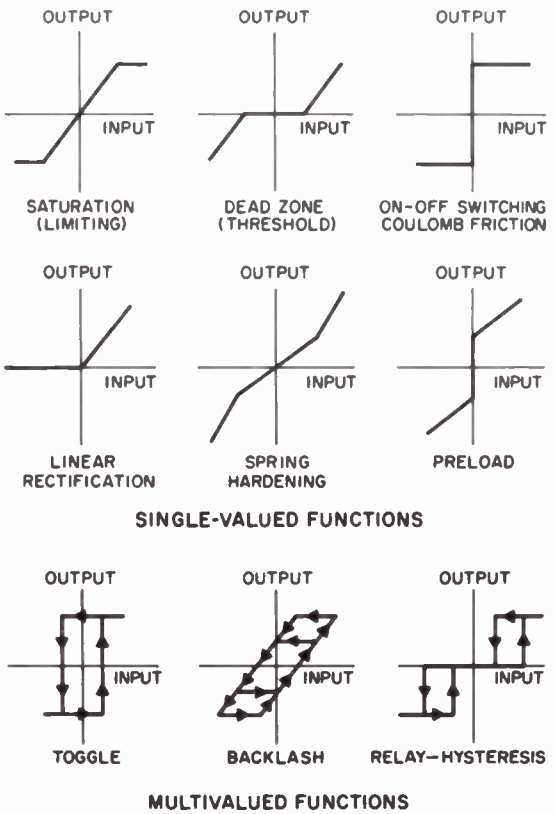

Fig. 28—Types of nonlinear elements.

(B) Numerical Method. The numerical method is a step-by-step process obtaining the solution to the differential equation as a table of corresponding values of independent and dependent variables. In theory any equation can be solved numerically, although the process may be quite complex.

Neither (A) nor (B) is discussed here but further information may be found in references 5–8 of the bibliography.

Describing-Function Technique

This technique is valuable in the analysis and design of an important class of nonlinear feedback control systems, in which the output of the nonlinear element is filtered by a linear element having low-pass frequency characteristics as it travels around the control loop. The object of the describing-function technique is to represent the actual nonlinearity of the system in terms of an equivalent linear system by considering only the fundamental component of the output waveform of the nonlinear element subject to a sinusoidal input.

Describing Function: The describing-function analysis is made of the following basic assumptions.

(A) The input to the nonlinear element n is a sinusoidal signal, and only the fundamental component of the output of n contributes to the input. The output response of a nonlinear element to a periodic signal consists of the fundamental frequency component of the input signal and its harmonics. Generally, the harmonic components are smaller in amplitude compared with the fundamental component. Further, in most control systems the system behaves as a low-pass filter and the higher harmonics are attenuated. If the higher harmonics are sufficiently small they can be neglected and the equivalent linear approximation may be justified.

(B) There is only one nonlinear element in the system. All nonlinearities in the system are lumped into one single nonlinear element n. Figure 29 shows a block diagram of a closed-loop system containing a nonlinear element n.

(C) The output of the lumped nonlinear element is a function only of the present value and past history of the input, i.e., n is not a function of time.

The describing function of a nonlinear element

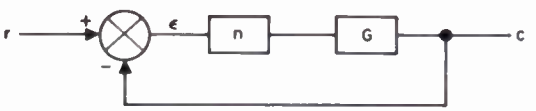

Fig. 29—Block diagram of nonlinear closed-loop system.

is defined as the ratio of the fundamental frequency component of the output as a complex quantity (amplitude and phase angle) to the amplitude of the sinusoidal input signal. If the input signal as applied to the nonlinear element n is described by

$$e_{in}(t) = X \sin\omega t$$

the output response $e_o(t)$ may generally take the form of

$$e_o(t) = (a_0X/2) + a_1X \sin\omega t + b_1X \cos\omega t + \sum_{n=2}^{\infty} a_nX \sin n\omega t + \sum_{n=2}^{\infty} b_nX \cos n\omega t + \text{subharmonics}.$$

The $(a_0/2)$ term is the dc component; a_n and b_n are the harmonic components.

The fundamental frequency component of the output may be expressed in terms of amplitude and phase angle as

$$e_{o1} = A(\omega, X)X \sin[\omega t + \phi(\omega, X)].$$

$A(\omega, X)X$ is the amplitude and $\phi(\omega, X)$ is the phase angle of the fundamental component. Both amplitude and phase angle are a function of the frequency and amplitude of the input signal. The describing function $N(\omega, X)$ by definition is

$$\begin{aligned} N(\omega, X) &= \{A(\omega, X)X \exp[j\phi(\omega, X)]/X\} \\ &= A(\omega, X) \exp[j\phi(\omega, X)] \\ &= A(\omega, X) \cos\phi(\omega, X) \\ &\quad + jA(\omega, X) \sin\phi(\omega, X). \end{aligned} \quad (1)$$

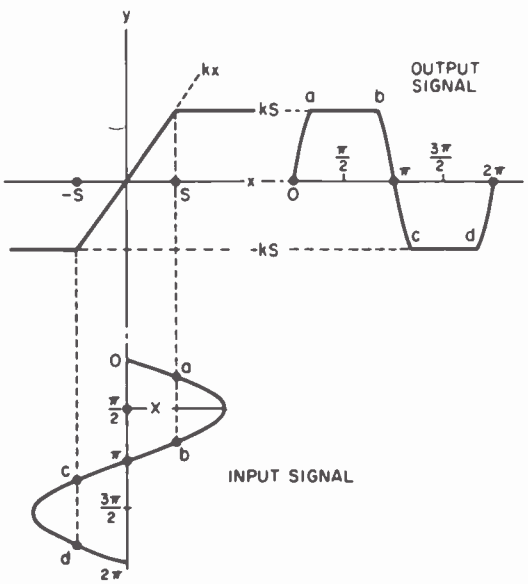

Fig. 30—Graphic representation of saturation.

The describing function $N(\omega, X)$ may be purely real or contain a phase angle depending on the type of nonlinearity. For single-valued nonlinear functions N is real, whereas for multivalued functions phase shift exists, generally lagging.

Calculation of a Describing Function: Calculation of the describing function involves performing a conventional Fourier analysis on the output waveform to obtain the fundamental component. The Fourier series expansion of the output waveform to an input sinusoidal $X \sin\omega t$ may be expressed as

$$e_o(t) = (a_0X/2) + a_1X \sin\omega t + b_1X \cos\omega t + a_2X \sin 2\omega t + b_2X \cos 2\omega t + \cdots.$$

For the describing function, only the coefficients of the fundamental frequency component are required. The coefficients may be obtained from the integrals

$$a_1 = (\pi X)^{-1} \int_0^{2\pi} f_o(t) \sin\omega t \cdot d(\omega t) \quad (2)$$

$$b_1 = (\pi X)^{-1} \int_0^{2\pi} f_o(t) \cos\omega t \cdot d(\omega t) \quad (3)$$

where $f_o(t)$ is the exact output of the nonlinear element expressed as a function of time. The describing function is then

$$|N(\omega, X)| = |a_1 + jb_1| = (a_1^2 + b_1^2)^{1/2}$$
$$\angle N(\omega, X) = \tan^{-1}(b_1/a_1).$$

Where the exact output function $f_o(t)$ is known, the above method is applicable. If the function is not known, a graphical Fourier expansion can be performed on the output waveform. Two examples describing the procedure for calculation of the describing function using the graphical method are given.

Example 1: *Saturation-Type Nonlinearity*. A nonlinear element with saturation is shown in Fig. 30.

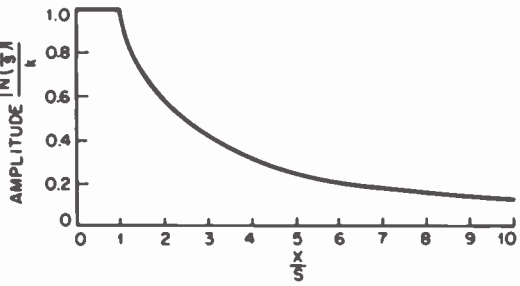

Fig. 31—Describing function for saturation (normalized amplitude).

The output y is held constant for input values greater than S. This region is called saturation or limiting. For input values less than S the output behaves linearly with the input. The input–output relationship can be expressed by

(A) $y=kx$ for $-S<x<S$

(B) $y=kS$ for $x>S$

(C) $y=-kS$ for $x<-S$.

The output is an odd function and thus only the sine term of the fundamental equation need be calculated. Furthermore, because of symmetry only the first quarter of the integration need be evaluated as follows:

$$a_1=(4/\pi X)\int_0^{\pi/2} f_o(t)\,\sin\omega t\cdot d(\omega t).$$

If the input is $x=X\sin\omega t$, then the output $f_o(t)=y$ is expressed by

$$f_o(t)=kX\sin\omega t \qquad X<S$$

and for X greater than S

$$f_o(t)=kX\sin\omega t \qquad 0<\omega t<\sin^{-1}(S/X)$$
$$=kS \qquad \sin^{-1}(S/X)<\omega t<\pi/2.$$

Therefore the coefficients a_1 are

$$a_1=k \qquad \text{for } X<S$$

and for X greater than S

$$a_1=(4/\pi X)\int_0^{\sin^{-1}(S/X)} kX\,\sin^2(\omega t)\cdot d(\omega t)$$
$$+(4/\pi X)\int_{\sin^{-1}(S/X)}^{\pi/2} kS\,\sin\omega t\cdot d(\omega t)$$
$$=(2k/\pi)[\phi+\tfrac{1}{2}(\sin 2\phi)]$$

where $\phi=\sin^{-1}(S/X)$.

The describing function N is given by

$$N=k \qquad X<S$$
$$N=k(2/\pi)[\phi+\tfrac{1}{2}(\sin 2\phi)] \qquad X>S.$$

The variation of amplitude of N with respect to X/S is plotted in Fig. 31. The phase angle is zero over the entire range.

Example 2: *Backlash-Type Nonlinearity*. For the second example a simple backlash-type nonlinearity of Fig. 32 is evaluated. The backlash is a multi-valued nonlinearity where the input–output relationship follows a different path dependent on

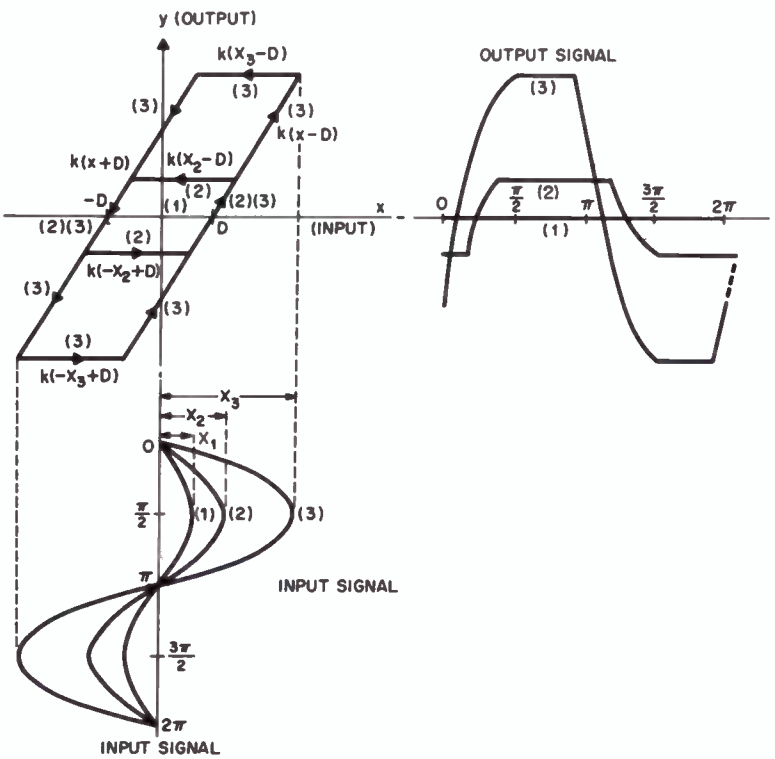

Fig. 32—Graphic representation of backlash nonlinearity. *E. Levinson, "Nonlinear Feedback Control Systems," Electro-Technology, p. 139, fig. 36; September 1962.*

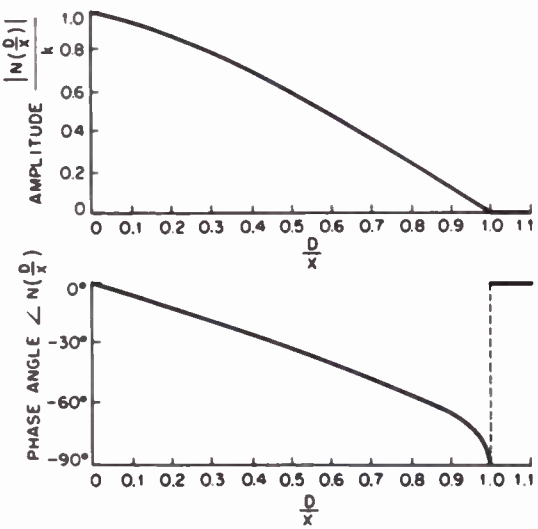

Fig. 33—Describing function for backlash (normalized amplitude and phase angle).

the input-signal amplitude (curves (1), (2), and (3)). After the steady state is established, the output $f_o(t)$ corresponding to different values of X of an input signal $x = X \sin\omega t$ are:

(A) For $X<D$ (curve 1):

$$f_o(t)=0.$$

(B) For $D<X<2D$ (curve 2):

$$f_o(t)=-k(X-D) \qquad 0<\omega t<\sin^{-1}[(2D/X)-1]$$

$$f_o(t)=k(X\sin\omega t-D) \qquad \sin^{-1}[(2D/X)-1]<\omega t<\tfrac{1}{2}\pi$$

$$f_o(t)=k(X-D) \qquad \tfrac{1}{2}\pi<\omega t<\pi+\sin^{-1}[(2D/X)-1]$$

$$f_o(t)=k(X\sin\omega t+D) \qquad \pi+\sin^{-1}[(2D/X)-1]<\omega t<\tfrac{3}{2}\pi$$

$$f_o(t)=-k(X-D) \qquad \tfrac{3}{2}\pi<\omega t<2\pi.$$

(C) For $X>2D$ (curve 3):

$$f_o(t)=k(X\sin\omega t-D) \qquad 0<\omega t<\tfrac{1}{2}\pi$$

$$f_o(t)=k(X-D) \qquad \tfrac{1}{2}\pi<\omega t<\pi-\sin^{-1}[1-(2D/X)]$$

$$f_o(t)=k(X\sin\omega t+D) \qquad \pi-\sin^{-1}[1-(2D/X)]<\omega t<\tfrac{3}{2}\pi$$

$$f_o(t)=-k(X-D) \qquad \tfrac{3}{2}\pi<\omega t<2\pi-\sin^{-1}[1-(2D/X)]$$

$$f_o(t)=k(X\sin\omega t-D) \qquad 2\pi-\sin^{-1}[1-(2D/X)]<\omega t<2\pi.$$

Solving for a_1 and b_1 of equations (2) and (3), for the three conditions above, yields the describing-function terms

$$a_1=0 \qquad X<D$$

$$a_1=(k/\pi)[\tfrac{1}{2}\pi+\theta+\tfrac{1}{2}(\sin 2\theta)] \qquad X>D$$

$$b_1=0 \qquad X<D$$

$$b_1=(-k/\pi)\cos^2\theta \qquad X>D$$

where

$$\theta=\sin^{-1}[1-(2D/X)]$$

or in terms of amplitude and phase angle

$$|N|=(k/\pi)\{[\tfrac{1}{2}\pi+\theta+\tfrac{1}{2}(\sin 2\theta)]^2+\cos^4\theta\}^{1/2}$$

$$\angle N=\tan^{-1}\left[-\left(\frac{\cos^2\theta}{\tfrac{1}{2}\pi+\theta+\tfrac{1}{2}(\sin 2\theta)}\right)\right].$$

The normalized amplitude and phase angle of the describing function N for different values of D/X is plotted in Fig. 33.

The describing function is calculated simply by determining the fundamental output component of the nonlinear element. The third-harmonic component may be obtained to estimate the accuracy of the describing-function analysis. Describing functions for some of the common nonlinear elements are given in Table 1.

Stability Analysis: The describing function N of the nonlinearity can be used to determine the stability of the system, providing the harmonics are sufficiently attenuated. In general, the describing function is a function of both frequency and amplitude of the input signal.

The closed-loop transfer function of the nonlinear feedback system for Fig. 34 is given by

$$(c/r)(\omega, X)=\frac{N(\omega, X)G(j\omega)}{1+N(\omega, X)G(j\omega)}.$$

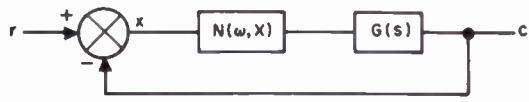

Fig. 34—Single-loop nonlinear system.

TABLE 1—DESCRIBING FUNCTIONS FOR COMMON NONLINEAR ELEMENTS.

DESCRIBING FUNCTION: $N(X)=a_1+jb_1$ or $|N(X)|=(a_1^2+b_1^2)^{1/2}$. $\angle N(X)=\tan^{-1}(b_1/a_1)$.

Characteristic	Describing-Function Coefficients	
A 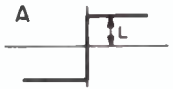	$a_1=4S/\pi X$ $b_1=0$	
B 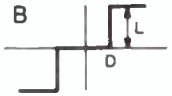	$a_1=(4S/\pi X)\cos\theta$ $b_1=0$	$\theta=\sin^{-1}(D/X)$
C 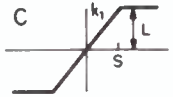	$a_1=(2k_1/\pi)[\theta+\frac{1}{2}(\sin 2\theta)]$ $b_1=0$	$\theta=\sin^{-1}(S/X)$
D	$a_1=(2k_1/\pi)[\frac{1}{2}\pi-\theta-\frac{1}{2}(\sin 2\theta)]$ $b_1=0$	$\theta=\sin^{-1}(D/X)$
E	$a_1=(2k_1/\pi)[\psi-\theta+\frac{1}{2}(\sin 2\psi)-\frac{1}{2}(\sin 2\theta)]$ $b_1=0$	$\psi=\sin^{-1}(S/X)$ $\theta=\sin^{-1}(D/X)$
F 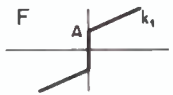	$a_1=k_1+(4A/\pi X)$ $b_1=0$	
G 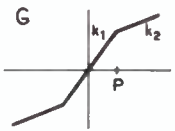	$a_1=k_2-[(k_2-k_1)/\pi](2\theta+\sin 2\theta)$ $b_1=0$	$\theta=\sin^{-1}(P/X)$

Characteristic	Describing-Function Coefficients	
H	$a_1=\frac{1}{2}k_1$ $b_1=0$	
I 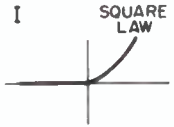	$a_1=4X/3\pi$ $b_1=0$	
J 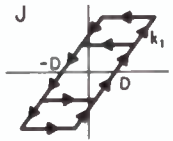	$a_1=(k_1/\pi)[\frac{1}{2}\pi+\theta+\frac{1}{2}(\sin 2\theta)]$ $b_1=-(k_1/\pi)\cos^2\theta$	$\theta=\sin^{-1}[1-(2D/X)]$
K 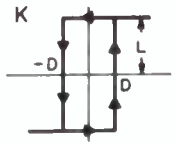	$a_1=(4L/\pi X)\cos\theta$ $b_1=-(4L/\pi X)\sin\theta$	$\theta=\sin^{-1}(D/X)$
L 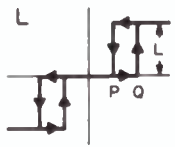	$a_1=(2L/\pi X)(\cos\theta+\cos\psi)$ $b_1=(2L/\pi X)(\sin\psi-\sin\theta)$	$\psi=\sin^{-1}(P/X)$ $\theta=\sin^{-1}(Q/X)$

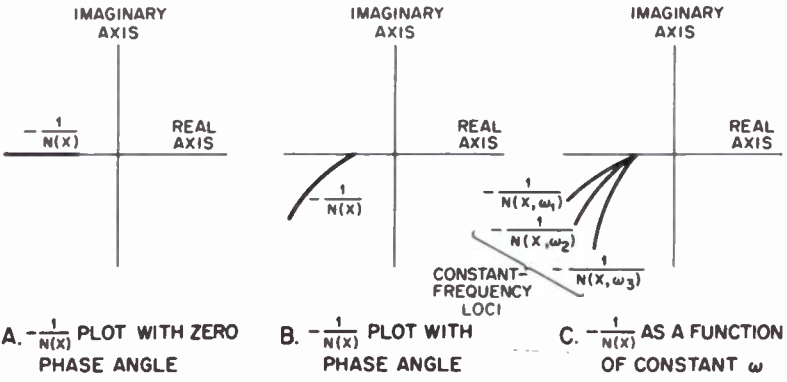

Fig. 35—Typical polar plots of various $N(\omega,X)$.

The characteristic equation of the system is

$$1+N(\omega, X)G(j\omega)=0 \qquad (4)$$

or

$$G(j\omega)=-[1/N(\omega, X)].$$

The condition of (4) must be satisfied for sustained oscillation of the output with zero input. Since $N(\omega, X)$ is a function of both frequency and amplitude, various combinations of ω and X can be found for oscillation. If there are no possible combinations satisfying the oscillatory condition, the system is stable. In the case of sustained oscillation, the oscillatory mode may be either stable or unstable. If a slight disturbance in amplitude or frequency occurs and the oscillation returns to its original value, the oscillation is stable (stable limit cycle). If the oscillation amplitude increases or decreases from the original value, the oscillation is unstable (unstable limit cycle). The stability of the closed-loop system may be evaluated analytically by directly solving the characteristic equation by any one of the modified linear graphical methods.

Polar Plot (Nyquist Diagram): The conventional Nyquist diagram must be modified to apply the Nyquist stability criteria to the frequency-response plot. In a linear system the critical point on the Nyquist diagram is -1. For nonlinear systems the $-[1/N(\omega, X)]$ locus corresponds to the critical point -1. To evaluate the stability of the system, both $-[1/N(\omega, X)]$ and the $G(j\omega)$ function are plotted on the polar plane. The describing function $N(\omega, X)$ generally is a function of both ω and X. If N is only a function of X, there will be one locus $-[1/N(x)]$ plotted as a function of X. If N is also a function of ω, a family of constant-frequency loci are plotted for different values of ω (see Fig. 35).

The stability of the system is determined by the following relationship between the $-[1/N(\omega, X)]$ locus and the $G(j\omega)$ plot (Fig. 36). If the $-[1/N(\omega, X)]$ lies to the left of the $G(j\omega)$ plot or is not enclosed, the system is *stable*. Conversely, if the $-[1/N(\omega, X)]$ lies to the right of the $G(j\omega)$ plot or is enclosed, the system is *unstable*. If the $-[1/N(\omega, X)]$ locus intersects with the $G(j\omega)$ plot, the system may have a *sustained oscillation*. In the case where N is a function of ω, the condition for sustained oscillation is satisfied if the ω of the $G(j\omega)$ plot at the intersecting point

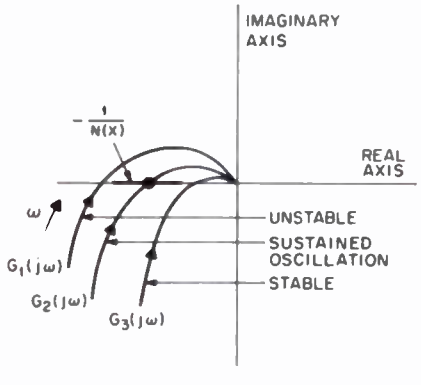

Fig. 36—Polar-plot stability criteria.

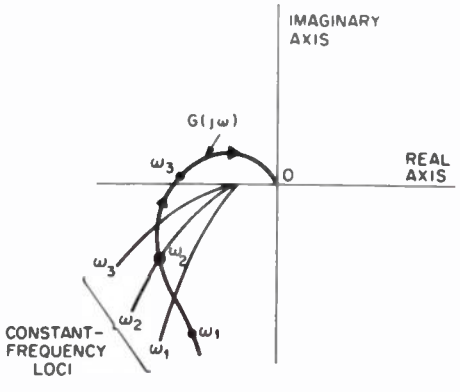

Fig. 37—Typical polar plot of $G(j\omega)$ and $-[1/N(\omega, X)]$ as a function of ω.

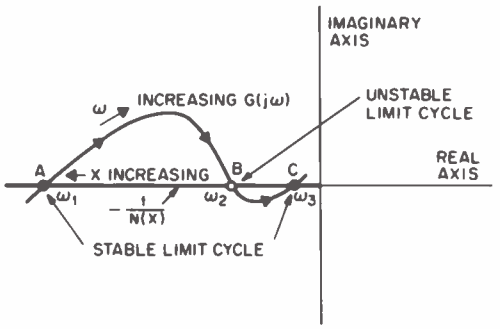

Fig. 38—Polar plot of stable and unstable limit cycles.

is the same ω of the $-[1/N(\omega, X)]$ locus (see Fig. 37).

The oscillation may be either stable or unstable. If the $G(j\omega)$ intersects with the $-[1/N(\omega, X)]$ locus at one point only, the oscillation is stable

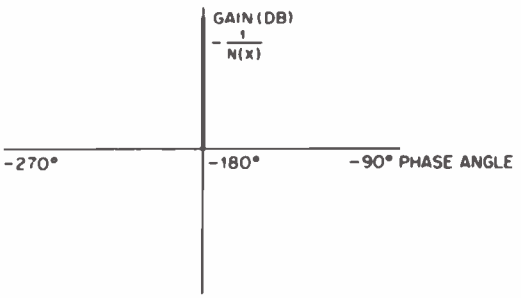

A. $-\frac{1}{N(X)}$ PLOT WITH ZERO PHASE ANGLE

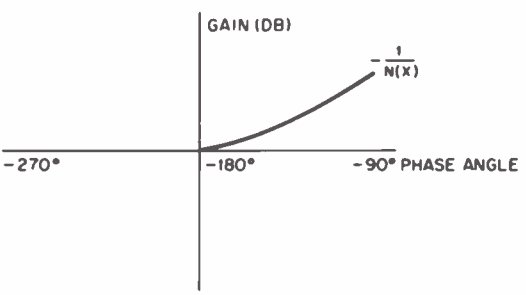

B. $-\frac{1}{N(X)}$ PLOT WITH PHASE ANGLE

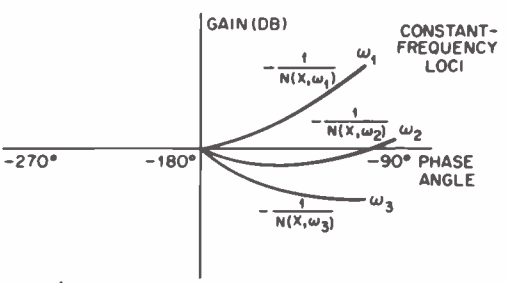

C. $-\frac{1}{N(X)}$ PLOT AS A FUNCTION OF CONSTANT ω

Fig. 39—Typical gain-phase plots of various $N(\omega, X)$.

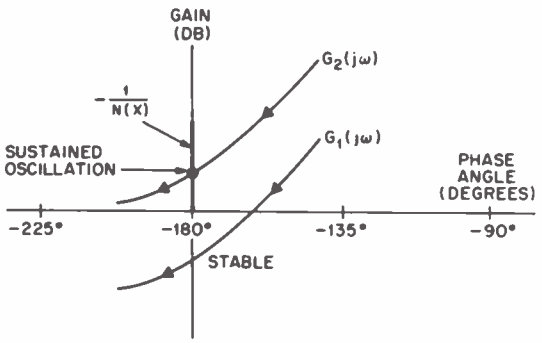

Fig. 40—Gain-phase plot stability criteria.

(stable limit cycle). If more points of intersection exist, the limit cycle may be either stable or unstable. The stability of the limit cycle is determined by the direction of the two loci at the crossover point.

By establishing the $G(j\omega)$ locus pointing in the direction of increasing frequency as a reference, if the $-[1/N(X)]$ locus pointing in the direction of increasing amplitude X crosses the $G(j\omega)$ locus from right to left, the limit cycle is stable. If the crossover occurs from left to right the limit cycle is unstable. A polar plot with both stable and unstable limit cycles is shown in Fig. 38.

Gain–Phase Plot: The gain–phase plot is the direct transfer of the polar plot from the polar coordinate to the rectangular coordinate. The ordinate is the gain in decibels and the abscissa is the phase angle in degrees.

The gain and phase angle of the two functions $G(j\omega)$ and $-[1/N(\omega, X)]$ are for $G(j\omega)$:

$$\text{Gain} \qquad 20 \log |G(j\omega)|$$

$$\text{Phase angle} \qquad \angle G(j\omega)$$

and for $N(X, \omega)$:

$$\text{Gain} \qquad -20 \log_{10} |N(\omega, X)|$$

$$\text{Phase angle} \qquad -180° - \angle N(\omega, X).$$

A typical gain–phase plot for various types of $N(\omega, X)$ is given in Fig. 39.

The system is stable if the $-(1/N)$ locus does not intersect with the $G(j\omega)$ plot. If the $-(1/N)$ locus intersects with the $G(j\omega)$ plot, the system has a sustained oscillation (Fig. 40).

In the case of sustained oscillation, there may be more than one point of intersection, as shown in Fig. 41. Points A and C are stable points (stable limit cycle) and point B is an unstable point (unstable limit cycle). The stability of the limit cycle is determined in a manner similar to that of

the polar plot, except that if the $-[1/N(X)]$ locus in the direction of increasing X crosses the $G(j\omega)$ locus pointing in the direction of increasing frequency from left to right the limit cycle is stable and if from right to left the limit cycle is unstable. Figure 42 is a typical gain–phase plot of $G(j\omega)$ and $-[1/N(\omega, X)]$, where $N(\omega, X)$ is a function of ω. The family of $-(1/N)$ plots are the constant-frequency loci. Point A is the location for sustained oscillation.

Root-Locus Plot: The root-locus plot must be modified to satisfy the following condition.

$$|N|\cdot|G(s)|=1$$
$$\angle N+\angle G(s)=(1+2m)180^\circ$$
$$m(\text{integer})=0, 1, \cdots.$$

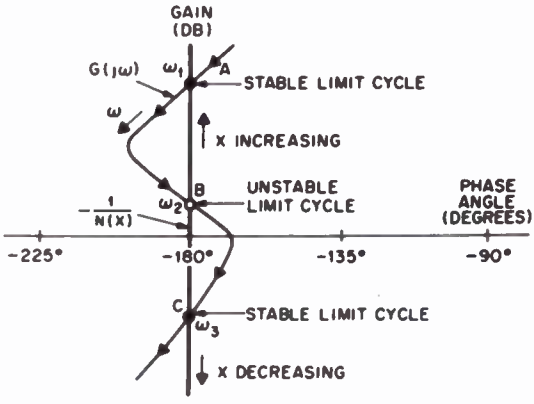

Fig. 41—Gain–phase plot of stable and unstable limit cycles.

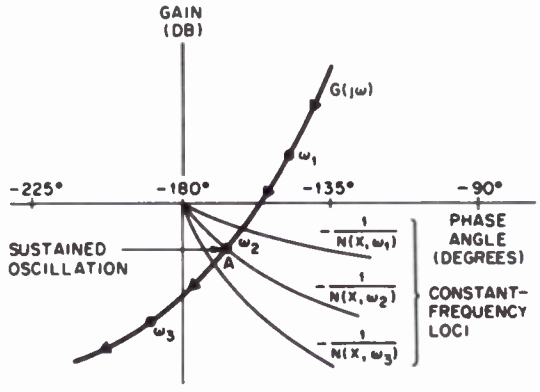

Fig. 42—Typical gain–phase plot of $G(j\omega)$ and $-[1/N(\omega, X)]$ as a function of ω.

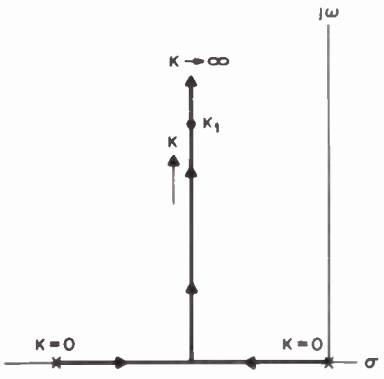

A. LINEAR (N = 1)

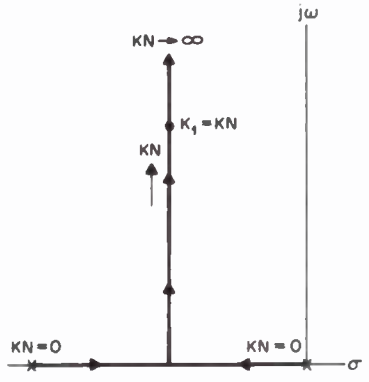

B. N(X) WITH ZERO PHASE ANGLE

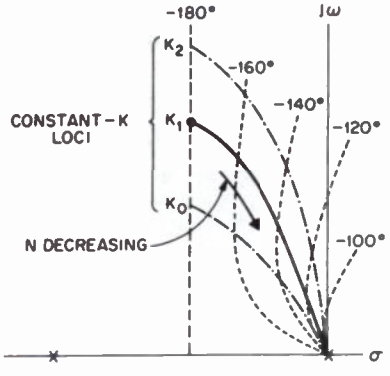

C. N(X) WITH PHASE ANGLE

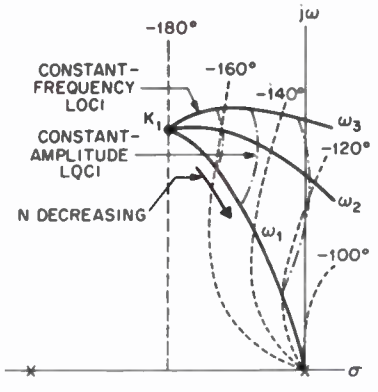

D. N(ω, X) AS A FUNCTION OF ω

Fig. 43—Typical root-locus plots of various $N(\omega, X)$.

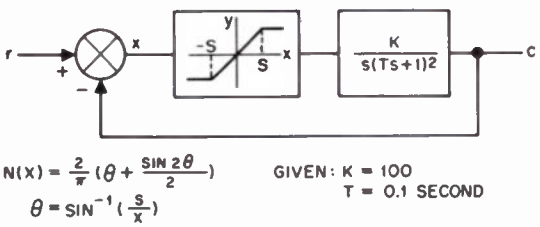

Fig. 44—Nonlinear system with saturation.

For cases of single-valued nonlinear functions where the phase angle is zero, the root-locus plot is identical to the linear case, except for the gain constant K. The gain constant K of a linear system (Fig. 43A) is modified to KN (Fig. 43B). If the root locus remains in the left half of the s plane for all values of KN, the system is stable. Conversely if the root locus extends into the right half of the s plane, the system is unstable. The value of KN corresponding to the crossover point of the root locus at the $j\omega$ axis yields sustained oscillation.

If the describing function N involves a phase angle, which is the case of multivalued functions, the root locus must take into consideration the phase angle of N. The root locus is then plotted for various fixed values of K, resulting with a family of constant-K loci (Fig. 43C). The stability criteria of the linear root-locus case still apply. When the describing function is a function of ω as well as X, a root locus must be plotted for each ω with the K value fixed, generating a family of constant-frequency loci (Fig. 43D). It is noted that for sustained oscillation the ω of the constant-frequency loci must intersect with the same ω of the $j\omega$ axis. When the root locus intersects the $j\omega$ axis more than once, stable and unstable limit cycles exist.

As an illustrated example, the stability of a closed-loop system with saturation shown in Fig. 44, and with backlash in Fig. 48, are evaluated using the analytical method, polar plot, gain–phase plot, and root-locus plot.

Example 3: *Closed-Loop System With Saturation.* The stability of the system to be evaluated is depicted in Fig. 44.

Analytical Method: The closed-loop transfer function is

$$(C/r)(\omega, R) = \frac{N(\omega, X)G(j\omega)}{1+N(\omega, X)G(j\omega)}$$

where $G(j\omega)$ is given as

$$G(j\omega) = K/j\omega(j\omega T+1)^2.$$

The characteristic equation of the system is

$$N(\omega, X)[K/j\omega(j\omega T+1)^2] = -1.$$

The condition for oscillation is

$$|N(X)|[K/\omega(\omega^2T^2+1)] = 1 \qquad (5)$$

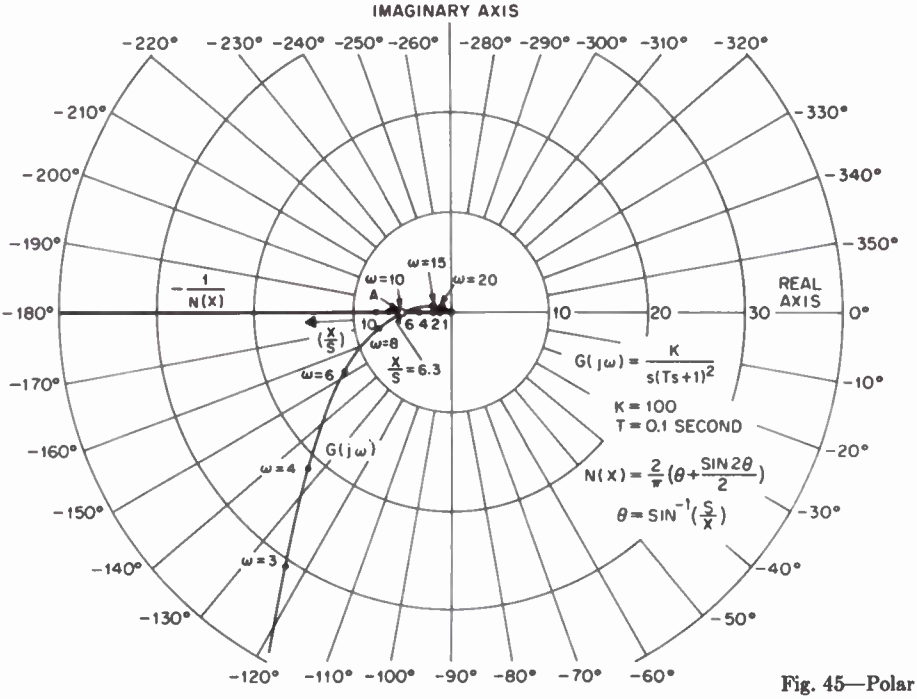

Fig. 45—Polar plot of example 3.

and

$$\angle N(X) - 90° - 2\tan^{-1}(\omega T) = -180°. \quad (6)$$

Solving (6) with phase angle $\angle N = 0$ yields

$$\omega T = 1 \qquad \text{or} \qquad \omega = 1/T$$

which satisfies the phase relation. Substituting this into (5) yields

$$|N(X)| = 2/KT.$$

For the example where $K = 100$, $T = 0.1$ second

$$N(S/X) = 0.2 \qquad \text{and} \qquad \omega = 10.$$

The expression for the describing function for saturation is given in Table 1C as

$$N(S/X) = (2k_1/\pi)[\theta + \tfrac{1}{2}(\sin 2\theta)], \quad \theta = \sin^{-1}(S/X)$$

and equating $N(S/X) = 0.2$, for $k = 1$ (unit slope) yields

$$S/X = 0.158 \qquad \text{or} \qquad X/S = 6.3.$$

The system has a sustained oscillation at a frequency of $f = 10/2\pi$ and the threshold-to-input-amplitude ratio S/X of 0.158, $(X/S = 6.3)$.

Polar Plot: The two loci, $G(j\omega)$ and $-[1/N(X/S)]$, are plotted on the polar plane for

$$G(\omega) = \frac{K}{\omega(1+\omega^2T^2)} = \frac{100}{\omega[1+(\omega^2/100)]}$$

$$\angle G(\omega) = -90° - 2\tan^{-1}(\omega T)$$

$$= -90° - 2\tan^{-1}(0.1\omega)$$

and

$$|N(X/S)|^{-1} = \left[\frac{2\theta}{\pi} + \frac{\sin 2\theta}{\pi}\right]^{-1}, \qquad \theta = \sin^{-1}(S/X)$$

$$\angle -[1/N(X/S)] = -180°.$$

The describing function for saturation may be obtained either by calculation using the procedure previously discussed or from Table 1C. The two loci are plotted in Fig. 45.

Gain–Phase Plot: The locus for $G(j\omega)$ is

$$20\log|G(j\omega)|$$

$$= 20\log K - 20\log\omega - 20\log(1+\omega^2T^2)$$

$$= 40 - 20\log\omega - 20\log[1+(\omega^2/100)]$$

$$\angle G(j\omega) = -90° - 2\tan^{-1}(\omega T)$$

$$= -90° - 2\tan^{-1}(0.1\omega).$$

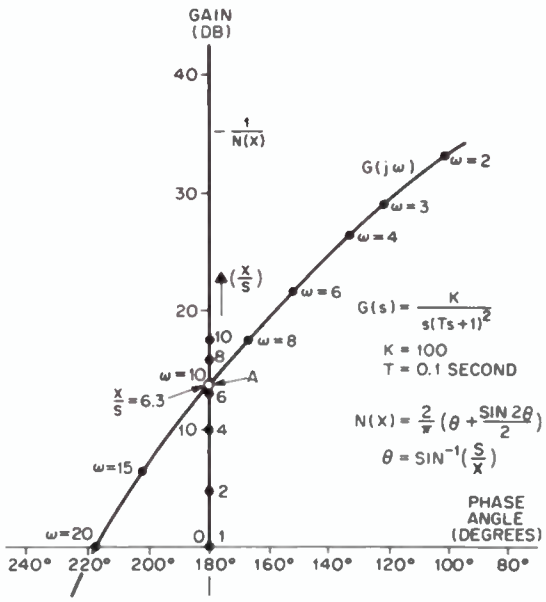

Fig. 46—Gain–phase plot of example 3.

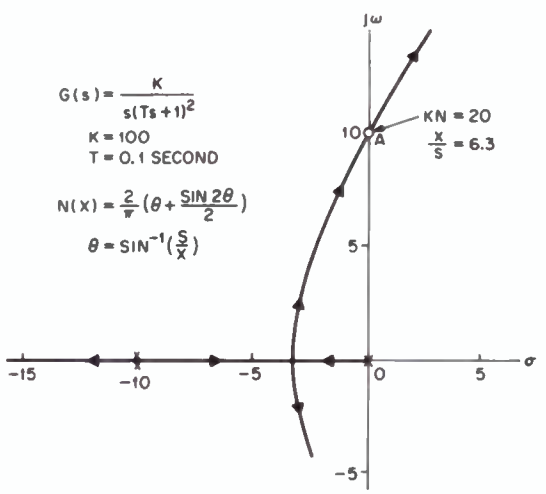

Fig. 47—Root-locus plot of example 3.

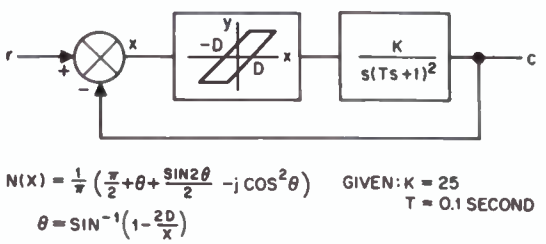

Fig. 48—Nonlinear system with backlash.

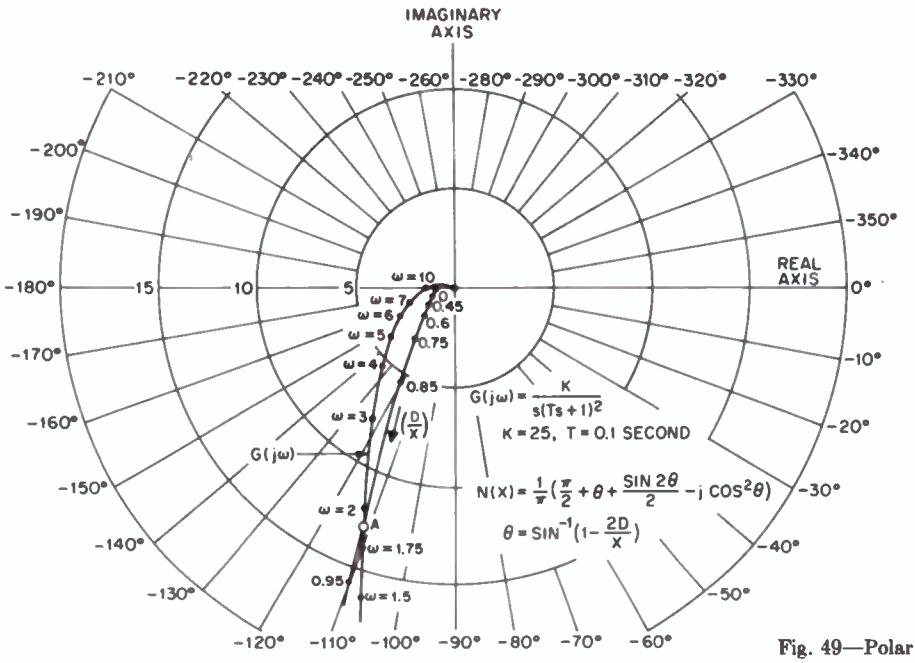

Fig. 49—Polar plot of example 4

The locus for $-[1/N(X)]$ is

$$20\log|-(1/N)(X/S)|$$

$$=-20\log[(2/\pi)\theta+\tfrac{1}{2}(\sin 2\theta)],\quad \theta=\sin^{-1}(S/X)$$

$$\angle -[1/N(X/S)]=-180^\circ.$$

The results are plotted in Fig. 46.

Root-Locus Plot: The root locus is plotted for

$$s(sT+1)=|N(X/S)|K$$

$$=|(2/\pi)[\theta+\tfrac{1}{2}(\sin 2\theta)]|\cdot 100,\quad \theta=\sin^{-1}(S/X)$$

and

$$90+2\tan^{-1}(\omega T)=+180^\circ+\angle N(X/S)$$

$$=180^\circ.$$

The root locus for the saturation case is plotted in Fig. 47. All three graphical methods yield the same results, that is, sustained oscillation occurs at the crossover point A of the two loci, at $\omega=10$ and $X/S=6.3$.

Example 4: *Closed-Loop System With Simple Backlash.* A system block diagram of a simple backlash nonlinear system is given in Fig. 48. The stability of the system for $K=25$, $T=0.1$ second is evaluated using the polar plot, gain–phase plot, and root-locus plot. The loci to be plotted follow.

Polar Plot:

$$|G(\omega)|=\frac{25}{\omega[(\omega^2/100)+1]}$$

$$\angle G(\omega)=-90^\circ-2\tan^{-1}(0.1\omega)$$

and

$$1/|N(D/X)|=\pi/\{[\tfrac{1}{2}\pi+\theta+\tfrac{1}{2}(\sin 2\theta)]^2+\cos^4\theta\}^{1/2}$$

$$\theta=\sin^{-1}[1-(2D/X)]$$

$$\angle -[1/N(D/X)]$$

$$=-180^\circ-\tan^{-1}\left[\frac{-\cos^2\theta}{\tfrac{1}{2}\pi+\theta+\tfrac{1}{2}(\sin 2\theta)}\right].$$

Gain–Phase Plot:

$$20\log|G(\omega)|=20\log 25-20\log\omega$$

$$-20\log[(\omega^2/100)+1]$$

$$\angle G(\omega)=-90^\circ-2\tan^{-1}(0.1\omega)$$

$$-20\log|N(D/X)|$$

$$=-20\log(\pi^{-1}\{[\tfrac{1}{2}\pi+\theta+\tfrac{1}{2}(\sin 2\theta)]^2+\cos^4\theta\}^{1/2})$$

$$\angle -[1/N(D/X)]$$

$$=-180^\circ-\tan^{-1}\left(\frac{-\cos^2\theta}{\tfrac{1}{2}\pi+\theta+\tfrac{1}{2}(\sin 2\theta)}\right)$$

$$\theta=\sin^{-1}[1-(2D/X)].$$

Root-Locus Plot:

$$s(0.1s+1)$$

$$= 25\left(\pi^{-1}\left\{\left[\tfrac{1}{2}\pi+\theta+\tfrac{1}{2}(\sin 2\theta)\right]^2+\cos^4\theta\right\}^{1/2}\right)$$

$$\angle s(0.1s+1) = 180^\circ+\tan^{-1}\left(\frac{-\cos^2\theta}{\tfrac{1}{2}\pi+\theta+\tfrac{1}{2}(\sin 2\theta)}\right)$$

$$\theta = \sin^{-1}[1-(2D/X)].$$

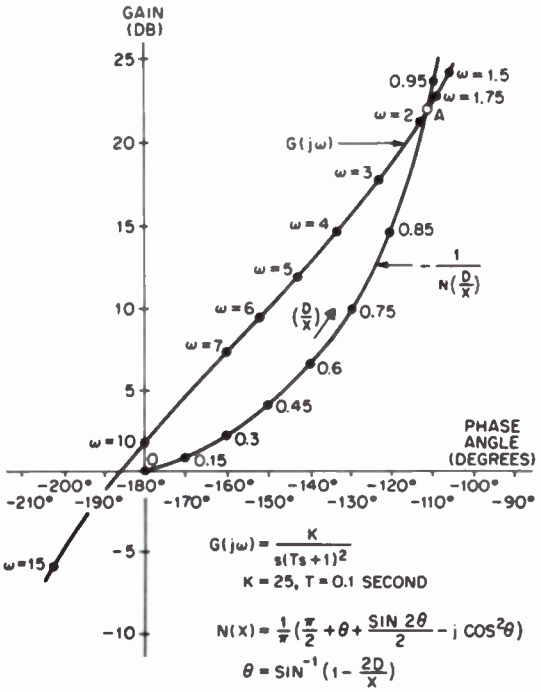

Fig. 50—Gain–phase plot of example 4.

The results are given in Figs. 49, 50, and 51. The system has a sustained oscillation at approximately $\omega = 1.85$, and the corresponding $N(D/X)$ is approximately equal to

$$|N(D/X)| = 0.08 \qquad \angle N(D/X) = -69^\circ$$

or

$$D/X = 0.925.$$

Phase-Plane Method

The phase-plane method of analysis is used to study the transient behavior of the nonlinear system. The systems to be considered are assumed to be so constituted that the system performance can be described in terms of an ordinary differential equation.

Restrictions of the Phase-Plane Method: The phase-plane method has the following restrictions.

(A) *The analysis is limited to systems described by the first and second order.* Differential equations to systems of higher order may be solved in the phase space; however, the results are complex and unwieldy.

(B) *The analysis can be used only for study of the transient response.* The forcing function of the differential equation is zero and, consequently, only the response to the initial condition is obtained. Simple forcing functions such as step and ramp functions with which, by appropriate substitutions, the characteristic equation may be made equal to zero can also be solved. It is extremely difficult to extend the forcing function to sinusoidal and complex functions.

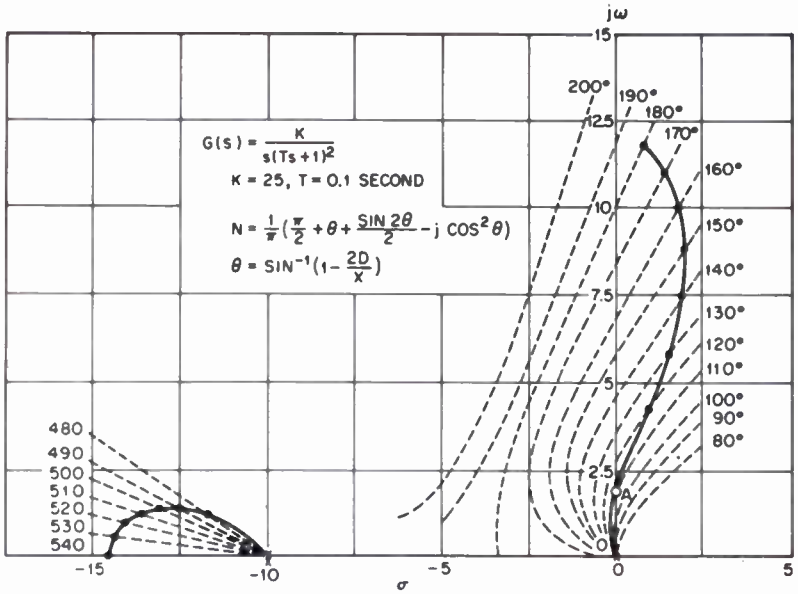

Fig. 51—Root-locus plot of example 4.

(C) *The analysis is limited to autonomous functions.* That is, the coefficients of the derivatives must be functions of x and $\dot{x}$ and not of time explicitly.

Phase Plane: The differential equation describing a second-order system may be expressed by

$$f_1(x, dx/dt, t)\,(d^2x/dt^2)+f_2(x, dx/dt, t)\,(dx/dt)+f_3(x, dx/dt, t)\,x=g(t).$$

The type of equations that can be evaluated in the phase plane is of the form

$$f_1(x, dx/dt)\,(d^2x/dt^2)+f_2(x, dx/dt)\,(dx/dt)+f_3(x, dx/dt)\,x=0. \quad (7)$$

The equation in which t does not appear explicitly is called "autonomous." By defining

$$\dot{x}=dx/dt$$

the equation may be rewritten as

$$f_1(x, \dot{x})\,(d\dot{x}/dt)+f_2(x, \dot{x})\dot{x}+f_3(x, \dot{x})x=0$$

or

$$dx/dt=P(x, \dot{x})=\dot{x} \quad (8)$$

$$d\dot{x}/dt=Q(x, \dot{x})=-[f_2(x, \dot{x})\dot{x}+f_3(x, \dot{x})x]/f_1(x, \dot{x}) \quad (9)$$

and further into the form of

$$\frac{(d\dot{x}/dt)}{(dx/dt)}=d\dot{x}/dx=Q(x, \dot{x})/P(x, \dot{x})=-[f_2(x, \dot{x})\dot{x}+f_3(x, \dot{x})x]/\dot{x}f_1(x, \dot{x}). \quad (10)$$

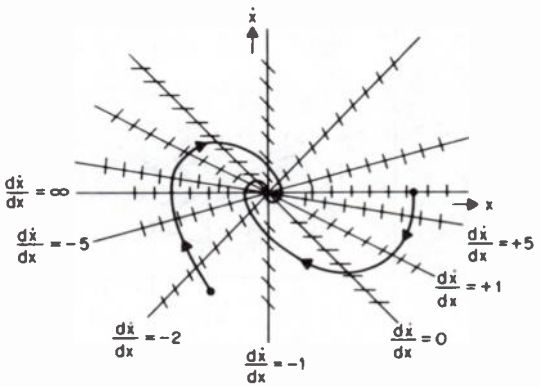

Fig. 52—Isocline method.

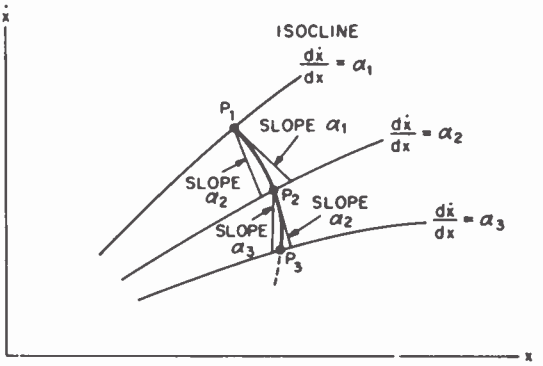

Fig. 53—Step-by-step slope averaging.

The second-order differential equation with respect to time is reduced to a first-order equation of x and $\dot{x}$.

The phase-plane diagram has the $\dot{x}$ as its ordinate and x as its abscissa. The plot of $\dot{x}$ as a function of x on the phase-plane diagram is termed *phase trajectory*. A family of phase trajectories is called the *phase portrait*.

The phase trajectory originates at a point corresponding to the initial condition $(x_0, \dot{x}_0)$ and moves to a new location at each increment of time. Generally, the increments of time are not portrayed on the trajectory and must be obtained by other means described in a later section. If the value of time at each point on the trajectory is obtained, the time response of $\dot{x}(t)$ and $x(t)$ can be plotted. The phase trajectory has a definite direction associated with time. When $\dot{x}$ is positive the trajectory moves from left to right, and for negative values of $\dot{x}$ all paths move from right to left. If the trajectory approaches the origin or some finite point on the phase plane as time goes to ∞, the system is stable. If the trajectory goes to ∞ with time, the system is unstable. If the trajectory approaches an enclosed path in the phase plane, the system has sustained oscillation. The enclosed path is called the limit cycle.

Construction of the Phase Portrait.

Method of Isoclines: The slope $d\dot{x}/dx$ of equation (10) is simply the slope of the trajectory in the phase plane. The locus of constant $d\dot{x}/dx$ is termed an *isocline* corresponding to the slope α, that is

$$\alpha=d\dot{x}/dx=-[f_2(x, \dot{x})/f_1(x, \dot{x})]-[f_3(x, \dot{x})/f_1(x, \dot{x})](x/\dot{x})=-g(x, \dot{x})-h(x, \dot{x})\,(x/\dot{x}).$$

The phase portrait is constructed by plotting a

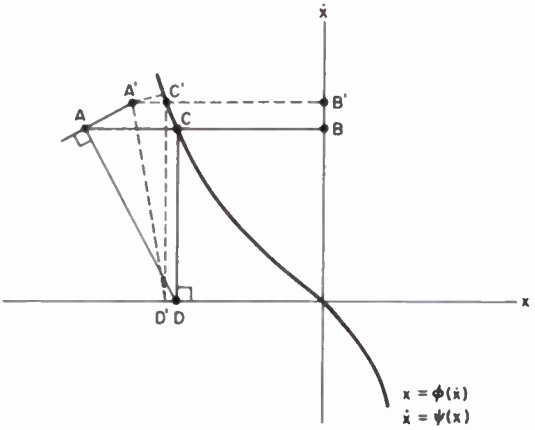

Fig. 54—Lienard's method.

large number of isoclines corresponding to the various slopes of the trajectory on the phase plane. All points located on the same isocline have the same slope α. Beginning at the location of the initial condition $(x_0, \dot{x}_0)$, the trajectory traverses in the clockwise direction, crossing each isocline at an angle corresponding to that slope α. Figure 52 shows the isocline for a damped, linear, second-order system. Isoclines for first- and second-order linear differential equations are straight lines.

For a more accurate method of sketching the trajectory, the method* of Fig. 53 is helpful. The

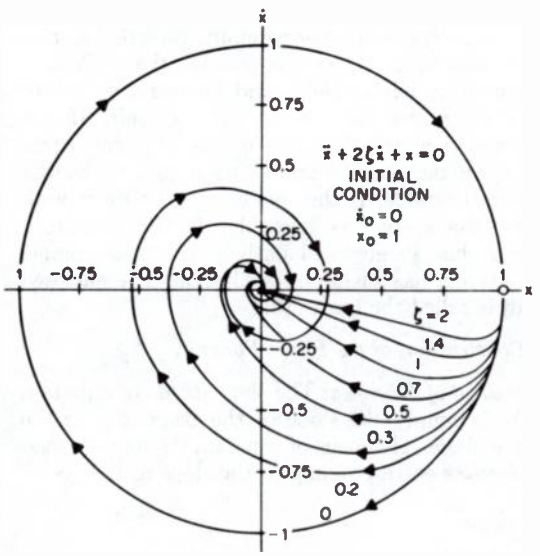

Fig. 55—Phase portrait of second-order system for various damping ratios ζ.

* A. A. Andronow and C. E. Chaikin, "Theory of Oscillations," Princeton University Press, Princeton, New Jersey; 1949: p. 248.

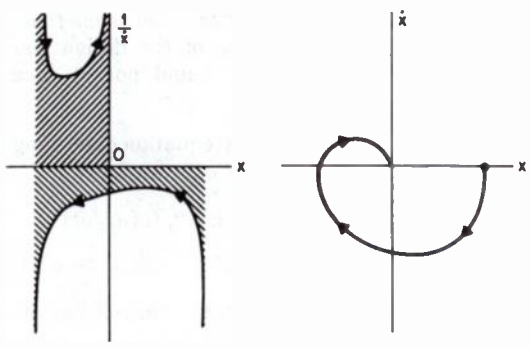

Fig. 56—Reciprocal plot of $\dot{x}$ for determining time.

method is a step-by-step construction using the average slope between the two adjacent isoclines. At point P_1 the slopes α_1 and α_2 are projected on the isocline of α_2. The halfway point of the two projected points is defined as P_2. The same procedure is repeated, determining points P_3, P_4, $\cdots$. The trajectory is obtained by connecting the various points P.

Lienard's Method: Lienard's graphic construction determines the slope of the trajectory at any point without the use of isoclines. With the slope at one point known, a short line segment with that slope

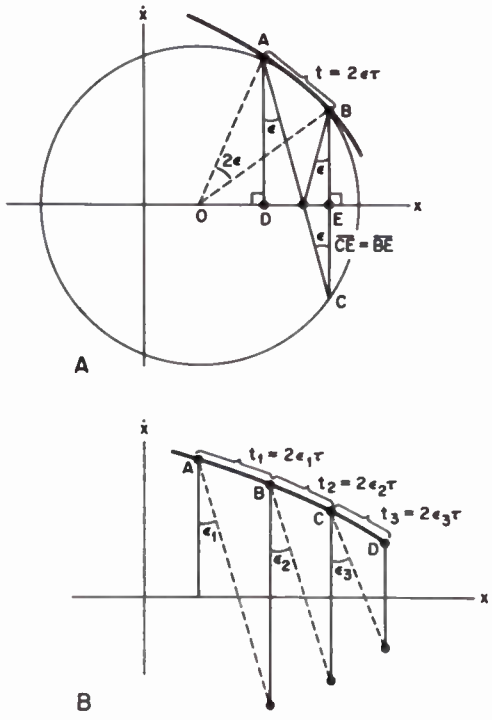

Fig. 57—Graphic construction for determining time.

can be projected to a new point and the procedure repeated. The construction procedure is as follows.

Referring to (10)

$$d\dot{x}/dx = -(1/\dot{x})\{[f_2(x,\dot{x})\dot{x}+f_3(x,\dot{x})x]/f_1(x,\dot{x})\}$$

$$= -(1/\dot{x})[f(x,\dot{x})].$$

The first step is to set

$$f(x,\dot{x})=0$$

and solve for either x or $\dot{x}$

$$x=\phi(\dot{x}) \quad \text{or} \quad \dot{x}=\psi(x).$$

The function $x=\phi(\dot{x})$ or $\dot{x}=\psi(x)$ is then plotted on the phase plane (Fig. 54).

The slope of the trajectory at location A is determined by the following procedure. Draw a horizontal line from A to B intersecting the curve $x=\phi(\dot{x})$ at C. Draw a line perpendicular to $\overline{AB}$ from C intersecting the x axis at D. Connect a line from A to D. The slope of the trajectory at point A is normal to the joining line $\overline{AD}$. Repeating the same procedure at a new point A′ the trajectory is carried forward. The trajectory may be constructed to any desired accuracy by selecting a small enough segment $\overline{AA'}$. A phase portrait of a second-order system for different values of damping ratio is shown in Fig. 55.

Determination of Time on the Phase Plane.

Time From Reciprocal Plot: This method is based on the relationship of time and the reciprocal plot of $\dot{x}$. Since

$$\dot{x}=dx/dt$$

dt may be expressed as

$$dt=dx/\dot{x}.$$

Integrating both sides yields

$$t=\int_{x_0}^{x_1}(1/\dot{x})\,dx.$$

Since $\dot{x}$ as a function of x is known from the phase plane, the reciprocal $1/\dot{x}$ may be plotted as a function of x, and the integral under the curve between any two points is the time required for the trajectory to change from one point to the other.

A typical reciprocal plot of $\dot{x}$ to determine time is shown in Fig. 56. The integration is in the direction of increasing time from right to left in the lower half-plane and vice versa in the upper half-plane.

In the vicinity of the x axis, the function $1/\dot{x}$ approaches infinity. Even with the integral unbounded the integral is finite; however, it is not readily evaluated graphically.

As an alternative method, the value of time may be evaluated from integration involving $\dot{x}$ instead of x. From the original differential equation (9)

$$d\dot{x}/dt=Q(x,\dot{x})$$

dt is written as

$$dt=[1/Q(x,\dot{x})]d\dot{x}$$

and therefore

$$t=\int_{\dot{x}_1}^{\dot{x}_2}[1/Q(x,\dot{x})]d\dot{x}.$$

The expression $1/Q(x,\dot{x})$ may be plotted as a function of $\dot{x}$ and graphic integration may be performed.

The two methods may be used alternately if the integral goes to infinity.

Graphic Construction: This method is based on the approximation of the phase trajectory by a series of circular arcs centered on the x axis (Fig. 57A). Consider the section of the path $\overline{AB}$ to be a segment of an arc centered on the x-axis 0. The angle of the arc $\overline{AB}$ is $\angle A0B=2\epsilon$. The time from A to B is given by $2\epsilon\tau$, where ϵ is measured in radians and τ is the ratio of the x and $\dot{x}$ scale factor.

$$\tau=\frac{\text{value of } x/\text{unit scale}}{\text{value of } \dot{x}/\text{unit scale}}.$$

On this basis, time from A to B of the path may be evaluated as follows.

Drop a line from A perpendicular to the x axis at point D. Drop a line from B perpendicular to the x axis, and scale an equal distance $\overline{BE}$ opposite the x-axis $\overline{CE}$. Draw a line $\overline{AC}$ connecting points A and C. Measure the angle $\angle CAD$ in radians. The time from point A to B is then

$$t=2\angle CAD\cdot\tau.$$

Repeat the procedure as the points move along the trajectory. A typical example is shown in Fig. 57B.

Singular Points: In a second-order system, the differential equation of the system may be described by two variables x and $\dot{x}$ in the following form.

$$dx/dt=P(x,\dot{x})$$

$$d\dot{x}/dt=Q(x,\dot{x}).$$

The points where dx/dt and $d\dot{x}/dt$ vanish are called *singular points*. At a singular point the system is in a state of equilibrium.

The importance of a singular point in the phase plane is how the trajectories of the phase portrait behave in the vicinity of the singular point. When the trajectory converges to the singular point the system is stable, whereas if it diverges the system is unstable. Typical types of singular points are described below.

Types of Singular Points: Besides stable and unstable equilibrium, the singular points may be classified into node, focus, center, and saddle points.

Consider, for example, a singular point at $x=a$ and $\dot{x}=b$ of equations (8) and (9). At a singular point the derivatives dx/dt and $d\dot{x}/dt$ are both zero, and the location may be solved in the phase plane by setting (8) and (9) equal to zero. A singular point exists at $x=a$, $\dot{x}=b$ and the functions P and Q can be expressed in terms of the Taylor series about those points; then

$$dx/dt=c_1(x-a)+c_2(\dot{x}-b)+c_3(x-a)^2 +c_4(x-a)(\dot{x}-b)+c_5(\dot{x}-b)^2+\cdots$$

$$d\dot{x}/dt=d_1(x-a)+d_2(\dot{x}-b)+d_3(x-a)^2 +d_4(x-a)(\dot{x}-b)+d_5(\dot{x}-b)^2+\cdots.$$

Taking a sufficiently small region around the singular point, the derivatives are dominated by the linear terms and hence quantities c_1, c_2, d_1, and d_2. By changing the variables, the singular point may be moved to the origin. Then the system equation may be rewritten as

$$dx/dt=p_1x+p_2\dot{x}=0$$

$$d\dot{x}/dt=q_1x+q_2\dot{x}=0$$

and the characteristic equation is

$$\lambda^2-(p_1+q_2)\lambda+(p_1q_2-p_2q_1)=0.$$

The roots of the characteristic equation determine the nature of the critical points. The roots are

$$\lambda=\tfrac{1}{2}\{(p_1+q_2)\pm[(p_1+q_2)^2-4(p_1q_2-p_2q_1)]^{1/2}\}.$$

There are six possible cases for the six types of singular points.

(A) The roots are real and are both negative.

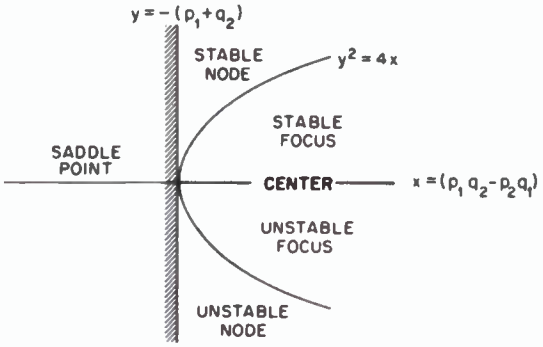

Fig. 59—Regions of various singular points.

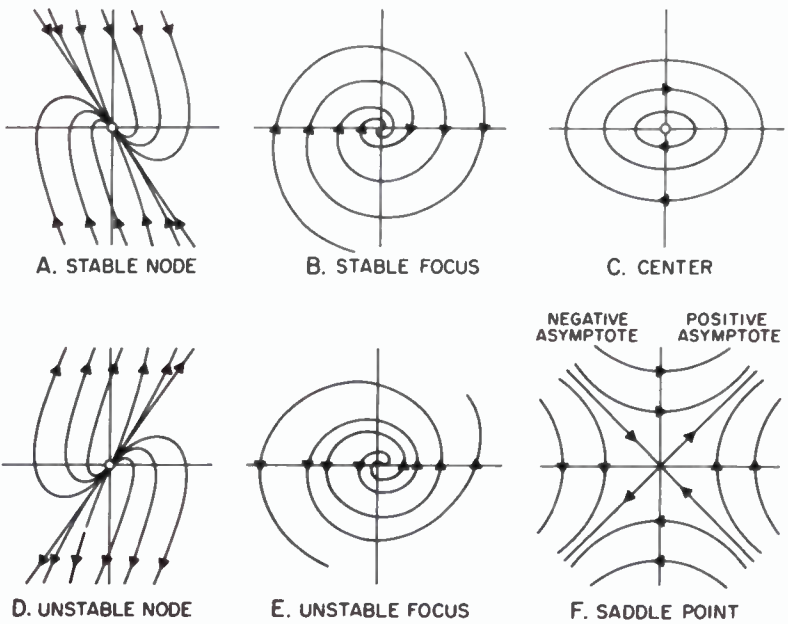

Fig. 58—Types of singular points.

If the initial condition is $x_0 \neq 0$, $\dot{x}_0 = 0$, the trajectory approaches the singular point without an overshoot or oscillation and is called a *stable node* (Fig. 58A).

(B) The roots are complex conjugate with negative real parts. The trajectory displays a spiraling response as it converges to the singular point as shown in Fig. 58B. This is called the *stable-focus* type singularity.

(C) The roots are conjugate and pure imaginary. The response exhibits a sustained oscillatory motion with the amplitude dependent on the initial condition. The trajectory displays a family of ellipses about the singular point, and is termed *center* (Fig. 58C).

(D) The roots are both positive real. The response in the time domain increases exponentially and is unstable. The portrait is the same as the stable node except the trajectory diverges from the singular point. This is termed *unstable node* (Fig. 58D).

(E) The roots are complex conjugate with positive real parts. The phase portrait is the same as the stable focus except the trajectory diverges from the singular points. This is termed the *unstable focus* (Fig. 58E).

(F) The roots are real with one negative and the other positive. The phase portrait consists of a family of curves of the hyperbolic type having $k_1 = (\lambda_1 - p_1)/p_2$ and $k_2 = (\lambda_2 - p_1)/p_2$ for its asymptotes. The direction of the paths is toward the singular point on the negative asymptote and away from the singular point on the positive asymptote. Singular points of this type are called *saddle points* and are unstable (Fig. 58F).

The six types of singularities correspond to the six regions of Fig. 59.

Limit Cycle and Existence Theorem.

Singular points alone do not provide a complete picture of the phase portrait required to determine the stability of the system.

A limit cycle differs from a center (singular point) in that a limit cycle results after a buildup or decay of a signal that eventually falls into an isolated closed path in the phase plane. A limit cycle may be either stable or unstable depending on whether all the neighboring paths spiral toward or spiral away from the limit cycle. The limit cycle may result from either soft or hard self-excitation. Figure 60 is a phase portrait of soft and hard self-excitation.

There is no concise way to determine the location of the limit cycle or whether a limit cycle

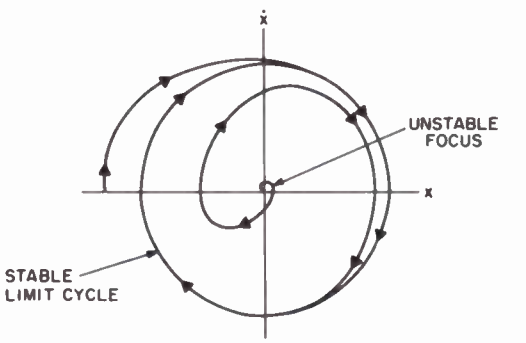

A. PORTRAIT OF SOFT SELF-EXCITATION

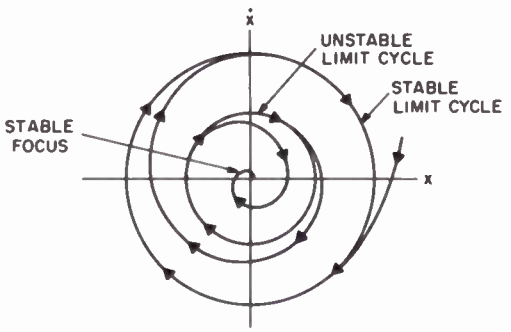

B. PORTRAIT OF HARD SELF-EXCITATION

Fig. 60—Phase portrait of a limit cycle.

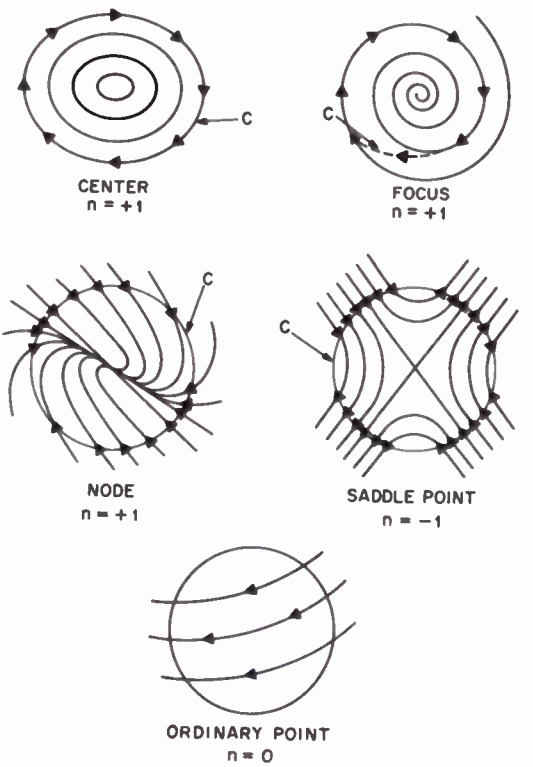

Fig. 61—Poincare's index. *From A. A. Andronow and C. E. Chaiken, "Theory of Oscillations," Princeton University Press, 1949: fig. 197, p. 211. Reprinted by permission.*

exists. Several theorems presented below may be useful.

Poincare's Index: The index of a closed curve C is determined by the number of revolutions of the vector $P(x, \dot{x}), Q(x, \dot{x})$ of the point $(x, \dot{x})$ on the curve C as it describes one complete cycle in the clockwise direction (Fig. 61).

(A) The index n of a closed curve C enclosing only ordinary points is zero.

(B) The index n of a closed curve C, enclosing a focus node or center is $+1$.

(C) The index n of a closed curve C enclosing a saddle point is -1.

(D) The index n of any closed curve C is the sum of the indices of all the singular points enclosed by C.

(E) The index n of every closed phase trajectory is $+1$. Therefore, a limit cycle must enclose at least one singular point other than a saddle point.

*Bendixson's First Theorem**: For the system described by the equations

$$dx/dt = P(x, \dot{x})$$

$$d\dot{x}/dt = Q(x, \dot{x})$$

no limit cycle exists in any region of the $x, \dot{x}$ phase plane within which the divergence $(\partial P/\partial x) + (\partial Q/\partial \dot{x})$ has an invariant sign and is not identically zero.

Bendixson's Second Theorem: If a trajectory remains inside a finite region and does not approach a singular point, it must itself be a limit cycle or else approach a stable limit cycle asymptotically.

Liapunov's Direct Method†: Liapunov's direct method is also known as the second method. Liapunov dealt with the stability of differential equations by two distinct methods. The first method presupposes a known explicit solution and is only applicable to some restricted cases. The direct method, on the other hand, does not require the knowledge of the solutions themselves.

Liapunov's Stability Criteria: Given a dynamic system described by an nth-order differential equation

$$\dot{x}_1 = f_1(x_1, x_2, \cdots, x_n)$$

$$\dot{x}_2 = f_2(x_1, x_2, \cdots, x_n)$$

$$\dot{x}_n = f_n(x_1, x_2, \cdots, x_n).$$

If a positive (negative) definite Liapunov function V can be chosen, such that the derivative with respect to time $\dot{V} = g(x_1, x_2, \cdots, x_n)$ is negative (positive) definite $(\dot{V} < 0)$, then the system is asymptotically stable.

Asymptotic stability implies that the state of the system converges to a stable equilibrium point as time approaches infinity. The condition $\dot{V} \leq 0$ permits the system to have a limit cycle. This is termed stable in the mathematical sense. If $\dot{V} > 0$ (same sign as V) the state of the system diverges and is unstable. The function $V(x)$ has the following properties.

(A) $V(x)$ is continuous together with its first derivative in a certain finite region Ω about the equilibrium point.

(B) $V(x) = 0$ at the equilibrium point.

(C) $V(x)$ is always positive outside the equilibrium point in the region Ω.

(D) $V(x)$ is called a Liapunov function if in addition $\dot{V} \leq 0$ in Ω.

There are no general rules for finding a Liapunov function. Usually, because of mathematical convenience, the function is chosen to have a positive definite quadratic form. Figure 62 illustrates an estimated region of stability derived from Bendixson's first theorem and Liapunov's direct method. The dynamic system under evaluation is the Lewis

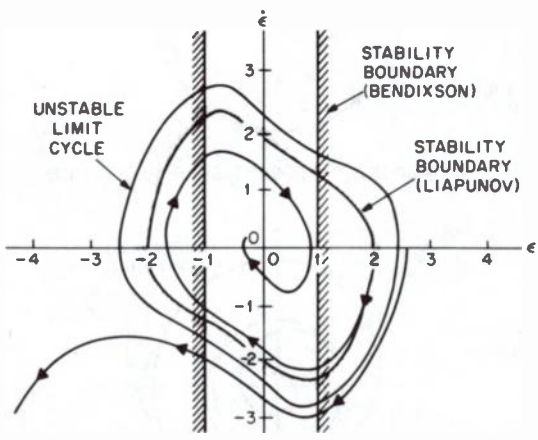

Fig. 62—Estimated region of stability using Bendixson's and Liapunov's methods. *From D. Graham and D. McRuer, "Analysis of Nonlinear Control Systems," fig. 8-22, ©1961, John Wiley & Sons, New York.*

* Proof may be obtained from Green's theorem setting $P d\dot{x} - Q dx = 0$ for limit cycle, I. S. Sokolnikof and R. M. Redheffer, "Mathematics of Physics and Modern Engineering," McGraw-Hill Book Company, New York, N. Y.; 1958: p. 391.

† J. LaSalle and S. Lefschetz, "Stability By Liapunov's Direct Method With Applications," Academic Press, New York; 1961.

servomechanism. It is noted that the region of stability obtained by Liapunov's method is much more accurate than Bendixson's results.

Application of the Phase-Plane Method to Nonlinear Systems: An illustrated example is presented using the phase-plane method to evaluate a hardening-type nonlinear feedback system.

Example 5: Piecewise Linear Analysis of a Nonlinear System. The block diagram of the nonlinear system to be evaluated is illustrated in Fig. 63. The system equation is given by

$$r-c=\epsilon$$

$$c=[K(\epsilon)/(Ts+1)s]\cdot\epsilon$$

or

$$T\ddot{\epsilon}+\dot{\epsilon}+K(\epsilon)=T\ddot{r}+\dot{r}=0, \qquad r=\text{constant}.$$

Since

$$\ddot{\epsilon}=\dot{\epsilon}(d\dot{\epsilon}/d\epsilon)$$

the system equation may be rewritten as

$$d\dot{\epsilon}/d\epsilon=-T^{-1}\{[\dot{\epsilon}+K(\epsilon)]/\epsilon\}$$

$$=Q(\epsilon,\dot{\epsilon})/P(\epsilon,\dot{\epsilon})$$

where

$$Q=-[\dot{\epsilon}+K(\epsilon)]/T$$

$$P=\dot{\epsilon}.$$

The singular point is determined by setting P and Q equal to zero.

For the slope K_1 the singular point is located at $\epsilon=0$ and $\dot{\epsilon}=0[\therefore K(0)=0]$ and for the slope K_2 the singular points are $\dot{\epsilon}=0$, $K(\epsilon_1)=0$; $\dot{\epsilon}=0$, $K(-\epsilon_1)=0$. The singular point on the phase plane is illustrated at the origin, at $\epsilon=+\epsilon_1$, and at $\epsilon=-\epsilon_1$. The type of singularities at the singular point is determined from the roots of the characteristic equation (assuming here that $T=0.5$, $K_1=0.5$, and $K_2=4.5$).

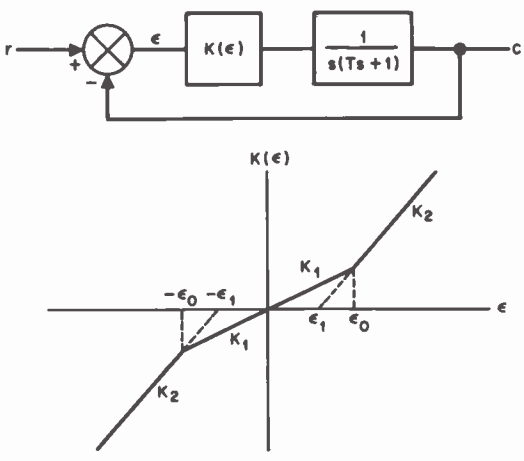

Fig. 63—Nonlinear system with spring "hardening".

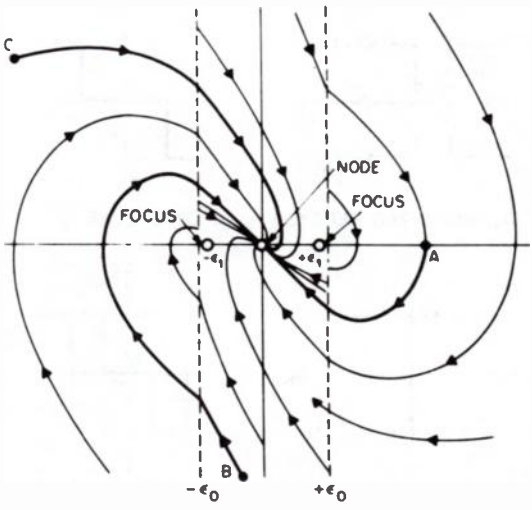

Fig. 64—Overall phase portrait.

The characteristic equation of the feedback system is given by

$$\lambda^2+(\lambda/T)+[K(\epsilon)/T]=0.$$

For $K_1=0.5$:

$$\lambda^2+2\lambda+1=0$$

stable node—roots are both negative real.

For $K_2=4.5$:

$$\lambda^2+2\lambda+9=0$$

stable focus—roots are conjugate complex with negative real parts.

Since the $K(\epsilon)$ function goes through a transition in slope at $\epsilon=\pm\epsilon_0$, the transition line is drawn vertical to the ϵ axis at $+\epsilon_0$ and $-\epsilon_0$.

In the first region, $+\epsilon_0<\epsilon<\infty$, the phase portrait is that of a stable focus at $\epsilon=+\epsilon_1$ (damping ratio $\zeta=1/3$).

In the second region, $-\epsilon_0<\epsilon<+\epsilon_0$, the phase portrait is that of a stable mode at the origin (damping ratio $\zeta=1$).

In the third region, $-\infty<\epsilon<-\epsilon_0$, the phase portrait is that of a stable focus at $\epsilon=-\epsilon_1$ (damping ratio $\zeta=1/3$).

Figure 64 is the overall phase portrait of the feedback system.

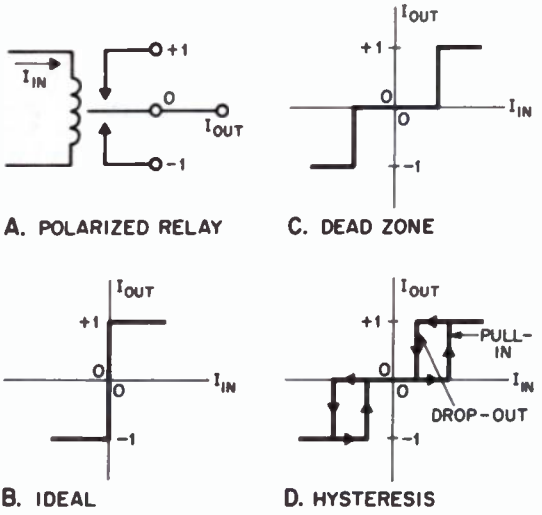

Fig. 65—Static characteristic of a relay.

RELAY CONTROL SYSTEM AND OPTIMUM SWITCHING

The system performance is termed "optimum" if the system is controlled to zero error in the minimum period of time. Relays are often used to achieve optimum performance in regulators and servo systems. The advantage of a relay is that it is economical and provides full power or torque capabilities of the control element (motor) to the load.

Characteristics of a Relay

The static characteristics of a relay may be idealized as a three-valued nonlinear device. The relay characteristics are shown in Fig. 65. In general, the relay has a threshold value (dead zone), which must be exceeded to close the contacts (Fig. 65C). A hysteresis loop is also present, that is, the pull-in and drop-out currents of a relay are of different values (Fig. 65D). Besides the static characteristics, a time delay that corresponds to the pull-in time after excitation must be considered for a dynamic representation. A simple block diagram of a relay servo system is shown in Fig. 66. A phase portrait of various combinations of relay characteristics are also illustrated in Fig. 67. It is noted that in the case where the time constant T of the lead equalizer is very large (Fig. 67F), relay chattering occurs as shown in Fig. 68. The chattering mode slows down the response, wears out the relay contacts, and must be avoided.

It is evident from the phase portraits that switching in the second and fourth quadrants of the phase plane is preferable to the first and third quadrants. Also, systems with lead equalizers show the best response, while the worst response occurs with pure time delay.

Optimum Switching

To achieve optimum performance of a relay servo system, the relay must be controlled and switched to the proper forcing function at the proper time. As an example, consider the ideal relay servo system of Fig. 69. The phase trajectory approaches the origin only if the initial point is located on the zero trajectories. The initial point at any other location will result in a continuous oscillation. The zero trajectories in this case are the optimum switching line. The initial point P_1 will be accelerated at full torque to a new location on the zero trajectory P_2, at which switching takes place and the deceleration torque moves the system to the origin. Finally, the deceleration torque is removed and the system is in an equilibrium state. The initial point P_1 was moved to the origin in a minimum period of time.

The optimum response is achieved by a controller detecting the difference between the state of the system and the optimum switching lines, and commanding switching when the two states coincide.

In a second-order system expressed by

$$\ddot{\epsilon}+2\zeta\dot{\epsilon}+\epsilon=\pm 1$$

for damping ratios of $\zeta \geq 1$, the switching lines are simple zero trajectories as shown in Fig. 70A, and for damping ratios $0 \leq \zeta < 1$ the switching line is complex as shown in Fig. 70B.

If the switching curves for optimum control are to remain invariant, only step and ramp inputs are admissible to the pure inertia servo, and only step inputs are admissible for inertia with viscous damping or coulomb friction-type servo.

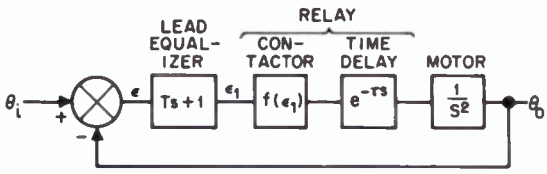

Fig. 66—Simple relay servo system. *From D. Graham and D. McRuer, "Analysis of Nonlinear Control Systems," fig. 9-4b, ©1961, John Wiley & Sons, New York.*

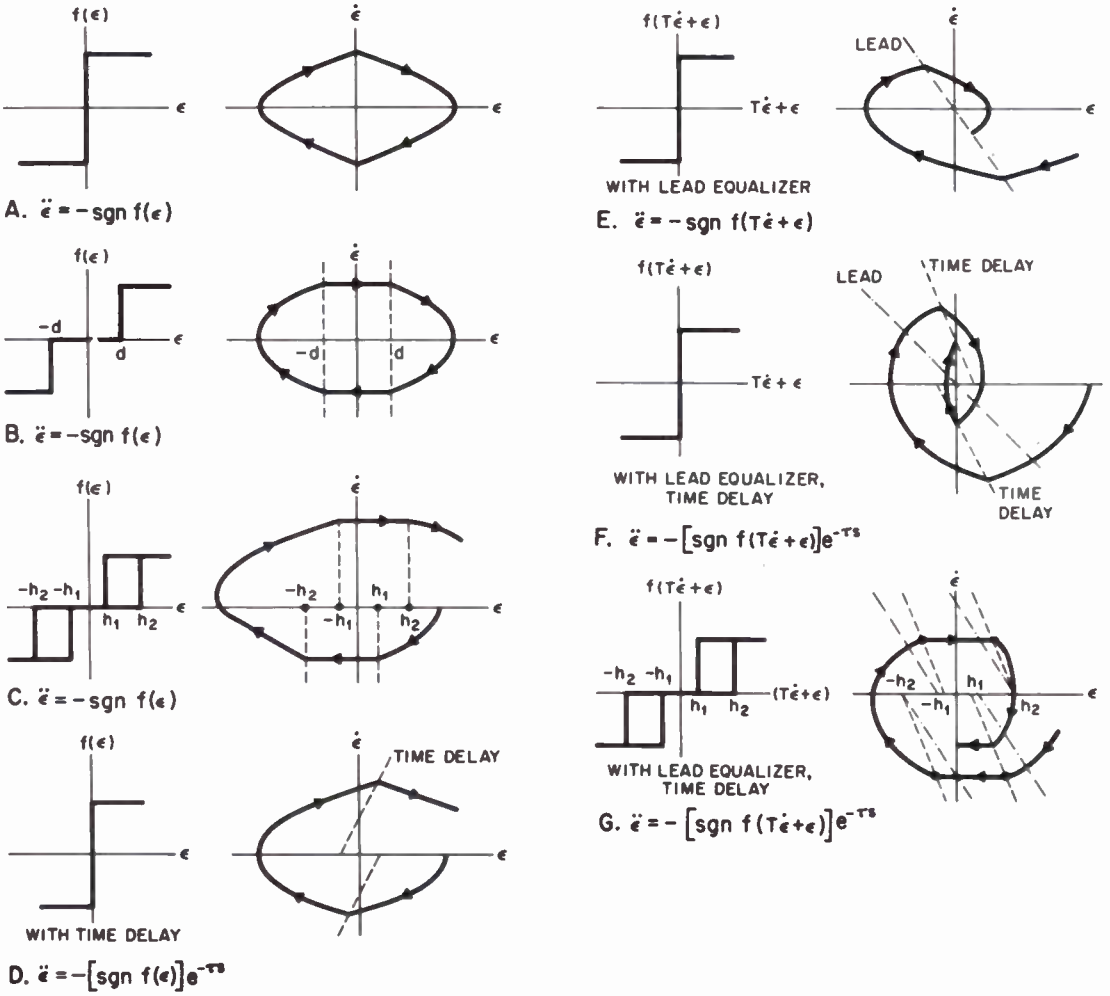

Fig. 67—Various phase portraits of the relay-controlled inertial servo system of Fig. 66. *From D. Graham and D. McRuer, "Analysis of Nonlinear Control Systems," parts of Table 9–1, © 1961, John Wiley & Sons, New York.*

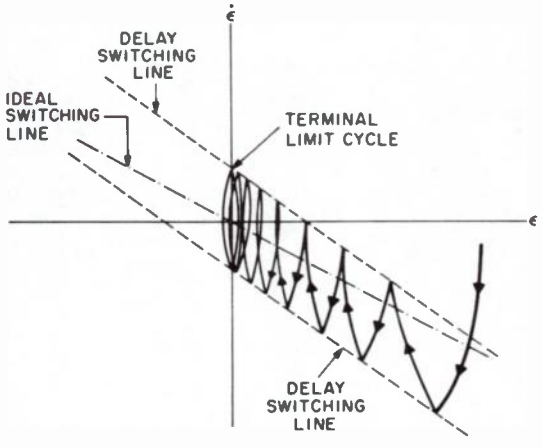

Fig. 68—Relay chattering. *From D. Graham and D. McRuer. "Analysis of Nonlinear Control Systems," fig. 9–8b, ©1961, John Wiley & Sons, New York.*

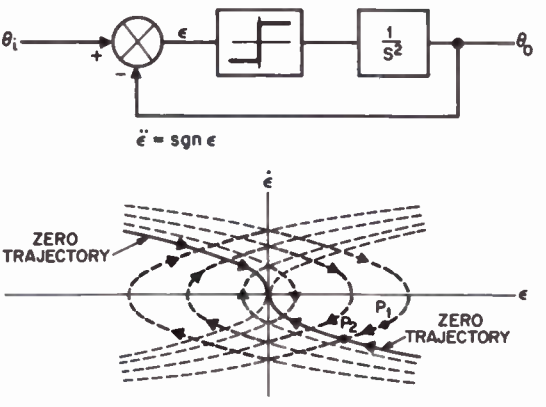

Fig. 69—Ideal relay servo system with inertia load. *From D. Graham and D. McRuer, "Analysis of Nonlinear Control Systems," fig. 9–9 (modified), ©1961, John Wiley & Sons, New York.*

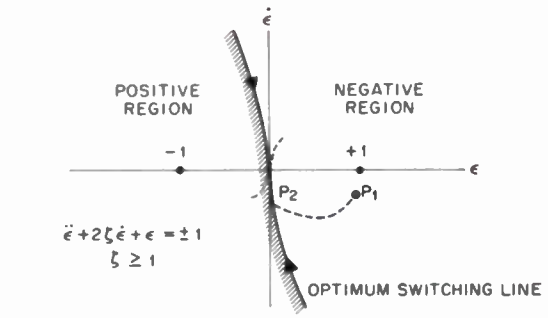

A. TYPICAL EXAMPLE FOR $\zeta \geq 1$

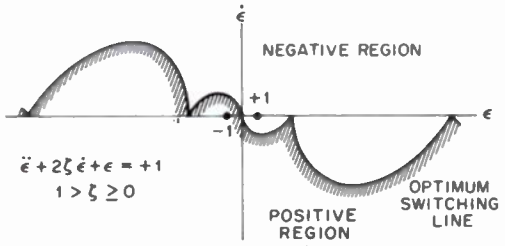

B. TYPICAL EXAMPLE FOR $0 \leq \zeta < 1$

Fig. 70—Typical optical switching lines for a second-order system. *Similar to H. S. Tsien, "Engineering Cybernetics," pp. 136-139, ©1954, McGraw-Hill Book Company, New York.*

Since the optimum switching line of the relay servo is restricted to a limited type of inputs, in practice, optimum performance of the system may be affected by errors in the controller, finite time delay in switching, and also by variation of the parameters in the control loop due to environmental change. Also, for inputs and loads other than those derived for optimum switching, the performance is nonoptimum.

BIBLIOGRAPHY

1. H. Chestnut and R. W. Mayer, "Servomechanism and Regulating System Design," vols. 1 and 2, John Wiley & Sons, New York; 1951 and 1955.
2. W. R. Evans, "Control System Dynamics," McGraw-Hill Book Co., New York; 1954.
3. J. G. Truxal, "Automatic Feedback Control System Synthesis," McGraw-Hill Book Co., New York; 1955.
4. H. S. Tsien, "Engineering Cybernetics," McGraw-Hill Book Co., New York; 1954.
5. N. W. McLachlan, "Ordinary Nonlinear Differential Equations in Engineering and Physical Sciences," University Press, Oxford; 1955.
6. E. L. Ince, "Ordinary Differential Equations," Dover Publications, New York; 1953.
7. W. J. Cunningham, "Introduction To Nonlinear Analysis," McGraw-Hill Book Co., New York; 1958.
8. F. B. Hildebrand, "Introduction to Numerical Analysis," McGraw-Hill Book Co., New York; 1956.
9. D. Graham and D. McRuer, "Analysis of Nonlinear Control Systems," John Wiley & Sons, New York; 1961.
10. J. E. Gibson, "Nonlinear Automatic Control," McGraw-Hill Book Co., New York; 1963.
11. A. A. Andronow and C. E. Chaiken, "Theory of Oscillations," Princeton University Press, Princeton, New Jersey; 1949.
12. E. Levinson, "Nonlinear Feedback Control Systems," *Electro-Technology*, vol. 70, no. 1 through 6; July–December 1962.
13. I. Flugge-Lotz, "Discontinuous Automatic Control," Princeton University Press, Princeton, New Jersey; 1953.
14. R. W. Bass, "Extension of Frequency Method of Analyzing Relay-Operated Servomechanism," Institute of Cooperative Research, Johns Hopkins University, Baltimore, Maryland.
15. S. S. L. Chang, "Synthesis of Optimum Control Systems," McGraw-Hill Book Co., New York; 1961.

CHAPTER 17
ELECTRON TUBES

ELECTRON EMISSION

All electron tubes* depend for their operation on the flow of electrons within the tube, either through high vacuum or an ionized gas. The electrons are emitted from a cathode surface as a result of one of four processes that are distinguished on the basis of the mechanism by which the electrons are enabled to leave the surface. These processes are elevated temperature (thermionic or primary emission); bombardment by other particles, generally electrons (secondary emission); the action of a high electric field (field emission); or the incidence of photons (photoemission).

Thermionic Emission

Thermionic emission occurs when the electrons in the cathode material have enough thermal energy to overcome the forces at the surface and escape.

The thermal emission of electrons from metals obeys the Richardson–Dushman equation

$$J_0 = AT^2 \exp(-11600\phi_0/T)$$

where J_0 is emission density in amperes/cm², A is a constant [amperes/cm²(K)²], ϕ_0 is the work function (electronvolts), and T is temperature in kelvins. A and ϕ_0 are characteristic of the specific material.

The current density given by this equation is usually referred to as the saturation emission current density. Typical constants are given in Table 1 for several commonly used cathode materials.

The maximum current of which a cathode is capable at the operating temperature is known as the saturation current and is normally taken as the value at which the current first fails to increase as the three-halves power of the voltage causing the current to flow. Thoriated-tungsten filaments for continuous-wave operation are usually assigned an available emission of approximately half the saturation value. Oxide-coated emitters do not have a well-defined saturation point and are designed empirically. The available emission from the cathode must be at least equal to the sum of the peak currents drawn by all the electrodes.

Figure 1 gives a plot of saturation current as a

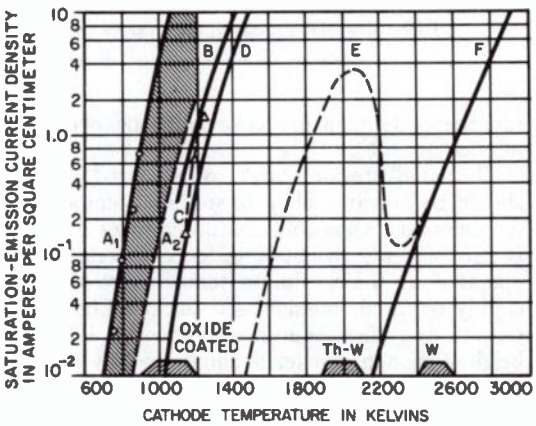

Fig. 1—Emission current density vs. cathode temperature for several types of thermionic emitters. The shaded blocks at the bottom of the figure show the normal operating range for three of the cathodes. Curves are given for (A) *The oxide-coated cathode.* Curve A_1 gives the saturation emission current density under pulsed conditions. Curve A_2 gives the direct-current saturation emission density. The position of this curve may vary substantially with environmental conditions. Direct-current densities much in excess of 0.5 amp/cm² lead to relatively short cathode life. (B) *The pressed nickel cathode.* Curve B shows the direct-current saturation emission current density obtained from a pressed nickel cathode. (C) *The impregnated nickel cathode.* Curve C shows the saturation emission current obtained from the impregnated nickel cathode. The measurements were taken with 40-microsecond pulses and a repetition rate of 60 pulses per second. (D) *Pressed and impregnated tungsten cathodes.* Curve D shows the saturation emission density obtained from pressed and impregnated tungsten cathodes based on $A = 2.5$ amps/cm² (K)² and $\phi_0 = 1.67$ electronvolts. (E) *The thoriated-tungsten cathode.* Curve E shows the measured saturation emission current density of an uncarburized thoriated-tungsten filament. (F) *Tungsten filaments.* Curve F shows the saturation emission current density of a tungsten filament based on $A = 70$ amps/cm² (K)² and $\phi_0 = 4.5$ electronvolts. *J. W. Gewartowski and H. A. Watson, "Principles of Electron Tubes," 1965: p. 42. Courtesy of D. Van Nostrand Company, Inc.*

* J. W. Gewartowski and H. A. Watson, "Principles of Electron Tubes," Van Nostrand, Princeton, New Jersey; 1965. J. Millman and S. Seely, "Electronics," 1st ed., McGraw-Hill Book Company, New York; 1941. K. R. Spangenberg, "Vacuum Tubes," 1st ed., McGraw-Hill Book Company, New York; 1948. A. H. W. Beck, "Thermionic Valves, Their Theory and Design," Cambridge University Press, London, England; 1953. "Standards on Electron Tubes: Definitions of Terms, 1950," Institute of Radio Engineers, New York.

TABLE 1—COMMONLY USED CATHODE MATERIALS.

Type	A	ϕ_0	Efficiency (milliamperes/watt)	Specific Emission (amp/cm²)	Emissivity (watts/cm²)	Operating Temperature (K)	Resistance Ratio (hot/cold)
Bright tungsten (W)	70	4.50	5–10	0.25–0.7	70–84	2500–2600	14/1
Thoriated tungsten (Th–W)	4	2.65	40–100	0.5–3.0	26–28	1950–2000	10/1
Tantalum (Ta)	37	4.12	10–20	0.5–1.2	48–60	2380–2480	6/1
Oxide coated (Ba–Ca–Sr)	*	1.0–1.3	50–150	0.5–2.5	3–5	1000–1150	2.5 to 5.5/1
Impregnated	2.4	1.65		1.8–5.4	2.6–3.8	1300–1400	

* The Richardson-Dushman equation does not apply to a composite surface of this type.

function of temperature for several types of emitters in common use.

Thoriated-tungsten and oxide-coated emitters should be operated close to specified temperature. A customary allowable heating-voltage deviation is ±5 percent. Bright-tungsten emitters may be operated at the minimum temperature that will supply required emission as determined by power-output and distortion measurements. Life of a bright-tungsten emitter is lengthened by lowering the operating temperature. Figure 2 shows a typical relationship between filament voltage and temperature, life, and emission.

Mechanical stresses in filaments due to the magnetic field of the heating current are proportional to I_f^2. Current flow through a cold filament should be limited to 150 percent of the normal operating value for large tubes, and 250 percent for medium types. Excessive starting current may easily warp or break a filament.

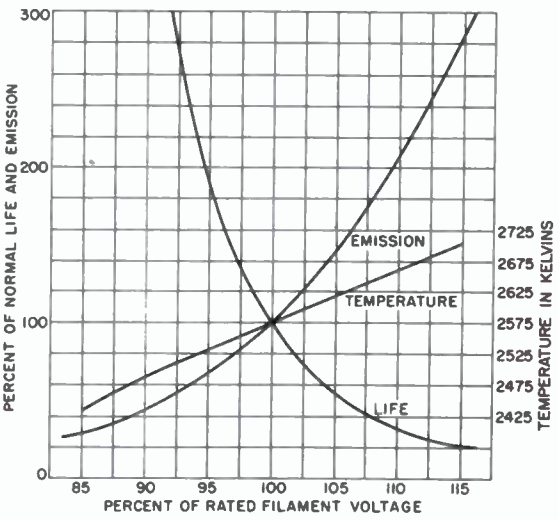

Fig. 2—Effect of change in filament voltage on the temperature, life, and emission of a bright-tungsten filament (based on 2575-kelvin normal temperature of filament).

Secondary Emission

When the surface of a solid is bombarded by charged particles having appreciable velocity, electrons are emitted from the solid. This is the process of secondary emission,* the most important case being when the bombarding particles are also electrons. One then differentiates between incident and emitted electrons by the terms primary and secondary, respectively. The latter term commonly describes all electrons collected from a secondary emitter; these electrons comprise three groups: (A) true secondaries, (B) inelastically reflected primaries, and (C) elastically reflected primaries. True secondaries are considered to be those of the solid which have been excited above the energy level required for escape across the surface barrier. The three groups are separable to a degree on the basis of energy as indicated in the energy distribution curve of Fig. 3. True secondaries constitute the bulk of emitted electrons at moderate primary energies and have a mode energy of at most a few electronvolts. Their distribution is almost independent of primary energy. Electrons in the rela-

* H. Bruining, "Physics and Applications of Secondary Electron Emission," McGraw-Hill Book Company, New York; 1954. O. Hackenberg and W. Brauer, "Secondary Electron Emission from Solids," Advances in Electronics and Electron Physics, Vol. XI, Academic Press; 1959. A. J. Dekker, "Secondary Electron Emission," Solid State Physics, Vol. 6, Academic Press, New York; 1958. R. Kollath, "Sekundarelektronen-Emission fester Korper bei Bestrahlung mit Elektronen," Handbuch der Physik, Band XXI, Springer-Verlag, Berlin; 1956.

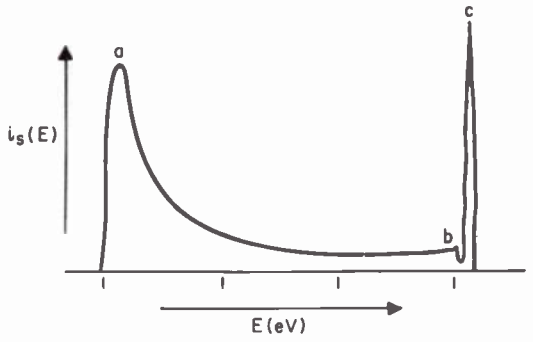

Fig. 3—Total energy distribution of secondary electrons.

tively flat interval within a, b constitute a mixture of true secondaries and inelastically reflected primaries. It has become customary to arbitrarily designate those emitted electrons having energies less than 50 electronvolts as true secondaries.

Total secondary yield δ, defined as the ratio of secondary to primary electron current, is independent of primary current but strongly dependent on primary energy as indicated in Fig. 4. The shape of the yield curve follows from generating and escape mechanisms; the former leading to an initial rise in yield with primary energy, and the latter causing an eventual reduction owing to increased penetration of primaries and a greater mean depth of escape of secondaries. Significant points of the yield curve are first and second crossover at which yield becomes unity, the maximum yield δ_m, and the primary energy eV_m at which the maximum occurs. For most insulators, first crossover occurs between 15 and 25 eV primary energy. Insulators generally exhibit higher yields than conductors, a property attributed to the absence of conduction electrons which tend to reduce the mean energy and the escape probability

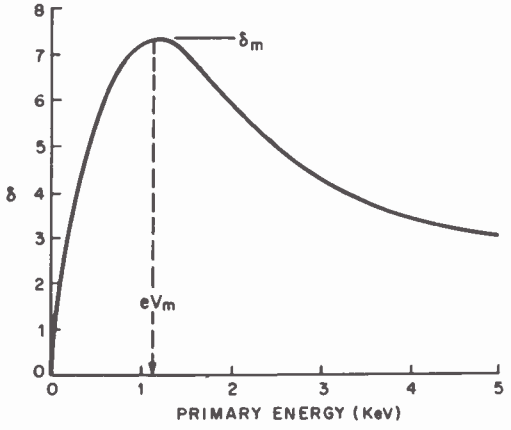

Fig. 4—Secondary-emission yield curve.

of secondaries through collision losses within the solid. The yield of insulators decreases noticeably as temperature is increased, owing to increasing electron–phonon interaction.

Secondary yield increases with angle of primary incidence, the effect being most pronounced at high primary energies. Yield is also a function of surface structure and may be minimized by employing physical trapping such as provided by a porous surface. Lowest yields are obtained for porous carbon deposits and highest yields for single crystal insulators having low electron affinity. Secondary yield may also be influenced by internal electric fields which tend to assist or retard the escape of secondaries. If such fields are strongly dependent on charge transport within the bombarded material, yield may become dependent on primary current which can in turn give rise to anomalous time-dependent effects. Barring such effects, it appears that the interaction time for the secondary-emission process is of the order of 10^{-12} second.

When the rate of bombardment by primary electrons becomes very low, as in single-electron counting, the statistical nature of the secondary-emission process becomes evident. The probability of obtaining $0, 1, 2, \cdots, n$ secondaries per incident primary is given by the Poisson distribution.

Commonly used secondary-emission materials are silver-magnesium or copper-beryllium alloy processed to provide a high-yield partly conductive surface film. Typically such surfaces exhibit yields of 2.5 to 4 at 100 eV primary energy.

Secondary emission is employed advantageously in the operation of many electron devices, such as camera tubes, storage tubes, and image intensifiers. A most important application lies in secondary-electron multiplication, which provides a means for amplifying very weak electron currents as in photomultiplier tubes. A conventional electron multiplier consists of a number of secondary-emitting dynodes operated at progressively higher potentials and terminated by an electron-collecting electrode. Electrons incident on the first dynode are multiplied, the resultant secondaries are accelerated to the second dynode where the process is repeated, and so on throughout the multiplier structure.

If the dynodes exhibit uniform yield characteristics, the overall amplification G obtained from a multiplier having n dynodes is

$$G = g^n$$

where g is the gain per dynode. The actual gain g may be slightly less than the secondary yield δ because of multiplier geometry. In the absence of appreciable space-charge effects, maximum gain is realized when the available potential is uniformly distributed across the dynode chain. An empirical relation for g may be obtained by approximating